frontiers | Research Topics

Translation of genetically engineered T cells in cancer immunotherapy

Edited by
Shao-An Xue, He Huang, Hakim Echchannaoui and Ralf-Holger Voss

Published in
Frontiers in Immunology
Frontiers in Oncology

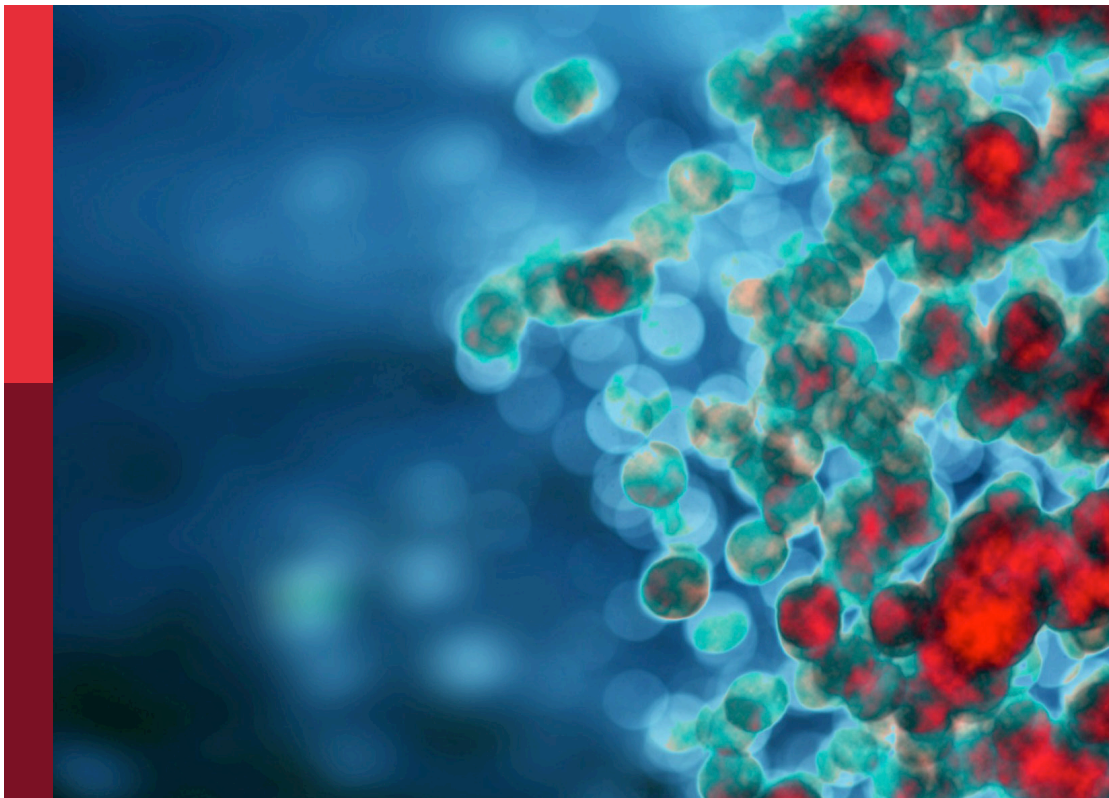

ISSN 1664-8714
ISBN 978-2-8325-3531-8
DOI 10.3389/978-2-8325-3531-8

About Frontiers

Frontiers is more than just an open access publisher of scholarly articles: it is a pioneering approach to the world of academia, radically improving the way scholarly research is managed. The grand vision of Frontiers is a world where all people have an equal opportunity to seek, share and generate knowledge. Frontiers provides immediate and permanent online open access to all its publications, but this alone is not enough to realize our grand goals.

Frontiers journal series

The Frontiers journal series is a multi-tier and interdisciplinary set of open-access, online journals, promising a paradigm shift from the current review, selection and dissemination processes in academic publishing. All Frontiers journals are driven by researchers for researchers; therefore, they constitute a service to the scholarly community. At the same time, the *Frontiers journal series* operates on a revolutionary invention, the tiered publishing system, initially addressing specific communities of scholars, and gradually climbing up to broader public understanding, thus serving the interests of the lay society, too.

Dedication to quality

Each Frontiers article is a landmark of the highest quality, thanks to genuinely collaborative interactions between authors and review editors, who include some of the world's best academicians. Research must be certified by peers before entering a stream of knowledge that may eventually reach the public - and shape society; therefore, Frontiers only applies the most rigorous and unbiased reviews. Frontiers revolutionizes research publishing by freely delivering the most outstanding research, evaluated with no bias from both the academic and social point of view. By applying the most advanced information technologies, Frontiers is catapulting scholarly publishing into a new generation.

What are Frontiers Research Topics?

Frontiers Research Topics are very popular trademarks of the *Frontiers journals series*: they are collections of at least ten articles, all centered on a particular subject. With their unique mix of varied contributions from Original Research to Review Articles, Frontiers Research Topics unify the most influential researchers, the latest key findings and historical advances in a hot research area.

Find out more on how to host your own Frontiers Research Topic or contribute to one as an author by contacting the Frontiers editorial office: frontiersin.org/about/contact

Translation of genetically engineered T cells in cancer immunotherapy

Topic editors

Shao-An Xue — University College London, United Kingdom

He Huang — Zhejiang University, China

Hakim Echchannaoui — University Medical Center, Johannes Gutenberg University Mainz, Germany

Ralf-Holger Voss — University Medical Centre, Johannes Gutenberg University Mainz, Germany

Citation

Xue, S.-A., Huang, H., Echchannaoui, H., Voss, R.-H., eds. (2023). *Translation of genetically engineered T cells in cancer immunotherapy*. Lausanne: Frontiers Media SA. doi: 10.3389/978-2-8325-3531-8

Table of contents

frontiers | Frontiers in Immunology

TYPE Editorial
PUBLISHED 07 September 2023
DOI 10.3389/fimmu.2023.1278677

OPEN ACCESS

EDITED AND REVIEWED BY
Gerald Willimsky,
Charité University Medicine Berlin, Germany

*CORRESPONDENCE
Ralf-Holger Voss
hvoss@uni-mainz.de
Shao-An Xue
shao-an.xue@ucl.ac.uk

RECEIVED 16 August 2023
ACCEPTED 23 August 2023
PUBLISHED 07 September 2023

CITATION
Voss R-H, Echchannaoui H, Huang H and Xue S-A (2023) Editorial: Translation of genetically engineered T cells in cancer immunotherapy. *Front. Immunol.* 14:1278677. doi: 10.3389/fimmu.2023.1278677

Editorial: Translation of genetically engineered T cells in cancer immunotherapy

Ralf-Holger Voss[1]*, Hakim Echchannaoui[2,3,4], He Huang[5] and Shao-An Xue[6,7]*

[1]Institute of Immunology, Department of Research Center for Immunotherapy, Laboratory U. Sahin, University Medical Center (UMC) of the Johannes Gutenberg University, Mainz, Germany, [2]Department of Hematology and Medical Oncology, University Medical Center, Johannes Gutenberg-University, Mainz, Germany, [3]German Cancer Consortium partner site Frankfurt/Mainz, Mainz, Germany, [4]University Cancer Center Mainz, Mainz, Germany, [5]Institute of Hematology, Zhejiang University, Hangzhou, China, [6]Surgery, Medical School, Faculty of Medical Sciences, University College London, London, United Kingdom, [7]Genetic Engineering Laboratory, School of Biological & Environmental Engineering, Xi'An University, Xi'An, China

KEYWORDS

genetic/cellular engineering, CAR-T, TCR-T, cancer immunotherapy, tumor specific/associated antigens, genome editing, immunosuppression, CAR toxicity

Editorial on the Research Topic
Translation of genetically engineered T cells in cancer immunotherapy

Genetically engineered T cells have made tremendous contributions to cancer immunotherapy. Chimeric antigen receptor (CAR)-modified T cells have demonstrated remarkable efficacy in hematological malignancies (1–5), however, clinical responses have not been convincing in solid tumors. T cell receptor (TCR)-engineered T cells showed promising results in some solid cancers (6–8), yet many hurdles remain to translate current genetically engineered T cells into more effective therapeutics, to achieve higher and durable clinical responses.

In this Research Topic, we compile recent advances in T cell immunotherapy, including the identification of new promising antigens, the optimisation of genetically modified TCR- and CAR-T cells to improve their persistence and reduce their toxicity. We also discuss strategies to overcome the suppressive tumor microenvironment (TME) and perspectives in T cell manufacturing.

1 Identification and validation of novel antigens for cancer immunotherapy

In recent years, tumor-specific mutated antigens, also called neoantigens (neoAgs) have emerged as a promising class of immunogenic antigens for immunotherapy (9). These antigens are exclusively expressed and presented on tumor cells, and represent an attractive therapeutic tool for solid tumors, in particular for TCR-engineered T cells (10).

In this Research Topic, Immisch et al. identified a neoepitope comprising Rac1P29S amino acid mutation, which is the third most common hotspot mutation in melanoma. They have not only isolated and characterised TCRs that can recognise this HLA-A*02:01-binding neoepitope, but also demonstrated TCR-T induced cytotoxicity against Rac1P29S expressing cancer cells *in vitro* and *in vivo* after adoptive T cell therapy.

Although neoAgs are considered as truly tumor-specific antigens (11), Amerongen et al. pursue the concept of identifying highly expressed tumor-associated antigens in ovarian cancer from pooled mRNAseq data bases, and a reverse immunology approach for the most prevalent HLA restriction elements. The candidate antigens comprising PRAME, CTCFL and CLDN6 exhibited a 20-fold higher expression in tumors compared to normal cells. High-avidity TCRs were isolated, cloned and characterised *in vitro* to exclude potential on/off-target-reactivities, and demonstrated potent antitumor activities, making these TCRs especially useful for adoptive therapy in ovarian cancers, generally considered as 'cold tumors' with less T-cell infiltrates.

2 Strategies to enhance expression, specificity, affinity, and (signaling) functions of the engineered molecules

Barden et al. addressed the issue of cross-activation of a CAR with the endogenous TCR in CAR-T cells. They found out that the antigen-dependent activation of T-cells by the triggered immunoreceptor (IR) exclusively results in phosphorylation of the CAR/CD3ζ or TCR/CD3ζ, respectively, thus excluding reciprocal cross-activation. This is in line with elaborate microscopy analyses elucidating their mutual spatial exclusion upon either IR activation. However, TCRs and CARs can co-operate by means of antigen recognition by the endogenous TCR and costimulation by CD28 incorporated in CD28/ζ CARs. Collectively, the authors claim that TCR/CD28 CAR-signaling may be exploited for Boolean logic "AND" gating (12), stressing the importance of endogenous TCRs for providing a non-TME tonic signaling for CAR-T persistence in patients.

TCR-based bispecific T cell engagers (TCE) are emerging therapeutics as recently reported by positive phase III clinical results of a gp100/HLA-A2-TCR/anti-CD3 bifunctional in melanoma patients (13). Unlike antibody-based TCE (14), which have been widely studied, little is known about how the formats of TCR-based TCE affect their potencies. In this context, Van Diest et al. recently developed a novel TCE format based on the soluble γ9δ2TCR-antiCD3 bispecific molecule (GAB) (15), and described an alternative design based on the multimerisation of GABs to improve their potency. Here, van Diest et al. could further enhance the fraction of GAB-dimers by shortening the linker length within the anti-CD3 scFv, and showed that GAB-dimers were superior in function, without apparent on-target/off-tumor reactivity.

3 Novel strategies for genetic engineering of T cells, including CAR-T and TCR-T cells

Hiltensperger and Krackhardt have reviewed in depth the TCR-T and CAR-T field, comprising several aspects, from the design of different generations of CARs for providing signal 1 to 3 in T-cell activation, prevention of TCR mispairing by TCR protein engineering and genome editing, the set up of allogeneic T-cell transfer to boost T-cell fitness and T-cell graft manufacturing, adverse events to reckon with and counteracting tumor escape, persistence of T-cells, to treatment modalities for solid cancers. The review also covers gene transfer shuttle systems, persistence of T-cells, gene delivery approaches *in vivo*, potentially arising adverse events such as on/off-target toxicities, and cellular and molecular strategies to force back tumor escape mechanisms and resistance of solid tumors in TME, and provides an overview of ongoing clinical trials.

Degirmencay et al. have explored how modifications of framework residues in the TCR variable domains affect TCR expression and function. They used bioinformatic and protein structural analyses to identify candidate amino acid residues in the framework of the variable β domain predicted to drive high TCR surface expression. Replacing these residues in poorly expressed TCRs resulted in improved surface expression and enhanced target specific killing by these engineered TCR-T. Their results corroborated improved expression and functionality, while at the same time reducing the risk of toxicity associated with TCR mispairing.

Autologous T cell engineering is not only costly but also time-consuming, limiting the number of patients who can benefit from this new therapy. Yu et al. developed an allogeneic approach by generating CD19-CAR T cells from cord blood of allogeneic donor, and demonstrated their anti-tumor activity *in vitro* and *in vivo* using a diffuse large B-cell lymphoma model (DLBCL). The rationale behind this idea is the higher proportion of naïve T-cells from cord blood that can be redirected into potent effector T cells, thus having a better anti-tumor activity. This strategy may provide a broader option for immunotherapy, offering readily accessible "off-the-shelf" cellular products.

4 Strategies for overcoming the immunosuppressive tumor microenvironment

In a previous study, TCR-T cells were engineered to disrupt PD-1 upregulation upon antigen encounter by CRISPR/Cas9 genome editing to minimise immunosuppression through PD-L1-positive tumor cells (16). Here, Kim et al. went on one step further and took advantage of the tightly regulated PDCD1 locus for replacing PD-1 by a pleiotropic cytokine such as IL-12 to positively affect the persistence of T-cells in TME. By this means, an inhibitory signal of PD-1 would be reversibly inverted into a stimulatory signal of IL-12 only in the presence of the tumor antigen recognised by the introduced TCR, and hence in a local (TME) and timely (as long as antigen is present) restricted manner so as to avert cytokine-induced toxicities.

5 Manufacturing platforms for vector production and cellular engineering

Niu et al. analysed the phenotype of lentivirally (LV) transduced versus PiggyBac transposon (PB)-transfected CAR-T cells *in vitro* and *in vivo*. They scrutinised biomarker expression rates and phenotype (effector versus central memory subsets), cytokine/chemokine secretions and cytolyses, including a transcriptomic approach, and

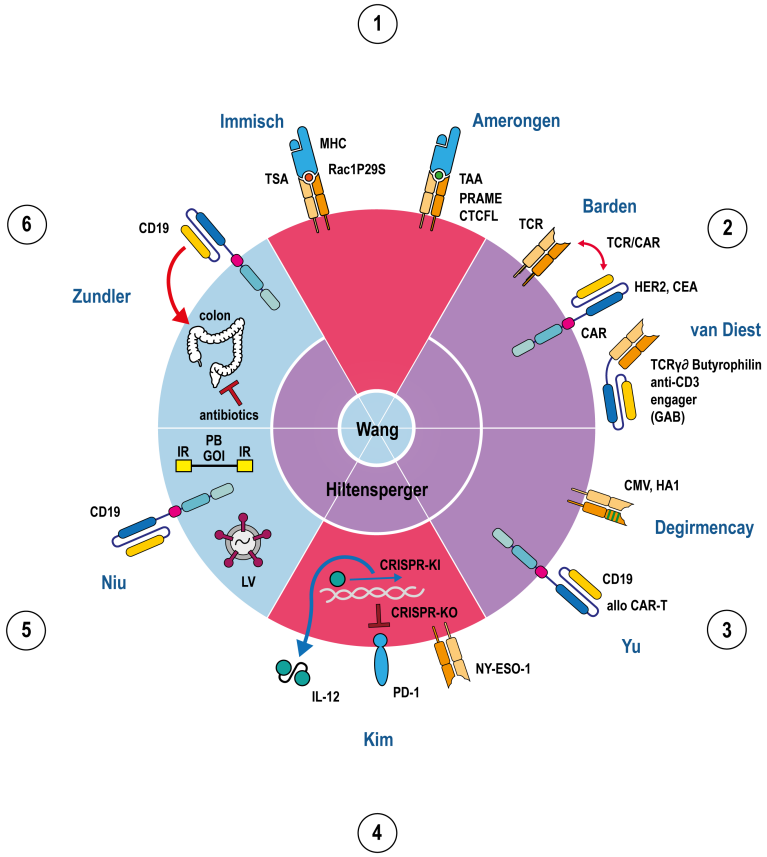

FIGURE 1
Apple pie chart attributing 11 articles (2 reviews, 8 original research articles, 1 case report) to the 6 topics 1.-6. listed in the Editorial summary in a clockwise manner. The 11 articles are indicated by their first author names. The 6 apple pie pieces are colour-coded according to their assigned articles covering either the subject TCR (red), CAR (blue), or both (purple). The review articles are shown in the center of the chart indicating to which topics they refer to. TCRs, CARs, MHCs, PD-1, IL-12, and GABs are depicted in a stylised fashion. The outline of the circle represents the T-cell membrane where all immunoreceptors (TCRs, CARs) are embedded. IL-12, GABs and MHCs are either soluble molecules or membrane proteins from target cells, respectively, and hence located outside the circle. Tumor antigens presented by MHC are indicated as coloured spheres, depending on the particular peptide. Antigen specificities of TCRs, CARs and GABs are denoted besides the stylised molecule. Helical DNA, lentivirus, recombinant transposon DNA, and colon are adumbrated as cell or body internal components and hence, located inside the circle. Red double/single arrows represent mutually interacting/inflammatory, a '⊥' inhibitory reactions, a blue arrow an activating reaction in transcription/translation, green lines in a TCR denotes point mutations in TCR Vβ domain. Abbreviations: TSA tumor specific antigen, TAA tumor associated antigen, TCR T-cell receptor, CAR chimeric antigen receptor, GAB gamma delta TCR anti-CD3 bispecific molecule, CMV cytomegalovirus, allo alloreactive, IL-12 interleukin 12, KO knock out, KI knock in, CRISPR clustered regularly interspaced short palindromic repeats, PD-1 programmed cell death protein 1, LV lentivirus, PB PiggyBac, IR inverted repeats, GOI gene of interest, Rac1P29S, PRAME, CTCFL, Her2, CEA, CMV, HA1, NY-ESO-1, CD19 represent processed or full length tumor/viral antigens, respectively.

validation of an *in vivo* tumor model. In PB- compared to LV-CAR-T, they reported on higher expression of IL-9, a cytokine that enhances anti-tumor responses, and on lower expression of IL-6, the hub cytokine triggering cytokine release syndrome, suggesting a favourable profile of the former manufacturing platform. Importantly, both systems control tumor cells comparably *in vivo*, in line with recently published work (17).

6 Strategies for reducing toxicity and improving safety

Although, CAR-T cell therapy approximates a consolidated mainstay in the treatment of several hematologic malignancies, adverse side effects may occur. In this Research Topic, Wang et al. reviewed CAR-T treatments in the context of multiple myeloma and potential toxicities, while Hiltensperger & Krackhardt covered CAR-T and TCR-T approaches in general, highlighting recent innovations capable of enhancing efficacy and reducing toxicity. Zundler et al. also reported a case of a rare complication in a patient treated with CD19 CAR-T for DLBCL, who developed chronic diarrhea with characteristics of inflammatory bowel disease-like colitis. Resolution of colitis occurred by using an antibiotic therapy that might have changed the intestinal microbiota, which most likely limited the stimulation of these intestinal infiltrating CAR-T cells.

Author contributions

RHV: Writing – review & editing, Conceptualization, Writing – original draft. HE: Writing – review & editing. HH: Writing – review & editing. SAX: Writing – original draft, Writing – review & editing, Conceptualization.

Funding

SAX is supported by the National Natural Science Foundation of China (NSFC-81972883).

Acknowledgments

We are in particular very grateful to Mr. Stefan Kindel, scientific illustrator of the University Medical Center Mainz, who prepared Figure 1 of this Editorial summary.

Conflict of interest

The authors declare that the research was conducted in the absence of any commercial or financial relationships that could be construed as a potential conflict of interest.

The author(s) declared that they were an editorial board member of Frontiers, at the time of submission. This had no impact on the peer review process and the final decision.

Publisher's note

References

1. Kalos M, Levine BL, Porter DL, Katz S, Grupp SA, Bagg A, et al. T cells with chimeric antigen receptors have potent antitumor effects and can establish memory in patients with advanced leukemia. *Sci Transl Med* (2011) 3(95):95ra73. doi: 10.1126/scitranslmed.3002842

2. Grupp SA, Kalos M, Barrett D, Aplenc R, Porter DL, Rheingold SR, et al. Chimeric antigen receptor-modified T cells for acute lymphoid leukemia. *New Engl J Med* (2013) 368(16):1509–18. doi: 10.1056/NEJMoa1215134

3. Maude SL, Laetsch TW, Buechner J, Rives S, Boyer M, Bittencourt H, et al. Tisagenlecleucel in children and young adults with B-cell lymphoblastic leukemia. *New Engl J Med* (2018) 378(5):439–48. doi: 10.1056/NEJMoa1709866

4. Boyiadzis MM, Dhodapkar MV, Brentjens RJ, Kochenderfer JN, Neelapu SS, Maus MV, et al. Chimeric antigen receptor (CAR) T therapies for the treatment of hematologic Malignancies: clinical perspective and significance. *J Immunother Cancer* (2018) 6(1):137. doi: 10.1186/s40425-018-0460-5

5. Ruella M, Maus MV. Catch me if you can: Leukemia Escape after CD19-Directed T Cell Immunotherapies. *Comput Struct Biotechnol J* (2016) 14:357–62. doi: 10.1016/j.csbj.2016.09.003

6. Robbins PF, Kassim SH, Tran TL, Crystal JS, Morgan RA, Feldman SA, et al. A pilot trial using lymphocytes genetically engineered with an NY-ESO-1-reactive T-cell receptor: long-term follow-up and correlates with response. *Clin Cancer Res* (2015) 21(5):1019–27. doi: 10.1158/1078-0432.CCR-14-2708

7. D'Angelo SP, Melchiori L, Merchant MS, Bernstein D, Glod J, Kaplan R, et al. Antitumor activity associated with prolonged persistence of adoptively transferred NY-ESO-1 (c259)T cells in synovial sarcoma. *Cancer Discov* (2018) 8(8):944–57. doi: 10.1158/2159-8290.CD-17-1417

8. Nagarsheth NB, Norberg SM, Sinkoe AL, Adhikary S, Meyer TJ, Lack JB, et al. TCR-engineered T cells targeting E7 for patients with metastatic HPV-associated epithelial cancers. *Nat Med* (2021) 27(3):419–25. doi: 10.1038/s41591-020-01225-1

9. Schumacher TN, Schreiber RD. Neoantigens in cancer immunotherapy. *Science* (2015) 348(6230):69–74. doi: 10.1126/science.aaa4971

10. Garber K. Driving T-cell immunotherapy to solid tumors. *Nat Biotechnol* (2018) 36(3):215–9. doi: 10.1038/nbt.4090

11. Coulie PG, Van den Eynde BJ, van der Bruggen P, Boon T. Tumour antigens recognized by T lymphocytes: at the core of cancer immunotherapy. *Nat Rev Cancer* (2014) 14(2):135–46. doi: 10.1038/nrc3670

12. Hamieh M, Mansilla-Soto J, Riviere I, Sadelain M. Programming CAR T cell tumor recognition: tuned antigen sensing and logic gating. *Cancer Discov* (2023) 13(4):829–43. doi: 10.1158/2159-8290.CD-23-0101

13. Nathan P, Hassel JC, Rutkowski P, Baurain JF, Butler MO, Schlaak M, et al. Overall survival benefit with tebentafusp in metastatic uveal melanoma. *N Engl J Med* (2021) 385(13):1196–206. doi: 10.1056/NEJMoa2103485

14. van de Donk N, Zweegman S. T-cell-engaging bispecific antibodies in cancer. *Lancet* (2023) 402(10396):142–58. doi: 10.1016/S0140-6736(23)00521-4

15. van Diest E, Hernandez Lopez P, Meringa AD, Vyborova A, Karaiskaki F, Heijhuurs S, et al. Gamma delta TCR anti-CD3 bispecific molecules (GABs) as novel immunotherapeutic compounds. *J Immunother Cancer* (2021) 9(11):e003850. doi: 10.1136/jitc-2021-003850

16. Stadtmauer EA, Fraietta JA, Davis MM, Cohen AD, Weber KL, Lancaster E, et al. CRISPR-engineered T cells in patients with refractory cancer. *Science* (2020) 367(6481):eaba7365. doi: 10.1126/science.aba7365

17. Lin Z, Liu X, Liu T, Gao H, Wang S, Zhu X, et al. Evaluation of Nonviral piggyBac and lentiviral Vector in Functions of CD19chimeric Antigen Receptor T Cells and Their Antitumor Activity for CD19(+) Tumor Cells. *Front Immunol* (2021) 12:802705. doi: 10.3389/fimmu.2021.802705

frontiers | Frontiers in Immunology

TYPE Review
PUBLISHED 22 December 2022
DOI 10.3389/fimmu.2022.1050522

OPEN ACCESS

EDITED BY
Shao-An Xue,
Xi'an University, China

REVIEWED BY
Nausheen Ahmed,
University of Kansas, United States
Estefanía García-Guerrero,
Institute of Biomedicine of Seville (CSIC), Spain

*CORRESPONDENCE
Yongxu Jia
jiayongxu111@126.com
Yanru Qin
yanruqin@163.com

†These authors have contributed equally to this work and share first authorship

SPECIALTY SECTION
This article was submitted to Cancer Immunity and Immunotherapy, a section of the journal Frontiers in Immunology

RECEIVED 21 September 2022
ACCEPTED 08 December 2022
PUBLISHED 22 December 2022

CITATION
Wang Z, Chen C, Wang L, Jia Y and Qin Y (2022) Chimeric antigen receptor T-cell therapy for multiple myeloma.
Front. Immunol. 13:1050522.
doi: 10.3389/fimmu.2022.1050522

Chimeric antigen receptor T-cell therapy for multiple myeloma

Zehua Wang†, Chen Chen†, Lei Wang, Yongxu Jia* and Yanru Qin*

Department of Oncology, The First Affiliated Hospital of Zhengzhou University, Zhengzhou, China

Multiple myeloma (MM) is a malignant plasma cell disorder that remains incurable for most patients, as persistent clonal evolution drives new mutations which confer MM high-risk signatures and resistance to standard care. The past two decades have significantly refashioned the therapeutic options for MM, especially adoptive T cell therapy contributing to impressive response rate and clinical efficacy. Despite great promises achieved from chimeric antigen receptor T-cell (CAR-T) therapy, the poor durability and severe toxicity (cytokine release syndrome and neurotoxicity) are still huge challenges. Therefore, relapsed/refractory multiple myeloma (RRMM), characterized by the nature of clinicopathologic and molecular heterogeneity, is frequently associated with poor prognosis. B Cell Maturation Antigen (BCMA) is the most successful target for CAR-T therapy, and other potential targets either for single-target or dual-target CAR-T are actively being studied in numerous clinical trials. Moreover, mechanisms driving resistance or relapse after CAR-T therapy remain uncharacterized, which might refer to T-cell clearance, antigen escape, and immunosuppressive tumor microenvironment. Engineering CAR T-cell to improve both efficacy and safety continues to be a promising area for investigation. In this review, we aim to describe novel tumor-associated neoantigens for MM, summarize the data from current MM CAR-T clinical trials, introduce the mechanism of disease resistance/relapse after CAR-T infusion, highlight innovations capable of enhanced efficacy and reduced toxicity, and provide potential directions to optimize manufacturing processes.

KEYWORDS

multiple myeloma, immunotherapy, chimeric antigen receptor cell therapy, resistance mechanism, efficacy, toxicity

1 Introduction

Multiple myeloma (MM) is a malignant plasma cell disorder that displays a myriad of manifestations including hypercalcemia, renal insufficiency, anemia, and bone destruction (CRAB) (1, 2). MM is the second most common hematological malignancy with an estimated 32270 new cases and 12830 deaths in the United States in 2020 (3). Genetic abnormities, mostly translocation and hyper-diploidy, result in dysregulated cancer-immunity cycle that allows MM to escape immune surveillance with an uncontrolled cell proliferation (4, 5). The past two decades have significantly refashioned the therapeutic options of MM, such as the availability of proteasome inhibitors (PI), immunomodulatory drugs (IMiDs), histone deacetylase inhibitors (HDACi), anti-CD38 monoclonal antibodies (mABs), antibody-drug conjugates (ADC), and selective inhibitors nuclear export (SINE) (6). However, MM remains incurable for most patients, as persistent clonal evolution drives new mutations which confer MM high-risk signatures and resistance to standard care (7, 8). Therefore, relapsed/refractory multiple myeloma (RRMM), characterized by the nature of clinicopathologic and molecular heterogeneity (9, 10), is frequently associated with poor prognosis (11).

Chimeric antigen receptor T-cell therapy (CAR-T) has shown exceptional success in the treatment of relapsed/refractory B-cell acute lymphoblastic leukaemia (B-ALL), B-cell chronic lymphoblastic leukaemia (B-CLL), and diffuse large B-cell Lymphoma (DLBCL) (12, 13), thereby motivating its application in RRMM (14). T cells are firstly isolated from the patients' or donors' blood and genetically modified in the laboratory to encode an artificial receptor, enabling CAR T cells to identify targets better and precisely destroy cancer cells. CAR T-cell functions with two major roles: 1) tumor-associated antigen (TAA) binding; 2) MHC-independent T-cell activation. Emerging as a novel immunotherapy, CAR T-cell therapy consists of an extracellular antigen recognition domain (scFv, Fab, Nb, and NKG2D ligand), a transmembrane domain, and an intracellular domain incorporating co-stimulation (CD28 or a 4-1BB) and signaling components (CD3zeta) (Figure 1) (15, 16). The interplay between tumor cell and CAR gives rise to an immunological synapse. This process could attack target cells through various pathways, such as the release of cytotoxic molecules, and the induction of apoptosis signal pathway, eventually leading to the activation of effector T cells and elimination of tumor cells (17).

Despite great promises achieved by CAR-T therapy, the poor durability and severe toxicity are still huge challenges. The mechanisms driving resistance and relapse after MM CAR T-cell therapy remain uncharacterized. Consequently, this review aims to describe candidate tumor-associated neoantigens for MM, provide a summary of efficacy and safety data from clinical trials, introduce mechanisms of disease resistance/relapse to CAR-T, and explore future innovations capable of enhanced efficacy and reduced toxicity, and provide potential directions to optimize manufacturing processes.

2 Candidate targets for multiple myeloma CAR-T

The key to design a successful CAR is to select a surface antigen that presents at high concentration on MM cells, but absent in non-malignant hematopoietic lineages or other tissues (18–21). The most important avenue is to discover novel TAAs to improve CAR-T therapy. Several targetable antigens are currently being evaluated regarding their safety and efficacy in clinical trials (Tables 1, 2). Potential targetable antigens for MM are summarized in Figure 2, including BCMA, CD19, SLAMF7, GPRC5D, CD138, CD38, CD70, NKG2DL, Kappa light chain.

2.1 BCMA

B cell maturation antigen (BCMA), a transmembrane glycoprotein belonging to tumor necrosis factor (TNF) receptor superfamily, is the most commonly used surface antigen target for multiple myeloma CAR-T. BCMA plays a critical role in differentiating B-cell to plasma cell and maintaining the survival of plasma cell (34, 35). BCMA is preferentially expressed on plasma cells, though limited BCMA-positive cells can be identified in normal tissues, such as the spleen, lymph nodes, and the stomach (36, 37). A European study involving 70 MM patients identified that surface BCMA expression on plasma cells (normal or malignant) was significantly higher ($P<0.001$) than non-plasma cells (38). The high expression of surface BCMA is associated with MM in several preclinical models and humans, making it an attractive target for MM (39–41). However, BCMA could be expressed at high or low concentrations in MM cells (36, 42, 43). In a United Kingdom study, 28 evaluable MM patients all expressed BCMA, and levels differed from low to moderate (42). Similarly, a UK study reported that all 64 patients with MM expressed surface BCMA at varying levels by immunohistochemistry (43). Since there is a considerable variation in BCMA expression on MM cells, patients may respond differently to BCMA-targeted CAR-T therapy. As surface BCMA level may serve as an independent prognostic factor, cytogenetic assessments are of great importance (43). It is anticipated that patients with high levels of BCMA may gain more benefits from BCMA-targeted CAR-T therapy. Thereby, all findings support that BCMA may be a promising target for MM CAR-T therapy.

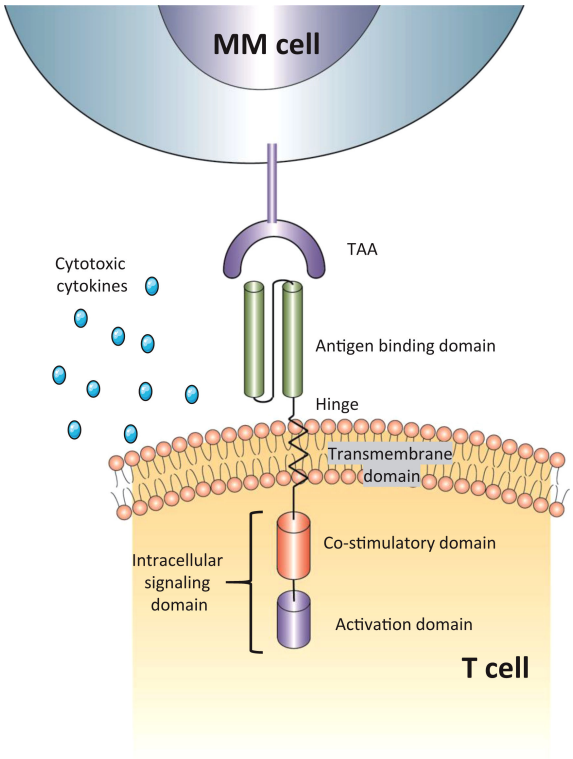

FIGURE 1
The structure of CAR-T cells. The antigen-binding domain is usually a single-chain variable fragment (scFv) but also has other structures; intracellular signaling domain include both co-stimulatory domain (CD28, 4-1BB) and activation domain (CD3zeta). TAA, tumor-associated antigen; MM cell, multiple myeloma cell.

The first BCMA-targeted MM CAR-T clinical trial was conducted by National Cancer Institute (NCT02215967) (44). A total of 24 patients with RRMM were enrolled. The notable findings of this study were the dose-dependence of efficacy and toxicity. The ORR was 20% among 10 patients receiving the lowest dose of 0.3-3.0 × 10^6 CAR-T cells/kg. However, of 16 patients treated with high-dose level, the ORR was 81% with 62.5% having very good partial response (VEGF) or better. Notably, the toxicity of low-dose CAR-T was generally modest and no patient with grade 3 or 4 cytokine release syndrome (CRS). By contrast, grade 3-4 CRS and neurotoxicity (NTX) were 25% and 4% among patients treated with highest dose (9 × 10^6 CAR-T cells/kg). Further, a statistically significant relationship (P = 0.04) between plasma cell burden and severe CRS had been reported from patients with high-dose level of CAR-T cells. Many BCMA-targeted CAR-T clinical trials are ongoing or completed (Table 1). Additionally, combination therapies are evaluated as well, such as associating BCMA CARs with tyrosine kinase inhibitor (NCT04603827), immunomodulators (NCT03070327, NCT04287660), nonspecific immune inhibitors (NCT03943472), and gamma-secrete inhibitor (NCT03502577).

2.2 Non-BCMA targets

Though a majority of MM CAR-T clinical trials target BCMA, but there are several studies focused on non-BCMA MM-associated neoantigens (Table 2).

2.2.1 CD19

Human CD19 antigen belongs to type-I transmembrane glycoprotein of the IgG immunoglobulin superfamily. In normal tissues, CD19 is specifically expressed throughout the development of B-cell lineage except for hematopoietic stem cells and terminal plasma cells, whereas it is absent on other hematopoietic lineages. In B-cell malignancies, its expression is widely distributed in relapsed/refractory B-cell acute lymphoblastic leukemia (R/R B-ALL) and relapsed/refractory B-cell non-Hodgkin lymphoma (R/R B-NHL) (45). Despite low expression of CD19 on MM cells, CD19 is expressed on the minor multiple myeloma stem cell (MMSC) subset that has been reported (46). MMSC is capable of self-renewal and drug-resistance. Thus, CD19 might be a potential target for MM. One clinical trial (NCT02135406) indicated that autologous stem cell transplantation (ASCT) followed by CD19-targeted CAR-T therapy (CTL019) infusion was safe and available in RRMM, leading to a longer PFS compared to patients with ASCT alone (47, 48).

2.2.2 SLAMF7

SLAMF7 belongs to the signaling lymphocyte activation molecule family (SLAMF). SLAMF7 is firstly documented in natural killer cells (49). It is also expressed on T cells, B cells, monocytes, macrophages, and dendritic cells. Over 95% of normal or malignant plasma cells of MM expressed SLAMF7 (50). Since SLAMF7 is also expressed in normal plasma cells, specific attacks on this target inevitably cause normal cell death. Thereby, SLAMF7 is an alternative but suboptimal choice for CAR-T cell therapy.

The function of SLAMF7 is poorly understood, but previous evidence indicates its similar role as growth factor contributing to myeloma cell proliferation (51, 52). It has been reported that SLAMF7-CAR T cells attack myeloma and confer selective fratricide of SLAMF7-positive normal lymphocytes (53). A conceivable side effect is the depletion of SLAMF7+ lymphocytes, including a substantial proportion of T cells, B cells, and NK cells. It would be reasonable to engineer SLAMF7-CAR T cells with a safety switch to terminate fratricide of normal lymphocytes. Inducible caspase 9 or herpes simplex virus thymidine kinase might be preferable choices for safety switch (54, 55).

10.3389/fimmu.2022.1050522

TABLE 1 Selected BCMA-targeted CAR-T clinical trials for MM.

Identifier	Target	Status	Phase	Enrollment	Study Population	Efficacy		Safety		Reference
						ORR (%)	Median PFS (month)	Grade > 3 CRS (%)	Grade > 3 NTX (%)	
NCT02215967	BCMA	Completed	I	24	RRMM	81	7.75	25	4	(22)
NCT02546167	BCMA	Completed	I	25	HRMM	48	2.7	32	12	(23)
NCT02658929	BCMA	Active	I	67	RRMM	76	8.8	6	3	(24)
NCT03274219	BCMA	Active	I	72	RRMM	55	11.9	4	6	(25)
NCT03975907	BCMA	Recruiting	I	62	RRMM	87.5	18.8	6	3	(26)
NCT03302403	BCMA	Active	I	18	RRMM	87.5	unknown	0	4	(27)
NCT03093168	BCMA	Unknown	I	10	RRMM	86	unknown	0	0	(28)
NCT04322292	BCMA	Recruiting	I	10	RRMM	95.2	unknown	5	0	(29)
NCT03661554	BCMA	Unknown	I	15	RRMM	88.2	12.1	2.9	0	(30)
NCT03090659	BCMA	Active	I-II	74	RRMM	87.8	18.04	9.5	0	(31)
NCT03548207	BCMA	Active	I-II	97	RRMM	96.9	unknown	4.1	9.3	(32)
NCT03716856	BCMA	Active	I	24	RRMM	87.5	unknown	0	4.2	(26, 33)

Abbreviations: RRMM, relapsed or refractory multiple myeloma; HRMM, high risk multiple myeloma; CRS, cytokine release syndrome; NTX, neurotoxicity; ORR, overall response rate; PFS, progression-free survival.

TABLE 2 Selected non-BCMA-targeted CAR-T clinical trials for MM.

Neoantigen	Expression on MM cells	Expression on hematopoietic cells	Expression on other cells	Identifier	Status	Phase	Enrollment	Efficacy	Safety
CD19	weak expression	B-cell lineage cells	absent	NCT02135406	completed	I	10	ORR: 80%	AE: 0%
SLAMF7	increased expression	NK cells, T cells, B cells, dendritic cells, monocytes, macrophages	absent	NCT03958656	completed	I	13	NA	NA
GPRC5D	high expression	B cells and plasma cells	epithelial cells	NCT04555551	active	I	17	ORR: 83%	G3+ CRS: 8%
CD138	high expression	Plasma cells	epithelial cells	NCT01886976	recruiting	I-II	10	ORR: 80%	AE: 0%
CD38	increased expression	NK cells, T cells, dendritic cells, neutrophils, and progenitor cells	epithelial cells	NCT03464916	active	I	72	NA	NA
CD70	increased expression	germinal center B cells, T cells	stromal cells of the thymic medulla	NCT04662294	recruiting	I	108	NA	NA
NKG2D	increased expression	NK cells, T cells	absent	NCT02203825	completed	I	12	NA	AE: 0%

MM, multiple myeloma; ORR, overall response rate; AE, adverse event; CRS, cytokine release syndrome; G3+, Grade 3-4; NA, not available.

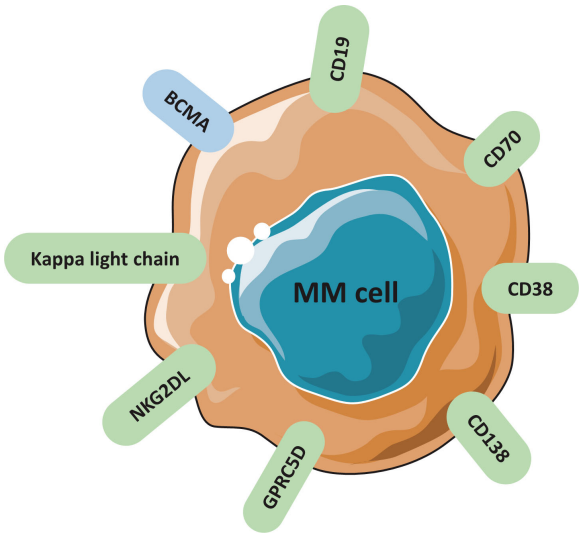

FIGURE 2
Candidate surface antigens found on MM cells and studied in clinical trials.

Several anti-SLAMF7 CAR constricts are evaluated in clinical trials, mostly as monotherapy (NCT03710421, NCT04142619, NCT04541368, NCT03958656, NCT04499339), or as dual CARs targeting both BCMA and SLAMF7 (NCT04795882, NCT04156269).

2.2.3 GPRC5D

The G protein-coupled receptor, class C group 5 member D (GPRC5D), is expressed on 98% of the CD138+ cells by quantitative immunofluorescence (56). Also, this surface receptor is primarily expressed on hair follicles, but also in multiple myeloma cells. Therefore, GPRC5D-targeted CAR-T was constructed by Smith et al., which displayed potent anti-MM effects on MM cell lines and xenografted models (56). Anti-GPRC5D was deemed safe and effective as no alopecia or any skin-related disorders were detected in a preclinical study (57). A series of GPRC5D-CAR T trials are ongoing, such as NCT05219721, NCT04555551, NCT05016778. MCARH109, as the first-in-class GPRC5D-targeted CAR T-cell therapy for MM, has a manageable safety profile and high rates of clinical response (ORR: 83%). More importantly, all 6 patients who relapsed after BCMA-targeted CAR-T responded to MCARH109.

2.2.4 CD138

As a major extracellular matrix (ECM) receptor, CD138 (syndecan-1) plays an important role in cell-cell and cell-matrix adhesion, and cell proliferation (58, 59). CD138 is widely expressed on normal and malignant plasma cells (60), but also expressed on the surface of mature epithelial cells that might cause skin toxicity. A prior study found that a high concentration of CD138 might be poor prognostic factor for MM (61). A CD138-directed CAR-T (CART-138) has been built incorporating with a 4-1BB domain (62). Relevant CD138-targeted CAR trials include single-target (NCT01886976, NCT03672318, NCT03196414, NCT03778346) and multi-target CAR-T products (NCT03271632). Based on current data (NCT01886976), the ORR achieved 80% and no toxicity has been reported, manifesting a good efficacy and tolerability. However, CD138 shedding and skin toxicity are major barriers for wide application of CD138-targeted CAR-T.

2.2.5 CD38

CD38, a transmembrane glycoprotein, is known to mediate cell adhesion, signal transduction, and Ca^{2+} regulation (63). CD38 is highly expressed on the surface of MM cells, though its expression in normal hematopoietic cells also have been detected, such as T cells, precursors of B cells, NK cells, and myeloid precursors (63). Some monoclonal antibodies against CD38 have been approved by FDA to treat multiple myeloma, such as Daratumumab. The success of mAb targeting CD38 in the treatment of MM has encouraged the development of CD38-targeted CAR T cells. Light-chain exchange technology brings potential to avoid accident damage to $CD38^{+}$ normal cells (64). A clinical trial (NCT0346491) investigated CD38-targeted CAR-T as a monotherapy for RRMM. In addition, dual CAR products are also tested in clinical trials, combing CD38 and BCMA (NCT03767751), CD38 and CD19 (NCT03125577).

2.2.6 CD70

Aberrant expression of CD70 has been found in hematological malignancies and solid tumors (65). Because of its limited expression on normal cells, CD70 holds great promises for monoclonal antibody-based therapy. A preclinical study supported that CD70-targeted CAR T-cell therapy was safe and effective (66). Further, related publications manifested that CD70 targeting CAR-T cells caused robust anti-tumor activity in both human cancer cells and animal models (67, 68). It is worth noting that a clinical trial (NCT04662294) on CD70 is recruiting RRMM patients, although no data has been reported yet. Importantly, an obvious advantage is a low risk of fratricidal killing caused by CD70 antibody, mainly because of the transient expression of CD70 on immune cells (8).

2.2.7 NKG2DL

NKG2D, a cell surface receptor binding to several ligands, is predominantly expressed on immune cytotoxic cells, such as NK cell and $CD8^{+}$ cytotoxic T cells. NKG2D ligands, such as MIC-A, MIC-B, and UL-16, are upregulated in many solid tumors or hematologic malignancies but absent on healthy tissue. NKG2D binds to corresponding ligands to prompt the secretion of proinflammatory cytokines and the activation of cytotoxic cells,

leading to immune elimination of MM cells (69). Due to the presence of a natural costimulatory domain, DAP10, there is no need to add this specific domain to NKG2D CARs. But a potential challenge is the poor persistency of T cells. To resolve this problem, patients should be treated with high doses or multiple infusions without compromising the toxicity (70). Satisfactorily, higher doses have the same safety profile with low doses, with no reports of CRS or NTX so far. We have identified one NKG2D CAR study (NCT03018405) in MM with an enrollment of 12 patients, but efficacy profile has not been published.

2.2.8 Kappa light chain

Although cell surface immunoglobulins are not expressed on all plasma cells, it is recognized that MM stem cells express surface immunoglobulins (71). Thereby, kappa light chain might be an ideal target for MM (71). Several monoclonal antibodies targeting kappa light chain have been developed and tested in clinical trials, such as MDX-1097 (72). But CAR-targeting kapa light chain is still a less explored field. In one trial conducted by Ramos et al., 4 of 7 RRMM patients responded to kappa-targeted CAR-T cell therapy, keeping disease stable for 2-17 months. In a phase-I trial of κ-CAR-T cells (NCT00881920), 16 patients with non-Hodgkin lymphoma/chronic lymphocytic leukemia or MM were enrolled. Notably, 4 of 7 patients with relapsed or refractory MM kept disease stable for 2-17 months (71).

3 Mechanisms of disease resistance/relapse after MM CAR-T

Despite the impressive ORR, over 50% of patients after BCMA-directed CAR-T would relapse or progress within 1-year (73). Another study showed a consistent preliminary trend that most MM patients who achieved MRD-negative to bb2121 have progressed in follow-up period (74). Thus, though CAR-T cells have the robust cytoreductive capacity to treat multiple myeloma, they cannot produce lasting immune surveillance. Currently, exact mechanism of disease resistance/relapse after MM CAR-T remains elusive, but there are several deductive mechanisms stated as following: 1) T cell-dependent resistance; 2) antigen-driven resistance (antigen escape, antigen shedding); 3) TME-related resistance. Some mechanisms are presented in Figure 3.

3.1 Poor persistence of CAR T cells

One study suggested that CAR-T cells were detectable up to 3 months after CAR-T injection and were gradually eliminated (73). At 12 months after infusion, only approximately 20% of patients had detectable engineered T cells (73). A lot of efforts have been made to figure out potential mechanisms leading to short persistence of CAR-T cells (73).

3.1.1 T cell clearance

CAR-T cells are immunogenicity, thereby they might be eliminated by adaptive immune response over time. Single-chain fragment variable (ScFv) is the most common antigen-binding counterpart in CAR-T constructs. Most of ScFvs in BCMA-directed CAR-T are derived from non-human species (73), which induce immunogenicity and thereby potentially limit the T-cell persistence. In legend-2 study (75), anti-ScFv antibodies were detected in 7 of 17 MM patients after receiving bi-epitope BCMA-targeting CAR-T (LCAR-B38M), and 6 of them had decreased CAR-T cells and experienced tumor recurrence. More specifically, camelid-derived ScFvs were used to assemble LCAR-B38M, specifically targeting two different epitopes of BCMA on MM cell surface. There are agreements that non-human ScFv can induce immunological reaction to produce anti-CAR antibodies, which eventually lead to T-cell clearance and constitute a higher risk of relapse after CAR-T. This observation also highlights the importance of manufacturing humanized ScFV.

3.1.2 Lack of memory characteristics

The differentiation stage of CAR-T cells affects their proliferation and survival, strongly correlating with their anti-tumor activity (76–78). The immunophenotype of T-cell used to manufacture CAR-T is considerably pivotal for T-cell persistence. Each subset of T cells possessed heterogeneity of proliferation and longevity (79). For example, naïve T-cells, stem memory T-cells, and central memory T-cells present the best proliferation capacity and delayed exhaustion or senescence (80). The enrichment of $CD27^+/CD45RO^-/CD8^+$ T cells with memory-like features is correlated with long-term remission (81, 82). Also, a high percentage of cytotoxic $CD8^+$ T cells with a naïve or stem memory characteristic are found to persist much longer and expand better *in vivo*, achieving superior outcomes after BCMA-targeted CAR-T treatment (23).

This view keeps in line with a previous finding that longer persistence of CAR-T cells *in vivo* expansion has been associated with better clinical remission and survival for recipient patients (83–86). One study also indicated that persistent CAR-T cells detected in peripheral blood tend to generate superior clinical response even among patients with high-grade diseases (87). Therefore, naïve cells and memory cells are important for CAR-T cell manufacture, mainly because they display sustained proliferation and longer persistence *in vivo*.

3.1.3 Impaired T cell fitness

The quality of T cells also profoundly affects their life span *in vivo*. Notably, malignancy itself and chemotherapy-related myelosuppression could hamper T-cell fitness (88). When

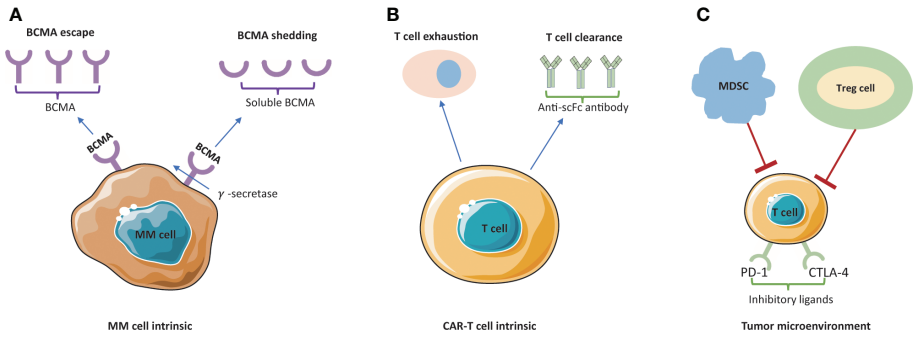

FIGURE 3
Mechanism of resistance/relapse to BCMA-targeted CAR-T cell therapy. **(A)** BCMA escape and BCMA shedding are blocking the antigen recognition by CAR-T cells. Membrane BCMA can be cleaved by γ–secretase and released to the plasma as soluble BCMA (sBCMA). **(B)** Poor persistence of CAR-T cells is mainly caused by T cell exhaustion and T cell clearance. **(C)** The tumor immunosuppressive microenvironment is mainly led by inhibitory ligands (PD-1 and CTLA-4) and suppressive immune cells (MDSC and Treg cells). MM, multiple myeloma; MDCS, myeloid-derived suppressor cells; Treg cell, T regulatory cells.

patients receive many lines of myeloma treatments, the composition of T cells would change over time. Furthermore, patients who underwent more lines of chemotherapies tended to have less early memory T cells *in vivo* (89).

3.1.4 T cell exhaustion

T-cell exhaustion is another potential culprit, mainly because of constitutive antigen-independent tonic signaling by CAR-T. A variety of factors are able to induce tonic signaling to form activating clusters, leading to off-target activation and T-cell exhaustion (90, 91). Optimizing the CAR to limit antigen-independent tonic signaling and increase antigen-dependent recognition could be beneficial for T-cell persistence. In an anti-GPRC5D model of CAR-T, an IgG4/IgG2-derived spacer with modifications has been raised by Smith and colleagues, which might delay T-cell exhaustion (57).

3.2 Antigen escape and shedding

Antigen escape and shedding are the most common causes of the failure of CAR-T cell strategy. First, downregulation of tumor antigen reduces the CAR-T cell targeting ability, weakening the tumor-killing effects. Second, increased antigen shedding into a soluble form could negatively affect the efficacy of CAR-T therapy.

BCMA represents an important target. Theoretically, nearly all MM patients express BCMA irrespective of newly diagnosed or relapsed (38). It remains controversial about whether BCMA expression level is associated with the response rate to BCMA-directed CAR-T cells. However, loss of BCMA expression was suspected in post-treatment residual MM cells. Based on existing findings, there is a transient phenomenon that BCMA disappeared after initial response and subsequently remerged over MM progression (92). Though MM relapse is mainly caused by BCMA-positive clones, cases of recurrence led by BCMA-negative target cells have been noticed (22, 93). For example, a recent study pointed out that BCMA-negative was suspected in 3 of 71 patients at disease progression (94).

BCMA shedding from plasma cells is mediated by γ-secretase, producing the soluble-BCMA (sBCMA) that serves as a circulatory biomarker. Previous literatures have demonstrated that sBCMA is associated with the tumor burden and the prognosis (41, 95). High levels of soluble-BCMA might competitively bind to ScFv and consequently interfere the precise recognition of MM cells by CAR-T cells (96). Inhibitors of γ-secretase avoid BCMA shedding from MM cells and reduce the interference of soluble BCMA. Intriguingly, based on preclinical data, soluble BCMA does not affect the function of novel BCMA-CAR T *in vitro* and *in vivo* (37). Up to date, there is no clear clinical evidence that the level of sBCMA could negatively affect the efficacy of BCMA-targeted CAR-T therapy.

Likewise, high levels of soluble SLAMF7 are associated with a worse response to elotuzumab, along with a shorter survival (97). In addition, soluble CD38 could reduce the anti-MM response of daratumumab (98). However, as a seven-transmembrane protein, the likelihood of GPRC5D shedding into serum is low (57, 99). It is interesting to find that GPRC5D expression is independent from BCMA, therefore it might be an alternative target for relapsed MM patients after BCMA-directed therapy due to BCMA loss or shedding (57).

3.3 TME suppression

The tumor microenvironment (TME) plays a critical role in drug-resistance mechanism. CAR T cells need to overcome

inhibitory signals and immunosuppressive cells existing in the TME. Immunosuppressive cells consist of T regulatory cells (Treg), B regulatory cells, myeloid-derived suppressor cells (MDSC), and plasmacytoid dendritic cells. These subsets may negatively affect the function of CAR-T cells (100–102). Besides, inaccessibility of MM cells by CAR-T cells forms another barrier. It is true MM cells generally reside in bone marrow microenvironment involving various cell types and extracellular matrix (ECM), which make CAR-T cells difficult to access MM (103). A recent study (104) about B-cell lymphoma reported a similar observation that many CD19-targted CAR-T cells did not successfully reach their target destination. Although mature CAR-T tracing method are still unmet needs, it is widely accepted that MM exploits immunosuppressive TME to block the efficacy of CAR-T cells and consequently lead to high risks of recurrence. PD1-PDL1 axis is another major cause of CAR T-cell dysfunction (105, 106). PD-1 expressed on activated T cells, is capable of binding with PD-L1 expressed by MM cells, eventually leading to exhausted state of T cells (107).

4 Strategies to improve the efficacy

For RRMM patients, poor persistence of T cells, antigen escape, and TME suppression restrict the durability of immune response and consequently limit the efficacy of CAR-T therapy in clinical settings. However, recently initiated studies have incorporated innovations to address above barriers (Figure 4, Table 3).

4.1 Enhancing CAR-T cell persistence

Optimizing CAR-T design is a potential strategy to enhance CAR-T cell persistence. The utility of fully human recognition domains, rather than those derived from mouse antibodies, is an attempt to reduce immunogenicity which usually leads to clearance of CAR-T cells by patients' immune system (22, 44, 75, 108, 109). Importantly, this strategy not only improves CAR-T cell persistence, but also simultaneously reduces cytokine storm. Besides, several studies demonstrated that the transmembrane region and co-stimulatory domain confer different properties of CAR-T cells that may influence efficacy and toxicity as well (110–125).

Another promising approach is to use less-differentiated T cells subsets that have a good proliferative capacity, such as naïve T cells, stem cell memory T cells (TSCM), central memory T cells (TCM). According to preclinical studies, CAR-T cells with memory phenotype presented superior engraftment, proliferation, and longevity compared to general CAR-T components (126, 127). Further, those who are treated with a defined ratio (1:1) of $CD4^+/CD8^+$ CAR-T cells, were monitored with more potent T cell expansion and fewer toxicities *in vivo* (128, 129).

In addition, lymphodepleting regimen may enhance the expansion of adoptively transferred T cells leading to superior persistence (130). First, lymphocytes depletion therapy before CAR-T could greatly reduce the risk of anti-CAR immune response. Second, a lymphodepleting environment is suitable for CAR-T cell expansion and persistence (80). It is known that IL-7 could assist $CD8^+$ cytotoxic T-cell to preserve a stem

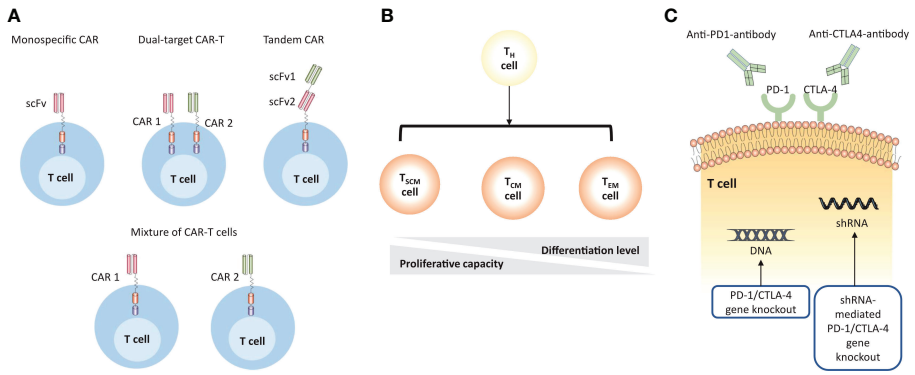

FIGURE 4
Strategies to improve the efficacy of MM CAR-T cell therapy. **(A)** CAR-T cell products are designed to target multiple TAAs to overcome antigen escape. The monospecific CAR has a single scFv; the dual-target CAR construct includes two separate monospecific CARs on the surface of T cells; the tandem CAR has two antigen-binding domains that are linked tandemly on one CAR protein; the mixture of CAR-T cells describes the simultaneous transduction of different types of CAR-T cells *in vivo*. **(B)** The persistence of CAR-T cells can be enhanced by using less-differentiated T cell subsets. **(C)** CAR-T cells can be engineered to overcome the immunosuppressive microenvironment by using immune checkpoint inhibitors or direct gene knockout.

memory phenotype *in vivo* (131), which is critical for T-cell expansion. All these data support the conclusion that more intense lymphodepletion may induce better CAR-T persistence and expansion.

4.2 Countering antigen escape

Increasing the density of BCMA expression is a critical area to counter antigen escape. The use of γ-secretase inhibitor (GSI) is able to increase BCMA expression on MM cells and reduce sBCMA levels by inhibiting the cleavage of surface BCMA (132). Preclinical models (133) have demonstrated that the presence of GSI could lead to a threefold to fivefold increase of BCMA expression level in MM cell lines. Particularly, when the density of BCMA is relatively low on the target cells, the administration of GSI may enhance the capacity of identifying MM cells. Great advancements in the efficacy of BCMA-targeted CAR T cells in combination with GSI have been observed in mouse models (133). Currently, several GSIs are being tested in clinical trials, even including patients with solid tumors (134). Future studies might discover other approaches to upregulate BCMA expression.

To address BCMA-negative clones, targeting two or more distinct antigens is underway. Due to the heterogeneity nature, targeting only one antigen at a time may not produce a long-lasting immunosurveillance in a large number of MM patients (135–137). More specifically, single target CAR-T only displays one single-chain variable fragment (ScFv) for antigen recognition, whereas dual-target CAR-T simultaneously contains co-stimulatory domain or tandem CAR molecules to overcome antigen escape and guarantee better identification. There are several strategies to achieve dual-target CAR-T products: 1) sequentially infusion of two CAR-T cells that respectively target different MM-associated antigen; 2) the same T cell displays two different CAR products; 3) One tandem CAR construct containing two antigen recognition moieties incorporated with one activation region (138). Available dual CAR products involved a combination of BCMA and CD19 (NCT04236011, NCT04162353), BCMA and SLAMF7 (NCT04662099, NCT04156269), BCMA and CD38 (NCT03767751). More details could be seen in Table 4.

4.3 Overcoming immunosuppression in the TME

CAR-T cells should preliminarily overcome direct T cell inhibitory signals presented in the TME. PD1-PDL1 is the best characterized pathway. Inhibition of the PD-1 signals could produce dramatic clinical benefits in a variety types of tumors (139). Recent studies have demonstrated that coadministration of immune checkpoint inhibitors (ICI) with CAR-T therapy brought increased efficacy in preclinical models (105). In addition to ICI, knockout of the PD-1 coding gene could be engineered by gene silencing techniques, such as short hairpin RNAs (140) and CRISPR-Cas9 (141). Also, armoured CAR T cells secreting cytokines or chemokines are able to alter the inflammatory microenvironment and support the functionality of CAR T cells (142). Further, the metabolic competition between tumor and immune cells in the TME may restrict nutrient availability and cause microenvironment acidosis, which could trigger T cell inhibitory pathways or otherwise hinder immune cell function (143). Intriguingly, the expression of the antioxidant enzyme catalase in CAR-T cells may overcome granulocyte-mediated oxidative stress *in vitro* (144). Modifying T cell metabolism is a promising area to boost efficacy, but further validation is needed in clinical application.

5 Strategies to reduce the toxicity

Overall, treatment-related toxicity of MM CAR-T therapy involves two major categories: 1) general toxicity caused by T cell activation and following systemic cytokine storm; 2) specific toxicity caused by the interaction between CARs and TAAs expressed on non-tumor cells, which is also termed as 'on-target, off-tumor' toxicity.

5.1 Systemic cytokine storm

The rapid immune activation responsible for the success of CAR-T strategy also stimulates treatment-related toxicity. The clinical complications caused by different CAR-T in MM are similar to those led by CD19-targeted CAR-T in ALL and DLBCL (84, 145, 146), including cytokine release syndrome (CRS) and neurotoxicity (NTX), and hematologic cytopenia, which might limit the wide application of CAR-T cell therapy in MM.

The most frequent toxicity is cytokine release syndrome (CRS), a constellation of symptoms involving fever, myalgia, hypoxia and hypertension, resulting from increased inflammatory cytokines like IL-6. IL-6 receptor antagonism *via* Tocilizumab and short-course steroids could be used for CRS management (147). Besides, CAR-T cell-associated HLH/MAS is a more severe systemic hyperinflammatory syndrome. CAR-T cell-induced HLH/MAS may be resistant to IL-6 receptor inhibitors, of which condition chemotherapy would be required (145).

Neurotoxicity (NTX), is the second major adverse effect, mainly because of the disruption of the blood-brain barrier and increased cerebrospinal fluid cytokine levels (148). NTX frequently occurs with or following CRS, presenting encephalopathy, delirium, aphasia, seizures, and life-threatening cerebral oedema (149). The consensus grading

TABLE 3 Mechanisms of resistance to MM CAR-T and strategies to overcome the resistance.

	Resistance Mechanism		Strategies	Clinical Trial
T-cell intrinsic	Poor persistence	T cell clearance due to Immunogenicity	Manufacturing humanized ScFv with decreased immunogenicity	NCT03602612
		Lack of memory characteristics	Memory T cell-enriched product • Culture with PI3K inhibitors • Transduction with stem-cell memory T cell • CAR constructs with specific CD4:CD8 ratio	NCT03274219 NCT03288493 NCT03338972
		Impaired T cell fitness	• Allogeneic CAR-T cells • Receiving treatment at earlier MM stage	NCT04093596 NCT04196491
		T cell exhaustion	Limit antigen-independent tonic signaling and increase antigen-dependent recognition	NA
MM intrinsic	Antigen Escape	BCMA escape BCMA shedding	• Dual-/Multi-target design • Increased BCMA expression with gamma-secretase inhibitors	NCT04935580 NCT03502577
TME	Inhibitory signals and immunosuppressive cells	PD1-PDL1-mediated T cell dysregulation Immunosuppressive cells: Treg, MDSC	• Combined with immune checkpoint inhibitors • Combined with immunomodulatory drugs	NA

MM, multiple myeloma; TME, tumor microenvironment; Treg, T regulatory cells; MDSC, myeloid-derived suppressor cells; NA, not available.

scheme proposed by ASBMT was applied extensively (149). Notably, the grade 3-4 CRS and NTX could be effectively managed by tocilizumab and supportive care. Also, management of NTX comprises of corticosteroids and IL-6 pathway antagonisms (145). A special form of NTX is referred to immune effector cell-associated neurotoxicity syndrome (ICANS), as transient encephalopathy, which is attributed to off-target cytokine production, as well as immune response of central nervous system (CNS). A mounting evidence suggests that ICANS could be characterized by atypical features and prolonged timeframes (150). And its management coincides with CRS interventions, such as cytokine inhibitors and corticosteroids. However, current understanding of ICANS is still limited. The mechanisms for ICANS after BCMA-targeted therapy need further elucidation (151).

Hematologic cytopenia is commonly reported following BCMA CAR-T cell therapy, manifesting as leukopenia, lymphopenia, anemia, neutropenia, and thrombocytopenia, which could increase the risks of infection, bleeding, fever, and bruising (146, 152–154). After infusion, CAR-T cells not only activate tumor-specific T-cell, but also induce non-specific T or B clones that target hematopoietic stem cell (HSC), neutrophils, platelets, and erythroid cells (155). Besides, the release of cytokines could drive differentiation but arrest maturation of HSC (156). Therefore, the IL-6 blockade may control hematologic cytopenia as well. The management of cytopenia also includes transfusion of blood cells and growth factors of hematopoietic stem cell transplantation (HSCT) (157, 158).

To counter systemic cytokine toxicity, CAR-T cells must reach a threshold level for activation but not exceed the level that

TABLE 4 Dual-target or multi-target strategy tested in early clinical trials.

Antigen	Identifier	Status	Enrollment	Population
BCMA × CD19	NCT04935580	recruiting	20	NDMM, HRMM
BCMA × CD19	NCT04714827	recruiting	24	RRMM
BCMA × CD19	NCT04236011	recruiting	15	RRMM
BCMA × CD38	NCT03767751	recruiting	80	RRMM
BCMA × SLAMF7	NCT04156269	unknown	12	RRMM
BCMA × CD38 × CD138 × CD56	NCT03271632	recruiting	20	RRMM
BCMA × CD19 × CD38 × NYESO-1	NCT03638206	recruiting	73	RRMM

RRMM, relapsed or refractory multiple myeloma; HRMM, high risk multiple myeloma; NDMM, newly diagnosed multiple myeloma.

would result in a series of cytokine secretion. Thus, therapeutic window for each CAR should be carefully considered. Researchers are currently engineering several innovations to control CAR expression or activity (Figure 5).

Firstly, 4-1BB co-stimulatory domain is associated with a much slower onset of T cell activation, increased T cell durability, and a lower risk of cytokine-related toxicity compared to CD28 domain. Therefore, inclusion of 4-1BB co-stimulatory domains might be less toxic in patients with heavy tumor burden. But CD28 is necessary to achieve the required threshold for T cell activation, especially for MM with a relatively low density of antigen or a low-affinity antigen-binding domain. Overall, the choice of co-stimulatory domain is critical to balance the efficacy and safety in CAR-T cell therapy.

Secondly, engineering 'suicide genes' into the CAR construct could induce apoptosis to eliminate CAR-T cells when treatment-related toxicity occurs. Co-expression of suicide receptors on MM CAR-T cells, such as CD20 and EGFR, could be attacked by rituximab (159–161) and cetuximab (162), respectively. Therefore, these FDA-approved antibodies provide a mean to deactivate CAR-T cells. Another strategy is to incorporate apoptosis-triggering fusion protein into CAR-T cells. iCasp9 is a well-characterized example, which can be triggered by dimerizing agents and subsequently drive rapid T cell depletion (163).

Thirdly, administration of small-molecular agents could control 'on or off switch' on CAR-T cells. Dasatinib, a tyrosine kinase inhibitor for CML and ALL. This agent enables the inhibition of LCK or intracellular signaling cascade, followed by destroying the downstream signal of activated CD3zeta. It has been demonstrated that dasatinib rapidly and reversibly hinder CAR-T cell activation, which provides a well-tolerated pharmacological toxicity switch without eradication of T cells (164). Alternatively, switch-off CARs (SMASh-CARs) provide another strategy to dynamically regulate T cell functionality *via*

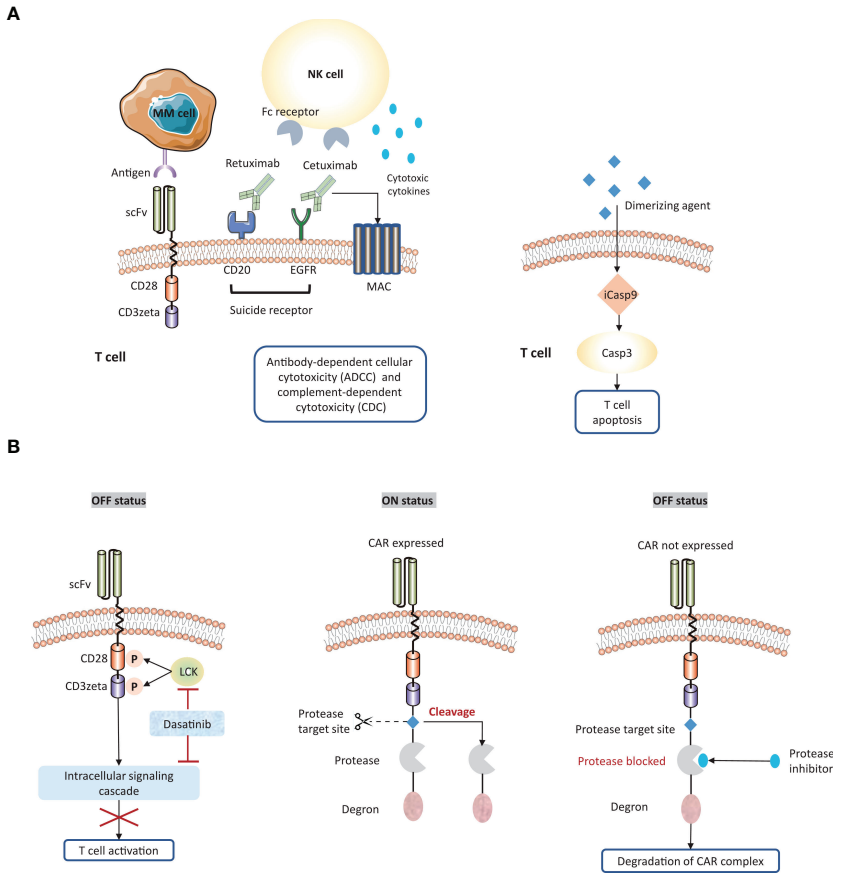

FIGURE 5
Strategies to overcome systemic cytokine toxicity. To counter systemic cytokine storm, several approaches are engineered to adjust CAR expression or activity. **(A)** Suicide gene system enables the elimination of CAR-T cells by following strategies: a) the activation of antibody-dependent cellular cytotoxicity (ADCC) or complement-dependent cytotoxicity (CDC); b) the induction of apoptosis pathway. **(B)** The 'ON/OFF switches' of CAR-T cells could be regulated by small molecular agents. scFv, single chain fragment variable; MAC, membrane attack complex; iCasp9, inducible caspase 9.

embedding a protease target, a protease, and a degron moiety (165). In the 'OFF' state, the degron moiety promotes the degradation of CAR-protease-degron complex. Protease inhibitors may function as the similar role to retain the degron structure. In the 'On' state, the protease target site is cleavage by protease leading to the removal of the degron from CAR protein, and consequently the CAR is expressed on the surface of T cells.

In addition, a more direct antagonism way is knockout of cytokine genes or expression of cytokine antagonists, both of which might provide opportunities to avert systemic toxicities. For example, the macrophage-activating and monocyte-activating cytokine GM-CSF can be antagonized by mutational inactivation and antibody lenzilumab, both of which can increase CAR T cell persistence while decreasing the risk of CRS.

5.2 On-target, off-tumor toxicity

Typically, CAR T cells are designed to target tumor-associated antigens (TAA). However, some TAAs are also expressed on the normal cells, leading to mistaken recognition and attack by CAR T cells. BCMA is a prominent TAA for CAR-T cell therapy in MM. However, the public transcriptomic datasets confirmed BCMA RNA expression in the caudate of normal human brains (166), indicating an on-target effect of anti-BCMA CAR-T therapy. Given the reports of phase-II ciltacel study, 12 of 97 patients were reported with non-ICANS neurotoxicity. 5 of 97 (5.2%) patients suffered from a cluster of movement and neurocognitive symptoms (3 with ≥ Grade 3 parkinsonism) (167). Among them, one patient developed a progressive movement disorder with symptoms of parkinsonism around three months after BCMA-targeted CAR-T cell infusion. By analyzing this case, one study demonstrated that BCMA expression on neurons and astrocytes in the basal ganglia (166). Therefore, BCMA-targeted CAR-T cells may hold the potential to cross the blood-brain barrier and induce a progressive neurocognitive or movement disorder by targeting the basal ganglia. Close monitoring of neurotoxicity is necessary in patients with BCMA-targeted CAR-T cell therapies.

Engineering strategies aims to overcome on-target, off-tumor toxicity mediated by CAR-T cell therapy (Figure 6). The first strategy is to enhance the specificity of antigen recognition. Targeting multiple TAA is a promising approach. Specifically, CAR protein could be disassembled into two separate receptors, one with CD3zeta domain and another with a co-stimulatory domain. Both receptors need to recognize different TAAs for CAR T cells activation. Preclinical models have observed the promises in such a strategy (168–170). Alternatively, the inhibitory CAR (iCAR) contains a special inhibitory region that is generally derived from immune checkpoint proteins, such as PD-1 and CTLA-4. The inhibitory signal could recognize an antigen expressed on healthy tissues but absent on tumor cells (171). Moreover, engineering chimeric co-stimulatory receptor enables T cells to recognize antigens that are enriched on tumor cells. The second strategy is to utilize logic gating or conditional system to control CAR-T cell activation, such as the phospho-antigens that could be identified by T cell receptor. For example, HIF-1α degradation pathway is exploited to restrict CAR expression to CAR-T cells located in hypoxia TME, thereby avoiding adverse effects on healthy tissues which are normally non-hypoxic (172).

6 Innovations of MM CAR-T manufacture

Novel agents and CAR-T manufacture platforms are especially noteworthy. Table 5 specifically focused on data of novel therapeutic agents for RRMM presented at major oncology meeting between 2020 and 2022, including Annual Society of Hematology (ASH) and American Society of Clinical Oncology (ASCO).

6.1 Role of allogeneic CAR-T

Currently, all FDA-approved CAR-T constructs are manufactured within autologous T cells isolated from the patients' blood. However, this individualized production process is somewhat costly and time-consuming, limiting the number of MM patients who can benefit from CAR-T therapy. First, the manufacture time of autological CAR-T cells is lengthy. Many patients with advanced stage of MM may be unable to benefit from this therapy (84, 186). Second, the production failure may be attributable to the insufficient T cells obtained from MM patients, as patients who previously received chemotherapy tend to undergo bone marrow suppression and lymphodepletion (88, 187). Third, the heterogeneity of apheresis CAR product is another underlying cause of preparation failure. There is a phenomenon that dysfunctional T subsets could result in inferior CAR-T products, consequently leading to poor efficacy and response rates (81, 188–191).

Allogeneic donor T cells provides an alternative to autological CAR-T cell therapy, which might potentially solve the manufacturing issues of inadequate T-cell number and suboptimal T-cell fitness for CAR-T production. CAR-T cells could be derived from HLA-matched allogeneic hemopoietic stem cell donors. Nevertheless, allogeneic CAR-T cell therapy has been associated with graft-versus-host (GVHD) and graft rejection. The engrafted allogeneic donor cells could launch an attack on recipient cells (192), whereas the host immune cells are able to eliminate allogeneic CAR-T cells. Recently, genetic modifications are explored to cope with T cell alloreactivity, such as TCR disruption and safety switch insertions (176). Genome-editing technologies include ZFN, TALEN, and CRISPR-Cas 9, all of which are used to generate universal

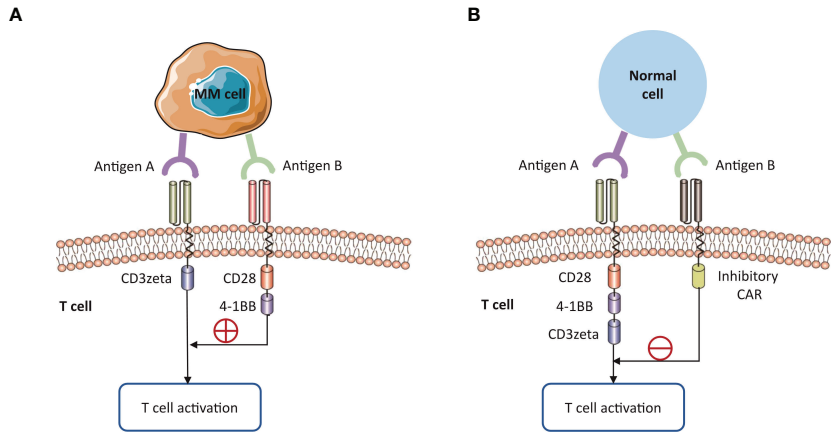

FIGURE 6
Strategies to overcome on-target, off-tumor toxicity. The expression of tumor-associated antigens on healthy tissues can lead to 'on-target, off-tumor' toxicity. **(A)** The specificity of CAR T cells is enhanced by targeting multiple TAAs. The activation domain and co-stimulatory domain should respectively bind to different antigens on MM cells for CAR T cell activation. **(B)** Alternative strategy is to use the inhibitory CAR against a specific non-tumor antigen, requiring the absence of this antigen on MM cells.

CAR-T cells (193). Ongoing clinical trials provide novel armamentarium for MM immunotherapy.

At ASH 2021, updated results of an open-label, phase-I clinical study (UNIVERSAL, NCT04093596) were reported to validate the feasibility of allogeneic anti-BCMA ALLO-715 for RRMM (176). ALLO-715 is a genetically modified anti-BCMA CAR-T product which employed TALEN technology to disrupt the TCR constant gene and CD52 gene to prevent GVHD and allow the use of anti-CD52 based lymphodepletion (194). At the time of data cut-off, 47 patients were enrolled; 42 patients received ALLO-715 infusion. Efficacy outcomes presented 61.5% ORR among patients with high doses. Safety prolife showed CRS occurred in 52.4% and there was no grade 4-5 CRS. Overall, the UNIVERSAL trial demonstrates the proof for allogeneic CAR-T therapy for MM, which might bring meaningful efficacy and tolerable toxicity. But this trial continues to enroll more patients and follow-up data will be updated in the future (176).

6.2 Rapid CAR-T manufacture platform

In the process of commercial manufacture, patients need to wait for around 3-4 weeks until CAR-T infusion, in whom disease might progress while waiting for CAR production. The first-in-human dual BCMA and CD19 targeted CAR was manufactured by a novel platform (FAST CAR platform) that significantly reduced the production time to only 24-36 hours (195). Latest results of this trial (NCT04236011) showed a high response with 100% (DL-1: 1×10^5/kg), 80% (DL-1: 2×10^5/kg), and 93.8% (DL-1: 3×10^5/kg) ORR, respectively. Also, 23 out of 28 patients (82.1%) suffered from grade 1-2 CRS and 2 patients (7.1%) with grade 3. The data presented promising efficacy and favorable safety of the BCMA-CD19 dual fast CAR-T for RRMM patients (182). This clinical trial is still ongoing and recruiting more patients.

At ASH 2021, a rapid manufacturing process that could both preserve the stemness of T cells to ensure longer durability and provide timely access for patients with aggressive disease, has been presented (28). Researchers developed a superior anti-BCMA CAR-T construct (PHE885) carrying a fully human anti-BCMA ScFv fused to 4-1BB/$CD3_{zeta}$ signaling domains and an innovative T-Charge manufacturing platform, which enables rapid and reliable patient access. More specifically, this novel manufacturing platform allows PHE885 to preserve a higher percentage of naïve/T_{SCM} cells, leading to effectively engraft, expand, and reject tumors. Based on this principle, a phase-I trial (NCT04318327) has been initiated and early data of this study will be presented in the future.

6.3 Modified manufacturing process to harvest early memory T-cell

CAR-T cells start to disappear at first 3-6 months after infusion, subsequently leading to the loss of disease control. An innovation is to enrich early memory T cells by modification of manufacturing process. JCARH125 is a well elaborated example. Its production is optimized to harvest early memory T-cell and increase T-cell fitness. Relevant clinical trial (EVOLVE) data

TABLE 5 Clinical trials of novel therapeutic agents for MM at recent oncology meetings, 2020-2022.

Product Name	Identifier	Target	Phase	Enrollment	Study Population	Country	Innovation	Clinical Update
P-BCMA-101	NCT03288493	BCMA	I-II	43	RRMM	United States	Using transposon-based system to enrich early memory T cells	ASH 2020 (173)
Orva-cel	NCT03430011 (EVOLVE)	BCMA	I-II	62	RRMM	United States	Fully human binder	ASCO 2020 (174)
JNJ-4528	NCT03548207 (CARTITUDE-1)	BCMA	I-II	17	RRMM	United States, Japan	A CAR-T therapy containing two BCMA-targeting single-domain antibodies	ASCO 2020 (175)
ALLO-715	NCT04093596 (UNIVERSAL)	BCMA	I	47	RRMM	United States	Allogeneic CAR-T product; Using TALEN technology to disrupt TCR constant gene	ASH 2021 (176)
CT053	NCT03975907 (LUMMICAR)	BCMA	I-II	14	RRMM	China	A fully human autologous CAR-T product	ASH 2021 (177)
ARI0002H	NCT04309981	BCMA	I-II	35	RRMM	Spanish	A lentiviral autologous second-generation CAR-T product	ASH 2021 (178)
PHE885	NCT04318327	BCMA	I	56	RRMM	United States	A novel CAR construct with an innovative T-charge manufacturing platform	ASH 2021 (179)
CT103A	ChiCTR1800018137	BCMA	I-II	71	RRMM	China	A fully human BCMA-specific CAR-T product	ASH 2021 (180)
bb2121	NCT03361748 (KarMMa)	BCMA	II	140	RRMM	Multicenter	Updated data of KarMMa trial	ASCO 2021 (181)
bb2121	NCT04196491 (KarMMa-4)	BCMA	I	13	NDMM	United States	Aiming at high-risk newly diagnosed MM patients	ASCO 2021 (24)
GC012F	NCT04236011	BCMA × CD19	I	28	RRMM	China	Rapid manufacture platform	ASCO 2022 (182)
CART-ddBCMA	NCT04155749	BCMA	I	25	RRMM	United States	An autologous CAR-T product that utilizes a novel, synthetic binding domain	ASCO 2022 (183)
OriCAR-017	NCT05016778	GPRC5D	I	11	RRMM	China	A novel CAR-T product with improvement in expansion and durability	ASCO 2022 (184)
Cilta-cel	NCT04133636 (CARTITUDE-2)	BCMA	II	19	RRMM	Multicenter	Update and supplement of CARTITUDE-1	ASCO 2022 (185)

RRMM, relapsed or refractory multiple myeloma; NDMM, newly diagnosed multiple myeloma; MM, multiple, myeloma; ASCO, American society of clinical oncology; ASH, American society of hematology.

have been previously presented in ASH 2018. According to the latest reporting at ASCO 2020 (174), a total of 44 patients who received higher doses (300×10^6, 450×10^6, 600×10^6) respectively achieved the ORR of 95%, 94%, and 71%. A promising finding is that functional CAR-T cells could be detected in 69% of cases at 6 months. P-BCMA-101 is an autologous BCMA-targeted CAR construct that consisted of a large number of stem cell memory cells. P-BCMA-101 was manufactured by a novel virus-free transposon "piggy-Bac" technology that preferentially transfect early memory T cells (196), thereby increasing efficacy while minimizing toxicity (173). A phase I-II study of P-BCMA-101 (NCT03288493) is being tested in RRMM patients and early data were reported in ASH 2018 (197). Current clinical data keep consistent with preclinical findings that the modifications of CAR production appear to have notably improved efficacy.

7 Conclusion

In this review, we summarized the current status and future innovations in CAR-T therapy for multiple myeloma. Clinical benefits of using CAR-T therapy to treat MM has been confirmed, but it does not lead to favorable durability and safety with current technologies. Numerous promising engineering approaches are underway to improve the efficacy and safety of CAR-T cell therapy, expanding this technology for a wider range of application and bring more benefits for MM patients.

Author contributions

YQ and YJ designed the study and reviewed the manuscript. ZW and CC participated in study design and wrote the original draft of the manuscript. ZW and CC was mainly responsible for the design of tables and figures. LW contributed to the conception of the paper. All authors contributed to the article and approved the submitted version.

Funding

This study was supported by the National Natural Science Foundation of China (grant no. 81872264).

Conflict of interest

The authors declare that the research was conducted in the absence of any commercial or financial relationships that could be construed as a potential conflict of interest.

Publisher's note

All claims expressed in this article are solely those of the authors and do not necessarily represent those of their affiliated organizations, or those of the publisher, the editors and the reviewers. Any product that may be evaluated in this article, or claim that may be made by its manufacturer, is not guaranteed or endorsed by the publisher.

References

1. Kehrer M, Koob S, Strauss A, Wirtz DC, Schmolders J. [Multiple myeloma - current status in diagnostic testing and therapy]. *Z fur Orthopadie und Unfallchirurgie* (2017) 155(5):575–86. doi: 10.1055/s-0043-110224

2. Michels TC, Petersen KE. Multiple myeloma: Diagnosis and treatment. *Am Family Physician* (2017) 95(6):373–83.

3. Padala SA, Barsouk A, Barsouk A, Rawla P, Vakiti A, Kolhe R, et al. Epidemiology, staging, and management of multiple myeloma. *Med Sci (Basel Switzerland)* (2021) 9(1):3. doi: 10.3390/medsci9010003

4. Kumar SK, Rajkumar V, Kyle RA, van Duin M, Sonneveld P, Mateos MV, et al. Multiple myeloma. *Nat Rev Dis Primers* (2017) 3:17046. doi: 10.1038/nrdp.2017.46

5. Casey M, Nakamura K. The cancer-immunity cycle in multiple myeloma. *ImmunoTargets Ther* (2021) 10:247–60. doi: 10.2147/itt.S305432

6. Kegyes D, Constantinescu C, Vrancken L, Rasche L, Gregoire C, Tigu B, et al. Patient selection for car T or bite therapy in multiple myeloma: Which treatment for each patient? *J Hematol Oncol* (2022) 15(1):78. doi: 10.1186/s13045-022-01296-2

7. Abramson HN. The multiple myeloma drug pipeline-2018: A review of small molecules and their therapeutic targets. *Clin lymphoma Myeloma Leukemia* (2018) 18(9):611–27. doi: 10.1016/j.clml.2018.06.015

8. Wu C, Zhang L, Brockman QR, Zhan F, Chen L. Chimeric antigen receptor T cell therapies for multiple myeloma. *J Hematol Oncol* (2019) 12(1):120. doi: 10.1186/s13045-019-0823-5

9. Ye CJ, Chen J, Liu G, Heng HH. Somatic genomic mosaicism in multiple myeloma. *Front Genet* (2020) 11:388. doi: 10.3389/fgene.2020.00388

10. Heng J, Heng HH. Genome chaos: Creating new genomic information essential for cancer macroevolution. *Semin Cancer Biol* (2022) 81:160–75. doi: 10.1016/j.semcancer.2020.11.003

11. Kumar SK, Dimopoulos MA, Kastritis E, Terpos E, Nahi H, Goldschmidt H, et al. Natural history of relapsed myeloma, refractory to immunomodulatory drugs and proteasome inhibitors: A multicenter imwg study. *Leukemia* (2017) 31 (11):2443–8. doi: 10.1038/leu.2017.138

12. Kochenderfer JN, Somerville RPT, Lu T, Yang JC, Sherry RM, Feldman SA, et al. Long-duration complete remissions of diffuse Large b cell lymphoma after anti-Cd19 chimeric antigen receptor T cell therapy. *Mol Therapy: J Am Soc Gene Ther* (2017) 25(10):2245–53. doi: 10.1016/j.ymthe.2017.07.004

13. Park JH, Rivière I, Gonen M, Wang X, Sénéchal B, Curran KJ, et al. Long-term follow-up of Cd19 car therapy in acute lymphoblastic leukemia. *New Engl J Med* (2018) 378(5):449–59. doi: 10.1056/NEJMoa1709919

14. Choi T, Kang Y. Chimeric antigen receptor (Car) T-cell therapy for multiple myeloma. *Pharmacol Ther* (2022) 232:108007. doi: 10.1016/j.pharmthera.2021.108007

15. van der Stegen SJ, Hamieh M, Sadelain M. The pharmacology of second-generation chimeric antigen receptors. *Nat Rev Drug Discovery* (2015) 14(7):499–509. doi: 10.1038/nrd4597

16. Jensen MC, Riddell SR. Designing chimeric antigen receptors to effectively and safely target tumors. *Curr Opin Immunol* (2015) 33:9–15. doi: 10.1016/j.coi.2015.01.002

17. Benmebarek MR, Karches CH, Cadilha BL, Lesch S, Endres S, Kobold S. Killing mechanisms of chimeric antigen receptor (Car) T cells. *Int J Mol Sci* (2019) 20(6):1283. doi: 10.3390/ijms20061283

18. Sadelain M, Rivière I, Riddell S. Therapeutic T cell engineering. *Nature* (2017) 545(7655):423–31. doi: 10.1038/nature22395

19. Srivastava S, Riddell SR. Engineering car-T cells: Design concepts. *Trends Immunol* (2015) 36(8):494–502. doi: 10.1016/j.it.2015.06.004

20. Lim WA, June CH. The principles of engineering immune cells to treat cancer. *Cell* (2017) 168(4):724–40. doi: 10.1016/j.cell.2017.01.016

21. Brudno JN, Kochenderfer JN. Recent advances in car T-cell toxicity: Mechanisms, manifestations and management. *Blood Rev* (2019) 34:45–55. doi: 10.1016/j.blre.2018.11.002

22. Brudno JN, Maric I, Hartman SD, Rose JJ, Wang M, Lam N, et al. T Cells genetically modified to express an anti-B-Cell maturation antigen chimeric antigen receptor cause remissions of poor-prognosis relapsed multiple myeloma. *J Clin Oncology: Off J Am Soc Clin Oncol* (2018) 36(22):2267–80. doi: 10.1200/jco.2018.77.8084

23. Cohen AD, Garfall AL, Stadtmauer EA, Melenhorst JJ, Lacey SF, Lancaster E, et al. B cell maturation antigen-specific car T cells are clinically active in multiple myeloma. *J Clin Invest* (2019) 129(6):2210–21. doi: 10.1172/jci126397

24. Usmani SZ, Berdeja JG, Truppel-Hartmann A, Fei Y, Wortman-Vayn H, Shelat S, et al. Karmma-4: Idecabtagene vicleucel (Ide-cel, Bb2121), a bcma-directed car T-cell therapy in high-risk newly diagnosed multiple myeloma. *J Clin Oncol* (2021) 39(15_suppl):TPS8053–TPS. doi: 10.1200/JCO.2021.39.15_suppl.TPS8053

25. Kumar SK, Baz RC, Orlowski RZ, Anderson LDJr., Ma H, Shrewsbury A, et al. Results from lummicar-2: A phase 1b/2 study of fully human b-cell maturation antigen-specific car T cells (Ct053) in patients with relapsed and/or refractory multiple myeloma. *Blood* (2020) 136(Supplement 1):28–9. doi: 10.1182/blood-2020-139802

26. Jie J, Hao S, Jiang S, Li Z, Yang M, Zhang W, et al. Phase 1 trial of the safety and efficacy of fully human anti-bcma car T cells in Relapsed/Refractory multiple myeloma. *Blood* (2019) 134(Supplement_1):4435. doi: 10.1182/blood-2019-126104

27. An G, Sui W, Wang T, Qu X, Zhang X, Yang J, et al. An anti-bcma car T-cell therapy (C-Car088) shows promising safety and efficacy profile in relapsed or refractory multiple myeloma. *Blood* (2020) 136(Supplement 1):29–30. doi: 10.1182/blood-2020-138734

28. Sperling AS, Nikiforow S, Nadeem O, Mo CC, Laubach JP, Anderson KC, et al. Phase I study of Phe885, a fully human bcma-directed car-T cell therapy for Relapsed/Refractory multiple myeloma manufactured in ≪2 days using the T-charge Tm platform. *Blood* (2021) 138(Supplement 1):3864. doi: 10.1182/blood-2021-146646

29. Han L, Gao Q, Zhou K, Zhou J, Yin Q-S, Fang B, et al. The clinical study of anti-bcma car-T with single-domain antibody as antigen binding domain. *J Clin Oncol* (2021) 39(15_suppl):8025. doi: 10.1200/JCO.2021.39.15_suppl.8025

30. Liu Y, Chen Z, Wei R, Shi L, He F, Shi Z, et al. Remission observed from a phase 1 clinical study of car-T therapy with safety switch targeting bcma for patients with Relapsed/Refractory multiple myeloma. *J Clin Oncol* (2018) 36 (15_suppl):8020. doi: 10.1200/JCO.2018.36.15_suppl.8020

31. Zhao WH, Wang BY, Chen LJ, Fu WJ, Xu J, Liu J, et al. Four-year follow-up of lcar-B38m in relapsed or refractory multiple myeloma: A phase 1, single-arm, open-label, multicenter study in China (Legend-2). *J Hematol Oncol* (2022) 15 (1):86. doi: 10.1186/s13045-022-01301-8

32. Madduri D, Berdeja JG, Usmani SZ, Jakubowiak A, Agha M, Cohen AD, et al. Cartitude-1: Phase 1b/2 study of ciltacabtagene autoleucel, a b-cell maturation antigen-directed chimeric antigen receptor T cell therapy, in Relapsed/Refractory multiple myeloma. *Blood* (2020) 136(Supplement 1):22–5. doi: 10.1182/blood-2020-136307

33. Hao S, Jin J, Jiang S, Li Z, Zhang W, Yang M, et al. Two-year follow-up of investigator-initiated phase 1 trials of the safety and efficacy of fully human anti-bcma car T cells (Ct053) in Relapsed/Refractory multiple myeloma. *Blood* (2020) 136(Supplement 1):27–8. doi: 10.1182/blood-2020-140156

34. Novak AJ, Darce JR, Arendt BK, Harder B, Henderson K, Kindsvogel W, et al. Expression of bcma, taci, and baff-r in multiple myeloma: A mechanism for growth and survival. *Blood* (2004) 103(2):689–94. doi: 10.1182/blood-2003-06-2043

35. Roex G, Timmers M, Wouters K, Campillo-Davo D, Flumens D, Schroyens W, et al. Safety and clinical efficacy of bcma car-T-Cell therapy in multiple myeloma. *J Hematol Oncol* (2020) 13(1):164. doi: 10.1186/s13045-020-01001-1

36. Bu DX, Singh R, Choi EE, Ruella M, Nunez-Cruz S, Mansfield KG, et al. Pre-clinical validation of b cell maturation antigen (Bcma) as a target for T cell immunotherapy of multiple myeloma. *Oncotarget* (2018) 9(40):25764–80. doi: 10.18632/oncotarget.25359

37. Carpenter RO, Evbuomwan MO, Pittaluga S, Rose JJ, Raffeld M, Yang S, et al. B-cell maturation antigen is a promising target for adoptive T-cell therapy of multiple myeloma. *Clin Cancer Res: an Off J Am Assoc Cancer Res* (2013) 19 (8):2048–60. doi: 10.1158/1078-0432.Ccr-12-2422

38. Seckinger A, Delgado JA, Moser S, Moreno L, Neuber B, Grab A, et al. Target expression, generation, preclinical activity, and pharmacokinetics of the bcma-T cell bispecific antibody Em801 for multiple myeloma treatment. *Cancer Cell* (2017) 31(3):396–410. doi: 10.1016/j.ccell.2017.02.002

39. Tai YT, Acharya C, An G, Moschetta M, Zhong MY, Feng X, et al. April And bcma promote human multiple myeloma growth and immunosuppression in the bone marrow microenvironment. *Blood* (2016) 127(25):3225–36. doi: 10.1182/blood-2016-01-691162

40. Sanchez E, Gillespie A, Tang G, Ferros M, Harutyunyan NM, Vardanyan S, et al. Soluble b-cell maturation antigen mediates tumor-induced immune deficiency in multiple myeloma. *Clin Cancer Res: an Off J Am Assoc Cancer Res* (2016) 22(13):3383–97. doi: 10.1158/1078-0432.Ccr-15-2224

41. Sanchez E, Li M, Kitto A, Li J, Wang CS, Kirk DT, et al. Serum b-cell maturation antigen is elevated in multiple myeloma and correlates with disease status and survival. *Br J Haematol* (2012) 158(6):727–38. doi: 10.1111/j.1365-2141.2012.09241.x

42. Quinn J, Glassford J, Percy L, Munson P, Marafioti T, Rodriguez-Justo M, et al. April Promotes cell-cycle progression in primary multiple myeloma cells: Influence of d-type cyclin group and translocation status. *Blood* (2011) 117(3):890–901. doi: 10.1182/blood-2010-01-264424

43. Lee L, Bounds D, Paterson J, Herledan G, Sully K, Seestaller-Wehr LM, et al. Evaluation of b cell maturation antigen as a target for antibody drug conjugate mediated cytotoxicity in multiple myeloma. *Br J Haematol* (2016) 174(6):911–22. doi: 10.1111/bjh.14145

44. Ali SA, Shi V, Maric I, Wang M, Stroncek DF, Rose JJ, et al. T Cells expressing an anti-B-Cell maturation antigen chimeric antigen receptor cause remissions of multiple myeloma. *Blood* (2016) 128(13):1688–700. doi: 10.1182/blood-2016-04-711903

45. Wang K, Wei G, Liu D. Cd19: A biomarker for b cell development, lymphoma diagnosis and therapy. *Exp Hematol Oncol* (2012) 1(1):36. doi: 10.1186/2162-3619-1-36

46. Johnsen HE, Bøgsted M, Schmitz A, Bødker JS, El-Galaly TC, Johansen P, et al. The myeloma stem cell concept, revisited: From phenomenology to operational terms. *Haematologica* (2016) 101(12):1451–9. doi: 10.3324/haematol.2015.138826

47. Garfall AL, Stadtmauer EA, Hwang WT, Lacey SF, Melenhorst JJ, Krevvata M, et al. Anti-Cd19 car T cells with high-dose melphalan and autologous stem cell transplantation for refractory multiple myeloma. *JCI Insight* (2018) 3(8):e120505. doi: 10.1172/jci.insight.120505

48. Garfall AL, Maus MV, Hwang WT, Lacey SF, Mahnke YD, Melenhorst JJ, et al. Chimeric antigen receptor T cells against Cd19 for multiple myeloma. *New Engl J Med* (2015) 373(11):1040–7. doi: 10.1056/NEJMoa1504542

49. Boles KS, Mathew PA. Molecular cloning of Cs1, a novel human natural killer cell receptor belonging to the Cd2 subset of the immunoglobulin superfamily. *Immunogenetics* (2001) 52(3-4):302–7. doi: 10.1007/s002510000274

50. Hsi ED, Steinle R, Balasa B, Szmania S, Draksharapu A, Shum BP, et al. Cs1, a potential new therapeutic antibody target for the treatment of multiple myeloma. *Clin Cancer Res: an Off J Am Assoc Cancer Res* (2008) 14(9):2775–84. doi: 10.1158/1078-0432.Ccr-07-4246

51. Tai YT, Dillon M, Song W, Leiba M, Li XF, Burger P, et al. Anti-Cs1 humanized monoclonal antibody Huluc63 inhibits myeloma cell adhesion and induces antibody-dependent cellular cytotoxicity in the bone marrow milieu. *Blood* (2008) 112(4):1329–37. doi: 10.1182/blood-2007-08-107292

52. Kikuchi J, Hori M, Iha H, Toyama-Sorimachi N, Hagiwara S, Kuroda Y, et al. Soluble Slamf7 promotes the growth of myeloma cells *Via* homophilic interaction with surface Slamf7. *Leukemia* (2020) 34(1):180–95. doi: 10.1038/s41375-019-0525-6

53. Gogishvili T, Danhof S, Prommersberger S, Rydzek J, Schreder M, Brede C, et al. Slamf7-car T cells eliminate myeloma and confer selective fratricide of Slamf7 (+) normal lymphocytes. *Blood* (2017) 130(26):2838–47. doi: 10.1182/blood-2017-04-778423

54. Bonini C, Ferrari G, Verzeletti S, Servida P, Zappone E, Ruggieri L, et al. Hsv-tk gene transfer into donor lymphocytes for control of allogeneic graft-Versus-Leukemia. *Sci (New York NY)* (1997) 276(5319):1719–24. doi: 10.1126/science.276.5319.1719

55. Hoyos V, Savoldo B, Quintarelli C, Mahendravada A, Zhang M, Vera J, et al. Engineering Cd19-specific T lymphocytes with interleukin-15 and a suicide gene to enhance their anti-Lymphoma/Leukemia effects and safety. *Leukemia* (2010) 24 (6):1160–70. doi: 10.1038/leu.2010.75

56. Smith EL, Harrington K, Staehr M, Masakayan R, Jones J, Long T, et al. T Cell therapy targeting G protein-coupled receptor class c group 5 member d (Gprc5d), a novel target for the immunotherapy of multiple myeloma. *Blood* (2018) 132(Supplement 1):589. doi: 10.1182/blood-2018-99-110471

57. Smith EL, Harrington K, Staehr M, Masakayan R, Jones J, Long TJ, et al. Gprc5d is a target for the immunotherapy of multiple myeloma with rationally designed car T cells. *Sci Trans Med* (2019) 11(485):eaau7746. doi: 10.1126/scitranslmed.aau7746

58. Sanderson RD, Turnbull JE, Gallagher JT, Lander AD. Fine structure of heparan sulfate regulates syndecan-1 function and cell behavior. *J Biol Chem* (1994) 269(18):13100–6. doi: 10.1016/S0021-9258(17)36804-7

59. Wijdenes J, Vooijs WC, Clément C, Post J, Morard F, Vita N, et al. A plasmocyte selective monoclonal antibody (B-B4) recognizes syndecan-1. *Br J Haematol* (1996) 94(2):318–23. doi: 10.1046/j.1365-2141.1996.d01-1811.x

60. Kambham N, Kong C, Longacre TA, Natkunam Y. Utility of syndecan-1 (Cd138) expression in the diagnosis of undifferentiated malignant neoplasms: A tissue microarray study of 1,754 cases. *Appl Immunohistochem Mol Morphol: AIMM* (2005) 13(4):304–10. doi: 10.1097/01.pai.0000159773.50905.7b

61. O'Connell FP, Pinkus JL, Pinkus GS. Cd138 (Syndecan-1), a plasma cell marker immunohistochemical profile in hematopoietic and nonhematopoietic neoplasms. *Am J Clin Pathol* (2004) 121(2):254–63. doi: 10.1309/617d-wb5g-nfwx-hw4l

62. Guo B, Chen M, Han Q, Hui F, Dai H, Zhang W, et al. Cd138-directed adoptive immunotherapy of chimeric antigen receptor (Car)-modified T cells for multiple myeloma. *J Cell Immunother* (2016) 2(1):28–35. doi: 10.1016/j.jocit.2014.11.001

63. Fernàndez JE, Deaglio S, Donati D, Beusan IS, Corno F, Aranega A, et al. Analysis of the distribution of human Cd38 and of its ligand Cd31 in normal tissues. *J Biol Regul Homeostatic Agents* (1998) 12(3):81–91.

64. Drent E, Themeli M, Poels R, de Jong-Korlaar R, Yuan H, de Bruijn J, et al. A rational strategy for reducing on-target off-tumor effects of Cd38-chimeric antigen receptors by affinity optimization. *Mol Therapy: J Am Soc Gene Ther* (2017) 25 (8):1946–58. doi: 10.1016/j.ymthe.2017.04.024

65. McEarchern JA, Smith LM, McDonagh CF, Klussman K, Gordon KA, Morris-Tilden CA, et al. Preclinical characterization of sgn-70, a humanized

antibody directed against Cd70. *Clin Cancer Res: an Off J Am Assoc Cancer Res* (2008) 14(23):7763–72. doi: 10.1158/1078-0432.Ccr-08-0493

66. Wang QJ, Yu Z, Hanada KI, Patel K, Kleiner D, Restifo NP, et al. Preclinical evaluation of chimeric antigen receptors targeting Cd70-expressing cancers. *Clin Cancer Res: an Off J Am Assoc Cancer Res* (2017) 23(9):2267–76. doi: 10.1158/1078-0432.Ccr-16-1421

67. Ge H, Mu L, Jin L, Yang C, Chang YE, Long Y, et al. Tumor associated Cd70 expression is involved in promoting tumor migration and macrophage infiltration in gbm. *Int J Cancer* (2017) 141(7):1434–44. doi: 10.1002/ijc.30830

68. Jin L, Ge H, Long Y, Yang C, Chang YE, Mu L, et al. Cd70, a novel target of car T-cell therapy for gliomas. *Neuro-oncology* (2018) 20(1):55–65. doi: 10.1093/neuonc/nox116

69. Wensveen FM, Jelenčić V, Polić B. Nkg2d: A master regulator of immune cell responsiveness. *Front Immunol* (2018) 9:441. doi: 10.3389/fimmu.2018.00441

70. Nikiforow S, Werner L, Murad J, Jacobs M, Johnston L, Patches S, et al. Safety data from a first-in-Human phase 1 trial of Nkg2d chimeric antigen receptor-T cells in Aml/Mds and multiple myeloma. *Blood* (2016) 128 (22):4052–. doi: 10.1182/blood.V128.22.4052.4052

71. Ramos CA, Savoldo B, Torrano V, Ballard B, Zhang H, Dakhova O, et al. Clinical responses with T lymphocytes targeting malignancy-associated K light chains. *J Clin Invest* (2016) 126(7):2588–96. doi: 10.1172/jci86000

72. Hutchinson AT, Jones DR, Raison RL. Preclinical and clinical development of an anti-kappa free light chain mab for multiple myeloma. *Mol Immunol* (2015) 67(2 Pt A):89–94. doi: 10.1016/j.molimm.2015.04.013

73. Raje N, Berdeja J, Lin Y, Siegel D, Jagannath S, Madduri D, et al. Anti-bcma car T-cell therapy Bb2121 in relapsed or refractory multiple myeloma. *New Engl J Med* (2019) 380(18):1726–37. doi: 10.1056/NEJMoa1817226

74. Raje NS, Berdeja JG, Lin Y, Munshi NC, Siegel DSD, Liedtke M, et al. Bb2121 anti-bcma car T-cell therapy in patients with Relapsed/Refractory multiple myeloma: Updated results from a multicenter phase I study. *J Clin Oncol* (2018) 36 (15_suppl):8007. doi: 10.1200/JCO.2018.36.15_suppl.8007

75. Xu J, Chen LJ, Yang SS, Sun Y, Wu W, Liu YF, et al. Exploratory trial of a biepitopic car T-targeting b cell maturation antigen in Relapsed/Refractory multiple myeloma. *Proc Natl Acad Sci United States America* (2019) 116 (19):9543–51. doi: 10.1073/pnas.1819745116

76. Gattinoni L, Lugli E, Ji Y, Pos Z, Paulos CM, Quigley MF, et al. A human memory T cell subset with stem cell-like properties. *Nat Med* (2011) 17(10):1290–7. doi: 10.1038/nm.2446

77. Hinrichs CS, Borman ZA, Cassard L, Gattinoni L, Spolski R, Yu Z, et al. Adoptively transferred effector cells derived from naive rather than central memory Cd8+ T cells mediate superior antitumor immunity. *Proc Natl Acad Sci United States America* (2009) 106(41):17469–74. doi: 10.1073/pnas.0907448106

78. Gattinoni L, Klebanoff CA, Palmer DC, Wrzesinski C, Kerstann K, Yu Z, et al. Acquisition of full effector function in vitro paradoxically impairs the in vivo antitumor efficacy of adoptively transferred Cd8+ T cells. *J Clin Invest* (2005) 115 (6):1616–26. doi: 10.1172/jci24480

79. Gattinoni L, Speiser DE, Lichterfeld M, Bonini C. T Memory stem cells in health and disease. *Nat Med* (2017) 23(1):18–27. doi: 10.1038/nm.4241

80. McLellan AD, Ali Hosseini Rad SM. Chimeric antigen receptor T cell persistence and memory cell formation. *Immunol Cell Biol* (2019) 97(7):664–74. doi: 10.1111/imcb.12254

81. Fraietta JA, Lacey SF, Orlando EJ, Pruteanu-Malinici I, Gohil M, Lundh S, et al. Determinants of response and resistance to Cd19 chimeric antigen receptor (Car) T cell therapy of chronic lymphocytic leukemia. *Nat Med* (2018) 24(5):563–71. doi: 10.1038/s41591-018-0010-1

82. Gattinoni L, Klebanoff CA, Restifo NP. Paths to stemness: Building the ultimate antitumour T cell. *Nat Rev Cancer* (2012) 12(10):671–84. doi: 10.1038/nrc3322

83. Hsieh EM, Scherer LD, Rouce RH. Replacing car-T cell resistance with persistence by changing a single residue. *J Clin Invest* (2020) 130(6):2806–8. doi: 10.1172/jci136872

84. Maude SL, Laetsch TW, Buechner J, Rives S, Boyer M, Bittencourt H, et al. Tisagenlecleucel in children and young adults with b-cell lymphoblastic leukemia. *New Engl J Med* (2018) 378(5):439–48. doi: 10.1056/NEJMoa1709866

85. Porter DL, Hwang WT, Frey NV, Lacey SF, Shaw PA, Loren AW, et al. Chimeric antigen receptor T cells persist and induce sustained remissions in relapsed refractory chronic lymphocytic leukemia. *Sci Trans Med* (2015) 7 (303):303ra139. doi: 10.1126/scitranslmed.aac5415

86. Kershaw MH, Westwood JA, Parker LL, Wang G, Eshhar Z, Mavroukakis SA, et al. A phase I study on adoptive immunotherapy using gene-modified T cells for ovarian cancer. *Clin Cancer Res: an Off J Am Assoc Cancer Res* (2006) 12(20 Pt 1):6106–15. doi: 10.1158/1078-0432.Ccr-06-1183

87. Louis CU, Savoldo B, Dotti G, Pule M, Yvon E, Myers GD, et al. Antitumor activity and long-term fate of chimeric antigen receptor–positive T cells in patients with neuroblastoma. *Blood* (2011) 118(23):6050–6. doi: 10.1182/blood-2011-05-354449

88. Das RK, Vernau L, Grupp SA, Barrett DM. Naïve T-cell deficits at diagnosis and after chemotherapy impair cell therapy potential in pediatric cancers. *Cancer Discovery* (2019) 9(4):492–9. doi: 10.1158/2159-8290.Cd-18-1314

89. Dancy E, Garfall AL, Cohen AD, Fraietta JA, Davis M, Levine BL, et al. Clinical predictors of T cell fitness for car T cell manufacturing and efficacy in multiple myeloma. *Blood* (2018) 132(Supplement 1):1886. doi: 10.1182/blood-2018-99-115319

90. Ajina A, Maher J. Strategies to address chimeric antigen receptor tonic signaling. *Mol Cancer Ther* (2018) 17(9):1795–815. doi: 10.1158/1535-7163.Mct-17-1097

91. Hudecek M, Sommermeyer D, Kosasih PL, Silva-Benedict A, Liu L, Rader C, et al. The nonsignaling extracellular spacer domain of chimeric antigen receptors is decisive for in vivo antitumor activity. *Cancer Immunol Res* (2015) 3(2):125–35. doi: 10.1158/2326-6066.Cir-14-0127

92. Susanibar Adaniya SP, Cohen AD, Garfall AL. Chimeric antigen receptor T cell immunotherapy for multiple myeloma: A review of current data and potential clinical applications. *Am J Hematol* (2019) 94(S1):S28–33. doi: 10.1002/ajh.25428

93. Green DJ, Pont M, Sather BD, Cowan AJ, Turtle CJ, Till BG, et al. Fully human bcma targeted chimeric antigen receptor T cells administered in a defined composition demonstrate potency at low doses in advanced stage high risk multiple myeloma. *Blood* (2018) 132(Supplement 1):1011. doi: 10.1182/blood-2018-99-117729

94. Munshi NC, Anderson LDJr., Shah N, Madduri D, Berdeja J, Lonial S, et al. Idecabtagene vicleucel in relapsed and refractory multiple myeloma. *New Engl J Med* (2021) 384(8):705–16. doi: 10.1056/NEJMoa2024850

95. Ghermezi M, Li M, Vardanyan S, Harutyunyan NM, Gottlieb J, Berenson A, et al. Serum b-cell maturation antigen: A novel biomarker to predict outcomes for multiple myeloma patients. *Haematologica* (2017) 102(4):785–95. doi: 10.3324/haematol.2016.150896

96. Chen CI, Bahlis N, Gasparetto C, Tuchman SA, Lipe BC, Baljevic M, et al. Selinexor, pomalidomide, and dexamethasone (Spd) in patients with relapsed or refractory multiple myeloma. *Blood* (2019) 134(Supplement_1):141. doi: 10.1182/blood-2019-122907

97. Ishibashi M, Soeda S, Sasaki M, Handa H, Imai Y, Tanaka N, et al. Clinical impact of serum soluble Slamf7 in multiple myeloma. *Oncotarget* (2018) 9 (78):34784–93. doi: 10.18632/oncotarget.26196

98. Nooka AK, Kaufman JL, Hofmeister CC, Joseph NS, Heffner TL, Gupta VA, et al. Daratumumab in multiple myeloma. *Cancer* (2019) 125(14):2364–82. doi: 10.1002/cncr.32065

99. Kodama T, Kochi Y, Nakai W, Mizuno H, Baba T, Habu K, et al. Anti-Gprc5d/Cd3 bispecific T-Cell-Redirecting antibody for the treatment of multiple myeloma. *Mol Cancer Ther* (2019) 18(9):1555–64. doi: 10.1158/1535-7163.Mct-18-1216

100. Oliva S, Troia R, D'Agostino M, Boccadoro M, Gay F. Promises and pitfalls in the use of pd-1/Pd-L1 inhibitors in multiple myeloma. *Front Immunol* (2018) 9:2749. doi: 10.3389/fimmu.2018.02749

101. Bonello F, D'Agostino M, Moscvin M, Cerrato C, Boccadoro M, Gay F. Cd38 as an immunotherapeutic target in multiple myeloma. *Expert Opin Biol Ther* (2018) 18(12):1209–21. doi: 10.1080/14712598.2018.1544240

102. Chauhan D, Singh AV, Brahmandam M, Carrasco R, Bandi M, Hideshima T, et al. Functional interaction of plasmacytoid dendritic cells with multiple myeloma cells: A therapeutic target. *Cancer Cell* (2009) 16(4):309–23. doi: 10.1016/j.ccr.2009.08.019

103. Hideshima T, Mitsiades C, Tonon G, Richardson PG, Anderson KC. Understanding multiple myeloma pathogenesis in the bone marrow to identify new therapeutic targets. *Nat Rev Cancer* (2007) 7(8):585–98. doi: 10.1038/nrc2189

104. Cazaux M, Grandjean CL, Lemaître F, Garcia Z, Beck RJ, Milo I, et al. Single-cell imaging of car T cell activity in vivo reveals extensive functional and anatomical heterogeneity. *J Exp Med* (2019) 216(5):1038–49. doi: 10.1084/jem.20182375

105. Yoon DH, Osborn MJ, Tolar J, Kim CJ. Incorporation of immune checkpoint blockade into chimeric antigen receptor T cells (Car-ts): Combination or built-in car-T. *Int J Mol Sci* (2018) 19(2):340. doi: 10.3390/ijms19020340

106. Moon EK, Wang LC, Dolfi DV, Wilson CB, Ranganathan R, Sun J, et al. Multifactorial T-cell hypofunction that is reversible can limit the efficacy of chimeric antigen receptor-transduced human T cells in solid tumors. *Clin Cancer Res: an Off J Am Assoc Cancer Res* (2014) 20(16):4262–73. doi: 10.1158/1078-0432.Ccr-13-2627

107. Gay F, D'Agostino M, Giaccone L, Genuardi M, Festuccia M, Boccadoro M, et al. Immuno-oncologic approaches: Car-T cells and checkpoint inhibitors. *Clin lymphoma Myeloma Leukemia* (2017) 17(8):471–8. doi: 10.1016/j.clml.2017.06.014

108. Lam N, Trinklein ND, Buelow B, Patterson GH, Ojha N, Kochenderfer JN. Anti-bcma chimeric antigen receptors with fully human heavy-Chain-Only antigen recognition domains. *Nat Commun* (2020) 11(1):283. doi: 10.1038/s41467-019-14119-9

109. Smith EL, Staehr M, Masakayan R, Tatake IJ, Purdon TJ, Wang X, et al. Development and evaluation of an optimal human single-chain variable fragment-derived bcma-targeted car T cell vector. *Mol Therapy: J Am Soc Gene Ther* (2018) 26(6):1447–56. doi: 10.1016/j.ymthe.2018.03.016

110. Shimasaki N, Jain A, Campana D. Nk cells for cancer immunotherapy. *Nat Rev Drug Discovery* (2020) 19(3):200–18. doi: 10.1038/s41573-019-0052-1

111. Liu E, Marin D, Banerjee P, Macapinlac HA, Thompson P, Basar R, et al. Use of car-transduced natural killer cells in Cd19-positive lymphoid tumors. *New Engl J Med* (2020) 382(6):545–53. doi: 10.1056/NEJMoa1910607

112. Depil S, Duchateau P, Grupp SA, Mufti G, Poirot L. 'Off-the-Shelf' allogeneic car T cells: Development and challenges. *Nat Rev Drug Discovery* (2020) 19(3):185–99. doi: 10.1038/s41573-019-0051-2

113. Ying Z, Huang XF, Xiang X, Liu Y, Kang X, Song Y, et al. A safe and potent anti-Cd19 car T cell therapy. *Nat Med* (2019) 25(6):947–53. doi: 10.1038/s41591-019-0421-7

114. Weinkove R, George P, Dasyam N, McLellan AD. Selecting costimulatory domains for chimeric antigen receptors: Functional and clinical considerations. *Clin Trans Immunol* (2019) 8(5):e1049. doi: 10.1002/cti2.1049

115. Rezvani K. Adoptive cell therapy using engineered natural killer cells. *Bone Marrow Transplant* (2019) 54(Suppl 2):785–8. doi: 10.1038/s41409-019-0601-6

116. Salter AI, Ivey RG, Kennedy JJ, Voillet V, Rajan A, Alderman EJ, et al. Phosphoproteomic analysis of chimeric antigen receptor signaling reveals kinetic and quantitative differences that affect cell function. *Sci Signaling* (2018) 11(544): eaat6753. doi: 10.1126/scisignal.aat6753

117. Brudno JN, Kochenderfer JN. Chimeric antigen receptor T-cell therapies for lymphoma. *Nat Rev Clin Oncol* (2018) 15(1):31–46. doi: 10.1038/nrclinonc.2017.128

118. Alabanza L, Pegues M, Geldres C, Shi V, Wiltzius JJW, Sievers SA, et al. Function of novel anti-Cd19 chimeric antigen receptors with human variable regions is affected by hinge and transmembrane domains. *Mol Therapy: J Am Soc Gene Ther* (2017) 25(11):2452–65. doi: 10.1016/j.ymthe.2017.07.013

119. Sabatino M, Hu J, Sommariva M, Gautam S, Fellowes V, Hocker JD, et al. Generation of clinical-grade Cd19-specific car-modified Cd8+ memory stem cells for the treatment of human b-cell malignancies. *Blood* (2016) 128(4):519–28. doi: 10.1182/blood-2015-11-683847

120. Geldres C, Savoldo B, Dotti G. Chimeric antigen receptor-redirected T cells return to the bench. *Semin Immunol* (2016) 28(1):3–9. doi: 10.1016/j.smim.2015.12.001

121. Zhao Z, Condomines M, van der Stegen SJC, Perna F, Kloss CC, Gunset G, et al. Structural design of engineered costimulation determines tumor rejection kinetics and persistence of car T cells. *Cancer Cell* (2015) 28(4):415–28. doi: 10.1016/j.ccell.2015.09.004

122. Teh BW, Harrison SJ, Worth LJ, Spelman T, Thursky KA, Slavin MA. Risks, severity and timing of infections in patients with multiple myeloma: A longitudinal cohort study in the era of immunomodulatory drug therapy. *Br J Haematol* (2015) 171(1):100–8. doi: 10.1111/bjh.13532

123. Blimark C, Holmberg E, Mellqvist UH, Landgren O, Björkholm M, Hultcrantz M, et al. Multiple myeloma and infections: A population-based study on 9253 multiple myeloma patients. *Haematologica* (2015) 100(1):107–13. doi: 10.3324/haematol.2014.107714

124. Xu Y, Zhang M, Ramos CA, Durett A, Liu E, Dakhova O, et al. Closely related T-memory stem cells correlate with in vivo expansion of Car.Cd19-T cells and are preserved by il-7 and il-15. *Blood* (2014) 123(24):3750–9. doi: 10.1182/blood-2014-01-552174

125. Zhang X, Sun S, Hwang I, Tough DF, Sprent J. Potent and selective stimulation of memory-phenotype Cd8+ T cells in vivo by il-15. *Immunity* (1998) 8 (5):591–9. doi: 10.1016/s1074-7613(00)80564-6

126. Petersen CT, Hassan M, Morris AB, Jeffery J, Lee K, Jagirdar N, et al. Improving T-cell expansion and function for adoptive T-cell therapy using ex vivo treatment with Pi3kδ inhibitors and vip antagonists. *Blood Adv* (2018) 2(3):210–23. doi: 10.1182/bloodadvances.2017011254

127. Morgan MA, Schambach A. Engineering car-T cells for improved function against solid tumors. *Front Immunol* (2018) 9:2493. doi: 10.3389/fimmu.2018.02493

128. Turtle CJ, Hanafi LA, Berger C, Hudecek M, Pender B, Robinson E, et al. Immunotherapy of non-hodgkin's lymphoma with a defined ratio of Cd8+ and Cd4+ Cd19-specific chimeric antigen receptor-modified T cells. *Sci Trans Med* (2016) 8(355):355ra116. doi: 10.1126/scitranslmed.aaf8621

129. Turtle CJ, Hanafi LA, Berger C, Gooley TA, Cherian S, Hudecek M, et al. Cd19 car-T cells of defined Cd4+:Cd8+ composition in adult b cell all patients. *J Clin Invest* (2016) 126(6):2123–38. doi: 10.1172/jci85309

130. Susanibar Adaniya S, Stadtmauer EA, Cohen AD. Car T cell therapy for multiple myeloma: What have we learned? *Leukemia* (2022) 36(6):1481–4. doi: 10.1038/s41375-022-01539-8

131. Cieri N, Camisa B, Cocchiarella F, Forcato M, Oliveira G, Provasi E, et al. Il-7 and il-15 instruct the generation of human memory stem T cells from naive precursors. *Blood* (2013) 121(4):573–84. doi: 10.1182/blood-2012-05-431718

132. Laurent SA, Hoffmann FS, Kuhn PH, Cheng Q, Chu Y, Schmidt-Supprian M, et al. Γ-secretase directly sheds the survival receptor bcma from plasma cells. *Nat Commun* (2015) 6:7333. doi: 10.1038/ncomms8333

133. Pont MJ, Hill T, Cole GO, Abbott JJ, Kelliher J, Salter AI, et al. Γ-secretase inhibition increases efficacy of bcma-specific chimeric antigen receptor T cells in multiple myeloma. *Blood* (2019) 134(19):1585–97. doi: 10.1182/blood.2019000050

134. Ran Y, Hossain F, Pannuti A, Lessard CB, Ladd GZ, Jung JI, et al. Γ-secretase inhibitors in cancer clinical trials are pharmacologically and functionally distinct. *EMBO Mol Med* (2017) 9(7):950–66. doi: 10.15252/emmm.201607265

135. Furukawa Y, Kikuchi J. Molecular basis of clonal evolution in multiple myeloma. *Int J Hematol* (2020) 111(4):496–511. doi: 10.1007/s12185-020-02829-6

136. Kumar SK, Rajkumar SV. The multiple myelomas - current concepts in cytogenetic classification and therapy. *Nat Rev Clin Oncol* (2018) 15(7):409–21. doi: 10.1038/s41571-018-0018-y

137. Bolli N, Avet-Loiseau H, Wedge DC, Van Loo P, Alexandrov LB, Martincorena I, et al. Heterogeneity of genomic evolution and mutational profiles in multiple myeloma. *Nat Commun* (2014) 5:2997. doi: 10.1038/ncomms3997

138. Yu S, Yi M, Qin S, Wu K. Next generation chimeric antigen receptor T cells: Safety strategies to overcome toxicity. *Mol Cancer* (2019) 18(1):125. doi: 10.1186/s12943-019-1057-4

139. Postow MA, Callahan MK, Wolchok JD. Immune checkpoint blockade in cancer therapy. *J Clin Oncology: Off J Am Soc Clin Oncol* (2015) 33(17):1974–82. doi: 10.1200/jco.2014.59.4358

140. Cherkassky L, Morello A, Villena-Vargas J, Feng Y, Dimitrov DS, Jones DR, et al. Human car T cells with cell-intrinsic pd-1 checkpoint blockade resist tumor-mediated inhibition. *J Clin Invest* (2016) 126(8):3130–44. doi: 10.1172/jci83092

141. Rupp LJ, Schumann K, Roybal KT, Gate RE, Ye CJ, Lim WA, et al. Crispr/Cas9-mediated pd-1 disruption enhances anti-tumor efficacy of human chimeric antigen receptor T cells. *Sci Rep* (2017) 7(1):737. doi: 10.1038/s41598-017-00462-8

142. Chmielewski M, Hombach AA, Abken H. Of cars and trucks: Chimeric antigen receptor (Car) T cells engineered with an inducible cytokine to modulate the tumor stroma. *Immunol Rev* (2014) 257(1):83–90. doi: 10.1111/imr.12125

143. Xu X, Gnanaprakasam JNR, Sherman J, Wang R. A metabolism toolbox for car T therapy. *Front Oncol* (2019) 9:322. doi: 10.3389/fonc.2019.00322

144. Ando T, Mimura K, Johansson CC, Hanson MG, Mougiakakos D, Larsson C, et al. Transduction with the antioxidant enzyme catalase protects human T cells against oxidative stress. *J Immunol (Baltimore Md: 1950)* (2008) 181(12):8382–90. doi: 10.4049/jimmunol.181.12.8382

145. Neelapu SS, Tummala S, Kebriaei P, Wierda W, Gutierrez C, Locke FL, et al. Chimeric antigen receptor T-cell therapy - assessment and management of toxicities. *Nat Rev Clin Oncol* (2018) 15(1):47–62. doi: 10.1038/nrclinonc.2017.148

146. Brudno JN, Kochenderfer JN. Toxicities of chimeric antigen receptor T cells: Recognition and management. *Blood* (2016) 127(26):3321–30. doi: 10.1182/blood-2016-04-703751

147. Grupp SA, Kalos M, Barrett D, Aplenc R, Porter DL, Rheingold SR, et al. Chimeric antigen receptor-modified T cells for acute lymphoid leukemia. *New Engl J Med* (2013) 368(16):1509–18. doi: 10.1056/NEJMoa1215134

148. Santomasso BD, Park JH, Salloum D, Riviere I, Flynn J, Mead E, et al. Clinical and biological correlates of neurotoxicity associated with car T-cell therapy in patients with b-cell acute lymphoblastic leukemia. *Cancer Discovery* (2018) 8 (8):958–71. doi: 10.1158/2159-8290.Cd-17-1319

149. Lee DW, Santomasso BD, Locke FL, Ghobadi A, Turtle CJ, Brudno JN, et al. Astct consensus grading for cytokine release syndrome and neurologic toxicity associated with immune effector cells. *Biol Blood Marrow Transpl: J Am Soc Blood Marrow Transplant* (2019) 25(4):625–38. doi: 10.1016/j.bbmt.2018.12.758

150. Mohyuddin GR, Banerjee R, Alam Z, Berger KE, Chakraborty R. Rethinking mechanisms of neurotoxicity with bcma directed therapy. *Crit Rev Oncol/Hematol* (2021) 166:103453. doi: 10.1016/j.critrevonc.2021.103453

151. Garcia Borrega J, Gödel P, Rüger MA, Onur ÖA, Shimabukuro-Vornhagen A, Kochanek M, et al. In the eye of the storm: Immune-mediated toxicities associated with car-T cell therapy. *HemaSphere* (2019) 3(2):e191. doi: 10.1097/hs9.0000000000000191

152. Strati P, Varma A, Adkins S, Nastoupil LJ, Westin J, Hagemeister FB, et al. Hematopoietic recovery and immune reconstitution after axicabtagene ciloleucel in patients with Large b-cell lymphoma. *Haematologica* (2021) 106(10):2667–72. doi: 10.3324/haematol.2020.254045

153. Nahas GR, Komanduri KV, Pereira D, Goodman M, Jimenez AM, Beitinjaneh A, et al. Incidence and risk factors associated with a syndrome of persistent cytopenias after car-T cell therapy (Pctt). *Leuk lymphoma* (2020) 61 (4):940–3. doi: 10.1080/10428194.2019.1697814

154. Fried S, Avigdor A, Bielorai B, Meir A, Besser MJ, Schachter J, et al. Early and late hematologic toxicity following Cd19 car-T cells. *Bone Marrow Transplant* (2019) 54(10):1643–50. doi: 10.1038/s41409-019-0487-3

155. Hegde M, Joseph SK, Pashankar F, DeRenzo C, Sanber K, Navai S, et al. Tumor response and endogenous immune reactivity after administration of Her2 car T cells in a child with metastatic rhabdomyosarcoma. *Nat Commun* (2020) 11 (1):3549. doi: 10.1038/s41467-020-17175-8

156. Juluri KR, Wu QV, Voutsinas J, Hou J, Hirayama AV, Mullane E, et al. Severe cytokine release syndrome is associated with hematologic toxicity following Cd19 car T-cell therapy. *Blood Adv* (2022) 6(7):2055–68. doi: 10.1182/bloodadvances.2020004142

157. Zhang X, Zhu L, Zhang H, Chen S, Xiao Y. Car-T cell therapy in hematological malignancies: Current opportunities and challenges. *Front Immunol* (2022) 13:927153. doi: 10.3389/fimmu.2022.927153

158. Huang R, Wang X, Zhang X. Unity brings strength: Combination of car-T cell therapy and hsct. *Cancer Lett* (2022) 549:215721. doi: 10.1016/j.canlet.2022.215721

159. Philip B, Kokalaki E, Mekkaoui L, Thomas S, Straathof K, Flutter B, et al. A highly compact epitope-based Marker/Suicide gene for easier and safer T-cell therapy. *Blood* (2014) 124(8):1277–87. doi: 10.1182/blood-2014-01-545020

160. Griffioen M, van Egmond EH, Kester MG, Willemze R, Falkenburg JH, Heemskerk MH. Retroviral transfer of human Cd20 as a suicide gene for adoptive T-cell therapy. *Haematologica* (2009) 94(9):1316–20. doi: 10.3324/haematol.2008.001677

161. Serafini M, Manganini M, Borleri G, Bonamino M, Imberti L, Biondi A, et al. Characterization of Cd20-transduced T lymphocytes as an alternative suicide gene therapy approach for the treatment of graft-Versus-Host disease. *Hum Gene Ther* (2004) 15(1):63–76. doi: 10.1089/10430340460732463

162. Wang X, Chang WC, Wong CW, Colcher D, Sherman M, Ostberg JR, et al. A transgene-encoded cell surface polypeptide for selection, in vivo tracking, and ablation of engineered cells. *Blood* (2011) 118(5):1255–63. doi: 10.1182/blood-2011-02-337360

163. Di Stasi A, Tey SK, Dotti G, Fujita Y, Kennedy-Nasser A, Martinez C, et al. Inducible apoptosis as a safety switch for adoptive cell therapy. *New Engl J Med* (2011) 365(18):1673–83. doi: 10.1056/NEJMoa1106152

164. Mestermann K, Giavridis T, Weber J, Rydzek J, Frenz S, Nerreter T, et al. The tyrosine kinase inhibitor dasatinib acts as a pharmacologic on/Off switch for car T cells. *Sci Trans Med* (2019) 11(499):eaau5907. doi: 10.1126/scitranslmed.aau5907

165. Juillerat A, Tkach D, Busser BW, Temburni S, Valton J, Duclert A, et al. Modulation of chimeric antigen receptor surface expression by a small molecule switch. *BMC Biotechnol* (2019) 19(1):44. doi: 10.1186/s12896-019-0537-3

166. Van Oekelen O, Aleman A, Upadhyaya B, Schnakenberg S, Madduri D, Gavane S, et al. Neurocognitive and hypokinetic movement disorder with features of parkinsonism after bcma-targeting car-T cell therapy. *Nat Med* (2021) 27 (12):2099–103. doi: 10.1038/s41591-021-01564-7

167. Berdeja JG, Madduri D, Usmani SZ, Jakubowiak A, Agha M, Cohen AD, et al. Ciltacabtagene autoleucel, a b-cell maturation antigen-directed chimeric antigen receptor T-cell therapy in patients with relapsed or refractory multiple myeloma (Cartitude-1): A phase 1b/2 open-label study. *Lancet (London England)* (2021) 398(10297):314–24. doi: 10.1016/s0140-6736(21)00933-8

168. Lanitis E, Poussin M, Klattenhoff AW, Song D, Sandaltzopoulos R, June CH, et al. Chimeric antigen receptor T cells with dissociated signaling domains exhibit focused antitumor activity with reduced potential for toxicity in vivo. *Cancer Immunol Res* (2013) 1(1):43–53. doi: 10.1158/2326-6066.Cir-13-0008

169. Kloss CC, Condomines M, Cartellieri M, Bachmann M, Sadelain M. Combinatorial antigen recognition with balanced signaling promotes selective tumor eradication by engineered T cells. *Nat Biotechnol* (2013) 31(1):71–5. doi: 10.1038/nbt.2459

170. Wilkie S, van Schalkwyk MC, Hobbs S, Davies DM, van der Stegen SJ, Pereira AC, et al. Dual targeting of Erbb2 and Muc1 in breast cancer using chimeric antigen receptors engineered to provide complementary signaling. *J Clin Immunol* (2012) 32(5):1059–70. doi: 10.1007/s10875-012-9689-9

171. Fedorov VD, Themeli M, Sadelain M. Pd-1- and ctla-4-Based inhibitory chimeric antigen receptors (Icars) divert off-target immunotherapy responses. *Sci Trans Med* (2013) 5(215):215ra172. doi: 10.1126/scitranslmed.3006597

172. Juillerat A, Marechal A, Filhol JM, Valogne Y, Valton J, Duclert A, et al. An oxygen sensitive self-decision making engineered car T-cell. *Sci Rep* (2017) 7:39833. doi: 10.1038/srep39833

173. Costello CL, Cohen AD, Patel KK, Ali SS, Berdeja JG, Shah N, et al. Phase 1/2 study of the safety and response of p-Bcma-101 car-T cells in patients with Relapsed/Refractory (R/R) multiple myeloma (Mm) (Prime) with novel therapeutic strategies. *Blood* (2020) 136(Supplement 1):29–30. doi: 10.1182/blood-2020-142695

174. Mailankody S, Jakubowiak AJ, Htut M, Costa LJ, Lee K, Ganguly S, et al. Orvacabtagene autoleucel (Orva-cel), a b-cell maturation antigen (Bcma)-directed car T cell therapy for patients (Pts) with Relapsed/Refractory multiple myeloma (Rrmm): Update of the phase 1/2 evolve study (Nct03430011). *J Clin Oncol* (2020) 38(15_suppl):8504. doi: 10.1200/JCO.2020.38.15_suppl.8504

175. Berdeja JG, Madduri D, Usmani SZ, Singh I, Zudaire E, Yeh T-M, et al. Update of cartitude-1: A phase Ib/Ii study of jnj-4528, a b-cell maturation antigen (Bcma)-directed car-T-Cell therapy, in Relapsed/Refractory multiple myeloma. *J Clin Oncol* (2020) 38(15_suppl):8505. doi: 10.1200/JCO.2020.38.15_suppl.8505

176. Mailankody S, Liedtke M, Sidana S, Matous JV, Chhabra S, Oluwole OO, et al. Universal updated phase 1 data validates the feasibility of allogeneic anti-bcma allo-715 therapy for Relapsed/Refractory multiple myeloma. *Blood* (2021) 138(Supplement 1):651. doi: 10.1182/blood-2021-145572

177. Chen W, Fu C, Cai Z, Li Z, Wang H, Yan L, et al. Sustainable efficacy and safety results from lummicar study 1: A phase 1/2 study of fully human b-cell maturation antigen-specific car T cells (Ct053) in Chinese subjects with relapsed and/or refractory multiple myeloma. *Blood* (2021) 138(Supplement 1):2821. doi: 10.1182/blood-2021-150124

178. Fernandez de Larrea C, Gonzalez-Calle V, Cabañas V, Oliver-Caldes A, Español-Rego M, Rodriguez-Otero P, et al. Results from a pilot study of Ari0002h, an academic bcma-directed car-T cell therapy with fractionated initial infusion and booster dose in patients with relapsed and/or refractory multiple myeloma. *Blood* (2021) 138(Supplement 1):2837. doi: 10.1182/blood-2021-147188

179. Bu D, Bennett P, Barton N, Bradshaw L, Pinon-Ortiz M, Li X, et al. Identification and development of Phe885: A novel and highly potent fully human anti-bcma car-T manufactured with a novel T-charge Tm platform for the treatment of multiple myeloma. *Blood* (2021) 138(Supplement 1):2770. doi: 10.1182/blood-2021-148390

180. Li C, Wang D, Song Y, Li J, Huang H, Chen B, et al. A phase 1/2 study of a novel fully human b-cell maturation antigen-specific car T cells (Ct103a) in patients with relapsed and/or refractory multiple myeloma. *Blood* (2021) 138 (Supplement 1):547. doi: 10.1182/blood-2021-152576

181. Larry D, Anderson J, Munshi NC, Shah N, Jagannath S, Berdeja JG, et al. Idecabtagene vicleucel (Ide-cel, Bb2121), a bcma-directed car T cell therapy, in relapsed and refractory multiple myeloma: Updated karmma results. *J Clin Oncol* (2021) 39(15_suppl):8016. doi: 10.1200/JCO.2021.39.15_suppl.8016

182. Du J, Jiang H, Dong B, Gao L, Liu L, Ge J, et al. Updated results of a multicenter first-in-Human study of Bcma/Cd19 dual-targeting fast car-T Gc012f for patients with Relapsed/Refractory multiple myeloma (Rrmm). *J Clin Oncol* (2022) 40(16_suppl):8005. doi: 10.1200/JCO.2022.40.16_suppl.8005

183. Frigault MJ, Rosenblatt J, Cook D, Cho HN, Depinho GD, Logan E, et al. Phase 1 study of cart-ddbcma in relapsed or refractory multiple myeloma. *J Clin Oncol* (2022) 40(16_suppl):8003. doi: 10.1200/JCO.2022.40.16_suppl.8003

184. Huang H, Hu Y, Zhang M, Ding X, Tang Y, He X, et al. Phase I open-label single arm study of Gprc5d car T-cells (Oricar-017) in patients with Relapsed/Refractory multiple myeloma (Polaris). *J Clin Oncol* (2022) 40(16_suppl):8004. doi: 10.1200/JCO.2022.40.16_suppl.8004

185. Donk NWCJVD, Agha ME, Cohen AD, Cohen YC, Anguille S, Kerre T, et al. Biological correlative analyses and updated clinical data of ciltacabtagene autoleucel (Cilta-cel), a bcma-directed car-T cell therapy, in patients with multiple myeloma (Mm) and early relapse after initial therapy: Cartitude-2, cohort b. *J Clin Oncol* (2022) 40(16_suppl):8029. doi: 10.1200/JCO.2022.40.16_suppl.8029

186. Schuster SJ, Svoboda J, Chong EA, Nasta SD, Mato AR, Anak Ö, et al. Chimeric antigen receptor T cells in refractory b-cell lymphomas. *New Engl J Med* (2017) 377(26):2545–54. doi: 10.1056/NEJMoa1708566

187. Singh N, Perazzelli J, Grupp SA, Barrett DM. Early memory phenotypes drive T cell proliferation in patients with pediatric malignancies. *Sci Trans Med* (2016) 8(320):320ra3. doi: 10.1126/scitranslmed.aad5222

188. Elavia N, Panch SR, McManus A, Bikkani T, Szymanski J, Highfill SL, et al. Effects of starting cellular material composition on chimeric antigen receptor T-cell expansion and characteristics. *Transfusion* (2019) 59(5):1755–64. doi: 10.1111/trf.15287

189. Philip M, Fairchild L, Sun L, Horste EL, Camara S, Shakiba M, et al. Chromatin states define tumour-specific T cell dysfunction and reprogramming. *Nature* (2017) 545(7655):452–6. doi: 10.1038/nature22367

190. Schietinger A, Philip M, Krisnawan VE, Chiu EY, Delrow JJ, Basom RS, et al. Tumor-specific T cell dysfunction is a dynamic antigen-driven differentiation program initiated early during tumorigenesis. *Immunity* (2016) 45(2):389–401. doi: 10.1016/j.immuni.2016.07.011

191. Tötterman TH, Carlsson M, Simonsson B, Bengtsson M, Nilsson K. T-Cell activation and subset patterns are altered in b-cll and correlate with the stage of the disease. *Blood* (1989) 74(2):786–92. doi: 10.1182/blood.V74.2.786.786

192. Kebriaei P, Singh H, Huls MH, Figliola MJ, Bassett R, Olivares S, et al. Phase I trials using sleeping beauty to generate Cd19-specific car T cells. *J Clin Invest* (2016) 126(9):3363–76. doi: 10.1172/jci86721

193. Zhao J, Lin Q, Song Y, Liu D. Universal cars, universal T cells, and universal car T cells. *J Hematol Oncol* (2018) 11(1):132. doi: 10.1186/s13045-018-0677-2

194. Mailankody S, Matous JV, Liedtke M, Sidana S, Malik S, Nath R, et al. Universal: An allogeneic first-in-Human study of the anti-bcma allo-715 and the anti-Cd52 allo-647 in Relapsed/Refractory multiple myeloma. *Blood* (2020) 136(Supplement 1):24–5. doi: 10.1182/blood-2020-140641

195. Jiang H, Dong B, Gao L, Liu L, Ge J, He A, et al. Clinical results of a multicenter study of the first-in-Human dual bcma and Cd19 targeted novel platform fast car-T cell therapy for patients with Relapsed/Refractory multiple myeloma. *Blood* (2020) 136(Supplement 1):25–6. doi: 10.1182/blood-2020-138614

196. Hermanson DL, Barnett BE, Rengarajan S, Codde R, Wang X, Tan Y, et al. A novel bcma-specific, centyrin-based car-T product for the treatment of multiple myeloma. *Blood* (2016) 128(22):2127–. doi: 10.1182/blood.V128.22.2127.2127

197. Gregory T, Cohen AD, Costello CL, Ali SA, Berdeja JG, Ostertag EM, et al. Efficacy and safety of p-Bcma-101 car-T cells in patients with Relapsed/Refractory (R/R) multiple myeloma (Mm). *Blood* (2018) 132(Supplement 1):1012. doi: 10.1182/blood-2018-99-111419

frontiers | Frontiers in Immunology

TYPE Original Research
PUBLISHED 05 January 2023
DOI 10.3389/fimmu.2022.1052090

OPEN ACCESS

EDITED BY
Hakim Echchannaoui,
Johannes Gutenberg University Mainz, Germany

REVIEWED BY
Demin Li,
University of Oxford, United Kingdom
Pierfrancesco Tassone,
Magna Græcia University, Italy

*CORRESPONDENCE
Jürgen Kuball
j.h.e.kuball@umcutrecht.nl

†These authors share first authorship

‡These authors share senior authorship

SPECIALTY SECTION
This article was submitted to Cancer Immunity and Immunotherapy, a section of the journal Frontiers in Immunology

RECEIVED 23 September 2022
ACCEPTED 15 December 2022
PUBLISHED 05 January 2023

CITATION
van Diest E, Nicolasen MJT, Kramer L, Zheng J, Hernández-López P, Beringer DX and Kuball J (2023) The making of multivalent gamma delta TCR anti-CD3 bispecific T cell engagers.
Front. Immunol. 13:1052090.
doi: 10.3389/fimmu.2022.1052090

The making of multivalent gamma delta TCR anti-CD3 bispecific T cell engagers

Eline van Diest[1†], Mara J. T. Nicolasen[1†], Lovro Kramer[1], Jiali Zheng[1], Patricia Hernández-López[1], Dennis X. Beringer[1‡] and Jürgen Kuball[1,2*‡]

[1]Center for Translational Immunology, University Medical Center Utrecht, Utrecht University, Utrecht, Netherlands, [2]Department of Hematology, University Medical Center Utrecht, Utrecht University, Utrecht, Netherlands

Introduction: We have recently developed a novel T cell engager concept by utilizing γ9δ2TCR as tumor targeting domain, named gamma delta TCR anti-CD3 bispecific molecule (GAB), targeting the phosphoantigen-dependent orchestration of BTN2A1 and BTN3A1 at the surface of cancer cells. GABs are made by the fusion of the ectodomains of a γδTCR to an anti-CD3 single chain variable fragment (scFv) (γδECTO-αCD3), here we explore alternative designs with the aim to enhance GAB effectivity.

Methods: The first alternative design was made by linking the variable domains of the γ and δ chain to an anti-CD3 scFv (γδVAR-αCD3). The second alternative design was multimerizing γδVAR-αCD3 proteins to increase the tumor binding valency. Both designs were expressed and purified and the potency to target tumor cells by T cells of the alternative designs was compared to γδECTO-αCD3, in T cell activation and cytotoxicity assays.

Results and discussion: The γδVAR-αCD3 proteins were poorly expressed, and while the addition of stabilizing mutations based on finding for αβ single chain formats increased expression, generation of meaningful amounts of γδVAR-αCD3 protein was not possible. As an alternative strategy, we explored the natural properties of the original GAB design (γδECTO-αCD3), and observed the spontaneous formation of γδECTO-αCD3-monomers and -dimers during expression. We successfully enhanced the fraction of γδECTO-αCD3-dimers by shortening the linker length between the heavy and light chain in the anti-CD3 scFv, though this also decreased protein yield by 50%. Finally, we formally demonstrated with purified γδECTO-αCD3-dimers and -monomers, that γδECTO-αCD3-dimers are superior in function when compared to similar concentrations of monomers, and do not induce T cell activation without simultaneous tumor engagement. In conclusion, a γδECTO-αCD3-dimer based GAB design has great potential, though protein production needs to be further optimized before preclinical and clinical testing.

KEYWORDS

tumor immunology, bispecific T cell engager, gamma delta TCR, protein engineering, Gamma Delta T cells

10.3389/fimmu.2022.1052090

Introduction

During the last decade, the introduction of immunotherapy has led to a significant improvement in treatment options for cancer patients. Many of these therapies aim to improve T lymphocyte mediated tumor recognition, for example by relieving the breaks on these cells by checkpoint inhibition, or by arming T cells with chimeric antigen receptors that induce cancer cell recognition (1). Another opportunity to use T cells for cancer therapy arose from the discovery that T cells can be redirected to tumor cells by a bispecific hybrid antibody (2), and since this initial discovery, many different bispecific antibodies to redirect T cells towards tumor cells have been developed (3). In general, bispecific antibodies combine a tumor binding domain, directed to a tumor associated antigen, with a T cell recruitment domain, most often binding to CD3ϵ. These bispecific antibodies, also called T cell engagers (TCE), can induce T cell mediated cytotoxicity towards tumor cells by simultaneously binding to the target antigen and CD3, without specific T cell receptor (TCR) - MHC engagement (4). Blinatumomab, a TCE directed against CD19 and CD3 is the first TCE construct that is FDA approved for the treatment of patients with refractory or relapsed pre-B-acute lymphoid leukemia (5). Recently a second TCE, Tebentafusp, targeting a gp100 peptide in HLA-A*02:01 and CD3, was FDA approved for the treatment of unresectable or metastatic uveal melanoma (6). Next to these two TCEs, a plethora of novel TCEs with different designs and tumor targets is currently in various stages of clinical development (7, 8).

The majority of TCEs utilize antibody-derived tumor binding domains, in the form of single chain variable fragments, antigen binding fragments, or full length antibodies (9). These antibody-derived binding domains can be engineered to bind to tumor associated antigens with very high affinity, which has been reported as beneficial for the development of highly potent TCEs (10, 11). A challenge that remains, however, is the selection of novel suitable target antigens for TCEs. On-target off- tumor toxicity remains a concern for high affinity TCEs when low levels of the target antigen are expressed on healthy tissue (12).

Most recently, we have developed a novel TCE concept, so called **g**amma delta TCR **a**nti-CD3 **b**ispecific molecules (**GABs**) by fusing ectodomains of a γδ T cell receptor (TCR) to an anti-CD3 single chain variable fragment ($\gamma\delta_{ECTO}$-αCD3) (13). This concept is based on the anti-tumor activity of γ9δ2 T cells, which are important players in the recognition of foreign pathogens, virally infected cells, and also cancer cells (14). Vγ9δ2 T cells, a specific γδT cell subset mainly found in the blood, recognize members of the butyrophilin (BTN) family, namely BTN2A1, through the gamma chain of their Vγ9δ2TCR, and additionally require BTN3A1 expression on the tumor cells for full activation (15–17). Recognition of the BTN2A1-BTN3A1 complex is induced by an intra-cellular accumulation of phosphoantigens (pAg) that can bind to the intracellular B30.2 domain of BTN3A1, which is modulated by RhoB (18, 19). pAg accumulation can be caused by microbial infection, but is also associated with cancerous transformation of cells (20). *In vitro* Vγ9δ2T cells recognize and lyse a broad spectrum of solid and hematological tumor cells (21, 22) and therefore provide an interesting tool box for the development of anti-cancer therapies (23). However, the activity of Vγ9δ2T cells is diverse when analyzed in a clonal population (17), and can be hampered by many inhibitory receptors, like NKG2A (24).

GABs are a means to utilize the favorable clonal properties of natural Vγ9δ2T cells, and, by engaging mainly αβ T lymphocytes, make it possible to overcome the general poor functionally of Vγ9δ2T cells in advanced stage cancer patients. Furthermore, GAB mediated tumor recognition is independent of the mutational load or tumor associated antigen expression of the tumor cells, thus introduces a novel tumor targeting concept to the TCE field. This concept would also overcome extensive and expensive T cell engineering concepts with defined Vγ9δ2TCRs (23, 25).

Critical for the GAB concept remains the rather low affinity of the Vγ9δ2 TCR for its ligands, which has been reported in the μM range (15, 16), a couple of magnitudes lower than the high affinity antibody derived domains generally used for tumor binding in TCEs. For αβTCR based TCEs, like Tebentafusp, the consensus is that affinity maturation of the αβTCR from μM to pM is required to create a functional TCE (26). While we have shown that for the GAB, affinity maturation of the γδTCR is not essential when naturally selected high affinity CDR3 sequences of the δ chain are used (13), we hypothesized that increasing the tumor binding avidity of the Vγ9δ2 TCR would further improve the effectivity of a GAB.

Most TCEs combine only one tumor- and one T cell engaging domain, similar to our original GAB design, however there are also higher valency constructs currently being developed (9, 27, 28). Often the rationale behind the use of these higher valency constructs is to increase the potency of the TCE by increasing the tumor binding avidity rather than the direct affinity maturation of the tumor binding domain (29). In this light,

we report here on the failures and success of different strategies to create multivalent GABs, and show that while attempts to express the γ and δ variable domains as a single chain linked to an anti-CD3 single chain variable fragment ($\gamma\delta_{VAR}$αCD3) were not successful, we observed $\gamma\delta_{ECTO}$-αCD3-dimers as a side product during the production process with the original $\gamma\delta_{ECTO}$-αCD3 GAB design, incorporating the full length γδTCR ectodomains. Although it is a technical challenge to achieve meaningful yields of $\gamma\delta_{ECTO}$-αCD3-dimers, $\gamma\delta_{ECTO}$-αCD3-dimers have improved *in vitro* potency compared to the monomeric form, while there is no evidence for non-specific T cell activation by bivalent CD3 engagement.

10.3389/fimmu.2022.1052090

Material and methods

Generation of bispecific constructs

Design of the original $\gamma\delta_{ECTO}$-αCD3 construct was reported previously (13). To force dimerization, the 3(G4S) linker between the OKT3 variable heavy and light chain was replaced by a G4S linker. To create the $\gamma\delta_{VAR}$-αCD3, the variable domains of the γ and δ chain linked to an anti-CD3 single chain variable fragment were cloned into a modified pcDNA3 vector (kind gift from protein facility LTI; UMCU) using BswI and SalI restriction sites, containing a 3' biotin acceptor peptide and His-tag after the SalI restriction site. From the N- to C-terminus the $\gamma\delta_{VAR}$ –αCD3 had the following design, Vδ-3(G4S)-Vγ-3(G4S)-VH-3(G4S)-VL. For constructing the single chain $\gamma\delta_{VAR}$ the C-terminus of the Vδ chain was linked to the N-terminus Vγ chain by a flexible linker with the sequence GSADDAKKDAAKKDGKS. Unless indicated otherwise, the TCR sequences used for the GAB constructs are derived from CL5 TCR (30) ($\gamma\delta_{VAR}$ and $\gamma\delta_{VAR}$-αCD3) or AJ8 TCR ($\gamma\delta_{ECTO}$-αCD3) (13). CDR3 sequences of all the TCRs used are indicated in Table 1. The anti CD3 single chain variable fragment (αCD3) was derived from the mAb OKT3 (32).

Cells and cell lines

PBMCS were isolated by Ficoll-Paque (GE Healthcare, cat no. Cytvia 17-1440-03)

from buffy coats obtained from Sanquin Blood Bank). αβT cells were expanded from PBMCs using CD3/CD28 dynabeads (Thermo Fisher scientific, cat no. 40203D) and (1.7×10^3 IU/ml of MACS GMP Recombinant Human interleukin (IL)-7 (Miltenyi Biotec, cat no. 130-095-361), and 1.5×10^2 IU/ml MACS GMP Recombinant Human IL-15 (Milteny Biotec, cat no. 130-095-762). HL60, RPMI 8226, and SSC9 stably expressing GFP-luciferase was generated by a previously described retroviral transduction protocol (30). The plasmid containing the GFP and luciferase transgenes was kindly provided by Jeanette Leusen (UMC Utrecht, Utrecht, Netherlands). The following cell lines were obtained from ATCC between 2010 and 2018, HL60 (CCL-240), RPMI 8226 (CCL-155), SCC9 (CRL-1629) and Daudi (CCL-213). Freestyle 293-F cells (R790-07) were obtained from Invitrogen. ML-1, HL60, RPMI 8226 and Daudi were cultured in RPMI (Gibco, cat no. 12017599), 10% FCS (Bodinco), 1% Pen/Strep (Invitrogen, cat no. 11548876). Freestyle 293-F in Freestyle expression medium (Gibco, cat no. 10319322). SCC9 in DMEM (Gibco, cat no. 31966047) 10% FCS, 1% Pen/Strep.

Expression and purification of bispecifics

Bap and His-tagged $\gamma\delta_{VAR}$ –αCD3, $\gamma\delta_{VAR}$, or $\gamma\delta_{ECTO}$-αCD3 were expressed in 293 F cells. 293 F cells were cultured in Gibco Freestyle Expression medium, as transfection reagent Polyethylenimine (PEI) (25 kDa linear PEI, Polysciences, cat no. 23966-1) was used. Transfection was performed using 293 F cells at a density of 1.10^6 cells/ml mixed with 1.25 μg DNA, 3.75 μg PEI and per million cells. DNA and PEI were pre-mixed in freestyle medium (1/30 of transfection volume), incubated for 20 minutes, and added dropwise to the cell cultures. The cultures were maintained shaking at 37°C 5% CO_2. To biotinylate the protein during expression, a vector containing the bacterial biotin ligase BirA was added to the transfection mix (10% of total DNA), and six hours after transfection, the medium was supplemented with 100 μM Biotin. Cell culture supernatant was harvested after 5 days and filtered through a 0.22 μm filter top (Milipore, Cat no. S2GPT02RE). Supernatant was adjusted to 25 mM Tris (Sigma Aldrich, cat no. 1185-53-1), 150 mM NaCl (Sigma Aldrich, 7647-14-5)

and 15 mM Imidazole (Merck, 288-32-4) (pH 8) and loaded on a 1 ml HisTrap HP column (GE healthcare, cat no. 17-5247-

TABLE 1 GAB sequences. Depicted are sequences used for generation of $y\delta_{ecto}$-αCD3.

GAB	REF	CDR3δ	CDR3γ
AJ8	(13)	CACDTAGGSWDTRQMFF	CALWEAQQELGKKIKVF
LM1	(30)	CACDTLLATDKLIF	CALWEAQQELGKKIKVF
A3	(17)	CACDAWGHTDKLIF	CALWEAQQELGKKIKVF
C4	(17)	CACDTLALGDTDKLIF	CALWEAQQELGKKIKVF
C5	(17)	CACDLLAPGDTSFTDKLIF	CALWEAQQELGKKIKVF
C7	(17)	CACDMGDASSWDTRQMFF	CALWEAQQELGKKIKVF
A3	(17)	CACDAWGHTDKLIF	CALWEAQQELGKKIKVF
CL5	(30)	CACDALKRTDTDKLIF	CALWEIQELGKKIKVF
6_2	(13)	CACDTLPGAGGADKLIF	CALWEVQELGKKIKVF
EPCR reactive γ4δ5 TCR	(31)	CAASSPIRGYTGSDKLIF	CATWDGFYYKKLFGSG

01) using the ÄKTA start purification system (GE healthcare). The column was washed with IMAC loading buffer (25 mM Tris,150 mM Nacl 15 mM Imidazole (pH 8), and protein was eluted using a linear imidazole gradient from 21 to 300 mM in 20 CV. Fractions containing the expressed protein were pooled, concentrated and buffer exchanged to TBS (25 mM tris, 150 mM NaCl, pH 8) using vivaspin 20 30kD spin columns (Sartorius, cat no. **VS2022**). Protein was diluted 100 times in IEX loading buffer (25 mM Tris pH 8), and loaded onto a HiTrap Q HP 1 ml column (GE healthcare, cat no. 17-1153-01) using the ÄKTA start purification system, for a second purification step. The column was washed with 10 column volumes IEX loading buffer, and protein was eluted using a linear NaCl gradient form 50 to 300 mM in 25 CV. Fractions containing the GAB were pooled, concentrated using vivaspin 20 30kD spin columns and examined by SDS-PAGE and staining with Instant blue protein stain (Sigma Aldrich, cat no. ISB1L). Protein concentration was measured by absorbance on Nanodrop and corrected for the Extinction coefficients. The protein was snap frozen and stored at -80°C and thawed before use.

Beads coated with variable domains of the γ and δ chains ($\gamma\delta_{VAR}$) for target cell staining

Biotinylated soluble $\gamma\delta_{VAR}$ was mixed with 5-7μm streptavidin-coated UV-beads (Spherotech) in excess to ensure fully coated beads, 10 μg $\gamma\delta_{VAR}$/mg microspheres. 7.5*104 cells, ML1 or K562, were incubated with 20 μl $\gamma\delta_{VAR}$ -UV beads (0.33 mg beads/ml) for 30 minutes at RT. The mixtures were fixed by adding 20 μl 2% formaldehyde for 15 minutes. The samples were washed once with 1% formaldehyde and analyzed on a BD FACSCanto II (BD).

Size exclusion chromatography and multi angle light scattering

Size exclusion chromatography was performed on a Yarra 3 uM SEC 3000 column (Phenomenex) using the high Performance Liquid Chromatography system (Shimadzu). The column was washed with SEC running buffer (100 mM Sodium Phosphate 150 mM NaCl pH 6.8) before loading of the samples. Protein samples were 5x diluted in SEC running buffer and filtered through a 0.22 uM centrifugal filter before loading on the column. For molecular weight characterization SEC was performed with online static light scattering (miniDAWN TREOS, Wyatt Technology) and differential refractive index (dRI, Shimadzu RID-10A) on a Shimadzu HPLC system. Data were analysed using the ASTRA software suite v.6.1.5 (Wyatt Technology).

IFNγ ELISA/Elispot

15.000 (Elispot) or 50.000 (ELISA) effector cells and 50.000 target cells were incubated together with or without GAB (different concentrations) for 16 hours at 37°C 5% CO_2. 30 or 100 μM pamidronate (calbiochem, cat no. 109552-15-0) was added to the target cells. For ELISA the supernatant was harvested after 16 hours, and the level of IFNγ was determined using the IFN gamma Human Uncoated ELISA Kit (Invitrogen, cat no. 15541107). For the Elispot assay the co-culture was done in nitrocellulose-bottomed 96-well plates (Millipore, cat no. MSIPN4550) precoated with α-IFNγ antibody (Mabtech, 3420-3-1000, clone 1-D1K 1:200). After 16 hours, the plates were washed with PBS and incubated with mAb7-B6-1 (II; Mabtech, cat no. 3420-6-1000) followed by Streptavadin-HRP (Mabtech, cat no. 3310-9) IFNγ spots were visualized with TMB substrate (Mabtech, cat no. 3651-10) and analyzed using A.EL.VIS ELISPOT Scanner and analysis software (A.EL.VIS).

Luciferase based cytotoxicity

5000 or 10000 target cells stably expressing luciferase were incubated with T cells at a 3:1 or 5:1 T cell to target cell ratio, with different $\gamma\delta_{ECTO}$-αCD3 concentrations (as indicated) in the presence of 30 or 100 μM pamidronate (calbiochem, cat no. 109552-15-0). After 16 hours, beetle luciferin (Promega, E1602) was added to the wells (125 μg/ml) and bioluminescence was measured on SoftMax Pro plate reader. The signal in treatment wells was normalized to the signal measured for targets and T cells only, which was assumed to represent 100% living cells.

Results

Variable domains of the γ and δ chains ($\gamma\delta_{VAR}$) are poorly expressed as a single chain fragment

The GAB design published to date is a fusion of ectodomains of a γδ T cell receptor (TCR) to an anti-CD3 single chain variable fragment ($\gamma\delta_{ECTO}$-αCD3) (Figure 1A) (13). We next explored strategies to increase the valency of GABs, in an effort to further increase potency. Multivalent tumor binding could be achieved, for example, by generating shorter single chain variable fragments as tumor- and T cell binding domains, and linking these in tandem with the desired stoichiometry (33). To test the feasibility of this approach, we constructed variable domains of the γ and δ chain ($\gamma\delta_{VAR}$) linked to an anti-CD3 single chain variable (αCD3) fragment with 1:1 stoichiometry ($\gamma\delta_{VAR}$-αCD3) (Figure 1B). $\gamma\delta_{VAR}$-αCD3 and the αCD3 alone (as a positive control) were expressed in HEK293F cells, and protein

10.3389/fimmu.2022.1052090

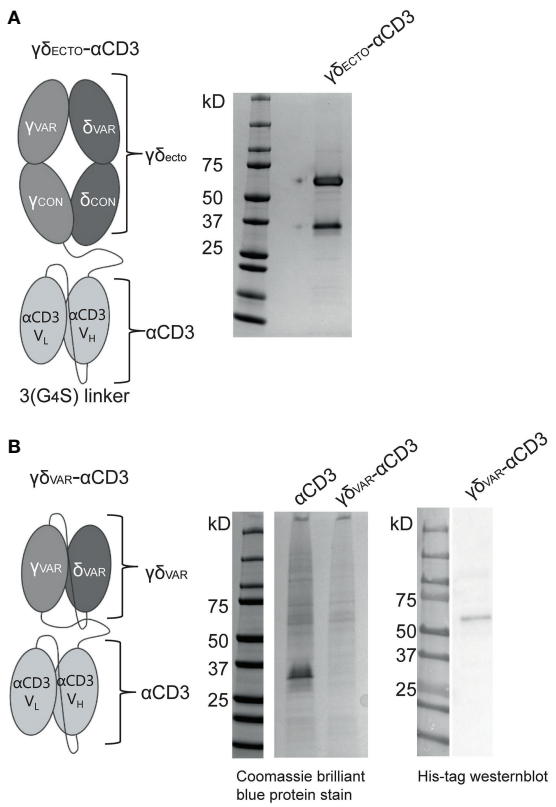

FIGURE 1
Expression of a $\gamma\delta_{Var}$–αCD3 bispecific molecule **(A)** Schematic representation of the $\gamma\delta_{ecto}$- αCD3, showing the extracellular (ecto) γδTCR (top), with the TCRγ chain connected to an anti-CD3 single chain variable fragment (αCD3) with the variable light (V_L)and heavy (V_H) and light chain (bottom) *via* a flexible linker. Purified GAB was run on SDS-page gel and stained with coomassie brilliant blue protein stain: visualizing the ectoγ-CD3scFV (59kD) and ectoδ chain (26 kD). **(B)** Schematic representation of the $\gamma\delta_{var}$–αCD3 with the Vδ-Vγ single chain TCR fragment (scTv) (top) linked to an anti-CD3 scFv (bottom) *via* a flexible linker. After HIS-tag purification the CD3scFv and $\gamma\delta_{Var}$ –αCD3 samples were run on SDS gel and visualized with coomassie brilliant blue protein stain. (left) or His-Tag western blot (right).

production was evaluated on a SDS gel after His-tag purification. While there was a visible band for the αCD3 alone around 30kD, we did not observe expression of the $\gamma\delta_{VAR}$-αCD3, which is expected at 62kD (Figure 1B left panel). We were able to visualize a band for the $\gamma\delta_{VAR}$-αCD3 using Western blot, indicating that this design does result in expressed protein, but yields are not comparable to quantities produced for αCD3 alone (Figure 1B right panel).

Stabilizing mutations reported from αβ variable T cell receptor single chains increase expression of $\gamma\delta_{VAR}$-αCD3 by three-fold

For αβTCR-derived single chains, expression yields are often very low compared to antibody-derived single chains, due to aggregation and misfolding of the protein (33). Therefore, introduction of stabilizing mutations is, in general, required to achieve successful expression of αβTCR-derived single chains (34–36). These stabilizing mutations are often unique for each TCR, and are usually identified by large random mutagenesis PCR screens. In an attempt to identify a more broadly applicable engineering strategy, Richman et al. compared stabilizing mutations found for several different αβTCR-derived single chains, and identified amino acids that were mutated in more than one stabilized αβTCR-derived single chain (35). To determine which of the regular occurring stabilizing mutation in single chain αβTCR would be suitable to include in our $\gamma\delta_{VAR}$, we aligned the sequences of variable domains of αβTCR 2C (PDB 1TCR) and γδTCR G115 (PDB 1HXM) (Supplementary Figure 1A) and their corresponding protein structures in PyMOL. Based on the location and chemical environment of the residues in the γδTCR and the potential benefit of mutations that are present in single chain αβTCRs, we selected six mutations to introduce in the γδTCR variable chains ($\gamma\delta_{VAR\text{-}MUT}$) (Supplementary Figure 1B). Three out of five mutations in the gamma chain were localized in the region of the variable domain that interacts with the constant domain in the full length TCR. These three mutations have the potential to either change polarity/hydrophobicity ($\gamma K_{13}V$ in orange and $\gamma I_{99}S$ blue) or flexibility ($\gamma V_{49}E$ in green) of the variable gamma chain (Supplementary Figure 1B) (35). Two other gamma chain mutations ($\gamma V_{49}E$ in blue and $\gamma I_{50}L$ in red) plus the delta chain mutation ($\delta M_{50}P$ in red) are located in in the variable γ- variable δ interface (in red, Supplementary Figure 1B).

$\gamma\delta_{VAR}$-αCD3 and $\gamma\delta_{VAR\text{-}MUT}$-αCD3 were expressed in HEK293F cells, and protein production was evaluated by western blot (Figure 2A). Introduction of the six mutations approximately tripled the expression yield of $\gamma\delta_{VAR\text{-}MUT}$-αCD3 when compared to $\gamma\delta_{VAR}$-αCD3 (Figure 2B). Despite the rather modest increase in expression by only threefold, we next performed a large-scale production and purification of the $\gamma\delta_{VAR\text{-}MUT}$-αCD3 (Figure 2C). To assess activity, the purified $\gamma\delta_{VAR\text{-}MUT}$-αCD3 and $\gamma\delta_{ECTO}$-αCD3 (as a positive control) were added to a co-culture of T lymphocytes, and the target cell line

10.3389/fimmu.2022.1052090

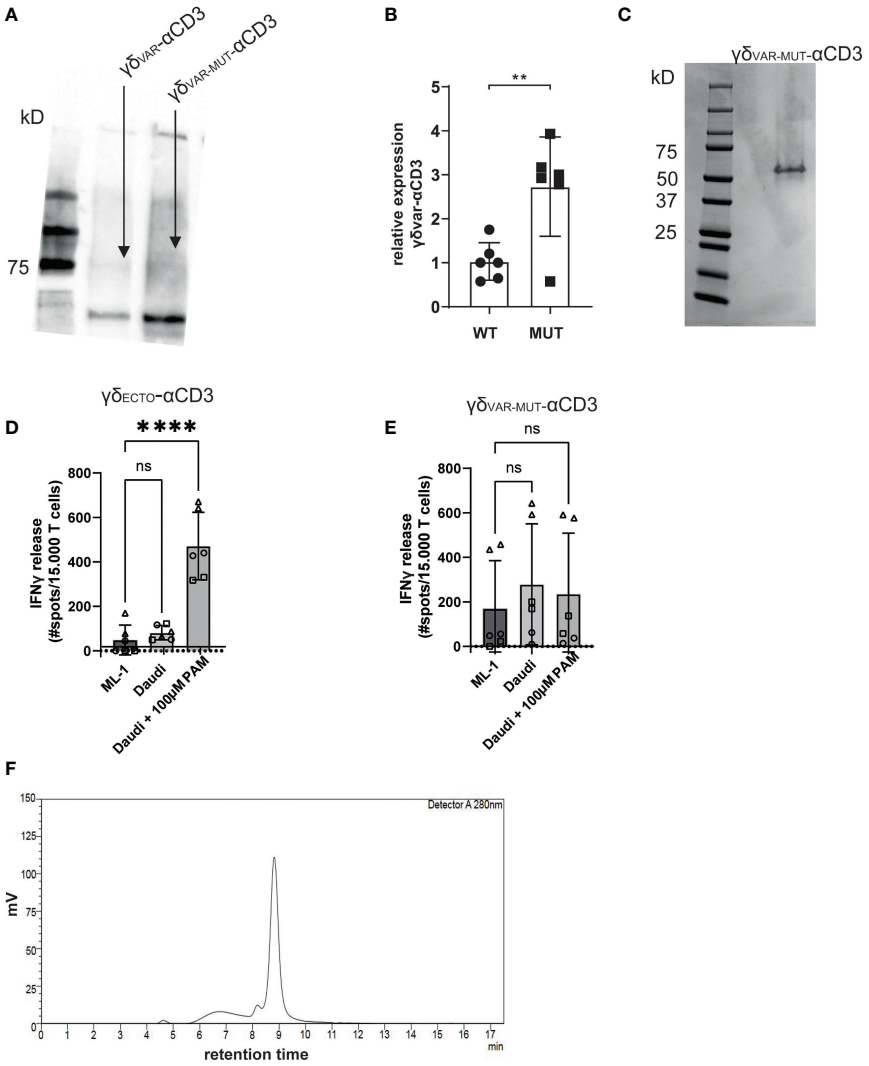

FIGURE 2
$\gamma\delta_{VAR\text{-}MUT}$–αCD3 does not redirect T cells to tumor cells **(A)** $\gamma\delta_{Var}$–αCD3 WT or with six stabilizing mutations, were expressed in HEK293F cells, and protein expression was visualized using His-Tag western blot. **(B)** Expression of $\gamma\delta_{Var}$–αCD3 6mut relative to the WT $\gamma\delta_{Var}$–αCD3. N=6 error bars represent SD, significance was calculated using an unpaired **p≤ 0.01. **(C)** SDS-PAGE analysis of purified $\gamma\delta_{VAR\text{-}MUT}$–αCD3. D\E) T lymphocytes were co-incubated with **(D)** $\gamma\delta_{ECTO}$-αCD3 or **(E)** $\gamma\delta_{VAR\text{-}MUT}$–αCD3 (5-10 µg/ml) and target cells ML-1 or Daudi, -/+ 100 µM pamidronate (PAM). IFNγ release was measured by ELISPOT. The different symbols represent three different experiments (two technical replicates). N=3, error bars represent SEM, significance was calculated using one-way ANOVA, ns not significant p>0.05, ****p≤ 0.0001. **(F)** Size exclusion chromatogram of the $\gamma\delta_{VAR\text{-}MUT}$–αCD3.

Daudi, previously shown to be recognized by γ9δ2 T cells (37). The unrecognized cell line ML-1 was used as a negative control, and additionally the Daudi cells were treated with the mevalonate pathway inhibitor pamidronate (PAM) to enhance γ9δ2TCR mediated recognition (30). While the $\gamma\delta_{ECTO}$-αCD3 only induced T cell activation against Daudi cells treated with PAM (Figure 2D), the $\gamma\delta_{VAR\text{-}MUT}$-αCD3 did not induce differential recognition of the target cell lines (Figure 2E). In one experiment the $\gamma\delta_{VAR\text{-}MUT}$-αCD3 induced nonspecific T cell activation, which could imply the presence of larger protein aggregates that can trigger T cell activation without target cell engagement. Size exclusion chromatography (SEC) of $\gamma\delta_{VAR\text{-}MUT}$-αCD3 protein confirmed that in addition to the monomeric $\gamma\delta_{VAR\text{-}MUT}$-αCD3 peak at 9 minutes, a large proportion of the $\gamma\delta_{VAR\text{-}MUT}$-αCD3, ~25%, was eluted before this monomeric peak, indicative of aggregated $\gamma\delta_{VAR\text{-}MUT}$-αCD3 (Figure 2F).

To assess the expression and folding properties of the $\gamma\delta_{VAR\text{-}MUT}$ specifically, $\gamma\delta_{VAR\text{-}MUT}$ was expressed in HEK293F cells and purified using ion exchange chromatography. The $\gamma\delta_{VAR\text{-}MUT}$ was eluted in several peaks (Figure 3A), indicating that there is a variation in the physical properties of the protein, which could

10.3389/fimmu.2022.1052090

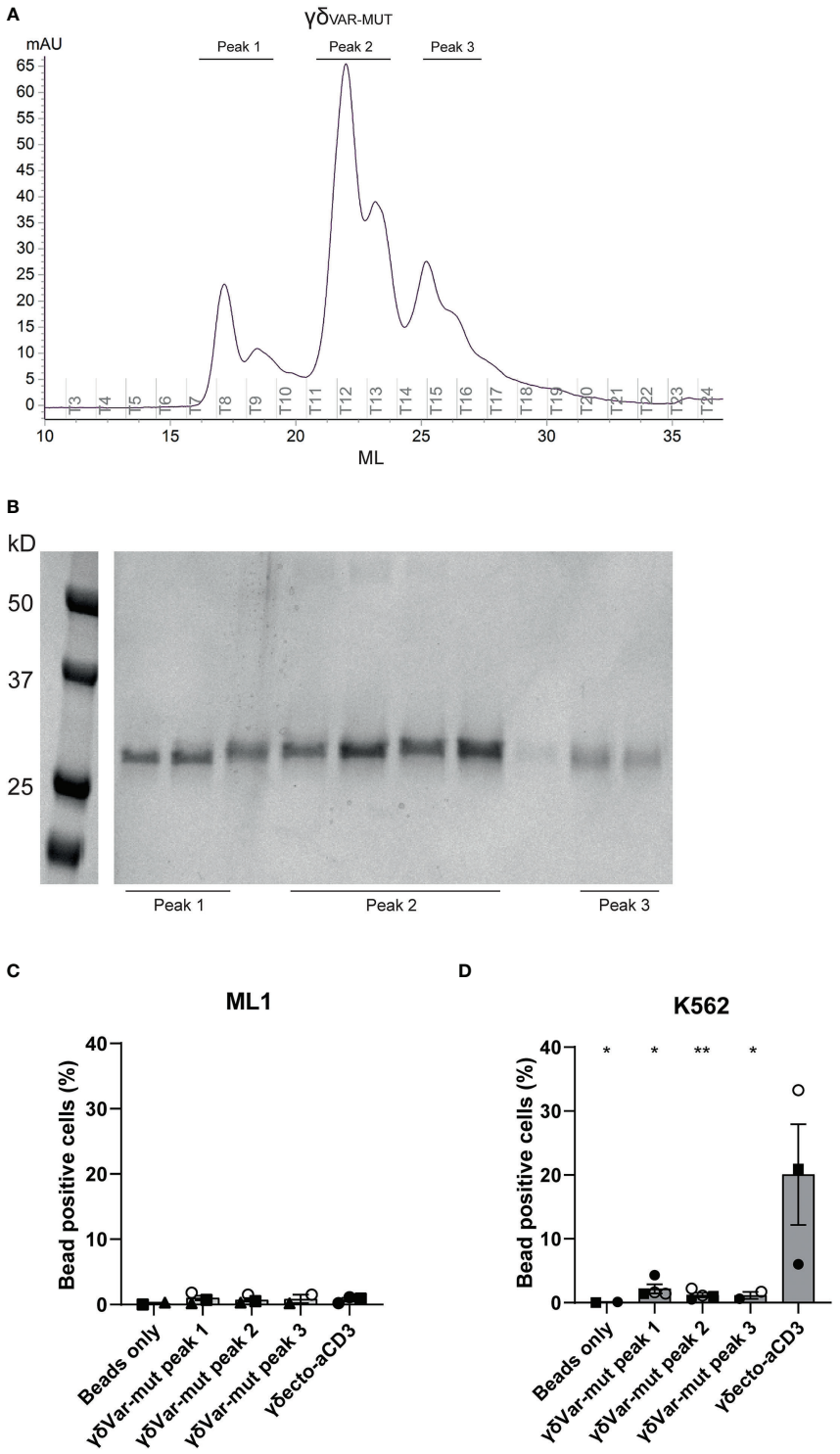

FIGURE 3
Expression and misfolding of single chain $\gamma\delta_{VAR\text{-}MUT}$. **(A)** $\gamma\delta_{var}$ with stabilizing mutations ($\gamma\delta_{VAR\text{-}MUT}$) were expressed in HEK29F cells and purified using ion exchange chromatography **(B)** the different protein elution fractions after ion exchange chromatography (IEX) were run on SDS gel and visualized by coomassie brilliant blue staining C/D) Fluorescent beads were coated with the indicated IEX protein elution peaks of $\gamma\delta_{VAR\text{-}MUT}$ or control $\gamma\delta_{ECTO}$ and incubated with ML1 **(C)** and K562 **(D)** cells. Graph shows % beads positive cells. The different symbols represent different experiments. Closed symbols represent protein elution fractions from batch 1, open symbols represent protein elution fractions from batch 2. N=3, error bars represent SEM, significance was calculated using a multiple comparison one-way ANOVA, comparing all means to the mean of γδecto, *=p≤ 0.05 **= p≤ 0.01.

10.3389/fimmu.2022.1052090

have an influence on its functionality. When the different fractions were evaluated on SDS gel, all contained the $\gamma\delta_{VAR-MUT}$ (Figure 3B). We have previously shown that it is possible to assess γ9δ2 TCR binding to target cells by coating soluble $\gamma\delta_{ECTO}$ on fluorescent streptavidin beads and evaluation of bead binding by flow cytometry (17). To test the $\gamma\delta_{VAR-MUT}$ in the different elution peaks for binding activity, the protein fractions corresponding to the separate peaks were coated on fluorescent streptavidin beads and assessed for K562 target cell binding by flow cytometry, ML-1 cells were used as a negative control. No staining was observed for beads coated with any of the $\gamma\delta_{VAR-MUT}$ elution peaks of the two cell lines, while beads coated with $\gamma\delta_{ECTO}$ specifically stained K562 cells and not the negative control cell line ML-1 (Figures 3C, D). Based on these results we can conclude that, similar to previous findings for αβTCR-derived single chains, in order for a $\gamma\delta_{VAR}$-αCD3 to be expressed and functional, extensive work would have to be performed to stabilize the γδ variable domain single chain format.

$\gamma\delta_{ECTO}$-αCD3 -dimer formation occurs naturally and is impacted by the linker length between the heavy and light chain of αCD3

As alternative strategy to increase valency of GABs, we next considered possibilities to generate a multivalent GAB by using the original $\gamma\delta_{ECTO}$-αCD3 design (Figure 1A). It has been reported previously that single chain fragments can cause protein oligomerization due to inter-chain variable heavy and light chain interactions, instead of the intended intra-chain heavy and light chain association (Figure 4A) (38, 39). To test whether the current $\gamma\delta_{ECTO}$-αCD3 design harboring an anti-CD3 single chain variable fragment with the heavy and light chain linked with a 3(G4S) flexible linker ($\gamma\delta_{ECTO}$-αCD3) results in multimerization of the $\gamma\delta_{ECTO}$-αCD3 molecules, $\gamma\delta_{ECTO}$-αCD3 were analyzed, using size exclusion chromatography (SEC) (Figure 4B). The SEC chromatogram of $\gamma\delta_{ECTO}$-αCD3 showed three peaks, with the peak at the highest retention time

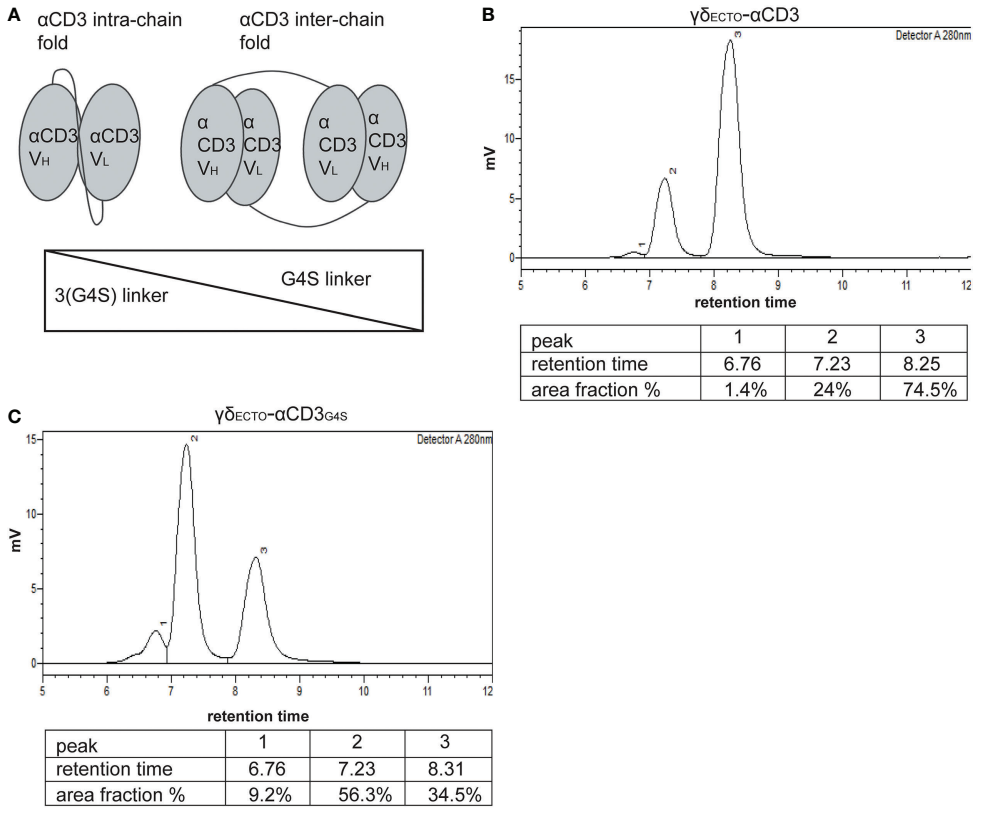

peak	1	2	3
retention time	6.76	7.23	8.25
area fraction %	1.4%	24%	74.5%

peak	1	2	3
retention time	6.76	7.23	8.31
area fraction %	9.2%	56.3%	34.5%

FIGURE 4
$\gamma\delta_{ecto}$-αCD3-dimers are formed by αCD3 dimerization, which is influenced by linker length between the heavy and the light chain. **(A)** Schematic representation of αCD3 either folded by with intra-chain interaction (left) or with inter-chain interaction of two αCD3s (right). B+C) Size exclusion chromatography of $\gamma\delta_{ecto}$-αCD3 comprising the linker 3(G4S) **(B)** or $\gamma\delta_{ecto}$-$\alpha CD3_{G4S}$ **(C)**.

(peak 3) containing the most protein, implying that there are indeed more size variants in the protein product. Separate analysis of the two major protein peaks (2 and 3) on SDS-PAGE showed the presence of both protein chains in the peaks, with no difference in relative signal intensity between the chains (Supplementary Figure 2A). The SEC was repeated with different protein batches, always resulting in a similar chromatogram, with a comparable ratio between the percentage area under the curve (AUC) of the 2 major peaks (Supplementary Figure 2B). Furthermore, varying the TCR sequence either by changing the CDR3 region of the Vδ2 or the complete Vγ9 or Vδ2 chain (Clone 5, 6_2, EPCR-reactive γδTCR) in the $\gamma\delta_{ecto}$-αCD3, did not influence the ratio of percentage AUC of the two size variants (Table 1 and Supplementary Figure 2C).

To determine the size of the GAB variants in both peaks we first used SEC-reference standards, containing 5 different molecules with known molecular weight. Based on the calibration curve the GAB variant peak 2 would have a molecular weight of around 310 kDa and the GAB variant in peak 3 would have a molecular mass of around 115 kDa (Supplementary Figure 2D). Assuming that the peak 3 would contain monomeric GAB, with a theoretical molecular mass of 85 kDa, this number deviates substantially. These large deviations in molecular mass are not uncommon when using SEC as the retention time is not only dictated by the size of the protein, but also by the shape (40). To formally determine the exact size of the $\gamma\delta_{ECTO}$-αCD3 protein in the SEC peaks, we performed size exclusion chromatography with multi angle light scattering (SEC-MALS). The MALS analysis provided the molar masses for the 2 major sized peaks, with peak 2 consisting of a protein with a molar mass 176.7 kDa, and peak 3 of a protein with a molar mass of 88.45 kDa, corresponding to dimeric and monomeric $\gamma\delta_{ECTO}$-αCD3 respectively (Supplementary Figure 2E), the small deviation from the theoretical molar mass, 171 kDa and 85.5 kDa, can be attributed to N-linked glycosylation of $\gamma\delta_{ECTO}$-αCD3 (Supplementary Figure 2F). While not determined in the SEC-MALS analysis, due to the small size, this means that peak 1 most likely contains trimerized $\gamma\delta_{ECTO}$-αCD3.

One of the factors influencing the single chain folding is the length of the linker between the two variable chains, with shorter linkers sterically hindering intra-chain interaction and thereby promoting inter-chain interactions (Figure 4A). Therefore, the flexible linker between the heavy and light chain of αCD3 was shortened from 15 to 5 amino acids (3(G4S) to G4S, $\gamma\delta_{ECTO}$-$\alpha CD3_{G4S}$). After production and purification, a sample of the $\gamma\delta_{ECTO}$-$\alpha CD3_{G4S}$ was analyzed by SEC (Figure 4C), showing an increase in the relative amount of dimeric $\gamma\delta_{ECTO}$-$\alpha CD3_{G4S}$ to over 50% of the total protein.

We conclude that it is possible to enhance the formation of naturally dimerized $\gamma\delta_{ECTO}$-αCD3 from approximately 20%, to over 50% by decreasing the linker length. Of note, there was no clear indication that larger aggregated oligomers, which could potentially cause non-specific T cell activation as seen for the $\gamma\delta_{VAR}$-αCD3, are present in either $\gamma\delta_{ECTO}$-αCD3 product.

$\gamma\delta_{ECTO}$-$\alpha CD3_{G4S}$ production is less efficient than $\gamma\delta_{ECTO}$-αCD3

Unfortunately, although the shorter G4S linker led to a higher percentage of dimer formed during protein expression, it also decreased total protein expression, as shown in a side by side comparison of expression medium of $\gamma\delta_{ECTO}$-αCD3 and $\gamma\delta_{ECTO}$-$\alpha CD3_{G4S}$ by western blot (Figure 5A). On average, the relative expression of the $\gamma\delta_{ECTO}$-$\alpha CD3_{G4S}$ compared to $\gamma\delta_{ECTO}$-αCD3 was decreased by two-fold, meaning that overall, while the G4S linker approximately doubles the proportion of formed dimer, it also causes a two-fold decrease in protein expression.

$\gamma\delta_{ECTO}$-αCD3-dimers are functionally superior to monomers

Despite the lower efficiency in the production of $\gamma\delta_{ECTO}$-$\alpha CD3_{G4S}$ compared to $\gamma\delta_{ECTO}$-αCD3, we tested whether, without further purification of the monomer and dimer fraction, differences in the activity between both constructs could be observed. $\gamma\delta_{ECTO}$-αCD3 and $\gamma\delta_{ECTO}$-$\alpha CD3_{G4S}$ were therefore titrated in a co-culture of T lymphocytes and SCC9 target cell line, and IFNγ release was determined by ELISPOT (Figure 5B). The $\gamma\delta_{ECTO}$-$\alpha CD3_{G4S}$ showed a slight increase in functional avidity, defined as IFNγ release, compared to the $\gamma\delta_{ECTO}$-αCD3, probably due to the higher percentage of dimer present in the $\gamma\delta_{ECTO}$–$\alpha CD3_{G4S}$ protein product. Next, we also tested the $\gamma\delta_{ECTO}$-αCD3 and $\gamma\delta_{ECTO}$-$\alpha CD3_{G4S}$ for direct target cell killing, using a luciferase-based cytotoxicity assay. Luciferase transduced target cell lines (RPMI8226 and SCC9) were co-cultured with T cells and different concentrations of $\gamma\delta_{ECTO}$-αCD3 and $\gamma\delta_{ECTO}$-$\alpha CD3_{G4S,}$ and the amount of viable cells was determined (Figure 5C). Again, we observed a slight, but not significant, increase target cell killing of the $\gamma\delta_{ECTO}$-$\alpha CD3_{G4S}$ compared to $\gamma\delta_{ECTO}$-αCD3.

We hypothesized that the lack of significance in activity was most likely a consequence of the still rather limited difference in the amount of dimers (20% and 50% dimer; Figures 4B, C), which made it difficult to formally asses the true value of dimers, when compared to monomers. As the shortening of the G4S linker also significantly decreased the expression efficiency of the $\gamma\delta_{ECTO}$-αCD3 protein, we decided to assess the impact of purified dimer and monomer fractions derived from the original design, namely $\gamma\delta_{ECTO}$-αCD3.

Preparative size exclusion chromatography was used to separate monomeric and dimeric $\gamma\delta_{ECTO}$-αCD3. As dimeric $\gamma\delta_{ECTO}$-αCD3 are, in theory, not only bivalent for tumor binding, but also for CD3 binding, the binding properties of

10.3389/fimmu.2022.1052090

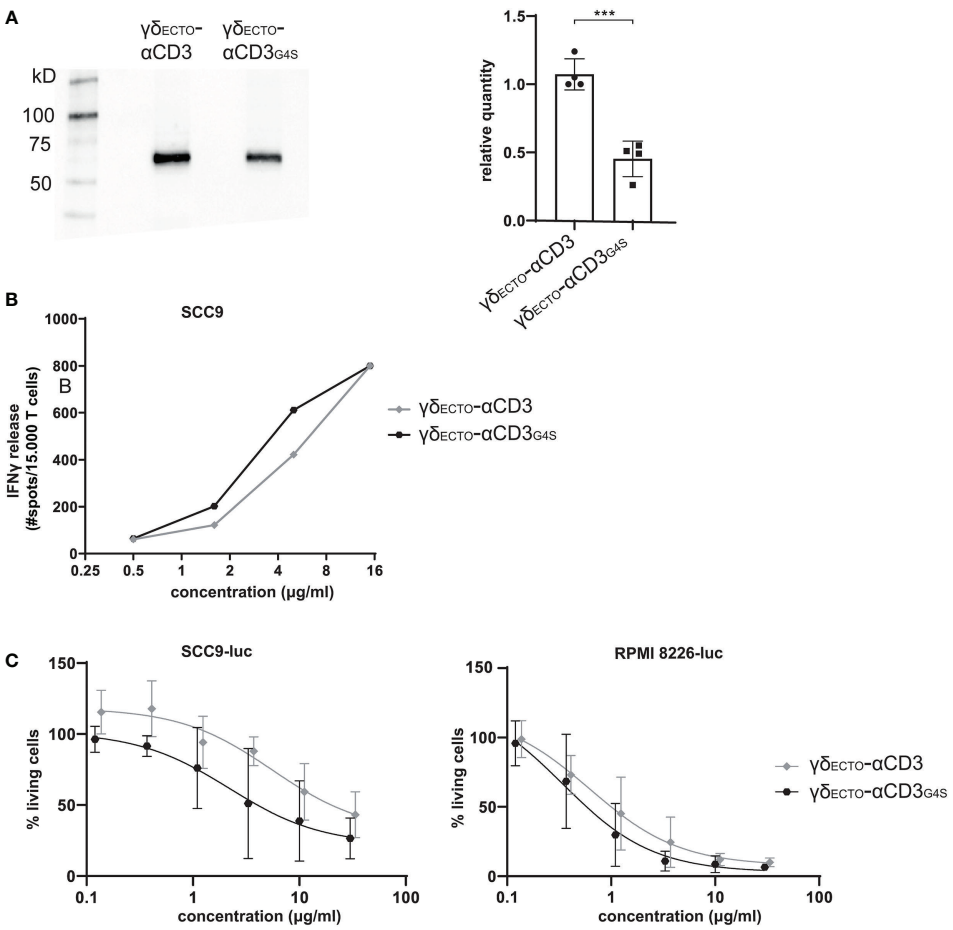

FIGURE 5
Functionality and expression of $\gamma\delta_{ecto}$-αCD3 and $\gamma\delta_{ecto}$-$\alpha CD3_{G4S}$. **(A)** Westernblot of unpurified expression medium with $\gamma\delta_{ecto}$-αCD3 and $\gamma\delta_{ecto}$-$\alpha CD3_{G4S}$ GAB. The ecto γ_{ecto}-αCD3 chain is visualized by α-HIS western blot B) T lymphocytes were co-incubated with SCC9 target cells in the presence of PAM (100 µM) and $\gamma\delta_{ecto}$-$\alpha CD3_{3(G4S)/G4S}$ (0.5-15 µg/ml) overnight. IFNγ was measured by ELISPOT C) Effector and luciferase transduced RPMI 8226 were co-incubated for 16 hours in the presence and absence of $\gamma\delta_{ecto}$-$\alpha CD3_{3(G4S)/G4S}$ at different concentrations and PAM (30 µM). Percentage viable cells was determined by comparing luminescence signal to the no $\gamma\delta_{ecto}$-αCD3 condition, representing 100% viability. N=4 **(A)**, N=2 **(B)**, N=4 **(C)**, error bars represent SD. Significance was calculated using an unpaired T-test ***P≤ 0.001.

monomeric and dimeric $\gamma\delta_{ECTO}$-αCD3 to T lymphocytes were first evaluated. Purified monomeric and dimeric $\gamma\delta_{ECTO}$-αCD3 were titrated and incubated with T lymphocytes, followed by a secondary staining using fluorochrome labeled panγδ-TCR antibody (Figure 6A). A comparison of the MFI between the dimer and the monomer showed an increase in T cell binding at lower $\gamma\delta_{ECTO}$-αCD3 concentrations for the dimeric form, compared to the monomer. This could be attributed to an increase in the CD3 binding avidity of the dimer protein, but might also be partially explained by the presence of two binding epitopes for the panγδ-TCR antibody in each dimeric $\gamma\delta_{ECTO}$-αCD3.

To test whether dimeric GABs are more potent than monomeric GABs to specifically activate T lymphocytes, we titrated monomeric or dimeric $\gamma\delta_{ECTO}$-αCD3 in a co-culture with T cells and target cells, either the non-recognized cell line HL60 (37) or one of the previously used recognized cell line RPMI8226 or SCC9. This titration showed that the dimeric $\gamma\delta_{ECTO}$-αCD3 was more potent compared to monomeric $\gamma\delta_{ECTO}$-αCD3, inducing more IFNγ release compared to monomer in a co-culture with recognized target cells, RPMI8226 and SCC9, while no IFNγ release was detected in the presence of the non-recognized target cell line HL60 for either dimeric or monomeric $\gamma\delta_{ECTO}$-αCD3 (Figure 6B). IFNγ release by T cells was significantly increased for dimeric $\gamma\delta_{ECTO}$-αCD3 at concentrations ≥ 0.6 µg/ml when co-cultured with RPMI8226 and SCC9 (Figure 6C).

A luciferase based killing assay was performed to directly compare the dimers and monomers of $\gamma\delta_{ECTO}$-αCD3 for the ability to induce target cell lysis. Luciferase transduced HL60,

10.3389/fimmu.2022.1052090

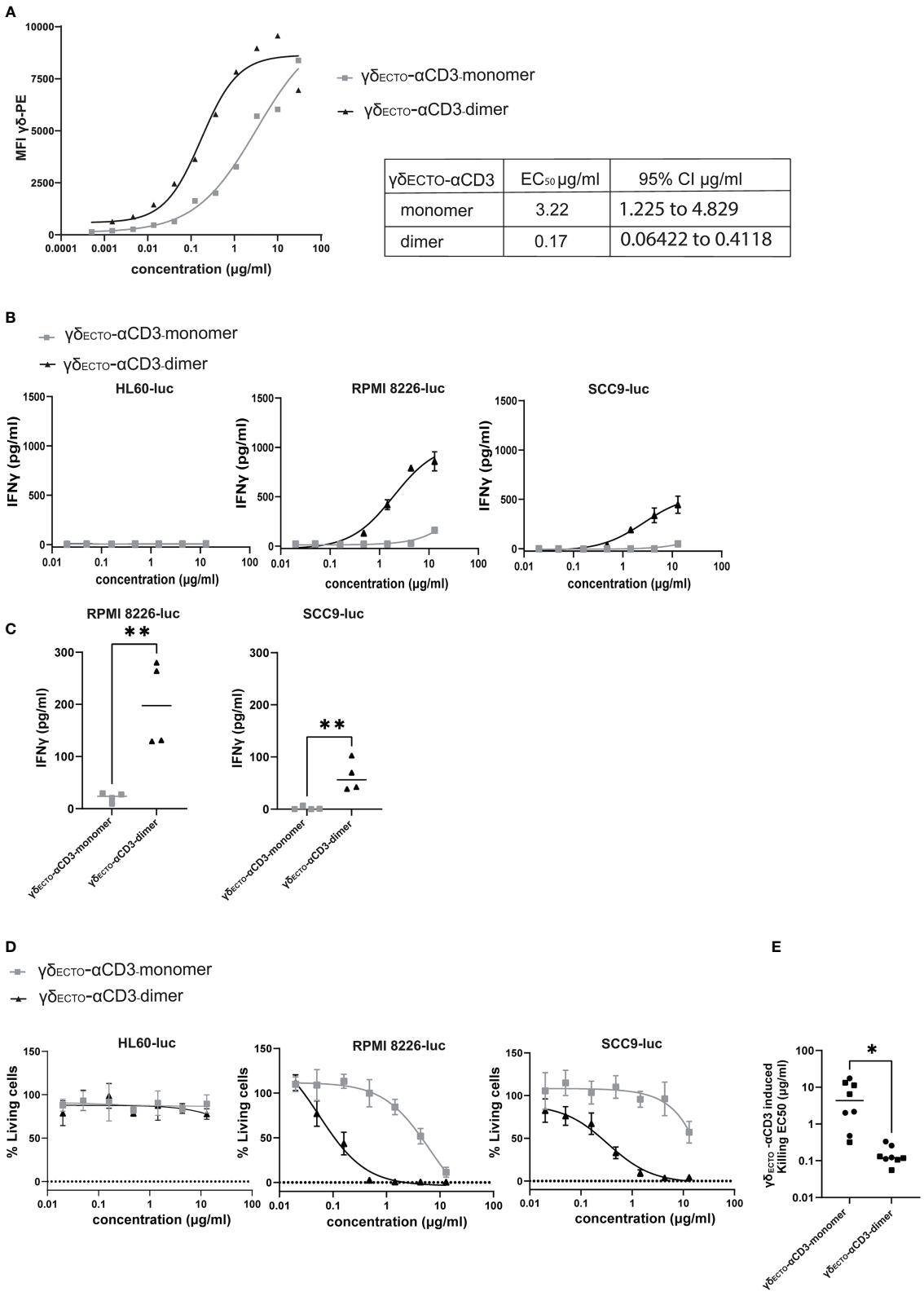

γδECTO-αCD3	EC50 μg/ml	95% CI μg/ml
monomer	3.22	1.225 to 4.829
dimer	0.17	0.06422 to 0.4118

FIGURE 6 (Continued)

FIGURE 6 (Continued)
$\gamma\delta_{ecto}$-αCD3-dimers are functionally superior **(A)** Coating of T lymphocytes with $\gamma\delta_{ecto}$-αCD3-monomers or dimers, followed by staining with fluorochrome labeled anti pan-γδ antibody. MFI was measured by flow cytometry, representative figure is shown N=3. **(B)** T cells were incubated with target cells, PAM (30 µM) and $\gamma\delta_{ecto}$-αCD3-monomers or dimers (0.02-15 µg/ml) for 20 hours. IFNγ release was measured by ELISA. Plots present mean + SD of duplicates of a representative assay, N=4 for all cell lines. **(C)** IFNγ release at a γδecto-αCD3 concentration at 0.6 µg/ml (as in B) for RPMI8226-luc and SCC9-luc. Unpaired t test was used to determine significance between the γδecto-αCD3 monomer and dimer conditions, ** P-value <0.01 (GraphPad Prism). Each dot represents the mean of biological replicate. **(D)** T lymphocytes and luciferase transduced HL60, RPMI8226, and SCC9 target cells were co-incubated for 20 hours in the presence and absence of $\gamma\delta_{ecto}$-αCD3-monomers or dimers at different concentrations and PAM (10 µM) at an E:T ratio of 5:1. Percentage viable cells was determined by comparing luminescence signal to the no GAB condition, representing 100% viability. Plots present mean + SD of triplicates of a representative assay, N=4 for all cell lines. **(E)** EC50 for each killing assay was determined in GraphPad Prism for RPMI8226-luc and SCC9-luc. Unpaired t test was used to determine significance between the γδecto-αCD3 monomer and dimer conditions, * P-value <0.05 (GraphPad Prism).

RPMI8226, and SCC9 targets cells were co-cultured with T cells and an increasing protein concentration. Neither monomeric nor dimeric $\gamma\delta_{ECTO}$-αCD3 did induce T cell mediated killing of the non-recognized target cell line HL60, in line with the lack of T cell activation in the cytokine release assay. Dimeric $\gamma\delta_{ECTO}$-αCD3 induced more target cell killing at lower protein concentrations for both tested recognized target cell lines RPMI8226 and SCC9, while monomeric $\gamma\delta_{ECTO}$-αCD3 induced efficient target cell lysis only at higher concentrations (Figure 6D), which is also reflected in the significant difference in EC_{50} between $\gamma\delta_{ECTO}$-αCD3 monomer and dimer (Figure 6E). In conclusion, our data shows that increasing the avidity of the γδTCR binding in the GAB format enhanced the potency *in vitro*, with the dimeric form of $\gamma\delta_{ECTO}$-αCD3 being superior to the monomeric form. Furthermore, bivalent CD3 engagement alone does not cause T cell activation, but requires target cell engagement.

Discussion

In this report we have explored different possibilities to increase the binding valency of previously described GABs (13). We show that dimers are a natural by-product of the recently reported $\gamma\delta_{ECTO}$-αCD3 design, and that $\gamma\delta_{ECTO}$-αCD3-dimers have higher activity when compared to $\gamma\delta_{ECTO}$-αCD3-monomers. However, all efforts to generate meaningful amounts of $\gamma\delta_{ECTO}$-αCD3-dimers, and strategies to increase valency by generating single chain formats derived from the variable domains the of the γδTCR ($\gamma\delta_{VAR}$-αCD3) were jeopardized by the lack of efficiency, and misfolding during protein production.

Identifying a means to increase valency of the GABs without compromising protein yields will be critical for further clinical translation, in order to guarantee sufficient amounts of protein during GMP-grade production, and to enter a clinical trial with the most active compound. There are several other TCEs described in literature that are multivalent in tumor binding, for example tandem diabodies (41) with two separate chains interacting to form four linked single chain variable fragments, or immunoglobulins with one or two extra antigen binding fragments attached (42, 43). These designs are, however, not easily translated to the GAB format, as we have shown here that the expression yield of a single chain $\gamma\delta_{VAR}$ was very low, and most of the expressed single chain $\gamma\delta_{VAR}$ was misfolded and not functional. This is not surprising, given the long journey required to develop stabilized αβTCR-derived single chains (34–36). While we have shown that the introduction of mutations, based on stabilizing mutations for αβTCR-derived single chains, increased expression efficiency of $\gamma\delta_{VAR}$ three-fold, further attempts to stabilize the single chain $\gamma\delta_{VAR}$ will be needed. Due to the inherent differences in sequence between variable domains of the αβ and γδ chains, non-optimal choices might have been made.

We next focused on the original $\gamma\delta_{ECTO}$-αCD3 design because of its sufficient stability, and observed spontaneous formation of monomers and dimers during expression. $\gamma\delta_{ECTO}$-αCD3-dimers are most likely formed by dimerization of αCD3 domains from two $\gamma\delta_{ECTO}$-αCD3 molecules. This assumption was supported by our observation that dimer formation could be enhanced by shortening the linker length between the variable heavy and light chain of the αCD3 fragment ($\gamma\delta_{ECTO}$-$\alpha CD3_{G4S}$). With a linker of 15 amino acids 20% of the $\gamma\delta_{ECTO}$-αCD3 protein was dimerized, which could be increased to over 50% by decreasing the linker length to only 5 amino acids in $\gamma\delta_{ECTO}$-$\alpha CD3_{G4S}$. The functional benefit of increased dimerization of the $\gamma\delta_{ECTO}$-$\alpha CD3_{G4S}$ was rather limited, and significant functional benefits could only be observed for $\gamma\delta_{ECTO}$αCD3-dimers when comparing purified dimers with purified monomers. Introduction of the shorter linker also decreased expression efficiency of the $\gamma\delta_{ECTO}$-$\alpha CD3_{G4S}$, which could be because this shorter linker is also more prone to cause larger misfolded oligomers that will be excluded during protein purification (38). Further clinical testing and development of the multivalent GABs using this αCD3 dimerized format is therefore not feasible. Addition of a dimerization domain to the C terminus of the αCD3 to induce association of two monovalent $\gamma\delta_{ECTO}$-αCD3 to form a dimer, as reported for other TCEs, could be a more efficient alternative (27, 44, 45).

Common dimerization domains cause symmetric dimerization of two identical molecules, thereby inducing a symmetric multivalent $\gamma\delta_{ECTO}$-αCD3 containing two tumor engaging- and two CD3 binding domains. We have shown in this report that the

dimerized αCD3 of $\gamma\delta_{ECTO}$-αCD3 did not result in a non-specific T cell activation, in line with observations for other TCE harboring two CD3 binding domains (41, 45). However, dual CD3 engagement and the risk for subsequent target cell independent T cell activation remains a concern in the field, and needs to be thoroughly investigated when designing a next generation of TCEs (29). In this light, the dock-and-lock method would be an interesting strategy to explore for the creation of a 2:1 valency GAB (44).

Despite the fact that our data imply that dimers are the preferred choice for further exploration to improve the potency of GABs, a potential downside of the introduction of additional multimerization domains in the GAB is that these larger multimers might substantially increase the space between the tumor- and CD3-binding domains, which could lead to a decreased activation efficacy, due to suboptimal immune synapse distances. The remarkable high potency of the FDA approved TCE blinatumomab is partially attributed to its small size, causing the formation of very tight immune synapses that are indistinguishable from naturally formed TCR-MHC synapses after target and T cell engagement (46). The overall effect of TCE size on efficacy is, however, also dependent on the exact binding epitope on the ligand. Chen et al. showed that while a smaller TCE was more efficient when binding to a membrane distal epitope, this effect was reversed when the binding epitope was more membrane proximal (47). As the exact binding mechanism and ligands for the γ9δ2 TCR are not yet completely elucidated (17), the optimal size and design for GABs is hard to predict, and is probably best determined by an experimental approach.

In conclusion, our data imply that dimerization of GAB is an interesting strategy for further preclinical development, however the road towards clinical translation is challenging, as engineering meaningful yields of dimers remains challenging.

Data availability statement

The raw data supporting the conclusions of this article will be made available by the authors, without undue reservation.

Author contributions

EvD, DXB and JK wrote the paper. EvD, MN, LK, JZ, PHL and DXB performed experiments. All authors contributed to the article and approved the submitted version.

Funding

Funding for this study was provided by KWF grant numbers 6790, 11393, 12586, 13043, 13493 to JK and 11979 to DB and JK.

Acknowledgments

We would like to thank Wout Oosterheert for his help with and the Structural Biochemistry group at Utrecht University for the use of the SEC-MALS. Figures 1A, B and Figure 4A were created using BioRender.com.

Conflict of interest

JK reports grants from Gadeta, Novartis, and Miltenyi Biotech and is the inventor on patents dealing with γδT cell-related aspects, as well as the co-founder and shareholder of Gadeta. EvD and DB are inventor on patents dealing with γδT cell-related aspects.

The remaining authors declare that the research was conducted in the absence of any commercial or financial relationships that could be construed as a potential conflict of interest.

Publisher's note

Supplementary material

The Supplementary Material for this article can be found online at: https://www.frontiersin.org/articles/10.3389/fimmu.2022.1052090/full#supplementary-material

References

1. Waldman AD, Fritz JM, Lenardo MJ. A guide to cancer immunotherapy: From T cell basic science to clinical practice. *Nat Rev Immunol* (2020) 20(11):651–68. doi: 10.1038/s41577-020-0306-5

2. Staerz UD, Bevan MJ. *Hybrid hybridoma producing a bispecific monoclonal antibody that can focus effector T-cell activity. Proc Natl Acad Sci U.S.A.* (1986) 83 (5):1453–7. doi: 10.1073/pnas.83.5.1453

3. Trabolsi A, Arumov A, Schatz JH. T Cell-activating bispecific antibodies in cancer therapy. *J Immunol* (2019) 203(3):585–92. doi: 10.4049/jimmunol.1900496

4. Brischwein K, Parr L, Pflanz S, Volkland J, Lumsden J, Klinger M, et al. Strictly target cell-dependent activation of T cells by bispecific single-chain antibody constructs of the BiTE class. *J Immunother* (2007) 30(8):798–807. doi: 10.1097/CJI.0b013e318156750c

5. Przepiorka D, Ko CW, Deisseroth A, Yancey CL, Candau-Chacon R, Chiu HJ, et al. FDA Approval: Blinatumomab. *Clin Cancer Res* (2015) 21(18):4035–9. doi: 10.1158/1078-0432.CCR-15-0612

6. Nathan P, Hassel JC, Rutkowski P, Baurain JF, Butler MO, Schlaak M, et al. Overall survival benefit with tebentafusp in metastatic uveal melanoma. *N Engl J Med* (2021) 385(13):1196–206. doi: 10.1056/NEJMoa2103485

7. Labrijn AF, Janmaat ML, Reichert JM, Parren P. Bispecific antibodies: a mechanistic review of the pipeline. *Nat Rev Drug Discovery* (2019) 18(8):585–608. doi: 10.1038/s41573-019-0028-1

8. Thakur A, Huang M, Lum LG. Bispecific antibody based therapeutics: Strengths and challenges. *Blood Rev* (2018) 32(4):339–47. doi: 10.1016/j.blre.2018.02.004

9. Brinkmann U, Kontermann RE. The making of bispecific antibodies. *MAbs* (2017) 9(2):182–212. doi: 10.1080/19420862.2016.1268307

10. Root AR, Cao W, Li B, LaPan P, Meade C, Sanford J, et al. Development of PF-06671008, a highly potent anti-P-cadherin/Anti-CD3 bispecific DART molecule with extended half-life for the treatment of cancer. *Antibodies (Basel)* (2016) 5(1). doi: 10.3390/antib5010006

11. Ellwanger K, Reusch U, Fucek I, Knackmuss S, Weichel M, Gantke T, et al. Highly specific and effective targeting of EGFRvIII-positive tumors with TandAb antibodies. *Front Oncol* (2017) 7:100. doi: 10.3389/fonc.2017.00100

12. Middelburg J, Kemper K, Engelberts P, Labrijn AF, Schuurman J, van Hall T. Overcoming challenges for CD3-bispecific antibody therapy in solid tumors. *Cancers (Basel)* (2021) 13(2). doi: 10.3390/cancers13020287

13. van Diest E, Hernández López P, Meringa AD, Vyborova A, Karaiskaki F, Heijhuurs S, et al. Gamma delta TCR anti-CD3 bispecific molecules (GABs) as novel immunotherapeutic compounds. *J Immunother Cancer* (2021) 9(11). doi: 10.1136/jitc-2021-003850

14. Bonneville M, O'Brien RL, Born WK. Gammadelta T cell effector functions: a blend of innate programming and acquired plasticity. *Nat.Rev.Immunol* (2010) 10(7):467–78. doi: 10.1038/nri2781

15. Rigau M, Ostrouska S, Fulford TS, Johnson DN, Woods K, Ruan Z, et al. Butyrophilin 2A1 is essential for phosphoantigen reactivity by γδ T cells. *Science* (2020) 367(6478). doi: 10.1126/science.aay5516

16. Karunakaran MM, Willcox CR, Salim M, Paletta D, Fichtner AS, Noll A, et al. Butyrophilin-2A1 directly binds germline-encoded regions of the Vγ9Vδ2 TCR and is essential for phosphoantigen sensing. *Immunity* (2020) 52(3):487–498.e6. doi: 10.1016/j.immuni.2020.02.014

17. Vyborova A, Beringer DX, Fasci D, Karaiskaki F, van Diest E, Kramer L, et al. γ9δ2T cell diversity and the receptor interface with tumor cells. *J Clin Invest* (2020) 130(9):4637–51. doi: 10.1172/JCI132489

18. Sebestyen Z, Scheper W, Vyborova A, Gu S, Rychnavska Z, Schiffler M, et al. RhoB mediates phosphoantigen recognition by Vγ9Vδ2 T cell receptor. *Cell Rep* (2016) 15(9):1973–85. doi: 10.1016/j.celrep.2016.04.081

19. Gu S, Sachleben JR, Boughter CT, Nawrocka WI, Borowska MT, Tarrasch JT, et al. *Phosphoantigen-induced conformational change of butyrophilin 3A1 (BTN3A1) and its implication on Vγ9Vδ2 T cell activation. Proc Natl Acad Sci U.S.A.* (2017) 114(35):E7311–:e7320. doi: 10.1073/pnas.1707547114

20. Gober HJ, Kistowska M, Angman L, Jenö P, Mori L, De Libero G. Human T cell receptor gammadelta cells recognize endogenous mevalonate metabolites in tumor cells. *J Exp Med* (2003) 197(2):163–8. doi: 10.1084/jem.20021500

21. Scheper W, Grunder C, Straetemans T, Sebestyen Z, Kuball J. Hunting for clinical translation with innate-like immune cells and their receptors. *Leukemia* (2014) 28(6):1181–90. doi: 10.1038/leu.2013.378

22. Scheper W, van Dorp S, Kersting S, Pietersma F, Lindemans C, Hol S, et al. γδT cells elicited by CMV reactivation after allo-SCT cross-recognize CMV and leukemia. *Leukemia* (2013) 27(6):1328–38. doi: 10.1038/leu.2012.374

23. Sebestyen Z, Prinz I, Dechanet-Merville J, Silva-Santos B, Kuball J. Translating gammadelta (gammadelta) T cells and their receptors into cancer cell therapies. *Nat Rev Drug Discovery* (2020) 19(3):169–84. doi: 10.1038/s41573-019-0038-z

24. Vyborova A, Janssen A, Gatti L, Karaiskaki F, Yonika A, van Dooremalen S, et al. γ9δ2 T-cell expansion and phenotypic profile are reflected in the CDR3δ repertoire of healthy adults. *Front Immunol* (2022) 13:915366. doi: 10.3389/fimmu.2022.915366

25. Dekkers JF, Alieva M, Cleven A, Keramati F, Wezenaar AKL, van Vliet EJ, et al. Uncovering the mode of action of engineered T cells in patient cancer organoids. *Nat Biotechnol* (2022). doi: 10.1038/s41587-022-01397-w

26. Liddy N, Bossi G, Adams KJ, Lissina A, Mahon TM, Hassan NJ, et al. Monoclonal TCR-redirected tumor cell killing. *Nat Med* (2012) 18(6):980–7. doi: 10.1038/nm.2764

27. Harwood SL, Alvarez-Cienfuegos A, Nuñez-Prado N, Compte M, Hernández-Pérez S, Merino N, et al. ATTACK, a novel bispecific T cell-recruiting antibody with trivalent EGFR binding and monovalent CD3 binding for cancer immunotherapy. *Oncoimmunology* (2017) 7(1):e1377874. doi: 10.1080/2162402x.2017.1377874

28. Bacac M, Colombetti S, Herter S, Sam J, Perro M, Chen S, et al. CD20-TCB with obinutuzumab pretreatment as next-generation treatment of hematologic malignancies. *Clin Cancer Res* (2018) 24(19):4785–97. doi: 10.1158/1078-0432.CCR-18-0455

29. Ellerman D. Bispecific T-cell engagers: Towards understanding variables influencing the in vitro potency and tumor selectivity and their modulation to enhance their efficacy and safety. *Methods* (2019) 154:102–17. doi: 10.1016/j.ymeth.2018.10.026

30. Grunder C, van DS, Hol S, Drent E, Straetemans T, Heijhuurs S, et al. γ9 and delta2CDR3 domains regulate functional avidity of T cells harboring γ9δ2TCRs. *Blood* (2012) 120(26):5153–62. doi: 10.1182/blood-2012-05-432427

31. Willcox CR, Pitard V, Netzer S, Couzi L, Salim M, Silberzahn T, et al. Cytomegalovirus and tumor stress surveillance by binding of a human γδ T cell antigen receptor to endothelial protein c receptor. *Nat Immunol* (2012) 13(9):872–9. doi: 10.1038/ni.2394

32. Arakawa F, Kuroki M, Kuwahara M, Senba T, Ozaki H, Matsuoka Y, et al. Cloning and sequencing of the VH and V kappa genes of an anti-CD3 monoclonal antibody, and construction of a mouse/human chimeric antibody. *J Biochem* (1996) 120 (3):657–62. doi: 10.1093/oxfordjournals.jbchem.a021462

33. Robinson RA, McMurran C, McCully ML, Cole DK, et al. Engineering soluble T-cell receptors for therapy. *FEBS J* (2021) 288:6159–73. doi: 10.1111/febs.15780

34. Gunnarsen KS, Kristinsson SG, Justesen S, Frigstad T, Buus S, Bogen B, et al. Chaperone-assisted thermostability engineering of a soluble T cell receptor using phage display. *Sci Rep* (2013) 3:1162. doi: 10.1038/srep01162

35. Richman SA, Aggen DH, Dossett ML, Donermeyer DL, Allen PM, Greenberg PD, et al. Structural features of T cell receptor variable regions that enhance domain stability and enable expression as single-chain ValphaVbeta fragments. *Mol Immunol* (2009) 46(5):902–16. doi: 10.1016/j.molimm.2008.09.021

36. Aggen DH, Chervin AS, Insaidoo FK, Piepenbrink KH, Baker BM, Kranz DM. Identification and engineering of human variable regions that allow expression of stable single-chain T cell receptors. *Protein Eng Des Sel* (2011) 24 (4):361–72. doi: 10.1093/protein/gzq113

37. Marcu-Malina V, Heijhuurs S, van Buuren M, Hartkamp L, Strand S, Sebestyen Z, et al. Redirecting αβ T cells against cancer cells by transfer of a broadly tumor-reactive γδT-cell receptor. *Blood* (2011) 118(1):50–9. doi: 10.1182/blood-2010-12-325993

38. Yamauchi S, Kobashigawa Y, Fukuda N, Teramoto M, Toyota Y, Liu C, et al. Cyclization of single-chain fv antibodies markedly suppressed their characteristic aggregation mediated by inter-chain VH-VL interactions. *Molecules* (2019) 24(14). doi: 10.3390/molecules24142620

39. Arndt KM, Müller KM, Plückthun A. Factors influencing the dimer to monomer transition of an antibody single-chain fv fragment. *Biochemistry* (1998) 37(37):12918–26. doi: 10.1021/bi9810407

40. Burgess RR. A brief practical review of size exclusion chromatography: Rules of thumb, limitations, and troubleshooting. *Protein Expr Purif* (2018) 150:81–5. doi: 10.1016/j.pep.2018.05.007

41. Reusch U, Duell J, Ellwanger K, Herbrecht C, Knackmuss SH, Fucek I, et al. A tetravalent bispecific TandAb (CD19/CD3), AFM11, efficiently recruits T cells for the potent lysis of CD19(+) tumor cells. *MAbs* (2015) 7(3):584–604. doi: 10.1080/19420862.2015.1029216

42. Bacac M, Fauti T, Sam J, Colombetti S, Weinzierl T, Ouaret D, et al. A novel carcinoembryonic antigen T-cell bispecific antibody (CEA TCB) for the treatment of solid tumors. *Clin Cancer Res* (2016) 22(13):3286–97. doi: 10.1158/1078-0432.CCR-15-1696

43. Slaga D, Ellerman D, Lombana TN, Vij R, Li J, Hristopoulos M, et al. Avidity-based binding to HER2 results in selective killing of HER2-overexpressing cells by anti-HER2/CD3. *Sci Transl Med* (2018) 10(463). doi: 10.1126/scitranslmed.aat5775

44. Chang CH, Rossi EA, Goldenberg DM. The dock and lock method: a novel platform technology for building multivalent, multifunctional structures of defined composition with retained bioactivity. *Clin Cancer Res* 200713(18 Pt 2):5586s–91s. doi: 10.1158/1078-0432.CCR-07-1217

45. Ahmed M, Cheng M, Cheung IY, Cheung NK. Human derived dimerization tag enhances tumor killing potency of a T-cell engaging bispecific antibody. *Oncoimmunology* (2015) 4(4):e989776. doi: 10.4161/2162402X.2014.989776

46. Kufer P, Lutterbüse R, Baeuerle PA. A revival of bispecific antibodies. *Trends Biotechnol* (2004) 22(5):238–44. doi: 10.1016/j.tibtech.2004.03.006

47. Chen W, Yang F, Wang C, Narula J, Pascua E, Ni I, et al. One size does not fit all: navigating the multi-dimensional space to optimize T-cell engaging protein therapeutics. *MAbs* (2021) 13(1):1871171. doi: 10.1080/19420862.2020.1871171

frontiers | Frontiers in Immunology

TYPE Original Research
PUBLISHED 30 January 2023
DOI 10.3389/fimmu.2023.1062365

OPEN ACCESS

EDITED BY
Ralf-Holger Voss,
Johannes Gutenberg University Mainz, Germany

REVIEWED BY
Chuan Jin,
Uppsala University, Sweden
Sisi He,
Zunyi Medical University, China

*CORRESPONDENCE
Chan Hyuk Kim
kimchanhyuk@kaist.ac.kr

SPECIALTY SECTION
This article was submitted to Cancer Immunity and Immunotherapy, a section of the journal Frontiers in Immunology

RECEIVED 05 October 2022
ACCEPTED 17 January 2023
PUBLISHED 30 January 2023

CITATION
Kim S, Park CI, Lee S, Choi HR and Kim CH (2023) Reprogramming of IL-12 secretion in the PDCD1 locus improves the anti-tumor activity of NY-ESO-1 TCR-T cells. *Front. Immunol.* 14:1062365. doi: 10.3389/fimmu.2023.1062365

Reprogramming of IL-12 secretion in the PDCD1 locus improves the anti-tumor activity of NY-ESO-1 TCR-T cells

Segi Kim, Cho I Park, Sunhwa Lee, Hyeong Ryeol Choi and Chan Hyuk Kim*

Department of Biological Sciences, Korea Advanced Institute of Science and Technology, Daejeon, Republic of Korea

Introduction: Although the engineering of T cells to co-express immunostimulatory cytokines has been shown to enhance the therapeutic efficacy of adoptive T cell therapy, the uncontrolled systemic release of potent cytokines can lead to severe adverse effects. To address this, we site-specifically inserted the *interleukin-12* (IL-12) gene into the PDCD1 locus in T cells using clustered regularly interspaced short palindromic repeats (CRISPR)/CRISPR-associated protein 9 (Cas9)-based genome editing to achieve T-cell activation-dependent expression of IL-12 while ablating the expression of inhibitory PD-1.

Methods: New York esophageal squamous cell carcinoma 1(NY-ESO-1)-specific TCR-T cells was investigated as a model system. We generated ΔPD-1-IL-12 -edited NY-ESO-1 TCR-T cells by sequential lentiviral transduction and CRISPR knock-in into activated human primary T cells.

Results: We showed that the endogenous *PDCD1* regulatory elements can tightly control the secretion of recombinant IL-12 in a target cell-dependent manner, at an expression level that is more moderate than that obtained using a synthetic NFAT-responsive promoter. The inducible expression of IL-12 from the *PDCD1* locus was sufficient to enhance the effector function of NY-ESO-1 TCR-T cells, as determined by upregulation of effector molecules, increased cytotoxic activity, and enhanced expansion upon repeated antigen stimulation in vitro. Mouse xenograft studies also revealed that PD-1-edited IL-12-secreting NY-ESO-1 TCR-T cells could eliminate established tumors and showed significantly greater in vivo expansion capacity than control TCR-T cells.

Discussion: Our approach may provide a way to safely harness the therapeutic potential of potent immunostimulatory cytokines for the development of effective adoptive T cell therapies against solid tumors.

KEYWORDS

immunotherapy, TCR-T, interleukin-12, CRISPR/Cas9, NY-ESO-1, PD-1

Introduction

Adoptive T-cell therapy (ACT) has shown successful clinical outcomes against some cancer types. For example, chimeric antigen receptor-T (CAR-T) cells exhibited a high proportion of complete responses against B cell malignancies (1, 2) and multiple myeloma (3). T cell receptor-T (TCR-T) cells or tumor-infiltrating lymphocytes (TILs) have shown objective clinical response in synovial carcinoma (4) and melanoma (5), although the longevity of their therapeutic effect was limited. However, the majority of patients with solid tumors do not benefit from these therapies, likely owing to the impaired function of T cells in the suppressive tumor microenvironment (TME) (6, 7). This suggests that modulation of immune responses within the TME is crucial for improving the efficacy of ACTs against solid tumors.

Co-delivery of cytokines in conjunction with conventional ACT has proven to be an attractive approach (8), since it can both directly enhance the activity of transferred T cells (9–12) and modulate inhibitory immune cells in the suppressive TME (13, 14). The cytokine, interleukin-12 (IL-12), which is mainly produced by activated antigen presenting cells (15), has been extensively studied owing to its potent immune-activating and tumor-suppressive activities. In T cells, IL-12 signaling induces pro-inflammatory Th1 responses (16) while inhibiting the induction of regulatory T and Th17 cells (17, 18). IL-12 is also known to promote IFN-γ secretion and the cytotoxic potential of CD8 T and natural killer (NK) cells (19, 20). In response to IL-12, tumor cells can upregulate antigen presentation (21) and myeloid-derived suppressor cells can be converted to exhibit a T cell-supportive phenotype (22, 23). These observations have led to the engineering of T cells to secrete exogenous IL-12, which has been demonstrated to enhance the cytotoxic activity of T cells, deplete tumor-associated macrophages, and recruit innate immune cells to improve tumor control in animal models (13, 24–26). However, since the systemic exposure of IL-12 is poorly tolerated (27, 28), high serum levels of IL-12 released from engineered T cells have caused life-threatening side effects in clinical investigations (29). Thus, the safe exploitation of the therapeutic effect of IL-12 in ACT requires a novel approach that will allow the cytokine to be delivered locally at the tumor site in a tightly controlled manner.

When T cells are activated upon the recognition of antigens *via* the TCR, transcriptional and posttranslational regulation tightly coordinate the exact up- and downregulation of multiple genes (30) whose activity dysregulation may result in failure to control disease or the development of an autoimmune condition (31). Thus, the reprogramming of genes whose expression levels are induced by TCR signaling provides an attractive strategy for controlling transgene expression in a target cell-dependent manner. One such gene candidate is the immune checkpoint receptor, programmed cell death 1 (PD-1), which is well characterized for its critical inhibitory effects on T cells as well as its inducible expression upon TCR activation (32). The transient expression of PD-1 rapidly declines to basal levels in the absence of TCR signaling, which critically minimizes transgene expression outside of the tumor tissue. Furthermore, ablating inhibitory PD-1 expression on T cells alone has shown benefits in maintaining robust T cell activity (33, 34), suggesting that PD-1 may be an optimal target for the reprogrammed expression of exogenous IL-12.

Here, we aimed to rewrite the *PDCD1* locus to express IL-12 instead of PD-1 in New York esophageal squamous cell carcinoma 1 (NY-ESO-1)-specific T cells. To this end, we used clustered regularly interspaced short palindromic repeats (CRISPR)/CRISPR-associated protein 9 (Cas9) technology with recombinant adeno-associated virus 6 (AAV6) donors to knock-in a recombinant single-chain IL-12 sequence. The targeted insertion of IL-12 into the *PDCD1* locus resulted in the strict regulation of IL-12 expression through antigen-dependent T cell activation while simultaneously inactivating the expression of endogenous PD-1. The secretion of IL-12 from the *PDCD1* locus enhanced the effector function of NY-ESO-1 TCR-T cells and promoted their proliferation during repetitive tumor challenges *in vitro*, leading to superior anti-tumor activity in xenograft models.

Materials and methods

Cell lines

The A375 cell line was purchased from the American Type Culture Collection (ATCC). A375 cells were genetically engineered with lentivirus to generate Zsgreen-2a-Luciferase- or PD-L1-overexpressed A375 (A375-ZF or A375-PDL1) cells. The Lenti-X™ 293T and AAVpro® 293T cell lines were purchased from Takara Bio. All cell lines were cultured in Dulbecco's modified Eagle's medium (DMEM; Welgene) supplemented with 10% heat-inactivated fetal bovine serum (Opti-Gold; Genedepot) and 1% penicillin/streptomycin (Gibco).

Lentivirus production and transduction

To produce lentiviruses, Lenti-X™ 293T cells were transiently transfected with a lentiviral backbone and three packaging plasmids: pMD2.G (#12259; Addgene), pMDLg/pRRE (#12251; Addgene), and pRSV-Rev (#12253; Addgene). Briefly, 10 μg of each DNA was mixed with 120 μg of PEI MAX (Polysciences) in Opti-MEM (Gibco) and incubated at 37°C for 10 min. The mixture was added dropwise into HEK293T cells that had been plated onto 150-mm^2 dishes 24 h before. After 6 h, the medium was replaced with fresh DMEM and the cells were maintained for 48 h. The culture supernatants containing lentivirus were collected and filtered using a 0.45-μm polyethersulfone membrane filter. Unpurified viral supernatants were used for the transduction of cell lines. For the transduction of human primary T cells, viral supernatants were further purified by ultracentrifugation. The viral supernatants were overlaid on 10% sucrose in Dulbecco's phosphate-buffered saline (DPBS) and then ultracentrifuged at 25,000 rpm for 2 h at 4°C. After centrifugation, the cleared supernatants were removed and DBPS was added to the lentivirus pellet without resuspension. After overnight incubation at 4°C, the virus was resuspended and stored at −80°C. To transduce the cells with lentivirus, 1 × 10^6 cells were mixed with purified or unpurified viruses in culture medium containing 30 μg of protamine sulfate (Sigma-Aldrich). Spin inoculation was performed by centrifugation at 1,000 × *g* for 90 min at 32°C, and thereafter the

cells were maintained at 37°C. After 24 h, the transduced cell medium was replaced with fresh culture medium.

AAV vector construction and production

The gene encoding human single-chain IL-12 (scIL-12; p40 and p35 subunits connected with the G6S linker), which was adopted from a previous report (25), was synthesized by Integrated DNA Technologies and cloned into the AAV-backbone plasmid (#20296; Addgene). The promoterless donor sequence encoded the knock-in donor genes flanked by two homology arms (614-bp left homology arm and 658-bp right homology arm), a self-cleaving T2A in-frame with a guide RNA cut site, followed by scIL-12, a self-cleaving P2A, truncated low-affinity nerve growth factor (tLNGFR), and the bovine growth hormone polyA signal (bGHpA).

For the production of recombinant AAV-6 virus, AAVpro® 293T cells were transiently transfected with an AAV backbone plasmid and two packaging plasmids (pHelper and pRC-6; #6665; Clontech). Briefly, a mixture of DNA and PEI MAX was transfected as described above for lentivirus production. After 6 h, the medium was replaced with fresh culture medium and the cells were maintained for 72 h. AAV was purified from both the culture supernatant and pelleted cells by iodixanol-based density gradient ultracentrifugation, as previously described (35). The titers of recombinant AAV6 were determined by quantitative PCR using inverted terminal repeat-targeting primers (36).

Single-guide RNA and Cas9 protein

The sequence of the guide RNA targeting exon 1 of the *PDCD1* locus (5′- GGCCAGGATGGTTCTTAGGT-3′) was designed using the web-based guide RNA design platform, CRISPR RGEN Tools (http://www.rgenome.net/). The single-guide RNA (sgRNA) was transcribed *in vitro* and purified as previously described (37). Immediately before electroporation, Cas9 protein (Enzynomics) and PDCD1 sgRNA were mixed at a 1:5 molar ratio and incubated for 10 min at 37°C to prepare the PD-1 targeting ribonucleoprotein (RNP).

Genetic engineering of human primary T cells

The blood of an anonymous healthy human donor was acquired from ASAN Medical Center (Seoul, Korea) under a protocol approved by the institutional review board. Peripheral blood mononuclear cells (PBMCs) were isolated from the whole blood by density gradient centrifugation using Sepmate-50 Tubes (STEMCELL Technologies) and cryopreserved in freezing medium (90% FBS/10% dimethylsulfoxide) until use. Frozen PBMCs were thawed and CD3+ human primary T cells were purified using a Pan T-cell isolation kit (Miltenyi Biotec). The resulting T cells were activated using Dynabeads Human T-Activator CD3/CD28 (Thermo Fisher Scientific) at a 1:1 bead-to-cell ratio. One day after activation, T cells were collected and transduced with a lentivirus encoding NY-ESO-1-specific TCR. After overnight incubation, the culture medium of the TCR-transduced T cells was replaced with fresh culture medium. Two days after transduction, the T cells were collected and the Dynabeads were magnetically removed to perform genome editing. A Neon Transfection System 10 µL Kit (Invitrogen) was used for the electroporation of CRISPR RNP. First, 1×10^6 NY-ESO-1 TCR-transduced T cells were resuspended in T buffer, mixed with PD-1-targeting RNP, and electroporated (1,400 V, 10 ms, 3 pulses). Electroporated T cells were transferred to fresh culture medium and maintained at 37°C for 15 min. The T cells were diluted to 0.5×10^6 cells mL^{-1} with culture medium, and recombinant AAV6 virus was added at a multiplicity of infection of 5×10^4. After 24 h, the culture medium was replaced with fresh culture medium with a cell density of 0.5×10^6 cells mL^{-1}. The medium was changed every 2 days. T cells were cultured in a T cell medium consisting of RPMI1640 (Gibco), 10% FBS (Gibco), 2 mM GlutaMAX (Gibco), 1 mM sodium pyruvate (Gibco), 55 µM 2-mercaptoethanol (Thermo Fisher Scientific), 10 mM HEPES (Sigma-Aldrich), and 1% non-essential amino acids (Gibco), supplemented with recombinant human interleukin-2 (300 IU mL^{-1}; BMI Korea).

Stimulation for detection of PD-1 and tLNGFR upregulation

To investigate activation-dependent transgene upregulation, 1×10^6 NY-ESO-1 TCR-T cells were stimulated with 5 µg of plate-coated CD3 antibody (clone, OKT3; Bio X Cell) and 2 µg of soluble CD28 antibody (clone, CD28.2; Bio X Cell). After 48 h, stimulated T cells were collected and PD-1 upregulation and tLNGFR expression were analyzed using flow cytometry.

Flow cytometry

For the detection of cell surface marker, 2×10^5 T cells were washed and probed with antibodies in FACS buffer (1% bovine serum albumin [BSA] in DPBS) for 20 min at 4°C. To exclude the dead cell population, cells were stained with the fixable vitality dye, eFluor 780 (65-0865-14; eBioscience) for 10 min at 25°C. After being washed with FACS buffer, the cells were probed with chloroform-conjugated specific antibodies. NY-ESO-1-targeting TCR expression was determined with allophycocyanin (APC)-conjugated TCR Vβ13.1 antibody (362410; BioLegend), and CD3ε and TCR α/β were detected with Alexa Fluor® 488 anti-human TCR α/β antibody (306712; BioLegend) and Brilliant Violet (BV)-421-conjugated CD3 antibody (300434; BioLegend). PD-1 upregulation was analyzed using BV421-conjugated CD279 antibody (367422; BioLegend). tLNGFR expression was analyzed using APC-conjugated CD271 antibody (130-113-418; Miltenyi Biotec). To detect CD4 and CD8, PerCP-CP/Cyanine5.5-conjugated CD4 antibody (357414; BioLegend) and APC-conjugated CD8 antibody (344722; BioLegend) were used. To determine differentiation status, BV421-conjugated CD45RO antibody (562641; BD Biosciences) and PE-conjugated CD197 antibody (560765; BD Biosciences) were used. To analyze intracellular proteins, surface-stained cells were fixed and permeabilized using a Cytofix/Cytoperm Fixation/Permeabilization Solution Kit (BD Biosciences). After being washed with intracellular

staining buffer (1% BSA, 0.1% sodium azide, and 0.1% saponin in DPBS), the cells were probed with following antibodies. IFN-γ secretion was detected with BV711-conjugated IFN- γ antibody (564039; BD Bioscience). The releases of granzyme B (GzmB) and perforin were detected using APC-conjugated GzmB antibody (396408; BioLegend) and PE-conjugated perforin antibody (353304; BioLegend), respectively. The percentage of proliferative cells after repeated stimulation was analyzed with APC-conjugated Ki67 antibody (556027; BD Biosciences). All flow cytometry data were acquired with a BD LSRFortessa X-20 Cell Analyzer (BD Biosciences) and analyzed using the FlowJo software (BD Biosciences).

Cytokine measurement

To detect IL-12 secretion after target-cell recognition, 2×10^5 A375 cells were plated on 24-well tissue culture plates. After 20–24 h, 5×10^5 NY-ESO-1 TCR-T cells resuspended in IL-2-free T cell culture medium were added to the A375 cells. After 2 days, the culture supernatant was collected and the secretion of IL-12 was measured using flow cytometry with a Human IL-12p70 Flex Set (BD Biosciences). To detect the releases of IFN-γ, TNF-α, IL-10, and IL-2, NY-ESO-1 TCR-T cells were co-cultured with A375 cells as described above and the cytokines released to the culture supernatant were measured using a cytometric bead array (CBA) assay with a Human th1/th2 Cytokine Kit (BD Biosciences).

Western blotting

For the detection of STAT-4 and phospho-STAT4 (p-STAT4), 2×10^6 NY-ESO-1 TCR-T cells were stimulated with 5 μg of plate-coated CD3 antibody for 72 h. To detect Bcl-xL upregulation, 2×10^5 A375 cells were plated on 24-well tissue culture plates for 24 h, after which 1×10^6 NY-ESO-1 TCR-T cells were added and maintained for 72 h. After stimulation, T cells were collected and lysed using NP-40 protein extraction buffer (Elpis Biotech) supplemented with a proteinase inhibitor cocktail (Sigma-Aldrich) and phosphatase inhibitor (Roche). The amount of protein in the lysates was quantified using a BCA protein assay kit (Thermo Fisher Scientific). Protein lysates (20 μg) from each sample were separated on precast 4%–12% Bis-Tris gradient gels (Invitrogen) using sodium dodecyl–sulfate polyacrylamide gel electrophoresis. Separated proteins were transferred to polyvinylidene fluoride (PVDF) membranes (Thermo Fisher Scientific) using an iBlot 2 Dry Blotting System (Thermo Fisher Scientific). Each membrane was blocked with 4% BSA in TBS with 0.5% Tween-20 (TBS-T) and probed with primary antibodies at 4°C overnight. The membranes were washed with TBS-T and incubated with secondary antibodies conjugated with horseradish peroxidase (HRP) at RT for 1 h. The following primary and secondary antibodies were used: anti-STAT4 (#2653, 1:1000; Cell Signaling), anti-phospho STAT4 (Tyr693) (#5267, 1:1000; Cell Signaling), anti-Bcl-xL (A19703, 1:1000; Abclonal, Wuhan, China), anti-actin (A2228, 1:20000; Sigma-Aldrich), anti-mouse IgG-HRP (#31430, 1:10000; Invitrogen), and anti-rabbit IgG-HRP (#31460, 1:10000; Invitrogen). Blot images were acquired using a ChemiDoc MP system (Bio-Rad) and processed using Image Lab software (Bio-Rad).

Cytotoxicity assay

First, 2×10^4 Zsgreen positive A375 cells were resuspended in 100 μL of culture medium and plated in 96-well tissue culture plates for 24 h. Then, 2×10^4 NY-ESO-1 TCR-T cells were resuspended in 100 μL of the culture medium, added into A375 cells, and maintained for 120 h. The green signal from A375 cells was monitored every 2 h using an IncuCyte S3 Live-Cell Analysis System (Sartorius).

Repeated tumor challenge

2×10^5 PD-L1-overexpressed A375 cells were plated on culture plates and incubated for 24 h. The culture medium were replaced with fresh culture medium containing 10 μg mL^{-1} mitomycin C (Sigma-Aldrich). After incubation at 37 °C for 3h, A375 cells were washed with DPBS three times. For co-culture, 1×10^6 NY-ESO-1 TCR-T cells were added into mitomycin C treated A375 cells. Four days later, T cells were counted using a Countess II Automated Cell Counter (Thermo Fisher Scientific) and re-challenged with fresh mitomycin C-pretreated A375-PDL1 cells. Three stimulations and cell counts were performed at intervals of four days. When the cells were counted, Trypan Blue (Gibco) was used to discriminate dead cells.

Xenograft mouse model

Animal care and experiments were performed according to a protocol approved by the Animal Care Committee of the Korea Advanced Institute of Science and Technology. First, 1×10^6 A375-ZF or A375-ZF-PDL1 cells were subcutaneously injected into the right flanks of 8–10-week-old male NSG mice (Jackson Laboratory). Mice were intravenously injected with 1×10^6 NY-ESO-1^+ TCR-T cells at 7 days after tumor injection in the A375-ZF model or at 6 days after tumor injection in the A375-ZF-PDL1 model. Tumor growth was monitored weekly using an IVIS® Lumina II *In Vivo* Imaging System (PerkinElmer). Quantification of the luminescent signal was performed using the Living Image software (PerkinElmer). To investigate the infiltration of T cells at tumor sites, A375-ZF-PDL1-engrafted NSG mice were euthanized at 6 days after T cell injection, and tumors were harvested. The collected tumors were roughly chopped into small fragments (2–4 mm) and incubated with 20 μg of DNase I (Sigma-Aldrich) and 125 μg of collagenase IV (Sigma-Aldrich) with gentle shaking for 1 h at 37°C. After being washed with DPBS, the cells were treated with ACK Lysing Buffer (Gibco) and filtered through a 70-μm nylon mesh filter. The resulting single-cell suspension was analyzed by flow cytometry.

Statistical analysis

All graph generations and statistical analyses were conducted using GraphPad Prism (GraphPad Software). Statistical significance was determined using two-tailed paired or unpaired Student's *t*-test, one-way analysis of variance (ANOVA) with Tukey's multiple comparisons, or two-way repeated-measures ANOVA with Holm-Sidak's multiple comparisons test. For all analyses, a *P*-value <0.05

was considered statistically significant (*$P < 0.05$, **$P < 0.01$, ***$P < 0.001$, ****$P < 0.0001$).

Results

ΔPD-1-IL-12-edited NY-ESO-1-specific T cells secrete IL-12 in an antigen-dependent manner

To insert the *IL-12* transgene into the *PDCD1* locus, we used CRISPR/Cas9 and AAV6-based knock-in systems, which have previously demonstrated robust and precise gene modifications in human T cells (38). To disrupt the *PDCD1* locus, we designed four sgRNAs targeting the first exon of *PDCD1* (Supplementary Figure 1A). We selected sgRNA#4 for further experiments because it resulted in a high knock-out efficiency (91.17%) when Cas9/sgRNA ribonucleoprotein (RNP) complexes were electroporated into activated human T cells (Supplementary Figure 1B). A promoterless AAV-6 donor matrix was designed to replace the endogenous PD-1 sequence with a single-chain IL-12 sequence, thus resulting in the expression of IL-12 under the control of *PDCD1* regulatory elements with concurrent knock-out of PD-1 expression. A self-cleaving P2A sequence was linked to the N-terminus of IL-12, followed by sequences encoding a self-cleaving T2A and truncated low-affinity nerve growth factor, tLNGFR, which was used as a surface marker to determine the knock-in efficiency (Figure 1A).

To edit the *PDCD1* locus of tumor-specific TCR-T cells that recognize the cancer testis antigen, NY-ESO-$1_{157–165}$ SLLMWITQV (NY-ESO-1 TCR-T cells) (39), we first transduced T cells with lentivirus encoding NY-ESO-1 TCR and then subsequently conducted Cas9 RNP/AAV6 knock-in into transduced T cells (Figure 1B). This process did not influence the viability or expansion of the resulting ΔPD-1-IL-12 edited NY-ESO-1-specific T cells (NE1ΔPD-1-IL-12) (Supplementary Figure 2). As a control group, NY-ESO-1 TCR-T cells treated only with Cas9 (NE1Cas9) or NY-ESO-1 TCR-T cells treated with Cas9/sgRNA RNP without AAV (NE1ΔPD-1) were generated. Five days after electroporation and AAV donor transduction, the surface expression of NY-ESO-1 TCR was measured in each group using flow cytometry (Figure 1C). We confirmed that CRISPR editing after lentiviral transduction did not affect the expression of the transduced NY-ESO-1 TCR, as there was no significant difference between the three groups in the positive percentage or mean fluorescence intensity (MFI) of NY-ESO-1 TCR.

Next, we examined whether CRISPR knock-out or knock-in was successfully achieved by performing flow cytometry on day 10 (Figure 1D). Before stimulation, neither PD-1 nor tLNGFR was expressed in any group. Upon stimulation with anti-CD3 and anti-CD28 antibodies, about 60% of NE1Cas9 T cells became PD-1 positive, whereas less than 10% of NE1ΔPD-1 or NE1ΔPD-1-IL-12 T cells expressed PD-1. Additionally, up to 30% of NE1ΔPD-1-IL-12 T cells displayed tLNGFR expression after stimulation (Figure 1E), indicating that the donor sequence was successfully inserted in frame and expressed under the endogenous *PDCD1* regulatory elements upon T cell activation. Flawless integration of the transgene was also confirmed by in-out PCR analysis of genomic DNA from NE1ΔPD-1-IL-12 T cells (Supplementary Figure 3).

After confirming the accurate insertion of transgenes, we investigated whether IL-12 could be secreted in a target cell-dependent manner (Figure 1F). Engineered NY-ESO-1 TCR-T cells were co-cultured with NY-ESO-1^+ A375 tumor cells for 48 h, and the amount of IL-12 secreted into the culture supernatants was analyzed using a CBA assay (Figure 1G). NE1Cas9 and NE1ΔPD-1 T cells did not produce IL-12 before co-culture, and NE1ΔPD-1-IL-12 T cells showed only slight leakage of IL-12 (2.662 pg/mL). Upon target cell recognition, NE1ΔPD-1-IL-12 T cells released approximately 20 pg/mL of IL-12 into the culture supernatant, whereas NE1Cas9 and NE1ΔPD-1 T cells showed minimal IL-12 release.

Given that *STAT4* is known as an early target gene of IL-12 signaling (40), we next examined the status of p-STAT4 in engineered T cells. Engineered NY-ESO-1 TCR-T cells were stimulated on anti-CD3-coated plates for 3 days and the levels of STAT4 and p-STAT4 were determined by western blotting (Figure 1H). Before stimulation, STAT-4 was not phosphorylated in any group. After stimulation, only NE1ΔPD-1-IL-12 T cells displayed a strong STAT-4 phosphorylation, which indicate the biological activity of the single-chain IL-12 released from the edited *PDCD1* locus. Overall, these results demonstrate that site-specific integration of the single-chain IL-12 gene into the *PDCD1* locus enabled functional IL-12 to be produced by NY-ESO-1-specific T cells in a target cell-dependent manner.

The endogenous PD-1 promoter tightly regulates the knock-in transgene

PD-1 expression is known to respond dynamically to TCR activation (41, 42). Here, we measured the expression levels of PD-1 and tLNGFR after stimulation of T cells to determine whether the transgenes inserted into the *PDCD1* locus would behave similarly (Figure 2A). The percentage of PD-1-positive cells in the NE1Cas9 T cells increased significantly at 2 days after stimulation, returned to almost baseline by day 4, and then re-elevated after the second stimulation. In contrast, minimal levels of PD-1-positive cells were detected in the NE1ΔPD-1 and NE1ΔPD-1-IL-12 T cell cells, confirming that the expression of inhibitory PD-1 was successfully abolished. Interestingly, the expression of tLNGFR was detected only in the NE1ΔPD-1-IL-12 T cells, where it showed kinetics similar to those of PD-1 expression in the NE1Cas9 T cells. These results indicate that our approach successfully utilizes the intrinsic regulatory mechanism of PD-1 to control transgene expression while simultaneously blocking the expression of endogenous PD-1.

As previously reported (25, 26), a synthetic promoter that responds to TCR activation could be used as an alternative strategy to our approach. Therefore, we next compared the expression patterns of a transgene inserted into the *PDCD1* locus with those controlled by a synthetic nuclear factor of activated T-cells (NFAT)-responsive promoter. To monitor expression, we used a transgene encoding a green fluorescent protein and tLNGFR (Zsgreen-2A-tLGNFR) which was either inserted site-specifically into the endogenous *PDCD1* locus using CRISPR knock-in (ΔPD-1-Zsgreen), or randomly integrated into the genome with the NFAT-responsive promoter using lentivirus (NFAT-Zsgreen, Figure 2B). After cells were stimulated with anti-CD3 and anti-CD28 antibodies, the upregulation of Zsgreen and tLNGFR was measured using flow

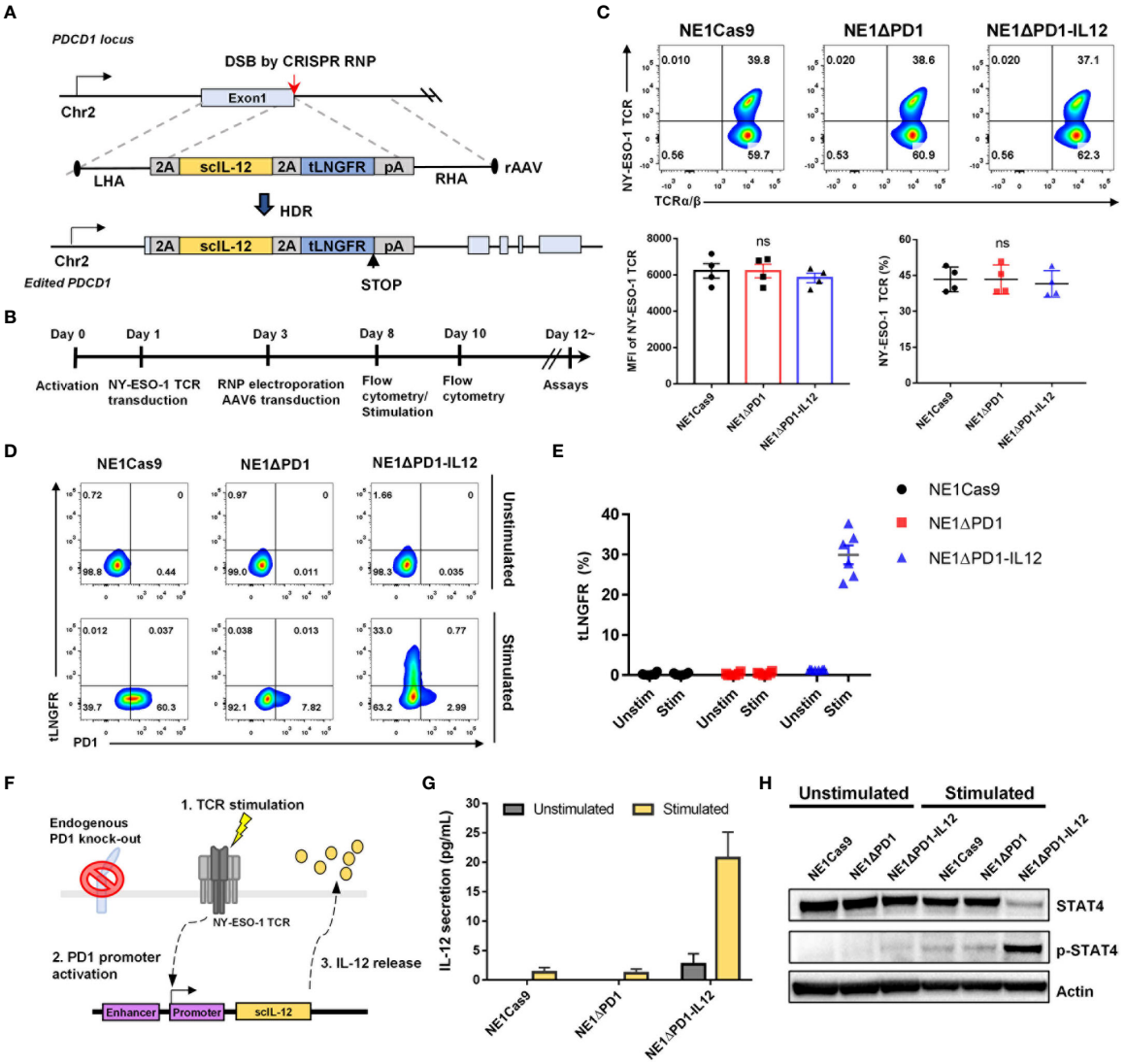

FIGURE 1
CRISPR-mediated *PDCD1* locus editing to generate ΔPD-1-IL-12-NY-ESO-1-specific T cells. **(A)** Schematic diagram for the targeted insertion of IL-12 into the PDCD1 locus using CRISPR RNP and AAV6 delivery (LHA and RHA: left and right homology arms, respectively, 2A: self-cleaving peptide, 2tLNGFR: truncated low-affinity nerve growth factor receptor, pA: polyA signal). **(B)** Timeline for the consecutive lentiviral transduction, electroporation, and AAV6 transduction to generate ΔPD-1-IL-12-edited NY-ESO-1-engineered T cells. **(C)** Five days after electroporation, the surface expression levels of NY-ESO-1 TCR on engineered T cells were analyzed using flow cytometry and the percentage and mean fluorescent intensity (MFI) of NY-ESO-1 TCR were quantified (n = 4; four independent experiments with four donors). Data were analyzed using one-way ANOVA. ns, not significant. **(D)** Representative flow cytometry plot of PD-1 and tLNGFR upregulation in engineered T cells two days after stimulation with αCD3 and αCD28. **(E)** Percentage of tLNGFR in engineered T cells before and after stimulation. Data are presented as the mean ± SEM (n = 6; six independent donors). **(F)** Schematic diagram of the stimulation-dependent release of targeted IL-12 from the edited PDCD1 locus. **(G)** After T cells were stimulated with A375 cells for 2 days, the amount of IL-12 secreted into the culture supernatant was measured using a CBA assay. Data are presented as the mean ± SEM (n = 3; three independent experiments with three donors). **(H)** Representative western blot image showing Tyr 693 phosphorylation of STAT-4 in NYESO1-ΔPD-1-IL-12 T cells before and after stimulation with αCD3 for 3 days (n = 3; three donors).

cytometry (Figure 2C). Before stimulation, we found that NFAT-Zsgreen T cells exhibit leaky expression of Zsgreen and tLNGFR, which was not observed in ΔPD-1-Zsgreen T cells. After stimulation, consistent with the results obtained from NE1ΔPD-1-IL-12 T cells, ΔPD-1-Zsgreen T cells displayed tightly controlled transgene expression that was upregulated on day 2 and returned to the baseline by day 4. NFAT-Zsgreen T cells also showed inducible transgene up-regulation at 2 day post-stimulation, but to a significantly higher level than that seen for ΔPD-1-Zsgreen T cells, as determined by the percentages (Figure 2D) and MFI (Figure 2E) of Zsgreen+ and tLNGFR+ cells. Furthermore, unlike ΔPD-1-Zsgreen T cells, NFAT-Zsgreen T cells exhibited significant levels of residual transgene expression on day 4. The significant levels of leaky transgene in NFAT-Zsgreen T cells, together with their high expression levels upon stimulation, may account for the unexpected toxicity observed in patients infused with NFAT-driven IL-12-expressing T cells (29). Collectively, these results suggest that, compared to the NFAT-responsive promoter, PD-1 regulatory elements can provide a better control of transgene expression without leakage and induce moderate levels of transgene expression with rapid kinetics, which could mitigate the potential toxicity of IL-12 secreted by engineered T cells.

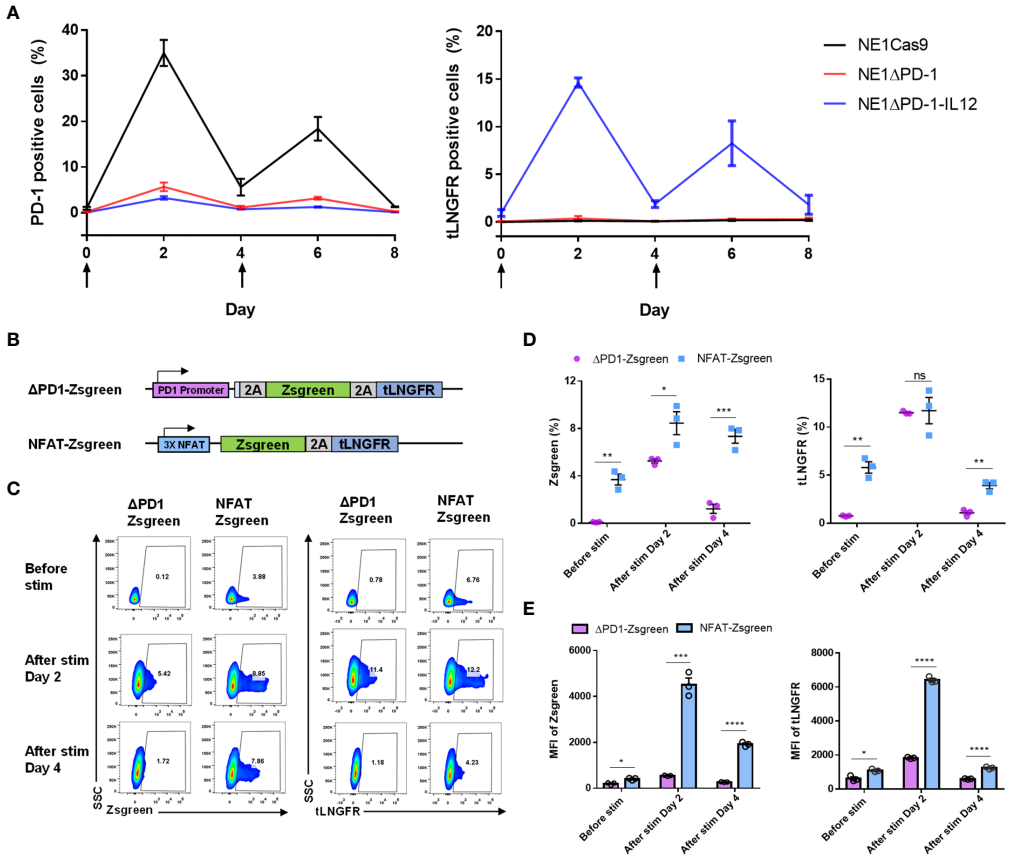

FIGURE 2
Tight control of transgene expression by the endogenous PDCD1 promoter. **(A)** Kinetics of PD-1 upregulation and tLNGFR expression in engineered T cells after two constitutive stimulations with αCD3 and αCD28. The arrow indicates the stimulation time points. Data are presented as the mean ± SEM (n = 3; independent experiments). **(B)** Schematic diagram of PD-1 promoter and NFAT-responsive promoter employed for expression of Zsgreen-2a-tLNGFR transgenes. **(C)** Representative flow cytometry plot for expression of Zsgreen and tLNGFR at 2-day intervals after stimulation with αCD3 and αCD28. **(D)** Percentage of Zsgreen and tLNGFR expression levels of engineered T cells in C. **(E)** MFI of Zsgreen and tLNGFR of engineered T cells in C. Data in D and E are presented as the mean ± SEM (n = 3; three independent experiments). P-values of D and E were determined by two-tailed unpaired t-test. *P<0.05, **P<0.01, ***P<0.001, and ****P<0.0001 were considered statistically significant. ns, not significant.

NE1ΔPD-1-IL-12 T cells exhibit enhanced effector function *in vitro*

Next, we investigated whether the IL-12 secreted from NE1ΔPD-1-IL-12 T cells could directly affect the effector function of TCR-T cells. As IL-12 signaling is known to be associated with increased IFN-γ production (19), we used intracellular flow cytometry to measure IFN-γ expression levels in engineered T cells co-cultured with A375 tumor cells for 24 h. Our results confirmed that NE1ΔPD-1-IL-12 T cells showed significantly higher proportions of IFN-γ-positive T cells and higher MFI compared to control T cells (Figure 3A). CBA-based analysis indicated that NE1ΔPD-1-IL-12 T cells produce higher levels of IFN-γ, TNF, and IL-10, but lower levels of IL-2, compared to control T cells (Figure 3B); this is consistent with the results from previous studies (13). NE1ΔPD-1-IL-12 T cells co-cultured with A375 tumor cells for 24 h also displayed higher expression of GzmB (Figures 3C, D), but no difference in the percentage or MFI for perforin, compared to control T cells (Supplementary Figures 4A, B). Next, we evaluated the cytotoxic function of the engineered TCR-T cells by co-culturing them with Zsgreen-overexpressing A375 cells. When the green signal on tumor cells was measured every 2 h by a live cell imaging system, NE1ΔPD-1-IL-12 T cells showed a more rapid decrease in the green signal compared to control T cells (Figure 3E). These results indicate that IL-12 secretion from the *PDCD1* locus enhances the effector function of NY-ESO-1-specific T cells, resulting in more efficient killing of target cancer cells.

IL-12 signaling has been reported to reprogram CD8+ T cells into effector memory and effector T cells (43, 44), which can elicit immediate effector functions in response to antigen recognition. Thus, we analyzed the differentiation status of the T cells before and after repeated exposure to target cells, based on the expression levels of CD45RO and C-C motif chemokine receptor 7 (CCR7) (Supplementary Figures 5A, B). Under homeostatic expansion conditions, the proportion of CD8+ T cells was similar among all three groups (Supplementary Figure 5C). After repeated stimulation, most T cells were skewed toward the CD8 phenotype, but the percentage remained similar in all groups. The proportion of effector memory CD8 T cells ($CD45RO^+CCR7^-$) was higher among NE1ΔPD-1-IL-12 T cells than in the control group (Figure 3F). The ratio of effector memory CD8 T cells to central memory CD8 T cells ($CD45RO^+CCR7^+$) was also increased in NE1ΔPD-1-IL-12 T cells (Figure 3G), indicating that *PDCD1*-driven-IL-12 secretion during the repetitive exposure to antigens had impacted the differentiation of $CD8^+$ T cells. Similar changes in effector and central memory T cell pool were observed in $CD4^+$ T cells (Supplementary Figures 5B, D).

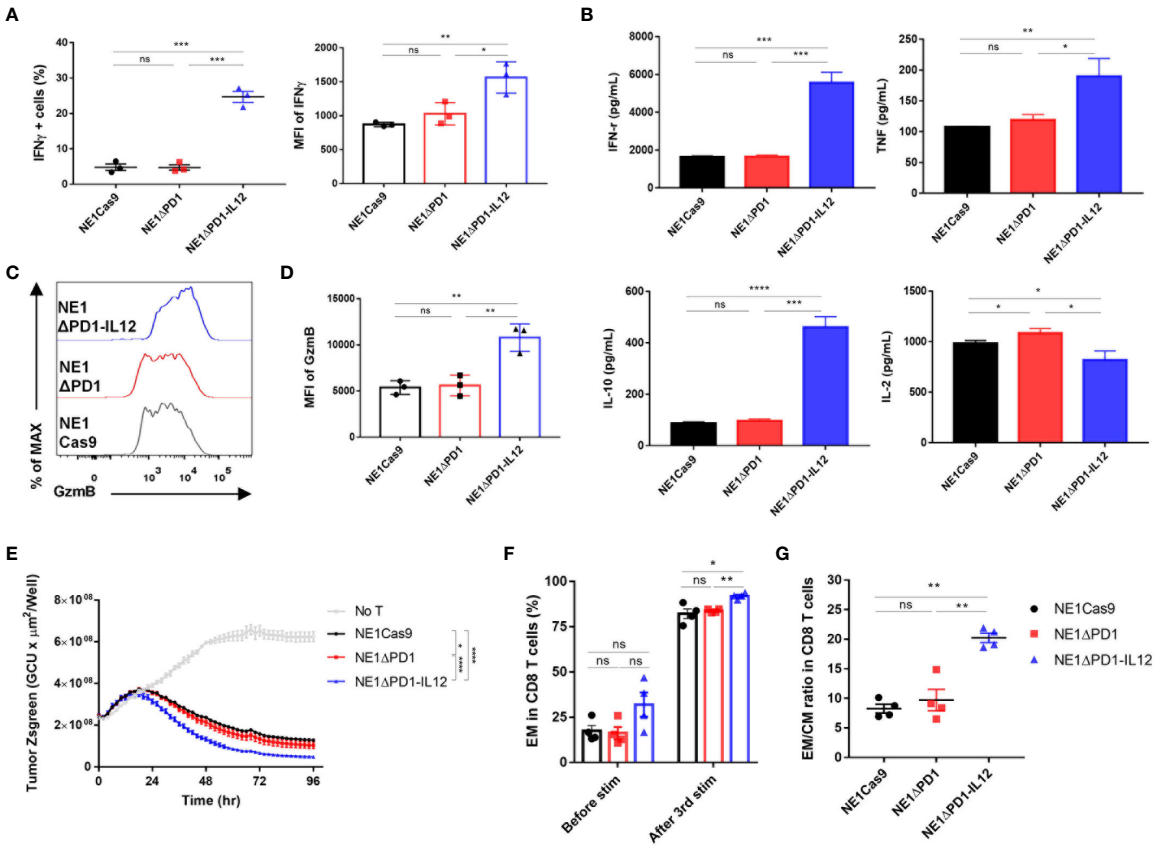

FIGURE 3
Enhanced effector function of ΔPD-1-IL-12-edited NY-ESO-1 TCR-T cells *in vitro* **(A)** Engineered T cells were co-cultured with A375 cells for 24 h. IFN-γ secretion was determined using flow cytometry. The percentage of IFN-γ positive cells and the MFI of IFN-γ were quantified. Data are presented as the mean ± SEM (n = 3; three independent experiments with three donors). **(B)** Engineered T cells were co-cultured with A375 cells for 48 h and the cytokines (IFN-γ, TNF, L-10, and IL-2) released into the culture supernatants were measured by CBA assay; results shown are representative of three experiments with three different donors. Data are presented as the mean ± SD of triplicates. **(C)** Engineered T cells were co-cultured with A375 cells for 48 h. The GzmB expression was determined by intracellular flow cytometric analysis. **(D)** The MFI of GzmB in the engineered T cells shown in **(C, E)** Engineered T cells were co-cultured with Zsgreen+ A375 cells for 96 h. The green signal from tumor cells was measured using IncuCyte every 2 h. A decrease in the green signal indicates that tumor cells were killed; results shown are representative of three experiments. Data are presented as the mean ± SD. **(F)** Percentage of effector memory CD8 T cells ($CD45RO^+/CCR7^-$) after a third repetitive stimulation with A375-PDL1 tumor cells. **(G)** The ratio of effector memory to central memory ($CD45RO^+/CCR7^+$) CD8 T cells in **(F)** Data of F and G are presented as the mean ± SEM (n = 4; individual donors). The *P*-values of A, B, and D were determined by two-tailed unpaired *t*-test. The *P*-value of E was determined by repeated-measures ANOVA followed by Holm-Sidak's multiple comparisons test. Data of F and G were compared by two-tailed paired *t*-test. *P<0.05, **P<0.01, ***P<0.001, and ****P<0.0001 were considered statistically significant. ns, not significant.

NE1ΔPD-1-IL-12 T cells greatly expand during chronic antigen stimulation

The immunosuppressive TME is believed to inhibit the proliferation and survival of adoptively transferred T cells (7, 45). Since proper T cell expansion is crucial for the success of T cell therapy (46, 47), we investigated the expansion ability during repeated tumor challenges. NY-ESO-1-specific T cells were repeatedly co-cultured with A375-PDL1 cells that had been pretreated with mitomycin C 3 times at 4-day intervals, and cell numbers and viability were monitored by cell counting with Trypan Blue staining (Figure 4A). After the first antigen stimulation, there was no difference in the number of cells among the three groups. However, after the second and third challenges, NE1ΔPD-1-IL-12 T cells were significantly more abundant than control T cells. Furthermore, although repeated stimulation gradually reduced the overall viability in all groups, NE1ΔPD-1-IL-12 T cells showed higher viability at all tested time points compared to control T cells (Figure 4B).

Next, we investigated whether this enhanced expansion of NE1ΔPD-1-IL-12 T cells was due to changes in apoptosis resistance or proliferative capacity. As a previous study demonstrated that IL-12 signaling inhibits TCR-induced T cell death by regulating caspases and anti-apoptotic molecules (48), we measured the percentage of annexin V-positive cells. However, we found no between-group difference after the third stimulation (Supplementary Figure 5A). We also found that the expression levels of the antiapoptotic marker, Bcl-xL, and the master anti-apoptotic regulator, c-FLIP, were similar in all groups (Supplementary Figures 5B, C). The levels of cleaved caspase-3 and -8 were also similar across all groups (Supplementary Figures 5D, E). These findings suggest that apoptosis resistance may not significantly contribute to the increased number of NE1ΔPD-1-IL-12 T cells observed following repeated stimulation. In contrast, when the proliferative capacity of T cells was evaluated by measuring Ki67 expression after the third

10.3389/fimmu.2023.1062365

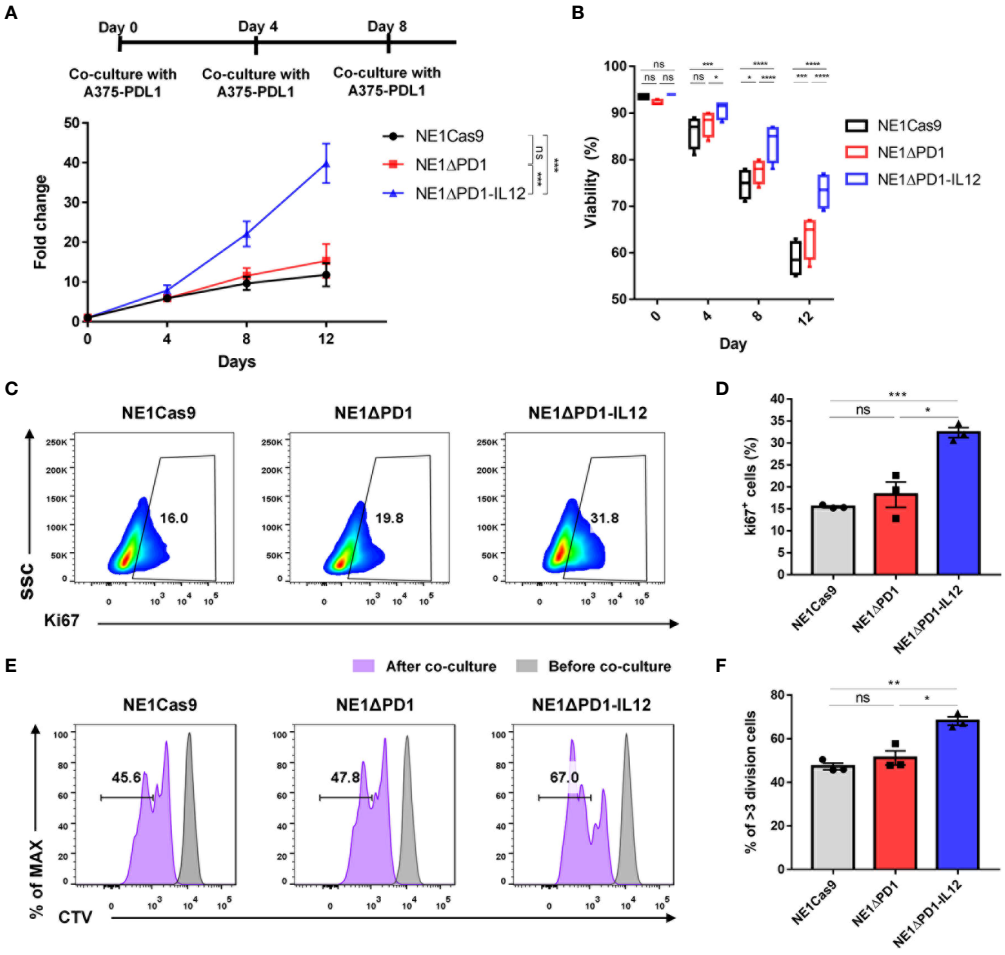

FIGURE 4
Enhanced cell expansion of ΔPD-1-IL-12-edited NY-ESO-1 TCR-T cells during repeated tumor challenge **(A)** The expansion engineered T cells was analyzed after repetitive stimulation with mitomycin C-pretreated A375-PDL1 cells three times every 4 d. Data are presented as the mean ± SEM (n = 4; four independent experiments with individual donors). **(B)** The viability of expanded T cells in A was measured using a Countess II automated cell counter with Trypan Blue staining. **(C)** Representative flow plot for Ki67 expression after the third stimulation in **(A, D)** The percentage of Ki67$^+$ T cells after the third stimulation (n = 3; individual donors). **(E)** Cell trace violet (CV)-stained engineered T cells were co-cultured with A375-PDL1 for 3 days. The diluted CTV intensity was measured by flow cytometry. **(F)** Percentage of diluted CTV stained T cells that divided more than three times in E (n = 3; individual donors). All data are presented as the mean ± SEM. The *P*-values of A and B were determined by repeated-measures ANOVA followed by Holm-Sidak's multiple comparisons test. *P*-values of D and F were determined by two-tailed unpaired *t*-test. *P<0.05, **P<0.01, ***P<0.001, and ****P<0.0001 were considered statistically significant. ns, not significant.

stimulation, NE1ΔPD-1-IL-12 T cells showed a significantly higher percentage of Ki67 positive cells compared to control T cells (Figures 4C, D). Consistent with this, NE1ΔPD-1-IL-12 T cells co-cultured with A375-PDL1 cells for 3 days showed a more divided cell population than the other groups, as determined by cell-trace violet dye staining (Figures 4E, F). Taken together, our results indicate that IL-12 production from the edited *PDCD1* locus contributed to expanding NY-ESO-1-specific T cells under chronic antigen stimulation by enhancing their proliferative capacity.

NE1ΔPD-1-IL-12 T cells exhibit superior anti-tumor activity *in vivo*

To investigate the therapeutic efficacy of NE1ΔPD-1-IL-12 T cells *in vivo*, we subcutaneously implanted immune-deficient NSG mice with 1 × 10^6 Zsgreen and firefly luciferase-overexpressing A375 cells (A375-ZF), followed by intravenous injection of 1 × 10^6 NY-ESO-1$^+$ TCR-T cells (Figure 5A). When the bioluminescent signal was measured weakly to monitor the tumor burden, the tumor cells were found to be completely eradicated in mice treated with NE1ΔPD-1-IL-12 T cells (Figure 5B, Supplementary Figures 7A, B). In contrast, NE1Cas9 and NE1ΔPD-1 T cells failed to control tumor growth in this xenograft model, suggesting that the secretion of IL-12 from TCR-T cells played a critical role in tumor control. We then carried out another *in vivo* experiment in which we used PD-L1-overexpressing A375 cells (A375-ZF-PDL1) to mimic a more immunosuppressive TME (Figure 5C). Under these experimental conditions, NE1Cas9 T cells had virtually no effect on tumor growth; NE1ΔPD-1 T cells cleared the tumor in one out of five mice, likely reflecting the effect of PD-1 knockout in the T cells; and NE1ΔPD-1-IL-12 T cells completely eradicated the tumors in all five

10.3389/fimmu.2023.1062365

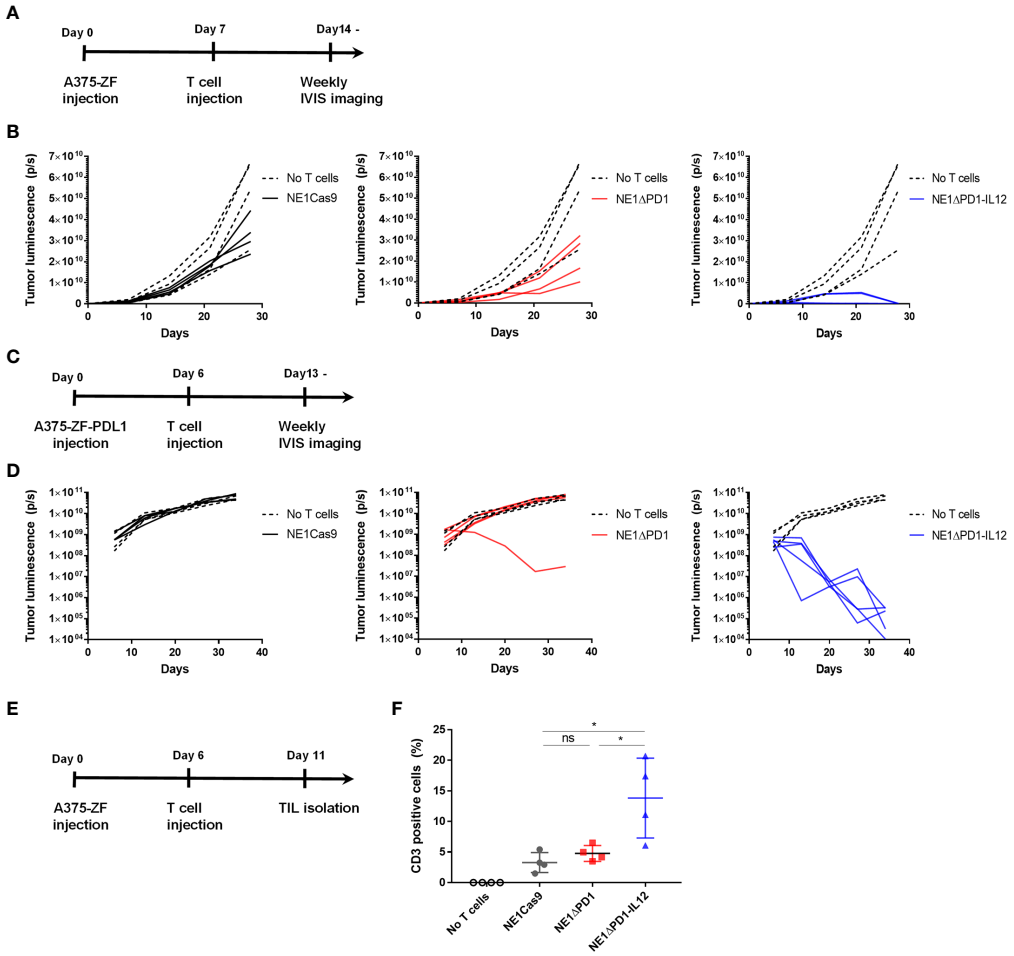

FIGURE 5
Enhanced anti-tumor activity of ΔPD-1-IL-12-edited NY-ESO-1 TCR-T cells *in vivo* **(A)** Timeline for *in vivo* experiment performed with A375-ZF tumor cells. Immunodeficient NSG mice were subcutaneously injected with 1 × 10^6 A375-ZF cells. After 7 days, 1 × 10^6 NY-ESO-1+ T cells were intravenously injected. The luminescence signal from tumor cells was measured weakly using an *in vivo* imaging system (IVIS). **(B)** Quantitative analysis of bioluminescent signal from individual mouse. ΔPD-1-IL-12 T cells exhibited superior anti-tumor activity (n = 4 mice per group). **(C)** Timeline for *in vivo* experiments performed using the PD-L1-overexpressed A375 model. Six days after subcutaneous injection of A375-ZF-PDL1 cells, 1 × 10^6 NY-ESO-1^+ T cells were intravenously injected. The luminescence signal from tumor cells was measured weekly using IVIS. **(D)** Quantitative analysis of bioluminescent signal from individual mouse. Tumors were cleared in only one of the PD-1 deleted NY-SO-1-treated mice. All NE1ΔPD-1-IL-12-treated mice were cured from tumors (n = 4 mice for no T cells and NE1Cas9, n = 5 mice for NE1ΔPD-1 and NE1ΔPD-1-IL-12). **(E)** Timeline for investigating engineered T cells infiltrated into the tumor site. A375-PDL1 tumor cells and NY-ESO-1 specific T cells were injected as in **(C)** At 11 d, the mice were sacrificed and tumors were harvested. Tumors were mechanically dissociated and the infiltrated T cells were analyzed by flow cytometry. **(F)** The percentage of CD3+ cells in tumor tissues (n = 4 mice per group). Data are presented as mean ± SEM. The *P*-value was determined by two-tailed unpaired *t*-test. *P<0.05 was considered statistically significant. ns, not significant.

mice, further demonstrating the potent anti-tumor activity of NE1ΔPD-1-IL-12 T cells (Figure 5C, Supplementary Figure 7C). Lastly, to determine the degree of T cell expansion *in vivo*, we analyzed isolated tumor tissues at 5 day after T cell injection (Figure 5E). The harvested tumors were mechanically dissociated and filtered to generate single-cell suspension and analyzed using flow cytometry (Supplementary Figure 8). We observed a significantly higher proportion of $CD3^+$ T cells in the mice treated with ΔPD-1-IL-12 T cells compared to those of the control groups (Figure 5F). Overall, consistent with the findings from our *in vitro* experiments, the results from *in vivo* xenograft models confirmed that the engineering of T cells to secrete IL-12 from the *PDCD1* locus can profoundly enhance the anti-tumor activity of NY-ESO-1-specific TCR-T cells.

Discussion

A variety of cofactors, including soluble factors such as cytokines or chemokines, as well as membrane-bound factors such as co-stimulatory receptors or cytokine receptors, have been employed to design ACTs with enhanced therapeutic potential (49–51). The co-delivery of exogenous cytokines has been extensively investigated because such factors have pleiotropic effects on both the therapeutic T cell itself and on other immune and non-immune cells of the TME (52). However, the constitutive secretion of some cytokines from circulating ACTs raises potential safety concerns, given that systemic administration of these cytokines often leads to severe side effects in patients due to on-target off-tumor toxicity (28, 53, 54). Therefore, a novel ACT engineering strategy that can limit their cytokine

expression within tumor tissues could help maximize the therapeutic benefits while minimizing the potential adverse effects.

To address this goal, we employed an endogenous genetic network influenced by TCR signaling to antigen-dependently control the expression of IL-12, a potent pro-inflammatory cytokine that has long been investigated in cancer immunotherapy. Based on reports that the *PDCD1* gene shows tight and dynamically regulated expression in response to T cell activation (32, 42), we selected this locus for targeted insertion of the *IL-12* gene using the CRISPR/Cas9 genome editing tool. This strategy enabled us to express IL-12 under the control of *PDCD1* regulatory elements strictly in response to T cell activation, with expression kinetics similar to those of endogenous PD-1. In this manner, the engineered T cells were expected to secrete IL-12 locally only upon encountering antigens within the tumor tissue. In addition, CRISPR editing of the *PDCD1* enabled us to simultaneously knock out the PD-1 gene, further empowering T cells to resist the functional exhaustion caused by inhibitory PD-1 signaling (45). Indeed, several studies have demonstrated that the disruption of PD-1 using CRISPR results in the enhanced anti-tumor activity of CAR-T cells (33, 55, 56), which was also partially observed in our *in vitro* and *in vivo* experiments with NY-ESO-1 T cells lacking PD-1 expression (NE1ΔPD-1 T cells).

Our results demonstrated that insertion of the *IL-12* gene into the *PDCD1* locus induces a more moderate expression level of IL-12 with a more strict reliance on TCR activation compared to that driven by the NFAT-responsive promoter. In a previous study, genetically engineered TILs expressing NFAT-IL-12 exhibited unexpected toxicity in patients (29), which may be attributable to a high amount of released IL-12. This report further described that low levels of leaky constitutive expression of IL-12 from the engineered TILs exert anti-proliferative effect, leading to difficulties in growing sufficient numbers of cells *ex vivo* and likely contributing to the poor persistence of cells *in vivo*. Another clinical study (NCT02498912) is currently underway using CAR-T cells engineered to release IL-12 from an internal ribosome entry site (IRES) positioned immediately after the CAR sequence in the vector (57, 58). The authors of this study hypothesized that the release of less IL-12 from IRES-IL-12 (200 pg/mL) compared to NFAT-IL-12 (50,000 pg/mL) might minimize potential IL-12-related toxicity issues. Of note, our ΔPD-1-IL-12-edited T cells secreted even fewer IL-12 (20 pg/mL) than the T cells engineered with NFAT-IL-12 or IRES-IL-12, and thus might offer even more benefits for preventing the potential adverse effects associated with IL-12. Nevertheless, a more thorough analysis with respect to potential IL-12-related safety concerns must be conducted before implementing our approach in clinical settings.

It is important to note that the moderate levels of IL-12 produced in our system were sufficient to elicit superior anti-tumor activity from ΔPD-1-IL-12-edited NY-ESO-1 T cells compared with non-edited NY-ESO-1 T cells in both *in vitro* cytotoxicity assays and *in vivo* xenograft mouse models. The expression of IL-12 in our system was significantly lower (20 pg/ml) than in previously reported systems such as IRES-IL-12 (200 pg/ml) (57), TET-IL-12 (1000 pg/ml) (59), and NFAT-IL-12 (5000 pg/ml) (29). Different copy numbers of the transgene as well as different promoter kinetics and strength may account for this difference. Unlike retroviral vector systems used in previous approaches, which randomly integrate multiple copies of transgenes into the host genome, our CRISPR knock-in system allows us to add a single copy of transgene per chromosome precisely and to control its expression through the endogenous transcription machinery of the PDCD1 locus. Even with the low levels of IL-12 released by activated T cells, we observed along with the increased production of pro-inflammatory cytokines, such as IFN-γ and TNF, the enhanced expression of GzmB, which is a major effector molecule of T cells for inducing apoptosis in tumor cells. This appears to be linked to the superior anti-tumor activity of PD-1-IL-12 edited T cells. We also found that the transient expression of IL-12 significantly enhanced the expansion of ΔPD-1-IL-12-edited T cells by promoting their proliferation upon repeated antigen stimulation. This enhanced proliferation is in sharp contrast to a previous report, which showed that continuous retroviral IL-12 expression has deleterious effects on T cell proliferation (25). The proliferation enhancement found in our system may be particularly important for the enhanced anti-tumor activity observed *in vivo* for ΔPD-1-IL-12-edited T cells. Collectively, our results suggest that the target-dependent and moderate expression of IL-12 derived from the *PDCD1* locus provides an effective strategy to enhance the anti-tumor function of TCR-T cells.

Several previous studies have demonstrated that IL-12 is involved in regulating not only T cells, but also a wide range of other immune cells, such as DCs and macrophages (13, 15, 24, 26). However, the severe immune-compromised state of NSG mice and a lack of cross-reactivity between human IL-12 and mouse IL-12 receptor proteins precluded us from investigating this axis in our study. The humanized mice model, in which human CD34+ HSCs are engrafted into NSG mice, may allow us to study the effects of IL-12 released by ΔPD-1-IL-12-edited T cells on other immune cell types in a more comprehensive manner.

In summary, we herein demonstrate that the inducible genetic circuit of PD-1 expression could be reprogrammed to secrete IL-12 in NY-ESO-1 TCR-T cells using CRISPR knock-in technology. The modest and tight expression of IL-12 from the *PDCD1* locus was sufficient to enhance the anti-tumor activity of NY-ESO-1 TCR-T cells. Our strategy could be extended to the controlled expression of other proteins of interest, such as antibodies, cytokines, chemokines, receptors, and transcription factors that may enhance or synergize with the function of T cells. Other genetic loci in addition to the *PDCD1* locus could also be explored in future studies. Lastly, our approach may provide a novel engineering approach for other adoptive T cell therapies, such as CAR-T, TIL, and virus-specific T cell therapies, against solid tumors.

Data availability statement

The original contributions presented in the study are included in the article/Supplementary Material. Further inquiries can be directed to the corresponding author.

Ethics statement

The animal study was reviewed and approved by Animal Care Committee of the Korea Advanced Institute of Science and Technology.

Author contributions

SK designed the study, performed the experiments, analyzed the data, and wrote the manuscript. CIP assisted in the *in vitro* and *in vivo* experiments. SL and HRC assisted in the *in vivo* experiments. CHK supervised the study and wrote the manuscript. All authors contributed to the article and approved the submitted version.

Funding

This work was supported by a grant from the Samsung Science & Technology Foundation (SRFC-MA1701-07, CHK).

Acknowledgments

We would like to thank Dr. Hee Jin Lee at ASAN Medical Center for providing blood samples from healthy donors.

Conflict of interest

The authors declare that the research was conducted in the absence of any commercial or financial relationships that could be construed as a potential conflict of interest.

Publisher's note

All claims expressed in this article are solely those of the authors and do not necessarily represent those of their affiliated organizations, or those of the publisher, the editors and the reviewers. Any product that may be evaluated in this article, or claim that may be made by its manufacturer, is not guaranteed or endorsed by the publisher.

Supplementary material

The Supplementary Material for this article can be found online at: https://www.frontiersin.org/articles/10.3389/fimmu.2023.1062365/full#supplementary-material

References

1. Schuster SJ, Bishop MR, Tam CS, Waller EK, Borchmann P, McGuirk JP, et al. Tisagenlecleucel in adult relapsed or refractory diffuse Large b-cell lymphoma. *N Engl J Med* (2019) 380(1):45–56. doi: 10.1056/NEJMoa1804980

2. Maude SL, Laetsch TW, Buechner J, Rives S, Boyer M, Bittencourt H, et al. Tisagenlecleucel in children and young adults with b-cell lymphoblastic leukemia. *N Engl J Med* (2018) 378(5):439–48. doi: 10.1056/NEJMoa1709866

3. Munshi NC, Anderson LDJr., Shah N, Madduri D, Berdeja J, Lonial S, et al. Idecabtagene vicleucel in relapsed and refractory multiple myeloma. *N Engl J Med* (2021) 384(8):705–16. doi: 10.1056/NEJMoa2024850

4. D'Angelo SP, Melchiori L, Merchant MS, Bernstein D, Glod J, Kaplan R, et al. Antitumor activity associated with prolonged persistence of adoptively transferred ny-Eso-1 (C259)T cells in synovial sarcoma. *Cancer Discovery* (2018) 8(8):944–57. doi: 10.1158/2159-8290.CD-17-1417

5. Dudley ME, Gross CA, Langhan MM, Garcia MR, Sherry RM, Yang JC, et al. Cd8+ enriched "Young" tumor infiltrating lymphocytes can mediate regression of metastatic melanoma. *Clin Cancer Res* (2010) 16(24):6122–31. doi: 10.1158/1078-0432.CCR-10-1297

6. Joyce JA, Fearon DT. T Cell exclusion, immune privilege, and the tumor microenvironment. *Science* (2015) 348(6230):74–80. doi: 10.1126/science.aaa6204

7. Binnewies M, Roberts EW, Kersten K, Chan V, Fearon DF, Merad M, et al. Understanding the tumor immune microenvironment (Time) for effective therapy. *Nat Med* (2018) 24(5):541–50. doi: 10.1038/s41591-018-0014-x

8. Bell M, Gottschalk S. Engineered cytokine signaling to improve car T cell effector function. *Front Immunol* (2021) 12:684642. doi: 10.3389/fimmu.2021.684642

9. Ma X, Shou P, Smith C, Chen Y, Du H, Sun C, et al. Interleukin-23 engineering improves car T cell function in solid tumors. *Nat Biotechnol* (2020) 38(4):448–59. doi: 10.1038/s41587-019-0398-2

10. Hurton LV, Singh H, Najjar AM, Switzer KC, Mi T, Maiti S, et al. Tethered il-15 augments antitumor activity and promotes a stem-cell memory subset in tumor-specific T cells. *Proc Natl Acad Sci U S A* (2016) 113(48):E7788–E97. doi: 10.1073/pnas.1610544113

11. Kunert A, Chmielewski M, Wijers R, Berrevoets C, Abken H, Debets R. Intra-tumoral production of Il18, but not Il12, by tcr-engineered T cells is non-toxic and counteracts immune evasion of solid tumors. *Oncoimmunology* (2017) 7(1):e1378842. doi: 10.1080/2162402X.2017.1378842

12. Liu L, Bi E, Ma X, Xiong W, Qian J, Ye L, et al. Enhanced car-T activity against established tumors by polarizing human T cells to secrete interleukin-9. *Nat Commun* (2020) 11(1):5902. doi: 10.1038/s41467-020-19672-2

13. Yeku OO, Purdon TJ, Koneru M, Spriggs D, Brentjens RJ. Armored car T cells enhance antitumor efficacy and overcome the tumor microenvironment. *Sci Rep* (2017) 7 (1):10541. doi: 10.1038/s41598-017-10940-8

14. Avanzi MP, Yeku O, Li X, Wijewarnasuriya DP, van Leeuwen DG, Cheung K, et al. Engineered tumor-targeted T cells mediate enhanced anti-tumor efficacy both directly and through activation of the endogenous immune system. *Cell Rep* (2018) 23(7):2130–41. doi: 10.1016/j.celrep.2018.04.051

15. Tugues S, Burkhard SH, Ohs I, Vrohlings M, Nussbaum K, Vom Berg J, et al. New insights into il-12-Mediated tumor suppression. *Cell Death Differ* (2015) 22(2):237–46. doi: 10.1038/cdd.2014.134

16. Athie-Morales V, Smits HH, Cantrell DA, Hilkens CM. Sustained il-12 signaling is required for Th1 development. *J Immunol* (2004) 172(1):61–9. doi: 10.4049/jimmunol.172.1.61

17. Cao X, Leonard K, Collins LI, Cai SF, Mayer JC, Payton JE, et al. Interleukin 12 stimulates ifn-Gamma-Mediated inhibition of tumor-induced regulatory T-cell proliferation and enhances tumor clearance. *Cancer Res* (2009) 69(22):8700–9. doi: 10.1158/0008-5472.CAN-09-1145

18. Khayrullina T, Yen JH, Jing H, Ganea D. *In vitro* differentiation of dendritic cells in the presence of prostaglandin E2 alters the il-12/Il-23 balance and promotes differentiation of Th17 cells. *J Immunol* (2008) 181(1):721–35. doi: 10.4049/jimmunol.181.1.721

19. Gerosa F, Paganin C, Peritt D, Paiola F, Scupoli MT, Aste-Amezaga M, et al. Interleukin-12 primes human Cd4 and Cd8 T cell clones for high production of both interferon-gamma and interleukin-10. *J Exp Med* (1996) 183(6):2559–69. doi: 10.1084/jem.183.6.2559

20. Parihar R, Dierksheide J, Hu Y, Carson WE. Il-12 enhances the natural killer cell cytokine response to ab-coated tumor cells. *J Clin Invest* (2002) 110(7):983–92. doi: 10.1172/JCI15950

21. Yue FY, Geertsen R, Hemmi S, Burg G, Pavlovic J, Laine E, et al. Il-12 directly up-regulates the expression of hla class I, hla class ii and icam-1 on human melanoma cells: A mechanism for its antitumor activity? *Eur J Immunol* (1999) 29(6):1762–73. doi: 10.1002/(SICI)1521-4141(199906)29:06<1762::AID-IMMU1762>3.0.CO;2-F

22. Kerkar SP, Goldszmid RS, Muranski P, Chinnasamy D, Yu Z, Reger RN, et al. Il-12 triggers a programmatic change in dysfunctional myeloid-derived cells within mouse tumors. *J Clin Invest* (2011) 121(12):4746–57. doi: 10.1172/JCI58814

23. Watkins SK, Egilmez NK, Suttles J, Stout RD. Il-12 rapidly alters the functional profile of tumor-associated and tumor-infiltrating macrophages in vitro and in vivo. *J Immunol* (2007) 178(3):1357–62. doi: 10.4049/jimmunol.178.3.1357

24. Liu Y, Di S, Shi B, Zhang H, Wang Y, Wu X, et al. Armored inducible expression of il-12 enhances antitumor activity of glypican-3-Targeted chimeric antigen receptor-engineered T cells in hepatocellular carcinoma. *J Immunol* (2019) 203(1):198–207. doi: 10.4049/jimmunol.1800033

25. Zhang L, Kerkar SP, Yu Z, Zheng Z, Yang S, Restifo NP, et al. Improving adoptive T cell therapy by targeting and controlling il-12 expression to the tumor environment. *Mol Ther* (2011) 19(4):751–9. doi: 10.1038/mt.2010.313

26. Chinnasamy D, Yu Z, Kerkar SP, Zhang L, Morgan RA, Restifo NP, et al. Local delivery of interleukin-12 using T cells targeting vegf receptor-2 eradicates multiple vascularized tumors in mice. *Clin Cancer Res* (2012) 18(6):1672–83. doi: 10.1158/1078-0432.CCR-11-3050

27. Cohen J. Il-12 deaths: Explanation and a puzzle. *Science* (1995) 270(5238):908. doi: 10.1126/science.270.5238.908a

28. Leonard JP, Sherman ML, Fisher GL, Buchanan LJ, Larsen G, Atkins MB, et al. Effects of single-dose interleukin-12 exposure on interleukin-12-Associated toxicity and interferon-gamma production. *Blood* (1997) 90(7):2541–8. doi: 10.1182/blood.V90.7.2541

29. Zhang L, Morgan RA, Beane JD, Zheng Z, Dudley ME, Kassim SH, et al. Tumor-infiltrating lymphocytes genetically engineered with an inducible gene encoding interleukin-12 for the immunotherapy of metastatic melanoma. *Clin Cancer Res* (2015) 21(10):2278–88. doi: 10.1158/1078-0432.CCR-14-2085

30. Smith-Garvin JE, Koretzky GA, Jordan MS. T Cell activation. *Annu Rev Immunol* (2009) 27:591–619. doi: 10.1146/annurev.immunol.021908.132706

31. Moulton VR, Tsokos GC. T Cell signaling abnormalities contribute to aberrant immune cell function and autoimmunity. *J Clin Invest* (2015) 125(6):2220–7. doi: 10.1172/JCI78087

32. Bally AP, Austin JW, Boss JM. Genetic and epigenetic regulation of pd-1 expression. *J Immunol* (2016) 196(6):2431–7. doi: 10.4049/jimmunol.1502643

33. Rupp LJ, Schumann K, Roybal KT, Gate RE, Ye CJ, Lim WA, et al. Crispr/Cas9-mediated pd-1 disruption enhances anti-tumor efficacy of human chimeric antigen receptor T cells. *Sci Rep* (2017) 7(1):737. doi: 10.1038/s41598-017-00462-8

34. Marotte L, Simon S, Vignard V, Dupre E, Gantier M, Cruard J, et al. Increased antitumor efficacy of pd-1-Deficient melanoma-specific human lymphocytes. *J Immunother Cancer* (2020) 8(1):e000311. doi: 10.1136/jitc-2019-000311

35. Crosson SM, Dib P, Smith JK, Zolotukhin S. Helper-free production of laboratory grade aav and purification by iodixanol density gradient centrifugation. *Mol Ther Methods Clin Dev* (2018) 10:1–7. doi: 10.1016/j.omtm.2018.05.001

36. Aurnhammer C, Haase M, Muether N, Hausl M, Rauschhuber C, Huber I, et al. Universal real-time pcr for the detection and quantification of adeno-associated virus serotype 2-derived inverted terminal repeat sequences. *Hum Gene Ther Methods* (2012) 23(1):18–28. doi: 10.1089/hgtb.2011.034

37. Kim S, Kim D, Cho SW, Kim J, Kim JS. Highly efficient rna-guided genome editing in human cells *Via* delivery of purified Cas9 ribonucleoproteins. *Genome Res* (2014) 24 (6):1012–9. doi: 10.1101/gr.171322.113

38. Eyquem J, Mansilla-Soto J, Giavridis T, van der Stegen SJ, Hamieh M, Cunanan KM, et al. Targeting a car to the trac locus with Crispr/Cas9 enhances tumour rejection. *Nature* (2017) 543(7643):113–7. doi: 10.1038/nature21405

39. Bethune MT, Li XH, Yu J, McLaughlin J, Cheng D, Mathis C, et al. Isolation and characterization of ny-Eso-1-Specific T cell receptors restricted on various mhc molecules. *Proc Natl Acad Sci USA* (2018) 115(45):E10702–E11. doi: 10.1073/pnas.1810653115

40. Morinobu A, Gadina M, Strober W, Visconti R, Fornace A, Montagna C, et al. Stat4 serine phosphorylation is critical for il-12-Induced ifn-gamma production but not for cell proliferation. *Proc Natl Acad Sci USA* (2002) 99(19):12281–6. doi: 10.1073/pnas.182618999

41. Tsushima F, Yao S, Shin T, Flies A, Flies S, Xu H, et al. Interaction between B7-H1 and pd-1 determines initiation and reversal of T-cell anergy. *Blood* (2007) 110(1):180–5. doi: 10.1182/blood-2006-11-060087

42. Ahn E, Araki K, Hashimoto M, Li W, Riley JL, Cheung J, et al. Role of pd-1 during effector Cd8 T cell differentiation. *Proc Natl Acad Sci USA* (2018) 115(18):4749–54. doi: 10.1073/pnas.1718217115

43. Chowdhury FZ, Ramos HJ, Davis LS, Forman J, Farrar JD. Il-12 selectively programs effector pathways that are stably expressed in human Cd8+ effector memory T cells in vivo. *Blood* (2011) 118(14):3890–900. doi: 10.1182/blood-2011-05-357111

44. Agarwal P, Raghavan A, Nandiwada SL, Curtsinger JM, Bohjanen PR, Mueller DL, et al. Gene regulation and chromatin remodeling by il-12 and type I ifn in programming for Cd8 T cell effector function and memory. *J Immunol* (2009) 183(3):1695–704. doi: 10.4049/jimmunol.0900592

45. Chauvin JM, Pagliano O, Fourcade J, Sun Z, Wang H, Sander C, et al. Tigit and pd-1 impair tumor antigen-specific Cd8(+) T cells in melanoma patients. *J Clin Invest* (2015) 125(5):2046–58. doi: 10.1172/JCI80445

46. Tang N, Cheng C, Zhang X, Qiao M, Li N, Mu W, et al. Tgf-beta inhibition *Via* crispr promotes the long-term efficacy of car T cells against solid tumors. *JCI Insight* (2020) 5(4):e133977. doi: 10.1172/jci.insight.133977

47. Savoldo B, Ramos CA, Liu E, Mims MP, Keating MJ, Carrum G, et al. Cd28 costimulation improves expansion and persistence of chimeric antigen receptor-modified T cells in lymphoma patients. *J Clin Invest* (2011) 121(5):1822–6. doi: 10.1172/JCI46110

48. Lee SW, Park Y, Yoo JK, Choi SY, Sung YC. Inhibition of tcr-induced Cd8 T cell death by il-12: Regulation of fas ligand and cellular flip expression and caspase activation by il-12. *J Immunol* (2003) 170(5):2456–60. doi: 10.4049/jimmunol.170.5.2456

49. Adachi K, Kano Y, Nagai T, Okuyama N, Sakoda Y, Tamada K. Il-7 and Ccl19 expression in car-T cells improves immune cell infiltration and car-T cell survival in the tumor. *Nat Biotechnol* (2018) 36(4):346–51. doi: 10.1038/nbt.4086

50. Feucht J, Sun J, Eyquem J, Ho YJ, Zhao Z, Leibold J, et al. Calibration of car activation potential directs alternative T cell fates and therapeutic potency. *Nat Med* (2019) 25(1):82–8. doi: 10.1038/s41591-018-0290-5

51. Zhang Q, Hresko ME, Picton LK, Su L, Hollander MJ, Nunez-Cruz S, et al. A human orthogonal il-2 and il-2rbeta system enhances car T cell expansion and antitumor activity in a murine model of leukemia. *Sci Transl Med* (2021) 13(625):eabg6986. doi: 10.1126/scitranslmed.abg6986

52. Briukhovetska D, Dorr J, Endres S, Libby P, Dinarello CA, Kobold S. Interleukins in cancer: From biology to therapy. *Nat Rev Cancer* (2021) 21(8):481–99. doi: 10.1038/s41568-021-00363-z

53. Dutcher JP, Schwartzentruber DJ, Kaufman HL, Agarwala SS, Tarhini AA, Lowder JN, et al. High dose interleukin-2 (Aldesleukin) - expert consensus on best management practices-2014. *J Immunother Cancer* (2014) 2(1):26. doi: 10.1186/s40425-014-0026-0

54. Conlon KC, Lugli E, Welles HC, Rosenberg SA, Fojo AT, Morris JC, et al. Redistribution, hyperproliferation, activation of natural killer cells and Cd8 T cells, and cytokine production during first-in-Human clinical trial of recombinant human interleukin-15 in patients with cancer. *J Clin Oncol* (2015) 33(1):74–82. doi: 10.1200/JCO.2014.57.3329

55. Hu W, Zi Z, Jin Y, Li G, Shao K, Cai Q, et al. Crispr/Cas9-mediated pd-1 disruption enhances human mesothelin-targeted car T cell effector functions. *Cancer Immunol Immunother* (2019) 68(3):365–77. doi: 10.1007/s00262-018-2281-2

56. Choi BD, Yu X, Castano AP, Darr H, Henderson DB, Bouffard AA, et al. Crispr-Cas9 disruption of pd-1 enhances activity of universal egfrviii car T cells in a preclinical model of human glioblastoma. *J Immunother Cancer* (2019) 7(1):304. doi: 10.1186/s40425-019-0806-7

57. Koneru M, Purdon TJ, Spriggs D, Koneru S, Brentjens RJ. Il-12 secreting tumor-targeted chimeric antigen receptor T cells eradicate ovarian tumors in vivo. *Oncoimmunology* (2015) 4(3):e994446. doi: 10.4161/2162402X.2014.994446

58. Koneru M, O'Cearbhaill R, Pendharkar S, Spriggs DR, Brentjens RJ. A phase I clinical trial of adoptive T cell therapy using il-12 secreting muc-16(Ecto) directed chimeric antigen receptors for recurrent ovarian cancer. *J Transl Med* (2015) 13:102. doi: 10.1186/s12967-015-0460-x

59. Alsaieedi A, Holler A, Velica P, Bendle G, Stauss HJ. Safety and efficacy of tet-regulated il-12 expression in cancer-specific T cells. *Oncoimmunology* (2019) 8 (3):1542917. doi: 10.1080/2162402X.2018.1542917

frontiers | Frontiers in Immunology

TYPE Original Research
PUBLISHED 01 February 2023
DOI 10.3389/fimmu.2023.1110482

OPEN ACCESS

EDITED BY
Ralf-Holger Voss,
Johannes Gutenberg University Mainz, Germany

REVIEWED BY
Michael Bachmann,
Helmholtz Association of German Research Centres (HZ), Germany
Phillip Kevin Darcy,
Peter MacCallum Cancer Centre, Australia

*CORRESPONDENCE
Hinrich Abken
hinrich.abken@ukr.de

SPECIALTY SECTION
This article was submitted to Cancer Immunity and Immunotherapy, a section of the journal Frontiers in Immunology

RECEIVED 28 November 2022
ACCEPTED 17 January 2023
PUBLISHED 01 February 2023

CITATION
Barden M, Holzinger A, Velas L, Mezősi-Csaplár M, Szöőr Á, Vereb G, Schütz GJ, Hombach AA and Abken H (2023) CAR and TCR form individual signaling synapses and do not cross-activate, however, can co-operate in T cell activation. *Front. Immunol.* 14:1110482. doi: 10.3389/fimmu.2023.1110482

CAR and TCR form individual signaling synapses and do not cross-activate, however, can co-operate in T cell activation

Markus Barden[1], Astrid Holzinger[1], Lukas Velas[2], Marianna Mezősi-Csaplár[3], Árpád Szöőr[3], György Vereb[3,4], Gerhard J. Schütz[2], Andreas A. Hombach[5,6] and Hinrich Abken[1]*

[1]Leibniz Institute for Immunotherapy (LIT), Division of Genetic Immunotherapy, University Regensburg, Regensburg, Germany, [2]Institute of Applied Physics, TU Wien, Vienna, Austria, [3]Department of Biophysics and Cell Biology, Faculty of Medicine, University of Debrecen, Debrecen, Hungary, [4]ELKH-DE Cell Biology and Signaling Research Group, Faculty of Medicine, University of Debrecen, Debrecen, Hungary, [5]Center for Molecular Medicine Cologne, University of Cologne, Cologne, Germany, [6]Department I Internal Medicine, University Hospital Cologne, Cologne, Germany

In engineered T cells the CAR is co-expressed along with the physiological TCR/CD3 complex, both utilizing the same downstream signaling machinery for T cell activation. It is unresolved whether CAR-mediated T cell activation depends on the presence of the TCR and whether CAR and TCR mutually cross-activate upon engaging their respective antigen. Here we demonstrate that the CD3ζ CAR level was independent of the TCR associated CD3ζ and could not replace CD3ζ to rescue the TCR complex in CD3ζ KO T cells. Upon activation, the CAR did not induce phosphorylation of TCR associated CD3ζ and, vice versa, TCR activation did not induce CAR CD3ζ phosphorylation. Consequently, CAR and TCR did not cross-signal to trigger T cell effector functions. On the membrane level, TCR and CAR formed separate synapses upon antigen engagement as revealed by total internal reflection fluorescence (TIRF) and fast AiryScan microscopy. Upon engaging their respective antigen, however, CAR and TCR could co-operate in triggering effector functions through combinatorial signaling allowing logic "AND" gating in target recognition. Data also imply that tonic TCR signaling can support CAR-mediated T cell activation emphasizing the potential relevance of the endogenous TCR for maintaining T cell capacities in the long-term.

KEYWORDS

immunotherapy, adoptive cell therapy, CAR, TCR, synapse

Introduction

Chimeric antigen receptors (CARs) can be remarkably powerful in redirecting a T cell response towards defined target cells (1) while utilizing the TCR/CD3 downstream signaling machinery for triggering T cell activation upon target engagement. Most "second generation" CARs in clinical application incorporate the CD3ζ signaling chain to provide the primary

signal together with the costimulatory domain to add the second signal in order to trigger T cell activation (2–5). While this type of CAR is efficacious in clinical application, little is known whether the endogenous TCR/CD3 complex affects the stability and function of the CAR and vice versa. This is a relevant issue since conventional CAR T cells express a functionally active TCR/CD3 complex with the consequence that the CAR competes with the TCR for downstream signaling molecules (6, 7). This situation may result in a functional cross-talk between CAR and TCR upon either target recognition. The issue is also of relevance when replacing the TCR α–chain locus of the endogenous TCR by the CAR encoding DNA sequence (8) thereby producing TCR-deficient CAR T cells. "Off-the-shelf" CAR T cell therapy also uses TCR^- T cells for manufacturing (9). In both situations, CAR redirected T cell activation would not compete with the endogenous TCR, however, would not get "help" by tonic TCR signaling.

The TCR associated CD3ζ chain is crucial for regulating the stability of the entire TCR complex and experiences a rapid turn-over on the T cell membrane independently of the other TCR chains (10). The impact of the TCR associated CD3ζ chain on the CD3ζ-based CAR with respect to expression and function was so far not addressed. Mutual co-regulation of the TCR and CAR would have substantial consequences for both CAR- and TCR-mediated T cell activation. This became most recently obvious when CAR T cells with genetically deleted TCR experienced reduced persistence *in vivo* compared to CAR T cells with the endogenous TCR (11). On the other hand, TCR^+ CAR T cells showed superior persistence implying that the CAR cannot fully substitute for the TCR in sustaining downstream functional capacities.

We asked whether the TCR affects a CD3ζ CAR, and vice versa, in T cell activation on the membrane level of chain phosphorylation and on the downstream level of effector functions. We revealed that TCR and CAR are co-regulated on the T cell surface and can complement in providing downstream T cell activation. However, there is no cross-phosphorylation of CAR and TCR CD3ζ signaling chains. Accordingly, the TCR is not recruited into the CAR synapse as revealed by TIRF and fast AiryScan microscopy. Such lack of cross-signaling allows Boolean logic "AND" gating during combinatorial antigen recognition through the TCR and CAR.

Materials and methods

Cell lines and cell culture

The murine T cell hybridoma line MD45 was described elsewhere (12). The human Jurkat T cell line (ATCC TIB-152), the N87 (ATCC CRL-5822) and the CA19–9^+ and CA19–9^- human tumor cell lines LS174T (ATCC CCL-188), H498 (ATCC CCL-254), H716 (ATCC CCL-251) and A375 (ATCC CRL-1619) were obtained from ATCC. Jurkat 76 cells lacking endogenous TCR expression (13) were kindly provided by Dr M.H.M. Heemskerk, Leiden, The Netherlands. Cell lines were cultured in RPMI 1640 medium supplemented with 10% (v/v) heat inactivated FCS. The N87 human gastric carcinoma cell line was cultured in Dulbecco's Modified Eagle Medium (DMEM) supplemented with 2 mM GlutaMAX, 10% (v/v) FCS and antibiotics. HEK293T cells are human embryonic kidney cells that express the SV40 large T antigen (14). Anti-CD3 mAb OKT3 and anti-CD28 mAb 15E8 were purified by affinity chromatography from supernatants of OKT3 hybridoma (ATCC CRL 8001) and 15E8 hybridoma cells (kindly provided by Dr. R. van Lier, Red Cross Central Blood Bank, Amsterdam, The Netherlands), respectively. The anti-BW431/26 idiotypic antibody BW2064 was described earlier (15). Recombinant ErbB2-Fc protein was purchased from R&D Systems, Wiesbaden, Germany. The PE-conjugated and the AF647-conjugated $F(ab')_2$ goat anti-human IgG antibody, goat anti-human IgG-UNLB antibody, goat anti-mouse IgG human ads-UNLB and rabbit anti-goat IgG (H+L)-UNLB antibody were purchased from Southern Biotechnology, Birmingham, AL, USA. PE-conjugated anti-CD3ζ mAb clone 6B10.2 and AF647-conjugated anti-TCR α/β mAb clone IP26 was purchased from BioLegend, San Diego, CA, USA. Fluorochrome-conjugated anti-human CD3 mAb was purchased from Miltenyi Biotec, Bergisch Gladbach, Germany. Fluorochrome-conjugated isotype controls were purchased from BD Biosciences, San Diego, CA, USA. Matched antibody pairs for capture and detection of human IFN-γ and IL-2 were purchased from BD Biosciences. Recombinant IL-2 was obtained from Endogen, Woburn, MA, USA. Alkaline phosphatase conjugated streptavidin was purchased from Roche Diagnostics, Mannheim, Germany. Peroxidase-labeled goat anti-human IgG Fc antibody and peroxidase-labeled anti-mouse IgG Fc antibody were purchased from Dako, Hamburg, Germany. Anti-actin antibody (clone 1A4) was purchased from Thermo Fisher Scientific, Dreieich, Germany. AF647-conjugated transferrin receptor monoclonal antibody (MEM-75) was purchased from Invitrogen, Regensburg, Germany.

Genome editing of Jurkat cells

Deletion of CD3ζ in Jurkat cells was performed by CRISPR/Cas9 mediated genome editing utilizing the CD3ζ CRISPR/Cas9 ko plasmid coding for a human CD3ζ guide RNA and the CD3ζ homology directed repair (HDR) plasmid for site specific integration of a puromycin resistance gene (both Santa Cruz Biotechnology, Dallas, TA, USA). Briefly, 5 x 10^6 Jurkat cells were transfected with 2 µg of each plasmid DNA utilizing the MACSfectin transfection system (Miltenyi Biotec) according to the manufacturer´s recommendations. Two days after transfection cells were further cultured in presence of 250 ng/ml puromycin (Sigma Aldrich, Taufkirchen, Germany). Puromycin resistant subclones were established and tested for expression of CD3ζ by flow cytometry and Western blot analysis.

Preparation of human T cells

Peripheral blood lymphocytes were obtained from healthy donors by Ficoll density centrifugation (Ethic approval 01-090 Cologne; Ethic approval 21-2224-101 Regensburg). T cells were initially activated by OKT3 (100–200 ng/ml) and 15E8 (50–100 ng/ml) antibodies and IL-2 (400–1,000 U/ml) and further cultured in the presence of IL–2 (100–500 U/ml).

Engineering and expression of CARs

Cloning and expression of CAR constructs were described previously (5, 16–19). MD45 T hybridoma cells with stable expression of ζ- and γ–chain CARs were generated as follows: The DNA for ζ- and γ–chain CARs in pRSV (50–100 µg) was transfected into 2 x 10^7 MD45 T cells by electroporation (one pulse, 250 V, 2400 µF) using a gene pulse electroporator (BioRad, Munich, Germany). After culture for two days, transfected cells with CAR expression were selected in the presence of G418 (2 mg/ml; Gibco, Eggenheim, Germany). For expression of CARs in peripheral blood T cells and Jurkat cells all CARs were cloned into the same retroviral expression vector as previously described (20). Transduction of T cells was previously described (5, 20, 21). Briefly, peripheral blood T cells were activated with anti–CD3 (100–200 ng/ml) and anti–CD28 (50–100 ng/ml) antibodies and IL–2 (400–1,000 U/ml). Cells were transduced on day 2–3 by co-cultivation with virus producing 293T cells or, alternatively, with γ-retrovirus containing supernatants. Retroviruses were transiently produced by 293T cells upon transfection with vector DNA and plasmids encoding the GALV envelope and MMLV derived gag/pol (21). For transient expression in non-lymphoid cells, CAR encoding DNAs were transfected in 293T cells. CAR expression was monitored by flow cytometry using an antibody against the common extracellular IgG1 Fc domain.

Immunofluorescence and flow cytometry

The CAR on the cell surface of engineered T cells was detected by FITC- or PE-labeled antibodies against the human IgG1 Fc domain and T cells were identified with fluorochrome-labeled anti–CD3 antibodies which recognize an epitope located on the ϵ-chain of the CD3 complex, respectively. Flow cytometry was performed using a FACScan™ cytofluorometer equipped with the FACScan™ research software type-B (BD Bioscience), a FACSCanto II flow cytometer equipped with the FACSDiva software (BD Bioscience), and FACSLyric flow cytometer equipped with FACSuite software (BD Bioscience). To monitor expression of the ζ–chain, cells were permeabilized and fixed utilizing the Cytofix/Cytoperm™ reagent kit (BD Bioscience) prior to incubation with the PE-conjugated anti-CD3ζ mAb (2 µg/ml).

Pulse chase labeling of CARs

CAR engineered cells (5 x 10^7 cells/ml) were washed twice in cold PBS, pH 7.6, and incubated with 100 µg/ml biotin-ε-amidocaproate-N-hydroxy-succinimidester (Sigma-Aldrich) for 60 min on ice. Cells were washed three times in RPMI 1640 medium, 10% (v/v) FCS, and incubated with or without the anti–IgG antibody (1 µg/ml) at 37°C to cross-link the CAR. Aliquots of cells (10^7 cells) were spun down at different time points and lysed by adding 100 µl lysis buffer (1% (v/v) NP40, 150 mM NaCl, 50 mM Tris/HCl, pH 8, 10 mM EDTA, 1 mM PMSF, 10 mM iodoacetamide. After 30 min on ice, the lysates were cleared by centrifugation. Nuclei free supernatants (100 µl) were stored at -20°C. Lysates were added to microtiter wells coated with anti–IgG antibody (1 µg/ml) and incubated for 2 h at room temperature. The bound biotinylated CAR was detected by alkaline phosphatase conjugated streptavidin (1:10,000). The reaction product was developed with pNPP (Sigma-Aldrich).

SDS PAGE and western blot analysis

For analysis of protein half-life on T cell surface, protein synthesis of CAR transfected cells (5 x 10^7/ml) was blocked by culture in the presence of cycloheximide (10 µg/ml). Cells were lysed (5 x 10^7) at different time points, lysates separated by SDS-PAGE in 8% (w/v) polyacrylamide gels under non-reducing conditions and subsequently blotted onto a PVDF membrane (Thermo Fisher Scientific). The membrane was probed with the peroxidase-labeled goat anti–human IgG Fc antibody to detect the CAR (1:10,000). For loading control blots were stripped and probed with an anti–actin antibody (0.5 µg/ml) and peroxidase-labeled anti–mouse IgG Fc antibody (1:5,000). Bands were visualized by chemoluminescence utilizing the "ECL Western blotting detection system" (Amersham Biosciences, Freiburg, Germany). Intensity of bands was densitometrically quantified utilizing the ImageJ software. Data were presented as percent of the intensity at time 0. To monitor expression of endogenous CD3ζ chain, lysates of non-modified and CD3ζ genome edited Jurkat cells were separated by SDS-PAGE in 12% (w/v) polyacrylamide gels under reducing conditions, blotted and probed with the anti–CD3ζ mAb (clone 4B10, Thermo Fisher Scientific). Bound antibodies were detected by a peroxidase-conjugated anti–mouse IgG antibody (Sigma Aldrich) at 1:5,000 dilution. Membranes were stripped and re-probed with the peroxidase-labeled anti–β-actin antibody (Santa Cruz Biotechnology) at 1:20,000 dilution. Bands were visualized by chemoluminescence. To monitor expression of phosphorylated CD3ζ, cells were resuspended in RIPA buffer and protein concentrations were determined by ROTI-Quant (Carl Roth, Karlsruhe, Germany). For Western blot analysis, lysates were electrophoresed by SDS-PAGE in 4–12% (w/v) Bis-Tris gels under reducing conditions, blotted and probed with the anti–phospho-CD247 (CD3 zeta) (Tyr142) mAb (clone EM-54, Thermo Fisher Scientific) at 1:1,000 and detected by the peroxidase-labeled anti-mouse IgG1 (γ–chain specific) antibody (Sigma-Aldrich) at 1:10,000 dilution. Membranes were stripped and re-probed with peroxidase-labeled anti–β-actin antibody (Santa Cruz Biotechnology) at 1:20,000 dilution. Bands were visualized by chemoluminescence (ChemiDoc Imaging System, BioRad).

Total internal reflection fluorescence microscopy

All images were recorded using a home-built setup based on an Olympus IX73 (Japan) microscope body equipped with a high NA objective (Carl Zeiss, alpha-plan apochromat, 1.46 NA, 100x, Germany), 488 nm and 640 nm excitation lasers (OBIS Laser box, Coherent, USA), a quad dichroic mirror (Di01-R405/488/532/635, Semrock, USA) and an emission filter (ZET405/488/532/642m, Chroma, USA). The emission path was split into two color

channels using a dichroic mirror (H 643 LPXR superflat, Chroma, USA) and emission filters (650/SP BrightLine HC Shortpass, Semrock, USA; 690/70 H Bandpass, AHF, Germany); the two color channels were imaged onto the same EM-CCD camera (Ixon Ultra, Andor, UK). Prior to measurements, CAR engineered T cells were labeled with either anti–TCRα/β AF647-conjugated full antibody, AF647-conjugated F(ab´)$_2$ goat anti–human IgG antibody or AF647-conjugated anti–transferrin receptor (TfR) monoclonal antibody, and seeded on glass slides coated either with recombinant HER2 protein or the anti–CD3 antibody OKT3. Cells were fixed 20 minutes post seeding and imaged by TIRF microscopy upon illumination at 488 nm for CAR-GFP and 640nm for TCR-AF647, for CAR-AF647, or for TfR-AF647. Data analysis was performed with custom Python code (version 3.6) utilizing the following libraries: numpy, mpl_toolkits, scipy, sdt, pandas, matplotlib, seaborn (22–24). The code is available upon request from the corresponding author. Data analysis was performed on regions of interest which included exclusively pixels above a user-defined threshold in at least one of the two color channels. To quantify the size of the contact region, the number of selected pixels was determined and multiplied by the pixel size of160x160 nm^2. To quantify the extent of CAR and TCR co-localization, the Pearson's correlation coefficient was calculated *via* $r = \frac{\sum (x-\bar{x})(y-\bar{y})}{\sqrt{\sum (x-\bar{x})^2 \sum (y-\bar{y})^2}}$, where x and y denote the intensity per pixel, and $\bar{x}$ and $\bar{y}$ the corresponding average.

Fast AiryScan and confocal microscopy

Images were recorded with an LSM 880 confocal laser scanning microscope (Carl Zeiss, Jena, Germany) equipped with an AiryScan/AiryScan Fast detection unit providing up to 120 nm lateral and 350 nm axial resolution (25) and a high NA water immersion objective (C-Apochromat, 1.2 NA, 40x). 488 nm and 633 nm excitation lasers were used to avoid spectral overlap, guided by a 488/543/633 nm triple dichroic mirror. Emission was detected in line switch mode through a 495-560BP/660LP dual band filter. Prior to the experiments CAR-transduced primary human T cells were labelled with either human anti–TCRα/β AF647-conjugated full antibody, AF647-conjugated F(ab´)$_2$ goat anti–human IgG antibody or AF647-conjugated anti–transferrin receptor (TfR) monoclonal antibody and seeded on HER2 expressing N87 target cells plated on eight-well tissue culture-treated chambered coverslips (ibidi, Gräfelfing, Germany). Images of live anti-HER2 CAR T cells forming contacts with the tumor target were recorded in AiryScan Fast mode. The chamber was incubated at 37°C during the measurement. 3D images of entire cells were captured by optical sectioning applying 0.23 µm step size along the z-axis. ZEN Black 2.3 software was used to process the acquired raw datasets where Wiener filter deconvolution with 3D reconstruction algorithm and automatic filter strength was applied. ZEN Blue 2.3 software was used to render 3D images for illustrative purposes. Confocal image of each analyzed cell was captured for overall orientation purposes. Differential distribution of CAR-GFP (green) and either CAR-AF647, TCR-AF647, or TfR-AF647 (red) in the synaptic contact region, the extrasynaptic membrane, and the whole cell membrane of AiryScan processed 3D images was quantified based on intensity values in the far red and in the green channels in 3D regions of interest generated using the software ImageJ/Fiji (26) with the 3DSuite plugin (27). 3D Mean Filtering was performed on voxels of 3x3x3 pixel radius (equivalent to 0.30x0.30x0.68 µm radius), then images were segmented based on intensity thresholding to acquire 3D regions of interest. 3D ROIs of the synaptic contact region were generated based on the CAR-GFP signal, and of the extrasynaptic membrane based on either CAR-AF647, TCR-AF647, or TfR-AF647. Each synaptic 3D ROI for all analyzed cells was manually verified based on the extent of the contact region visible in the confocal images to exclude ROIs outside the contact region. Each extrasynaptic 3D ROI for all analyzed cells was manually verified to exclude any non-contacting anti-HER2 CAR T cells in the field of view. Whole cell 3D ROIs were generated by merging the synaptic and extrasynaptic membrane ROIs. Mean intensity of the synaptic contact region, the extrasynaptic membrane, and the whole cell membrane was quantified in both green and red channels. Relative intensity values were generated by dividing the mean intensity values of the synaptic contact region and the extrasynaptic membrane by the mean intensity of the whole cell membrane. Pixel-wise correlation was quantified based on intensity values recorded for CAR-GFP (green) and either CAR-AF647, TCR-AF647, or TfR-AF647 (red) in the synaptic contact region and the extrasynaptic membrane 3D ROIs, including only pixels that were, in at least one of the channels, above the threshold determined as the intersect of intensity histograms from the cell-containing and cell-free areas, i.e. expectedly high cross-correlation of non-labeled areas was excluded from analysis. Pearson's correlation coefficient was calculated separately for each slice in the 3D images using a custom ImageJ/Fiji plugin. The development of this code will be published separately and will be available at GitHub and the Fiji updater. Average PCC values of all slices for each individual cell were calculated and their mean was plotted with SD as error bars across all cells from at least 3 independent experiments. As an exception to this procedure, for control PCC values, only one AiryScan Fast 2D slice was imaged for each unstimulated cell given the relatively high spatial mobility of unengaged lymphocytes. GraphPad Prism 5 software was used for statistical analysis.

Activation of CAR engineered Jurkat cells

Microtiter plates were coated with anti–human IgG antibody, that binds to the CAR, and the anti–CD3 antibody OKT3 (5 µg/ml each). CAR engineered or non-modified Jurkat T cells (5 x 10^4/well) were incubated in coated plates for 48 h and IL–2 in the supernatant was determined by ELISA with a solid phase anti–human IL–2 (2 µg/ml) capture and a biotinylated anti–human IL–2 detection antibody (0.5 µg/ml) (BD Bioscience). The reaction product was visualized with a peroxidase-streptavidin-conjugate (1:10,000) and ABTS (Roche Diagnostics).

Activation of CAR T cells

CAR T cells (0.32 x 10^4–5 x 10^4 cells/well) were co-cultivated for 24–48 h in 96-well round bottom plates with tumor cells (2–5 x 10^4 cells/well). Supernatants were removed and tested for IFN–γ as described below. Specific target cell lysis of CAR T cells was

determined by XTT assay as previously described (28). Viability of target cells without T cells was calculated as the OD-mean of six wells containing only tumor cells subtracted by the background OD-mean of wells with medium only. Non-specific formation of formazan by T cells was determined from ODs of triplicate wells containing exclusively T cells and in same numbers as in the corresponding experimental wells. Viability of target cells in experimental wells was calculated by: viability (%) = [OD(experimental wells - corresponding number of T cells)]/[OD(tumor cells only - medium)] x 100. Cytotoxicity (%) was calculated by: cytotoxicity (%) = 100 - viability (%). Alternatively, CAR T cells (2.5–5 x 10^4 cells/well) were incubated in 96 well microwell plates coated with the agonistic anti–CD3 (1 μg/ml), anti–CD28 (5 μg/ml), anti–TCR (4 μg/ml), anti–IgG (1 μg/ml) antibodies, anti–idiotypic antibody (BW2064/36; 8 μg/ml) or recombinant HER2-Fc protein (8 μg/ml), respectively. After 48 h supernatants were tested for IFN–γ and IL–2 by ELISA utilizing solid phase bound anti–IFN–γ and anti–IL–2 capture antibodies (each 1 μg/ml) and biotinylated anti–IFN–γ (0.5 μg/ml) and anti–IL–2 detection antibodies (1 μg/ml), respectively. The reaction product was visualized as described above.

Results

Physiologically, the TCR associated CD3ζ chain rapidly recycles on the cell membrane independently of the other TCR components (10). We asked whether a CD3ζ chain CAR is subjected to the same rapid turn-over and tested a set of CARs with the CD3ζ or the FcεRI γ signaling chain (Figure 1A); the other domains of the respective CARs were the same; the CARs were expressed by the same vector. The ζ–chain CARs were consistently present at lower levels on the T cell surface compared to the corresponding γ–chain CARs. Exchange of the intracellular ζ- and γ–chains reciprocally altered the CAR levels on the cell membrane, while exchange of the transmembrane domains did not, indicating that the different CAR levels on the T cell surface were due to the intracellular moiety. For comparison, the γ- and ζ–chain CARs were present at equal levels in non-T cells like HEK293T cells (Figure 1A) indicating that the different CAR levels are due to their expression in T cells, most likely due to the presence of the endogenous TCR/CD3 complex.

We addressed whether the different ζ- and γ–chain CAR levels go along with different protein half-life times on the T cell surface. Blocking protein synthesis and Western blot analyses revealed that the ζ–chain CAR had a shorter half-life time than the γ–chain CAR in engineered MD45 T cells (Figure 1B). CAR cross-linking by an anti –IgG antibody, that binds to the common extracellular CAR domain, resulted in rapid degradation of both γ- and ζ–chain CARs as expected. This goes in line with a recent study showing that antigen encounter results in rapid ubiquitination and, as a consequence of internalization and lysosomal degradation, downregulation of CARs (29). Pulse-chase analysis revealed that the ζ–chain CAR molecules on the cell surface more rapidly declined than the γ–chain CARs (Figure 1C). Taken together, the ζ–chain CAR experienced a higher turnover on the T cell membrane and a shorter half-life time than the γ–chain CAR.

To record CAR-driven T cell effector functions, peripheral blood T cells were engineered with ζ- and γ–chain CARs with specificity for CA19–9. Recording the cytotoxic activity against CA19–9^+ and CA19–9^- cancer cells revealed that the ζ–chain CAR induced higher cytolytic activity and higher IFN–γ release than the γ–chain CAR indicating a higher potency of the ζ–chain CAR in T cell activation (Figure 1D). This was the case despite a lower expression level and lower half-life time compared to the γ–chain CAR on the T cell surface.

Half-life time and rapid turn-over may affect T cell activation in the presence of soluble target antigen. This is a clinically relevant scenario since a substantial number of CAR-targetable surface antigens are also shed by cancer cells which may block the CAR redirected T cell activation. To address the issue, we engineered T cells with the ζ- and γ–chain CAR, respectively, with the same anti–CA19–9 binding domain and co-incubated CAR T cells with CA19–9^+ target cells in the presence of increasing concentrations of soluble CA19–9 (Figure 1E). The induction of lytic activity triggered by the γ–chain CAR was blocked by soluble CA19–9 whereas the activity by the ζ–chain CAR was less affected. We assumed that the rapid turn-over and shorter half-life of the ζ–chain CAR goes along with a rapid replacement by antigen-free CAR chains on surface and thereby a higher resistance towards blocking by soluble antigen.

We asked whether a ζ–chain CAR can substitute for the CD3ζ chain in reconstituting the endogenous TCR, and whether the endogenous CD3 of the TCR affects the expression level of the CD3ζ CAR independently of the TCR αβ chains. To address the issue, we deleted the endogenous CD3ζ chain of Jurkat cells by CRISPR/Cas9 mediated gene editing. Flow cytometry and Western blot analysis demonstrated efficient knockout of the endogenous CD3ζ in engineered Jurkat cells; consequently, no TCR was expressed (Figures 2A, B). For comparison, TCR deficient Jurkat76 cells express the endogenous CD3ζ chain as reported (13).

We engineered Jurkat cells without endogenous CD3ζ and/or CD3/TCR expression, respectively, with ζ- and γ–chain CARs (Figure 2C). While the CARs were properly expressed by Jurkat cells, the CARs did not rescue TCR expression in CD3ζ KO Jurkat cells (Figure 2D). Expression of the endogenous CD3 was not altered by the respective CARs in Jurkat cells. Same data were obtained upon engineering blood T cells (Figure 2E). More importantly, ζ–chain CARs were expressed at lower levels in both TCR^- $CD3ζ^+$ Jurkat76 cells and in TCR^- $CD3ζ^-$ Jurkat E4 cells compared to the γ–chain CAR indicating that the lower levels of ζ-CARs on T cell surface did not depend on the presence of the TCR or TCR/CD3 complex. With respect to CAR triggered functionality, the ζ- and γ–chain CARs were as active in CD3ζ KO cells as in TCR^+ $CD3ζ^+$ Jurkat cells indicated by cytokine release upon CAR stimulation (Figure 2F). For comparison, engineered CD3ζ KO Jurkat cells did not respond upon CD3 stimulation despite the presence of the ζ–chain CAR.

Taken together we concluded that, firstly, the CAR and the CD3/TCR complex are independently regulated on the membrane surface and that the ζ- and γ–chain CARs function independently of the presence of the endogenous CD3/TCR complex in T cells. Secondly, the ζ–chain CAR did not replace CD3ζ in rescuing TCR expression in CD3ζ KO cells.

To address whether there is a cross-signaling at the very early stage of TCR and CAR mediated activation, we recorded by Western blot analysis the phosphorylated CD3ζ (pCD3ζ) of the CAR and of

10.3389/fimmu.2023.1110482

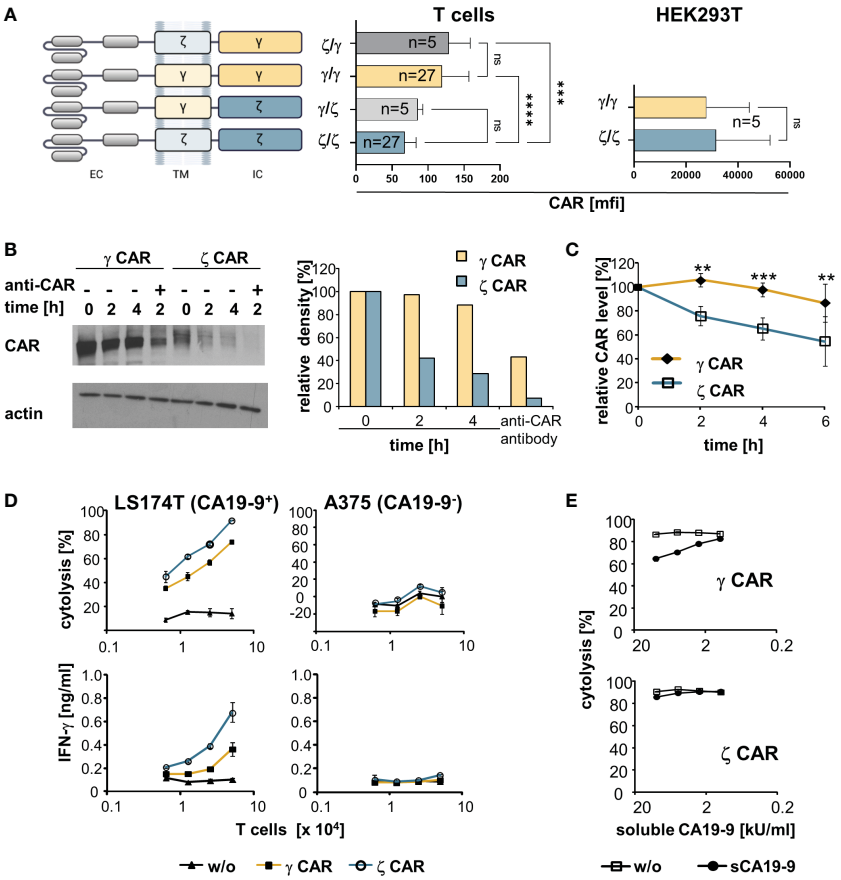

FIGURE 1
CARs with an intracellular CD3ζ chain are superior over γ–chain CARs in T cell activation despite lower cell surface expression and shorter half-life on the T cell surface. **(A)** Schematic representation of CARs with their respective transmembrane (TM) and intracellular (IC) signaling domains consisting of the respective CD3ζ (ζ) or the FcεRI γ (γ) chain. All CARs harbour the same extracellular domain (EC) and were expressed by the same promoter in the same retroviral vector backbone. Cells were engineered with the respective CARs. CAR expression was monitored by an anti–IgG Fc antibody that detects the common extracellular CAR IgG1-Fc spacer domain. Background staining was determined by an isotype control antibody. Data represent the mean values of mean fluorescence intensity (mfi) ± SD. **(B)** MD45 cells were engineered with a ζ or a γ CAR, respectively, and incubated with cycloheximide (10 µg/ml) to block protein synthesis. For comparison, the CARs were additionally cross-linked by an anti–IgG (anti–CAR) antibody, that binds to the extracellular CAR spacer domain, for 2 h to induce CAR internalization. At different time points, 10^7 cells were lysed and proteins separated by SDS-PAGE on 8% (w/v) polyacrylamide gels under non-reducing conditions. CARs were detected by the anti–IgG Fc-POD antibody (1:10,000), actin was detected by the anti–actin antibody (0.5 µg/ml). Relative density of CAR bands was quantified utilizing the ImageJ software 1.48 and presented as percent of the initial amount at t=0. Data from a representative experiment out of three are shown. **(C)** Pulse-chase CAR labeling. CAR transfected cells were surface-labeled with biotin as described in Materials and Methods, washed and stimulated at 37°C by an anti–IgG antibody (1 µg/ml) directed against the IgG extracellular CAR domain. Aliquots of cells (5 x 10^6 cells) were lysed at different time points and lysates were subjected to ELISA plates coated with an anti–IgG1 mAb (1 µg/ml) to capture the CAR. Bound labeled CARs were detected by streptavidin POD and visualized with ABTS. OD at time point 0 was set at 100% and relative ODs at indicated time points were calculated. Numbers represent the mean values of three independent experiments ± SD. **(D)** CAR redirected T cell activation. T cells with ζ- or γ–chain anti–CA19–9 CAR were expanded in the presence of IL–2 and co-cultivated (0.625–5 x 10^4 cells/well) for 48 h with CA19–9^+ LS174T or CA19–9^- A375 tumor cells (5 x 10^4 cells/well). Supernatants were analyzed for IFN–γ by ELISA, target cell lysis was determined by the XTT assay. Data represent mean values ± SD of two independent experiments. w/o, without CAR. **(E)** Activation of CAR T cells in the presence of soluble CA19–9 antigen. Anti–CA19–9 CAR T cells (5 x 10^4 cells/well) were co-cultivated for 48 h with CA19–9^+ LS174T cells (5 x 10^4 cells/well) in the presence of serial dilutions of supernatants of H498 tumor cells containing about 20,000 U/ml of soluble CA19–9 (sCA19–9). Target cell lysis was determined by the XTT assay. For control, cells were co-cultivated in the presence of supernatants of the CA19–9^- cell line H716 lacking soluble CA19–9 (w/o). Data represent mean values ± SD of technical triplicates. For comparison of two groups, significant differences were determined by Student´s T test. For comparisons of three or more groups, one-way ANOVA with Tukey's *post hoc* test was used. p-values < 0.05 were considered statistically significant (**p<0.01; ***p<0.001; ****p<0.0001; ns, not significant).

TCR-associated, endogenous CD3ζ chain on stimulation. TCR stimulation increased phosphorylation of the TCR associated endogenous CD3ζ chain, but not of the CAR CD3ζ domain (Figure 3). Vice versa, stimulation of the CAR resulted in an increased phosphorylation of the CAR CD3ζ chain but not of the TCR CD3ζ chain. The same pattern was obtained with CD28-CD3ζ CAR engineered cells; phosphorylation of CAR CD3ζ increased upon CAR stimulation but not upon TCR/CD3 stimulation; pCD3ζ of the TCR, but not of the CAR, increased upon TCR/CD3 stimulation.

We also investigated whether CAR-associated CD28 signaling can induce CD3ζ signaling through the TCR. Stimulation of the CD28 CAR, that lacks the CD3ζ domain, did not produce TCR CD3ζ phosphorylation; increase in pCD3ζ occurred upon TCR/CD3 stimulation as control (Figure 3). We concluded that CD28-CD3ζ CAR stimulation did not induce phosphorylation of the endogenous TCR CD3ζ chain indicating that no substantial cross-signaling between the TCR/CD3 and the CAR at the stage of CD3ζ phosphorylation occurred.

10.3389/fimmu.2023.1110482

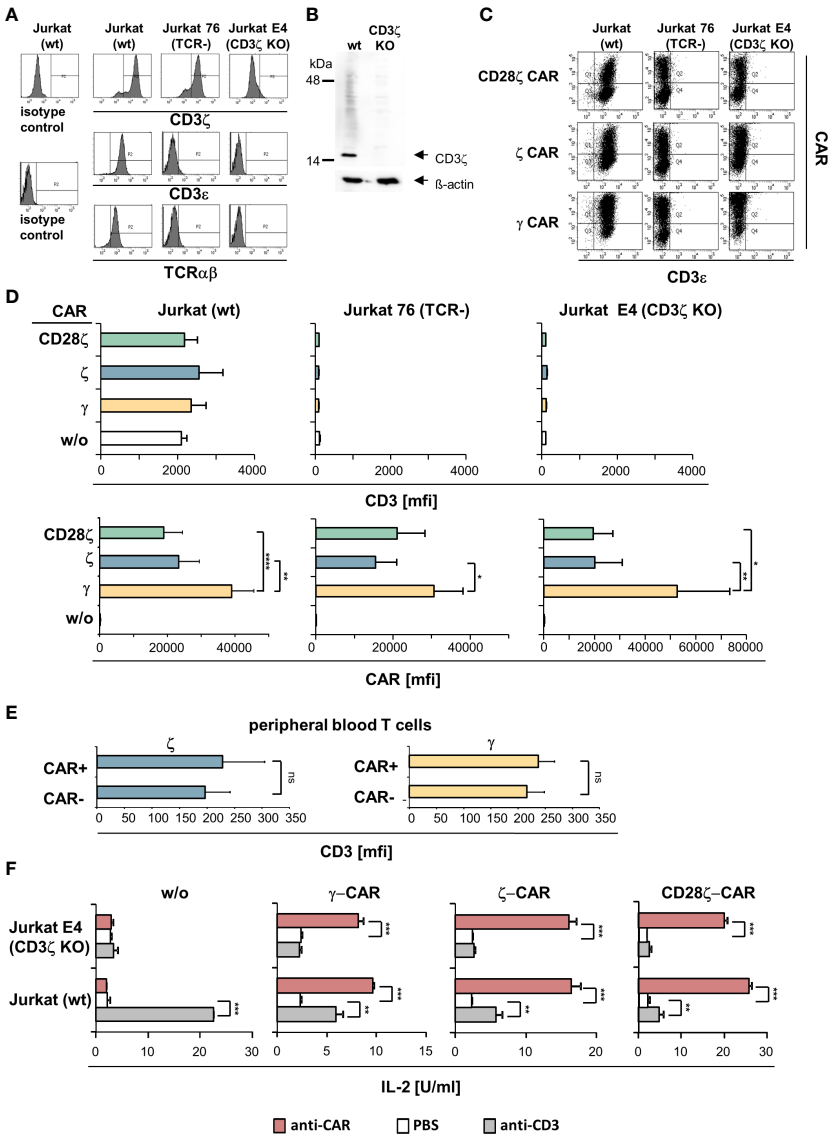

FIGURE 2
ζ CARs did not rescue the CD3/TCR complex in CD3ζ KO Jurkat cells. **(A)** The CD3ζ locus in Jurkat cells was deleted by CRISPR/Cas9 engineering as described in Materials and Methods. Non-modified Jurkat cells (wt), Jurkat76 cells lacking TCR (TCR$^-$) and Jurkat E4 CD3ζ knock-out (KO) cells were tested by flow cytometry for intracellular CD3ζ expression and for surface expression of CD3ε and TCR, respectively. Histograms of a representative analysis are shown. **(B)** Western blots of genome edited Jurkat cells. Lysates of non-modified (wt) and CD3ζ KO Jurkat cells (5 µg protein lysate/lane) were separated by SDS PAGE, blotted, probed with a mouse anti–human CD3ζ antibody (1:500) and detected by a HRP-conjugated anti–mouse antibody (1:5,000). Blots were re-probed with an anti–β-actin antibody (1:20,000). **(C)** TCR$^+$ Jurkat (wt), Jurkat76 (TCR$^-$) and Jurkat E4 (CD3ζ KO) cells were engineered with the CD28ζ, ζ or γ CAR, respectively. Expression of CARs and surface expression of CD3 was recorded by flow cytometry and mean fluorescence intensity (mfi) was determined. Dot plots of a typical experiment and mean values of 5 independent experiments ± SD **(D)** are shown. Significant differences were determined by Student´s T test. **(E)** Peripheral blood T cells engineered with ζ–chain and γ–chain CAR, respectively, were stained for CAR and CD3 expression and analyzed by flow cytometry. CAR$^+$ and CAR$^-$ T cells were gated and mean fluorescence intensity (mfi) of CD3 was determined. Data represent mean values of 4 healthy donors ± SD. Statistical differences were determined by Student´s T test. **(F)** Jurkat (wt) and Jurkat E4 (CD3ζ KO) cells with and without CAR, respectively, were stimulated through the CAR and CD3 by incubation on 96-well plates (4 x 10^4 cells/well) coated with the agonistic anti–CD3 antibody OKT3 or anti–IgG Fc antibody (5 µg/ml each) that binds to the CAR extracellular domain. After 48 h supernatants were tested for IL–2 by ELISA. Values represent the means of technical triplicates ± SD. Significant differences were determined by Student´s T test. A representative experiment out of two is shown. p-values <0.05 were considered statistically significant (*p<0.05; **p<0.01; ***p<0.001; ****p<0.001; ns, not significant).

To investigate whether CAR and TCR are recruited into similar regions during immunological synapse formation, we engineered peripheral blood T cells with Her2-specific CD28-CD3ζ CARs linked to GFP (Figure 4A). The distribution of CAR and TCR in the contact region between CAR T cell and immobilized Her2 molecules was recorded *via* TIRF microscopy. The CAR was localized by its linked GFP and verified by staining with an AF647-conjugated anti–CAR antibody; the TCR was localized by an anti–TCRαβ AF647-conjugated antibody; the transferrin receptor (TfR) was localized by an anti-TfR AF647-conjugated antibody (Figure 4B). There was no difference in size of the contact regions formed by the T cell on surfaces coated either with Her2 as CAR target or with the anti–CD3 antibody OKT3 as TCR target (Figure 4C). While there was no indication for synapse formation of anti

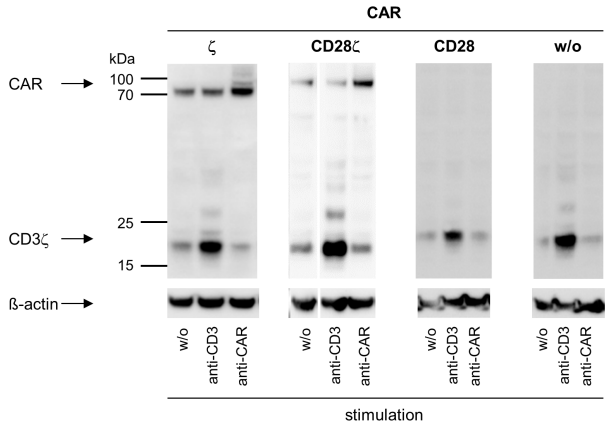

FIGURE 3
ζ CARs and TCR/CD3 do not cross-activate through their CD3ζ chains. CAR engineered Jurkat cells were recorded for CD3ζ phosphorylation by Western blot analysis. Non-modified (w/o) Jurkat cells or Jurkat cells engineered with ζ CAR, CD28 CAR or CD28ζ CAR (5 x 10^6 cells each) were subjected stimulation through their TCR by incubation with the agonistic mouse anti–CD3 antibody OKT3 (10 µg/ml) for 10 min followed by an anti –mouse IgG antibody (10 µg/ml) for cross-linking for 3 min (ζ CAR, CD28 CAR and w/o CAR) or 1 min (CD28ζ CAR). Alternatively, cells were stimulated through the CAR independently of the binding domain by incubation with a goat anti–human IgG antibody (10 µg/ml) for 10 min followed by an anti –goat IgG antibody (10 µg/ml) for cross-linking for 3 min (ζ CAR, CD28 CAR and w/o CAR) or 1 min (CD28ζ CAR). Lysates were separated by SDS PAGE and blotted membranes were probed with the anti–phospho-CD247 (CD3ζ) (Tyr142) antibody (clone EM-54) (1:1,000) followed by a peroxidase-conjugated anti–mouse IgG1 antibody (1:10,000) for detection. Blots were re-probed with an anti–human β-actin antibody (1:20,000).

–Her2 CARs on the OKT3 antibody coated surface, recognition of the cognate antigen Her2 led to an accumulation of anti–Her2 CARs in the contact region, but not of the TCR (Figure 4D). Notably, the Pearson's correlation coefficient (PCC) between CAR and TCR distribution was not different compared to the negative distribution (Figure 4E, median PCC = 0.384). As negative control, the TfR, that is distributed on the cell surface independently of the CAR and TCR, showed no substantial correlation with the CAR distribution (median PCC = 0.306). As positive control, the GFP-CAR signal strongly correlated with the signal of anti–CAR antibody (median PCC = 0.949).

The distribution of CAR and TCR in the contact region between anti-Her2 CAR T cell and $Her2^+$ tumor cell was studied by 3D fast AiryScan microscopy (Figure 4F; Supplementary Figure 1A; Supplementary Video 1, 2, 3). The analysis confirmed accumulation of the anti–Her2 CAR, but not of the TCR, in the synaptic region (Figure 4G). In fact, TCR was present at lower mean intensities in the synaptic than in the extra-synaptic regions (Supplementary Figure 1B), making up a significant difference after normalization to the entire membrane intensity. In anti-Her2 CAR T cells engaging $Her2^+$ tumor cells, PCC between CAR and TCR in the synapse was not different from the TfR negative control (mean PCC_{CAR_TCR} = 0.149; PCC_{CAR_TfR} = 0.040), while the GFP-CAR signal showed a strong correlation with the anti–CAR antibody as positive control signal (mean PCC_{CAR_CAR} = 0.628) (Figure 4H). No co-distribution of the CAR with the TCR or the TfR as control occurred when the synaptic region, the extra-synaptic region, and the unstimulated CAR T cell membranes were compared (Figure 4H). Taken together, data indicate that the CAR synapse formed upon engagement of cognate antigen did not recruit the TCR into the same region.

As cross-signaling between the CAR and TCR/CD3 can occur at more downstream steps in the activation pathway at the level of effector functions, we recorded cytokine production as a near final step in the activation of effector functions. CAR engineered T cells were stimulated through the CAR, CD3 and TCR, respectively, and IFN–γ and IL–2 release was recorded. The threshold for IFN–γ release by TCR and CD3 activation, respectively, was not altered by the presence of a CD3ζ or CD28-CD3ζ CAR compared to unmodified T cells (Figure 5A). While CD3ζ–chain signaling by the CAR was sufficient for IFN–γ secretion, IL–2 release required additional CD28 co-stimulation as provided through the CD28-CD3ζ CAR as expected. No IL–2 release occurred upon TCR or CD3 stimulation in the presence of the CD28-CD3ζ CAR indicating that the co-expressed CD28 CAR domain was not cross-activated by TCR stimulation to complement for IL–2 release.

While TCR and CAR did not cross-activate upon engagement of either cognate antigen, we assessed whether CAR and TCR can complement in T cell activation when both are engaging their respective target. T cells were engineered with a CD28 CAR lacking the CD3ζ domain and recognizing CEA or HER2, respectively. CAR T cells were stimulated through the CAR by binding to their cognate antigen or through their TCR/CD3 (Figure 5B). Simultaneous binding to the respective CAR ligand and to an agonistic anti–CD3 antibody induced IL–2 release indicating successful complementation of the TCR/CD3 signaling with CAR CD28 signaling; IL–2 release was not obtained upon TCR/CD3 or CAR stimulation alone. For control, the CD28-CD3ζ CAR induced IL–2 upon binding to the CAR ligand without additional TCR stimulation; stimulation of CD3 plus CD28 independently of the CAR also induced IL–2 release. Data indicate that CAR and TCR/CD3 could complement in the downstream T cell activation pathway when engaging their respective cognate ligand.

Discussion

Nearly all CARs used in clinical trials signal through the CD3ζ chain by engaging downstream signaling proteins associated with the

10.3389/fimmu.2023.1110482

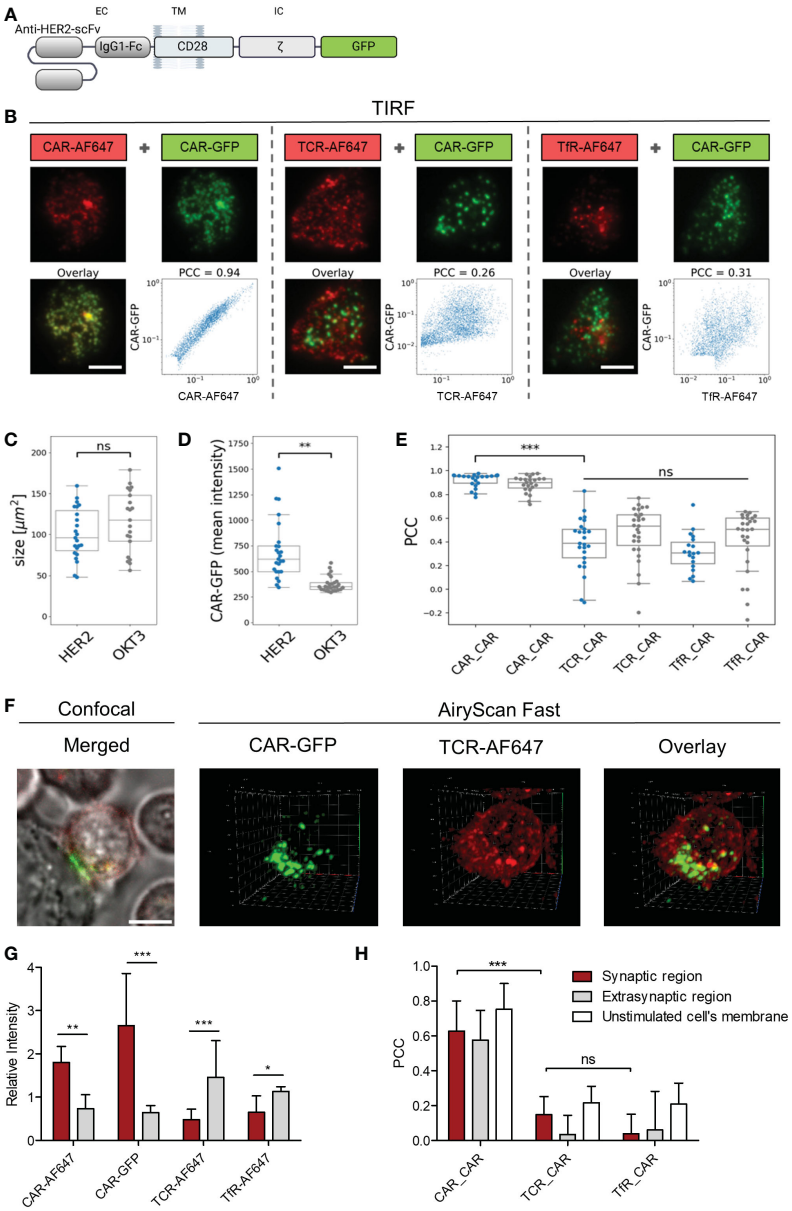

FIGURE 4
ζ CAR engagement of antigen induced clustering without TCR integration. Anti–HER2 CAR T cells were labeled with either AF647–conjugated F(ab´)$_2$ goat anti–human IgG antibody that recognizes the CAR, anti–TCRα/β AF647-conjugated antibody, or AF647-conjugated anti–transferrin receptor (TfR) antibody. **(A)** Schematic representation of the used anti–HER2 CD28ζ CAR linked to GFP at the intracellular site (IC). **(B)** Cells were seeded onto surfaces coated with HER2 protein or anti–CD3 antibody OKT3 and contacts were formed for 20 minutes. Cells were fixed and TIRF microscopy was used to image the localization of CAR-GFP (green) and either CAR-AF647, TCR-AF647, or TfR-AF647 (red). Scale bar represents 5 μm. For each cell, the pixel-wise correlation of the brightness values recorded in the red and in the green channel were plotted along the x- and the y-axis, respectively. Pearson's correlation coefficient (PCC) for each cell was calculated. Contact size **(C)** and Mean intensity **(D)** of anti–HER2 CAR-GFP plated on HER2 (blue) and OKT3 coated slides (grey) are displayed for n≥16 cells per group in a Whisker box plot. Statistical differences were determined by Wilcoxon-Mann-Whitney test with Python code (**p<0.01). **(E)** PCC for CAR-GFP and TCR-AF647 was calculated for anti–HER2 CAR T cells plated on HER2 (blue) and OKT3 (grey) coated slides and displayed for n≥24 cells per group in a Whisker box plot. Statistical differences were determined by Kruskal-Wallis test with Dunn's post-hoc test performed with Python code (***p<0.001). **(F)** Labelled anti-HER2 CAR T cells were seeded on HER2 expressing N87 target cells plated on chambered coverslips. 3D fluorescence images of live anti-HER2 CAR T cells forming contacts with the tumor target were recorded in AiryScan Fast mode. Confocal images of each analyzed cell were recorded as controls. **(G)** Differential 3D distribution of CAR-GFP and either CAR-AF647, TCR-AF647, or TfR-AF647 in the synaptic contact region and the extrasynaptic membrane was normalized to total intensity ($n_{CAR\text{-}GFP}$=11, $n_{TCR\text{-}AF647}$ = 11, $n_{CAR\text{-}AF647}$ = 10, $n_{TfR\text{-}AF647}$ = 6; 3D images contained approximately 50-80 slices). **(H)** PCC for CAR-GFP and either CAR-AF647, TCR-AF647, or TfR-AF647 in the synaptic contact region and the extrasynaptic membrane was quantified separately for each slice and averaged for each individual cell and presented as the mean of multiple cells across 3 independent experiments. 2D AiryScan Fast images of unstimulated cells were used as control (n_{CAR_CAR}=15, n_{TCR_CAR}=7, n_{TfR_CAR}=14). Data are presented as mean ± SD (*p<0.05, **p<0.01, ***p<0.001; ns, not significant).

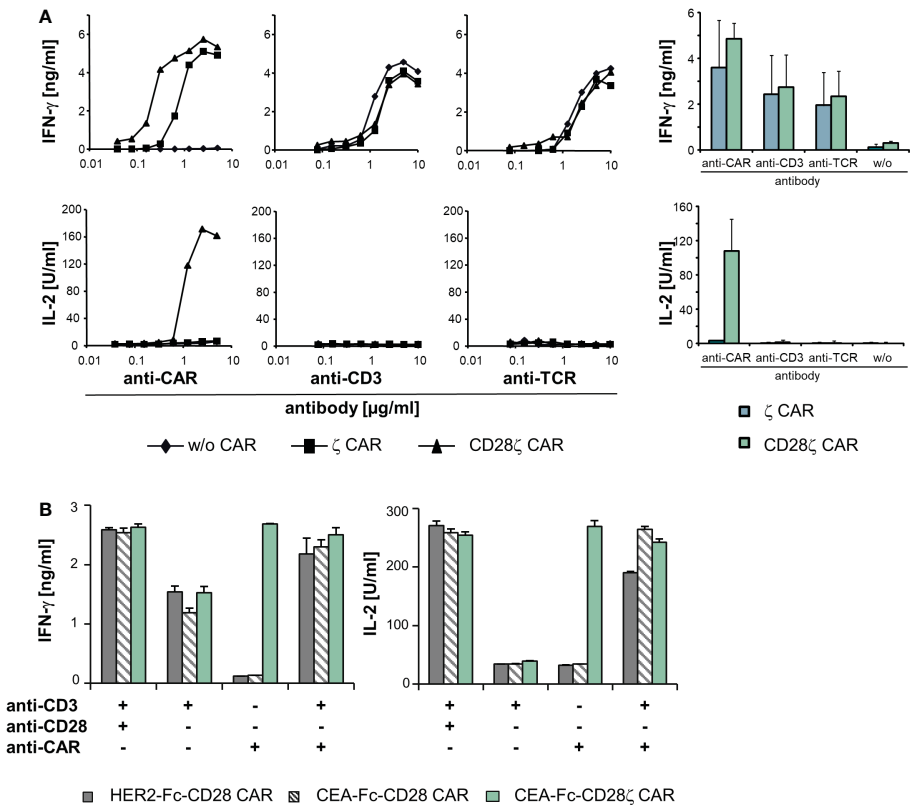

FIGURE 5
The TCR/CD3 complex and ζ–chain CARs can complement in signaling. **(A)** T cells of healthy donors (5 x 10^4 cells/well) were engineered with a ζ or CD28ζ CAR, respectively, and cultivated for 48 h in micro-titer plates that were coated with serial dilutions (starting from 10 µg/ml) of an anti–IgG1 Fc antibody for CAR activation or an agonistic anti–CD3 and anti–TCR antibody, respectively. Data from a representative T cell donor are shown; data from four donors were accumulated in mean values ± SD. **(B)** T cells (5 x 10^4 cells/well) expressing an anti-HER2-Fc-CD28, anti-CEA-Fc-CD28 or anti-CEA-Fc-CD28ζ CAR were cultivated for 48 h in micro-titer plates coated with an agonistic anti–CD3 (1 µg/ml) and anti–CD28 (5 µg/ml) antibody, respectively, or the anti–idiotypic antibody BW2064/36 (8 µg/ml), directed against the binding domain of the anti–CEA CAR, or recombinant HER2-Fc protein (8 µg/ml) recognized by the anti–HER2 CAR, respectively. Combinations of antibodies and/or antigen were used as indicated. Culture supernatants were analyzed for IFN–γ or IL–2 by ELISA as indicated. Numbers represent mean values of technical triplicates ± SD. A representative experiment out of at least three experiments is shown.

endogenous TCR/CD3 complex (6, 7). The impact of TCR/CD3 on the CAR redirected T cell activation and vice versa was so far not addressed. A mutual functional interaction is a relevant issue since CAR engineered T cells harbor in addition a functionally active TCR that may interfere with or add to CAR-mediated signaling.

Physiologically, the endogenous CD3ζ stabilizes the CD3/TCR complex; in the absence of CD3ζ, the levels of TCRαβ chains are substantially reduced (30, 31). Moreover, CD3ζ has a rapid turnover on the cell membrane independently of the other TCR components (10). Here we revealed that CD3ζ–chain CARs likewise have a shorter half-life and are expressed at lower levels on the T cell membrane than the FcεRI γ–chain CARs. The low expression levels are mediated by the CAR intracellular CD3ζ and not by the transmembrane domain; the effect holds also true for the second generation CD28-CD3ζ CAR. In contrast to the situation in T cells, γ–chain CARs are less expressed in Fc receptor expressing cells compared with the ζ–chain CARs, like macrophages and neutrophils (32–36); in non-lymphoid cells both γ- and ζ–chain CARs are expressed at similar levels. In CD3ζ KO and in TCR^- Jurkat cells the ζ–chain CARs were also less expressed than the γ–chain CARs indicating that the levels of ζ–chain CARs on the T cell surface are affected by downstream elements of the TCR/CD3 complex and not by the presence of the TCR and CD3ζ themselves. Notably, the expression level does not correlate with the activation capacity since CD3ζ CARs require less amounts of antigen than γ–chain CARs to activate engineered T cells.

At the membrane receptor level, the CAR does not co-recruit the TCR into its synapse as revealed by TIRF and fast AiryScan microscopy; vice versa, the TCR does not recruit the CAR into its synapse (37). Consequently, CAR and TCR do not cross-signal with respect to CD3ζ phosphorylation; TCR/CD3 stimulation did not result in increase in CAR CD3ζ phosphorylation and, conversely, CAR stimulation did not increase TCR/CD3 phosphorylation. The conclusion holds true for both the CD3ζ and the CD28-CD3ζ CAR. In line with this finding, costimulatory CD28 signaling through the CD28 CAR did not increase TCR/CD3ζ phosphorylation. However, there is a convergence in TCR and CAR downstream signaling, since the adaptor protein LAT, which is a linker between proximal and distal signaling events, becomes phosphorylated by each TCR and CAR activation, although at different levels (38).

We asked whether lack of cross-signaling at the early step was associated with lack of cross-activation of downstream pathways like the release of effector molecules including cytokines. To address this

scenario in a well-defined antigen stimulation assay, we took advantage of the different signaling requirements for IFN–γ and IL–2 release; IFN–γ release indicates CD3ζ signaling while IL–2 release depends on combined CD3ζ and CD28 signaling in T cells. Using these cytokines as indicators, we revealed that signaling through TCR/CD3 did not activate CAR-associated CD28 and vice versa (Figure 6). However, TCR/CD3 stimulation can complement with CAR-provided CD28 co-stimulation when both TCR and CAR are engaging their respective cognate antigen; signaling through only the TCR or the CD28 CAR was not sufficient. Taken together data indicate lack of cross-signaling between CAR and TCR not only on the level of the cell membrane associated kinases but also in the downstream pathway of effector molecules. In addition to our findings, potential physical interaction between CAR and endogenous signaling molecules can occur. Muller et al. showed that CAR T cells harboring a CD28-derived transmembrane domain form heterodimers with the endogenous CD28; such CAR-CD28 heterodimers can activate CAR T cells (39). The number of molecules captured in heterodimers may differ and the functional consequences still need thorough investigation.

Our conclusions are of relevance for clinical applications in various aspects. Firstly, T cells will undergo terminal differentiation towards hypo-responsive cells with terminally differentiated KLRG-1$^+$ CD57$^+$ CD7$^-$ phenotype once extensively stimulated through their TCR. In a previous study we revealed that hypo-responsiveness of CMV-specific late-stage CD8$^+$ T cells is due to reduced TCR synapse formation compared to younger cells which is the result of galectin-mediated membrane-anchoring of TCR components (40). However, transgenic CAR expression and CAR triggering produced full effector functions in TCR hypo-responsive T cells indicating that the defect is restricted to TCR membrane components while synapse formation of the transgenic CAR was not blocked. CAR engineered late-stage T cells released cytokines and mediated redirected cytotoxicity as efficiently as younger effector T cells. Together with our recent analysis, data presented here sustain the model that CAR mediated activation occurs TCR-independently and can by-pass hypo-responsiveness of late-stage T cells upon repetitive TCR encounter.

Secondly, we do not expect an increase in signaling through the endogenous TCR in presence of a CAR, for instance, when EBV-specific T cells are used for a CAR redirected anti–tumor attack (41). Clinical observation indicates that both CAR and TCR can trigger T cells as TCR stimulation of virus-specific T cells in addition to CAR engagement of antigen enhances expansion of CAR T cells and finally their anti–leukemic function (42). Moreover, TCR and CAR can complement in signaling when simultaneously engaging their respective cognate antigen. This is of benefit when achieving complementation in target recognition; one target is recognized by the TCR, the other by the CD28 CAR as shown in our model system. Complementing in activation while lacking cross-signaling is the basis for creating Boolean logic "AND" gating by co-signaling through a CD28 CAR without primary signal while the latter is provided by signaling through the TCR upon engagement of its respective antigen. In this situation, only engagement of both targets will be capable to sustain a lasting T cell activation. The combination may also be used for specific T cell inhibition using an inhibitory CAR that dampens TCR driven activation upon CAR antigen recognition.

The concept of combinatorial antigen recognition was primarily introduced by Kloss et al. (43) aiming at complementing signals between two CARs, one CAR harboring a suboptimal activation signal and the other CAR harboring a costimulatory signal. So-called RevCARs are a further improvement as they represent an artificial receptor platform for controllable T cell activation (44). Herein, universal receptors are redirected by adaptor molecules to the respective targets allowing dosing of the adaptor molecules, flexible targeting and, notably in this context, combinatorial antigen recognition. Again, prerequisite for successful "AND" gating is lack of dimerization and cross-talk between the signaling receptors.

Thirdly, we do not expect altered CAR signaling under conditions where the endogenous CD3ζ chain is down-regulated as it occurs under chronic inflammatory conditions (45). CAR redirected T cell activation does not depend on primary TCR signals as it is mediated through the CAR intrinsic CD3ζ and costimulatory domain. However, the presence of the endogenous TCR/CD3 substantially prolongs the persistence of CAR T cells in a mouse model compared to TCR β–chain KO cells (11). This is the case despite similar CAR

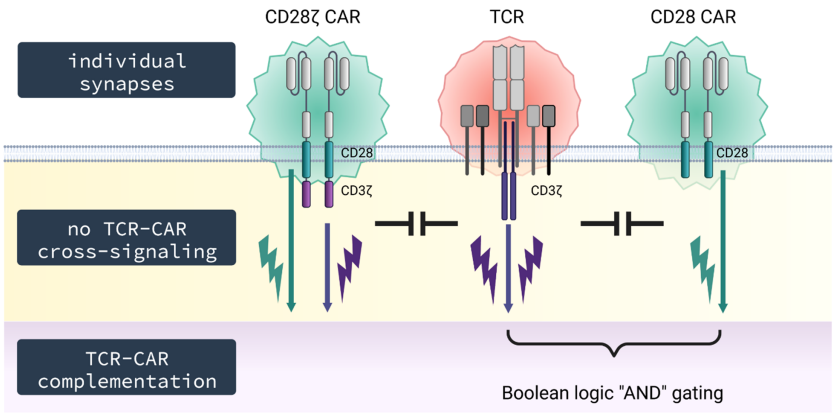

FIGURE 6
Schematic diagram. TCR and CAR do not co-integrate into the same synapse and signal independently upon engagement of their respective antigen without cross-signaling on the membrane level; however, TCR and CAR can complement in signaling upon simultaneous engagement of their respective cognate antigens, thereby providing T cell activation by both CD3 through the TCR and costimulation through the CAR.

expression in both cells indicating the impact of the endogenous TCR/CD3 on sustaining CAR T cell function. The "tonic" activation through the TCR and thereby an active downstream signaling cascade, although at low levels, seems to be crucial for the overall therapeutic success given the less persistence of CAR redirected TCR KO T cells and the pivotal impact of CAR T cell persistence on their efficacy in controlling leukemia/lymphoma in the long-term. Along with this hypothesis, in patients treated with CAR engineered allogeneic TCR KO T cells only contaminating TCR^+ CAR T cells, but not TCR^- CAR T cells, persisted while producing TCR signaling and finally graft-versus-host disease (9).

Taken together, CD3ζ CARs are similarly regulated as the CD3ζ chain of the TCR. However, the CAR cannot substitute for CD3ζ within the TCR complex underlining the concept that CAR and TCR form individual synapses in structure as verified by microscopic analyses and in function as shown by phospho-CD3ζ analyses. This specific situation allows logic "AND" gating by combinatorial target recognition through TCR and CAR. On the other hand, CAR engineered TCR KO T cells, designed for allogeneic "off-the-shelf" therapy, lack TCR support through "tonic" signaling and likely may lose functional capacities in the long-term.

Data availability statement

The raw data supporting the conclusions of this article will be made available by the authors, without undue reservation.

Author contributions

MB, AH, LV and MM-C conducted, designed, and analyzed experiments. AS, GV, AAH, GS, and HA interpreted the data and wrote the manuscript. All authors contributed to the article and approved the submitted version.

Funding

This research was funded by the German Federal Ministry of Education and Research through the CD20 CAR-TIME consortium within the funding program "Innovations for Individualized Medicine" (Fkz 01EK1507A-C), the European Union through the EN-ACTI2NG consortium (H2020-MSCA-ITN-2016 GA HYPERLINK "tel:721358" 721358), the Center of Molecular Medicine Cologne (CMMC), and the National Research, Development and Innovation Office, Hungary (OTKA K143771, FK132773 and GINOP- HYPERLINK "tel:23215201600044" 2.3.2-15-2016-00044).

Acknowledgments

The authors would like to thank Birgit Hops, Petra Hoffmann and Danuta Chrobok (Cologne) and Linda Otzelberger, Anja Pavlica, Charlotte Schenkel and Dorothea Weber-Steffens (Regensburg) for excellent technical assistance. We also thank Dr. M.H.M. Heemskerk for kindly providing Jurkat76 cells. Parts of Figure 1, 4, 6 were created with BioRender (Biorender.com) for which the authors have a license.

Conflict of interest

The authors declare that the research was conducted in the absence of any commercial or financial relationships that could be construed as a potential conflict of interest.

Publisher's note

Supplementary material

The Supplementary Material for this article can be found online at: https://www.frontiersin.org/articles/10.3389/fimmu.2023.1110482/full#supplementary-material

SUPPLEMENTARY FIGURE 1
Distribution of CAR, TCR and TfR in unstimulated and synapse forming cells. **(A)** Confocal and AiryScan Fast 2D fluorescence images of live anti-HER2 CAR T cells forming contacts with the tumor target. (B) Mean intensity of CAR-AF647, CAR-GFP, TCR-AF647, and TfR-AF647 in the synaptic region, extrasynaptic region, and both regions.

SUPPLEMENTARY VIDEO 1
3D distribution of CAR-GFP and CAR-AF647 in the synaptic contact region of one exemplary cell. 3D fluorescence images of live anti-HER2 CAR T cells forming contacts with the tumor target were recorded in AiryScan Fast mode.

SUPPLEMENTARY VIDEO 2
3D distribution of CAR-GFP and TCR-AF647 in the synaptic contact region and the extrasynaptic membrane of one exemplary cell. 3D fluorescence images of live anti-HER2 CAR T cells forming contacts with the tumor target were recorded in AiryScan Fast mode.

SUPPLEMENTARY VIDEO 3
3D distribution of CAR-GFP and TfR-AF647 in the synaptic contact region and the extrasynaptic membrane of one exemplary cell. 3D fluorescence images of live anti-HER2 CAR T cells forming contacts with the tumor target were recorded in AiryScan Fast mode.

References

1. Porter DL, Hwang W-T, Frey NV, Lacey SF, Shaw PA, Loren AW, et al. Chimeric antigen receptor T cells persist and induce sustained remissions in relapsed refractory chronic lymphocytic leukemia. *Sci Transl Med* (2015) 7:303ra139. doi: 10.1126/scitranslmed.aac5415

2. Golumba-Nagy V, Kuehle J, Hombach AA, Abken H. CD28-ζ CAR T cells resist TGF-β repression through IL-2 signaling, which can be mimicked by an engineered IL-7 autocrine loop. *Mol Ther J Am Soc Gene Ther* (2018) 26:2218–30. doi: 10.1016/j.ymthe.2018.07.005

3. Long AH, Haso WM, Shern JF, Wanhainen KM, Murgai M, Ingaramo M, et al. 4-1BB costimulation ameliorates T cell exhaustion induced by tonic signaling of chimeric antigen receptors. *Nat Med* (2015) 21:581–90. doi: 10.1038/nm.3838

4. Chandler NJ, Call MJ, Call ME. T Cell activation machinery: Form and function in natural and engineered immune receptors. *Int J Mol Sci* (2020) 21:7424. doi: 10.3390/ijms21197424

5. Hombach A, Wieczarkowiecz A, Marquardt T, Heuser C, Usai L, Pohl C, et al. Tumor-specific T cell activation by recombinant immunoreceptors: CD3 zeta signaling and CD28 costimulation are simultaneously required for efficient IL-2 secretion and can be integrated into one combined CD28/CD3 zeta signaling receptor molecule. *J Immunol Baltim Md 1950* (2001) 167:6123–31. doi: 10.4049/jimmunol.167.11.6123

6. Salter AI, Ivey RG, Kennedy JJ, Voillet V, Rajan A, Alderman EJ, et al. Phosphoproteomic analysis of chimeric antigen receptor signaling reveals kinetic and quantitative differences that affect cell function. *Sci Signal* (2018) 11:eaat6753. doi: 10.1126/scisignal.aat6753

7. Ramello MC, Benzaïd I, Kuenzi BM, Lienlaf-Moreno M, Kandell WM, Santiago DN, et al. An immunoproteomic approach to characterize the CAR interactome and signalosome. *Sci Signal* (2019) 12:eaap9777. doi: 10.1126/scisignal.aap9777

8. MacLeod DT, Antony J, Martin AJ, Moser RJ, Hekele A, Wetzel KJ, et al. Integration of a CD19 CAR into the TCR alpha chain locus streamlines production of allogeneic gene-edited CAR T cells. *Mol Ther* (2017) 25:949–61. doi: 10.1016/j.ymthe.2017.02.005

9. Qasim W, Zhan H, Samarasinghe S, Adams S, Amrolia P, Stafford S, et al. Molecular remission of infant b-ALL after infusion of universal TALEN gene-edited CAR T cells. *Sci Transl Med* (2017) 9:eaaj2013. doi: 10.1126/scitranslmed.aaj2013

10. Ono S, Ohno H, Saito T. Rapid turnover of the CD3 zeta chain independent of the TCR-CD3 complex in normal T cells. *Immunity* (1995) 2:639–44. doi: 10.1016/1074-7613(95)90008-x

11. Stenger D, Stief TA, Kaeuferle T, Willier S, Rataj F, Schober K, et al. Endogenous TCR promotes *in vivo* persistence of CD19-CAR-T cells compared to a CRISPR/Cas9-mediated TCR knockout CAR. *Blood* (2020) 136:1407–18. doi: 10.1182/blood.2020005185

12. Eshhar Z, Waks T, Gross G, Schindler DG. Specific activation and targeting of cytotoxic lymphocytes through chimeric single chains consisting of antibody-binding domains and the gamma or zeta subunits of the immunoglobulin and T-cell receptors. *Proc Natl Acad Sci U.S.A.* (1993) 90:720–4. doi: 10.1073/pnas.90.2.720

13. Rosskopf S, Leitner J, Paster W, Morton LT, Hagedoorn RS, Steinberger P, et al. A jurkat 76 based triple parameter reporter system to evaluate TCR functions and adoptive T cell strategies. *Oncotarget* (2018) 9:17608–19. doi: 10.18632/oncotarget.24807

14. Graham FL, Smiley J, Russell WC, Nairn R. Characteristics of a human cell line transformed by DNA from human adenovirus type 5. *J Gen Virol* (1977) 36:59–74. doi: 10.1099/0022-1317-36-1-59

15. Hombach A, Koch D, Sircar R, Heuser C, Diehl V, Kruis W, et al. A chimeric receptor that selectively targets membrane-bound carcinoembryonic antigen (mCEA) in the presence of soluble CEA. *Gene Ther* (1999) 6:300–4. doi: 10.1038/sj.gt.3300813

16. Heuser C, Hombach A, Lösch C, Manista K, Abken H. T-Cell activation by recombinant immunoreceptors: impact of the intracellular signalling domain on the stability of receptor expression and antigen-specific activation of grafted T cells. *Gene Ther* (2003) 10:1408–19. doi: 10.1038/sj.gt.3302023

17. Hombach A, Sircar R, Heuser C, Tillmann T, Diehl V, Kruis W, et al. Chimeric anti-TAG72 receptors with immunoglobulin constant fc domains and gamma or zeta signalling chains. *Int J Mol Med* (1998) 2:99–103. doi: 10.3892/ijmm.2.1.99

18. Schmidt P, Kopecky C, Hombach A, Zigrino P, Mauch C, Abken H. Eradication of melanomas by targeted elimination of a minor subset of tumor cells. *Proc Natl Acad Sci U.S.A.* (2011) 108:2474–9. doi: 10.1073/pnas.1009069108

19. Chmielewski M, Hombach A, Heuser C, Adams GP, Abken H. T Cell activation by antibody-like immunoreceptors: Increase in affinity of the single-chain fragment domain above threshold does not increase T cell activation against antigen-positive target cells but decreases selectivity. *J Immunol* (2004) 173:7647–53. doi: 10.4049/jimmunol.173.12.7647

20. Weijtens ME, Willemsen RA, Hart EH, Bolhuis RL. A retroviral vector system "STITCH" in combination with an optimized single chain antibody chimeric receptor gene structure allows efficient gene transduction and expression in human T lymphocytes. *Gene Ther* (1998) 5:1195–203. doi: 10.1038/sj.gt.3300696

21. Golumba-Nagy V, Kuehle J, Abken H. Genetic modification of T cells with chimeric antigen receptors: A laboratory manual. *Hum Gene Ther Methods* (2017) 28:302–9. doi: 10.1089/hgtb.2017.083

22. Schrangl L. Sdt-python: Python library for fluorescence microscopy data analysis. (2020). doi: 10.5281/zenodo.4604495

23. Harris CR, Millman KJ, van der Walt SJ, Gommers R, Virtanen P, Cournapeau D, et al. Array programming with NumPy. *Nature* (2020) 585:357–62. doi: 10.1038/s41586-020-2649-2

24. Virtanen P, Gommers R, Oliphant TE, Haberland M, Reddy T, Cournapeau D, et al. SciPy 1.0: fundamental algorithms for scientific computing in Python. *Nat Methods* (2020) 17:261–72. doi: 10.1038/s41592-019-0686-2

25. Huff J, Bergter A, Birkenbeil J, Kleppe I, Engelmann R, Krzic U. The new 2D superresolution mode for ZEISS airyscan. *Nat Methods* (2017) 14:1223–3. doi: 10.1038/nmeth.f.404

26. Schindelin J, Arganda-Carreras I, Frise E, Kaynig V, Longair M, Pietzsch T, et al. Fiji: an open-source platform for biological-image analysis. *Nat Methods* (2012) 9:676–82. doi: 10.1038/nmeth.2019

27. Ollion J, Cochennec J, Loll F, Escudé C, Boudier T. TANGO: a generic tool for high-throughput 3D image analysis for studying nuclear organization. *Bioinformatics* (2013) 29:1840–1. doi: 10.1093/bioinformatics/btt276

28. Jost LM, Kirkwood JM, Whiteside TL. Improved short- and long-term XTT-based colorimetric cellular cytotoxicity assay for melanoma and other tumor cells. *J Immunol Methods* (1992) 147:153–65. doi: 10.1016/s0022-1759(12)80003-2

29. Li W, Qiu S, Chen J, Jiang S, Chen W, Jiang J, et al. Chimeric antigen receptor designed to prevent ubiquitination and downregulation showed durable antitumor efficacy. *Immunity* (2020) 53:456–470.e6. doi: 10.1016/j.immuni.2020.07.011

30. Marin AV, Jiménez-Reinoso A, Briones AC, Muñoz-Ruiz M, Aydogmus C, Pasick LJ, et al. Primary T-cell immunodeficiency with functional revertant somatic mosaicism in CD247. *J Allergy Clin Immunol* (2017) 139:347–349.e8. doi: 10.1016/j.jaci.2016.06.020

31. Blázquez-Moreno A, Pérez-Portilla A, Agúndez-Llaca M, Dukovska D, Valés-Gómez M, Aydogmus C, et al. Analysis of the recovery of CD247 expression in a PID patient: insights into the spontaneous repair of defective genes. *Blood* (2017) 130:1205–8. doi: 10.1182/blood-2017-01-762864

32. Dombrowicz D, Flamand V, Miyajima I, Ravetch JV, Galli SJ, Kinet JP. Absence of fc epsilonRI alpha chain results in upregulation of fc gammaRIII-dependent mast cell degranulation and anaphylaxis. evidence of competition between fc epsilonRI and fc gammaRIII for limiting amounts of FcR beta and gamma chains. *J Clin Invest* (1997) 99:915–25. doi: 10.1172/JCI119256

33. Kraft S, Wessendorf JH, Hanau D, Bieber T. Regulation of the high affinity receptor for IgE on human epidermal langerhans cells. *J Immunol Baltim Md 1950* (1998) 161:1000–6. doi: 10.4049/jimmunol.161.2.1000

34. Borkowski TA, Jouvin MH, Lin SY, Kinet JP. Minimal requirements for IgE-mediated regulation of surface fc epsilon RI. *J Immunol Baltim Md 1950* (2001) 167:1290–6. doi: 10.4049/jimmunol.167.3.1290

35. van Vugt MJ, Heijnen IA, Capel PJ, Park SY, Ra C, Saito T, et al. FcR gamma-chain is essential for both surface expression and function of human fc gamma RI (CD64) in vivo. *Blood* (1996) 87:3593–9. doi: 10.1182/blood.V87.9.3593

36. Roberts MR, Cooke KS, Tran AC, Smith KA, Lin WY, Wang M, et al. Antigen-specific cytolysis by neutrophils and NK cells expressing chimeric immune receptors bearing zeta or gamma signaling domains. *J Immunol Baltim Md 1950* (1998) 161:375–84. doi: 10.4049/jimmunol.161.1.375

37. Beppler C, Eichorst J, Marchuk K, Cai E, Castellanos CA, Sriram V, et al. Hyperstabilization of T cell microvilli contacts by chimeric antigen receptors. *J Cell Biol* (2023) 222:e202205118. doi: 10.1083/jcb.202205118

38. Salter AI, Rajan A, Kennedy JJ, Ivey RG, Shelby SA, Leung I, et al. Comparative analysis of TCR and CAR signaling informs CAR designs with superior antigen sensitivity and in vivo function. *Sci Signal* (2021) 14:eabe2606. doi: 10.1126/scisignal.abe2606

39. Muller YD, Nguyen DP, Ferreira LMR, Ho P, Raffin C, Valencia RVB, et al. The CD28-transmembrane domain mediates chimeric antigen receptor heterodimerization with CD28. *Front Immunol* (2021) 12:639818. doi: 10.3389/fimmu.2021.639818

40. Rappl G, Riet T, Awerkiew S, Schmidt A, Hombach AA, Pfister H, et al. The CD3-zeta chimeric antigen receptor overcomes TCR hypo-responsiveness of human terminal late-stage T cells. *PLos One* (2012) 7:e30713. doi: 10.1371/journal.pone.0030713

41. Savoldo B, Rooney CM, Di Stasi A, Abken H, Hombach A, Foster AE, et al. Epstein Barr Virus specific cytotoxic T lymphocytes expressing the anti-CD30zeta artificial chimeric T-cell receptor for immunotherapy of Hodgkin disease. *Blood* (2007) 110:2620–30. doi: 10.1182/blood-2006-11-059139

42. Lapteva N, Gilbert M, Diaconu I, Al-Sabbagh M, Rollins LA, Naik S, et al. T Cell receptor stimulation enhances the expansion and function of CD19 chimeric antigen receptor-expressing T cells. *Clin Cancer Res* (2019) 25:7340–7350. doi: 10.1158/1078-0432.CCR-18-3199

43. Kloss CC, Condomines M, Cartellieri M, Bachmann M, Sadelain M. Combinatorial antigen recognition with balanced signaling promotes selective tumor eradication by engineered T cells. *Nat Biotechnol* (2013) 31:71–5. doi: 10.1038/nbt.2459

44. Feldmann A, Hoffmann A, Kittel-Boselli E, Bergmann R, Koristka S, Berndt N, et al. A novel revcar platform for switchable and gated tumor targeting. *Blood* (2019) 134:5611. doi: 10.1182/blood-2019-128436

45. Berg L, Rönnelid J, Klareskog L, Bucht A. Down-regulation of the T cell receptor CD3 zeta chain in rheumatoid arthritis (RA) and its influence on T cell responsiveness. *Clin Exp Immunol* (2000) 120:174–82. doi: 10.1046/j.1365-2249.2000.01180.x

frontiers | Frontiers in Immunology

TYPE Original Research
PUBLISHED 16 February 2023
DOI 10.3389/fimmu.2023.1119498

OPEN ACCESS

EDITED BY
Hakim Echchannaoui,
Johannes Gutenberg University Mainz, Germany

REVIEWED BY
Yong-Chen Lu,
University of Arkansas for Medical Sciences, United States
Frank Momburg,
German Cancer Research Center (DKFZ), Germany
Ram Babu Undi,
University of Oklahoma Health Sciences Center, United States

*CORRESPONDENCE
Gerald Willimsky
gerald.willimsky@charite.de

†These authors share last authorship

SPECIALTY SECTION
This article was submitted to Cancer Immunity and Immunotherapy, a section of the journal Frontiers in Immunology

RECEIVED 08 December 2022
ACCEPTED 02 February 2023
PUBLISHED 16 February 2023

CITATION
Immisch L, Papafotiou G, Gallarín Delgado N, Scheuplein V, Paschen A, Blankenstein T and Willimsky G (2023) Targeting the recurrent Rac1P29S neoepitope in melanoma with heterologous high-affinity T cell receptors. *Front. Immunol.* 14:1119498. doi: 10.3389/fimmu.2023.1119498

Targeting the recurrent Rac1P29S neoepitope in melanoma with heterologous high-affinity T cell receptors

Lena Immisch[1,2,3], George Papafotiou[1,2,3], Nerea Gallarín Delgado[1], Vivian Scheuplein[4], Annette Paschen[5,6], Thomas Blankenstein[4,7†] and Gerald Willimsky[1,2,3,7*†]

[1]Institute of Immunology, Charité-Universitätsmedizin Berlin, corporate member of Freie Universität Berlin and Humboldt-Universität zu Berlin, Berlin, Germany, [2]German Cancer Research Center, Heidelberg, Germany, [3]German Cancer Consortium, partner site Berlin, Berlin, Germany, [4]Max Delbrück Center for Molecular Medicine in the Helmholtz Association, Berlin, Germany, [5]Department of Dermatology, University Hospital Essen, University of Duisburg-Essen, Essen, Germany, [6]German Cancer Consortium, partner site Essen, Essen, Germany, [7]Berlin Institute of Health at Charité-Universitätsmedizin Berlin, Berlin, Germany

Recurrent neoepitopes are cancer-specific antigens common among groups of patients and therefore ideal targets for adoptive T cell therapy. The neoepitope F**S**GEYIPTV carries the Rac1P29S amino acid change caused by a c.85C>T missense mutation, which is the third most common hotspot mutation in melanoma. Here, we isolated and characterized TCRs to target this HLA-A*02:01-binding neoepitope by adoptive T cell therapy. Peptide immunization elicited immune responses in transgenic mice expressing a diverse human TCR repertoire restricted to HLA-A*02:01, which enabled isolation of high-affinity TCRs. TCR-transduced T cells induced cytotoxicity against Rac1P29S expressing melanoma cells and we observed regression of Rac1P29S expressing tumors *in vivo* after adoptive T cell therapy (ATT). Here we found that a TCR raised against a heterologous mutation with higher peptide-MHC affinity (Rac2P29L) more efficiently targeted the common melanoma mutation Rac1P29S. Overall, our study provides evidence for the therapeutic potential of Rac1P29S-specific TCR-transduced T cells and reveal a novel strategy by generating more efficient TCRs by heterologous peptides.

KEYWORDS

neoantigen, TCR gene therapy, melanoma, Rho (Rho GTPase), humanized mouse models

Introduction

Adoptive T cell therapy (ATT) as a treatment option against cancer is coming of age, so far primarily with remarkable efficiencies against non-solid leukemia and lymphoma, for example using chimeric antigen receptor modified T cells (CAR-Ts) targeting the lineage-specific surface protein CD19 (1). Targeting cancer mutations by reactivating neoepitope-

specific T cells using checkpoint blockade has shown therapeutic success in half of the patients harboring solid cancers with high mutational load but is hampered in patients with tumors carrying lower numbers of mutations (2). Therefore, TCR gene therapy, the genetic modification of autologous patient T cells by introducing a therapeutic TCR and thus grafting of new antigen specificities onto patients' T cells, may be a valuable alternative. Since TCR gene therapy allows for targeting proteins independent of cellular localization it broadens the spectrum of target antigens. Therefore, it also allows for targeting somatic mutations, so called neoantigens, that come with the best possible risk-benefit ratio because these are truly cancer-specific mutant antigens not expressed in normal tissue (3).

Rac (Ras-related C3 botulinum toxin substrate) proteins are a subfamily of the Rho family of GTPases involved in many cellular processes including cell migration, cytoskeleton reorganization and cell transformation (4). Due to its role to control a variety of cellular functions, aberrant Rac signaling is often involved in tumorigenesis (5, 6). The Rac family comprises the homologous proteins Rac1, Rac2 and Rac3; this study focused on Rac1 and Rac2, for which point mutations in tumors have been described. A single-nucleotide variant (SNV) at position 85C>T leads to the Rac1P29S amino acid change with a strong UV signature. Following mutations in Braf V600 and Nras Q61, Rac1 P29 is the third most commonly mutated protooncogene in cutaneous melanomas and with up to 9% of sun-exposed melanomas carrying this mutation the most common cancer-associated recurrent missense mutation among the family of small Rho GTPases (7, 8). The Rac1 mutation occurred in both Braf and Nras mutant melanomas (7, 8), but a higher percentage of Braf/Nras wild type melanomas possess the Rac1P29S mutation (9). In addition, both Braf and Nras mutations also occur in benign naevi and seem insufficient to cause progression towards melanoma (10), altogether suggesting that Rac1P29S could also be a driving event independently of these oncogenes (11). Additionally, the mutation confers resistance to Braf inhibition by vemurafenib and dabrafenib *in vitro*, suggesting a role of Rac1P29S mutation as a biomarker for Raf inhibitor resistance in melanoma patients (12). It has furthermore been reported that Rac1P29S upregulates PD-L1 expression in melanoma (13), and thus may contribute to immune evasion. Due to its importance in proliferation, metastasis and drug resistance, Rac1 is an important therapeutic target in melanoma, but so far is considered undruggable, which makes targeting Rac1P29S in melanoma a challenge.

Other Rho GTPase members also harbor mutations in homologous residues, but these are less frequently found in tumorigenesis (<1% incidence), such as Rac2 (P29L) and Rhot (P30L) (8). The P29L (c.86C>T) mutation in Rac2 was not only detected in melanoma but also in a breast cancer samples, confirming an important role of the P29 position in oncogenesis (14, 15).

Since mutant Rac1 is specifically expressed on cancer cells and is important for the perpetual growth and survival of tumor cells, it is a promising target candidate for TCR gene therapy, a methodology that equips patient T cells with anti-cancer specificity. Additionally, the mutation is found in a large percentage of cancer patients and presented by a frequent HLA-molecule. Here, we explore the Rac1P29S mutation together with the less frequent Rac2P29L mutation as targets for adoptive T cells therapy.

Materials and methods

Peptide immunization of mice

Mutation-specific T cells were generated in ABabDII mice expressing a diverse human TCR repertoire restricted to HLA-A*02:01 (16). The mice are additional deficient for mouse TCR and mouse MHC I expression. Mice were immunized by subcutaneous injection of 100 µg Rac1P29S (F**S**GEYIPTV), Rac2P29L (F**L**GEYIPTV) or RhotP30L (F**L**EEVPPRA) peptide in a 1:1 solution of incomplete Freund's adjuvant and PBS containing 50 µg CpG. After priming, the mice received the same immunization twice as boosts in a three weeks interval. To assess $CD8^+$ T cell responses, peripheral T cells were restimulated *in vitro* with either 10^{-6} M peptide, PBS as a negative control, or 10^6 Dynabeads mouse T activator CD3/CD28 (Gibco) as a positive control. After 2h, Brefeldin A (BD) was added to the cultures and after overnight culturing, specific $CD8^+$ T cells were measured by intracellular IFNγ staining (PE anti-mouse IFNγ XMG1.2, Biolegend).

Isolation and cloning of TCRs

To isolate specific TCRs, immunized mice were sacrificed; splenocytes and lymphocytes from inguinal lymph nodes were prepared and $CD4^+$ T cells were depleted using microbeads (Miltenyi Biotec). $1x10^6$ splenocytes were cultured in T cell media (TCM, RPMI (Gibco™) containing 10% FCS (Pan Biotech), 1 mM HEPES (Gibco™), 100 IU/ml PenStrep (Gibco™), 50 µM 2-Mercaptoethanol (Gibco™)) supplemented with 100 IU/ml IL-2 (Peprotech) for 10 days in the presence of 10^{-8} M or 10^{-9} M peptide. Reactive T cells were either sorted using a Rac1-specific tetramer (pA2-tetramer, Beckman Coulter) or the mouse IFNγ secretion assay (Miltenyi). Four hours prior to the *in vitro* assessment of IFNγ secretion, cells were stimulated with a peptide concentration of 10^{-6} M. To sort IFNγ-secreting $CD8^+$ T cells, cells were stained with anti-mouse CD3-APC (145-2C11, Biolegend) and anti-mouse CD8-PerCP (53-6.7, Biolegend) at 4°C for 30 minutes. For sorting of tetramer-positive T cells, staining was done with PE-labeled pA2-tetramer, anti-mouse CD3-APC and anti-mouse CD8-PerCP. T cells were subsequently sorted (BD FACS Aria III) into RTL lysis buffer for RNA isolation with RNeasy Micro Kit (QIAGEN). SMARTer™ RacE cDNA Amplification Kit (Clontech Laboratories) was used to synthesize first-strand cDNA synthesis and 5'-RACE PCR. The TCR sequence was specifically amplified using 0.1 µM universal primer (5'-ctaatacgactcactatagggcaagcagtggtatcaacgcagagt-3') and either 0.1 µM hTRAC (5'-cggccactttcaggaggaggattcggaac-3') or hTRBC (5'–ccgtagaactggacttgacagcggaagtgg-3') specific primer and 1U Phusion® HotStart II polymerase (Thermo Scientific) from 1-2 µl of the reverse transcriptase reaction. The amplicons were analyzed on an agarose gel and specific bands were cut out and cloned using a Zero Blunt® TOPO® PCR cloning kit (Life Technologies). A T3 primer (5'-aattaaccctcactaaaggg-3') was used to sequence plasmids from isolated individual clones (Eurofins Genomics). Dominant TCR-α/β chains were selected and corresponding TCR-α/β chains were linked using a P2A element and constant regions of the TCRs were exchanged

with mouse constant regions. The codon-optimized TCR cassettes were synthesized by GeneArt (Thermo Fisher Scientific) and cloned into an MP71 vector.

Plasmid constructs and cDNA synthesis

All retroviral packaging plasmid vectors were based on plasmid MP71 (17). Plasmids MP71-A2 encoding HLA-A*02:01, and MP71-CDK4-R24L-i-GFP encoding the full-length cDNA of CDK4 harboring the R24L mutation and co-expressing EGFP through an IRES element, were a kind gift from M. Leisegang. To construct MP71-CDK4R24L-P2A-GFP, a P2A-EGFP fragment was PCR amplified from plasmid pcDNA3.1-Hygro(+)-M7PG (kind gift V. Anastasopoulou) using primer CDK4-P2A_F (5'-acataaggatgaaggtaatccggagggcagcggcgccacc aac-3') combined with GFP-PRE_Rev (5'-aatggcggtaagatgctcgaatttcatttgtacagctcgtccatgc-3'). Produced amplicons bear homologies to the above plasmids and can serve to prime overlap extension PCR (OE-PCR), replacing the IRES-EGFP elements with P2A-EGFP. In brief, the respective OE-PCR amplicon was mixed in a 200 molar excess ratio to 10 ng of MP71-CDK4-R24L-i-GFP, in 25 µl PCR reactions and were cycled, using 52° C annealing temperature and a 7-minute extension time at 72°C, for 21 cycles. Reactions were subsequently digested with DpnI and transformed into competent E. coli. All PCRs described were performed using Q5, High fidelity 2x Master mix (NEB). Unless stated otherwise, all other constructs were synthesized by GeneArt Gene Synthesis, ThermoFischer Scientific and are followed by an AAY sequence and EGFP.

Cells and cell culture

The retroviral packaging cell lines 293GP-GLV (producing amphotropic retroviral vectors) and Plat-E (producing ecotropic retroviral vectors) were cultured in DMEM supplemented with 10% FCS (18, 19). TAP-deficient T2 cells (RRID : CVCL_2211, ATCC: CRL-1992) and human PBMCs were cultured in T cell media (TCM, RPMI (Gibco™) containing 10% FCS (Pan Biotech), 1 mM HEPES (Gibco™), 100 IU/ml PenStrep (Gibco™), 50 µM 2-Mercaptoethanol (Gibco™). Mouse T cells were cultured in mouse T cell media (mTCM, RPMI (Gibco™) containing 10% FCS (Pan Biotech), 100 IU/ml PenStrep (Gibco™), 50 µM 2-Mercaptoethanol (Gibco™) and Sodium Pyruvate). The cell lines Mel624 (RRID : CVCL_8054), UKRV-Mel-21a (referred to hereafter as Mel21a) (20), Mel20aI (RRID : CVCL_A157), MaMel085 (called here Mel085) (RRID : CVCL_A220), Mel55b (RRID : CVCL_A190), HepG2 (RRID : CVCL_0027), SH-SY5Y (RRID : CVCL_0019), were cultured in RPMI (Gibco™) supplemented with 10% FCS (Pan Biotech) and 100 IU/ml PenStrep (Gibco™). MC703 cells were kindly provided by M. Leisegang and are described in (21). The panel of EBV–transformed lymphoblastoid B cell lines [LCLs (22)] were cultured in RPMI supplemented with 10% FCS, 1x antibiotic-antimycotic, 1mM sodium pyruvate and 1x non-essential amino acids.

Retroviral transduction of TCRs into primary T cells

TCR gene transfer was carried out as described before (17, 23). In brief, for retrovirus generation, 293GP-GLV cells were transfected with MP71 vector carrying the respective TCR cassettes using Lipofectamine 3000 (ThermoFisher Scientific). On the same day, PBMCs from healthy donors were seeded on plates coated with 5 µg/ml anti-CD3 (OKT3, Invitrogen) and 1 µg/ml anti-CD28 antibodies (CD28.2, Invitrogen) in TCM supplemented with 100 IU/ml IL-2 (Peprotech). 48 hours later, the virus supernatant was harvested, filtered and supplemented with 8 µg/ml protamine sulfate (Sigma-Aldrich) and 100 IU/ml IL-2, before spinoculation with the activated T cells at 800g for 90 minutes at 32°C was performed. The next day, a second supernatant was harvested from the same 293GP-GLV cells, transferred to a RetroNectin (Takara Bio) coated plate and centrifuged at 3200g for 90 minutes at 4°C. The PBMCs were harvested, supplemented with 100 IU/ml IL-2 and 8 µg/ml protamine sulfate and spinoculated with the virus-containing plates at 800g for 30 minutes at 32°C. After the second transduction, T cells were expanded for 10 days, before being transferred to low IL-2 (10 IU/ml). After 48 hours, transduced T cells were harvested, analyzed for TCR expression by flow cytometry and frozen for future experiments. To detect the transduction rate of the TCRs transduced into primary T cells, the following antibodies were used in a 1:100 dilution at 4°C for 30 min: anti-human CD3-PerCP (UCHT1, Biolegend), anti-human CD8-APC (HIT8a, Biolegend) and anti-mouse TCR β chain-PE (H57-597, Biolegend).

For mouse transductions, Plat-E cells were transfected with MP71 vector carrying the respective TCR cassettes using Lipofectamine 3000 (ThermoFisher Scientific). On the following day, spleen cells were isolated from HHD mice (24) and erythrocytes were lysed by ammonium chloride treatment. $2x10^6$/ml cells were incubated in mTCM supplemented with 1 µg/ml anti-mouse CD3, 0.1 µg/ml antimouse CD28 antibodies (BD Biosciences (BD), Franklin Lakes, NJ, USA) and 10 IU/ml human IL-2 (Proleukin S, Novartis, Basel, Switzerland). On the next day, $1x10^6$ cells were transduced by spinoculation in 24-well non-tissue culture-treated plates pre-coated with 12.5 µg/ml RetroNectin (TaKaRa, Otsu, Japan) and virus particles (3200 x g, 90 min, 4°C) in 1ml mTCM supplemented with 10 IU/ml IL-2 and $4x10^5$ mouse T-Activator beads (Life Technologies). A second transduction was performed on the following day by spinoculation with 1 ml virus supernatant (+ 10 IU/ml IL-2). T cells were expanded in mTCM (+ 50 ng/ml IL-15 (Miltenyi Biotec) for 10 days. TCR transduction rate was measured by flow cytometry using the following antibodies in a 1:100 dilution at 4° C for 30 min: anti-mouse CD3-BV421 (UCHT1, Biolegend), anti-mouse CD8-APC (HIT8a, Biolegend) and FITC-labeled anti-human TCR Vβ22 (IMMU 546, Beckman Coulter), Vβ9 (MKB1, Biolegend) and Vβ1 (BL37.2, Beckman Coulter) for TCRs 22894, 5934 and 14/35, respectively. These antibody combinations were also used to stain blood from adoptively transferred HHDxRag$^{-/-}$ mice [(21); see below].

10.3389/fimmu.2023.1119498

Retroviral transduction of tumor cell lines

Mel085-A2 and SH-SY5Y-A2 cells were generated by transfecting MP71-HLA-A*02:01 into 293GP-GLV cells using Lipofectamine 3000 (ThermoFisher Scientific). 48 hours after transfection, 293GP-GLV virus-containing supernatant was harvested, supplemented with 8 µg/ml protamine sulfate and transferred to the respective glioma cell line. Cells and virus supernatant were spinoculated at 800g for 90 minutes at 32°C. The medium was changed to the respective growth medium 6 hours later. To analyze successful transduction, flow cytometry was used to determine the fraction of GFP-positive cells. HLA-A*02:01 transduction was confirmed by flow cytometry using an anti-human HLA-A*02:01-APC (BB7.2, Biolegend) specific antibody and an APC mIgG2b, k isotype control (MPC-11, Biolegend). Mel55, Mel085-A2 and Mel20aI cells expressing CDK4R24L-GFP were generated by retroviral transduction using MP71 plasmid expressing the R24L mutant CDK4 full-length cDNA followed by a P2A element and GFP. MC703 cells were transduced with a triple epitope construct of Rac1P29S nonamer separated by AAY proteasomal cleavage sites tagged with GFP (5'LTR – $(P29S)_3$ – GFP – PRE – 3'LTR).

Co-culture experiments

All co-culture experiments to detect IFNγ secretion were conducted using $1x10^4$ - $1x10^5$ transduced T cells with $1x10^4$ -$1x10^5$ target cells as indicated for 22-24 hours in a 96 well plate. As a positive control for the T cell activation, 50 ng/ml PMA (Phorbol-12-myristat-13-acetat, (Calbiochem) and 1 µg/ml Ionomycin (Calbiochem) were added to the transduced T cells. T2 cells were loaded with the labelled peptides (JPT Peptide Technologies GmbH) at the indicated concentrations. Secreted IFNγ amounts in the supernatant were measured by ELISA (BD OptEIA; BD Biosciences). Alanine-exchanged Rac1/2 peptides (all JPT Peptide Technologies GmbH, >95% purity) were added at 10^{-5} M or 10^{-9} M.

Cytotoxicity assay

The cytotoxic potential of transduced T cells was analyzed using the live cell imaging system IncuCyte Zoom (Essen Bioscience). 3-$5x10^3$ GFP positive target cells were resuspended in TCM without phenol red and seeded into flat-bottom 96 well plates. The following day, transduced T cells in a 5:1 or 15:1 (effector: target) ratio were added to the respective wells in triplicates. GFP expression in target cells was determined every hour over a time period of 72 hours at 37° C and 5% CO2. For analysis, the average of GFP total area (µm²/image) in the target cells co-cultured with the respective TCR-transduced T cells was calculated and normalized to the average of GFP total area (µm²/image) of the same target cells co-cultured with mock-transduced T cells (% of mock T cells).

Tumor challenge and adoptive T cell transfer

12-20 weeks old HHDxRag$^{-/-}$ mice (21) were injected with $1x10^6$ MC703-FSG tumor cells and tumor growth was measured 2-3 times a week. When tumors reached a tumor size of 300-1000 mm^3 (mean treatment group tumor size ~500 mm^3), mice were intravenously injected with TCR-engineered T cells obtained from HHD mice in 100µl PBS (adjusted to $1x10^6$ CD8$^+$TCR$^+$ HHD T cells per mouse). Tumor volume was determined by caliper measurement of the tumor parameters (x,y,z) according to the formula (xyz)/2. Mice were sacrificed and tumors isolated when tumors reached the maximum tolerable size.

Statistical analysis

Statistical analysis was conducted using GraphPad prism software. Statistics (standard deviation (SD), t-test, two-way ANOVA) are indicated in the figure legends. If not stated otherwise, significance is given as ns = not significant, p<0.001 *** and p<0.0001 ****.

Results

High affinity Rac1/2-specific TCRs were successfully isolated after peptide immunization

The Rho GTPase mutations, Rac1P29S and Rac2P29L and RhotP30L create epitopes (Rac1P29S$_{28-36}$ F**S**GEYIPTV, Rac2P29L$_{28-36}$ F**L**GEYIPTV and RhotP30L$_{29-37}$ F**L**EEVPPRA) predicted to bind HLA-A*02:01 with high affinity of 18.2 nM, 2.3 nM and 27.7 nM, respectively (Table 1) (25). Peptides binding to MHC class I molecules are defined as strong binders with an IC_{50} value <50 nM

TABLE 1 Prediction of binding of peptides to MHC class I molecules [NetMHC 4.0 DTU Health Tech (25)].

	Peptide	HLA	Affinity (nM)
Rac1P29S	F**S**GEYIPTV	HLA-A*02:01	18.2
Rac2P29L	F**L**GEYIPTV	HLA-A*02:01	2.3
Rac1/2 wt	F**P**GEYIPTV	HLA-A*02:01	573.0
RhotP30L	F**L**EEVPPRA	HLA-A*02:01	27.7
Rhot wt	F**P**EEVPPRA	HLA-A*02:01	21063.3

(26, 27). In contrast to the wildtype peptide, the Rho GTPase mutant epitopes are predicted strong binders, with the less frequent mutant Rac2P29L epitope being the strongest.

To study the potential of the recurrent Rac1P29S mutation as a target for ATT, we isolated and characterized TCRs against Rac1P29S. Additionally, TCRs were also raised against Rac2P29L, a mutation that differs in one amino acid but has a higher predicted peptide-MHC affinity than Rac1P29S. Mutant peptides were used to immunize ABabDII mice, a transgenic mouse model expressing an HLA-A*02:01-restricted diverse human TCR repertoire (16). Peripheral T cells of Rac1 and Rac2 mutant peptide immunized mice showed an immune response upon restimulation, measured by intracellular IFNγ responsiveness (Figures 1A–C). Repeated immunization of ABabDII mice with the RhotP30L peptide-epitope did not result in a $CD8^+$ T cell response (data not shown). To isolate specific TCRs, we cultured splenocytes of responsive mice in the presence of the respective mutant peptide for 10 days and sorted either peptide HLA-A*02:01 tetramer positive (pA2 $tetramer^+$) T cells (Figure 1D) or $IFN\gamma^+$ $CD8^+$ T cells (Figure 1E). We identified dominant α and β chains of the responsive mice #22894 (Rac2 mutant immunized), #A12B20 and #5934 (Rac1 mutant immunized) (Table 2). After replacing of the human constant regions by murine ones in order to reduce mispairing between endogenous and transduced TCR chains, the constructs comprising TCRβ-P2A-TCRα cloned into pMP71 vector were retrovirally transduced into human T cells of healthy donors. Successful transduction of the three Rac1/2-specific TCRs, as well as a well-characterized CDK4R24L-specific TCR (14/35) as control, was measured by staining for the murine constant β chain in $CD8^+$ T cells and analyzed by flow cytometry (Supplementary Figure 1A). We found $CD8^+$ and TCR^+ double positive T cells at similar percentages ranging from 26.3% to 34.6% of $CD3^+$ T cells.

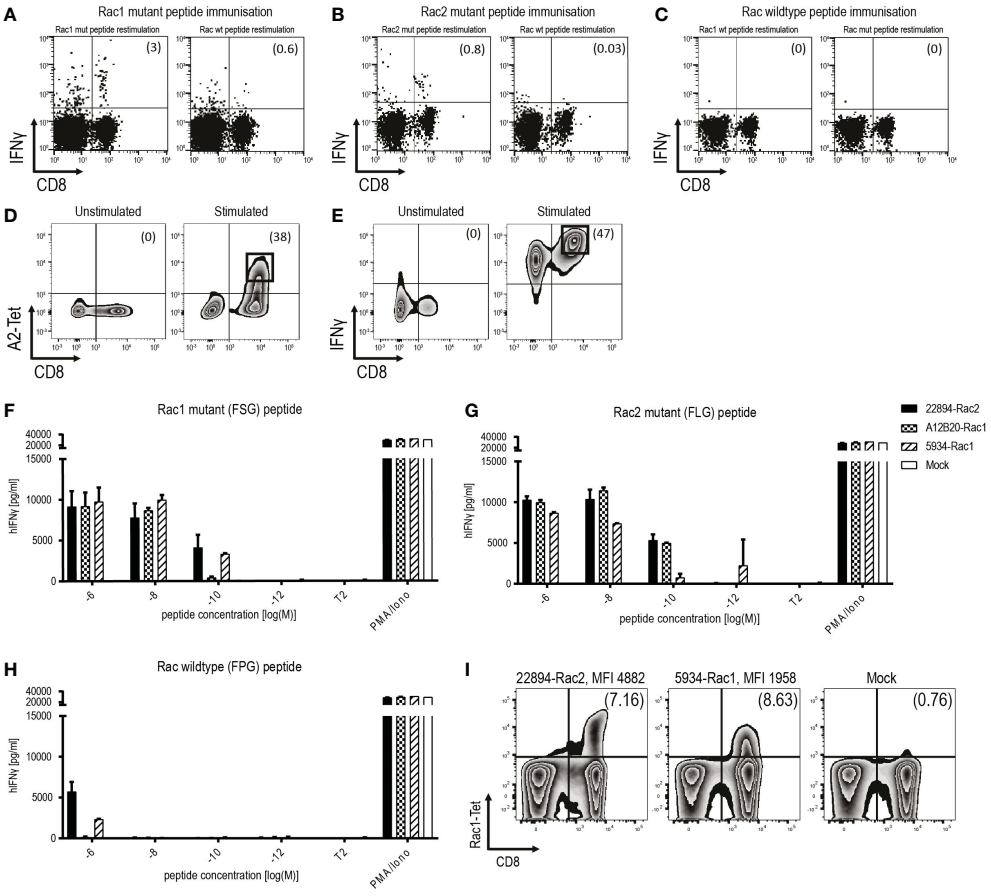

FIGURE 1
Identification and isolation of mutant Rac1/2-specific, high-affinity TCRs in ABabDII mice. **(A-C)** Representative examples of *ex vivo* intracellular IFNγ staining of peripheral T cells obtained from ABabDII mice immunized with **(A)** Rac1P29S mutant peptide, **(B)** Rac2P29L mutant peptide or **(C)** Rac wild type peptide. Splenocytes were restimulated with the indicated peptide 7 days after the last immunization of ABabDII mice. Numbers in brackets represent percent of $CD8^+$ T cells **(D)** Representative pA2 tetramer staining of mutant Rac1-specific $CD8^+$ T cells 10 days after spleen cell culture in the presence of 10^{-9} M mutant Rac1 peptide. Cells were gated on lymphocytes and $CD3^+$ T cells. Numbers in brackets represent percent of pA2 $tetramer^+$ $CD8^+$ T cells, unstimulated splenocytes served as a negative control. Sorted cells are depicted in squares. **(E)** Identification of $IFN\gamma^+$ $CD8^+$ T cells using IFNγ-capture assay depicted by representative staining of mutant Rac1-specific $CD8^+$ T cells 10 days after spleen cell culture in the presence of 10^{-8} M mutant Rac1 peptide. Cells were gated on lymphocytes and $CD3^+$ T cells, unstimulated splenocytes served as a negative control. Numbers in brackets represent percent $IFN\gamma^+CD8^+$ T cells. Sorted cells were depicted in squares. **(F-H)** TCR-transduced T cells were co-cultured with peptide-loaded T2 cells ($1x10^4$ cells, 1:1 ratio) for 22 hours in triplicates. IFNγ levels were determined in an ELISA assay. PMA and Ionomycin (P/I) stimulation served as a positive control, non-loaded T2 cells as a negative control. T2 cells were loaded with indicated concentrations of **(F)** Rac1 mutant peptide (F**S**GEYIPTV), **(G)** Rac2 mutant peptide (F**L**GEYIPTV) or **(H)** Rac wild type peptide (F**P**GEYIPTV). **(I)** Affinity of the TCRs to its peptide-MHC complex was determined using a mutant Rac1-specific pA2 tetramer. Binding to the pA2 tetramer is indicated by mean fluorescence intensity (MFI). The experiment was performed three times with similar results and graphs represent means of triplicate cultures ± SD.

To determine the functional avidity of the isolated TCRs, TAP-deficient T2 cells were loaded with titrated amounts of Rac1 mutant (FSG) peptide (Figure 1F), Rac2 mutant (FLG) peptide (Figure 1G) and as a negative control Rac wild type (FPG) peptide (Figure 1H). The two TCRs isolated after Rac1 mutant peptide immunization showed high affinity to their respective peptide down to a concentration of 10^{-9} M for TCR A12B20-transduced, and 10^{-10} M for TCR 5934-transduced T cells. Interestingly, also the TCR 22894, isolated after immunization with the Rac2 mutant peptide showed high functional avidity towards the Rac1 mutant peptide down to a concentration of 10^{-10} M. When loaded with the Rac2P29L peptide, the mutant Rac1-specific TCRs also recognized the Rac2 mutant peptide (Figure 1G). The Rac wild type (FPG) peptide was only recognized when co-cultured with the T cells in the highest peptide concentrations of 10^{-6} M. Since the Rac2P29L mutation is less common in human cancers, the subsequent experiments focused primarily on the Rac1P29S mutation as a target for ATT. To determine the binding strength of the TCRs to the Rac1 peptide-MHC (pMHC) complex, we stained the two TCRs 22894 and 5934 that performed best in the affinity assays with a mutant Rac1-specific pA2 tetramer. As depicted in Figure 1I, the heterologous Rac2-specific TCR 22894-transduced T cells showed a higher MFI of 4889 compared to the Rac1-specific TCR 5934-transduced T cells (MFI 1958).

Mutant Rac1/2-specific T cells showed cytotoxicity against melanoma cell lines naturally expressing mutant Rac1

Next, we aimed to confirm the recognition of tumor cell lines that endogenously express the respective mutation. Presence of the Rac1P29S mutation in cell lines Mel55, Mel085, and Mel20aI has been confirmed by Sanger sequencing, interestingly Mel55 has lost the Rac wild type allele (data not shown). All tumor cells were GFP positive, as they were retrovirally transduced to express the positive control CDK4R24L coupled to GFP (Supplementary Figure 2A). Since Mel085 melanoma cells are HLA-A*02:01 negative, they were in addition retrovirally transduced to express HLA-A*02:01 as confirmed by flow cytometry (Supplementary Figure 2B). The other two cell lines are naturally HLA-A*02:01 positive. To analyze T cell reactivity against the natural occurring Rac1P29S mutation, the mutant Rac1 harboring melanoma cells were co-cultured with TCR-transduced T cells over 72 hours and cytotoxicity was measured by the decrease in GFP expressing target cells determined by live-cell imaging. Rac1-specific TCR 5934-transduced T cells showed cytotoxicity against all three cell lines (Figures 2A–C, left panels). The Mel085-A2 cells were also partially lysed by the Rac2-specific 22894 TCR-transduced T cells (Figure 2B, left panel), whereas all three Rac1/2-specific TCR-transduced T cell groups (TCRs 5934, A12B20 and 22894) were able to elicit cytotoxicity against Mel20aI cells (Figure 2C, left panel). The positive control CDK4-specific TCR 14/35-transduced T cells (28) lysed all CDK4R24L overexpressing target cells (Figures 2A–C, left panels). These experiments prove that the melanoma cell lines generally are able to process and present neoantigens. It further shows that the *in silico* predicted Rac1P29S epitope similarly is naturally processed and recognized by TCR-redirected T cells, which also could be confirmed when recombinantly mutant Rac1 cDNA was expressed in tumor cells (data not shown). As a positive control, all three cell lines were exogenously loaded with mutant Rac1P29S peptide. It showed that these peptide-loaded cells were efficiently recognized and lysed by the Rac1/2-specific TCR-transduced T cells (Figures 2A–C, right panels).

Mutant Rac1P29S triple epitope was recognized by Rac1/2-specific T cells *in vivo*

The two Rac1/2-specific TCRs that performed best *in vitro*, Rac2P29L-specific TCR 22484 and Rac1P29S-specific TCR 5934, were used to evaluate their ability to reject tumors *in vivo*. The fibrosarcoma cells MC703 (21), which were generated in an HLA-A*02:01-transgenic mouse (HHD, chimeric HLA-A*02:01/H-2D^{b}) (24), were transduced with the Rac1P29S triple epitope FSGEYIPTV coupled to GFP. Recognition of these cells was confirmed *in vitro* with and without loaded Rac1 mutant peptide (Figure 3A). As shown before, both TCR-transduced T cells recognized the target, recognition by Rac1-specific TCR 5934 was slightly higher compared to the heterologous Rac2-specific TCR 22894. Before the MC703-FSG cells were injected into HHDxRag$^{-/-}$ mice, the expression of FSG-GFP and HLA-A*02:01 was determined by flow cytometry (Figure 3B). Notably, 99% of injected cells were double positive. When tumors reached an average size of 300-500 mm^3, mice were treated with 1x10^6 TCR-transduced HHD T cells. As a negative control, mice were also treated with the irrelevant CDK4-specific TCR 14/35 or left untreated. As depicted in Figure 3C and Supplementary Figure 3A (respective SD and significance depicted in Supplementary Figures 3C, D), Rac1/2-specific 22894 and 5934 TCR-transduced T cells were able to induce regression, while CDK4-specific 14/35 TCR-transduced T cells treated tumors progressively grew after ATT. Interestingly, the heterologous Rac2-specific 22894 TCR-transduced T cells showed greater efficacy in tumor regression

TABLE 2 List of isolated Rac 1/2 -specific TCRs.

TCR	α chain	Frequency α chain	β chain	Frequency β chain	Immunization
A12B20	TRAV12-2*02 –CAAQSARQLTF –TRAJ22*01	3/12	TRBV20-1*01(/02) –CSARDLITDTQYF –TRBJ2-3*01	7/11	Rac1P29S$_{28\text{-}36}$
5934	TRAV13-1*01–CAASRGGAQKLVF – TRAJ54*01	12/15	TRBV3-1*01 –CASSQLAGGPLYNEQFF –TRBJ2-1*01	14/14	Rac1P29S$_{28\text{-}36}$
22894	TRAV13-1*03 – CAVGANNLFF – TRAJ39*01	8/13	TRBV2*01 – CAASMGNAGNMLTF – TRBJ2-7*01	10/12	Rac2P29L$_{28\text{-}36}$

Name of TCR, frequency and details of the alpha and beta chains as well as the CDR3 region are listed.

compared to the Rac1-specific TCR 5934. To investigate the differences in therapeutic outcome when targeting Rac1P29S$^+$ MC703-FSG tumors with either Rac1- or Rac2-specific T cells, we monitored the human TCR-transduced HHD$^+$ T cells after transfer into tumor-bearing mice in the second experiment (Figure 3D and Supplementary Figures 3A, B). On day 7 after ATT high numbers of CD8$^+$ Vβ22$^+$ 22894 T cells were detected, while T cell expansion of CD8$^+$ Vβ9$^+$ 5934 T cells was significantly lower. Similarly, target antigen irrelevant CD8$^+$ Vβ1$^+$ 14/35 T cells showed no amplification on day 7. When analyzing transferred T cells on day 21 it showed that 22894 T cells persisted at a significant higher level in comparison to 5934 and irrelevant 14/35 T cells. Of note, only CD8$^+$ but not CD8$^-$ human TCR$^+$ T cells expanded *in vivo* in response to Rac1P29S expressing MC703-FSG tumors (Supplementary Figure 3B).

To investigate potential reasons for tumor relapse after initial regression, we reisolated the MC703-FSG tumors and analyzed GFP as well as HLA-A*02:01 expression by flow cytometry (Figure 4A). Mice treated with the more efficient Rac2-specific 22894 TCR-transduced T cells showed almost complete loss of FSG-GFP expression down to 8%, while tumors treated with Rac1-specific 5934 TCR-transduced T cells showed partial loss (38% double positive T cells). Tumors treated with CDK4-specific 14/35 TCR-transduced T cells, which did not have any selective pressure on outgrowing FSG-GFP negative tumors, only showed a reduction in HLA-A*02:01 expression. These data suggest that tumors in the 22894 and 5934 TCR treated groups regressed due to target-specific lysis by T cells but subsequently FSG-GFP negative cells led to relapse. As shown in Figure 3B, the injected cells were composed of 1% antigen-negative cells, explaining this outgrowth and the selective pressure induced by target-specific TCR-transduced T cells. To confirm this hypothesis, we co-cultured reisolated tumors with a new batch of TCR-transduced T cells (Figure 4B). In line with previous data, tumors isolated from mice that were treated with Rac2-specific 22894 TCR-transduced T cells were not recognized by Rac1-specific 5934 TCR-transduced T cells, most likely due to outgrowth of antigen-negative variants. Tumors isolated from Rac1-specific 5934 TCR treated mice were partly recognized, while CDK4-specific 14/35 TCR treated tumors induced comparable IFNγ levels to MC703-FSG control cells which were not previously injected into mice. These *in vivo* data suggest that there might be a potential for ATT with heterologous TCRs that were isolated after immunization with peptides with stronger predicted peptide-MHC binding.

Recognition pattern and alloreactivity of Rac1/2-specific T cells

To exclude off-target toxicity of the Rac1/2-specific TCRs, we determined their recognition pattern with an alanine scan. To do so, TAP-deficient T2 cells were loaded with Rac1/2 peptides containing single alanine exchanges at concentrations of 10^{-9} M and 10^{-5} M and co-cultured with the respective TCRs. Using a threshold of 50% reduction compared to Rac1/2 unmodified peptide, we identified x (4)-Y-I-P-T-V as the recognition pattern for the TCRs 5934-Rac1 and 22894-Rac2 and F-x(2)-E-x(2)-P-x-V for TCR A12B20-Rac1 (Supplementary Figures 4A–C). We found one peptide in the G Protein Subunit Alpha Z (GNAZ) protein (A-A-A-D-Y-I-P-T-V, IC_{50} = 23.16 nM) with the same recognition pattern as the TCRs 22894-

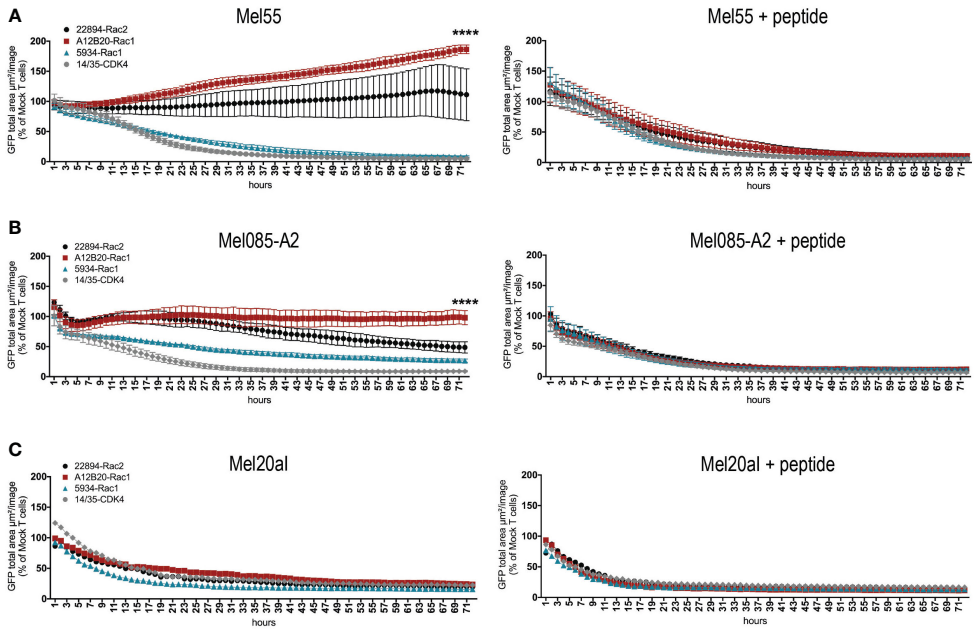

FIGURE 2
Rac1/2-specific T cells showed cytotoxicity against melanoma cell lines naturally expressing Rac1P29S. **(A-C)** 15x10^3 transduced CD8$^+$ T cells were co-cultured as triplicates at a 5:1 E:T ratio with **(A)** Mel55 cells, **(B)** Mel085-A2 and as singlets at a 15:1 E:T ratio with **(C)** Mel20al cells. Right panels show the same cell line loaded with 10^{-6} Rac1 mutant peptide. Cells were retrovirally transduced to express CDK4R24L full-length cDNA. Cytotoxicity was observed over 72 hours using the live cell imaging system IncuCyte Zoom (Essen Bioscience). Values were calculated by normalizing the average GFP total area (µm^2/image) in the target cells co-cultured with the respective TCR-transduced T cells to the average of that co-cultured with mock transduced T cells. The experiment was performed three times with similar results, for triplicate cultures graphs represent means ± SD. Cytotoxicity was compared at 72h using two-way ANOVA, only significant results are depicted.

10.3389/fimmu.2023.1119498

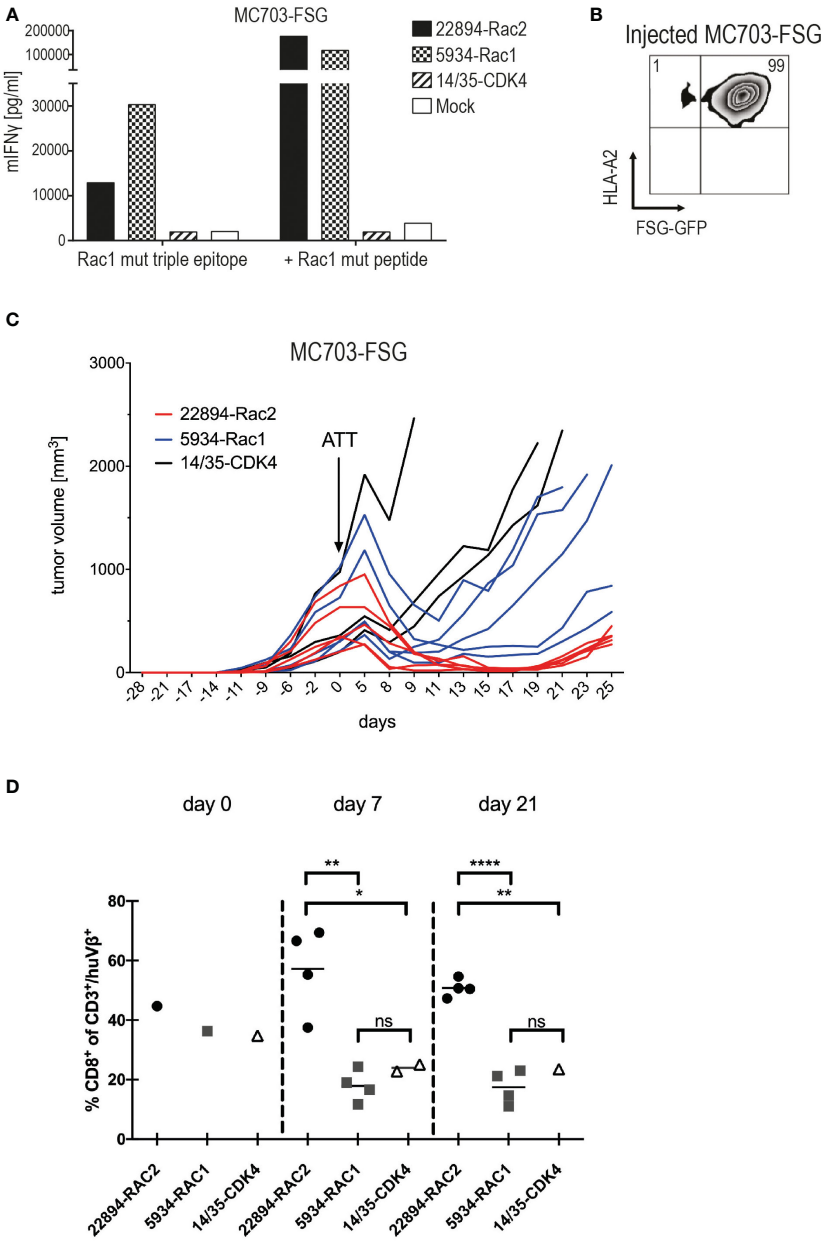

FIGURE 3
Heterologous Rac2-specific 22894 TCR-transduced T cells elicited tumor regression upon ATT. **(A)** TCR-transduced murine T cells were co-cultured with the mouse tumor cell line MC703 expressing FSG triple epitope (5'LTR - $(P29S)_3$ - GFP - PRE - 3'LTR) ($1x10^5$, 1:1 ratio) for 24 hours. IFNγ levels were determined in an ELISA assay. Cells were loaded with 10^{-6}M Rac1 mutant FSG peptide as a control. The experiment was performed at least three times, one representative experiment is shown. **(B)** FSG-GFP and HLA-A*02:01 expression of MC703-FSG cells before injection measured by flow cytometry. Number indicates percentage. **(C)** $1x10^6$ MC703-FSG cells were injected into HHDxRag$^{-/-}$ mice. Rac1/2-specific T cells were injected 28 days after tumor inoculation (arrow) at an average tumor size of 472 mm^3 (n=5, 22894-Rac2, red lines), 514 mm^3 (n=5, 5934-Rac1, blue lines) and 512 mm^3 (n=3, 14/35-CDK4, black lines), respectively. The experiment was performed two times with similar results (Supplementary Figure 3A), standard deviation (SD) and significance is shown in Supplementary Figure 3C. **(D)** Mutant Rac2- but not Rac1-specific TCR gene-modified T cells show rapid amplification upon recognition of Rac1P29S$^+$ FSG-GFP tumor cells. 22894, 5934 and 14/35 TCR-transduced T cells were identified by staining with anti-human Vβ22, Vβ9 and Vβ1 antibodies, respectively, and number of CD8$^+$/huTCR$^+$ T cells within the adoptively transferred CD3$^+$/huTCR$^+$ T cells was calculated. Of note, CD4$^+$/huTCR$^+$ T cells do not recognize Rac1P29S target cells (data not shown). Treatment groups were compared by unpaired t-test: d7, ** p=0.0022; * p=0.0378; d21, **** p<0.0001; ** p=0.0038; ns = not significant.

Rac2 and 5934-Rac1. We observed cross-recognition of GNAZ (AAA) peptide in a peptide titration assay (Supplementary Figure 4D) and in an assay using a mouse cell line transduced to express a GNAZ triple 35mer (Supplementary Figure 4E). However, human cell lines endogenously expressing GNAZ in high amounts (https://www.proteinatlas.org/ENSG00000128266-GNAZ/cell+line) were not recognized by TCR-transduced human T cells (Supplementary Figure 4F), demonstrating that this epitope is not processed and presented naturally in sufficient amounts. Since GNAZ is also highly expressed in brain tissue further evaluation of potential cross-reactivity will be necessary (29) to justify clinical application of TCRs 22894-Rac2 and 5934-Rac1 in high-risk patients in order to

10.3389/fimmu.2023.1119498

allow for effective tumor-killing without causing dose-limiting pathology in normal somatic tissues (30). For the Rac1-specific TCR A12B20 we identified a peptide in the Nibrin protein (F-R-I-E-Y-E-P-L-V, IC_{50} = 439 nM) with the same recognition pattern. Using a peptide titration assay we excluded cross-reactivity of TCR A12B20-Rac1 to this peptide (Supplementary Figure 4G).

Since the TCRs were isolated from transgenic mice expressing HLA-A*02:01 but no other HLAs, we tested for MHC alloreactivity using a panel of EBV-transformed lymphoblastoid B cell lines (LCLs) expressing different MHC class I molecules (Supplementary Table 1). No allorecognition of the Rac2-specific TCR 22894 (Supplementary Figure 5A) and Rac1-specific TCR 5934 (Supplementary Figure 5B) was observed using two different donors. In contrast, TCR A12B20-Rac1 transduced T cells recognized the LCL cell lines Bello and WT49. No shared HLA-A, -B or-C between these cell lines was detected, therefore, more research may be required to determine the scope of the allorecognition mediated by TCR A12B20-Rac1 (Supplementary Figure 5C).

Discussion

In this study, we investigated the potential of three Rac1P29S-specific TCRs derived after immunization of human TCR gene loci transgenic mice with peptide-epitopes containing either Rac1P29S or Rac2P29L mutation. We detected high affinity of all three TCRs transduced into human PBMCs against both the mutant Rac1 and the mutant Rac2 peptide-epitope loaded on TAP-deficient T2 cells. This indicates that the one amino acid change in the epitopes is only responsible for the binding affinity to MHC class I complexes (anchor residue) but not to the TCR, which was also confirmed by detecting the TCR recognition pattern by an alanine scan. Therefore, also the heterologous Rac2P29L-derived TCR can potentially be used clinically to target the more frequent melanoma mutation Rac1P29S. By demonstrating cytotoxicity of our TCR-transduced T cells against three melanoma cell lines harboring the Rac1P29S mutation we proved natural processing and presentation of the predicted Rac1P29S peptide epitope, a necessity not always given for *in silico* predicted neoepitopes but essential for clinical application in an adoptive T cell transfer setting (31, 32). Nevertheless, the three tested cell lines were recognized by the TCR-transduced T cells with varying efficacy. While the Mel20aI cells were lysed by all three TCR-transduced T cells (22894-Rac2, 5934-Rac1 and A12B20-Rac1), the Mel085-A2 and Mel55 cells were not recognized by A12B20. Due to their role in signaling, cell cycle and migration variable recognition might be caused by intrinsic properties of oncogenic Rac GTPase mutants, such as expression too low to be recognized by lower affinity TCRs.

The two TCRs which performed best in the cytotoxicity assays against the Rac1 mutation were subsequently used for *in vivo* studies. Interestingly, when we stained the TCRs with a mutant Rac1-specific pA2 tetramer, the 22894 Rac2-derived TCR showed higher staining intensity than the 5934 Rac1-derived TCR, suggesting that we isolated a TCR with higher affinity after immunization with a heterologous

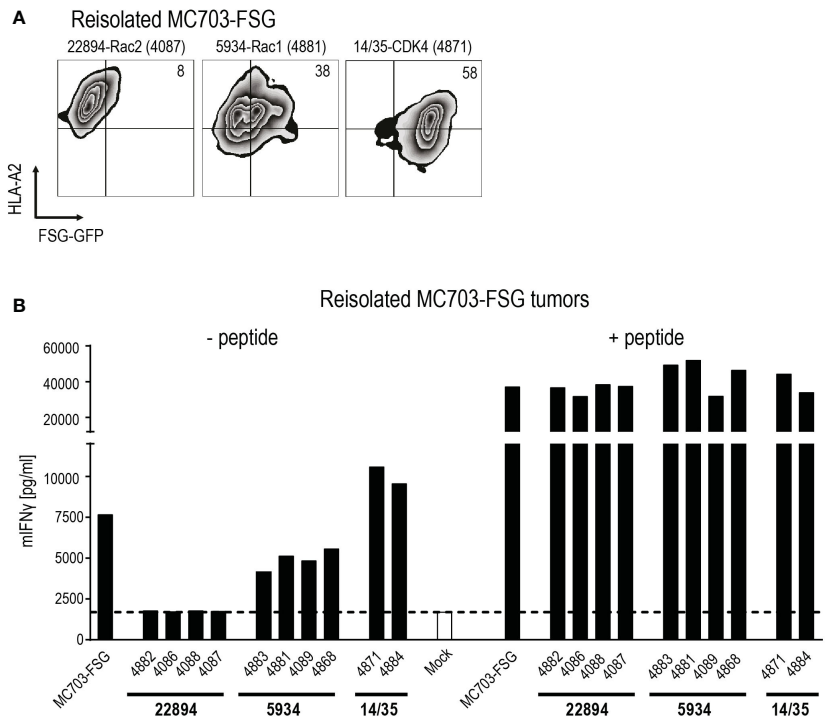

FIGURE 4
Tumor relapse upon transfer of heterologous mutant Rac2-specific T cells exclusively is due to selection of antigen-negative cancer cells. **(A)** Reisolated tumors were analyzed for HLA-A*02:01 and Rac1P29S FSG-GFP expression by flow cytometry. Numbers in plots indicate percentages. One representative plot per treatment group is depicted, mouse is indicated by numbers in parenthesis. **(B)** Recognition of reisolated tumors was measured in an IFNγ ELISA. Tumors were co-cultured with 5934 TCR-transduced T cells ($1x10^5$, 1:1 ratio) for 24 hours. PMA and Ionomycin (P/I) stimulation served as positive control. Cells were loaded with 10^{-6} M Rac1 mutant FSG peptide as control. Mock serves as negative control with no T cells added.

peptide. For HLA-A*02:01 leucine is the dominant anchor amino acid residue at position 2 (33). Thus, the hydrophobic leucine mutation in Rac2P29L at the primary anchor position 2 of the epitope (34) induces stronger binding to the HLA-A*02:01 molecule than the polar serine mutation in Rac1P29S [NetMHC 4.0, IC_{50} 2.3 nM versus 18.2 nM (Table 1)]. The phenomenon of enhancing HLA binding and T cell activation by anchor position modification has already been described as altered peptide ligand immunity where modified peptides may act as super-agonists (35, 36). In line with this finding, 22894 TCR-transduced T cells did also induce stronger regression of Rac1P29S expressing tumors in a syngeneic HLA-A2–transgenic mouse model after adoptive T cell therapy. Furthermore, upon antigen encounter, amplification of 22894 TCR-transduced $CD8^+$ T cells was significantly higher when compared to that of the $CD8^+$ T cells modified with 5934 Rac1-derived TCR, despite comparable T cell transduction rates and comparable recognition of $Rac1P29S^+$ tumor cells *in vitro*. Similar observations *in vivo* have been made with a CDK4R24C-derived human TCR that induced more effective rejection and tumor-specific $CD8^+$ T cell amplification when tumors expressed the isogenic CDK4R24L mutation (21). The exclusive selection of antigen-negative tumor cells by the heterologous Rac2-specific T cells that led to tumor relapse in our *in vivo* model argues for a strong T cell pressure. Such a selection phenomenon has also been seen in the clinic, when exclusively tumors relapsed under T cell pressure by Kras-specific T cells that had lost the respective restriction element (37). Since there are several recurrent neoantigens that harbor different mutations in the same hotspot region (e. g. Kras, p53), our finding might support the notion of using a heterologous peptide with higher predicted peptide MHC affinity for immunization to isolate TCRs with higher affinity and *in vivo* efficacy.

Our approach thus describes an *in vivo* affinity maturation that is still controlled by thymic selection and may lower the risk of off-target toxicity (38). As the mouse model, we isolated the TCRs from, only expresses human HLA-A2 and is therefore not tolerant for other HLA molecules, we in addition excluded the possibility of alloreactivity by LCL assays and alanine scans. We found that at least the two TCRs with highest clinical potential (22894 and 5934) were not alloreactive against other HLA expressing cell lines. TCR A12B20 showed alloreactivity against two LCLs and was therefore excluded from further use. The recognition pattern of the TCRs was detected in an alanine scan. For the identical recognition pattern of TCRs 5934 and 22894 we found one epitope derived from the GNAZ protein with an overlapping pattern. However, human cell lines naturally expressing this protein were not recognized and, therefore, we minimized the risk of off-target toxicity.

While *in vitro* the Rac1-specific 5934 TCR-transduced T cells performed slightly better in cytotoxicity and IFNγ release, the Rac2-specific 22894 TCR-transduced T cells expanded significantly better *in vivo* and induced more potent regression of the Rac1P29S expressing tumor cells. Discrepancies between *in vitro* and *in vivo* T cell responses have been described, e.g. when analyzing a TCR recognizing the mutant CDK4 isoforms R24L and R24C (21). Therefore, *in vivo* validation of targets and TCRs in suitable mouse models remains unavoidable so far.

In conclusion, we showed that the recurrent neoepitope $Rac1P29S_{28\text{-}36}$ is naturally processed and presented and can be successfully targeted with high-affinity TCR-transduced T cells. Rac1P29S-derived TCR 5934 as well as a heterologous Rac2P29L-derived TCR 22894 elicited cytotoxicity against melanoma cell lines naturally expressing the Rac1P29S mutation and induced regression against Rac1P29S expressing tumors *in vivo*. These data suggest that both TCRs show clinical potential of adoptive T cell therapy in HLA-A2 positive melanoma patients expressing the Rac1P29S mutation and open an avenue for using TCRs raised by a heterologous peptide with higher efficacy.

Data availability statement

The original contributions presented in the study are included in the article/Supplementary Material. Further inquiries can be directed to the corresponding author.

Ethics statement

All animal experiments were performed according to institutional and national guidelines and regulations and were approved by the Landesamt für Gesundheit und Soziales Berlin (H0086/16 and G0112/16).

Author contributions

GW designed the study. LI, GP, NG, VS, and AP conducted experiments and provided material. LI, GP, TB, and GW analyzed data and wrote the manuscript. TB and GW are joint last authors. All authors contributed to the article and approved the submitted version.

Funding

Funding was provided by grants from the German Research Foundation (SFB-TR36), the Berlin Institute of Health (CRG-1), Deutsche Krebshilfe (111546), DKTK joint funding (NEO-ATT), European Union (ERC Advanced Grant 882963) and the Helmholtz-Gemeinschaft, Zukunftsthema ‘Immunology and Inflammation’ (ZT-0027).

Acknowledgments

We thank Sabrina Horn, Kathrin Borgwald and Mathias Pippow for excellent technical support.

Conflict of interest

GW and TB are inventors on filed patent applications for the T-cell receptors described in the study WO2014083173A1, WO2022219155A1.

The remaining authors declare that the research was conducted in the absence of any commercial or financial relationships that could be construed as a potential conflict of interest.

The reviewer FM declared a shared affiliation with the authors LI, GP, and GW to the handling editor at the time of review.

Publisher's note

All claims expressed in this article are solely those of the authors and do not necessarily represent those of their affiliated organizations, or those of the publisher, the editors and the reviewers. Any product that may be evaluated in this article, or claim that may be made by its manufacturer, is not guaranteed or endorsed by the publisher.

Supplementary material

The Supplementary Material for this article can be found online at: https://www.frontiersin.org/articles/10.3389/fimmu.2023.1119498/full#supplementary-material

References

1. Finck AV, Blanchard T, Roselle CP, Golinelli G, June CH. Engineered cellular immunotherapies in cancer and beyond. *Nat Med* (2022) 28(4):678–89. doi: 10.1038/s41591-022-01765-8

2. Rizvi NA, Hellmann MD, Snyder A, Kvistborg P, Makarov V, Havel JJ, et al. Cancer immunology. mutational landscape determines sensitivity to pd-1 blockade in non-small cell lung cancer. *Science* (2015) 348(6230):124–8. doi: 10.1126/science.aaa1348

3. Blankenstein T, Leisegang M, Uckert W, Schreiber H. Targeting cancer-specific mutations by T cell receptor gene therapy. *Curr Opin Immunol* (2015) 33:112–9. doi: 10.1016/j.coi.2015.02.005

4. Davidson G, Coassolo S, Kieny A, Ennen M, Pencreach E, Malouf GG, et al. Dynamic evolution of clonal composition and neoantigen landscape in recurrent metastatic melanoma with a rare combination of driver mutations. *J Invest Dermatol* (2019) 139(8):1769–78 e2. doi: 10.1016/j.jid.2019.01.027

5. Porter AP, Papaioannou A, Malliri A. Deregulation of rho gtpases in cancer. *Small GTPases* (2016) 7(3):123–38. doi: 10.1080/21541248.2016.1173767

6. Mack NA, Whalley HJ, Castillo-Lluva S, Malliri A. The diverse roles of rac signaling in tumorigenesis. *Cell Cycle* (2011) 10(10):1571–81. doi: 10.4161/cc.10.10.15612

7. Krauthammer M, Kong Y, Ha BH, Evans P, Bacchiocchi A, McCusker JP, et al. Exome sequencing identifies recurrent somatic Rac1 mutations in melanoma. *Nat Genet* (2012) 44(9):1006–14. doi: 10.1038/ng.2359

8. Hodis E, Watson IR, Kryukov GV, Arold ST, Imielinski M, Theurillat JP, et al. A landscape of driver mutations in melanoma. *Cell* (2012) 150(2):251–63. doi: 10.1016/j.cell.2012.06.024

9. Cancer Genome Atlas N. Genomic classification of cutaneous melanoma. *Cell* (2015) 161(7):1681–96. doi: 10.1016/j.cell.2015.05.044

10. Blokx WA, van Dijk MC, Ruiter DJ. Molecular cytogenetics of cutaneous melanocytic lesions - diagnostic, prognostic and therapeutic aspects. *Histopathology* (2010) 56(1):121–32. doi: 10.1111/j.1365-2559.2009.03452.x

11. Lionarons DA, Hancock DC, Rana S, East P, Moore C, Murillo MM, et al. Rac1 (P29s) induces a mesenchymal phenotypic switch *Via* serum response factor to promote melanoma development and therapy resistance. *Cancer Cell* (2019) 36(1):68–83 e9. doi: 10.1016/j.ccell.2019.05.015

12. Watson IR, Li L, Cabeceiras PK, Mahdavi M, Gutschner T, Genovese G, et al. The Rac1 P29s hotspot mutation in melanoma confers resistance to pharmacological inhibition of raf. *Cancer Res* (2014) 74(17):4845–52. doi: 10.1158/0008-5472.CAN-14-1232-T

13. Vu HL, Rosenbaum S, Purwin TJ, Davies MA, Aplin AE. Rac1 P29s regulates pd-L1 expression in melanoma. *Pigment Cell Melanoma Res* (2015) 28(5):590–8. doi: 10.1111/pcmr.12392

14. Kawazu M, Ueno T, Kontani K, Ogita Y, Ando M, Fukumura K, et al. Transforming mutations of rac guanosine triphosphatases in human cancers. *Proc Natl Acad Sci USA* (2013) 110(8):3029–34. doi: 10.1073/pnas.1216141110

15. Sjoblom T, Jones S, Wood LD, Parsons DW, Lin J, Barber TD, et al. The consensus coding sequences of human breast and colorectal cancers. *Science* (2006) 314(5797):268–74. doi: 10.1126/science.1133427

16. Li LP, Lampert JC, Chen X, Leitao C, Popovic J, Muller W, et al. Transgenic mice with a diverse human T cell antigen receptor repertoire. *Nat Med* (2010) 16(9):1029–34. doi: 10.1038/nm.2197

17. Engels B, Cam H, Schuler T, Indraccolo S, Gladow M, Baum C, et al. Retroviral vectors for high-level transgene expression in T lymphocytes. *Hum Gene Ther* (2003) 14(12):1155–68. doi: 10.1089/104303403322167993

18. Ghani K, Wang X, de Campos-Lima PO, Olszewska M, Kamen A, Riviere I, et al. Efficient human hematopoietic cell transduction using Rd114- and galv-pseudotyped retroviral vectors produced in suspension and serum-free media. *Hum Gene Ther* (2009) 20(9):966–74. doi: 10.1089/hum.2009.001

19. Morita S, Kojima T, Kitamura T. Plat-e: An efficient and stable system for transient packaging of retroviruses. *Gene Ther* (2000) 7(12):1063–6. doi: 10.1038/sj.gt.3301206

20. Sun Y, Sijts AJ, Song M, Janek K, Nussbaum AK, Kral S, et al. Expression of the proteasome activator Pa28 rescues the presentation of a cytotoxic T lymphocyte epitope on melanoma cells. *Cancer Res* (2002) 62(10):2875–82.

21. Leisegang M, Kammertoens T, Uckert W, Blankenstein T. Targeting human melanoma neoantigens by T cell receptor gene therapy. *J Clin Invest* (2016) 126(3):854–8. doi: 10.1172/JCI83465

22. Obenaus M, Leitao C, Leisegang M, Chen X, Gavvovidis I, van der Bruggen P, et al. Identification of human T-cell receptors with optimal affinity to cancer antigens using antigen-negative humanized mice. *Nat Biotechnol* (2015) 33(4):402–7. doi: 10.1038/nbt.3147

23. Uckert W, Becker C, Gladow M, Klein D, Kammertoens T, Pedersen L, et al. Efficient gene transfer into primary human Cd8+ T lymphocytes by mulv-10a1 retrovirus pseudotype. *Hum Gene Ther* (2000) 11(7):1005–14. doi: 10.1089/10430340050015310

24. Pascolo S, Bervas N, Ure JM, Smith AG, Lemonnier FA, Perarnau B. Hla-A2.1-Restricted education and cytolytic activity of Cd8(+) T lymphocytes from Beta2 microglobulin (Beta2m) hla-A2.1 monochain transgenic h-2db Beta2m double knockout mice. *J Exp Med* (1997) 185(12):2043–51. doi: 10.1084/jem.185.12.2043

25. Jurtz V, Paul S, Andreatta M, Marcatili P, Peters B, Nielsen M. Netmhcpan-4.0: Improved peptide-mhc class I interaction predictions integrating eluted ligand and peptide binding affinity data. *J Immunol* (2017) 199(9):3360–8. doi: 10.4049/jimmunol.1700893

26. Zhao W, Sher X. Systematically benchmarking peptide-mhc binding predictors: From synthetic to naturally processed epitopes. *PloS Comput Biol* (2018) 14(11):e1006457. doi: 10.1371/journal.pcbi.1006457

27. Sette A, Sidney J, del Guercio MF, Southwood S, Ruppert J, Dahlberg C, et al. Peptide binding to the most frequent hla-a class I alleles measured by quantitative molecular binding assays. *Mol Immunol* (1994) 31(11):813–22. doi: 10.1016/0161-5890(94)90019-1

28. Wolfel T, Hauer M, Schneider J, Serrano M, Wolfel C, Klehmann-Hieb E, et al. A P16ink4a-insensitive Cdk4 mutant targeted by cytolytic T lymphocytes in a human melanoma. *Science* (1995) 269(5228):1281–4. doi: 10.1126/science.7652577

29. Cakmak-Gorur N, Radke J, Rhein S, Schumann E, Willimsky G, Heppner FL, et al. Intracellular expression of Flt3 in purkinje cells: Implications for adoptive T-cell therapies. *Leukemia* (2019) 33(4):1039–43. doi: 10.1038/s41375-018-0330-7

30. Morgan RA, Chinnasamy N, Abate-Daga D, Gros A, Robbins PF, Zheng Z, et al. Cancer regression and neurological toxicity following anti-Mage-A3 tcr gene therapy. *J Immunother* (2013) 36(2):133–51. doi: 10.1097/CJI.0b013e3182829903

31. Immisch L, Papafotiou G, Popp O, Mertins P, Blankenstein T, Willimsky G. H3.3k27m mutation is not a suitable target for immunotherapy in hla-A2⁺ patients with diffuse midline glioma. *J Immunother Cancer* (2022) 10(10):1-7. doi: 10.1136/jitc-2022-005535

32. Willimsky G, Beier C, Immisch L, Papafotiou G, Scheuplein V, Goede A, et al. *In vitro* proteasome processing of neo-splicetopes does not predict their presentation *in vivo*. *Elife* (2021) 10:1-22. doi: 10.7554/eLife.62019

33. Falk K, Rotzschke O, Stevanovic S, Jung G, Rammensee HG. Allele-specific motifs revealed by sequencing of self-peptides eluted from mhc molecules. *Nature* (1991) 351 (6324):290–6. doi: 10.1038/351290a0

34. Sidney J, Assarsson E, Moore C, Ngo S, Pinilla C, Sette A, et al. Quantitative peptide binding motifs for 19 human and mouse mhc class I molecules derived using positional scanning combinatorial peptide libraries. *Immunome Res* (2008) 4:2. doi: 10.1186/1745-7580-4-2

35. Galloway SAE, Dolton G, Attaf M, Wall A, Fuller A, Rius C, et al. Peptide super-agonist enhances T-cell responses to melanoma. *Front Immunol* (2019) 10:319. doi: 10.3389/fimmu.2019.00319

36. Katsara M, Minigo G, Plebanski M, Apostolopoulos V. The good, the bad and the ugly: How altered peptide ligands modulate immunity. *Expert Opin Biol Ther* (2008) 8 (12):1873–84. doi: 10.1517/14712590802494501

37. Tran E, Robbins PF, Lu YC, Prickett TD, Gartner JJ, Jia L, et al. T-Cell transfer therapy targeting mutant kras in cancer. *N Engl J Med* (2016) 375(23):2255–62. doi: 10.1056/NEJMoa1609279

38. Cameron BJ, Gerry AB, Dukes J, Harper JV, Kannan V, Bianchi FC, et al. Identification of a titin-derived hla-A1-Presented peptide as a cross-reactive target for engineered mage A3-directed T cells. *Sci Transl Med* (2013) 5(197):197ra03. doi: 10.1126/scitranslmed.3006034

frontiers | Frontiers in Immunology

TYPE Review
PUBLISHED 06 March 2023
DOI 10.3389/fimmu.2023.1121030

OPEN ACCESS

EDITED BY
Ralf-Holger Voss,
Johannes Gutenberg University Mainz, Germany

REVIEWED BY
Hinrich Abken,
Regensburg Center for Interventional Immunology (RCI), Germany
Bipulendu Jena,
Independent Researcher, San Diego, United States

*CORRESPONDENCE
Michael Hiltensperger
michael.hiltensperger@tum.de
Angela M. Krackhardt
angela.krackhardt@tum.de

SPECIALTY SECTION
This article was submitted to Cancer Immunity and Immunotherapy, a section of the journal Frontiers in Immunology

RECEIVED 11 December 2022
ACCEPTED 15 February 2023
PUBLISHED 06 March 2023

CITATION
Hiltensperger M and Krackhardt AM (2023) Current and future concepts for the generation and application of genetically engineered CAR-T and TCR-T cells. *Front. Immunol.* 14:1121030. doi: 10.3389/fimmu.2023.1121030

Current and future concepts for the generation and application of genetically engineered CAR-T and TCR-T cells

Michael Hiltensperger[1,2]* and Angela M. Krackhardt[1,2,3,4]*

[1]German Cancer Consortium (DKTK), partner site Munich and German Cancer Research Center (DKFZ), Heidelberg, Germany, [2]IIIrd Medical Department, Klinikum rechts der Isar, School of Medicine, Technical University of Munich, Munich, Germany, [3]Center for Translational Cancer Research (TranslaTUM), School of Medicine, Technical University of Munich, Munich, Germany, [4]Bavarian Cancer Research Center (BZKF), Erlangen, Germany

Adoptive cell therapy (ACT) has seen a steep rise of new therapeutic approaches in its immune-oncology pipeline over the last years. This is in great part due to the recent approvals of chimeric antigen receptor (CAR)-T cell therapies and their remarkable efficacy in certain soluble tumors. A big focus of ACT lies on T cells and how to genetically modify them to target and kill tumor cells. Genetically modified T cells that are currently utilized are either equipped with an engineered CAR or a T cell receptor (TCR) for this purpose. Both strategies have their advantages and limitations. While CAR-T cell therapies are already used in the clinic, these therapies face challenges when it comes to the treatment of solid tumors. New designs of next-generation CAR-T cells might be able to overcome these hurdles. Moreover, CARs are restricted to surface antigens. Genetically engineered TCR-T cells targeting intracellular antigens might provide necessary qualities for the treatment of solid tumors. In this review, we will summarize the major advancements of the CAR-T and TCR-T cell technology. Moreover, we will cover ongoing clinical trials, discuss current challenges, and provide an assessment of future directions within the field.

KEYWORDS

genetically engineered T cells, cancer immunotherapy, adoptive cell therapy (ACT), CAR-T cells, TCR-T cells, CAR (chimeric antigen receptor), TCR (T cell receptor)

1 Introduction

Cancer immunotherapies, specifically immune checkpoint inhibition (ICI), have shown high efficacy in the treatment of an increasing number of cancer entities (1). However, a significant portion of patients does not respond to ICI and there is an unmet medical need in these patients for alternative treatment options. One promising new avenue for the treatment of refractory tumors is the field of adoptive T-cell therapy with hundreds of ongoing clinical trials (2). This cell-based personalized therapy either utilizes

the patients' own tumor-infiltrating lymphocytes (TIL) or uses genetically modified T cells with engineered chimeric antigen receptors (CAR) or T cell receptors (TCR) to target and kill tumor cells. Its most prominent form is CAR-T cell therapy, which shows great efficacy in certain hematological cancers and several CAR-T cell therapies have already been approved by the Food and Drug Administration (FDA) for the treatment of blood cancers (2). CAR designs have undergone many iterations in a short amount of time and led to impressive improvements over previous generations of CAR formats. However, their effectiveness in the treatment of solid tumors so far is limited. On the other hand, TCR-T cell therapies have not yet been approved for clinical application but are currently tested in early clinical trials (2). TCR-T cells are not restricted to surface antigens and are more sensitive regarding the level of antigens on the tumor cell compared to CAR-T cells (3). Their dependence on a specific human leukocyte antigen (HLA) composition of the patients, however, restricts this therapy to specific patient populations. Here, we will give an overview of the vast field of CAR-T and TCR-T cell therapy from the manufacturing processes and their impact on the antitumor activity of the T cell product to the feasibility of potential strategies to improve the treatment of refractory tumors.

2 Design of engineered CAR and TCR formats

Endogenous and engineered TCRs recognize peptide-HLA complexes on target cells representing the antigen of interest. Engineered TCRs in general do not deviate from the classical TCR structure of an α-/β-chain heterodimer and are able to form functional TCR-CD3 complexes (Figure 1, left). Upon antigen recognition the two intracellular CD3ζ domains induce downstream TCR signaling. In contrast, CARs are designed as single molecules that consists of a single-chain variable fragment (scFV), a hinge domain, a transmembrane domain, and intracellular costimulatory signaling domains (Figure 1, right). Antigen recognition is facilitated by the scFV, a fusion protein of the light and heavy chain variable regions of an antibody that are connected by a peptide linker (4). Contrary to engineered or endogenous TCRs, CARs cannot assemble CD3 complexes and antigen recognition of surface antigens by the scFV is HLA-independent. First-generation CARs proved the feasibility of the concept by showing that coupling to an intracellular CD3ζ domain is sufficient for downstream signaling upon antigen recognition (5). The next iteration to the format included a costimulatory signaling domain, CD28 or 4-1BB, proximal to the membrane to incorporate both primary and costimulatory signaling with increased IL-2 production (6). To enhance antitumor activity and potentially increase persistence of CAR-T cells, a second costimulatory domain was added in third-generation CARs (7, 8). There is a number of third-generation CAR-T cells currently tested in clinical studies (NCT03676504 (9); NCT04049513 (10)) that showed good safety profiles and will evaluate their persistence in patients with $CD19^+$ malignancies. One interesting finding in support of this comes from a phase I clinical trial (NCT01853631) that observed greater expansion and longer persistence of CD19 third-generation (CD28 and 4-1BB) CAR-T cells compared to second-generation (CD28) cells when infused simultaneously in patients with r/r NHL (11). A new concept was applied in fourth-generation CARs or T cells redirected for antigen-unrestricted cytokine-initiated killing (TRUCKs). TRUCKs combine the introduction of a CAR with a transgenic expression cassette consisting of synthetic nuclear factor of activated T-cells (NFAT) response elements with an IL-2 minimal promoter and transgenes. CD3ζ-mediated signaling ultimately leads to the phosphorylation of NFAT, its translocation into the nucleus, and the expression of the transgenes (12). Because the TRUCK concept is dependent on CD3ζ-mediated NFAT translocation, it is applicable not only for CAR-T but also for

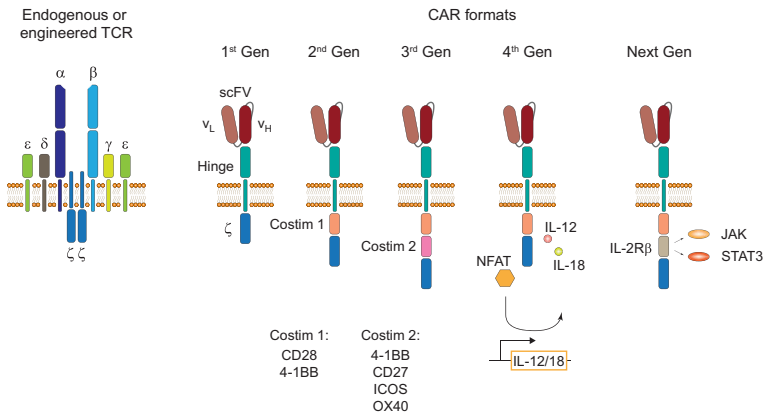

FIGURE 1
TCR and CAR formats. Structure of an endogenous or genetically engineered T cell receptor (TCR)-CD3 complex (left). Generations of chimeric antigen receptors (CARs) and their structural differences (right). First-generation (1st Gen) CARs only consist of a single-chain variable fragment (scFV), a hinge domain/spacer, and an intracellular CD3ζ signaling domain. Second- (2nd Gen) and third-generation (3rd Gen) CARs include one or two costimulatory domains, respectively. Fourth-generation (4th Gen) CARs or T cells redirected for antigen-unrestricted cytokine-initiated killing (TRUCKs) include a transgenic expression cassette for nuclear factor of activated T-cells (NFAT)-mediated transgene expression. Next-generation (Next Gen) CARs include a truncated intracellular domain of cytokine receptors with a STAT-binding motif for JAK/STAT signaling.

TCR-T cells (13). The most common transgenic proteins for this approach are IL-12 and IL-18 (14–17) but many other cytokines and enzymes are currently explored (12). The TRUCK concept is of particular interest for the treatment of solid tumors by combining T cell-mediated killing with immune modulation of the tumor microenvironment (TME) through the secretion of cytokines. IL-12 and IL-18 secretion in the TME might augment the antitumor cascade by attracting and activating macrophages and NK cells (13). Since CAR constructs do not have a specific domain for cytokine-mediated signaling (also known as signal 3), novel developments include CARs with a truncated intracellular domain of cytokine receptors (e.g. IL-2 receptor β (IL-2Rβ) domain) and a STAT3-binding motif to induce JAK/STAT signaling (18). This approach prevented terminal differentiation *in vitro* and showed increased persistence and antitumor activity in preclinical tumor models compared to second-generation CAR-T cells (18) but this format likely needs further evaluation to prove its translational potential.

CAR-T cells have inherently lower antigen sensitivity compared to canonical T cells and tonic CAR signaling has been associated with CAR-T cell exhaustion (3, 19). This is likely at least in part due to the differences in signaling modalities of a TCR-CD3 complex that contains 10 immunoreceptor tyrosine-rich activation motifs (ITAMs) compared to conventional CARs that only contain three ITAMs (20). To engage the endogenous CD3 signaling complex with antibody-mediated antigen recognition, a double-chain chimeric receptor, termed synthetic TCR and antigen receptor (STAR), fused the constant α and β domain to the light and heavy chain variable regions of an antibody has been developed (21). Upon antigen recognition, STAR has been demonstrated to provide TCR-like signaling with superior antigen sensitivity and antitumor activity compared to a second-generation CAR-T cell in solid tumor mouse models. This might be an interesting new design, however, a potential risk for increased on-target off-tumor toxicity due to its enhanced antigen sensitivity could limit its clinical application and needs to be investigated.

3 Manufacturing of genetically engineered T cells

Genetically engineered T cell products were initially developed in open self-operated bioreactors that are common in academic institutions. However, these systems require well-trained staff and rigorous hygiene monitoring to avoid contaminations. Therefore, with the clinical successes of CAR-T cell therapies, the production has shifted not only in industrial facilities but also in academic institutions more and more to closed and semi- or fully-automated platforms (22–25). Most advances to the manufacturing platforms for CAR-T cells are likely transferable for the production of TCR-T cells with some modifications to the protocols. Therefore, TCR-T cell therapies greatly benefit from the innovations in the ACT field which were set in motion by the clinical approval of CAR-T cell therapies. The general workflow of CAR-T and TCR-T cell therapy is depicted in Figure 2 and will be summarized in this chapter in detail.

3.1 Cell collection and handling

For the generation of genetically engineered T cells, leukocytes are collected either from patients (autologous) or healthy donors (allogeneic). Notably, all FDA-approved CAR-T cell therapies to date are using patient-derived autologous cells but there is a number of clinical trials investigating the use of donor-derived allogeneic cells (2). Leukapheresis is the method of choice for the collection of leukocytes due to its availability at health care centers, patient tolerability, and its high yield of T cells for manufacturing (27, 28). Collected cells are either used fresh for direct manufacturing or more commonly cryopreserved for later handling. Cryopreservation takes place at the clinical center or in some cases at the manufacturing center. Although, cryopreservation has an impact on cell viability, on-site manufacturing of genetically engineered T cells is often not feasible – with the exception of a few academical clinical studies (NCT03676504 (9)) – and CAR-T cell generation can be achieved with frozen cells (29). There are differences of the cryopreservation procedure across clinical and manufacturing centers for different T cell products, regarding freezing media composition and durations, but their impact on the final product quality has not yet been comparably assessed.

3.2 Impact of starting cell composition on antitumor immunity

The cellular composition of the starting material is paramount for the success to engineer a functional CAR-T cell product with

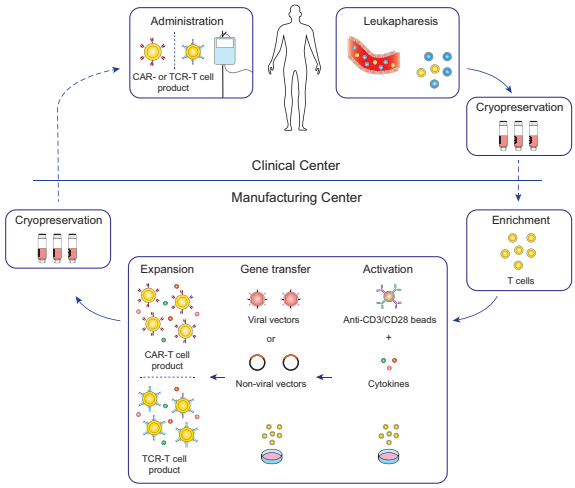

FIGURE 2
Workflow for conventional CAR-T and TCR-T cell therapy. For most conventional CAR-T and TCR-T cell therapies, autologous patient-derived leukocytes are collected by leukapheresis at clinical centers (top) and after cryopreservation shipped to manufacturing centers (bottom). Enriched T cells are genetically engineered with either CARs or TCRs and after expansion cryopreserved and shipped to the clinical centers for infusion into the patients. Lymphodepleting chemotherapy is generally recommended in the week before infusion to increase engraftment of the genetically engineered T cells (26).

long-lived antitumor properties. Enrichment of T cells from the leukapheresis product can be achieved with magnetic separation beads and all approved CAR-T cell therapies to date either use $CD4^+$ and $CD8^+$ T cells in a combined or a separate culture setting. Thus, CAR-T cell therapies are not limited to only generating $CD8^+$ CAR-T cell responses but also utilize $CD4^+$ CAR-T cells to improve their antitumor response in a synergistic fashion (30, 31). $CD4^+$ T cells show more plasticity compared to $CD8^+$ T cells and are comprised of T helper (Th) subsets and regulatory T (Treg) cells (32). Perturbation of $CD4^+$ subsets and generation of Treg cells in particular might have an impact on the clinical response. In a recent study, the expansion of CAR-Treg cells has been associated with resistance to CD19 CAR-T cell therapy (33). Therefore, differentiation of $CD4^+$ T cells to an "optimal" antitumor phenotype and limited generation of CAR-Treg cells during manufacturing might be essential to improve ACT. Separate manufacturing and administration of $CD4^+$ and $CD8^+$ T cells is already applied for the CD19 CAR-T cell therapy Breyanzi to reduce variability between the $CD4^+$ and $CD8^+$ CAR-T cell composition and to administer it in a dose-defined manner (34). In a clinical trial of a CD22 CAR-T cell therapy in children and young adults with $CD22^+$ B-cell neoplasms, the change of the manufacturing protocol to $CD4^+$ and $CD8^+$ T cell selection improved manufacturing feasibility and reduced variability, however, this led to increased inflammatory toxicities and warranted dose de-escalation (35). The overall complete remission rate was still very high with 70% but may indicate CAR-T cell-induced toxicities based on the ratio of $CD4^+/CD8^+$ cells in the CAR-T cell product. In some cases separate manufacturing of $CD4^+$ and $CD8^+$ CAR-T cells could compromise CAR-T cell expansion. This has been the case in a third-generation CD20 CAR-T cell therapy where changing from $CD4^+/CD8^+$ selection to a combined culture setting improved manufacturing feasibility and clinical response rates (36). Moreover, enrichment and differentiation of specific memory T cell subsets, like multipotent T memory stem (TSCM) cells, may improve the antitumor responses of CAR-T cells (37, 38). This might be due to a certain level of stemness of the T cells that comes with higher T cell persistence and less susceptibility to exhaustion (39–41). Overall, the impact of the cellular composition during manufacturing on the antitumor efficacy of T cell therapies still needs to be compared in future clinical studies.

3.3 Activation conditions during manufacturing

T cells are activated for efficient gene transfer and expansion which is commonly achieved by using anti-CD3/CD28 paramagnetic beads for viral transduction (42). However, this approach was reported to favor the expansion of $CD4^+$ T cells over $CD8^+$ T cells in non-enriched products (43) and could lead to even inefficient expansion of $CD8^+$ T cells in some cases (44). This is likely due to the importance of CD28-mediated signaling in $CD4^+$ T cells while 4-1BB costimulation is superior for the expansion of $CD8^+$ memory T cells (44). To overcome this, current protocols have introduced cytokine cocktails in addition to anti-CD3/CD28 beads to support the expansion and to skew the differentiation into a phenotype with inherent good antitumor characteristics (45–49). For example, the cytokine IL-2 is used in standard protocols for its mitogenic effects on T cells and its potential benefits on T cell effectiveness in the context of tumor immunity (50).

In addition, the activation conditions and strength of the stimuli during manufacturing could also determine if the genetically engineered T cells are prone to exhaustion upon encountering their cognate antigen on the tumor cells. Soluble anti-CD3 antibodies together with mononuclear cells have been shown to result in a similar expansion efficacy of $CD8^+$ T cells compared to anti-CD3/CD28 beads but induced a less terminally differentiated phenotype as well as less antigen-induced cell death and more expansion in previously activated $CD8^+$ T cells (51). Acquisition of terminal differentiated effector functions during manufacturing actually may lead to impaired antitumor immunity *in vivo* (52). Due to the sensitive nature of T cell activation and differentiation and their impact on antitumor immunity and longevity of the genetically engineered T cells, new methods are constantly investigated. The Expamer technology is an interesting new approach for time-controlled initiation and termination by using soluble Strep-Tactin multimers that can be assembled with Twin-Strep-tag conjugated anti-CD3 and anti-CD28 Fab fragments and dissociated by adding non-toxic D-biotin (53). Soluble addition and inactivation of Expamer components for T cell activation is particularly attractive for large-scale production and might be useful to avoid overstimulation and subsequent apoptosis. On the other hand, less rigid surfaces for immobilization of anti-CD3/CD28 binders might be a better alternative since they have been shown to induce higher IL-2 production and expansion of $CD4^+$ and $CD8^+$ T cells ex vivo (54). Consistent with this, an antigen-presenting cell (APC)-mimetic scaffold that consists of a fluid lipid bilayer supported by mesoporous silica micro-rods and attached with anti-CD3/CD28 antibodies promoted two- to tenfold greater expansion compared to anti-CD3/CD28 paramagnetic beads (55). However, lipid bilayer systems might be less appealing compared to bead-based approaches for activation when it comes to large-scale manufacturing due to their increased technical complexity regarding handling and ease of removal. More studies that compare the effects of different activation conditions on the final T cell product for ACT will be necessary in the future in order to understand their impact on the clinical efficacy.

3.4 Gene transfer methods

Viral vectors are used for all approved CAR-T cell therapies and most clinical trials for CAR- and TCR-T cell therapies due to their efficiency for stable gene transfer (56). Lentiviral (LV) and γ-retroviral vectors are the vectors of choice for cell engineering since they can carry larger genetic constructs and integrate the target gene into the genome of the engineered T cells compared to other viral vectors (57, 58). However, streamlining the generation of large quantities of viral vectors for manufacturing is a challenge and ensuring that no residual viral vectors or accidently transduced

malignant cells are given to the patients comes with extensive and costly safety testing (59, 60). This presents difficulties for scaling out manufacturing and for making these therapies more affordable to meet the increasing demand for ACT. Therefore, non-viral approaches are currently investigated in early trials. Transposon-based gene delivery approaches, such as Sleeping Beauty (SB) or PiggyBac (PB) transposons, are cheaper and can carry larger genetic constructs compared to viral vectors while still integrating their target gene (61). SB transposition has already been used successfully for the manufacturing of CD19 or SLAMF7 CAR-T cells in early clinical trials without severe toxicity (62–65). In addition, automation of SB transposition was feasible and could be very attractive for large-scale manufacturing (25). Although PB transposition was also successful for the manufacturing of CAR-T cells and even showed an inclination to promote the generation of desired TSCM CAR-T cells (66, 67), a recent clinical trial observed the formation of CAR-T cell lymphoma in two out of ten patients (68, 69). This presented the first cases of malignant lymphoma derived from CAR-T cells and the investigators of the study caution for regular follow-ups of the patients receiving CAR-T cell therapies, especially when new methods for gene transfer are applied (69). The underlying causes for the observed malignant transformation in this study using the PB system is not fully understood yet. Insertional mutagenesis did not seem to be the cause since the pattern of integration of the CAR transgene was comparable to other studies using PB and in line with studies using viral systems (68). However, transcriptional upregulation of surrounding regions by the transgene promotor was observed but how these alterations may be involved in malignant transformation needs to be further addressed. The authors of the study do not think that this finding is an inherent problem with the PB system but rather it might be based on their manufacturing methodology with high-voltage electroporation and high concentration of transposon and transposase (69). Understanding the underlying mechanisms will help to develop safer manufacturing protocols and better safety readouts in the future.

Genome editing is a promising novel approach not only for the generation of genetically engineered autologous but also for "off-the-shelf" allogeneic T cells that might solve manufacturing challenges and excessive cost that are inherent to autologous T-cell therapies. In particular, clustered regularly interspaced short palindromic repeat (CRISPR)-Cas9 has already been used for the generation and clinical application of CAR-T cells with tolerable adverse events in cancer patients (70, 71). Multifactorial genome editing holds great potential for ACT with genetically engineered T cell in the future but will need further optimization and extensive safety monitoring to assess the risks for harmful off-target events. More information about CRISPR-Cas9 genome editing for the generation of engineered T cells is reviewed in (72, 73).

3.5 Shortening manufacturing time of genetically engineered T cells

An important avenue for optimizing the manufacturing process of genetically engineered T cells is reducing the manufacturing time. This will reduce the cost and will scale-up manufacturing due to a faster turn-around of the engineered T cells. Most importantly, it might reduce mortality of patients with rapidly progressing cancers by reducing the vein-to-vein time. Standard protocols for CAR-T cell therapy culture CAR-T cells for 11 to 24 days which leads to a high number of harvested CAR-T cells (45–48). Interestingly, reducing the culture time of CD19 CAR-T cells to only 3 days increased their antitumor activity even at a 6-fold lower dose in a human xenograft model of acute lymphoblastic leukemia (ALL) (74). This could be due to an enriched proportion of stem-like T cells in the CAR-T product at reduced culture times. Remarkable manufacturing times haven been achieved with the FastT CAR-T next-day manufacturing platform, that was recently evaluated in a clinical trial for B-cell ALL (NCT03825718 (75)). Next day manufacturing with activation, LV transduction, and without expansion was feasible for all 25 patients with a tolerable safety profile and promising efficacy. Moreover, CD19 FasT CAR-T cells showed less exhaustion and a younger cellular phenotype compared to conventionally manufactured CAR-T cells *in vitro* but evaluation in larger clinical studies is needed. In addition, the T-Charge platform was used for manufacturing of CD19 CAR-T-cells in a phase I study with promising efficacy and safety profile (NCT03960840 (76)). The manufacturing time was less than 2 days and culturing time only took 24 hours. This approach also preserved naïve T and TSCM cells in the final CAR-T cell product which might increase the persistence of the genetically engineered T cells in patients. Rapid manufacturing of CAR-T cells was even demonstrated without activation and expansion within 24 hours and showed improved anti-leukemic activity in mouse xenograft models when compared to their conventionally manufactured counterparts (77). These new approaches seem to have great potential to reduce the vein-to-vein time which would greatly benefit the patients. However, since most of the T cell expansion takes place in the patients, this could mean that adverse events might be more difficult to predict in a temporal fashion upon therapy administration. Therefore, these new methods will have to be thoroughly tested in clinical trials with rigorous monitoring to ensure non-inferiority in efficacy and safety in comparison to standard long-time manufacturing procedures. Improving and standardizing manufacturing protocols for genetically engineered T cells, with every step potentially having an extensive impact on the antitumor activity and safety, is especially difficult since in-depth manufacturing protocols of approved CAR-T therapies are not publicly available. This will present a challenge for the future but overcoming this roadblock by greater exchange could fuel innovation and accessibility of these groundbreaking new therapies.

4 Targeted gene delivery *in vivo*

Due to the high cost of ex vivo T cell manufacturing, long vein-to-vein times which are problematic for highly progressive cancers, and the risk of manufacturing failure, targeted *in vivo* programming of T cells could be a viable alternative. DNA-carrying nanoparticles have been demonstrated to translocate into the nucleus of T cells followed by CAR expression in the targeted T cells (78). In addition,

in vivo administration of mRNA nanocarriers for the delivery of antitumor CARs or antiviral TCRs showed transient expression in T cells and comparable disease regression in mice compared to their ex vivo manufactured counter parts (79). These carrier systems are inexpensive and can be manufactured in large scale for broader distribution but their safety profile and efficacy regarding long-term disease remission is still largely unclear. The transient expression will likely reduce certain safety concerns, such as programing of malignant cells by accident and rendering them resistant to therapy (59) or the formation of CAR-T lymphoma (69). However, the lack of long-term T memory formation could hinder the efficacy of the treatment and might lead to earlier relapses compared to ex vivo manufactured T cells. Thus, their efficacy compared to more established approaches, such as bispecific T cell engagers (BiTEs), might not be superior.

Viral approaches have also been tested for long-term programing of T cells *in vivo*. Adeno-associated virus (AAV) vector achieved introduction of CARs in humanized mice and resulted in tumor regression (80). The AAV-based gene therapy LUXTURNA for the treatment of patients with *RPE65*-mediated inherited retinal dystrophy (81) is the first of its kind that received FDA approval, which could increase the interest for AVV vectors also for the clinical application of T cell programming *in vivo* for the treatment of cancer. A strategy for targeted *in vivo* engineering of a CD19 CAR was shown in a study using CD8α-chain targeted LVs (82). Although the specificity for CD8 T cells was good with this approach, NK and NKT cells also showed transduction for the CD19 CAR since they are also expressing the targeted CD8α-chain. LV targeting to $CD3^+$ T cells was also feasible by using bispecific antibody tandem fragments that bind the mutant E2 glycoprotein on Sindbis pseudotyped lentiviral vector (SINV-LV) and CD3 on T cells, achieving specific *in vivo* introduction of a CD19 CAR into T cells with good antitumor efficacy in a human B cell tumor xenograft model (83). Despite the early preclinical and clinical successes of viral *in vivo* transduction for cell engineering and gene therapy, this strategy comes with much higher safety risks compared to ex vivo manufacturing of genetically engineered T cells and it remains to been seen if it can meet the high safety requirements.

5 Specific requirements of gene transfer techniques for TCR-T cells

Many advances of the manufacturing processes for CAR-T cell therapies are likely transferable to TCR-T cell therapies. However, one specific problem for the generation of TCR-T cells is that introduction of an engineered TCR into a T cell can cause mispairing of the engineered α- or β-chains with the endogenous chains. This presents an unpredictable risk since mispaired TCRs have unknown reactivity that never went through thymic selection and could result in the formation of TCRs against self-peptides and thereby autoimmunity or graft-versus-host disease (GvHD) (84, 85). Although earlier clinical trials with TCR-T cells that retained their endogenous TCR did not observe GvHD (86), ways to prevent the safety risk of mispairing would be beneficial. Therefore, a number of strategies have been developed to avoid mispairing events with varying success as illustrated in Figure 3.

Insertion of an extra disulfide bond into the constant domains, murinization of the constant domains or domain swapping all led to the reduction of mispairing events but could not prevent it completely (Figures 3B–D (85, 87, 88)). Only CD3ζ fusion chains or single-chain TCR (scTCR) constructs abolished mispairing but do not form a TCR complex with the endogenous CD3γ, δ, and ε subunits (Figures 3E, F (89, 90)). Further elimination of the constant β domain and the addition of an intracellular costimulatory CD28 or 4-1BB domain has been reported which resembles the CAR structure and signaling modalities (Figure 3G (91, 92)). However, this altered structure has reduced sensitivity compared to the native TCR-CD3 complex as is the case for conventional CARs (3). Therefore, a more recent scTCR scaffold tried to incorporate the assembly of the native CD3 complex to harness the benefits of classical TCR signaling (Figure 3H (93)). This 3-domain scTCR consists of a vα-linker-vβ fragment fused to the cβ-domain and utilizes co-expression of the cα-domain with very little mispairing occurring. In addition, insertion of a disulfide bond between the vα-domain and a linker residue in close proximity to the vβ-domain was sufficient to prevent residual mispairing (93). Although this might provide a safe alternative for the introduction of engineered TCRs without the danger of mispairing events, the design of stable scTCRs could present a technical challenge for a number of TCRs. Stability engineering might be a potential solution for this limitation, since distinct regions in the vα- and vβ-domains have already been shown to be critical for surface expression and stability of scTCRs (94, 95).

Alterations from the native TCR structure could lead to a higher immunogenicity and reduced persistence of genetically engineered T cells if the constructs deviate greatly from the native format. Thus, another approach to avoid mispairing without altering the TCR structure is to knock-out the endogenous α- and β-chain. Orthotopic TCR α- and β-chain replacement (OTR) was done by CRISPR-Cas9 genome editing and was recently used in a phase I clinical trial to achieve endogenous TCR replacement with neoantigen-specific TCRs (neoTCRs) in 16 patients with refractory solid cancers (Figure 3I (70, 96, 97)). Insertion of the engineered TCR construct into exon 1 of the TRAC locus disrupts the endogenous α-chain and CRISPR-mediated knockout of the TRBC locus causes disruption of the endogenous β-chain. Another advantage of OTR is that there is no competition for the CD3 subunits with the endogenous TCR to form core TCR-CD3 complexes (98). However, cell-surface expression of the introduced TCRs can be inefficient in some cases with this editing approach. In the recent trial mentioned above, out of the 37 neoTCRs generated for 16 patients, cell-surface expression of neoTCR positive cells ranged from 1.9 to 46.8% of the live cell product (97). This might potentially be a matter of protocol optimization since changes to the medium formulation and the electroporation device increased the knock-in efficiency from 13.4% to 23% in the same study. Moreover, chromosomal aberrations at the chromosome 7 and 14 target sites were observed and are an indication for potential *TRAC : TRBC* translocations. Off-target editing and on-target mutagenesis present a major concern for

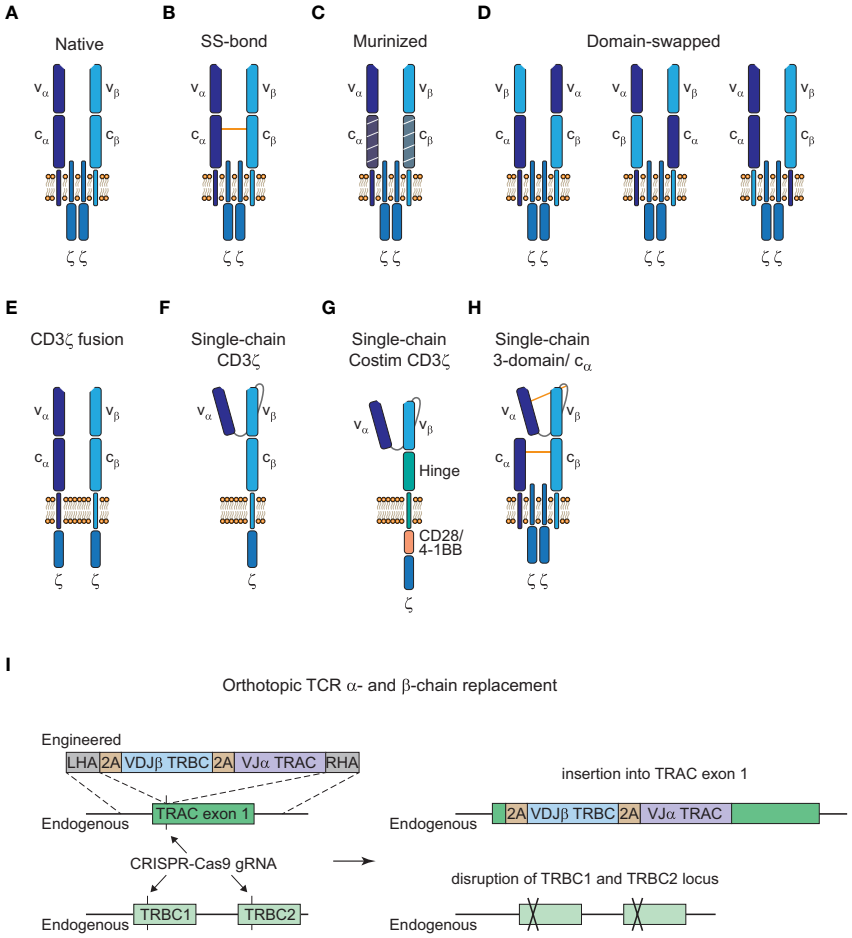

FIGURE 3
Strategies to avoid TCR mispairing. **(A)**, Native structure of a T cell receptor (TCR) α:β heterodimer (CD3ε, CD3δ, and CD3γ subunits are not shown here). **(B)**, Engineered TCR α:β heterodimer with an extra disulfide (SS) bond between the constant α and β domain. **(C)**, Engineered TCR α:β heterodimer with murine constant α- and β-domain. **(D)**, Engineered TCR α:β heterodimer with α- and β-domain swapping of the variable (left), constant (middle) or transmembrane (right) domains. **(E)**, Engineered TCR α:β heterodimer with a fused intracellular CD3ζ domain. **(F)**, Engineered single-chain TCR with a fused intracellular CD3ζ domain. **(G)**, Engineered single-chain TCR with a hinge domain instead of a constant and transmembrane β domain and inclusion of a costimulatory (Costim) and a CD3ζ domain. **(H)**, Engineered 3-domain single-chain TCR with an extra SS bond between the constant α and β domain and the variable α domain and a linker residue in close proximity to the variable β domain. A constant α domain is co-expressed with the 3-domain single-chain TCR. **(I)**, Orthotopic TCR α- and β-chain replacement with CRISPR-Cas9 gene editing. Engineered TCR construct is introduced into exon 1 of TRAC with a left homology arm (LHA) and a right homology arm (RHA). The endogenous TRAC locus is disrupted by the insertion of the engineered TCR construct and the endogenous TRBC1/TRBC2 gene locus is disrupted with another guide RNA (gRNA).

CRISPR-mediated approaches since they could lead to functional alterations or even malignant transformation of the edited cells (99, 100). Close monitoring of patients will be crucial for these newer approaches and further efforts will be necessary to understand and to reduce unwanted DNA aberrations for clinical application (101).

6 Genetically engineered allogeneic T cells

To date, all approved CAR-T cell therapies are utilizing patient-derived autologous T cells. However, since only heavily pretreated patients are applicable for immunotherapy with CAR-T cells, their T cell compartment is often compromised (27). This can result in reduced fitness or even manufacturing failure of the autologous CAR-T cell product (102, 103). Moreover, personalized production for each patient is challenging and very costly (as described above) and does not allow for mass production to meet the increasing demand for ACT. "Off-the-shelf" allogeneic T cells could be an approach to overcome these limitations. Because unaltered allogeneic T cells could lead to GvHD but also elimination of the genetically engineered T cells in the patient, a number of strategies have been developed to reduce these risks.

For the treatment of relapsed or refractory (r/r) B-cell ALL an allogeneic CD19 CAR- (NCT02808442 and NCT02746952) and a

CD19/CD22 dual-targeting CAR-T cell therapy (NCT04154709) have shown manageable safety profiles and anti-leukemic activity (104, 105). CRISPR-Cas9 genome editing was used to disrupt the *TRAC* and *CD52* gene locus allowing severe lymphodepletion with alemtuzumab prior to adoptive T cell transfer to reduce the risk for elimination of allogeneic engineered T cells by the host. In another first-in-human phase I clinical trial (NCT04637763), early positive results of an allogeneic CD19 CAR-T cell therapy for the treatment of r/r B cell non-Hodgkin lymphoma (B-NHL) were reported (106). Cas9 and CRISPR hybrid RNA-DNA (chRDNA) guides were used for reduced off-target editing (107) to introduce the CD19 CAR into the *TRAC* gene locus and disrupt it in the process (108). In addition, PD-1 was knocked out with the aim to improve persistence and antitumor activity of the genetically engineered T cells. No GvHD was observed and the therapy was generally well tolerated with promising clinical response rates. Another targeted approach is the use of a TRAC-specific ARCUS nuclease for site-specific introduction of the construct and disruption of the endogenous TCR to avoid GvHD (109). An allogeneic CD19 CAR-T cell therapy using this editing approach showed promising results in a Phase I/IIa clinical trial (NCT03666000) for the treatment of r/r B-NHL and B-cell ALL and could potentially be used for the treatment of relapsed patients with lymphomas that previously received autologous CAR-T cells. All 11 patients showed an objective response rate (ORR) after six months but no reported GvHD.

Genome editing also allows for the generation of fratricide-resistant CAR-T cells. This has been shown in a phase I clinical trial (NCT04538599) for a CD7 CAR T cell therapy for the treatment of T-cell lymphoma and CD7-expressing acute myeloid leukemia (AML) (110). Because CD7 is also expressed on normal T cells, CD7 was knocked-out to avoid fratricide and a number of additional edits (knock-out of TCR and HLA-II, knock-in of an NK cell inhibitor) were performed to avoid GvHD of the allogeneic CAR-T cell product.

Allogeneic TCR-T cells were also successfully tested in an investigator-initiated Phase I/II clinical trial (NCT01640301) for patients with AML receiving allogeneic hematopoietic cell transplantation (HCT) with high risk of relapse (111). Epstein-Bar virus (EBV)-specific $CD8^+$ T cells from the HCT donor were transduced with a TCR that recognizes the AML-associated intracellular antigen Wilms' Tumor Antigen 1 (WT1). Patients with HLA-A*0201 expression that received an allogeneic HCT and had no detectable disease at day 28 post-HCT were given engineered WT1-specific T cells prophylactically. All 12 patients showed relapse-free survival at a median of 44 months and compared very favorable to a similar risk group of 88 patients with 54% relapse-free survival. These results encourage the use of allogeneic consolidating ACT as a strategy for the prevention of AML relapses after HCT. In addition, allogenic HA-1-specific TCR-T cell therapy for the treatment of HLA-A*0201 positive patients with r/r ALL after allogeneic HCT is currently explored in a dose-escalation study (NCT03326921).

Preliminary results from early clinical studies with allogeneic engineered T cells that we described here are encouraging regarding their efficacy and risk of GvHD, however, this approach is still in its early stages and we will need to wait out larger clinical studies to assess its clinical value in the future.

7 Current challenges and potential strategies to improve CAR-T and TCR-T cell therapies

CAR-T cell therapies showed remarkable efficacy in certain B cell malignancies but struggle when it comes to myeloid malignancies and solid tumors. Challenges for CAR-T and TCR-T cell therapies that limit their clinical efficacy are severe adverse events, limited tumor infiltration, and persistence of genetically engineered T cells, as well as tumor immune evasion by loss of antigen. In particular, the complex nature of the immunosuppressive TME in solid tumors (112) is limiting T-cell infiltration and is promoting their exhaustion through presentation of inhibitory ligands on the tumor cells. There are a number of approaches with the aim to improve ACT by overcoming tumor antigen escape and increasing tumor specificity, and a selection of strategies will be highlighted here (Figure 4).

7.1 Adverse events associated with genetically engineered T cells

Immunotherapies with genetically engineered T cells are often accompanied by moderate to severe adverse events, limiting their clinical application in certain cases. The most common and severe adverse event of therapies with engineered T cells is cytokine release syndrome (CRS), which was first observed in clinical studies and did not occur in preclinical models at the time (113). Moreover, immune effector cell-associated neurotoxicity syndrome (ICANS), often referred as neurotoxicity, is very common in patients receiving CD19 CAR-T cells (114). Symptoms of CRS range from mild fever to life-threatening manifestations up to multi-organ system failure (115). Follow-up of patients receiving engineered T cells and monitoring for signs of CRS is vital to manage moderate to severe cases of CRS with anti-IL6 receptor agonist tocilizumab alone or in combination with corticosteroids, together with extensive supportive care (116). Symptoms of ICANS include headache, encephalopathy, tremor, and seizures, that are usually self-limiting, but rare lethal cases have been reported as well (117). Severe cases are often managed with corticosteroids, while tocilizumab is mostly ineffective in the treatment of ICANS, contrary to its effectiveness in CRS (116). Cross-talk between the engineered T cells and other immune cells, especially macrophages, can lead to the induction of systemic inflammation in the form of CRS which might cause leakiness of the blood brain barrier and symptoms of ICANS (116). Therefore, ICANS is often associated and correlates with the severity of CRS in patients, but it has also been reported in some cases in the absence of CRS (117).

On-target off-tumor toxicity is another challenge for adoptive T-cell therapies. In contrast to CRS and ICANS, this adverse event is not caused indirectly by associated endogenous immune cells but directly by the engineered T cells recognizing their cognate antigen or a cross-reactive antigen on healthy tissues. In particular, TCR-T cells warrant careful screening to avoid severe toxicity caused by autoreactivity due to lethal cases of tissue damage in the heart and

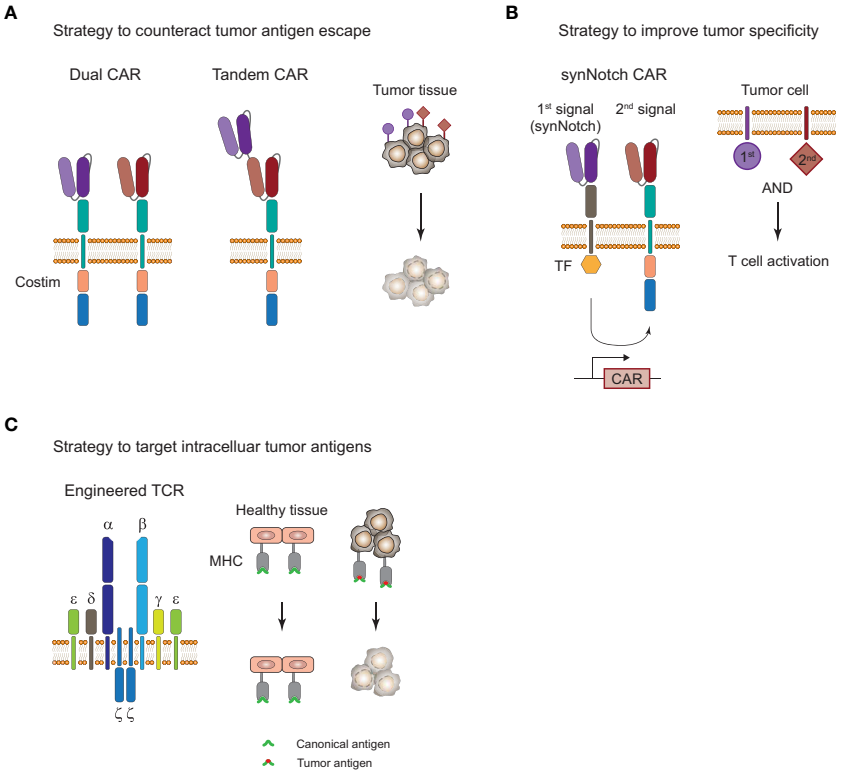

FIGURE 4
Strategies to improve adoptive T-cell therapy for the treatment of tumors. **(A)**, Strategy to overcome tumor antigen escape by using bi-specific dual or tandem CAR-T cells. **(B)**, Strategy for increased tumor specificity and reduced off-tumor toxicity with a synthetic Notch (synNotch) receptor. Encounter of a primary antigen (purple) leads to translocation of a transcription factor (TF) into the nucleus and expression of a CAR that recognizes a secondary antigen (red) on the tumor cell. T cell activation and tumor cell killing only occurs in the presence of both antigens and spares healthy tissues that only express the primary antigen. **(C)**, Targeting of intracellular antigens by using genetically engineered TCR-T cells. Peptide-major histocompatibility complex (MHC) tumor-associated or tumor-specific antigens of mutated intracellular proteins are promising targets for the treatment of solid tumors. Tumor surface antigens are often expressed to some extent on healthy tissues and can cause severe off-tumor toxicity.

brain in two early clinical trials targeting MAGE-A3 positive cancers (118, 119). As these TCRs were affinity enhanced, on-target off-tumor toxicity was likely increased. However, recent studies with affinity enhanced TCRs targeting MAGE-A4 showed clinical efficacy in the absence of severe TCR-T cell-mediated toxicity (120–122), indicating the necessity to investigate each single modified TCR for such risks although also non-modified TCRs have the potential for cross-reactivity. These cases highlight the difficulties of screening methods for TCR candidates to exclude potential common and individualized severe autoreactivity, which is highly difficult to be tested sufficiently at the preclinical level, but also indicate that TCRs have the potential to represent safe therapies with promising efficacy.

For the use of allogeneic CAR-T and TCR-T cells, a potential additional adverse event risk is allo-reactivity of allogeneic engineered T cells against foreign MHC molecules or minor histocompatibility antigens on host cells that can lead to GvHD. As described above, early clinical trials suggest that gene editing for the removal of the endogenous TCR is a viable strategy to avoid GvHD. Moreover, the use of allogeneic engineered T cells post-HCT, HLA-matching of the donor cells, and the use of non-αβ T cells are potential strategies (123). However, it remains to be seen how durable the persistence of allogeneic engineered T cells with these strategies is compared to their autologous counterparts, since elimination of the allogeneic T cells by the host immune system is a serious concern here.

Moreover, accompanying therapies, such as lymphodepletion prior to T-cell therapy, can add to hematological toxicities like cytopenia, which is a common adverse event with often unknown origin (26). Overall, this highlights the complex clinical landscape in regard to adverse events of CAR-T and TCR-T cell therapies and the need for better preclinical models to predict them early on (113).

7.2 Persistence of genetically engineered T cells

Persistence of CD19 CAR-T cells for up to 10 years has been reported in two patients with chronic lymphocytic leukemia after remission (124). While $CD8^+$ CAR-T cells were abundantly found in the initial response, it was almost exclusively $CD4^+$ CAR-T cells that were present during long-term remission. However, poor T cell persistence has been reported in many CAR-T (125) and TCR-T cell (97) clinical trials against a variety of tumor entities and is often likely the reason for limited clinical efficacy or relapses. Therefore, administration of lymphodepleting regimens is commonly

performed prior to the engineered T-cell therapy to increase T cell persistence (26).

Preclinical studies observed less exhaustion and improved antitumor activity of CAR-T cells with PD-1 knock-out (126, 127). Therefore, PD-1 knock-out is currently explored for the treatment of tumors with CAR-T (108, 125) and TCR-T cells (70) as a strategy to protect the engineered T cells from exhaustion and to enhance their persistence. Stadtmauer et al. used CRISPR-Cas9 genome editing to remove the endogenous TCR and PD-1 and introduced an engineered TCR specific for the cancer-testis antigens (CTAs) NY-ESO-1 and LAGE-1 to treat two patients with refractory melanoma and one with sarcoma. Engineered T cells trafficked to the sites of the tumor and reduction of the target antigens, likely as a response to the immune pressure of the TCR-T cells, was observed for both melanoma patients. Interestingly, no toxicity was observed and persistence of the TCR-T cells was increased in all three patients with at least 9 months compared to previous trials with T cells that retained their endogenous TCR and PD-1 expression. However, the number of patients in this first-in-human phase I clinical trial is low (NCT03399448) and expansion of the study is necessary. It also remains to be elucidated if the prolonged persistence is based on the ablation of PD-1 or in part on the removal of the endogenous TCR. Moreover, PD-1 ablation was also reported to cause increased functional exhaustion and cell death along greater activation in a CD19 CAR-T cell therapy (128). Results from knock-out experiments of PD-1 in mice with a chronic lymphocytic choriomeningitis virus (LCMV) infection showed that $CD8^+$ T cell exhaustion can not only occur in the absence of PD-1 but PD-1 even protected the cells from overstimulation and terminal differentiation to an exhausted effector phenotype at the site of infection (129). Suggesting that PD-1 could be relevant to fine-tune T cell responses in certain environments, such as high antigen load as is the case in viral infections. In that context, transient blockade of PD-1 with ICI could be superior over PD-1 ablation but our understanding how PD-1 signaling modulates gene expression during T cell responses remains enigmatic and needs to be further elucidated. A recent study showed that genes associated with survival and proliferation are resistant to PD-1-mediated inhibition while effector functions are regulated by it based on the TCR signal strength (130). Due to the context-dependent functions of PD-1 signaling, it remains to be seen if PD-1 ablation of genetically engineered T cells is an effective way of improving T cell persistence depending on the tumor entity and antigen load.

Moreover, a number of costimulatory switch receptors have been reported to prevent exhaustion of genetically engineered T cells and might increase their persistence (131–133). Switch receptors consist of the extracellular portion of an inhibitory receptor (e.g. PD-1, TIGIT, TIM-3) and the intracellular signaling domain of a costimulatory receptor (e.g. CD28, 4-1BB). Reports from the preclinical studies are encouraging with improved antitumor activity and persistence of genetically engineered T cells armored with these switch receptors, however, these signaling axes are complicated in nature. Tipping the scale from exhaustion to activation and not just balancing it as is the case with anti-PD-1/PD-L1 ICI might lead to overstimulation and a dysfunctional T cell phenotype.

Tonic endogenous TCR signaling was also associated with improved persistence of CAR-T cells in recent studies (125, 134). Removal of the endogenous TCR and PD-1 in mesothelin (MPTK)-specific CAR-T cells for the treatment of solid tumors resulted in poor persistence of the TCR-deficient CAR-T cells beyond 6 weeks in a phase I clinical trial with 15 patients (NCT03545815 (125)). Surprisingly, it was the TCR-positive CAR-T cells that became the main fraction after infusion in three patients despite their rare presence in the infused cell product. The authors replicated these findings in mice and hypothesized that tonic TCR signaling plays a beneficial role in CAR-T cell persistence. Off note, this was in the scenario of low-level engraftment and might be different when using lymphodepletion to increase engraftment. In line with these observations, another study also observed reduced persistence for TCR-deficient CD19 CAR-T cells in animal models (134). The role of tonic TCR signaling for the longevity of CAR-T cells (19) needs to be further addressed especially in the context of allogenic CAR-T cell therapies, where the removal of the endogenous TCR is already common practice to prevent GvHD (108, 109). TCR-T cells with endogenous TCR replacement are likely not affected due to tonic signaling of the introduced TCR as indicated by the results from Statdmauer et al.

7.3 Potential strategies to overcome tumor antigen escape

A common form of tumor resistance to ACT is tumor antigen escape by loss or downregulation of surface antigens or peptide-HLA complexes (135). Targeting multiple antigens by engineering T cells with a dual CAR or a tandem CAR could reduce the risk of tumor antigen escape (Figure 4A). Preliminary results from a phase I study (NCT03233854) with a CD19/CD22 bispecific CAR showed clinical efficacy but antigen escape in relapses was mostly observed for CD19 and not CD22 antigen, suggesting that there was less immune pressure of the CAR-T cells on the CD22 target (136). This is supported by the observation that CD22 scFV ligation in the bispecific CAR showed less cytokine secretion than for CD19 scFV. Another bispecific CD19/CD22 CAR that uses a tandem approach showed good efficacy in 6 patients with r/r B-ALL and observed one relapse of blast cells with loss of CD19 antigen and diminished CD22 expression 5 months after treatment (NCT03185494 (137)). The single construct approach for multi-specific CAR-T cells might affect the antigen binding capabilities based on the design of the linkers and it could be favorable to use a bi- or tricistronic design that expresses individual CAR molecules on the same cell to avoid these problems. This has been done for tricistronic CD19/CD20/CD22 tri-specific CAR-T cells that were able to target B-lineage ALL independent of CD19 expression *in vitro* and in animal models (138). Results from a phase I study (NCT03289455) with bicistronic CD19/CD22 bispecific CAR-T cells for the treatment of 15 patients with r/r B-ALL showed 86% CR and one-year overall survival and event-free survival of 60% and 32%, respectively (139). Dual targeting of B7-H3 and CD70, which are overexpressed in a variety of solid tumors, with a tandem CAR elicited superior tumor control and overall survival in a lung cancer and

melanoma xenograft model (140). Moreover, infusing patients with a mixture of mono-specific CAR-T cells or TCR-T cells with different specificity could also be a viable option and has recently been done for patients with solid tumors that received up to three neoTCR-T cells with different specificity (97).

Multi-targeting of different antigens seems to be viable strategy to overcome tumor antigen escape and preliminary results suggest that it might increase antitumor immunity against tumor cells that co-express multiple antigens. However, this approach is limited so far by the number of known promising tumor antigens and will benefit from the discovery of additional tumor-associated and tumor specific antigens in the future.

7.4 Potential strategies for the treatment of solid tumors

The treatment of solid tumors is one of the most difficult areas in the field. Limited T-cell infiltration into the tumor as well as T cell exhaustion due to the immunosuppressive TME poses a high risk for an insufficient response to the treatment. In addition, the heterogeneity of antigen expression and the lack of truly tumor-specific surface antigens in solid tumors (112) can cause severe off-tumor toxicity in healthy tissues. Due to the difficulty of identifying tumor-specific surface antigens on solid tumors as targets for CAR-T cell therapies, strategies with higher specificity and less off-tumor toxicity have been developed, such as the synthetic Notch (synNotch) receptor designs (Figure 4B). Recognition of a primary antigen by the synNotch receptor cleaves an orthogonal transcription factor from the cytoplasmatic tail and induces the expression of a CAR that can recognize a secondary antigen on the tumor cell (141). T cell activation and tumor cell killing only occurs if both antigens are expressed on the tumor cell. This concept has been applied in a number of preclinical studies for solid tumor models and demonstrated improved specificity for the treatment of solid tumors (142, 143). SynNotch circuits can also be used to improve the specificity of engineered TCRs for selective killing of tumor cells, which has been demonstrated for a SynNotch-TCR against melanoma cells *in vitro* (144).

TCR-T cells are inherently equipped for the recognition of intracellular antigens through peptide-HLA presentation which opens up a treasure trove of tumor-associated or tumor-specific antigens that could be exploited for TCR-T cell therapy of solid tumors (Figure 4C). As mentioned above, a preliminary study showed the feasibility and efficacy of TCR-T cells in two melanoma and one sarcoma patient (70) and clinical trials for the treatment of MAGE-A4 positive solid tumors showed clinical efficacy in subset of patients with an ORR of 24% (9/38) (121). Foy et al. demonstrated recently the feasibility of TCR-T cell therapy targeting personalized neoantigens (97). A combinatorial screening approach with whole exome sequencing (WES) and RNA sequencing of the patients' tumors was used to predict potential neoantigens. In a next step, multimeric labeled peptide-HLA complexes were generated for reactivity assessment of the predicted neoantigens in peripheral blood of patients and neoTCRs were identified and manufactured for 16 patients. Despite this impressive demonstration of feasibility of such a complex workflow in a clinical setting, efficacy and T cell persistence was limited. However, there are over a hundred clinical trials with adoptive TCR-T cell transfer registered in clinicaltrials.gov with the majority of them for the treatment of solid tumors (145). Hurdles for TCR-T cell therapy include its dependency on a specific HLA genotype, restricting it to a specific patient population in most cases, and its susceptibility to HLA-downregulation. Moreover, intracellular antigens can also be targeted with TCR-like CARs that use scFV molecules that recognize specific peptide-MHC complexes. Recently, a phase I clinical trial with a TCR-like CAR T-cell therapy targeting MAGE-A4 peptide-HLA-A*02:01 complexes for the treatment of solid tumors has been initiated (146) and evaluation of the clinical efficacy of more TCR-like CAR formats in clinical trials will be of great interest for the use of this concept. Overall, combinatorial approaches with a variety of different interventions will likely be necessary for the treatment of solid tumors in the future in order to overcome their complex mechanisms of immune evasion.

8 Future perspective

Adoptive immunotherapies with genetically engineered T cells for the treatment of refractory tumors is a new breakthrough therapy with promising efficacy in certain cancers. However, its application is held back by manufacturing difficulties, severe adverse events, regulatory challenges, and extremely high costs. There are a number of strategies how limitations are currently addressed. Automated and expedited manufacturing processes might have an impact on both product quality as well as costs. Approaches with allogeneic donor T cells may improve availability but also provide "off-the shelf" therapies and therefore substantially result in cost reduction. Due to the HLA-restriction of TCR-T cell therapies, it seems unlikely that companies will go through the expensive process of testing this type of therapy in tumor types where CAR-T cell therapies are already showing good efficacy at this point. Therefore, TCR-T cells are mostly tested in solid tumors where the lack of good surface targets limit CAR-T cell therapy. At the moment, TCR-T cells are usually targeting tumor-associated antigens but first tumor-specific studies have demonstrated their feasibility and personalized approaches might be more prevalent in the future. Improving tools to predict potential on-target off-tumor toxicity is especially crucial for TCR-T cells due to their higher antigen sensitivity compared to CAR-T cells, especially for affinity enhanced TCRs. This is in particular important for time-saving clinical translation of newly identified, optimized or personalized TCR constructs. Additionally, the development of novel preclinical models for the prediction of associated adverse events like CRS and ICANS is necessary to develop novel strategies to exclude most severe adverse events before clinical testing in the future (113). The number of clinical studies exploring new strategies and the speed the field is innovated upon is impressive. However, it is difficult for the regulation of these novel and complex therapies to keep up with this speed, and standardization of certain manufacturing steps will likely be necessary to ensure safety and comparability of T cell

products for patients in the future. To make these therapies more commonly available and explore their benefit not only for refractory tumors but also at earlier stages of disease, their costs and resources for manufacturing must become more sustainable for the health care system (60, 147).

One of the major challenges is the development of novel strategies in case of resistance. Personalized combinatorial approaches to target multiple antigens and to neutralize the immunosuppressive TME probably will be necessary for the treatment of solid tumors but also resistant hematological malignancies in the future.

While ACT with genetically engineered T cells is mainly used as a therapy for cancer, its potential for the treatment of other diseases is more and more realized. Preliminary results of CD19 CAR-T cell therapy in patients with refractory systemic lupus erythematosus (SLE) showed that it was well tolerated and highly effective (148). Exploring its use for other autoimmune but also genetic diseases might open up effective novel options for treatment failures in the future.

Author contributions

MH conceptualization, writing, drawing of figures, review and editing. AK conceptualization, writing, review and editing. All authors contributed to the article and approved the submitted version.

Funding

This work was funded by the Deutsche Forschungsgemeinschaft (DFG, German Research Foundation) –SFB-TRR 338/1 2021–452881907 (to AMK/A03) and the German Cancer Consortium (DKTK), partner site Munich.

Conflict of interest

The authors declare that the research was conducted in the absence of any commercial or financial relationships that could be construed as a potential conflict of interest.

Publisher's note

References

1. Robert C. A decade of immune-checkpoint inhibitors in cancer therapy. *Nat Commun* (2020) 11(1):3801. doi: 10.1038/s41467-020-17670-y

2. Saez-Ibanez AR, Upadhaya S, Partridge T, Shah M, Correa D, Campbell J. Landscape of cancer cell therapies: trends and real-world data. *Nat Rev Drug Discov* (2022) 21(9):631–2. doi: 10.1038/d41573-022-00095-1

3. Harris DT, Hager MV, Smith SN, Cai Q, Stone JD, Kruger P, et al. Comparison of T cell activities mediated by human TCRs and CARs that use the same recognition domains. *J Immunol* (2018) 200(3):1088–100. doi: 10.4049/jimmunol.1700236

4. Jayaraman J, Mellody MP, Hou AJ, Desai RP, Fung AW, Pham AHT, et al. CAR-T design: Elements and their synergistic function. *EBioMedicine* (2020) 58:102931. doi: 10.1016/j.ebiom.2020.102931

5. Irving BA, Weiss A. The cytoplasmic domain of the T cell receptor zeta chain is sufficient to couple to receptor-associated signal transduction pathways. *Cell* (1991) 64 (5):891–901. doi: 10.1016/0092-8674(91)90314-O

6. Finney HM, Lawson AD, Bebbington CR, Weir AN. Chimeric receptors providing both primary and costimulatory signaling in T cells from a single gene product. *J Immunol* (1998) 161(6):2791–7. doi: 10.4049/jimmunol.161.6.2791

7. Milone MC, Fish JD, Carpenito C, Carroll RG, Binder GK, Teachey D, et al. Chimeric receptors containing CD137 signal transduction domains mediate enhanced survival of T cells and increased antileukemic efficacy in vivo. *Mol Ther* (2009) 17 (8):1453–64. doi: 10.1038/mt.2009.83

8. Zhong XS, Matsushita M, Plotkin J, Riviere I, Sadelain M. Chimeric antigen receptors combining 4-1BB and CD28 signaling domains augment PI3kinase/AKT/Bcl-XL activation and CD8+ T cell-mediated tumor eradication. *Mol Ther* (2010) 18 (2):413–20. doi: 10.1038/mt.2009.210

9. Schubert M-L, Schmitt A, Neuber B, Hückelhoven-Krauss A, Kunz A, Wang L, et al. Third-generation CAR T cells targeting CD19 are associated with an excellent safety profile and might improve persistence of CAR T cells in treated patients. *Blood* (2019) 134(Supplement_1):51–. doi: 10.1182/blood-2019-125423

10. George P, Dasyam N, Giunti G, Mester B, Bauer E, Andrews B, et al. Third-generation anti-CD19 chimeric antigen receptor T-cells incorporating a TLR2 domain for relapsed or refractory b-cell lymphoma: a phase I clinical trial protocol (ENABLE). *BMJ Open* (2020) 10(2):e034629. doi: 10.1136/bmjopen-2019-034629

11. Ramos CA, Rouce R, Robertson CS, Reyna A, Narala N, Vyas G, et al. *In vivo* fate and activity of second- versus third-generation CD19-specific CAR-T cells in b cell non-hodgkin's lymphomas. *Mol Ther* (2018) 26(12):2727–37. doi: 10.1016/j.ymthe.2018.09.009

12. Chmielewski M, Abken H. TRUCKS, the fourth-generation CAR T cells: Current developments and clinical translation. *Adv Cell Gene Ther* (2020) 3(3):e84. doi: 10.1002/acg2.84

13. Kunert A, Chmielewski M, Wijers R, Berrevoets C, Abken H, Debets R. Intra-tumoral production of IL18, but not IL12, by TCR-engineered T cells is non-toxic and counteracts immune evasion of solid tumors. *Oncoimmunology* (2017) 7(1):e1378842. doi: 10.1080/2162402X.2017.1378842

14. Dragon AC, Zimmermann K, Nerreter T, Sandfort D, Lahrberg J, Kloss S, et al. CAR-T cells and TRUCKs that recognize an EBNA-3C-derived epitope presented on HLA-B*35 control Epstein-Barr virus-associated lymphoproliferation. *J Immunother Cancer* (2020) 8(2):e000736. doi: 10.1136/jitc-2020-000736

15. Chmielewski M, Abken H. CAR T cells releasing IL-18 convert to T-bet(high) FoxO1(low) effectors that exhibit augmented activity against advanced solid tumors. *Cell Rep* (2017) 21(11):3205–19. doi: 10.1016/j.celrep.2017.11.063

16. Zimmermann K, Kuehle J, Dragon AC, Galla M, Kloth C, Rudek LS, et al. Design and characterization of an "All-in-One" lentiviral vector system combining constitutive anti-G(D2) CAR expression and inducible cytokines. *Cancers (Basel)* (2020) 12(2):375. doi: 10.3390/cancers12020375

17. Glienke W, Dragon AC, Zimmermann K, Martyniszyn-Eiben A, Mertens M, Abken H, et al. GMP-compliant manufacturing of TRUCKs: CAR T cells targeting GD (2) and releasing inducible IL-18. *Front Immunol* (2022) 13:839783. doi: 10.3389/fimmu.2022.839783

18. Kagoya Y, Tanaka S, Guo T, Anczurowski M, Wang CH, Saso K, et al. A novel chimeric antigen receptor containing a JAK-STAT signaling domain mediates superior antitumor effects. *Nat Med* (2018) 24(3):352–9. doi: 10.1038/nm.4478

19. Ajina A, Maher J. Strategies to address chimeric antigen receptor tonic signaling. *Mol Cancer Ther* (2018) 17(9):1795–815. doi: 10.1158/1535-7163.MCT-17-1097

20. Guy CS, Vignali KM, Temirov J, Bettini ML, Overacre AE, Smeltzer M, et al. Distinct TCR signaling pathways drive proliferation and cytokine production in T cells. *Nat Immunol* (2013) 14(3):262–70. doi: 10.1038/ni.2538

21. Liu Y, Liu G, Wang J, Zheng ZY, Jia L, Rui W, et al. Chimeric STAR receptors using TCR machinery mediate robust responses against solid tumors. *Sci Transl Med* (2021) 13(586):eabb5191. doi: 10.1126/scitranslmed.abb5191

22. Lock D, Mockel-Tenbrinck N, Drechsel K, Barth C, Mauer D, Schaser T, et al. Automated manufacturing of potent CD20-directed chimeric antigen receptor T cells for clinical use. *Hum Gene Ther* (2017) 28(10):914–25. doi: 10.1089/hum.2017.111

23. Castella M, Caballero-Banos M, Ortiz-Maldonado V, Gonzalez-Navarro EA, Sune G, Antonana-Vidosola A, et al. Point-Of-Care CAR T-cell production (ARI-0001) using a closed semi-automatic bioreactor: Experience from an academic phase I clinical trial. *Front Immunol* (2020) 11:482. doi: 10.3389/fimmu.2020.00482

24. Jackson Z, Roe A, Sharma AA, Lopes F, Talla A, Kleinsorge-Block S, et al. Automated manufacture of autologous CD19 CAR-T cells for treatment of non-hodgkin lymphoma. *Front Immunol* (2020) 11:1941. doi: 10.3389/fimmu.2020.01941

25. Lock D, Monjezi R, Brandes C, Bates S, Lennartz S, Teppert K, et al. Automated, scaled, transposon-based production of CAR T cells. *J Immunother Cancer* (2022) 10 (9):e005189. doi: 10.1136/jitc-2022-005189

26. Wall DA, Krueger J. Chimeric antigen receptor T cell therapy comes to clinical practice. *Curr Oncol* (2020) 27(Suppl 2):S115–S23. doi: 10.3747/co.27.5283

27. Allen ES, Stroncek DF, Ren J, Eder AF, West KA, Fry TJ, et al. Autologous lymphapheresis for the production of chimeric antigen receptor T cells. *Transfusion* (2017) 57(5):1133–41. doi: 10.1111/trf.14003

28. Harrer DC, Heidenreich M, Fante MA, Muller V, Haehnel V, Offner R, et al. Apheresis for chimeric antigen receptor T-cell production in adult lymphoma patients. *Transfusion* (2022) 62(8):1602–11. doi: 10.1111/trf.17030

29. Panch SR, Srivastava SK, Elavia N, McManus A, Liu S, Jin P, et al. Effect of cryopreservation on autologous chimeric antigen receptor T cell characteristics. *Mol Ther* (2019) 27(7):1275–85. doi: 10.1016/j.ymthe.2019.05.015

30. Liadi I, Singh H, Romain G, Rey-Villamizar N, Merouane A, Adolacion JR, et al. Individual motile CD4(+) T cells can participate in efficient multikilling through conjugation to multiple tumor cells. *Cancer Immunol Res* (2015) 3(5):473–82. doi: 10.1158/2326-6066.CIR-14-0195

31. Sommermeyer D, Hudecek M, Kosasih PL, Gogishvili T, Maloney DG, Turtle CJ, et al. Chimeric antigen receptor-modified T cells derived from defined CD8+ and CD4+ subsets confer superior antitumor reactivity in vivo. *Leukemia* (2016) 30(2):492–500. doi: 10.1038/leu.2015.247

32. Zhou L, Chong MM, Littman DR. Plasticity of CD4+ T cell lineage differentiation. *Immunity* (2009) 30(5):646–55. doi: 10.1016/j.immuni.2009.05.001

33. Good Z, Spiegel JY, Sahaf B, Malipatlolla MB, Ehlinger ZJ, Kurra S, et al. Post-infusion CAR TReg cells identify patients resistant to CD19-CAR therapy. *Nat Med* (2022) 28(9):1860–71. doi: 10.1038/s41591-022-01960-7

34. Abramson JS, Palomba ML, Gordon LI, Lunning MA, Wang M, Arnason J, et al. Lisocabtagene maraleucel for patients with relapsed or refractory large b-cell lymphomas (TRANSCEND NHL 001): a multicentre seamless design study. *Lancet* (2020) 396(10254):839–52. doi: 10.1016/S0140-6736(20)31366-0

35. Shah NN, Highfill SL, Shalabi H, Yates B, Jin J, Wolters PL, et al. CD4/CD8 T-cell selection affects chimeric antigen receptor (CAR) T-cell potency and toxicity: Updated results from a phase I anti-CD22 CAR T-cell trial. *J Clin Oncol* (2020) 38 (17):1938–50. doi: 10.1200/JCO.19.03279

36. Shadman M, Yeung C, Redman MW, Lee SY, Lee DH, Ramachandran A, et al. Third generation CD20 targeted CAR T-cell therapy (MB-106) for treatment of patients with Relapsed/Refractory b-cell non-Hodgkin lymphoma. *Blood* (2020) 136 (Supplement 1):38–9. doi: 10.1182/blood-2020-136440

37. Joedicke JJ, Grosskinsky U, Gerlach K, Kunkele A, Hopken UE, Rehm A. Accelerating clinical-scale production of BCMA CAR T cells with defined maturation stages. *Mol Ther Methods Clin Dev* (2022) 24:181–98. doi: 10.1016/j.omtm.2021.12.005

38. Arcangeli S, Bove C, Mezzanotte C, Camisa B, Falcone L, Manfredi F, et al. CAR T cell manufacturing from naive/stem memory T lymphocytes enhances antitumor responses while curtailing cytokine release syndrome. *J Clin Invest* (2022) 132(12): e150807. doi: 10.1172/JCI150807

39. Gattinoni L, Klebanoff CA, Restifo NP. Paths to stemness: building the ultimate antitumour T cell. *Nat Rev Cancer* (2012) 12(10):671–84. doi: 10.1038/nrc3322

40. Deng Q, Han G, Puebla-Osorio N, Ma MCJ, Strati P, Chasen B, et al. Characteristics of anti-CD19 CAR T cell infusion products associated with efficacy and toxicity in patients with large b cell lymphomas. *Nat Med* (2020) 26(12):1878–87. doi: 10.1038/s41591-020-1061-7

41. Locke FL, Rossi JM, Neelapu SS, Jacobson CA, Miklos DB, Ghobadi A, et al. Tumor burden, inflammation, and product attributes determine outcomes of axicabtagene ciloleucel in large b-cell lymphoma. *Blood Adv* (2020) 4(19):4898–911. doi: 10.1182/bloodadvances.2020002394

42. Yang S, Rosenberg SA, Morgan RA. Clinical-scale lentiviral vector transduction of PBL for TCR gene therapy and potential for expression in less-differentiated cells. *J Immunother* (2008) 31(9):830–9. doi: 10.1097/CJI.0b013e31818817c5

43. Laux I, Khoshnan A, Tindell C, Bae D, Zhu X, June CH, et al. Response differences between human CD4(+) and CD8(+) T-cells during CD28 costimulation: implications for immune cell-based therapies and studies related to the expansion of double-positive T-cells during aging. *Clin Immunol* (2000) 96(3):187–97. doi: 10.1006/clim.2000.4902

44. Zhang H, Snyder KM, Suhoski MM, Maus MV, Kapoor V, June CH, et al. 4-1BB is superior to CD28 costimulation for generating CD8+ cytotoxic lymphocytes for adoptive immunotherapy. *J Immunol* (2007) 179(7):4910–8. doi: 10.4049/jimmunol.179.7.4910

45. Brentjens RJ, Riviere I, Park JH, Davila ML, Wang X, Stefanski J, et al. Safety and persistence of adoptively transferred autologous CD19-targeted T cells in patients with relapsed or chemotherapy refractory b-cell leukemias. *Blood* (2011) 118(18):4817–28. doi: 10.1182/blood-2011-04-348540

46. Ramos CA, Ballard B, Zhang H, Dakhova O, Gee AP, Mei Z, et al. Clinical and immunological responses after CD30-specific chimeric antigen receptor-redirected lymphocytes. *J Clin Invest* (2017) 127(9):3462–71. doi: 10.1172/JCI94306

47. Kochenderfer JN, Dudley ME, Feldman SA, Wilson WH, Spaner DE, Maric I, et al. B-cell depletion and remissions of malignancy along with cytokine-associated toxicity in a clinical trial of anti-CD19 chimeric-antigen-receptor-transduced T cells. *Blood* (2012) 119(12):2709–20. doi: 10.1182/blood-2011-10-384388

48. Turtle CJ, Hanafi LA, Berger C, Gooley TA, Cherian S, Hudecek M, et al. CD19 CAR-T cells of defined CD4+:CD8+ composition in adult b cell ALL patients. *J Clin Invest* (2016) 126(6):2123–38. doi: 10.1172/JCI85309

49. Alizadeh D, Wong RA, Yang X, Wang D, Pecoraro JR, Kuo CF, et al. IL15 enhances CAR-T cell antitumor activity by reducing mTORC1 activity and preserving their stem cell memory phenotype. *Cancer Immunol Res* (2019) 7(5):759–72. doi: 10.1158/2326-6066.CIR-18-0466

50. Besser MJ, Schallmach E, Oved K, Treves AJ, Markel G, Reiter Y, et al. Modifying interleukin-2 concentrations during culture improves function of T cells for adoptive immunotherapy. *Cytotherapy* (2009) 11(2):206–17. doi: 10.1080/14653240802590391

51. Li Y, Kurlander RJ. Comparison of anti-CD3 and anti-CD28-coated beads with soluble anti-CD3 for expanding human T cells: differing impact on CD8 T cell phenotype and responsiveness to restimulation. *J Transl Med* (2010) 8:104. doi: 10.1186/1479-5876-8-104

52. Gattinoni L, Klebanoff CA, Palmer DC, Wrzesinski C, Kerstann K, Yu Z, et al. Acquisition of full effector function *in vitro* paradoxically impairs the *in vivo* antitumor efficacy of adoptively transferred CD8+ T cells. *J Clin Invest* (2005) 115(6):1616–26. doi: 10.1172/JCI24480

53. Poltorak MP, Graef P, Tschulik C, Wagner M, Cletiu V, Dreher S, et al. Expamers: a new technology to control T cell activation. *Sci Rep* (2020) 10(1):17832. doi: 10.1038/s41598-020-74595-8

54. O'Connor RS, Hao X, Shen K, Bashour K, Akimova T, Hancock WW, et al. Substrate rigidity regulates human T cell activation and proliferation. *J Immunol* (2012) 189(3):1330–9. doi: 10.4049/jimmunol.1102757

55. Cheung AS, Zhang DKY, Koshy ST, Mooney DJ. Scaffolds that mimic antigen-presenting cells enable ex vivo expansion of primary T cells. *Nat Biotechnol* (2018) 36 (2):160–9. doi: 10.1038/nbt.4047

56. Bulcha JT, Wang Y, Ma H, Tai PWL, Gao G. Viral vector platforms within the gene therapy landscape. *Signal Transduct Target Ther* (2021) 6(1):53. doi: 10.1038/s41392-021-00487-6

57. Naldini L, Blomer U, Gallay P, Ory D, Mulligan R, Gage FH, et al. *In vivo* gene delivery and stable transduction of nondividing cells by a lentiviral vector. *Science* (1996) 272(5259):263–7. doi: 10.1126/science.272.5259.263

58. Qian W, Wang Y, Li RF, Zhou X, Liu J, Peng DZ. Prolonged integration site selection of a lentiviral vector in the genome of human keratinocytes. *Med Sci Monit* (2017) 23:1116–22. doi: 10.12659/MSM.903094

59. Ruella M, Xu J, Barrett DM, Fraietta JA, Reich TJ, Ambrose DE, et al. Induction of resistance to chimeric antigen receptor T cell therapy by transduction of a single leukemic b cell. *Nat Med* (2018) 24(10):1499–503. doi: 10.1038/s41591-018-0201-9

60. Lin JK, Lerman BJ, Barnes JI, Boursiquot BC, Tan YJ, Robinson AQL, et al. Cost effectiveness of chimeric antigen receptor T-cell therapy in relapsed or refractory pediatric b-cell acute lymphoblastic leukemia. *J Clin Oncol* (2018) 36(32):3192–202. doi: 10.1200/JCO.2018.79.0642

61. Rostovskaya M, Fu J, Obst M, Baer I, Weidlich S, Wang H, et al. Transposon-mediated BAC transgenesis in human ES cells. *Nucleic Acids Res* (2012) 40(19):e150. doi: 10.1093/nar/gks643

62. Kebriaei P, Singh H, Huls MH, Figliola MJ, Bassett R, Olivares S, et al. Phase I trials using sleeping beauty to generate CD19-specific CAR T cells. *J Clin Invest* (2016) 126(9):3363–76. doi: 10.1172/JCI86721

63. Srour SA, Singh H, McCarty J, de Groot E, Huls H, Rondon G, et al. Long-term outcomes of sleeping beauty-generated CD19-specific CAR T-cell therapy for relapsed-refractory b-cell lymphomas. *Blood* (2020) 135(11):862–5. doi: 10.1182/blood.2019002920

64. Magnani CF, Gaipa G, Lussana F, Belotti D, Gritti G, Napolitano S, et al. Sleeping beauty-engineered CAR T cells achieve antileukemic activity without severe toxicities. *J Clin Invest* (2020) 130(11):6021–33. doi: 10.1172/JCI138473

65. Prommersberger S, Reiser M, Beckmann J, Danhof S, Amberger M, Quade-Lyssy P, et al. CARAMBA: a first-in-human clinical trial with SLAMF7 CAR-T cells prepared by virus-free sleeping beauty gene transfer to treat multiple myeloma. *Gene Ther* (2021) 28(9):560–71. doi: 10.1038/s41434-021-00254-w

66. Barnett BE, Hermanson DL, Smith JB, Wang X, Tan Y, Martin CE, et al. piggyBacTM-produced CAR-T cells exhibit stem-cell memory phenotype. *Blood* (2016) 128(22):2167. doi: 10.1182/blood.V128.22.2167.2167

67. Li C, Sun Y, Wang J, Tang L, Jiang H, Guo T, et al. PiggyBac-generated CAR19-T cells plus lenalidomide cause durable complete remission of triple-hit Refractory/Relapsed DLBCL: A case report. *Front Immunol* (2021) 12:599493. doi: 10.3389/fimmu.2021.599493

68. Bishop DC, Clancy LE, Simms R, Burgess J, Mathew G, Moezzi L, et al. Development of CAR T-cell lymphoma in 2 of 10 patients effectively treated with piggyBac-modified CD19 CAR T cells. *Blood* (2021) 138(16):1504–9. doi: 10.1182/blood.2021010813

69. Micklethwaite KP, Gowrishankar K, Gloss BS, Li Z, Street JA, Moezzi L, et al. Investigation of product-derived lymphoma following infusion of piggyBac-modified CD19 chimeric antigen receptor T cells. *Blood* (2021) 138(16):1391–405. doi: 10.1182/blood.2021010858

70. Stadtmauer EA, Fraietta JA, Davis MM, Cohen AD, Weber KL, Lancaster E, et al. CRISPR-engineered T cells in patients with refractory cancer. *Science* (2020) 367: eaba7365. doi: 10.1126/science.aba7365

71. Lu Y, Xue J, Deng T, Zhou X, Yu K, Deng L, et al. Safety and feasibility of CRISPR-edited T cells in patients with refractory non-small-cell lung cancer. *Nat Med* (2020) 26(5):732–40. doi: 10.1038/s41591-020-0840-5

72. Razeghian E, Nasution MKM, Rahman HS, Gardanova ZR, Abdelbasset WK, Aravindhan S, et al. A deep insight into CRISPR/Cas9 application in CAR-T cell-based tumor immunotherapies. *Stem Cell Res Ther* (2021) 12(1):428. doi: 10.1186/s13287-021-02510-7

73. Dimitri A, Herbst F, Fraietta JA. Engineering the next-generation of CAR T-cells with CRISPR-Cas9 gene editing. *Mol Cancer* (2022) 21(1):78. doi: 10.1186/s12943-022-01559-z

74. Ghassemi S, Nunez-Cruz S, O'Connor RS, Fraietta JA, Patel PR, Scholler J, et al. Reducing ex vivo culture improves the antileukemic activity of chimeric antigen receptor (CAR) T cells. *Cancer Immunol Res* (2018) 6(9):1100–9. doi: 10.1158/2326-6066.CIR-17-0405

75. Yang J, He J, Zhang X, Li J, Wang Z, Zhang Y, et al. Next-day manufacture of a novel anti-CD19 CAR-T therapy for b-cell acute lymphoblastic leukemia: first-in-human clinical study. *Blood Cancer J* (2022) 12(7):104. doi: 10.1038/s41408-022-00694-6

76. Flinn IW, Jaeger U, Shah NN, Blaise D, Briones J, Shune L, et al. A first-in-Human study of YTB323, a novel, autologous CD19-directed CAR-T cell therapy manufactured using the novel T-charge TM platform, for the treatment of patients (Pts) with Relapsed/Refractory (r/r) diffuse Large b-cell lymphoma (DLBCL). *Blood* (2021) 138:740. doi: 10.1182/blood-2021-146268

77. Ghassemi S, Durgin JS, Nunez-Cruz S, Patel J, Leferovich J, Pinzone M, et al. Rapid manufacturing of non-activated potent CAR T cells. *Nat BioMed Eng* (2022) 6 (2):118–28. doi: 10.1038/s41551-021-00842-6

78. Smith TT, Stephan SB, Moffett HF, McKnight LE, Ji W, Reiman D, et al. *In situ* programming of leukaemia-specific T cells using synthetic DNA nanocarriers. *Nat Nanotechnol* (2017) 12(8):813–20. doi: 10.1038/nnano.2017.57

79. Parayath NN, Stephan SB, Koehne AL, Nelson PS, Stephan MT. *In vitro*-transcribed antigen receptor mRNA nanocarriers for transient expression in circulating T cells in vivo. *Nat Commun* (2020) 11(1):6080. doi: 10.1038/s41467-020-19486-2

80. Nawaz W, Huang B, Xu S, Li Y, Zhu L, Yiqiao H, et al. AAV-mediated *in vivo* CAR gene therapy for targeting human T-cell leukemia. *Blood Cancer J* (2021) 11 (6):119. doi: 10.1038/s41408-021-00508-1

81. Russell S, Bennett J, Wellman JA, Chung DC, Yu ZF, Tillman A, et al. Efficacy and safety of voretigene neparvovec (AAV2-hRPE65v2) in patients with RPE65-mediated inherited retinal dystrophy: a randomised, controlled, open-label, phase 3 trial. *Lancet* (2017) 390(10097):849–60. doi: 10.1016/S0140-6736(17)31868-8

82. Agarwal S, Weidner T, Thalheimer FB, Buchholz CJ. *In vivo* generated human CAR T cells eradicate tumor cells. *Oncoimmunology* (2019) 8(12):e1671761. doi: 10.1080/2162402X.2019.1671761

83. Huckaby JT, Landoni E, Jacobs TM, Savoldo B, Dotti G, Lai SK. Bispecific binder redirected lentiviral vector enables in vivo engineering of CAR-T cells. *J Immunother Cancer* (2021) 9(9):e002737. doi: 10.1136/jitc-2021-002737

84. Bendle GM, Linnemann C, Hooijkaas AI, Bies L, de Witte MA, Jorritsma A, et al. Lethal graft-versus-host disease in mouse models of T cell receptor gene therapy. *Nat Med* (2010) 16(5):565–70. 1p following 70. doi: 10.1038/nm.2128

85. van Loenen MM, de Boer R, Amir AL, Hagedoorn RS, Volbeda GL, Willemze R, et al. Mixed T cell receptor dimers harbor potentially harmful neoreactivity. *Proc Natl Acad Sci USA* (2010) 107(24):10972–7. doi: 10.1073/pnas.1005802107

86. Rosenberg SA. Of mice, not men: no evidence for graft-versus-host disease in humans receiving T-cell receptor-transduced autologous T cells. *Mol Ther* (2010) 18 (10):1744–5. doi: 10.1038/mt.2010.195

87. Cohen CJ, Zhao Y, Zheng Z, Rosenberg SA, Morgan RA. Enhanced antitumor activity of murine-human hybrid T-cell receptor (TCR) in human lymphocytes is associated with improved pairing and TCR/CD3 stability. *Cancer Res* (2006) 66 (17):8878–86. doi: 10.1158/0008-5472.CAN-06-1450

88. Bethune MT, Gee MH, Bunse M, Lee MS, Gschweng EH, Pagadala MS, et al. Domain-swapped T cell receptors improve the safety of TCR gene therapy. *Elife* (2016) 5:e19095. doi: 10.7554/eLife.19095

89. Willemsen RA, Weijtens ME, Ronteltap C, Eshhar Z, Gratama JW, Chames P, et al. Grafting primary human T lymphocytes with cancer-specific chimeric single chain and two chain TCR. *Gene Ther* (2000) 7(16):1369–77. doi: 10.1038/sj.gt.3301253

90. Sebestyen Z, Schooten E, Sals T, Zaldivar I, San Jose E, Alarcon B, et al. Human TCR that incorporate CD3zeta induce highly preferred pairing between TCRalpha and beta chains following gene transfer. *J Immunol* (2008) 180(11):7736–46. doi: 10.4049/jimmunol.180.11.7736

91. Aggen DH, Chervin AS, Schmitt TM, Engels B, Stone JD, Richman SA, et al. Single-chain ValphaVbeta T-cell receptors function without mispairing with endogenous TCR chains. *Gene Ther* (2012) 19(4):365–74. doi: 10.1038/gt.2011.104

92. Stone JD, Harris DT, Soto CM, Chervin AS, Aggen DH, Roy EJ, et al. A novel T cell receptor single-chain signaling complex mediates antigen-specific T cell activity and tumor control. *Cancer Immunol Immunother* (2014) 63(11):1163–76. doi: 10.1007/s00262-014-1586-z

93. Knies D, Klobuch S, Xue SA, Birtel M, Echchannaoui H, Yildiz O, et al. An optimized single chain TCR scaffold relying on the assembly with the native CD3-complex prevents residual mispairing with endogenous TCRs in human T-cells. *Oncotarget* (2016) 7(16):21199–221. doi: 10.18632/oncotarget.8385

94. Richman SA, Aggen DH, Dossett ML, Donermeyer DL, Allen PM, Greenberg PD, et al. Structural features of T cell receptor variable regions that enhance domain stability and enable expression as single-chain ValphaVbeta fragments. *Mol Immunol* (2009) 46(5):902–16. doi: 10.1016/j.molimm.2008.09.021

95. Gunnarsen KS, Hoydahl LS, Neumann RS, Bjerregaard-Andersen K, Nilssen NR, Sollid LM, et al. Soluble T-cell receptor design influences functional yield in an e. coli chaperone-assisted expression system. *PLoS One* (2018) 13(4):e0195868. doi: 10.1371/journal.pone.0195868

96. Schober K, Muller TR, Gokmen F, Grassmann S, Effenberger M, Poltorak M, et al. Orthotopic replacement of T-cell receptor alpha- and beta-chains with preservation of near-physiological T-cell function. *Nat BioMed Eng* (2019) 3 (12):974–84. doi: 10.1038/s41551-019-0409-0

97. Foy SP, Jacoby K, Bota DA, Hunter T, Pan Z, Stawiski E, et al. Non-viral precision T cell receptor replacement for personalized cell therapy. *Nature* (2022). doi: 10.1038/s41586-022-05531-1

98. Heemskerk MH, Hagedoorn RS, van der Hoorn MA, van der Veken LT, Hoogeboom M, Kester MG, et al. Efficiency of T-cell receptor expression in dual-specific T cells is controlled by the intrinsic qualities of the TCR chains within the TCR-CD3 complex. *Blood* (2007) 109(1):235–43. doi: 10.1182/blood-2006-03-013318

99. Zhang XH, Tee LY, Wang XG, Huang QS, Yang SH. Off-target effects in CRISPR/Cas9-mediated genome engineering. *Mol Ther Nucleic Acids* (2015) 4(11): e264. doi: 10.1038/mtna.2015.37

100. Kosicki M, Tomberg K, Bradley A. Repair of double-strand breaks induced by CRISPR-Cas9 leads to large deletions and complex rearrangements. *Nat Biotechnol* (2018) 36(8):765–71. doi: 10.1038/nbt.4192

101. Naeem M, Majeed S, Hoque MZ, Ahmad I. Latest developed strategies to minimize the off-target effects in CRISPR-Cas-Mediated genome editing. *Cells* (2020) 9 (7):1608. doi: 10.3390/cells9071608

102. Park JH, Riviere I, Gonen M, Wang X, Senechal B, Curran KJ, et al. Long-term follow-up of CD19 CAR therapy in acute lymphoblastic leukemia. *N Engl J Med* (2018) 378(5):449–59. doi: 10.1056/NEJMoa1709919

103. Maude SL, Laetsch TW, Buechner J, Rives S, Boyer M, Bittencourt H, et al. Tisagenlecleucel in children and young adults with b-cell lymphoblastic leukemia. *N Engl J Med* (2018) 378(5):439–48. doi: 10.1056/NEJMoa1709866

104. Benjamin R, Graham C, Yallop D, Jozwik A, Mirci-Danicar OC, Lucchini G, et al. Genome-edited, donor-derived allogeneic anti-CD19 chimeric antigen receptor T cells in paediatric and adult b-cell acute lymphoblastic leukaemia: results of two phase 1 studies. *Lancet* (2020) 396(10266):1885–94. doi: 10.1016/S0140-6736(20)32334-5

105. Hu Y, Zhou Y, Zhang M, Ge W, Li Y, Yang L, et al. CRISPR/Cas9-engineered universal CD19/CD22 dual-targeted CAR-T cell therapy for Relapsed/Refractory b-cell acute lymphoblastic leukemia. *Clin Cancer Res* (2021) 27(10):2764–72. doi: 10.1158/1078-0432.CCR-20-3863

106. Nastoupil LJ, O'Brien S, Holmes HE, Dsouza L, Hart D, Matsuda E, et al. P1455: first-in-human trial of cb-010, a crispr-edited allogeneic anti-cd19 car -t cell therapy with a pd-1 knock out, in patients with relapsed or refractory b cell non-hodgkin lymphoma (antler study). *Hemasphere* (2022) 6(Suppl):1337–8. doi: 10.1097/01.HS9.0000848676.15840.df

107. Donohoue PD, Pacesa M, Lau E, Vidal B, Irby MJ, Nyer DB, et al. Conformational control of Cas9 by CRISPR hybrid RNA-DNA guides mitigates off-target activity in T cells. *Mol Cell* (2021) 81(17):3637–49.e5. doi: 10.1016/j.molcel.2021.07.035

108. O'Brien S, Nastoupil LJ, Essell J, Dsouza L, Hart D, Matsuda E, et al. A first-in-Human phase 1, multicenter, open-label study of CB-010, a next-generation CRISPR-edited allogeneic anti-CD19 CAR-T cell therapy with a PD-1 knockout, in patients with Relapsed/Refractory b cell non-Hodgkin lymphoma (ANTLER study). *Blood* (2022) 140(Supplement 1):9457–8. doi: 10.1182/blood-2022-168128

109. Shah BD, Jacobson C, Solomon SR, Jain N, Johnson MC, Vainorius M, et al. Allogeneic CAR-T PBCAR0191 with intensified lymphodepletion is highly active in patients with Relapsed/Refractory b-cell malignancies. *Blood* (2021) 138(Supplement 1):302. doi: 10.1182/blood-2021-150609

110. Hu Y, Zhou Y, Zhang M, Zhao H, Wei G, Ge W, et al. Genetically modified CD7-targeting allogeneic CAR-T cell therapy with enhanced efficacy for relapsed/refractory CD7-positive hematological malignancies: a phase I clinical study. *Cell Res* (2022) 32(11):995–1007. doi: 10.1038/s41422-022-00721-y

111. Chapuis AG, Egan DN, Bar M, Schmitt TM, McAfee MS, Paulson KG, et al. T Cell receptor gene therapy targeting WT1 prevents acute myeloid leukemia relapse post-transplant. *Nat Med* (2019) 25(7):1064–72. doi: 10.1038/s41591-019-0472-9

112. Anderson NM, Simon MC. The tumor microenvironment. *Curr Biol* (2020) 30 (16):R921–R5. doi: 10.1016/j.cub.2020.06.081

113. Donnadieu E, Luu M, Alb M, Anliker B, Arcangeli S, Bonini C, et al. Time to evolve: predicting engineered T cell-associated toxicity with next-generation models. *J Immunother Cancer* (2022) 10(5):e003486. doi: 10.1136/jitc-2021-003486

114. Hay KA. Cytokine release syndrome and neurotoxicity after CD19 chimeric antigen receptor-modified (CAR-) T cell therapy. *Br J Haematol* (2018) 183(3):364–74. doi: 10.1111/bjh.15644

115. Shimabukuro-Vornhagen A, Godel P, Subklewe M, Stemmler HJ, Schlosser HA, Schlaak M, et al. Cytokine release syndrome. *J Immunother Cancer* (2018) 6(1):56. doi: 10.1186/s40425-018-0343-9

116. Morris EC, Neelapu SS, Giavridis T, Sadelain M. Cytokine release syndrome and associated neurotoxicity in cancer immunotherapy. *Nat Rev Immunol* (2022) 22 (2):85–96. doi: 10.1038/s41577-021-00547-6

117. Santomasso BD, Park JH, Salloum D, Riviere I, Flynn J, Mead E, et al. Clinical and biological correlates of neurotoxicity associated with CAR T-cell therapy in patients with b-cell acute lymphoblastic leukemia. *Cancer Discov* (2018) 8(8):958–71. doi: 10.1158/2159-8290.CD-17-1319

118. Cameron BJ, Gerry AB, Dukes J, Harper JV, Kannan V, Bianchi FC, et al. Identification of a titin-derived HLA-A1-presented peptide as a cross-reactive target for engineered MAGE A3-directed T cells. *Sci Transl Med* (2013) 5(197):197ra03. doi: 10.1126/scitranslmed.3006034

119. Morgan RA, Chinnasamy N, Abate-Daga D, Gros A, Robbins PF, Zheng Z, et al. Cancer regression and neurological toxicity following anti-MAGE-A3 TCR gene therapy. *J Immunother* (2013) 36(2):133–51. doi: 10.1097/CJI.0b013e3182829903

120. Sanderson JP, Crowley DJ, Wiedermann GE, Quinn LL, Crossland KL, Tunbridge HM, et al. Preclinical evaluation of an affinity-enhanced MAGE-A4-specific T-cell receptor for adoptive T-cell therapy. *Oncoimmunology* (2020) 9 (1):1682381. doi: 10.1080/2162402X.2019.1682381

121. Hong DS, Van Tine BA, Biswas S, McAlpine C, Johnson ML, Olszanski AJ, et al. Autologous T cell therapy for MAGE-A4(+) solid cancers in HLA-A*02(+) patients: a phase 1 trial. *Nat Med* (2023) 29(1):104–14. doi: 10.1038/s41591-022-02128-z

122. D'Angelo SP, Tine BAV, Attia S, Blay J-Y, Strauss SJ, Morales CMV, et al. SPEARHEAD-1: A phase 2 trial of afamitresgene autoleucel (Formerly ADP-A2M4) in patients with advanced synovial sarcoma or myxoid/round cell liposarcoma. *J Clin Oncol* (2021) 39(15_suppl):11504–. doi: 10.1200/JCO.2021.39.15_suppl.11504

123. Depil S, Duchateau P, Grupp SA, Mufti G, Poirot L. 'Off-the-shelf' allogeneic CAR T cells: development and challenges. *Nat Rev Drug Discov* (2020) 19(3):185–99. doi: 10.1038/s41573-019-0051-2

124. Melenhorst JJ, Chen GM, Wang M, Porter DL, Chen C, Collins MA, et al. Decade-long leukaemia remissions with persistence of CD4(+) CAR T cells. *Nature* (2022) 602(7897):503–9. doi: 10.1038/s41586-021-04390-6

125. Wang Z, Li N, Feng K, Chen M, Zhang Y, Liu Y, et al. Phase I study of CAR-T cells with PD-1 and TCR disruption in mesothelin-positive solid tumors. *Cell Mol Immunol* (2021) 18(9):2188–98. doi: 10.1038/s41423-021-00749-x

126. Cherkassky L, Morello A, Villena-Vargas J, Feng Y, Dimitrov DS, Jones DR, et al. Human CAR T cells with cell-intrinsic PD-1 checkpoint blockade resist tumor-mediated inhibition. *J Clin Invest* (2016) 126(8):3130–44. doi: 10.1172/JCI83092

127. Guo X, Jiang H, Shi B, Zhou M, Zhang H, Shi Z, et al. Disruption of PD-1 enhanced the anti-tumor activity of chimeric antigen receptor T cells against hepatocellular carcinoma. *Front Pharmacol* (2018) 9:1118. doi: 10.3389/fphar.2018.01118

128. Kalinin RS, Ukrainskaya VM, Chumakov SP, Moysenovich AM, Tereshchuk VM, Volkov DV, et al. Engineered removal of PD-1 from the surface of CD19 CAR-T cells results in increased activation and diminished survival. *Front Mol Biosci* (2021) 8:745286. doi: 10.3389/fmolb.2021.745286

129. Odorizzi PM, Pauken KE, Paley MA, Sharpe A, Wherry EJ. Genetic absence of PD-1 promotes accumulation of terminally differentiated exhausted CD8+ T cells. *J Exp Med* (2015) 212(7):1125–37. doi: 10.1084/jem.20142237

130. Shimizu K, Sugiura D, Okazaki IM, Maruhashi T, Takegami Y, Cheng C, et al. PD-1 imposes qualitative control of cellular transcriptomes in response to T cell activation. *Mol Cell* (2020) 77(5):937–50.e6. doi: 10.1016/j.molcel.2019.12.012

131. Liu X, Ranganathan R, Jiang S, Fang C, Sun J, Kim S, et al. A chimeric switch-receptor targeting PD1 augments the efficacy of second-generation CAR T cells in advanced solid tumors. *Cancer Res* (2016) 76(6):1578–90. doi: 10.1158/0008-5472.CAN-15-2524

132. Zhao S, Wang C, Lu P, Lou Y, Liu H, Wang T, et al. Switch receptor T3/28 improves long-term persistence and antitumor efficacy of CAR-T cells. *J Immunother Cancer* (2021) 9(12):e003176. doi: 10.1136/jitc-2021-003176

133. Hoogi S, Eisenberg V, Mayer S, Shamul A, Barliya T, Cohen CJ. A TIGIT-based chimeric co-stimulatory switch receptor improves T-cell anti-tumor function. *J Immunother Cancer* (2019) 7(1):243. doi: 10.1186/s40425-019-0721-y

134. Stenger D, Stief TA, Kaeuferle T, Willier S, Rataj F, Schober K, et al. Endogenous TCR promotes *in vivo* persistence of CD19-CAR-T cells compared to a CRISPR/Cas9-mediated TCR knockout CAR. *Blood* (2020) 136(12):1407–18. doi: 10.1182/blood.2020005185

135. Majzner RG, Mackall CL. Tumor antigen escape from CAR T-cell therapy. *Cancer Discov* (2018) 8(10):1219–26. doi: 10.1158/2159-8290.CD-18-0442

136. Spiegel JY, Patel S, Muffly L, Hossain NM, Oak J, Baird JH, et al. CAR T cells with dual targeting of CD19 and CD22 in adult patients with recurrent or refractory b cell malignancies: a phase 1 trial. *Nat Med* (2021) 27(8):1419–31. doi: 10.1038/s41591-021-01436-0

137. Dai H, Wu Z, Jia H, Tong C, Guo Y, Ti D, et al. Bispecific CAR-T cells targeting both CD19 and CD22 for therapy of adults with relapsed or refractory b cell acute lymphoblastic leukemia. *J Hematol Oncol* (2020) 13(1):30. doi: 10.1186/s13045-020-00856-8

138. Fousek K, Watanabe J, Joseph SK, George A, An X, Byrd TT, et al. CAR T-cells that target acute b-lineage leukemia irrespective of CD19 expression. *Leukemia* (2021) 35(1):75–89. doi: 10.1038/s41375-020-0792-2

139. Cordoba S, Onuoha S, Thomas S, Pignataro DS, Hough R, Ghorashian S, et al. CAR T cells with dual targeting of CD19 and CD22 in pediatric and young adult patients with relapsed or refractory b cell acute lymphoblastic leukemia: a phase 1 trial. *Nat Med* (2021) 27(10):1797–805. doi: 10.1038/s41591-021-01497-1

140. Yang M, Tang X, Zhang Z, Gu L, Wei H, Zhao S, et al. Tandem CAR-T cells targeting CD70 and B7-H3 exhibit potent preclinical activity against multiple solid tumors. *Theranostics* (2020) 10(17):7622–34. doi: 10.7150/thno.43991

141. Roybal KT, Rupp LJ, Morsut L, Walker WJ, McNally KA, Park JS, et al. Precision tumor recognition by T cells with combinatorial antigen-sensing circuits. *Cell* (2016) 164(4):770–9. doi: 10.1016/j.cell.2016.01.011

142. Srivastava S, Salter AI, Liggitt D, Yechan-Gunja S, Sarvothama M, Cooper K, et al. Logic-gated ROR1 chimeric antigen receptor expression rescues T cell-mediated toxicity to normal tissues and enables selective tumor targeting. *Cancer Cell* (2019) 35 (3):489–503.e8. doi: 10.1016/j.ccell.2019.02.003

143. Choe JH, Watchmaker PB, Simic MS, Gilbert RD, Li AW, Krasnow NA, et al. SynNotch-CAR T cells overcome challenges of specificity, heterogeneity, and persistence in treating glioblastoma. *Sci Transl Med* (2021) 13:eabe7378. doi: 10.1126/scitranslmed.abe7378

144. Williams JZ, Allen GM, Shah D, Sterin IS, Kim KH, Garcia VP, et al. Precise T cell recognition programs designed by transcriptionally linking multiple receptors. *Science* (2020) 370(6520):1099–104. doi: 10.1126/science.abc6270

145. Shafer P, Kelly LM, Hoyos V. Cancer therapy with TCR-engineered T cells: Current strategies, challenges, and prospects. *Front Immunol* (2022) 13:835762. doi: 10.3389/fimmu.2022.835762

146. Okumura S, Ishihara M, Kiyota N, Yakushijin K, Takada K, Kobayashi S, et al. Chimeric antigen receptor T-cell therapy targeting a MAGE A4 peptide and HLA-A*02:01 complex for unresectable advanced or recurrent solid cancer: protocol for a multi-institutional phase 1 clinical trial. *BMJ Open* (2022) 12(11):e065109. doi: 10.1136/bmjopen-2022-065109

147. Arnaudo L. On CAR-ts, decentralized in-house models, and the hospital exception. routes for sustainable access to innovative therapies. *J Law Biosci* (2022) 9 (2):lsac027. doi: 10.1093/jlb/lsac027

148. Mackensen A, Muller F, Mougiakakos D, Boltz S, Wilhelm A, Aigner M, et al. Anti-CD19 CAR T cell therapy for refractory systemic lupus erythematosus. *Nat Med* (2022) 28(10):2124–32. doi: 10.1038/s41591-022-02017-5

frontiers | Frontiers in Immunology

TYPE Original Research
PUBLISHED 21 March 2023
DOI 10.3389/fimmu.2023.1121973

OPEN ACCESS

EDITED BY
Ralf-Holger Voss,
Johannes Gutenberg University Mainz, Germany

REVIEWED BY
Gerald Willimsky,
Charité Universitätsmedizin Berlin, Germany
Eliana Ruggiero,
San Raffaele Hospital (IRCCS), Italy

*CORRESPONDENCE
Mirjam H. M. Heemskerk
m.h.m.heemskerk@lumc.nl

SPECIALTY SECTION
This article was submitted to Cancer Immunity and Immunotherapy, a section of the journal Frontiers in Immunology

RECEIVED 12 December 2022
ACCEPTED 06 February 2023
PUBLISHED 21 March 2023

CITATION
van Amerongen RA, Tuit S, Wouters AK, van de Meent M, Siekman SL, Meeuwsen MH, Wachsmann TLA, Remst DFG, Hagedoorn RS, van der Steen DM, de Ru AH, Verdegaal EME, van Veelen PA, Falkenburg JHF and Heemskerk MHM (2023) PRAME and CTCFL-reactive TCRs for the treatment of ovarian cancer. *Front. Immunol.* 14:1121973. doi: 10.3389/fimmu.2023.1121973

PRAME and CTCFL-reactive TCRs for the treatment of ovarian cancer

Rosa A. van Amerongen[1], Sander Tuit[1], Anne K. Wouters[1], Marian van de Meent[1], Sterre L. Siekman[1], Miranda H. Meeuwsen[1], Tassilo L. A. Wachsmann[1], Dennis F. G. Remst[1], Renate S. Hagedoorn[1], Dirk M. van der Steen[1], Arnoud H. de Ru[2], Els M. E. Verdegaal[3], Peter A. van Veelen[2], J. H. Frederik Falkenburg[1] and Mirjam H. M. Heemskerk[1]*

[1]Department of Hematology, Leiden University Medical Center, Leiden, Netherlands, [2]Center for Proteomics and Metabolomics, Leiden University Medical Center, Leiden, Netherlands, [3]Department of Medical Oncology, Oncode Institute, Leiden University Medical Center, Leiden, Netherlands

Recurrent disease emerges in the majority of patients with ovarian cancer (OVCA). Adoptive T-cell therapies with T-cell receptors (TCRs) targeting tumor-associated antigens (TAAs) are considered promising solutions for less-immunogenic 'cold' ovarian tumors. In order to treat a broader patient population, more TCRs targeting peptides derived from different TAAs binding in various HLA class I molecules are essential. By performing a differential gene expression analysis using mRNA-seq datasets, PRAME, CTCFL and CLDN6 were selected as strictly tumor-specific TAAs, with high expression in ovarian cancer and at least 20-fold lower expression in all healthy tissues of risk. In primary OVCA patient samples and cell lines we confirmed expression and identified naturally expressed TAA-derived peptides in the HLA class I ligandome. Subsequently, high-avidity T-cell clones recognizing these peptides were isolated from the allo-HLA T-cell repertoire of healthy individuals. Three PRAME TCRs and one CTCFL TCR of the most promising T-cell clones were sequenced, and transferred to CD8+ T cells. The PRAME TCR-T cells demonstrated potent and specific antitumor reactivity *in vitro* and *in vivo*. The CTCFL TCR-T cells efficiently recognized primary patient-derived OVCA cells, and OVCA cell lines treated with demethylating agent 5-aza-2′-deoxycytidine (DAC). The identified PRAME and CTCFL TCRs are promising candidates for the treatment of patients with ovarian cancer, and are an essential addition to the currently used HLA-A*02:01 restricted PRAME TCRs. Our selection of differentially expressed genes, naturally expressed TAA peptides and potent TCRs can improve and broaden the use of T-cell therapies for patients with ovarian cancer or other *PRAME* or *CTCFL* expressing cancers.

KEYWORDS

ovarian cancer, PRAME, CTCFL, CLDN6, TCR gene transfer, T-cell therapy, immunotherapy, allogeneic HLA

Background

Ovarian cancer (OVCA) is the fifth most lethal cancer type among women (1). Due to lack of specific symptoms, 58% of the ovarian cancer patients are diagnosed at an advanced or metastatic stage. These advanced stages have 5-year survival rates of only 30%, compared to about 80% for earlier stages (2). Ovarian cancer is a heterogeneous malignancy, with five distinct histotypes of which high-grade serous ovarian cancer (HGSC) is the most frequent type covering 70% of all ovarian cancers (3). Although late-stage patients initially respond well to standard treatments like debulking surgery, platinum- and taxane-based chemotherapy, or more recently poly (ADP-ribose) polymerase inhibitors, recurrent disease emerges in the majority of patients (4–6). Also immunotherapies such as, infusion of tumor infiltrating lymphocytes (TILs), anti-cancer vaccination, treatment with immune checkpoint inhibitors, and adoptive T-cell therapies using chimeric antigen receptors (CARs) or T-cell receptors (TCRs) are being explored in ovarian cancer patients (7–9). CARs are restricted to target epitopes of proteins located at the cell membrane, with limited options for ovarian cancer. TCRs can target more antigens, since peptides derived from both intra- and extracellular proteins can be processed and presented in human leukocyte antigen (HLA) and thus recognized by TCRs.

Ovarian cancer is in general classified as an immunogenic tumor, with CD8+ T-cell rich tumors associating with prolonged survival (10–12). Furthermore, immune escape mechanisms correlate with poor survival, such as HLA downregulation and increased expression of immune inhibitory molecules (13). For T-cell infiltrated tumors ('hot' tumors), immune checkpoint inhibitors or infusion of TILs may be good strategies. However, in most ovarian tumors the tumor mutation burden (TMB) is low, resulting in limited T-cell infiltration, lack of antitumor-reactive T cells, and consequently 'cold' tumors (13, 14). For those 'cold' tumors, adoptive T-cell therapies with TCR-engineered T cells (TCR-T cells) targeting tumor-associated antigens (TAAs) are considered promising solutions (8). In clinical trials with ovarian cancer patients, TCRs targeting cancer-testis antigens (CTAs) NY-ESO-1, MAGE-A4 and more recently PRAME have been investigated (8). Preclinically, T cells targeting MSLN, CCNA1, CLDN6, and several MAGE-A family members have been investigated for ovarian cancer as well (15–18). Yet, targeting more TAAs is desired and target antigens restricted by more HLA alleles are essential, as most of the investigated TCRs are HLA-A*02:01 restricted. Ideal TAAs to target ovarian cancer would be those that are highly and homogenously expressed in tumors, without expression in healthy tissues. Co-expression in tissues from reproductive organs would be tolerable, as expression in the reproductive compartment does not form an unacceptable toxicity risk for ovarian cancer patients. In addition, protein expression or options to induce expression in case of variable expression are required. For example, DNA-demethylating agents have shown the potential to induce expression of some CTAs, thereby contributing to increased recognition by CTA-specific T cells (19–21). T cells targeting TAAs can be found in the T-cell repertoire of either healthy individuals or patients. If TAAs are also expressed in healthy tissues, self-tolerance is established during negative selection whereby high-avidity self-reactive T cells are centrally deleted from the autologous-HLA (auto-HLA) T-cell repertoire. Self-tolerance can be circumvented by searching for TAA-specific T cells in the allogeneic-HLA (allo-HLA) T-cell repertoire, as we previously demonstrated for several B-cell restricted antigens and WT1 (22–24). Since these T cells of the allo-HLA T-cell repertoire have not been subjected to negative selection, the safety should be carefully evaluated.

In order to treat a broader patient population, we searched for strictly tumor-specific TAAs in ovarian cancer and high-affinity TCRs targeting these TAAs. By combining mRNA-seq datasets of healthy and tumor tissues, we selected preferentially expressed antigen of melanoma (PRAME), CCCTC-binding factor (CTCFL), and Claudin-6 (CLDN6) as TAAs with high expression in ovarian cancer and at least 20-fold lower expression in all healthy tissues of risk. We identified peptides derived from the selected targets in the HLA class I ligandome of primary OVCA patient samples as well as cell lines. To target the identified peptides we isolated high-avidity T-cell clones from the allo-HLA T-cell repertoire of 25 healthy individuals. Using panels of primary patient-derived ovarian cancer cells, OVCA cell lines and healthy cell subsets, we ultimately selected three PRAME TCRs and one CTCFL TCR with potent and specific antitumor reactivity *in vitro* and *in vivo*. These TCRs are promising candidates for the treatment of patients with ovarian cancer.

Abbreviations: OVCA, ovarian cancer; TCR, T-cell receptor; TAA, tumor-associated antigen; DAC, 5-aza-2′-deoxycytidine; HGSC, high-grade serous ovarian cancer; TIL, tumor infiltrating lymphocyte; CAR, chimeric antigen receptor; HLA, human leukocyte antigen; TMB, the tumor mutation burden; TCR-T cells, TCR-engineered T cells; CTA, cancer-testis antigen; auto-HLA, autologous-HLA; allo-HLA, allogeneic-HLA; PRAME, preferentially expressed antigen of melanoma; CTCFL, CCCTC-binding factor; CLDN6, claudin-6; TCGA, The Cancer Genome Atlas; GTEx, Genotype Tissue Expression; HPA, Human Protein Atlas; RLE, relative log expression; FC, fold change; AML, acute myeloid leukemia; MACS, magnetic-activated cell sorting; FACS, fluorescence-activated cell sorting; qPCR, quantitative polymerase chain reaction; TCM, T-cell medium; mDCs, mature CD14-derived dendritic cells; imDCs, immature CD14-derived dendritic cells; PBMCs, peripheral blood mononuclear cells; PTECs, proximal tubular epithelial cells; PHA, phytohemagglutinin; E:T, effector-to-target; DMSO, dimethyl sulfoxide; DE, differentially expressed; pMHC-multimer, peptide MHC-multimer; EBV-LCL, Epstein-Barr virus transformed lymphoblastoid cell lines; mTCR, murine TCR.

Materials and methods

Differential gene expression analysis

Publicly available datasets [The Cancer Genome Atlas (TCGA) (https://www.cancer.gov/tcga); Genotype Tissue Expression (GTEx) (25); Human Protein Atlas (HPA) (26)] were accessed through the online resource Recount2 (https://jhubiostatistics.shinyapps.io/recount/) (27). Read alignment against the hg38 reference genome and mRNA quantification were part of the Recount2 pre-processing pipeline. Raw count tables were obtained and combined into one

comprehensive dataset. For each distinct primary cancer tissue from the TCGA 30 samples were randomly chosen. Random sampling was also applied for the GTEx dataset, with maximum number of 20 samples, if available. Regarding the HPA dataset, all samples were included (3-5 samples per tissue). The compiled dataset consisted of a total of 2202 samples and was normalized utilizing the EdgeR package and its Relative Log Expression (RLE) method (28, 29) in R (v3.4.3). Finally, the dataset was filtered to retain only those genes showing evidence of expression in ovarian cancer, as defined by a minimum mean of 100 read counts (16855 genes in total). Differential gene expression analysis was performed using the EdgeR package after fitting a quasi-likelihood negative binomial generalized log-linear model to the count data. Genes were defined to be DE in ovarian cancer when they exhibited an absolute minimum fold change (FC) of ≥ 20 and FDR adjusted p-value of ≤ 0.05. Mean expression in ovarian cancer was compared against most of the healthy tissues present in the dataset, only tissues from reproductive organs and tumors were excluded.

Sample collection for peptide elution

Seven solid primary OVCA patient samples derived from different patients (2 – 20 gram) were collected and dissociated using the gentleMACS (Miltenyi Biotec) procedure (Supplemental Methods). Also one ascites OVCA patient sample ($6*10^9$ cells) and three primary acute myeloid leukemia (AML) samples (65 – $500*10^9$ cells) were collected. Furthermore, various cell lines were expanded up to at least $2*10^9$ cells (Supplementary Table 3). Cell lines transduced with HLA alleles, CLDN6 and/or CTCFL were first enriched for marker gene expression *via* magnetic-activated cell sorting (MACS) or fluorescence-activated cell sorting (FACS). HLA typing of all samples/cell lines was performed and gene expression was quantified by Quantitative Polymerase Chain Reaction (qPCR) (Supplemental Methods).

HLA class I-peptide elution procedure, fractionation and mass spectrometry

Cell pellets were lysed and subjected to an immunoaffinity column to collect bound peptide-HLA complexes. Peptides were subsequently separated, fractionated and analyzed by data-dependent MS/MS (Supplemental Methods). Proteome Discoverer V.2.1 (Thermo Fisher Scientific) was used for peptide and protein identification, using the mascot search node for identification (mascot V.2.2.04) and the UniProt Homo Sapiens database (UP000005640; Jan 2015; 67,911 entries). Peptides were in-house synthesized using standard Fmoc chemistry and PE-conjugated pMHC-multimers were generated with minor modifications (Supplemental Methods).

Cell culture

T cells were cultured in T-cell medium (TCM) and (re) stimulated every 10-14 days with PHA and irradiated autologous feeders (Supplemental Methods). OVCA cell lines COV-318/-362.4/-413b/-434/-504/-641 were established at the department of Medical Oncology (LUMC, NL) (30). OVCA cell lines OVCAR-3 and SK-OV-3 were obtained from the ATCC and A2780 from the ECACC. Primary patient-derived OVCA cells were either isolated from bulk tumor tissue using gentle MACS and immediately frozen (OVCA-L11) or isolated from the ascites fluid by centrifugation (>70% EpCAM positive cells and >95% CD45 negative cells) and immediately frozen (OVCA-L23). Both OVCA-L11 and OVCA-L23 were derived from an HLA-A*02:01 positive OVCA patient. The primary patient-derived OVCA cells (p0) were thawed three days before being used as target cells in screening experiments. Additionally, primary patient-derived OVCA-L23 cells expanded *in vitro* which allowed retroviral introduction of HLA-A*24:02 or B*07:01, followed by MACS-enrichment. OVCA-L23 cells transduced with HLA-A*24:02 or B*07:01 (passage 10) were included as target cells in screening experiments. Tumor cell lines and primary patient-derived OVCA cells were cultured in different media (Supplemental Methods). CD14-derived mature and immature dendritic cells (mDCs and imDCs), and activated CD19 cells were isolated from peripheral blood mononuclear cells (PBMCs) of different healthy donors and generated as previously described (24). Purity of the generated cells was assessed using flow cytometry (Supplemental Methods). Fibroblasts and keratinocytes, both cultured from skin biopsies, were cultured as previously described (24). PTECs derived from kidney tubules were isolated and cultured as previously described (31).

Isolation of OVCA-specific T cells by pMHC-multimer enrichment

Buffy coats of healthy donors were collected after informed consent (Sanquin). PBMCs were isolated using Ficoll gradient separation and incubated with the selection of pMHC-multimers for 1 hour at 4°C or 15 minutes at 37°C. pMHC-multimers were only included if the healthy donor was negative for the restricted HLA allele. pMHC-multimer bound cells were MACS enriched using anti-PE MicroBeads (Miltenyi Biotec/130-048-801). The positive fraction was stained with CD8 (AF700) and CD4, CD14 and CD19 (FITC). pMHC-multimer and CD8 positive cells were single-cell sorted using an Aria III cell sorter (BD Biosciences) in a 96 well round bottom plate containing $5x10^4$ irradiated PBMCs (35Gy) and $5x10^3$ EBV-JY cells (55Gy) in 100 µL TCM with 0.8 µg/mL phytohemagglutinin (PHA). T-cell recognition was assessed 10 – 14 days after stimulation, followed by restimulation or storage of the selected T-cell clones.

T-cell reactivity assays

T-cell recognition was measured by an IFN-γ ELISA (Sanquin or Diaclone). 5,000 T cells were cocultured overnight with target cells in various effector-to-target (E:T) ratios in 60 µL TCM in 384-well flat-bottom plates (Greiner Bio-One). To upregulate HLA expression, all adherent target cells were treated with 100 IU/mL IFN-γ (Boehringer Ingelheim) for 48 hours before coculture. All T cells and target cells

were washed thoroughly before coculture to remove expansion-related cytokines. Supernatants were transferred during the ELISA procedure using the Hamilton Microlab STAR Liquid Handling System (Hamilton company) and diluted 1:5, 1:25 and/or 1:125 to quantify IFN-γ production levels within the linear range of the standard curve. T-cell mediated cytotoxicity was measured in a 6-hour ^{51}chromium release assay (Supplemental Methods).

TCR identification and TCR gene transfer to CD8+ T cells

TCR α and β chains of the selected T-cell clones were identified by sequencing with minor modifications (Supplemental Methods). The TCR α (VJ) and β (VDJ) regions were codon optimized, synthesized, and cloned in MP71-TCR-flex retroviral vectors by Baseclear. The MP71-TCR-flex vector already contains codon-optimized and cysteine-modified murine TCR α and β constant domains to optimize TCR expression and increase preferential pairing (32). Apart from the OVCA-specific TCRs, a murinized CMV-specific TCR (NLVPMVATV peptide presented in HLA-A*02:01) was included as a negative control. CD8+ T cells were isolated from PBMCs of different donors by MACS and TCRs were introduced *via* retroviral transduction two days after stimulation with PHA and irradiated autologous feeders. Seven days after stimulation, CD8+ T cells were MACS enriched for murine TCR. Ten days after stimulation, purity of TCR-T cells was checked by flow cytometry and used in functional assays (more details in Supplemental Methods).

In vivo model

NOD-scid-IL2Rgamma^{null} (NSG) mice (The Jackson Laboratory) were intravenously (i.v.) injected with 2*10^6 U266 multiple myeloma (MM)_cells. U266 cells were transduced with and enriched for Luciferase-tdTomato Red and HLA-A24 (NGFR) when indicated. On day 14, mice were treated i.v. with 5*10^6 purified PRAME TCR-T cells (n = 6) or CMV TCR-T cells (n = 4). TCR-T cells were used seven days after second stimulation with PHA and irradiated autologous feeder cells. Tumor outgrowth (average radiance) was measured at regular intervals after intraperitoneal injection of 150 mL 7.5 mM D-luciferine (Cayman Chemical) using a CCD camera (IVIS Spectrum, PerkinElmer). All mice were sacrificed when control mice reached an average luminescence of 1*10^7 p/s/cm^2/sr. This study was approved by the national Ethical Committee for Animal Research (AVD116002017891) and performed in accordance with Dutch laws for animal experiments.

DAC treatment

DAC (5-aza-2′-deoxycytidine) (A3656, Sigma-Aldrich) was solved in dimethyl sulfoxide (DMSO). Target cells were at 50% confluency at start of treatment and were treated with 1 μM DAC on day 1 and 4. DMSO treated cells served as negative control. On day 7, cells were harvested for T-cell reactivity assays and RNA isolation to determine gene expression by qPCR.

Statistical analysis

Statistical analysis was performed using GraphPad Prism software (Version 9.0.1.). Statistical tests used are indicated in the figure legends, $P < 0.05$ was considered significant. Significance levels are indicated as p <.05 *, p <.01 **, p <.001 ***, and p <.0001 ****.

Study approval

Samples of healthy donors and AML patients were used from the LUMC Biobank for Hematological Diseases, after approval by the Institutional Review Board of the LUMC (approval number 3.4205/010/FB/jr) and the METC-LDD (approval number HEM 008/SH/sh). The OVCA patient samples were obtained according to the Code of Conduct for Responsible Use of human tissues or in the context of study L18.012 that was approved by the Institutional Review Board of the LUMC (approval number L18.012) and Central Committee on Research Involving Human Subjects (approval number NL63434.000.17). Studies were conducted in accordance with the Declaration of Helsinki and after obtaining informed consent.

Results

Interrogation of mRNA-seq data reveals differentially expressed genes in ovarian cancer

To identify genes with immuno-therapeutic potential in ovarian cancer, we obtained mRNA-seq data of 2202 samples from three independent sources (TCGA, GTEx, and HPA) representing 120 different healthy or tumor tissues. We combined these tissues into one comprehensive dataset to perform an elaborate differential gene expression analysis (Figure 1A and Supplementary Table 1). Genes were defined to be differentially expressed (DE) in ovarian cancer when they exhibited an absolute FC of ≥ 20 compared to the different healthy tissues present in the dataset, using the mean expression values. Tissues from reproductive organs were excluded from this comparison, as expression in the reproductive compartment does not form an unacceptable toxicity risk for ovarian cancer patients. The FC values for all 16,855 genes with ≥ 100 read counts in ovarian cancer are listed in Supplementary Table 2, of which 9 genes were DE with a FC ≥ 20 in ovarian cancer. We plotted for all genes the minimum FC against the adjusted p-value to visualize the minimal extent of differential expression in ovarian cancer (Figure 1B).

Six of the nine DE genes are not expressed on protein level and were therefore not considered target candidates for T-cell therapy.

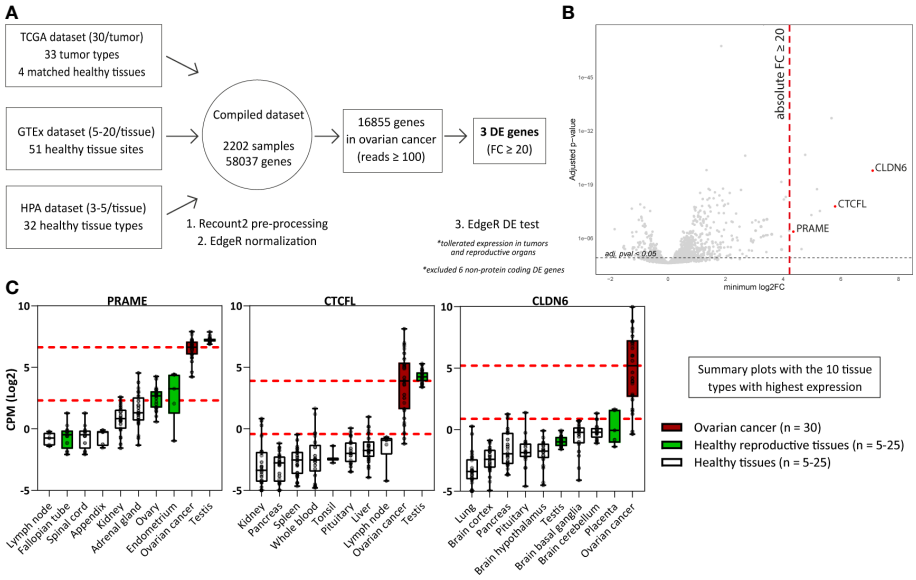

FIGURE 1
Differential gene expression analysis reveals genes associated with High-Grade Serous Ovarian Carcinoma. **(A)** Scheme depicting the differential gene expression analysis strategy. **(B)** Plot displaying for all genes the minimum FC against the adj. p-val. Indicated in red are the three identified DE genes (FC ≥ 20; adj. p-val ≤ 0.05). Indicated in grey are non-DE genes and non-protein coding genes. **(C)** Boxplots depicting *PRAME*, *CTCFL* and *CLDN6* expression in ovarian cancer (TCGA data, n = 30) and the 9 healthy tissue types with highest gene expression (HPA and/or GTEx data, n = 5-25). Overlapping healthy tissue types within the HPA and GTEx were combined when possible. Boxplots extend from first to third quartile, the horizontal line represent the median expression value. The whiskers represent minimum and maximum expression. The upper and lower red dashed lines represent the median expression value and the 20 times lower expression value, respectively. (Adj. p-val: false discovery rate adjusted p-value, DE, differentially expressed; FC, fold change; GTEx, genotype-tissue expression; HPA, human protein atlas; CPM Log2, log2-transformed counts per million; minimum log2FC, log2 fold change; TCGA, The cancer genome atlas).

SLC25A3P1, small nuclear RNU1-27P and small nuclear RNU1-28P are pseudogenes which are assumed not to be translated (33). Furthermore, microRNA MIR3687-1, antisense RNA ELFN1-AS1 and an uncharacterized long non-coding RNA gene are classified as non-protein coding RNAs, although they do exhibit several gene regulating functions of other genes (34). The final three genes, PRAME, CTCFL and CLDN6, were considered interesting target candidates. These genes were at least 20 times higher expressed in ovarian cancer compared with healthy tissues, except for some reproductive organs (Supplementary Figure 1, summarized in Figure 1C). In line with their classification as CTA, *PRAME* and *CTCFL* were highly expressed in testis (35). *PRAME* was also found to be expressed in healthy endometrium and ovary, and *CLDN6* in placenta. According to the TCGA data, in particular *PRAME* is expressed in various other tumor types as well (Supplementary Figure 2).

To confirm expression of the three selected genes in ovarian cancer, we quantified gene expression by qPCR in primary solid tumor patient samples and malignant ascites patient samples, and in OVCA cell lines (Figure 2A). We quantified relative gene expression compared with three housekeeping genes. *PRAME* and *CLDN6* expression was demonstrated in most primary patient samples and OVCA cell lines. Expression of *CTCFL* was high (>30% relative expression) in 10/12 solid tumor patient samples, but limited expression was observed in ascites patient samples and cell lines.

PRAME, CTCFL and CLDN6-derived peptides identified in the HLA class I ligandome

The number of previously identified peptides derived from PRAME, CTCFL and CLDN6 binding in different common HLA class I molecules is limited, as well as solid evidence of processing and presentation in the context of HLA class I on ovarian tumors. The PRAME TCRs currently investigated in clinical trials all target the SLLQHLIGL or VLDGLDVLL peptide presented in HLA-A*02:01. To establish a dataset of peptides that can be targeted by TCRs, we determined the HLA class I ligandome of eight primary OVCA patient samples and two OVCA cell lines (Supplementary Tables 3A, B). In order to enlarge the dataset, various tumor cell lines and primary AML patient samples expressing the selected genes were additionally included (Supplementary Table 3C), some of these cell lines were transduced with CTCFL, CLDN6 and/or HLA class I molecules (Supplementary Table 3D). All best scoring peptides for each gene with preferably a minimal Best Mascot Ion score of 20 and a mass accuracy of 10 ppm were considered in the

10.3389/fimmu.2023.1121973

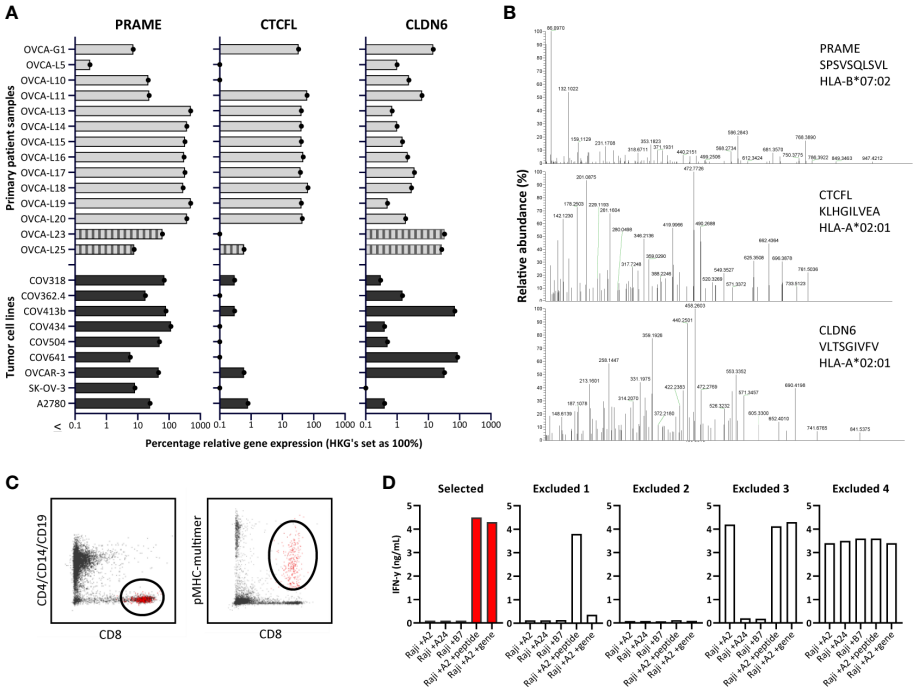

FIGURE 2
Identification of PRAME, CTCFL and CLDN6 peptides and T-cell clones. **(A)** PRAME, CTCFL (TvX) and CLDN6 mRNA gene expression in 14 OVCA patient samples (12 solid tumor tissues and 2 malignant ascites samples (OVCA-L23 and OVCA-L25)), and 9 OVCA cell lines. Expression was measured by qPCR and is shown as percentage relative to the three HKGs *GUSB*, *VPS29* and *PSMB4*, which was set at 100%. **(B)** Example of three OVCA-derived peptides identified in our HLA ligandome analyses. Shown are the mass spectra of the eluted peptides, including the gene, peptide sequence and HLA restriction. All eluted peptides were validated by comparing tandem mass spectra of eluted peptides and synthetic peptides, as shown in Supplementary Figure 3. **(C)** Representative flow cytometry plots of the pMHC-multimer enriched cell population in 1 of the 25 healthy donors. Shown is the gating strategy of the single-cell sorted population (depicted in red), gated on CD8 (Alx700) +, pMHC-multimer (PE) + and CD4/CD14/CD19 (FITC) -. **(D)** Examples of recognition patterns based on IFN-γ production (ng/mL) of selected and excluded T-cell clones during the first T-cell screenings. T-cell clones were cocultured with Raji cells transduced with various HLA alleles, combined with loading of OVCA peptides (1 μM) or transduction of OVCA genes (E:T=1:6). Excluded 1 – 4 represent T-cell clones lacking potency and/or specificity. (HKGs, housekeeping genes; OVCA, primary ovarian cancer sample).

first round of selection. As CLDN6 and CTCFL share homology with ubiquitously expressed family members, only those peptides that were unique for the target genes and did not demonstrate major sequence overlap with Claudin-family members (n=47) or paralog CTCF (n=6) were selected. In addition, we only continued with peptides binding to common HLA molecules according to netMHC peptide binding algorithm that matched with the HLA typing of the material from which the peptides originated (Supplementary Tables 3A–D) (36). Identified peptides were validated by comparing mass spectra of eluted peptides and synthetic peptides (Figure 2B and Supplementary Figure 3). HLA binding was confirmed by stable pMHC-monomer refolding. In total 23 PRAME peptides, 8 CTCFL peptides and 3 CLDN6 peptides were validated (Supplementary Table 4). As a result of alternative splicing, at least 15 protein variants derived from CTCFL isoforms are known (37). 7/8 CTCFL peptides are present in all 15 CTCFL variants, 1/8 CTCFL peptides, KLHGILVEA in HLA-A*02:01, is only located in the unique region of CTCFL variant 13 (Supplementary Figures 4A, B) (37). Since no substantial differences in gene expression were observed between variant 13 and the other CTCFL variants we also continued with this peptide (Supplementary Figure 4C).

OVCA-reactive T-cell clones isolated from the allo-HLA T-cell repertoire of 25 healthy donors

To isolate high-avidity T cells reactive against PRAME-, CTCFL- and CLDN6-derived peptides, peptide MHC-multimers (pMHC-multimers) were generated for a selection of 17 peptides binding in different common HLA class I alleles (Table 1). Of these peptides 16 were identified in our mass spectrometry analysis and 1 peptide was previously identified (38). These pMHC-multimers were incubated with PBMCs of 25 healthy HLA typed donors, pMHC-multimer+ cells were enriched by MACS, and pMHC-multimer+ CD8+ cells were subsequently single-cell sorted (Figure 2C). pMHC-multimers were only included if the donor was negative for the HLA allele, to ensure identification of T cells from the allogeneic T-cell repertoire, and thereby circumventing self-tolerance. On average $618*10^6$ PBMCs were used per donor and between 21 and 368 pMHC-multimer+ CD8+ T-cell clones could be expanded after single-cell sorting. To test for functional peptide-specificity, T-cell clones were cocultured with Raji cells loaded with a pool of all target peptides. T-cell clones specifically recognizing the peptide pool were subsequently tested for recognition of target cells

10.3389/fimmu.2023.1121973

TABLE 1 Included PRAME, CTCFL and CLDN6 HLA class I peptides.

Gene	Peptide	HLA	Sample/cell line source	BMI
PRAME	QLLALLPSL	A*02:01	TMD8 +A2, EBV-5098	37
PRAME	LYVDSLFFL	A*24:02	x	x
PRAME	SPRRLVELAGQSL	B*07:02	COV413b, AML-6711, TMD8 +B7, EBV-5098	30
PRAME	MPMQDIKMIL	B*07:02	TMD8 +B7, AML-6498	25
PRAME	SPSVSQLSVL	B*07:02	COV413b, EBV-5098, TMD8 +B7, AML-3374, U266	65
PRAME	LPRELFPPL	B*07:02	EBV-5098, K562+B7	26
PRAME	MPMQDIKMIL	B*35:01	TMD8 +B7, AML-6498	25
PRAME	LPRELFPPL	B*35:01	EBV-5098, K562+B7	26
PRAME	YEDIHGTLHL	B*40:01	COV362.4, U266	42
CTCFL	CSAVFHERY	A*01:01	K562+A1	43
CTCFL	RSDEIVLTV	A*01:01	K562+A1	37
CTCFL	KLHGILVEA	A*02:01	K562+A2	12
CTCFL	DSKLAVSL	B*08:01	K562+B8	35
CTCFL	AETTGLIKL	B*40:01	COV362.4	51
CLDN6	GPSEYPTKNYV	A*01:01	EBV-9603 +CLDN6	25
CLDN6	VLTSGIVFV	A*02:01	EBV-6519 +CLDN6	23
CLDN6	DSKARLVL	B*08:01	EBV-9603 +CLDN6	37

Overview of the 17 OVCA gene-derived peptides included in our T-cell search. For each peptide identified in our HLA ligandome analyses, the gene, HLA binding restriction, sample/cell line source, and BMI are listed. Details of the samples and cell lines are listed in Supplementary Table 1. The LYVDSLFFL peptide binding in A*24:02 was included based on literature (38). BMI, best Mascot ion score.

transduced with OVCA genes, to select T-cell clones potent enough to recognize endogenously processed and presented peptide. T-cell clones that were only reactive against peptide-loaded cells, nonreactive, reactive against one specific HLA allele independent of added peptides, or reactive against all target cells were excluded (Figure 2D). In addition to our search in healthy donors, we searched within the allogeneic T-cell repertoire of an AML patient after HLA-mismatched stem cell transplantation that was published previously (39).

In total, 56 T-cell clones specific for 6/9 PRAME and 3/5 CTCFL peptides that recognized cells transduced with the respective OVCA gene were selected of which 28 clones are shown in Supplementary figure 5A, B. For CLDN6, T-cell clones were isolated that recognized peptide-loaded target cells (Supplementary figure 5C), however, CLDN6 transduced cells were not recognized and therefore these CLDN6-specific T-cell clones were not of sufficient avidity and excluded from further screenings.

T-cell clones selected as clinical TCR candidates for the treatment of ovarian cancer patients

To select TCR candidates for clinical development, 3 additional screenings were performed. First, tumor recognition was assessed using a panel of naturally expressing *PRAME* or *CTCFL* positive tumor cell lines, all expressing the target HLA allele. OVCA cell lines were included to screen the PRAME T-cell clones and for the CTCFL T-cell clones K562 and Ca Ski cell lines were included since OVCA cell lines did not express *CTCFL* (Figure 2A). Second, cross-reactivity with other peptides presented in the target HLA allele was assessed using a panel of *PRAME* or *CTCFL* negative tumor cell lines and healthy cell subsets. Third, HLA cross-reactivity was assessed using a panel of Epstein-Barr virus transformed lymphoblastoid cell lines (EBV-LCL) expressing all HLA alleles with an allele frequency ≥ 1% present in the Caucasian population. In total, four T-cell clones were selected as TCR candidates for clinical development. Three T-cell clones target a PRAME-derived peptide: clone DSK3 specific for QLLALLPSL in HLA-A*02:01 (PRAME/QLL/A2), clone 16.3C1 specific for LYVDSLFFL in HLA-A*24:02 (PRAME/LYV/A24) and clone 8.10C4 specific for SPSVSQLSVL in B*07:02 (PRAME/SPS/B7). One T-cell clone targets a CTCFL-derived peptide: clone 39.2E12 specific for KLHGILVEA in HLA-A*02:01 (CTCFL/KLH/A2). These T-cell clones effectively recognized all *PRAME* or *CTCFL* positive OVCA/tumor cell lines (Figure 3A). Of the *PRAME* and *CTCFL* negative cells, only clone $8.10C4^{PRAME/SPS/B7}$ showed low recognition of *PRAME* negative healthy imDCs (Figure 3B). To prevent unwanted toxicity, this recognition should be investigated further using TCR-T cells. Furthermore, clone $16.3C1^{PRAME/LYV/A24}$ showed cross-reactivity against HLA-B*37:01 and HLA-B*38:01 positive EBV-LCLs (Figure 3C). The global frequencies of these HLA alleles are low (HLA-B*37:01: 3.23% and HLA-B*38:01:

10.3389/fimmu.2023.1121973

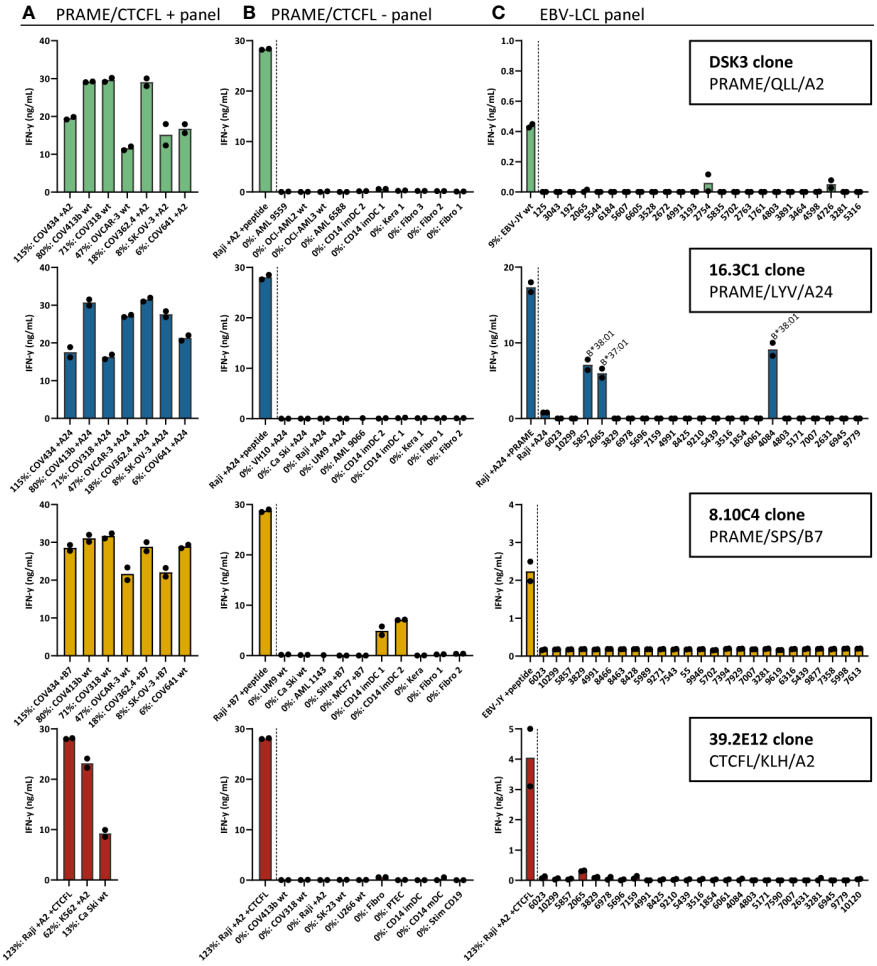

FIGURE 3
Recognition patterns of the selected T-cell clones recognizing *PRAME* or *CTCFL* positive tumor cells, without substantial peptide or HLA cross-reactivity. Recognition patterns based on IFN-γ production (ng/mL) after overnight coculture assays with **(A)** *PRAME* or *CTCFL* positive tumor cell lines, **(B)** PRAME or CTCFL-negative tumor cell lines and healthy cell subsets, and **(C)** 25 EBV-LCLs, expressing all HLA alleles with an allele frequency ≥ 1% present in the Caucasian population. The HLA allele in **(C)** is depicted if an HLA allele is recognized by the T-cell clone, meeting the requirement that all EBV-LCLs with this HLA allele are recognized. All cell lines in **(A, B)** express the HLA allele that presents the targeted peptide, either wildtype or the HLA allele was introduced by transduction (+A2, +A24 or +B7). Percentage relative *PRAME* or *CTCFL* expression is depicted, as determined by qPCR. Bars represent mean and symbols depict technical duplicates. (EBV-LCL: Epstein-Barr virus transformed lymphoblastoid cell lines).

1.72%) (40). The excluded T-cell clones exhibited either limited recognition of *PRAME* or *CTCFL* positive OVCA/tumor cell lines (25/56), or were cross-reactive against peptides in commonly expressed HLA alleles (27/56).

High-affinity PRAME TCRs reactive against OVCA cells

To investigate the clinical potential of the selected PRAME T-cell clones for TCR gene therapeutic strategies, the TCR α and β chains were sequenced and transferred using retroviral vectors into CD8+ T cells of at least four different donors. TCR-T cells were enriched based on murine TCR (mTCR) expression and functionally tested. In Figure 4A we demonstrated, by pMHC-multimer staining, that PRAME TCR-T cells efficiently expressed the three newly identified TCRs at the cell surface. As a reference, the previously identified HSS3 TCR$^{PRAME/SLL/A2}$ (patent: WO2016142783A2) that will be clinically tested in the near future was included (39). Most TCR-T cells exhibited high peptide sensitivity in peptide titration experiments, only TCR 8.10C4$^{PRAME/SPS/B7}$ demonstrated limited peptide sensitivity (Figure 4B). Additionally, ovarian cancer reactivity of the different PRAME TCR-T cells was studied against various OVCA tumor cell lines and primary patient-derived ovarian cancer cells (OVCA-L23) (Figure 4C). The OVCA-L23 cells positive for HLA-A*02:01 expanded *in vitro* which allowed additional retroviral introduction of HLA-A*24:02 or B*07:01. Uncultured OVCA-L23 (p0) cells were therefore included as target for TCR DSK3$^{PRAME/QLL/A2}$ and HLA-A*24:02 or B*07:01 transduced cells (p10) were included as targets for all the PRAME TCR-T cells. All PRAME TCR-T cells recognized the primary patient-derived OVCA-L23

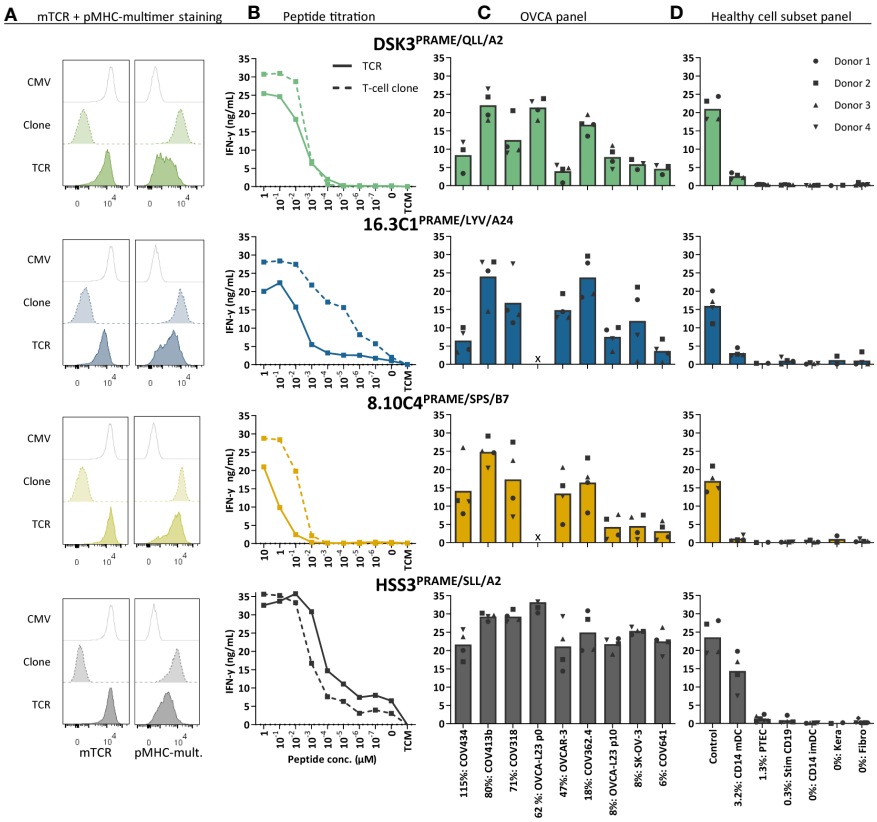

FIGURE 4
Three new PRAME TCR-T cells recognize *PRAME* positive OVCA cells and mature DCs. The three new PRAME TCRs and clinically tested HSS3 TCR were introduced *via* retroviral transduction in CD8+ cells of four different donors. **(A)** Representative flow cytometry plots of purified CMV and PRAME TCR-T cells, and their parental PRAME T-cell clones stained with murine TCR (mTCR) and the PRAME-specific pMHC-mult. **(B)** IFN-γ production (ng/mL) of TCR-T cells and their parental T-cell clones cocultured overnight with Raji cells (transduced with HLA-A2, A24 or B7) loaded with titrated peptide concentrations (E:T = 1:6). **(C)** IFN-γ production of TCR-T cells cocultured with OVCA cells (E:T = 1:6). All OVCA cells express the HLA allele that presents the targeted peptide, either wildtype or the HLA allele was introduced by transduction. Primary malignant ascites patient sample OVCA-L23 (wildtype HLA-A2) was either passage 0 (included for TCR DSK3 and HSS3) or passage 10 transduced with HLA-A24 or B7 (included for all TCRs). **(D)** IFN-γ production of TCR-T cells cocultured with several healthy cell subsets (E:T = 1:4 for keratinocytes, fibroblasts, PTECs and CD14+, 1:6 for CD19+). Cell subsets were isolated from multiple HLA-A2+, A24+ and/or B7+ donors. **(C-D)** Percentage relative *PRAME* expression is depicted, as determined by qPCR. Bars represent mean and symbols depict averaged duplicate values from four different donors tested in two independent experiments. (E:T, effector:target ratio; imDCs and mDCs, immature and mature dendritic cells; pMHC-mult, peptide MHC-multimers; PTECs, proximal tubular epithelial cells; OVCA, primary ovarian carcinoma sample).

cells as well as all seven PRAME positive OVCA tumor cell lines. In addition, the specificity of the PRAME TCR-T cells was tested against various healthy cell subsets. By qPCR relative *PRAME* expression was observed in mDCs (3.2%), PTECs (1.3%) and stimulated CD19 cells (0.3%) (Supplementary Figure 6). mDCs were slightly recognized by the PRAME TCRs, as was previously observed for the HSS3 TCR$^{PRAME/SLL/A2}$ (39), but no other reactivity was observed (Figure 4D). Although clone 8.10C4$^{PRAME/SPS/B7}$ had exhibited some reactivity against imDCs (Figure 3B), the TCR-T cells did not show any signs of recognition in repeated experiments (Figure 4D).

Anti-OVCA cytotoxic reactivity was further investigated in a six-hour ^{51}chromium release assay. Transfer of the different PRAME TCRs to CD8+ T cells of four different donors resulted in efficient killing of OVCA tumor cell lines and the primary patient-derived OVCA cells (OVCA-L23 p0 or p10) (Figure 5A). Comparable killing percentages were observed by positive control TCR HSS3$^{PRAME/SLL/A2}$ (Figure 5A), and peptide-loaded targets were similarly lysed (Supplementary Figure 7). No off-target killing of Raji cells (0% *PRAME*), imDCs (0% *PRAME*), and target HLA negative COV362.4 cells was observed (Figure 5B). *In vivo* killing potential of the PRAME TCRs was tested in an established model for multiple myeloma (MM) (23), since *PRAME* is also expressed in MM. Despite low *PRAME* expression (4%), all three newly identified PRAME TCR-T cells and positive control TCR HSS3$^{PRAME/SLL/A2}$ reduced tumor burden for at least 6 days after infusion (Figure 5C). TCR 16.3C1$^{PRAME/LYV/A24}$ and the positive control demonstrated the strongest effect. In conclusion, the three PRAME TCRs (DSK3$^{PRAME/QLL/A2}$, 16.3C1$^{PRAME/LYV/A24}$ and 8.10C4$^{PRAME/SPS/B7}$) demonstrated potent antitumor reactivity *in vitro* and *in vivo* without harming healthy cell subsets *in vitro* and are considered promising TCRs for TCR gene therapy.

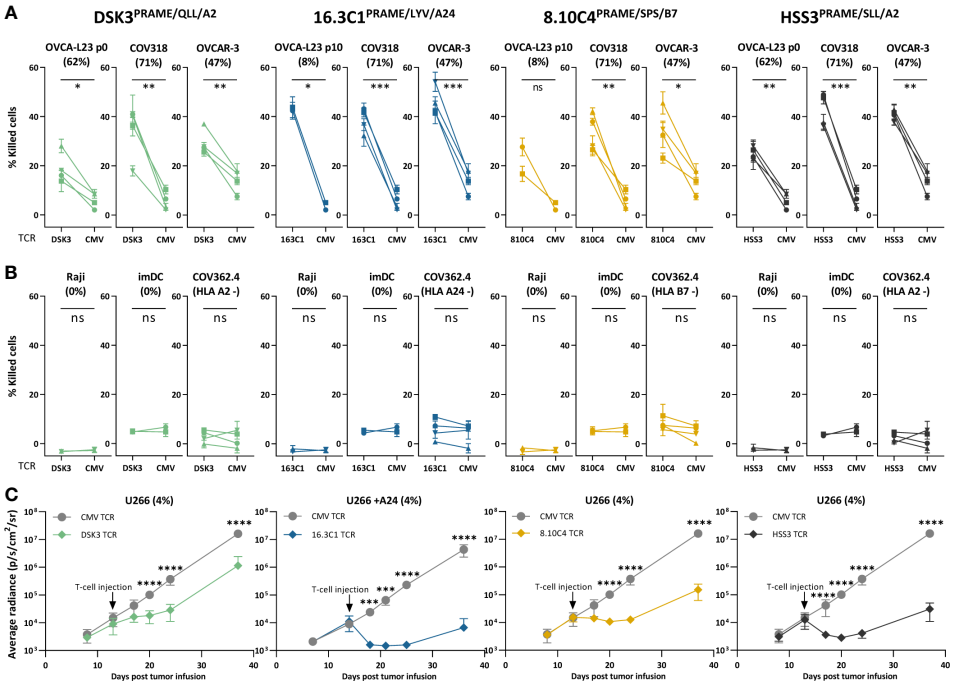

FIGURE 5
PRAME TCR-T cells kill OVCA cells *in vitro* and demonstrate *in vivo* killing potential in an established MM model. **(A, B)** Purified PRAME TCR-T cells were tested for cytotoxic capacity in a 6-hour ^{51}Cr-release assay at E:T ratio 10:1 against **(A)** primary OVCA patient samples and OVCA cell lines, and **(B)** *PRAME* negative cells (Raji and imDCs), or target HLA negative cells (COV362.4). Except for COV362.4, all target cells expressed the target HLA alleles, either wildtype or Td. COV318 and OVCAR-3 were Td with A24, Raji cells were Td with A2, A24 or B7. Primary malignant ascites patient sample OVCA-L23 (wildtype HLA-A2) was either passage 0 (included for TCR DSK3 and HSS3) or passage 10 Td with A24 or B7 (included for TCR 16.3C1 and 8.10C4). imDCs were isolated from PBMCs of a A2+, A24+ and B7+ donor. Percentage relative *PRAME* expression is depicted, as determined by qPCR. Cytotoxic capacity of PRAME TCR- and CMV TCR-T cells were compared using a paired t-test (two-sided). Mean and SD of technical triplicates are depicted for four donors tested in two independent experiments. **(C)** NSG mice engrafted with 2*10^6 U266 MM cells Td with *Luc2* luciferase. Mice were i.v. treated with 5*10^6 PRAME or CMV TCR-T cells 14 days after tumor infusion. Mean and SD of tumor outgrowth (average radiance measured by bioluminescence imaging) over time on the ventral side are depicted. N=6 for PRAME TCR-T cells and n=4 for CMV TCR-T cells. Tumor outgrowth in mice treated with PRAME or CMV-TCR T cells was compared for each time point using two-way ANOVA on log-transformed data, followed by Bonferroni *post-hoc* analysis. Only significant results are depicted. (ANOVA, analysis of variance, E:T, effector:target ratio; ns, not significant; imDCs, immature dendritic cells; MM, multiple myeloma; OVCA, primary ovarian carcinoma sample; Td, transduced). Meaning of the * are listed in the M&M. Significance levels are indicated as p <.05 *, p <.01 **, p <.001 ***, and p <.0001 ****. ns, not significant.

High-affinity CTCFL TCR reactive against DAC treated OVCA cells

Next, the CTCFL-specific TCR 39.2E12$^{CTCFL/KLH/A2}$ was tested for anti-ovarian cancer reactivity and specificity. Generated CTCFL TCR-T cells efficiently expressed the TCR at the cell surface (Figure 6A) and demonstrated high peptide sensitivity in a peptide titration (Figure 6B). CTCFL TCR-T cells generated from three different donors recognized primary patient-derived OVCA-L11 cells harvested from an HLA-A*02:01 positive patient (Figure 6C). Furthermore, in line with the lack of *CTCFL* expression in any of the included healthy cell subsets (Supplementary Figure 6), healthy cell subsets were not recognized by CTCFL TCR-T cells (Figure 6D).

Despite high *CTCFL* expression in primary OVCA patient samples, OVCA tumor cell lines did not express *CTCFL* (Figure 2A). In contrast, cervical cancer cell line Ca Ski is positive for CTCFL and this correlates with expression in part of primary cervical carcinoma samples (Supplementary Figure 2B). As demonstrated in Figure 6E, the Ca Ski cells were efficiently recognized by the CTCFL TCR-T cells. Since *CTCFL* expression is epigenetically regulated and treatment with demethylating agent DAC has previously been shown to upregulate expression of *CTCFL* in OVCA tumor cell lines (42), we investigated whether DAC can make tumor cell-lines more susceptible to CTCFL-mediated killing. Seven days of DAC treatment clearly resulted in *CTCFL* upregulation in OVCA cell lines, compared to not treated cells (Figure 6E). In line with the upregulation, recognition of DAC-treated OVCA tumor cell lines COV413b and A2780 was significantly increased for CTCFL TCR-T cells (Figure 6E). *CTCFL* upregulation by DAC was restricted to tumor cells, as DAC treatment of healthy fibroblasts did not upregulate *CTCFL* expression and did not induce recognition by CTCFL TCR-T cells (Figure 6F). In line with increased cytokine production, cytotoxic capacity of CTCFL TCR-T cells towards DAC-treated COV413b was significantly increased (Figure 6G). DAC treatment did not increase killing by allo-HLA-A*02:01 T cells (Figure 6G) neither did it influence killing of peptide-loaded target cells (Supplementary Figure 8), suggesting DAC treatment does not generally increase susceptibility of these target cells to T-cell mediated killing. In OVCA tumor cell lines we also observed increased *PRAME* expression after DAC treatment, which slightly increased

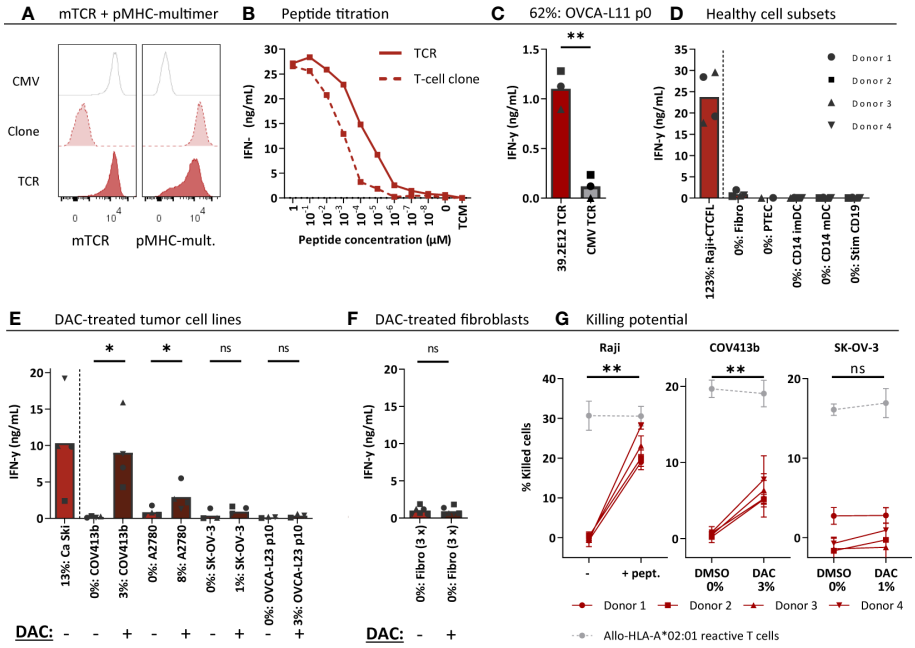

FIGURE 6
CTCFL TCR-T cells recognize and kill (DAC-treated) *CTCFL* positive OVCA cells. CD8+ cells of four different donors were retrovirally transduced to express the 39.2E12$^{CTCFL/KLH/A2}$ TCR and purified. **(A)** Representative flow cytometry plots of purified CMV and CTCFL TCR-T cells, and the parental CTCFL T-cell clone stained with murine TCR (mTCR) and the CTCFL-specific pMHC-mult. **(B)** IFN-γ production (ng/mL) of the TCR-T cells and parental T-cell clone cocultured overnight with Raji cells transduced with HLA-A*02:01 and loaded with titrated peptide concentrations (E:T = 1:6). **(C–F)** IFN-γ production of TCR-T cells cocultured with **(C)** single viable cells of primary patient-derived sample OVCA-L11 passage 0 (E:T 1:6), **(D)** healthy cell subsets of multiple donors (E:T = 1:4 for fibroblasts, PTECs and CD14+, and 1:6 for CD19+), **(E)** 7 days 1 μM DAC or DMSO treated tumor cells (E:T = 1:6), and **(F)** 7 days 1 μM DAC or DMSO treated fibroblasts. Bars represent mean and symbols depict averaged duplicate values from three or four different donors tested in two independent experiments. **(G)** Cytotoxic capacity of CTCFL TCR-T cells in a 6-hour ^{51}Cr-release assay against Raji cells loaded with the KLH peptide, and COV413b and SK-OV-3 treated with 7 days 1 μM DAC or DMSO. Mean and SD depict technical triplicates from four different donors tested in two independent experiments, at E:T ratio 10:1. Cytotoxic capacity of an allo-HLA-A*02:01 reactive T-cell clone recognizing HKG USP11 is shown for the different conditions (41). **(B–G)** All target cells express HLA-A*02:01, either wildtype or the HLA allele was introduced by transduction (Raji, SK-OV-3, A2780). Percentage relative *CTCFL* (TvX) expression is depicted, as determined by qPCR. **(D)** IFN-γ production of CTCFL TCR- and CMV TCR-T cells compared using a paired t-test (two-sided). **(E–G)** IFN-γ production and cytotoxicity of CTCFL TCR-T cells cocultured with DMSO and DAC-treated cells, or Raji cells loaded with and without peptide, compared using a paired t-test (two-sided). (ns, not significant; DAC, 5-aza-2′-deoxycytidine; imDCs and mDCs, immature and mature dendritic cells; pMHC-mult, peptide MHC-multimers; PTECs, proximal tubular epithelial cells; OVCA, primary ovarian carcinoma sample). Meaning of the * are listed in the M&M. Significance levels are indicated as p <.05 *, p <.01 **. ns, not significant.

recognition and killing potential by HLA-A*02:01-restricted PRAME TCR-T cells (Supplementary Figure 9). In conclusion, CTCFL-specific TCR 39.2E12$^{CTCFL/KLH/A2}$ demonstrate anti-OVCA reactivity against (DAC-treated) *CTCFL* positive tumor cells without harming healthy cell subsets and is considered a promising TCR for TCR gene therapy of ovarian cancer.

Discussion

In this study, we describe the selection of PRAME, CTCFL and CLDN6 as strictly tumor-specific targets for patients with ovarian cancer. We identified 34 peptides derived from these genes in the HLA class I ligandome of OVCA patient samples as well as various tumor cell lines. For nine peptides we identified potent T-cell clones in the allo-HLA T-cell repertoire of healthy donors, demonstrating these peptides can be recognized by T cells. We made a final selection of four potent and specific TCRs recognizing PRAME or CTCFL peptides presented in different HLA alleles. The three PRAME TCRs, recognizing peptides in HLA-A*02:01, -A*24:02 or -B*07:01, are an essential addition to the currently used TCRs. We demonstrated that these PRAME TCRs exhibit potent antitumor reactivity *in vitro* and *in vivo*. The CTCFL TCR recognizing an HLA-A*02:01 restricted peptide is, to our knowledge, the first CTCFL TCR described to date. The CTCFL TCR-T cells efficiently recognized primary patient-derived OVCA cells, and OVCA cell lines treated with epigenetically regulator DAC. Overall, the four TCRs are considered promising candidates for TCR gene transfer strategies in patients suffering from ovarian cancer or other *PRAME* or *CTCFL* expressing cancers.

We aimed to identify strictly tumor-specific TAAs in ovarian cancer by only selecting DE genes with a FC ≥ 20 compared to all healthy tissues of risk. Not all antigens currently targeted in clinical studies with ovarian cancer patients fulfilled these strict criteria. CAR-T cells targeting extracellular proteins CLDN6, mucin16, mesothelin, folate receptor-α and HER2, are currently investigated in ovarian cancer patients (43). The DE fold change values calculated in our analysis were respectively 137, 12, 6, 3 and 1 (Supplementary table 2). According to our DE criteria (FC ≥ 20), we consider CLDN6 a strictly tumor-specific target for ovarian cancer

patients. For the other targets the difference between expression in OVCA patient samples and some of the healthy tissues was lower, suggesting possible on-target off-tumor toxicity risks and a narrow therapeutic window (44). Moreover, we question whether the frequently studied TCR targets NY-ESO-1 and MAGE-A4 are optimal targets for the majority of ovarian cancer patients, since the mean expression levels were low in the included TCGA OVCA samples (mean read count ¾ 100).

Currently three clinical studies targeting CLDN6 are ongoing in ovarian cancer patients: a CLDN6 CAR (NCT04503278 (45)), CLDN6 bispecific T cell engager (NCT05317078 (46)) and CLDN6 CAR-NK (NCT05410717). In our study, thus far only T cells reactive against CLDN6 peptide-loaded cells, but not against CLDN6 transduced cells were identified. We, however, anticipate that the three identified CLDN6 peptides can be used for identification of more potent CLDN6-reactive TCRs in the future. To our knowledge these are the first validated CLDN6 peptides found in the HLA ligandome. In general, the number of unique CLDN6-derived peptides will be limited due to shared homology with ubiquitously expressed Claudin-family members. This also counts for CTCFL which has homology with its ubiquitously expressed paralog CTCF. Based on serious side effects in patients treated with a TCR targeting MAGE-A3 and -A9, that was cross-reactive with MAGE-A12 expressed in brain (47), overlap or minor differences in peptide sequences between tumor and ubiquitously expressed antigens is probably not acceptable. Recently two TCRs targeting CLDN6 peptides that were predicted to bind to HLA-A*02:01 or HLA-DR*04:04 have been identified (15). Considering the shared homology of the HLA-A*02:01 binding peptide with CLDN9, the safety of this TCR has to be carefully evaluated.

The three identified PRAME TCRs demonstrated potent and specific antitumor reactivity *in vitro* and *in vivo* and pose a valuable addition to the currently used TCRs targeting the SLL or VLD peptide presented in HLA-A*02:01. Only TCR 16.3C1$^{PRAME/LYV/A24}$ showed HLA cross-reactivity against the globally infrequent alleles HLA-B*37:01 (3.23%) and HLA-B*38:01 (1.72%) (40) (Figure 3C), implicating this TCR is not suitable for the group of patients expressing these HLA alleles. Furthermore, clone 8.10C4$^{PRAME/SPS/B7}$ demonstrated some reactivity against *PRAME* negative imDCs. However, given the lack of reactivity by the TCR-T cells towards imDCs, we hypothesize the reactivity is a result of non-TCR mediated recognition, for example induced by a killer immunoglobulin-like receptor expressed on the T-cell clone. Given the broad and high *PRAME* expression in many tumor types (Supplementary Figure 2), we expect the PRAME TCRs to be valuable for treatment of other *PRAME* positive tumors as well. PRAME-reactive TCRs are currently investigated in a variety of tumor types: myeloid and lymphoid neoplasms (NCT03503968), acute myeloid leukemia, myelodysplastic syndrome and uveal melanoma (NCT02743611), and various solid tumors including ovarian cancer (NCT03686124 (48) and a TCR/anti-CD3 bispecific fusion protein in NCT04262466 (49)). Especially for PRAME our strategy to isolate high-avidity T cells in the allo-HLA T-cell repertoire was essential, since low *PRAME* expression in mDCs (3.2%) and PTECs (1.3%) (Supplementary Figure 6) implicate self-tolerance to PRAME in the autologous T-cell repertoire. Previously, we indeed demonstrated that PRAME-specific T-cell clones derived from the autologous T-cell repertoire lacked reactivity against endogenously processed PRAME and showed lower peptide sensitivity compared with T-cell clones derived from the allo-HLA T-cell repertoire (39). Apart from the T-cell repertoire, selecting the accurate peptide is crucial for clinical efficacy of TCR-based therapy as well. We identified 23 naturally expressed PRAME peptides, of which 8 peptides were presented in HLA-A*02:01. We were not able to identify the often used VLD peptide presented in HLA-A*02:01, which may suggest this peptide is not optimally processed and presented in PRAME positive tumor cells.

Although CTCFL has been proposed as an attractive tumor target given the restricted expression profile and several oncogenic properties, studies investigating CTCFL-targeting therapies are still limited. CTCFL, also named brother of the regulator of imprinted sites (BORIS), is a DNA binding protein and plays a central role in gene regulation by acting as a transcription factor of testis-specific genes, including some CTAs (50). By interfering with cellular processes such as apoptosis, proliferation and immortalization, CTCFL exhibits several oncogenic properties (50). In ovarian cancer *CTCFL* expression indeed correlates with advanced stage and decreased survival (51). In other tumor types *CTCFL* expression has also been detected, although expression data have been contradictory (52). According to the TCGA data, *CTCFL* is mainly expressed in ovarian cancer (Supplementary Figure 2). We also demonstrated high *CTCFL* expression in most primary OVCA patient samples, and demonstrated reactivity of the CTCFL TCR-T cells against the primary patient-derived OVCA cells of an HLA-A*02:01 positive OVCA patient. With the exception of the cervical cancer cell line Ca Ski, no expression was observed in OVCA tumor cell lines (Figure 2A). Since *CTCFL* expression is epigenetically regulated, treatment with demethylating agent DAC has previously been shown to upregulate *CTCFL* in OVCA cell lines (42). We also observed increased expression of *CTCFL*, leading to increased reactivity by the CTCFL TCR-T cells against DAC-treated OVCA cell lines (Figures 6E, G). We also demonstrated this for the HSS3$^{PRAME/SLL/A2}$ TCR-T cells (Supplementary Figure 9), which is in line with previous findings using PRAME-reactive T cells and DAC-treated leukemic cell lines (20). These preclinical findings demonstrate that pre-treatment with DAC may increase reactivity of transferred TCR-T cells in patients. However, clinical data on effectivity or potential toxicity risks, if DAC upregulates gene expression also in non-malignant cells, is limited.

In summary, we present a selection of strictly and highly expressed DE genes in ovarian tumors, combined with a set of naturally expressed peptides. We expect this selection to broaden the applicability of T-cell therapies in patients with ovarian cancer. In addition, we consider the three PRAME TCRs (DSK3$^{PRAME/QLL/A2}$, 16.3C1$^{PRAME/LYV/A24}$ and 8.10C4$^{PRAME/SPS/B7}$) and CTCFL TCR (39.2E12$^{CTCFL/KLH/A2}$) to be promising candidates for the treatment of patients with ovarian cancer, and also for other *PRAME* or *CTCFL* expressing cancers.

Data availability statement

The mass spectrometry proteomics data have been deposited to the ProteomeXchange Consortium *via* the PRIDE (53) partner repository with the dataset identifier PXD040651.

Ethics statement

The studies involving human participants were reviewed and approved by Institutional Review Board of the LUMC (approval number 3.4205/010/FB/jr) and the METC-LDD (approval number HEM 008/SH/sh), for samples of LUMC Biobank for Hematological Diseases. For the OVCA samples this was approved by the Institutional Review Board of the LUMC (approval number L18.012) and Central Committee on Research Involving Human Subjects (approval number NL63434.000.17). The patients/participants provided their written informed consent to participate in this study. The animal study was reviewed and approved by National Ethical Committee for Animal Research (AVD116002017891).

Author contributions

RA designed, performed, analyzed, and interpreted all experiments and wrote the manuscript. ST performed the differential gene expression analysis. AW, MM and SS performed *in vitro* experiments. MHM and TW performed *in vivo* experiments. DR performed qPCR and constructed retroviral expression vectors. RH determined TRAV and TRBV usage and constructed retroviral expression vectors. DS generated and analyzed peptide elution data and produced pMHC-multimers. AR performed and analyzed mass spectrometry experiments. EV provided ovarian cancer patient samples and cell lines. PV produced and analyzed MS data. JF supervised the study and revised the manuscript. MH designed and interpreted the experiments, conceptualized and supervised the study, and revised the manuscript. All authors contributed to the article and approved the submitted version.

Funding

The research in this study was funded by Health Holland (grant number LSHM15011) and Bellicum Pharmaceuticals (unrestricted grant). The funder Bellicum Pharmaceuticals was not involved in the study design, collection, analysis, interpretation of data, the writing of this article, or the decision to submit it for publication.

Acknowledgments

The authors thank the operators of the LUMC Flow cytometry Core Facility (Leiden University Medical Center, the Netherlands) for providing expert technical assistance in flow cytometric cell sorting and Jaap D.H. van Eendenburg (Department of Pathology, Leiden University Medical Center, the Netherlands) for providing the OVCAR-3 and A2780 cell lines.

Conflict of interest

The authors declare that the research was conducted in the absence of any commercial or financial relationships that could be construed as a potential conflict of interest.

Publisher's note

Supplementary material

The Supplementary Material for this article can be found online at: https://www.frontiersin.org/articles/10.3389/fimmu.2023.1121973/full#supplementary-material

References

1. Siegel RL, Miller KD, Fuchs HE, Jemal A. Cancer statistics, 2022. *A Cancer J Clin* (2022) 72(1):7–33. doi: 10.3322/caac.21708

2. Howlader N NA, Krapcho M, Miller D, Brest A, Yu M, Ruhl J, et al. *SEER cancer statistics review, 1975-2017* (2020). Bethesda, MD: National Cancer Institute. cited Based on November 2019 SEER data submission, posted to the SEER web site, April 2020.

3. Vaughan S, Coward JI, Bast RC, Berchuck A, Berek JS, Brenton JD, et al. Rethinking ovarian cancer: Recommendations for improving outcomes. *Nat Rev Cancer* (2011) 11(10):719–25. doi: 10.1038/nrc3144

4. Hennessy BT, Coleman RL, Markman M. Ovarian cancer. *Lancet* (2009) 374 (9698):1371–82. doi: 10.1016/S0140-6736(09)61338-6

5. Freimund AE, Beach JA, Christie EL, Bowtell DDL. Mechanisms of drug resistance in high-grade serous ovarian cancer. *Hematol/Oncol Clinics North America* (2018) 32(6):983–96. doi: 10.1016/j.hoc.2018.07.007

6. Konstantinopoulos PA, Lheureux S, Moore KN. PARP inhibitors for ovarian cancer: Current indications, future combinations, and novel assets in development to target DNA damage repair. *Am Soc Clin Oncol Educ Book* (2020) 40:e116–31. doi: 10.1200/EDBK_288015

7. Coukos G, Tanyi J, Kandalaft LE. Opportunities in immunotherapy of ovarian cancer. *Ann Oncol* (2016) 27:i11–5. doi: 10.1093/annonc/mdw084

8. Wu JWY, Dand S, Doig L, Papenfuss AT, Scott CL, Ho G, et al. T-Cell receptor therapy in the treatment of ovarian cancer: A mini review. *Front Immunol* (2021) 12:672502. doi: 10.3389/fimmu.2021.672502

9. Yang C, Xia B-R, Zhang Z-C, Zhang Y-J, Lou G, Jin W-L. Immunotherapy for ovarian cancer: Adjuvant, combination, and neoadjuvant. *Front Immunol* (2020) 11. doi: 10.3389/fimmu.2020.577869

10. Santoiemma PP, Reyes C, Wang L-P, McLane MW, Feldman MD, Tanyi JL, et al. Systematic evaluation of multiple immune markers reveals prognostic factors in ovarian cancer. *Gynecol Oncol* (2016) 143(1):120–7. doi: 10.1016/j.ygyno.2016.07.105

11. Sato E, Olson SH, Ahn J, Bundy B, Nishikawa H, Qian F, et al. Intraepithelial CD8+ tumor-infiltrating lymphocytes and a high CD8+/regulatory T cell ratio are

associated with favorable prognosis in ovarian cancer. *Proc Natl Acad Sci U.S.A.* (2005) 102(51):18538–43. doi: 10.1073/pnas.0509182102

12. Clarke B, Tinker AV, Lee C-H, Subramanian S, van de Rijn M, Turbin D, et al. Intraepithelial T cells and prognosis in ovarian carcinoma: Novel associations with stage, tumor type, and BRCA1 loss. *Modern Pathol* (2009) 22(3):393–402. doi: 10.1038/modpathol.2008.191

13. Rodriguez GM, Galpin KJC, McCloskey CW, Vanderhyden BC. The tumor microenvironment of epithelial ovarian cancer and its influence on response to immunotherapy. *Cancers* (2018) 10(8):242. doi: 10.3390/cancers10080242

14. Alexandrov LB, Nik-Zainal S, Wedge DC, Aparicio SAJR, Behjati S, Biankin AV, et al. Signatures of mutational processes in human cancer. *Nature* (2013) 500 (7463):415–21. doi: 10.1038/nature12477

15. Matsuzaki J, Lele S, Odunsi K, Tsuji T. Identification of claudin 6-specific HLA class I- and HLA class II-restricted T cell receptors for cellular immunotherapy in ovarian cancer. *OncoImmunology* (2022) 11(1):2020983. doi: 10.1080/2162402X.2021.2020983

16. Anderson KG, Voillet V, Bates BM, Chiu EY, Burnett MG, Garcia NM, et al. Engineered adoptive T-cell therapy prolongs survival in a preclinical model of advanced-stage ovarian cancer. *Cancer Immunol Res* (2019) 7(9):1412–25. doi: 10.1158/2326-6066.CIR-19-0258

17. Teck AT, Urban S, Quass P, Nelde A, Schuster H, Letsch A, et al. Cancer testis antigen cyclin A1 harbors several HLA-A*02:01-restricted T cell epitopes, which are presented and recognized in vivo. *Cancer Immunol Immunother* (2020) 69(7):1217–27. doi: 10.1007/s00262-020-02519-6

18. de Rooij MAJ, Remst DFG, van der Steen DM, Wouters AK, Hagedoorn RS, Kester MGD, et al. A library of cancer testis specific T cell receptors for T cell receptor gene therapy. *Mol Ther Oncolytics* (2023) 28:1–14. doi: 10.1016/j.omto.2022.11.007

19. Almstedt M, Blagitko-Dorfs N, Duque-Afonso J, Karbach J, Pfeifer D, Jäger E, et al. The DNA demethylating agent 5-aza-2′-deoxycytidine induces expression of NY-ESO-1 and other cancer/testis antigens in myeloid leukemia cells. *Leuk Res* (2010) 34 (7):899–905. doi: 10.1016/j.leukres.2010.02.004

20. Yan M, Himoudi N, Basu BP, Wallace R, Poon E, Adams S, et al. Increased PRAME antigen-specific killing of malignant cell lines by low avidity CTL clones, following treatment with 5-Aza-2'-Deoxycytidine. *Cancer Immunol Immunother* (2011) 60(9):1243–55. doi: 10.1007/s00262-011-1024-4

21. Pollack SM, Li Y, Blaisdell MJ, Farrar EA, Chou J, Hoch BL, et al. NYESO-1/LAGE-1s and PRAME are targets for antigen specific T cells in chondrosarcoma following treatment with 5-Aza-2-Deoxycitabine. *PloS One* (2012) 7(2):e32165. doi: 10.1371/journal.pone.0032165

22. Jahn L, van der Steen DM, Hagedoorn RS, Hombrink P, Kester MG, Schoonakker MP, et al. Generation of CD20-specific TCRs for TCR gene therapy of CD20low b-cell malignancies insusceptible to CD20-targeting antibodies. *Oncotarget* (2016) 7(47):77021–37. doi: 10.18632/oncotarget.12778

23. Meeuwsen MH, Wouters AK, Jahn L, Hagedoorn RS, Kester MGD, Remst DFG, et al. A broad and systematic approach to identify b cell malignancy-targeting TCRs for multi-antigen-based T cell therapy. *Mol Ther* (2022) 30(2):564-78 doi: 10.1016/j.ymthe.2021.08.010

24. van Amerongen RA, Hagedoorn RS, Remst DFG, Assendelft DC, van der Steen DM, Wouters AK, et al. WT1-specific TCRs directed against newly identified peptides install antitumor reactivity against acute myeloid leukemia and ovarian carcinoma. *J ImmunoTher Cancer* (2022) 10(6):e004409. doi: 10.1136/jitc-2021-004409

25. Lonsdale J, Thomas J, Salvatore M, Phillips R, Lo E, Shad S, et al. The genotype-tissue expression (GTEx) project. *Nat Genet* (2013) 45(6):580–5. doi: 10.1038/ng.2653

26. Uhlén M, Fagerberg L, Hallström BM, Lindskog C, Oksvold P, Mardinoglu A, et al. Proteomics. tissue-based map of the human proteome. *Science* (2015) 347 (6220):1260419. doi: 10.1126/science.1260419

27. Collado-Torres L, Nellore A, Kammers K, Ellis SE, Taub MA, Hansen KD, et al, et al. Reproducible RNA-seq analysis using recount2. *Nat Biotechnol* (2017) 35(4):319–21. doi: 10.1038/nbt.3838

28. Robinson MD, McCarthy DJ, Smyth GK. edgeR: A bioconductor package for differential expression analysis of digital gene expression data. *Bioinformatics* (2010) 26 (1):139–40. doi: 10.1093/bioinformatics/btp616

29. McCarthy DJ, Chen Y, Smyth GK. Differential expression analysis of multifactor RNA-seq experiments with respect to biological variation. *Nucleic Acids Res* (2012) 40 (10):4288–97. doi: 10.1093/nar/gks042

30. van den Berg-Bakker CA, Hagemeijer A, Franken-Postma EM, Smit VT, Kuppen PJ, van Ravenswaay Claasen HH, et al. Establishment and characterization of 7 ovarian carcinoma cell lines and one granulosa tumor cell line: Growth features and cytogenetics. *Int J Cancer* (1993) 53(4):613–20. doi: 10.1002/ijc.2910530415

31. Nauta AJ, de Haij S, Bottazzi B, Mantovani A, Borrias MC, Aten J, et al. Human renal epithelial cells produce the long pentraxin PTX3. *Kidney Int* (2005) 67(2):543–53. doi: 10.1111/j.1523-1755.2005.67111.x

32. Linnemann C, Heemskerk B, Kvistborg P, Kluin RJ, Bolotin DA, Chen X, et al. High-throughput identification of antigen-specific TCRs by TCR gene capture. *Nat Med* (2013) 19(11):1534–41. doi: 10.1038/nm.3359

33. Poliseno L, Salmena L, Zhang J, Carver B, Haveman WJ, Pandolfi PP. A coding-independent function of gene and pseudogene mRNAs regulates tumour biology. *Nature* (2010) 465(7301):1033–8. doi: 10.1038/nature09144

34. Ling H, Fabbri M, Calin GA. MicroRNAs and other non-coding RNAs as targets for anticancer drug development. *Nat Rev Drug Discovery* (2013) 12(11):847–65. doi: 10.1038/nrd4140

35. Wang C, Gu Y, Zhang K, Xie K, Zhu M, Dai N, et al. Systematic identification of genes with a cancer-testis expression pattern in 19 cancer types. *Nat Commun* (2016) 7 (1):10499. doi: 10.1038/ncomms10499

36. Andreatta M, Nielsen M. Gapped sequence alignment using artificial neural networks: Application to the MHC class I system. *Bioinformatics* (2015) 32(4):511–7. doi: 10.1093/bioinformatics/btv639

37. Consortium, T.U. UniProt: The universal protein knowledgebase in 2021. *Nucleic Acids Res* (2020) 49(D1):D480–9. doi: 10.1093/nar/gkaa1100

38. Ikeda H, Lethé B, Lehmann F, van Baren N, Baurain JF, de Smet C, et al. Characterization of an antigen that is recognized on a melanoma showing partial HLA loss by CTL expressing an NK inhibitory receptor. *Immunity* (1997) 6(2):199–208. doi: 10.1016/S1074-7613(00)80426-4

39. Amir AL, van der Steen DM, van Loenen MM, Hagedoorn RS, de Boer R, Kester MD, et al. PRAME-specific allo-HLA-restricted T cells with potent antitumor reactivity useful for therapeutic T-cell receptor gene transfer. *Clin Cancer Res* (2011) 17 (17):5615–25. doi: 10.1158/1078-0432.CCR-11-1066

40. Bui HH, Sidney J, Dinh K, Southwood S, Newman MJ, Sette A. Predicting population coverage of T-cell epitope-based diagnostics and vaccines. *BMC Bioinf* (2006) 7:153. doi: 10.1186/1471-2105-7-153

41. Amir AL, van der Steen DM, Hagedoorn RS, Kester MG, van Bergen CA, Drijfhout JW, et al. Allo-HLA-reactive T cells inducing graft-versus-host disease are single peptide specific. *Blood* (2011) 118(26):6733–42. doi: 10.1182/blood-2011-05-354787

42. Woloszynska-Read A, James SR, Link PA, Yu J, Odunsi K, Karpf AR. DNA Methylation-dependent regulation of BORIS/CTCFL expression in ovarian cancer. *Cancer Immun* (2007) 7:21.

43. Yan W, Hu H, Tang B. Advances of chimeric antigen receptor T cell therapy in ovarian cancer. *Onco Targets Ther* (2019) 12:8015–22. doi: 10.2147/OTT.S203550

44. Watanabe K, Kuramitsu S, Posey AD, June CH. Expanding the therapeutic window for CAR T cell therapy in solid tumors: The knowns and unknowns of CAR T cell biology. *Front Immunol* (2018) 9. doi: 10.3389/fimmu.2018.02486

45. Reinhard K, Rengstl B, Oehm P, Michel K, Billmeier A, Hayduk N, et al. An RNA vaccine drives expansion and efficacy of claudin-CAR-T cells against solid tumors. *Science* (2020) 367(6476):446–53. doi: 10.1126/science.aay5967

46. Pham E, Henn A, Sable B, Wahl J, Conner K, Matthes K, et al. Abstract 5202: AMG 794, a claudin 6-targeted half-life extended (HLE) bispecific T cell engager (BITE®) molecule for non-small cell lung cancer and epithelial ovarian cancer. *Cancer Res* (2022) 82(12_Supplement):5202–2. doi: 10.1158/1538-7445.AM2022-5202

47. Morgan RA, Chinnasamy N, Abate-Daga D, Gros A, Robbins PF, Zheng Z, et al. Cancer regression and neurological toxicity following anti-MAGE-A3 TCR gene therapy. *J Immunother* (2013) 36(2):133–51. doi: 10.1097/CJI.0b013e3182829903

48. Wermke M, Tsimberidou A-M, Mohamed A, Mayer-Mokler A, Satelli A, Reinhardt C, et al. 959 safety and anti-tumor activity of TCR-engineered autologous, PRAME-directed T cells across multiple advanced solid cancers at low doses – clinical update on the ACTengine® IMA203 trial. *J ImmunoTher Cancer* (2021) 9(Suppl 2): A1009–9. doi: 10.1136/jitc-2021-SITC2021.959

49. Moureau S, Vantellini A, Schlosser F, Robinson J, Harper J, Shankar A, et al. Abstract 5572: IMC-F106C, a novel and potent immunotherapy approach to treat PRAME expressing solid and hematologic tumors. *Cancer Res* (2020) 80 (16_Supplement):5572–2. doi: 10.1158/1538-7445.AM2020-5572

50. Debaugny RE, Skok JA. CTCF and CTCFL in cancer. *Curr Opin Genet Dev* (2020) 61:44–52. doi: 10.1016/j.gde.2020.02.021

51. Hillman JC, Pugacheva EM, Barger CJ, Sribenja S, Rosario S, Albahrani M, et al. BORIS expression in ovarian cancer precursor cells alters the CTCF cistrome and enhances invasiveness through GALNT14. *Mol Cancer Res* (2019) 17(10):2051–62. doi: 10.1158/1541-7786.MCR-19-0310

52. de Necochea-Campion R, Ghochikyan A, Josephs SF, Zacharias S, Woods E, Karimi-Busheri F, et al. Expression of the epigenetic factor BORIS (CTCFL) in the human genome. *J Trans Med* (2011) 9(1):213. doi: 10.1186/1479-5876-9-213

53. Perez-Riverol Y, Bai J, Hewapathirana S, García-Seisdedos D, Kamatchinathan S, et al. The PRIDE database resources in 2022: A Hub for mass spectrometry-based proteomics evidences. *Nucleic Acids Res* (2022) 50(D1):D543–52. doi: 10.1093/nar/gkab1038

frontiers | Frontiers in Immunology

TYPE Original Research
PUBLISHED 12 April 2023
DOI 10.3389/fimmu.2023.1148890

OPEN ACCESS

EDITED BY
Ralf-Holger Voss,
Johannes Gutenberg University
Mainz, Germany

REVIEWED BY
Nishant Kumar Singh,
Ragon Institute, United States
Caroline Arber,
Centre Hospitalier Universitaire Vaudois
(CHUV), Switzerland

*CORRESPONDENCE
Hans J. Stauss
h.stauss@ucl.ac.uk

SPECIALTY SECTION
This article was submitted to
Cancer Immunity
and Immunotherapy,
a section of the journal
Frontiers in Immunology

RECEIVED 20 January 2023
ACCEPTED 28 March 2023
PUBLISHED 12 April 2023

CITATION
Degirmencay A, Thomas S, Mohammed F,
Willcox BE and Stauss HJ (2023)
Modifications outside CDR1, 2 and 3 of the
TCR variable β domain increase TCR
expression and antigen-specific function.
Front. Immunol. 14:1148890.
doi: 10.3389/fimmu.2023.1148890

Modifications outside CDR1, 2 and 3 of the TCR variable β domain increase TCR expression and antigen-specific function

Abdullah Degirmencay[1], Sharyn Thomas[1], Fiyaz Mohammed[2], Benjamin E. Willcox[2] and Hans J. Stauss[1]*

[1]Institute of Immunity and Transplantation, Division of Infection and Immunity, University College London, London, United Kingdom, [2]Cancer Immunology and Immunotherapy Centre, Institute for Immunology and Immunotherapy, University of Birmingham, Edgbaston, Birmingham, United Kingdom

T cell receptor (TCR) gene modified T cells are a promising form of adoptive cellular therapy against human malignancies and viral infections. Since the first human clinical trial was carried out in 2006, several strategies have been developed to improve the efficacy and safety of TCR engineered T cells by enhancing the surface expression of the introduced therapeutic TCRs whilst reducing the mis-pairing with endogenous TCR chains. In this study, we explored how modifications of framework residues in the TCR variable domains affect TCR expression and function. We used bioinformatic and protein structural analyses to identify candidate amino acid residues in the framework of the variable β domain predicted to drive high TCR surface expression. Changes of these residues in poorly expressed TCRs resulted in improved surface expression and boosted target cell specific killing by engineered T cells expressing the modified TCRs. Overall, these results indicate that small changes in the framework of the TCR variable domains can result in improved expression and functionality, while at the same time reducing the risk of toxicity associated with TCR mis-pairing.

KEYWORDS

TCR-T therapy, TCR (T cell receptor), TCRV, T cell function, framework engineering

Introduction

The engineering of T cells with genes encoding TCR chains, or chimeric antigen receptors (CARs) is an efficient strategy to produce cells for antigen-specific T cell therapy in the clinical setting (1). TCR gene therapy typically relies on transferring antigen-specific T cell receptor alpha and beta chains into the autologous T cells obtained from patients (2). Several promising clinical benefits have been obtained using TCR gene therapy to target tumour associated antigens, cancer testis antigens and viral antigens (3–14). Nonetheless,

certain drawbacks with this therapy have diminished its clinical efficacy and may pose a safety risk. For example, low expression levels of introduced TCRs may reduce T cell avidity and prevent recognition of target cells expressing low level of TCR-recognised target antigens (15). The expression levels of TCRs are determined by the amino acid composition of the variable alpha and variable beta domains, resulting in 'dominant' TCRs that are highly expressed on the surface of engineered T cells, and 'weak' TCRs that are poorly expressed (16).

A major safety concern relates to potential mis-pairing of endogenous and introduced TCR chains, which was shown to result in fatal autoimmunity in murine models of TCR gene therapy (17, 18), although such toxicities have not been observed in patients. Mis-pairing occurs between endogenous (end) α and introduced (int) β chains or vice versa during the pairing step of TCR chains in the endoplasmic reticulum (ER). Mis-pairing results in two additional receptor combinations ($\alpha_{end}\beta_{int}$, $\alpha_{int}\beta_{end}$) in transduced cells. In total, four different receptor combinations can result, $\alpha\beta_{end}$, $\alpha\beta_{int}$, $\alpha_{end}\beta_{int}$, $\alpha_{int}\beta_{end}$, only one of which is desired, namely $\alpha\beta_{int}$.

Heemskerk et al. demonstrated that the quality of the endogenous TCR is a determining factor in the surface expression of introduced TCR, hence it is important that introduced TCRs are dominant over their endogenous competitor (19). To date, multiple strategies have been developed to improve the efficacy of TCR therapy and to tackle the issues of mis-pairing and suboptimal surface expression. These include TCR constant region murinisation (20, 21), introduction of an additional disulphide bond between Cα and Cβ (22, 23), codon optimisation (24), TCR domain swapping (25), single chain TCRs (26–29) and addition of accessory or co-stimulatory molecules (30, 31). Ablating the endogenous TCR using the zinc-finger (32), CRISPR (29, 33–35) or TALEN (36) technology has been employed to eliminate TCR mis-pairing and improve TCR expression levels.

TCR framework engineering is a technology that can improve TCR safety and efficacy, without the need for additional gene deletion, thus avoiding the safety concerns of the zinc-finger, CRISPR and TALEN technologies (16). Our previous framework engineering work has mostly focused on the TCR variable alpha domain (TRAV), without fully exploring the role of the TCR variable beta domain (TRBV). Here, we have analysed the framework amino acids of TRBV to further optimise TCR expression and antigen-specific function. We discovered that single amino acid changes in the TRBV framework region can enhance performance, and when combined with previously identified TRAV residue changes enable optimal TCR expression and function.

Methods

TCR gene usage

The weak1 TCR expressed the TRAV13-2/TRBV7-3 variable gene segments, the CMV1 TCR expressed TRAV24/TRBV6-5, the HA1.m2 TCR expressed TRAV13-1/TRBV7-9, and the HA1.m7 TCR expressed TRAV25/TRBV7-9.

Cell culture

TCRαβ-deficit human Jurkat76 cells, HLA-$A2^+$ T2 cells and human PBMCs were cultured in RPMI 1640 medium (Lonza) supplemented with 10% FCS, 1% L-Glutamine (Gibco, 2mM) and 1% Penicillin/Streptomycin (100U/ml). HEK293T (Human embryonic kidney epithelial) packaging cells were cultured in IMDM (Lonza) supplemented with 10% FCS, 1% L-Glutamine (Gibco, 2mM) and 1% Penicillin/Streptomycin (100U/ml).

Primary human peripheral blood mononuclear cells

Human PBMCs were obtained from volunteer donors *via* the National Health Blood Transfusion Service (Approved by UCL Research Ethics Committee, Project ID/Title: 15887/001) and stored in the Biobank facility based at the Royal Free Hospital, London, UK, until use. 48h prior to retroviral transduction, bulk PBMCs were activated at $1x10^6$ cells/ml with 20µl anti-CD3/CD28 dyne beads (Gibco) and 30U/ml Roche IL-2.

Retroviral vector and *In vitro* mutagenesis

Retroviral constructs were designed and produced as previously described (16). General structure of a TCR construct was consisting of a V5 sequence, a TCRα chain, a viral P2A sequence, two Myc sequence, a TCRβ chain, a viral T2A sequence, and truncated murineCD19.

In vitro mutagenesis was employed to implement the identified residue changes in TCR chains. Mutated primers were designed using the Agilent *in vitro* mutagenesis primer design tool. Quickchange II XL Site-Directed Mutagenesis Kit (Agilent Technologies) was used to change the framework region amino acid residues by PCR as per protocol. Produced DNAs were sent for Sanger sequencing to verify the presence of intended amino acid changes.

Retrovirus production and transduction of the cells

1.8-2.0 x 10^6 HEK293T packaging cells were plated in 10-cm tissue culture dishes in 8ml complete IMDM media. On the following day, cells underwent a 100% media change with 5ml fresh complete IMDM media 30 minutes prior to the transfection. Transfection master mix A was prepared with 1.5µg pCl-ampho retroviral packaging vector and 2.6µg of TCR DNA with dH_2O to a final volume of 50µl. Master mix B was composed of 150µl Opti-MEM media and 10µl FugeneHD (Promega. Master mixes A and B were mixed and incubated for 20 minutes at room temperature, and then added to the transfection plates by droplets. On Day1 post transfection, cells were 100% media changes and given 5ml fresh complete RPMI media. On Day2 post transfection, retroviral supernatants were harvested either used directly for a transduction of the target cells or stored in -80° C freezer. Non-TC treated, 750 ul Retronectin (Takara) overnight coated 24-well plate was used in the

transduction of the pre-activated bulk hPBMCs. Following the collecting of the Retronectin, 24-well plate were blocked by 2% BSA-PBS (Sigma-Aldrich) for 30 mins. Following the incubation, wells were washed with PBS by 2x times. Then, 500ul viral supernatant and $5x10^5$ Jurkat76 or 1x106 bulk hPBMCs were added each well, and the transduction was done by centrifuge with 32°C, 2000rpm, 1h30 mins configurations. Following the transduction, supernatant in each well was discarded, and cells were supplied with 2ml complete RPMI while bulk hPBMCs received additional 10U/ml Roche IL-2. On Day-3/4 post transduction, cells were stained for Live/dead, anti-human CD3, anti-mouse CD19, anti-human CD8, anti-Myc, anti-V5. Data was collected by LSRFortessa (BD Biosciences) and the analysis was done by FlowJo software. While transduced Jurkat76 cells pre-gated on live, singlets and CD19+, transduced bulk hPBMCs pre-gated on live, singlets, CD19+, CD3+CD8+. V5/TCRα and Myc/TCRβ staining was used for determining TCR expression in both Jurkat76 and bulk hPBMCs.

Antibodies and peptides

The following antibodies were used: anti-human CD3-FITC (Clone: HIT3A; BD), anti-mouse CD19-eFluor450 (Clone: 1D3; Invitrogen), mouse anti-c-Myc (Bio-Rad), rabbit polyclonal V5-APC (abcam), anti-mouse IgG1-PE (Invitrogen), anti-human CD3-PE-Cy7 (Clone: SK7; Biolegend), anti-human CD8-FITC (Clone: OKT8) and Live/Dead-eFluor780 (Invitrogen), anti-human IL-2-APC (Clone: MQ1-17H12, eBioscience) and anti-human IFN-γ-PE (Invitrogen). Peptides used were: pCMVpp65 (NLVPMVATV) for CMV1 TCR and the pHA1 (VLHDDLLEA) for HA-1.m2 and HA-1.m7 TCRs. The pHA2 (YIGEVLVSV) peptide was used as a control peptide in the functional assays.

Killing assay

7-10 days post-transduced bulk hPBMCs were employed in killing assays. HLA-$A2^+$ T2 cells were loaded with cognate peptide were labelled with 0.02uM CFSE whilst cells loaded with control peptide were labelled with 0.2uM CFSE. Following peptide loading for 2h, T2 cells were mixed at 1:1 ratio and $1x10^5$ transduced bulk-T cells were co-cultured with $1x10^5$ mixed T2 cells for 18 hours. Cells were stained with anti-human CD3 Ab and Live/Dead antibodies, and data acquisition was done by LSRFortessa and analysed by FlowJo software. Antigen specific killing of T cells was calculated as % Specific Killing = 100- [(Relevant/Irrelevant T2 cells with T cells)/(Relevant/Irrelevant T2 cells with no T cells)]*100.

TCR structural modelling

The weak TCR that was most extensively tested in our study comprised of TRAV13-2 and TRBV7-3. A molecular model of the TRAV13-2/TRBV7-3 TCR complex was generated as described previously (16). Models of weak to strong TCRs incorporating the 11 variable domain framework residues were generated using the I-TASSER (Iterative Threading ASSEmbly Refinement) server (37). For all modelling studies with I-TASSER, the target sequences were initially threaded through the PDB library by the meta threading server, LOMETS2. Continuous fragments were excised from LOMETS2 alignments and structurally reassembled *via* replica-exchange Monte Carlo simulations. The simulation trajectories were then clustered and used as the initial state for second round I-TASSER assembly simulations. Finally, lowest energy structural models were selected and refined by fragment-guided molecular dynamic simulations to optimize polar interactions and omit steric clashes. Analysis of molecular interactions was carried using the CCP4 suite (38). Model visualization was performed with COOT (39) and structural figures were generated using PyMOL (The PyMOL Molecular Graphics System, Version 1.8 Schrödinger, LLC).

Intracellular cytokine staining

$3x10^5$ T2 cells were stimulated with either relevant or irrelevant peptide for 2 hours. Then they were washed and re-suspended in RPMI and co-cultured with 7-10-day post-transduced $3x10^5$ bulk-T cells for 18 hours. Cells were stained with surface markers and washed. Then they were fixed by BD Cytofix/Cytoperm Kit and incubated for 20 minutes at 4°C. Afterwards they were washed and stained for IL-2 and IFN-γ and incubated for 1 hour at 4°C. Data acquisition was done by LSRFortessa and analysed by FlowJo software.

Results

A single amino acid change in the framework of TRBV improves TCR expression in human Jurkat76 cells

In order to select additional candidate residues in the TRBV framework, we exploited a previous bioinformatics analysis that identified amino acid positions that were highly enriched in a library of more than 130,000 TCRs with a 'dominant' expression profile compared to a similar number of TCRs with a 'weak' expression profile (16). We had previously employed this analysis to identify framework mutations at TCR-α96, TCR-β9, and TCR-β10 that substantially increased TCR expression and functionality (16). Here, we focussed on 11 additional amino acid residues in TCR-β that showed a highly significant enrichment in the 'dominant' library, were distal to the CDR1, 2 and 3 loops (Figures 1A, B), and based on TCR structural modelling were predicted to affect the stability of the Vβ domain. We mutated a TCR from the 'weak' expression library comprised of TRAV13-2 and TRBV7-3 (weak 1-TCR), changing the amino acids of the selected candidate residues to those present in the 'dominant' library.

In vitro mutagenesis was employed to substitute these residues in the weak TCR, followed by transduction into human Jurkat76 cells to assess TCR expression levels. Truncated murineCD19 (mCD19) was used to identify transduced cells, and V5 and Myc tags located at the N-terminus of the TCRα and TCRβ chain, respectively, were used to measure the expression levels of each TCR chain (Figures 2A–C).

10.3389/fimmu.2023.1148890

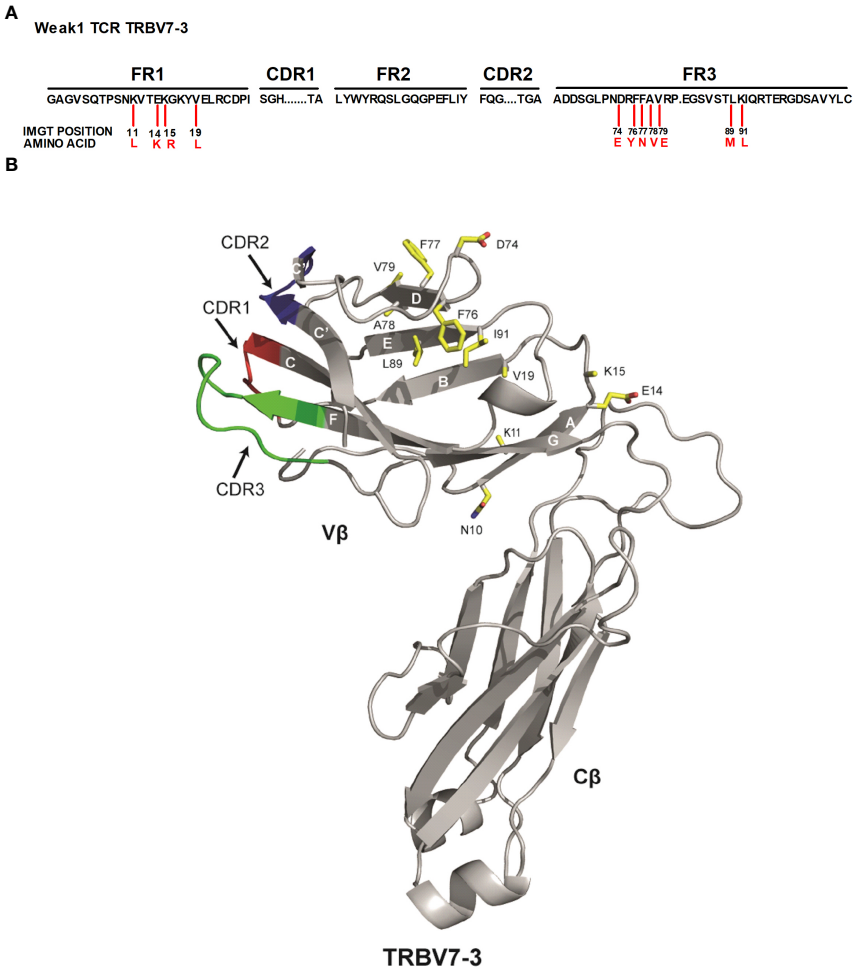

FIGURE 1
Identified 11 TRBV framework residues are distal to the CDR parts **(A)** Representation of the candidate residues assessed. Numbers in black indicate the IMGT positions in the TCRβ framework regions that were substituted with the amino acids indicated in red. FR framework region, CDR complementarity determining region. **(B)** The published 3-D structure of the 3PL6 TCR (TRAV13-1/TRBV7-3) was used as a model for the weak 1 TCR (TRAV13-2/TRBV7-3) used in this study. The location of each of the 11 residues that were changed in the weak 1 TCR Vβ domain to enhance TCR surface expression is indicated. Also included is location of residue at position 10.

One of the candidate residues tested (mutant β11) was able to significantly increase TCR expression levels in Jurkat76 cells (Figures 2C, D). The single amino acid change from lysine to leucine at position Vβ-11 resulted in a 2-fold increase in TCRβ, TCRα and CD3 expression levels in Jurkat76 cells (Figure 2D).

Combinations of amino acid changes can further improve TCR expression in Jurkat76 cells

Next, we tested whether combinations of amino acid changes could further improve expression of the weak TCR. Combining the change of Vβ residue 11 with the previously identified TCRβ10 (N>Y) mutation that is predicted to enhance the stability of Vβ-Cβ interaction (16), resulted in a small, but non-significant improvement of TCR expression compared to the single amino acid change at position 11 only (Figure 2E). However, combining various Vβ modifications with the TCR-α96 framework mutation previously identified (a single amino acid change from proline (P) to leucine (L) at position 96 of the Vα domain) doubled TCRα, β and CD3 expression levels compared to modifications in the Vβ domain alone. In the weak1 TCR, all tested Vβ modifications combined with L96 in the Vα domain achieved similar high levels of expression in Jurkat76 cells.

Next, we tested which modifications are best able to achieve optimal expression of three HLA-A0201-restricted TCRs specific for the minor histocompatibility antigen HA-1 or for cytomegalovirus (CMV). All TCRs demonstrated improved expression when only Vβ residues 10 and 11 were modified, with the most impressive improvement seen with the HA-1.m7 TCR, followed by the HA1.m2 and CMV1 TCR. Adding the TCR-α96 (P>L) modification to the TCR-β10-11 mutated chains of the 3 antigen-specific TCRs only marginally improved the expression levels (Figure 2F). This indicates that the impact of introducing leucine 96 in Vα is TCR dependent, as it increased expression of the weak1-TCR substantially (Figure 2E), but only marginally increasing the expression of the three antigen-specific TCRs (Figure 2F). Of note, the modifications had a relative small effect on the CMV TCR,

10.3389/fimmu.2023.1148890

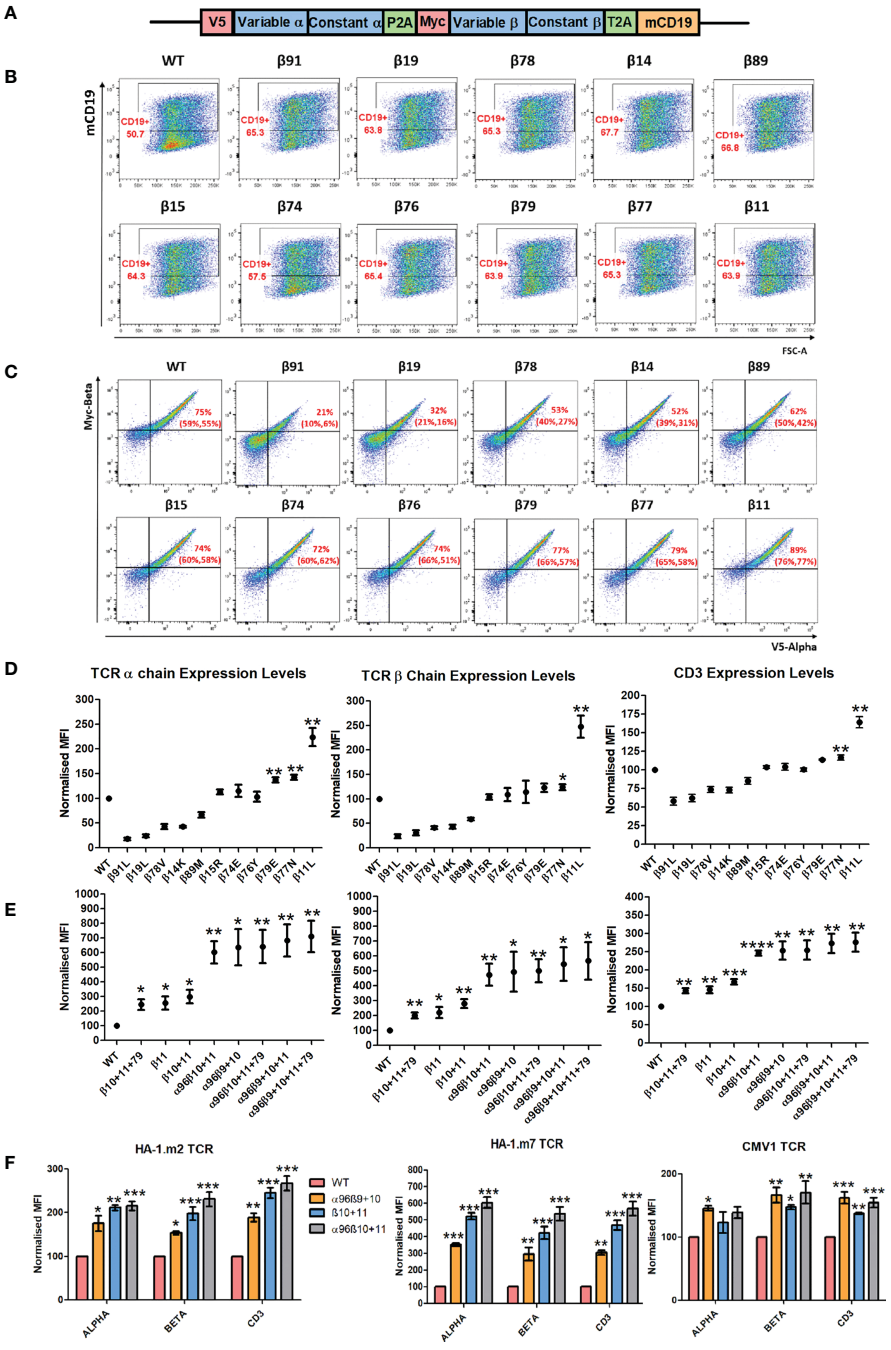

FIGURE 2
Single and combinations of amino-acid TRBV framework residue replacements can improve TCR expression in Jurkat76 cells. **(A)** Schematic representation of the retroviral vector that was used to transfer TCRs into Jurkat76 and primary T cells. Anti-V5 and anti-Myc Abs were used to determine the expression levels of TCRα and TCRβ respectively. Anti-murine CD19 Abs were used to determine transduction efficiency. mCD19 truncated murine CD19 sequence. **(B)** Representative example of three independent experiments showing Jurkat76 cells transduced with either the weak1 wild-type (WT) TCR or weak TCR constructs with the indicated single TCRβ chain amino-acid residue swap. Shown is mCD19 expression levels, indicating transduction efficiency. **(C)** Representative plots of three independent experiments showing TCRα and TCRβ expression in CD19+ gated Jurkat76 cells expressing WT or single amino-acid TCRβ chain residue modified versions of the Weak1 TCR. Numbers in brackets demonstrate the percentage of introduced TCR+ cells of the repeated experiments **(D)** Representative graphs of three independent experiments showing MFI (median fluorescence intensity) of TCRα, TCRβ and CD3 expression in CD19+ gated Jurkat76 cells transduced with WT or single amino-acid TCRβ versions of the weak1 TCR. MFI (Mean+/- SEM) data has been normalised to WT expression. Unpaired t test was applied, *: p<0.05, **: p<0.01 **(E)** Representative graphs of three independent experiments showing MFI of TCRα, TCRβ and CD3 expression in CD19+ gated Jurkat76 cells transduced with either weak1 WT TCR or TCRs with either 1 amino-acid TCRβ chain residue change, or residue combinations as indicated. MFI (Mean+/- SEM) data has been normalised to the WT TCR expression. Unpaired t test was applied, *: p<0.05, **: p<0.01 **(F)** Jurkat76 cells were transduced with either WT TCRs or 3 TCR versions with the indicated residue modifications for 3 different antigen specific TCRs (HA1.m2, HA1.m7 and CMV1 pp65). Shown is a representative example of three independent experiments showing MFI values of TCRα, TCRβ and CD3 in CD19+ gated cells. MFI (Mean+/- SEM) data has been normalised to WT expression. One-way ANOVA, Dunnett's Multiple Comparison Test, *: p<0.05, **: p<0.01, ***: p<0.001 (Residue changes were as followed: HA1.m2: α96P>L, β10H>Y, β11K>L, HA1.m7: α96T>L, β10H>Y, β11K>L.

10.3389/fimmu.2023.1148890

enhancing expression by only 1.5-fold, while the same modifications enhanced HA-1.m7 TCR expression by 6-fold (Figure 2F). This is probably due to the fact that the unmodified CMV TCR already displays strong surface expression, while the HA-1.m7 TCR is poorly expressed in the absence of Vα and Vβ modifications.

Our modelling approaches highlighted a likely molecular mechanism underlying this effect (Figure 3). K11β is a semi-buried residue that protrudes from strand A and its positively charged side chain is in close proximity to the non-polar Vβ domain core region. The positive effect of L11β on TCR expression can be explained by its protrusion from strand A into the hydrophobic core. Replacing K11β with L11β predicts that the leucine side chain is likely to stabilise the hydrophobic core by mediating multiple non-polar interactions with V19β (strand B) and L23β (strand B) (Figure 3). Therefore, the L11β substitution likely enhances the stabilisation of the hydrophobic core of the Vβ domain.

TCR modifications improve expression and reduce mis-pairing in primary human T cells

In the next set of experiments, we assessed how modifications of the three antigen-specific TCRs above affected their expression and mis-pairing in primary human T cells (Figure 4A). T cells were transduced with wild type TCRs or with versions containing Vβ modifications, either alone or in combination with the TCR-α96 (P>L) Vα domain modification. Following flow cytometry, transduced cells were identified by gating on CD19+ T cells, and levels of V5 and myc staining served to assess expression of the introduced α and β chain, respectively. The analyses demonstrated that transduction of wild type TCRs generated T cells that mostly expressed mis-paired TCRs consisting of introduced α and endogenous β chain (Figure 4A, Q3 in the FACS plots), or introduced β and endogenous α chain (Q1). All modifications increased the number of T cells expressing both the introduced α as well as the introduced β chain (Q2). Although the modification of position 10 and 11 of Vβ increased the number of T cells in Q2 expressing the introduced α and β chains, it also increased mis-pairing between the modified β and the endogenous α chain (Q1). For all three TCRs tested the modification of both Vβ and Vα was required to increase the number of T cells expressing both chains, and also reduce TCR mis-pairing (Figure 4A). Figures 4B, C display the summary of TCR expression in gated CD4+ T cells and in CD8+ T cells, respectively. It shows that the previously identified changes at 96α,9β,10β and the new combination of 96α, 10β, 11β were equally effective in increasing the percentage of T cells expressing both introduced TCR chains, except for the CMV1 TCR where only the new combination of 96α, 10β, 11β significantly increased CD4+ and CD8+ T cell numbers expressing both TCR chains. Finally, Figures 4D, E illustrates that the TCR modifications not only increased the numbers of CD4+ and CD8+ T cells expressing both chains, but the displayed MFI values indicate that the surface expression levels of the introduced chains was also increased compared to the MFI seen with the wild type TCRs. Together, the data show that the TCR modifications increased both the number of T cells expressing both chains, as well as the amount of TCR found on the surface of these T cells.

TCR modifications improve antigen-specific effector function

In the final set of experiments, we tested whether TCR modification improved the antigen-specific killing activity of primary human T cells. Transduced T cells were co-cultured with CFSE-high target cells pulsed with an irrelevant peptide, and CFSE-low targets pulsed with the TCR-recognised cognate peptide. Although T cells transduced with wild type TCRs were able to kill the relevant target cells, the modified TCRs displayed much

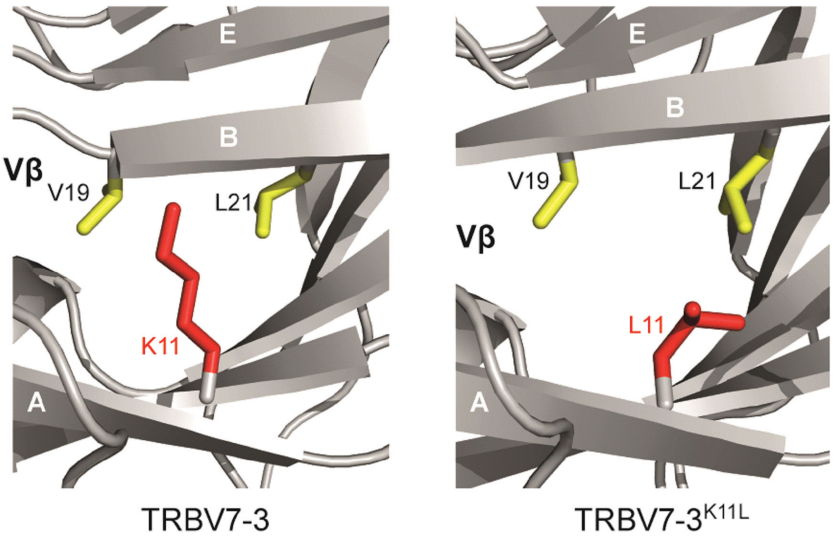

FIGURE 3
Structural modelling provides insight into the mechanistic role of framework residues in TCR stability. The change of K11β to L11β improves non-polar interactions within a hydrophobic core of the β chain. Left hand figure, lysine at position 11. Right hand figure, leucine at position 11.

10.3389/fimmu.2023.1148890

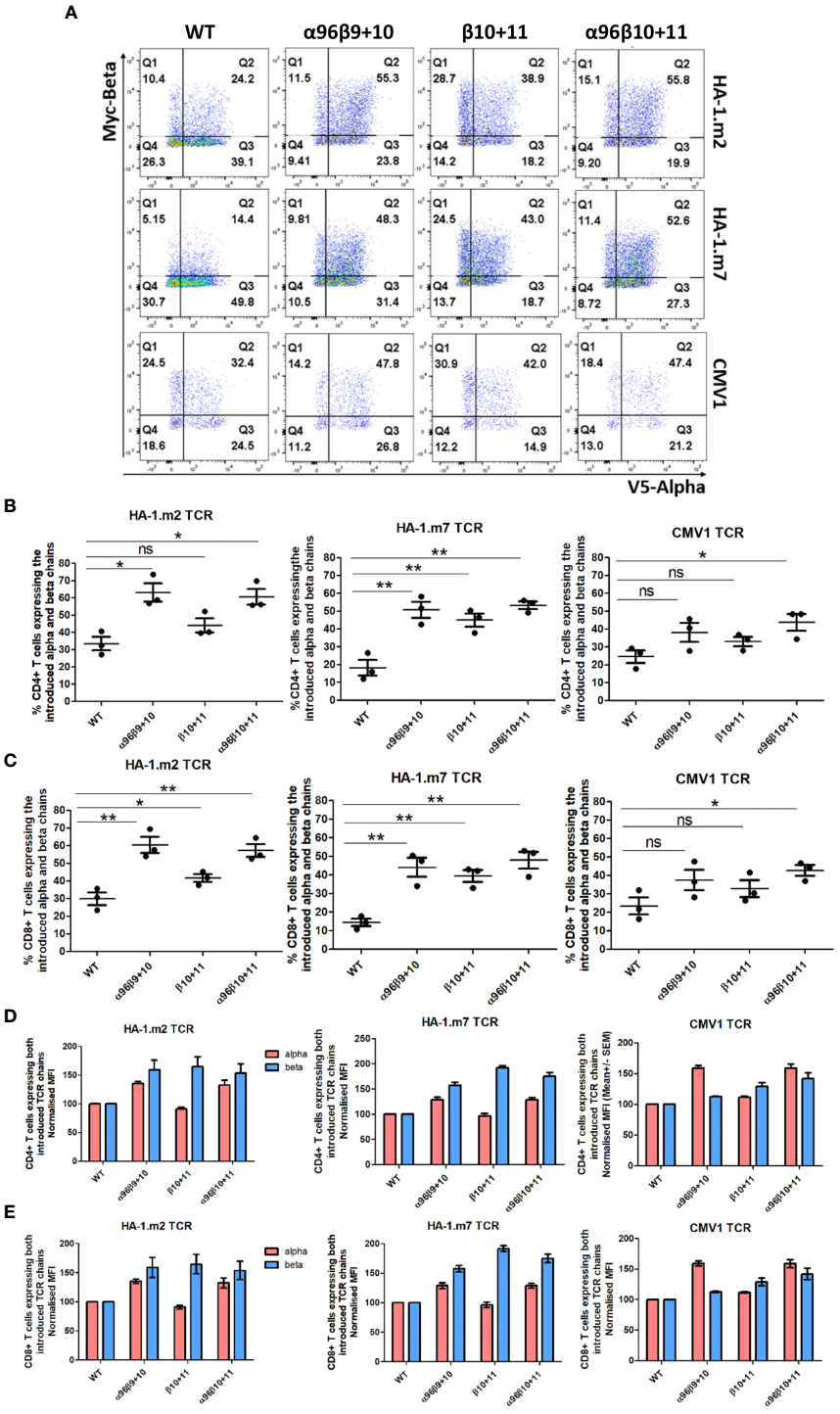

FIGURE 4
Alpha and beta chain residue modifications elevated introduced TCRs expression and reduced mis-pairing in human primary T cells. Human activated PBMCs were transduced with either WT TCR or TCRs with the indicated modified residue changes for 3 antigen specific TCRs (CMV1 pp65, HA1.2 and HA1.m7). Shown are representative examples of three independent experiments. **(A)** FACS plot show introduced TCRα chain and TCRβ chain expression in CD8+CD19+ gated cells. **(B)** Graphs show the percentage of cells expressing both the introduced α chain and introduced β chain in CD4+CD19+ gated T cells. Unpaired t test, *: p<0.05, **: p<0.01, ns: non-significant. **(C)** Graph show the percentage of cells expressing both the introduced α chain and introduced β chain in CD8-CD19+ gated T cells. Unpaired t test, *: p<0.05, **: p<0.01, ns: non-significant **(D)** The MFI (Mean+/- SEM) values of the introduced TCRα and TCRβ chain in CD8+CD19+ gated T cells. MFI values are normalised to WT expression. **(E)** The MFI (Mean+/- SEM) values of the introduced TCRα and TCRβ chain in CD4+CD19+ gated T cells. MFI values are normalised to WT expression.

10.3389/fimmu.2023.1148890

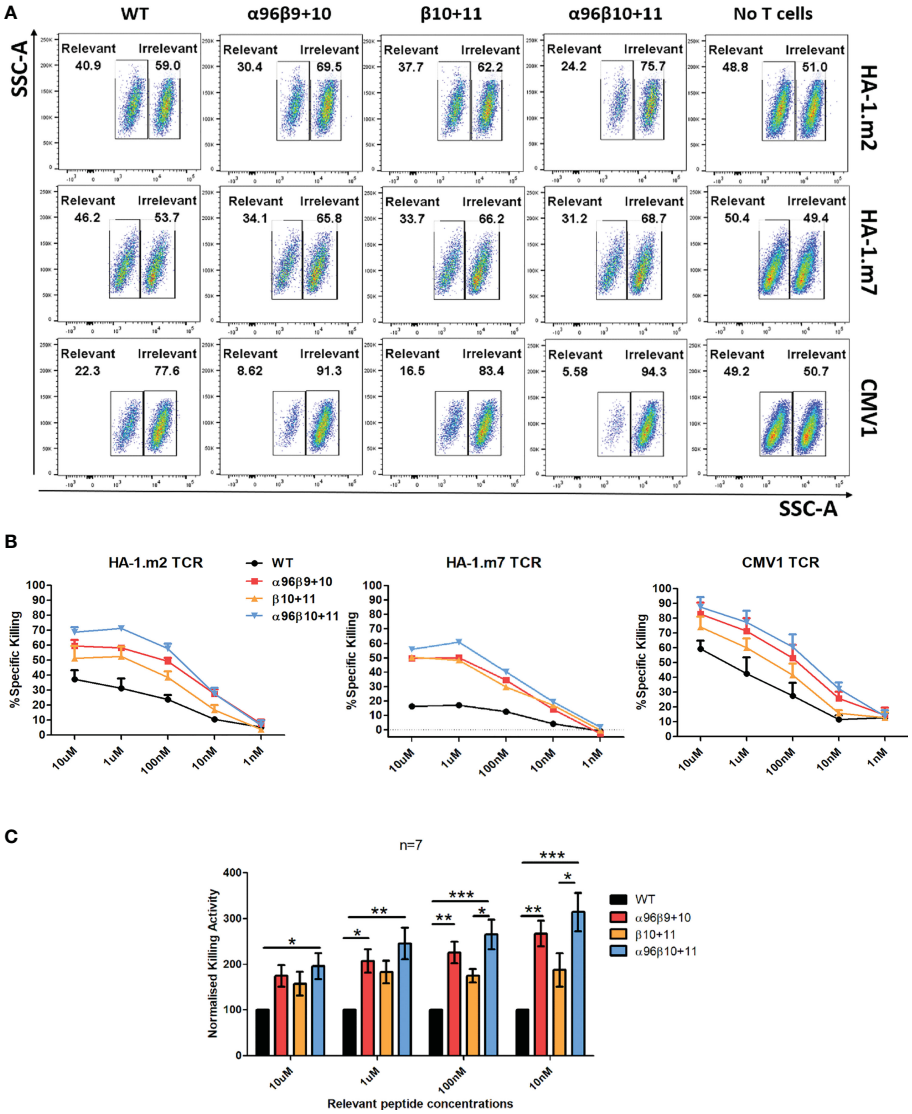

FIGURE 5
Enhanced cytotoxicity was observed with T cells expressing the residue modified TCRs. Human activated PBMCs were transduced and rested for 8-10 days and then used in subsequent assays. **(A)** Cell were co-cultured with T2 cells labelled with 10μM cognate peptide (low CFSE) or control peptide (high CFSE) mixed at 1:1 ratio (Effector: Target = 2:1). **(B)** Cell were co-cultured T2 cells labelled with 10μM – 1nM cognate peptide (low CFSE) or control peptide (high CFSE) mixed at 1:1 ratio (Effector: Target = 2:1). The following day, cells were stained for CD3 and Live/Dead and acquisition was collected on FACS. 'No T cells' control is 1:1 cognate or control peptide pulsed, CFSE labelled T2 cells only. Representative graphs demonstrating the specific killing activity of T cells transduced with either wild type or residue modified versions of HA-1.m2 (n=3), HA-1.m7 (n=1) and CMV1 (n=3) TCRs. Specific killing is: %= {100- [(Relevant/Irrelevant with T cells)/(Relevant/Irrelevant with no T cells)]*100} **(C)** Pooled relative killing data of all three TCRs tested in 7 independent experiments. At each peptide concentration the killing activity of the modified TCRs is relative to the killing activity seen with each wild type TCR which is set as 100. One-way ANOVA, Tukey Multiple Comparison Test was applied, *: p<0.05, **: p<0.01, ***: p<0.001.

improved killing activity (Figure 5A). Vβ modification alone resulted in improved killing, but the most efficient antigen-specific killing was seen when the Vβ and the Vα96 modifications were combined (Figures 5A, B). Interestingly, in all experiments the TCRs modified at the positions 96α,10β,11β showed slightly higher killing activities compared with the previously identified combination 96α,9β,10β. A comparison of the pooled killing data of all three TCRs showed that the 96α,10β,11β modification identified in this study displayed the most significant improvement in target cell killing at all peptide concentrations tested (Figure 5C).

Discussion

In this study, we have demonstrated that modifying several framework residues away from CDR1, 2 and 3 can improve TCR expression and T cell antigen specific function, while at the same time reducing mis-pairing of the introduced and endogenous TCR chains. We selected 11 candidate Vβ residues by analysing our previously created bioinformatic dataset and candidate TCR structure. TCR-deficient Jurkat76 cells and primary human T cells were transduced with modified TCRs to identify the effects of each residue change on TCR expression. Results indicated that a single amino acid change at

the 11th position of the TCRVβ domain resulted in a 2-fold increase of the TCR and CD3 in Jurkat76 cells. Combination with several other Vβ residue changes did not lead to any significant improvement compared to Vβ 11 only. However, introduction of the Vα 96 P>L modification we identified previously along with several β chain modifications enhanced expression of the Weak1 TCR.

We know from our previous work (16) that framework amino acid modifications do not cause any alteration in the mRNA expression levels of the introduced TCRs. It is well established that following their production, TCRα and TCRβ chains complete their pairing in the ER. Interaction of these two paired TCR chains with CD3 is pivotal to maintain their intact structure, otherwise they are degraded (40). Jurkat76 cell experiments indicated that not all TCRα and TCRβ chains produced in the ER migrate to the cell surface. Even though the TCR chains are produced in the ER, some may not complete proper folding to become fully functional TCR proteins; alternatively, they may complete folding, but because of low stability, they may not pair efficiently and subsequently undergo degradation in the ER. It is likely that residue substitutions enhancing TCR surface expression play a role in improving the folding and stability of the nascent TCR chains, thereby facilitating heterodimeric pairing and assembly with CD3 chains, ultimately enhancing migration of the residue modified TCRs to the T cell surface. Surprisingly, a number of candidate TCRβ framework mutations we tested caused a reduction in TCR expression, despite the fact they were identified as enriched in 'strong' TCRs, and appeared to be structurally relatively conservative. One possible explanation is that dominant TCR libraries show enrichment of complete V gene sequences that contain residues that drive high TCR folding, stability and expression, but may also contain genetically linked V gene residues that may impair TCR expression. Consistent with this possible explanation, we previously demonstrated that some amino acid residues enriched in dominant TCR-Vα chains did impair TCR surface expression, and that changing these residues to amino acids that were present in weak TCRs did actually improve TCR expression (16).

Primary human T cell experiments with HA-1.m2, HA-1.m7 and CMV1 TCRs revealed that the same residue changes elicited similar improvements in CD4+ and CD8+ T cell numbers bearing the introduced TCRs and their expression levels. By assessing the presence of V5 and Myc tags at the N-terminus site of TCRα and TCRβ, respectively, the expression level of each TCR chain could be measured independently. That also enabled assessment of cell numbers expressing mis-paired TCRs. All residue modified constructs increased the number of T cells expressing both introduced TCR chains compared to that of wild type TCRs. In addition, residue modifications decreased the number of cells expressing the mis-paired TCRs, while the wild type form of each antigen specific TCR displayed higher number of cells expressing either introduced-β-endogenous-α or vice versa mis-paired versions. We observed that modifications of both TCRα and TCRβ are required to improve the expression of the introduced TCR chains while ensuring less mis-paired TCR formations. Published work has shown that codon optimisation and the replacement of the human TCR α/β constant domains with murine domains can reduce mis-pairing and increase expression of correctly paired TCRs. In pilot experiments we saw that the TCR framework engineering approach described here improves correct TCR pairing more effectively than codon optimisation. Although murine constant regions were most effective in improving correct TCR pairing in human T cells, this approach is not suitable for clinical application as murine constant domains are immunogenic and likely to cause rejection of the engineered T cells in patients. To reduce the rejection risk, groups have identified a minimal set of 9 murine residues that were sufficient to enhance TCR expression in human T cells (41, 42). Our preliminary data showed that TCRs containing 3 residue changes in the variable framework region were more efficiently expressed in human T cells than TCRs containing the minimal set of 9 murine residues in the constant region. This suggests that the framework technology described here is superior to the previously described 'murinization' technology in terms of TCR expression and reduction of immunogenicity related to 3 amino acid changes compared to 9 residue alterations. Another important observation with residue modifications was that they conferred increased dominance to the TCRs. Transduction of TCRs into polyclonal primary human T cells provided a means to assess dominance, given the T cell repertoire naturally contains an immense variety of different TCRs, with diverse expression profiles ranging from weak to strong. These experiments clearly indicated that relative to wild type TCRs, introduction of residue modified TCRs decreased the percentage of cells expressing solely naturally dominant endogenous TCRs. Therefore, residue modification conferred increased dominance to the introduced TCRs, allowing more successful competition with the endogenous TCR repertoire, and ultimately increasing percentage expression.

We have also observed that the impact of residue modifications on TCR expression and T cell function may vary depending on the initial quality of a TCR. While the performance of TCRs with a 'weak' expression profile can be elevated dramatically by residue modification, the effects may be more limited on TCRs with a 'strong' expression profile. We recorded remarkably low HA-1.m7 wild type TCR expression in TCR-deficient Jurkat76 cells, suggesting that even in the absence of an endogenous competitor, this TCR did not form a TCR complex efficiently. Nevertheless, with framework residue modifications (α96β10+11), its performance was substantially improved in both Jurkat76 cells and primary T cells, resulting in increased numbers of T cells expressing the introduced TCR, 10-fold increased antigen-specific cytokine production, and augmented cytolysis. While the CMV1 TCR, which is a strong TCR based on Jurkat76 cell experiments and wild type TCR functional assay results, also benefited from the residue changes (with α96β10 +11) in all the categories, performance gains were limited relative to the modified HA-1.m7 TCR.

Another advantage of residue modification is that it endows T cells with increased sensitivity. Intracellular cytokine staining demonstrated that modified TCRs retained peptide specific cytokine production without non-specific activity against irrelevant peptide (Supplementary Figure 1). In killing assays, we observed an increased sensitivity of T cells expressing the residue modified TCRs. Killing assay results indicated more than 100-fold increase in antigen sensitivity for T cells bearing residue modified (α96β10+11) HA-1 TCRs. This probably arises from the enhancements observed in the TCR expression level of the introduced TCRs. As the density of the

antigen specific TCRs on the T cell surface increases, decreased antigen becomes sufficient to elicit an antigen specific response. Considering the hostile tumour environment in which there may be a scarcity of tumour specific or tumour associated antigen presentation to T cells, framework engineering seems promising route to equip T cells with an increased target sensitivity.

In this study, we have demonstrated that by substituting as few as three amino acids in the framework region of TCR variable domains, it is possible to improve the expression level of the introduced TCR and ultimately augment T cell antigen specific function. We observed that TCRα and TCRβ framework residue modifications are required for an optimal TCR expression and enhanced T cell function. The ultimate goal of TCR-T therapy relies on achieving expression of antigen specific TCR in T cells as effectively and safely as possible. Integration of framework engineering technology into this therapeutic approach holds substantial promise, namely to further exploit the potential of TCR therapy by augmenting both its efficacy and safety.

Data availability statement

The raw data supporting the conclusions of this article will be made available by the authors, without undue reservation.

Author contributions

AD designed and conducted experiments, analysed data and wrote the paper. ST designed experiments and wrote the paper. FM and BW designed experiments and wrote the paper. HS initiated the study, designed experiments, analysed data and wrote the paper. All authors contributed to the article and approved the submitted version.

Funding

AD is holding a PhD scholarship which is sponsored by the Republic of Türkiye Ministry of National Education.

Conflict of interest

Author HS is co-founder of Quell Therapeutics, and has a consultant contract and shares. He also has shares in Kuur Therapeutics and is scientific advisor for Pan CancerT.

The remaining authors declare that the research was conducted in the absence of any commercial or financial relationships that could be construed as a potential conflict of interest.

Publisher's note

Supplementary material

The Supplementary Material for this article can be found online at: https://www.frontiersin.org/articles/10.3389/fimmu.2023.1148890/full#supplementary-material

References

1. Watanabe K, Nishikawa H. Engineering strategies for broad application of TCR-t- and CAR-t-cell therapies. *Int Immunol* (2021) 33:551–62. doi: 10.1093/intimm/dxab052

2. Holler A, Zech M, Ghorashian S, Pike R, Hotblack A, Veliça P, et al. Expression of a dominant T-cell receptor can reduce toxicity and enhance tumor protection of allogeneic T-cell therapy. *Haematologica* (2016) 101:482–90. doi: 10.3324/haematol.2015.132712

3. Morgan RA, Dudley ME, Wunderlich JR, Hughes MS, Yang JC, Sherry RM, et al. Cancer regression in patients after transfer of genetically engineered lymphocytes. *Sci (1979)* (2006) 314:126–9. doi: 10.1126/science.1129003

4. Kageyama S, Ikeda H, Miyahara Y, Imai N, Ishihara M, Saito K, et al. Adoptive transfer of MAGE-A4 T-cell receptor gene-transduced lymphocytes in patients with recurrent esophageal cancer. *Clin Cancer Res* (2015) 21:2268–77. doi: 10.1158/1078-0432.CCR-14-1559

5. Rapoport AP, Stadtmauer EA, Binder-Scholl GK, Goloubeva O, Vogl DT, Lacey SF, et al. NY-ESO-1-specific TCR-engineered T cells mediate sustained antigen-specific antitumor effects in myeloma. *Nat Med* (2015) 21:914–21. doi: 10.1038/nm.3910

6. Robbins PF, Kassim SH, Tran TLN, Crystal JS, Morgan RA, Feldman SA, et al. A pilot trial using lymphocytes genetically engineered with an NY-ESO-1-reactive T-cell receptor: Long-term follow-up and correlates with response. *Clin Cancer Res* (2015) 21:1019–27. doi: 10.1158/1078-0432.CCR-14-2708

7. Robbins PF, Morgan RA, Feldman SA, Yang JC, Sherry RM, Dudley ME, et al. Tumor regression in patients with metastatic synovial cell sarcoma and melanoma using genetically engineered lymphocytes reactive with NY-ESO-1. *J Clin Oncol* (2011) 29:917–24. doi: 10.1200/JCO.2010.32.2537

8. Nagarsheth NB, Norberg SM, Sinkoe AL, Adhikary S, Meyer TJ, Lack JB, et al. TCR-engineered T cells targeting E7 for patients with metastatic HPV-associated epithelial cancers. *Nat Med* (2021) 27:419–25. doi: 10.1038/s41591-020-01225-1

9. Tawara I, Kageyama S, Miyahara Y, Fujiwara H, Nishida T, Akatsuka Y, et al. Safety and persistence of WT1-specific T-cell receptor gene2transduced lymphocytes in patients with AML and MDS. *Blood* (2017) 130:1985–94. doi: 10.1182/blood-2017-06-791202

10. Chapuis AG, Egan DN, Bar M, Schmitt TM, McAfee MS, Paulson KG, et al. T Cell receptor gene therapy targeting WT1 prevents acute myeloid leukemia relapse post-transplant. *Nat Med* (2019) 25:1064–72. doi: 10.1038/s41591-019-0472-9

11. Doran SL, Stevanović S, Adhikary S, Gartner JJ, Jia L, Kwong MLM, et al. T-Cell receptor gene therapy for human papillomavirus-associated epithelial cancers: A first-in-human, phase I/II study. *J Clin Oncol* (2019) 37:2759–68. doi: 10.1200/JCO.18.02424

12. Linette GP, Stadtmauer EA, Maus MV, Rapoport AP, Levine BL, Emery L, et al. Cardiovascular toxicity and titin cross-reactivity of affinity-enhanced T cells in myeloma and melanoma. *Blood* (2013) 122:863–71. doi: 10.1182/blood-2013-03-490565

13. Johnson LA, Morgan RA, Dudley ME, Cassard L, Yang JC, Hughes MS, et al. Gene therapy with human and mouse T-cell receptors mediates cancer regression and targets normal tissues expressing cognate antigen. *Blood* (2009) 114:535–46. doi: 10.1182/blood-2009-03-211714

14. Morgan RA, Chinnasamy N, Abate-Daga D, Gros A, Robbins PF, Zheng Z, et al. Cancer regression and neurological toxicity following anti-MAGE-A3 TCR gene therapy. *J Immunotherapy* (2013) 36:133–51. doi: 10.1097/CJI.0b013e3182829903

15. van Loenen MM, de Boer R, Amir AL, Hagedoorn RS, Volbeda GL, Willemze R, et al. Mixed T cell receptor dimers harbor potentially harmful neoreactivity. *Proc Natl Acad Sci U.S.A.* (2010) 107:10972–7. doi: 10.1073/pnas.1005802107

16. Thomas S, Mohammed F, Reijmers RM, Woolston A, Stauss T, Kennedy A, et al. Framework engineering to produce dominant T cell receptors with enhanced antigen-specific function. *Nat Commun* (2019) 10:1–15. doi: 10.1038/s41467-019-12441-w

17. Bendle GM, Linnemann C, Hooijkaas AI, Bies L, de Witte MA, Jorritsma A, et al. Lethal graft-versus-host disease in mouse models of T cell receptor gene therapy. *Nat Med* (2010) 16(5):565–70. doi: 10.1038/nm.2128

18. Rosenberg SA. Of mice, not men: No evidence for graft-versus-host disease in humans receiving T-cell receptor-transduced autologous T cells. *Mol Ther* (2010) 18 (10):1744–5. doi: 10.1038/mt.2010.195

19. Heemskerk MHM, Hagedoorn RS, van der Hoorn MAWG, van der Veken LT, Hoogeboom M, Kester MGD, et al. Efficiency of T-cell receptor expression in dual-specific T cells is controlled by the intrinsic qualities of the TCR chains within the TCR-CD3 complex. *Blood* (2007) 109(1):235–43. doi: 10.1182/blood-2006-03-013318

20. Cohen CJ, Zhao Y, Zheng Z, Rosenberg SA, Morgan RA. Enhanced antitumor activity of murine-human hybrid T-cell receptor (TCR) in human lymphocytes is associated with improved pairing and TCR/CD3 stability. *Cancer Res* (2006) 66:8878–86. doi: 10.1158/0008-5472.CAN-06-1450

21. Voss RH, Kuball J, Engel R, Guillaume P, Romero P, Huber C, et al. Redirection of T cells by delivering a transgenic mouse-derived MDM2 tumor antigen-specific TCR and its humanized derviative is governed by the CD8 coreceptor and affects natural human TCR expression. *Immunol Res* (2006) 34:67–87. doi: 10.1385/IR:34:1:67

22. Cohen CJ, Li YF, El-Gamil M, Robbins PF, Rosenberg SA, Morgan RA. Enhanced antitumor activity of T cells engineered to express T-cell receptors with a second disulfide bond. *Cancer Res* (2007) 67:3898–903. doi: 10.1158/0008-5472.CAN-06-3986

23. Kuball J, Dossett ML, Wolfl M, Ho WY, Voss RH, Fowler C, et al. Facilitating matched pairing and expression of TCR chains introduced into human T cells. *Blood* (2007) 109(6):2331–8. doi: 10.1182/blood-2006-05-023069

24. Xue SA, Gao L, Thomas S, Hart DP, Xue JZ, Gillmore R, et al. Development of a wilms' tumor antigen-specific T-cell receptor for clinical trials: Engineered patient's T cells can eliminate autologous leukemia blasts in NOD/SCID mice. *Haematologica* (2010) 95:126–34. doi: 10.3324/haematol.2009.006486

25. Bethune MT, Gee MH, Bunse M, Lee MS, Gschweng EH, Pagadala MS, et al. Domain-swapped t cell receptors improve the safety of TCR gene therapy. *Elife* (2016) 5:e19095. doi: 10.7554/eLife.19095

26. Aggen DH, Chervin AS, Schmitt TM, Engels B, Stone JD, Richman SA, et al. Single-chain VαVβ T-cell receptors function without mispairing with endogenous TCR chains. *Gene Ther* (2012) 19:365–74. doi: 10.1038/gt.2011.104

27. Knies D, Klobuch S, Xue SA, Birtel M, Echchannaoui H, Yildiz O, et al. An optimized single chain TCR scaffold relying on the assembly with the native CD3-complex prevents residual mispairing with endogenous TCRs in human T-cells. *Oncotarget* (2016) 7:21199–221. doi: 10.18632/oncotarget.8385

28. Voss RH, Thomas S, Pfirschke C, Hauptrock B, Klobuch S, Kuball J, et al. Coexpression of the T-cell receptor constant α domain triggers tumor reactivity of single-chain TCR-transduced human T cells. *Blood* (2010) 115(25):5154–63. doi: 10.1182/blood-2009-11-254078

29. Xue SA, Chen Y, Voss RH, Kisan V, Wang B, Chen KK, et al. Enhancing the expression and function of an EBV-TCR on engineered T cells by combining Sc-TCR design with CRISPR editing to prevent mispairing. *Cell Mol Immunol* (2020) 17:1275–7. doi: 10.1038/s41423-020-0396-9

30. Govers C, Sebestyén Z, Roszik J, van Brakel M, Berrevoets C, Szöőr Á, et al. TCRs genetically linked to CD28 and CD3ϵ do not mispair with endogenous TCR chains and mediate enhanced T cell persistence and anti-melanoma activity. *J Immunol* (2014) 193(10):5315–26. doi: 10.4049/jimmunol.1302074

31. Stone JD, Harris DT, Soto CM, Chervin AS, Aggen DH, Roy EJ, et al. A novel T cell receptor single-chain signaling complex mediates antigen-specific T cell activity and tumor control. *Cancer Immunology Immunotherapy* (2014) 63:1163–76. doi: 10.1007/s00262-014-1586-z

32. Provasi E, Genovese P, Lombardo A, Magnani Z, Liu PQ, Reik A, et al. Editing T cell specificity towards leukemia by zinc finger nucleases and lentiviral gene transfer. *Nat Med* (2012) 18(5):807–15. doi: 10.1038/nm.2700

33. Legut M, Dolton G, Mian AA, Ottmann OG, Sewell AK. CRISPR-mediated TCR replacement generates superior anticancer transgenic t cells. *Blood* (2018) 131:311–22. doi: 10.1182/blood-2017-05-787598

34. Schober K, Müller TR, Gökmen F, Grassmann S, Effenberger M, Poltorak M, et al. Orthotopic replacement of T-cell receptor α- and β-chains with preservation of near-physiological T-cell function. *Nat BioMed Eng* (2019) 3:974–84. doi: 10.1038/s41551-019-0409-0

35. Morton LT, Reijmers RM, Wouters AK, Kweekel C, Remst DFG, Pothast CR, et al. Simultaneous deletion of endogenous TCRαβ for TCR gene therapy creates an improved and safe cellular therapeutic. *Mol Ther* (2020) 28:64–74. doi: 10.1016/j.ymthe.2019.10.001

36. Osborn MJ, Webber BR, Knipping F, Lonetree CL, Tennis N, DeFeo AP, et al. Evaluation of TCR gene editing achieved by TALENs, CRISPR/Cas9, and megaTAL nucleases. *Mol Ther* (2016) 24:570–81. doi: 10.1038/mt.2015.197

37. Zhang Y. I-TASSER server for protein 3D structure prediction. *BMC Bioinf* (2008) 9:1–8. doi: 10.1186/1471-2105-9-40

38. Winn MD, Ballard CC, Cowtan KD, Dodson EJ, Emsley P, Evans PR, et al. Overview of the CCP4 suite and current developments. *Acta Crystallogr D Biol Crystallogr* (2011) 67:235–42. doi: 10.1107/S0907444910045749

39. Emsley P, Cowtan K. Coot: Model-building tools for molecular graphics. *Acta Crystallogr D Biol Crystallogr* (2004) 60:2126–32. doi: 10.1107/S0907444904019158

40. Klausner RD, Lippincott-Schwartz J, Bonifacino JS. The T cell antigen receptor: insights into organelle biology. *Annu Rev Cell Biol* (1990) 6:403–31. doi: 10.1146/annurev.cb.06.110190.002155

41. Bialer G, Horovitz-Fried M, Ya'acobi S, Morgan RA, Cohen CJ. Selected murine residues endow human tcr with enhanced tumor recognition. *J Immunol* (2010) 184 (11):6232–41. doi: 10.4049/jimmunol.0902047

42. Sommermeyer D, Uckert W. Minimal amino acid exchange in human tcr constant regions fosters improved function of tcr gene-modified t cells. *J Immunol* (2010) 184(11):6223–41. doi: 10.4049/jimmunol.0902055

frontiers | Frontiers in Immunology

TYPE Original Research
PUBLISHED 09 May 2023
DOI 10.3389/fimmu.2023.1068625

OPEN ACCESS

EDITED BY
Ralf-Holger Voss,
Johannes Gutenberg University
Mainz, Germany

REVIEWED BY
Reona Leo Sakemura,
Mayo Clinic, United States
Tingxuan Gu,
Zhengzhou University, China
Yixiong Zhou,
Shanghai Jiao Tong University, China

*CORRESPONDENCE
Wei Chen
cw0226@foxmail.com
Xiaopeng Zhang
zhangxp@bmi.ac.cn

†These authors have contributed equally to this work

RECEIVED 13 October 2022
ACCEPTED 14 April 2023
PUBLISHED 09 May 2023

CITATION
Niu A, Zou J, Hu X, Zhang Z, Su L, Wang J, Lu X, Zhang W, Chen W and Zhang X (2023) Differences in the phenotypes and transcriptomic signatures of chimeric antigen receptor T lymphocytes manufactured *via* electroporation or lentiviral transfection.
Front. Immunol. 14:1068625.
doi: 10.3389/fimmu.2023.1068625

Differences in the phenotypes and transcriptomic signatures of chimeric antigen receptor T lymphocytes manufactured *via* electroporation or lentiviral transfection

Anna Niu[1†], Jintao Zou[1†], Xuan Hu[1], Zhang Zhang[1], Lingyu Su[1,2], Jing Wang[1], Xing Lu[1,2], Wei Zhang[2], Wei Chen[1*] and Xiaopeng Zhang[1*]

[1]Beijing Institute of Biotechnology, Beijing, China, [2]Nanhu Laboratory, Jiaxing, Zhejiang, China

Chimeric antigen receptor (CAR)-T cell therapy is an innovative treatment for CD19-expressing lymphomas. CAR-T cells are primarily manufactured via lentivirus transfection or transposon electroporation. While anti-tumor efficacy comparisons between the two methods have been conducted, there is a current dearth of studies investigating the phenotypes and transcriptome alterations induced in T cells by the two distinct manufacturing methods. Here, we established CAR-T signatures using fluorescent imaging, flow cytometry, and RNA-sequencing. A small fraction of CAR-T cells that were produced using the PiggyBac transposon (PB CAR-T cells) exhibited much higher expression of CAR than those produced using a lentivirus (Lenti CAR-T cells). PB and Lenti CAR-T cells contained more cytotoxic T cell subsets than control T cells, and Lenti CAR-T cells presented a more pronounced memory phenotype. RNA-sequencing further revealed vast disparities between the two CAR-T cell groups, with PB CAR-T cells exhibiting greater upregulation of cytokines, chemokines, and their receptors. Intriguingly, PB CAR-T cells singularly expressed IL-9 and fewer cytokine release syndrome-associated cytokines when activated by target cells. In addition, PB CAR-T cells exerted faster *in vitro* cytotoxicity against CD19-expressing K562 cells but similar *in vivo* anti-tumor efficacy with Lenti CAR-T. Taken together, these data provide insights into the phenotypic alterations induced by lentiviral transfection or transposon electroporation and will attract more attention to the clinical influence of different manufacturing procedures.

KEYWORDS

chimeric antigen receptor T lymphocyte, piggyBac transposon, lentiviral transfection, phenotype, transcriptomic signature

1 Introduction

Chimeric antigen receptor (CAR)-T cell therapy has been revolutionized in hematologic malignancies with the recent development and emergence of adoptive cell therapy. CARs consist of two major functional components: extracellular recognition and intracellular signal transduction molecules. CARs comprise a single chain variable fragment (scFv), transmembrane region, co-stimulation signaling domain, CD28 (1) or 4-1BB (2) domain, and CD3ζ domain, which elicit profound and durable anti-B cell leukemia responses (3). CAR-T cell therapy targeting CD19 was first approved by the US Food and Drug Administration in 2017 (4). The overall response rate of patients with B cell acute lymphoblastic leukemia is 73%–83% (5–7) with an annual cost of up to $1,615,000 (8). However, side effects, cytokine release syndrome (9), and neurotoxicity (10) caused by CAR-T cells are concerning barriers, and some patients achieve only about 50% remission after receiving CAR-T cell therapy (11, 12). To achieve an optimized risk/benefit ratio in patients receiving CAR-T cell therapy, all factors affecting antigen binding, exhaustion, duration, and signaling activation should be considered during the design and manufacturing process, as even slight alterations in the CAR design will alter the function and side effects of CAR-T cell therapy (13).

The CAR gene transfer method may represent a critical factor that affects the phenotype of CAR-T cells. The predominant manufacturing procedures have been confirmed to be safe and effective and primarily involve lentiviral/retroviral transfection or transposon electroporation (14, 15). Although replication-competent lentivirus/retrovirus have been shown to cause oncogenesis of gene-modified cells, data for 375 manufactured T cell products with self-inactivated lentivirus/retrovirus exhibited low safety risk for HIV and oncology patients (16). The lentiviral/retroviral transfection system packages RNA encoding transgenes and essential viral genome components, such as the Rev responsive element (RRE), 5′ long terminal repeat (LTR), 3′ LTR, and Psi elements (17). Following infection of target cells, the RNA is reverse transcribed into DNA and subsequently integrated into the cell genome (18). Transposon systems generally comprise two vectors encoding the enzyme and transgenes. In comparison, when electroporated into cells and expressed, transposase excises transposons from the plasmid and integrates them into the target genome. In particular, the PiggyBac transposon system can efficiently transpose between vectors and chromosomes via a "no footprint cut-and-paste" mechanism. Recently, electroporation of CAR plasmids into T cells was introduced, and their safety and efficacy were assessed (19). We previously reported an optimized electroporation method for constructing functional CAR-T cells (20). In phase I clinical trials, the transposon system achieved a 2200–2500 fold expansion of CAR-T cells with 84% positivity after co-culturing with feeder cells (19). Moreover, the use of minicircle vectors in this system was less likely to cause genomic damage during mutagenesis (21).

Lentivirus and transposon systems expose T cells to considerably different stimuli. More specifically, the integrated fragments differ due to the essential viral genome compounds required by the lentivirus for reverse transcription and nuclear translocation, whereas reverse transcription is not required in the transposon system. Additionally, the mode of entry into the cells (viral infection versus electroporation) differs between the two methods.

Functional comparisons of CAR-T cells produced using the two manufacturing processes have been conducted in mouse xenograft models by different groups (21, 22) and have shown similar anti-tumor efficacy; however, there is a lack of comprehensive data on the perturbation of intracellular signaling networks and transcriptomes of T cells subjected to the distinct manufacturing methods. Hence, in the current study, we sought to explore phenotypic differences between CAR-T cells produced via lentiviral transfection (Lenti CAR-T cells) or PiggyBac transposon electroporation (PB CAR-T cells) using transcriptome analysis and flow cytometry. We then determined the potential effects of these differences on the anti-tumor efficacy of CAR-T cells.

2 Materials and methods

2.1 Primary cells and cell lines

Peripheral blood mononuclear cells (PBMCs) were isolated by density gradient centrifugation using Ficoll Paque Plus (Cytiva, USA) from whole blood samples obtained from healthy donors. The PBMCs were cultured in Xvivo 15 medium (Lonza, Belgium), and cryopreserved in fetal bovine serum (FBS) containing 10% dimethyl sulfoxide. CD19-expressing luciferase-tagged K562 cells (Shanghai Genechem Co., Ltd.) were cultured in Iscove's Modified Dulbecco's Medium (Lonza, Belgium) supplemented with 10% FBS and used as target cells for the assessment of CAR-T cell cytotoxicity. Raji cells were cultured in RPMI 1640 medium supplemented with 10% FBS and used for the assessment of CAR-T cell efficacy *in vivo*.

2.2 Construction of CD19-targeting CAR transposon and lentiviral vectors

Constructs containing CD19-targeting CAR molecules—including a CD8a signal peptide, clone FMC63 CD19-targeting scFv, CD8a transmembrane domain, 4-1BB domain, and CD3ζ domain—and TagGFP2 separated by a P2A sequence, were produced. CAR expression was controlled by the EF-1α promoter. The consensus EF-1α promoter and CD19-targeting CAR open reading frame (ORF) were cloned into the pLenti lentiviral gene expression vector (Origene, USA) and PiggyBac dual promoter vector (System Biosciences, USA).

2.3 Electroporation of the CD19-targeting CAR transposon

Electroporation was performed as previously described (20), with slight modifications. In brief, PBMCs were stimulated with anti-CD3/CD28-coated beads (Thermo Fisher Scientific, USA) at a

bead-to-cell ratio of 1:1 for 3 days. Then cells were counted and washed twice to remove the beads. Next, 1×10^6 primary T cells were resuspended with 2.1 μg plasmids in 20 μL electroporation buffer containing approximately 0.7 μg of the Super PiggyBac transposase vector and 1.4 μg of the CD19-targeting CAR transposon vector. The resulting mixture was immediately transferred to 20-μL electroporation tubes and subjected to electroporation condition (voltage = 500 V, time = 20 ms) within an electroporator (Celetrix CTX-1500A LE, USA) and then gently transferred into pre-warmed Xvivo 15 medium without antibiotics.

2.4 Manufacturing of CD19-targeting CAR-T cells *via* lentiviral transfection

Lentivirus generation was performed as described previously (22), with slight modifications. Second-generation lentiviral vectors were also produced. The pLenti CD19-targeting CAR vector was co-transfected into 293T cells with the packaging vector and the spike glycoprotein of the vesicular stomatitis virus (VSV-G)-expressing vector. Lentivirus was concentrated from the medium supernatant with a lentivirus concentrator kit (Oligobio, China), detected via flow cytometry, resuspended in phosphate buffer saline without Mg^{2+} and Ca^{2+}, and frozen at -80°C. PBMCs were cultured for 24 hours before activation, suspended at a concentration of 1×10^6 cells/mL, and incubated with anti-CD3/CD28-coated beads (Thermo Fisher Scientific, USA) at a bead-to-cell ratio of 1:1. After activation, T cells were infected with lentivirus at a multiplicity of infection of 3.0. The media was refreshed 24 hours post-transfection.

2.5 Flow cytometry analysis

1×10^6 CAR-T cells were stained with protein L labeled with iFluor647 (GenScript, USA). iFluor647 was detected using GUAVA easyCyte HT after separate detection of dead cells using acridine orange/propidium iodide staining. Analysis of CAR-T cells was conducted using the method described by Blom et al. (23). In brief, manufactured T cells were stained with live/dead dye from the Zombie Aqua Fixable Viability Kit (BioLegend) and primary antibodies, according to manufacturers' protocols, including Alexa Fluor 700 conjugated anti-human CD3 antibody (Clone UCHT1), PE-Cy7 conjugated anti-human CD4 antibody (Clone RPA-T4), PerCP-Cy5.5 conjugated anti-human CD8 antibody (Clone SK1), APC conjugated anti-human CD69 antibody (Clone FN50), Brilliant Violet 605 anti-human CD62L antibody (Clone DREG-56), PE/Dazzle 594 anti-human CD45RO antibody (Clone UCHL1), Brilliant Violet 421 anti-human PD-1 antibody (Clone EH12.2H7), APC-conjugated anti-human CD107a (Clone H4A3), and PE-conjugated anti-human Granzyme B (Clone QA18A28). Gates for CD62L, CD45RO, PD-1, and Granzyme B fluorescence were further validated using fluorescence minus one control. Peripheral blood collected from mice at 3 weeks post-infusion with T/CAR-T cells were stained with PE-Cy7 conjugated anti-human CD3 antibody (Clone UCHT1), Pacific Blue conjugated anti-human CD45 (Clone HI30), and FITC conjugated anti-human CD19 antibody (Clone HIB19). All antibodies used in this study and their corresponding isotypes were purchased from BioLegend company. The positives of each marker were gated against an isotype control. The data were analyzed using FlowJo V10.8.1.

2.6 RNA extraction, library construction, sequencing, and validation

The PBMCs samples were collected from healthy donors and samples from each donor were divided into three groups: control T (untreated), Lenti CAR-T, and PB CAR-T. After manufacturing, CAR-T cells were isolated with the flow cytometer Sony MA900. The samples were frozen in liquid nitrogen until RNA extraction. Total RNA was extracted from CAR-T cells using RNAiso Plus (Takara, Japan). RNA quality was evaluated by Nanodrop spectrophotometer (Thermo Fisher Scientific, USA). The NEBNext Ultra RNA Library Prep Kit for Illumina reagent was used to prepare the RNA library. The reference genome files were downloaded from genome websites (https://www.ncbi.nlm.nih.gov/genome/51?genome_assembly_id=1820449). The filtered reads were mapped to the reference genome using the HISAT2 version 2.0.5. MicroRNAs were isolated using a miRNeasy Micro Kit (QIAGEN, Germany) according to the manufacturer's instructions. Quality was assessed with an Agilent 4200 TapeStation, and quantity was determined using a Qubit 2.0 Fluorometer (Thermo Fisher Scientific, USA). The samples were sent to Shanghai Personal Biotechnology Co,. Ltd. for mRNA library construction and sequencing on an Illumina HiSeq platform (Illumina).

To perform RT-qPCR validation, total RNA sample (1 μg) was used for synthesis of cDNA and PCR amplification using the HiScript II One Step RT-PCR Kit (Vazyme, China) as manufacturers' protocols described. Primers for RT-qPCR analysis were synthesized by Sangon Biotech Co., Ltd. (Shanghai, China). RT-qPCR was carried out with the Bio-Rad CFX384 Touch real-time PCR detection system. The relative expression levels of the selected genes were analyzed using the comparative CT method ($2^{-\Delta\Delta CT}$). Each RT-qPCR analysis was repeated at least 4 times and *β-actin* was used as the reference control.

2.7 Principle component analysis and pathway analysis

Comparison was made between the Read Count values for each gene as the original expression of that gene. The expression was then standardized with fragments per kilobase of exon per million mapped fragments (FPKM). Differences in gene expression were analyzed with DESeq software (version 1.39.0) under the following screening conditions: $\log_2$ fold change > 1, P-value < 0.05. Principal component analysis (PCA) was then performed as described previously (24). Kyoto Encyclopedia of Genes and Genomes (KEGG) analysis was performed using differentially expressed genes with an adjusted P-value of ≤ 0.01. The number of

differentially enriched genes in KEGG pathway was calculated. Gene Set Enrichment Analysis (GSEA, https://www.gsea-msigdb.org) was performed to investigate distinct genesets between PB and Lenti CAR-T groups.

2.8 Enzyme-linked immunosorbent assay

After CAR-T cells manufacturing or coculturing with target cells, cytokine analysis was performed by using ELISA, according to the manufacturers' protocols. The concentration of IFN-γ, TNF-α, GM-CSF, CXCL10, IL-6, IL-10, IL-12, and CCL2 was measured by an Ella automated immunoassay kit (Bio-Techne, USA). Concentrations of IL-9 and Granzyme B were determined using enzyme-linked immunosorbent assay kits (Dakewei, China or Neobioscience, China).

2.9 *In vitro* anti-tumor efficacy

Luciferase-expressing K562 CD19 cells were co-cultured with CAR-T cells at desired effector-to-target (E:T) ratios for either 4 or 24 hours. Following co-culture, luciferin substrate was introduced to the system at a final concentration of 0.3 mg/mL. Relative luminescence units (RLUs) were measured using a SpectraMax M5 plate reader (Molecular Devices, CA). The lysis rates of tumor cells were calculated by the following formula: %tumor cell lysis =100% × (1 – RLU (experimental -background)/(target cell max-background).

The cytotoxicity of CAR-T cells was further evaluated using the xCELLigence Real-Time Cellular Analysis DP platform (Agilent Technologies, CA). This system measures a dimensionless parameter called cell index (CI) to determine the viability of the cell and tumor lysis rate. Briefly, K562-CD19-luc cells were plated at a concentration of 2.5×10^4 cells per well in 200 μL of cell culture medium in 16-well E-plates. After seeding, the cells were cultured on the xCELLigence instrument in a humidified incubator at 37°C with 5% CO_2 for 24 hours. Subsequently, T/CAR-T cells were seeded onto the E-plates at an E:T ratio of 2.5:1. Continuous impedance measurements were then monitored every 5 minutes for up to 72 hours. Four replicates were set for each group. The cell index was normalized to the time point of addition of the T/CAR-T cells. The lysis rates of tumor cells were calculated by the following formula: $[1 - \text{Normalized CI}_{\text{treatment}}/\text{Normalized CI}_{\text{target only}}] \times 100\%$.

2.10 *In vivo* anti-tumor efficacy

Six-week-old NSG (NOD-*Prkdc*^{scid}*Il2rg*^{em1}/Smoc) mice were intravenously injected with 1×10^6 Raji cells *via* the tail vein. Two weeks after tumor cell inoculation, the mice received intravenous treatment with 1.5×10^6 CAR-T cells. Serum samples were collected at 4 hours and 24 hours post-infusion of CAR-T cells. Peripheral blood samples were obtained three weeks post-infusion and analyzed for the presence of $CD19^+$ Raji cells by flow cytometry. Animals used in this study were reviewed and approved by the Animal Care and Use Committee of the Beijing Institute of Biotechnology.

2.11 Statistical analysis

Data were presented as the mean ± standard deviation (SD) in triplicate. Flow cytometry data were analyzed using BD FlowJo software (version 10.8.1). To determine *P*-values, one-way ANOVA with Tukey's multiple comparison test or student's *t*-test was applied. GraphPad Prism 9.0 was used to perform statistical analyses.

3 Results

3.1 Production of CAR-T cells by electroporation and lentiviral transfection

T cells isolated from healthy donors were used to manufacture Lenti CAR-T cells and PB CAR-T cells. To minimize technical bias, both manufacturing processes were carried out following the same schedule (Figure 1A). The two vector systems share a consensus ORF and promoter (Figure 1B). Higher green and red fluorescent intensities of PB CAR T cells were shown in Figure 1C, compared with Lenti CAR-T cells. Moreover, the percentage of CAR-positive T cells was adjusted to approximately 30% for both groups on day 6 (Figures 1D, E). The mean fluorescence intensity (MFI) values of PB CAR-T cells were significantly higher than those of Lenti CAR-T cells (Figure 1F), suggesting relatively weak expression of CAR molecules following lentiviral transfection. The reduced CAR expression in Lenti CAR-T cells may be attributed to excessive viral elements integrated into the genome of the target cells.

3.2 Analysis of CAR-T cell cytotoxicity, activation, and exhaustion

Flow cytometry was performed to characterize the two CAR-T cell groups. The analysis pipeline was shown in Supplementary Figure 1. The $CD4^+$ and $CD8^+$ gates divided the T cells into four subsets: $CD4^+$, $CD8^+$, $CD4^+$ $CD8^+$ (double-positive, DP), and $CD4^-$ $CD8^-$ (double-negative, DN). These subsets were further gated using CD69, granzyme B, and programmed cell death-1 (PD-1) as markers of T cell activation, cytotoxicity, and exhaustion, respectively (25). Given that the DP T cell subset only accounted for ~6% of the total T cells, markers of DP T cells were not analyzed.

Granzyme B, secreted by cytotoxic T lymphocytes, triggers target cell DNA cleavage and apoptosis by binding to its receptor and being released by perforin (26). The proportion of granzyme B^+ cells was consistently high, ranging from 80% to 90% across all groups (Figures 2A–D), as evidenced by CD107a staining (Supplementary Figure 2A, B). Following CAR transfection, the proportion of granzyme B^+ cells in the PB groups slightly increased. (Figures 2A–C), with the CAR-T cell groups exhibiting the highest proportion of granzyme B^+ cells in the $CD8^+$ subset (Figures 2C). No significant difference was observed in CD69 expression between PB CAR-T cells and Lenti CAR-T cells (Supplementary Figures 2C–2F). Expression of PD-1, which is a member of the CD28 superfamily that negatively regulates T cells upon activation by

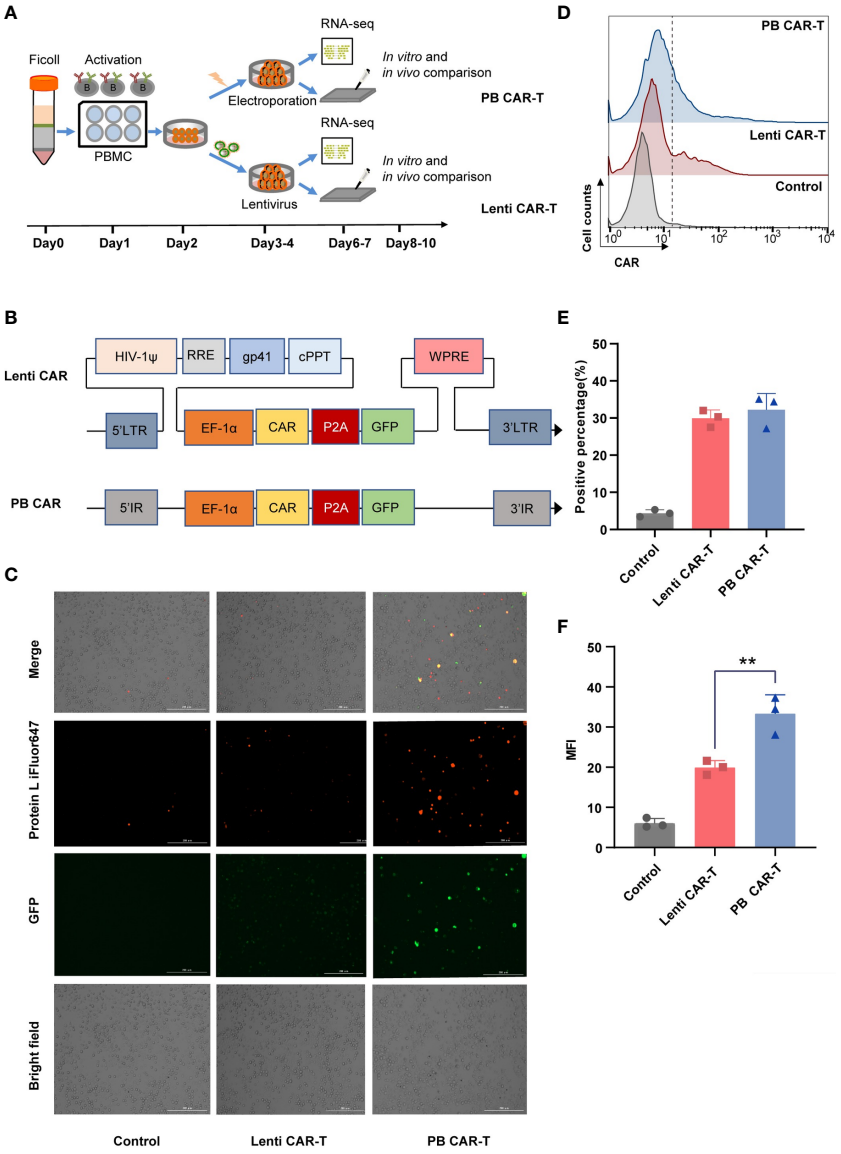

FIGURE 1
Production of CAR-T cells *via* PiggyBac transposon electroporation or lentiviral transfection. **(A)** CAR-T cell manufacturing schedule. **(B)** CAR insertion fragments used in the study. The scFv of CAR is derived from mAb clone FMC63 that binds human CD19 and was generated by fusing the VL and VH regions via a 3× G4S linker peptide. The scFv was attached to modified human CD8a hinge and CD8a transmembrane regions that were fused to the 4-1BB (cytoplasmic) and CD3ζ (cytoplasmic) domains. **(C)** Representative fluorescent images of CAR-positive T cells. Transfection efficiency after 48 hours was demonstrated by fluorescence microscopy images with Bio-Tek Cytation 5. **(D–F)** Flow cytometry detection of CAR expression on the surface of transduced CAR-T cells on day 6. Lenti CAR-T cells and PB CAR-T were generated by Lentivirus transfection and plasmid electroporation, respectively. **(D)** iFluor 647 Protein L that binds to the variable light chains of scFv can be used for the detection of CAR expression in 1 × 10^6 cells at a 1:100 dilution ratio. Untransduced T cells were used as control groups. Representative flow cytometry plots of CAR-positive T cells. **(E)** Statistical analysis of CAR-positive percentages (n = 3). **(F)** Statistical analysis of mean fluorescent intensity (MFI) values represents the mean fluorescence intensity of iFluor 647 protein L (n = 3). One-way ANOVA with Tukey's multiple comparison test. $^{**}P < 0.01$.

PD-L1 or PD-L2 (27), was similar in T cells before and after CAR insertion (Supplementary Figure 3), indicating that neither manufacturing process induced T cell exhaustion.

3.3 Fewer PB CAR-T cells exhibit a memory phenotype than Control T cells

CD62L and CD45RO are major plasma membrane markers that distinguish central memory (CM; $CD45RO^+CD62L^+$) T cells from effector memory (EM; $CD45RO^+CD62L^-$) T cells (23). T_{EM} function as rapid effectors by migrating to inflamed sites through surface chemokine receptors and adhesion proteins, whereas T_{CM} shares certain cell plasma membrane markers with naive T cells (28). The proportion of T cells with a CM phenotype, compared with those of the EM phenotype, was higher in each group (Figures 3A–D; Supplementary Figure 4). Within the total T cell population, the frequency of CM was higher than that of EM (Supplementary Table 1). Compared with control T cells, the proportion of PB CAR-T cells with an EM phenotype (Figure 3A), or CM

10.3389/fimmu.2023.1068625

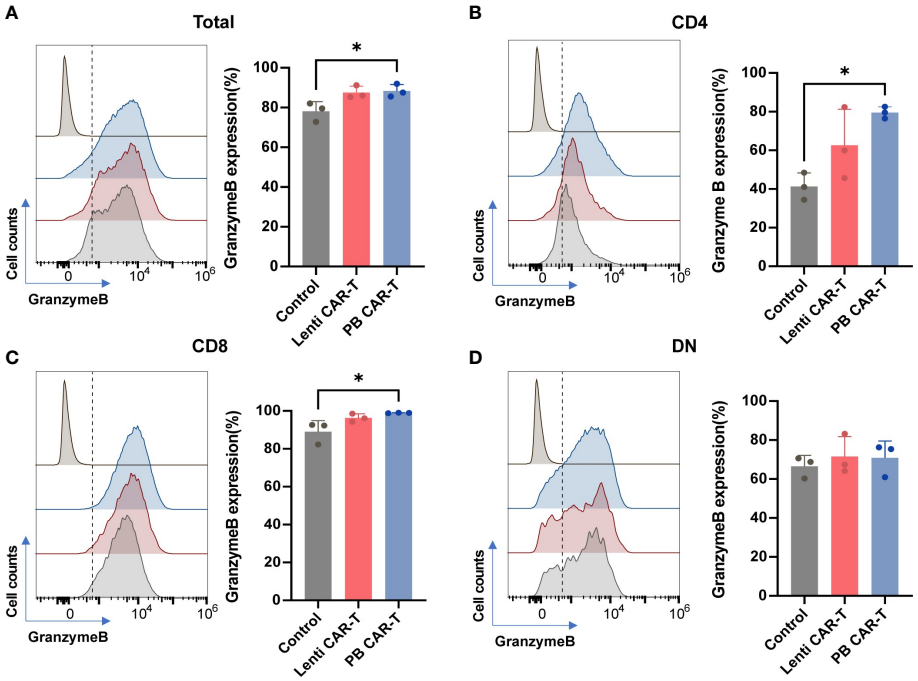

FIGURE 2
Flow cytometry analysis of granzyme B expression of total T cells and T cell subsets. CAR-T cells at day 3 post-transfection were analyzed using flow cytometry. Representative histogram images and statistical analysis of granzyme B expression in total T cells **(A)** and $CD4^+$ **(B)**, $CD8^+$ **(C)**, and double negative (DN) **(D)** T cell subsets (n = 3). Isotype controls were presented in the upper first lane. One-way ANOVA with Tukey's multiple comparison test. *$P < 0.05$.

phenotype, was lower in the total cell population and $CD4^+$ subsets (Figures 3A, B). No significant difference was observed in memory phenotypes among the $CD8^+$ and DN subsets (Figures 3C, D). Collectively, these data suggest that fewer PB CAR-T cells exhibit a pronounced memory phenotype, which may be due to the susceptibility of memory T cells to electroporation in the manufacturing process (29).

3.4 Transcriptomic comparison of Lenti and PB CAR-T cells

To identify transcriptome-wide alterations induced by the different manufacturing methods, RNA-sequencing (RNA-seq) was conducted on samples obtained from three healthy donors. PCA analysis revealed a marked transcriptomic difference between Lenti and PB CAR-T cells (Figures 4A, B), suggesting that Lenti and PB CAR-T cells may be two distinct cell populations despite their similar flow cytometry profiles. To gain a more comprehensive understanding of the functions of differentially expressed genes in PB CAR-T cells compared to Lenti CAR-T cells, we conducted KEGG pathway annotations and enrichment analysis. Our results revealed that 67 pathways were significantly overrepresented (adjusted $P < 0.05$), including "cytokine-cytokine receptor interaction", "chemokine signaling pathway," and "viral protein interaction with cytokine and cytokine receptor" (Figure 4C). T cells execute their functions primarily by secreting various cytokines and chemokines (23). The hierarchical clustering (Figure 4D) and GSEA analysis (Supplementary Figure 5) of "cytokine-cytokine receptor interaction" pathway revealed the upregulated cytokine synthesis in PB CAR-T. To further validate the transcriptomic difference between the two CAR-Ts, we employed RT-qPCR to quantify the transcription of upregulated genes in PB CAR-T. The RT-qPCR assays confirmed that the mRNA levels of *gm-csf*, *cxcl13*, *ifn-γ*, *il9*, *serpine1*, *il17f*, *il3*, and *ccl22* were higher in the PB CAR-T groups than the Control T groups. Furthermore, in comparison to Lenti CAR-T cells, the majority of these genes exhibited elevated mRNA levels in PB CAR-T cells (as demonstrated in Supplementary Figure 6). These findings suggest that PB CAR-T cells may possess a proinflammatory phenotype.

3.5 PB CAR-T cells create an intensive cytokine microenvironment *in vitro*

To validate the differences detected by RNA-seq, we performed a quantitative cytokine analysis using ELISA. Numerous cytokines were released into the media by PB CAR-T cells, including IFN-γ, granzyme B, interleukin (IL)-6, tumor necrosis factor (TNF)-α, Granulocyte-macrophage colony-stimulating factor (GM-CSF), CXCL10, IL-9, and CCL2 (Figures 5A–H). Of these, IL-6, IL-9, IFN-γ, TNF-α, and GM-CSF are critical soluble mediators of cytokine storms (30). These data suggested that the electroporation of PB transposon vectors induced the release of numerous high-concentration cytokines and a cytokine storm-like microenvironment *in vitro*, which differed markedly from the cytokine profile associated with CAR-T cells produced via lentiviral transfection. To further investigate the effects of the electroporation

10.3389/fimmu.2023.1068625

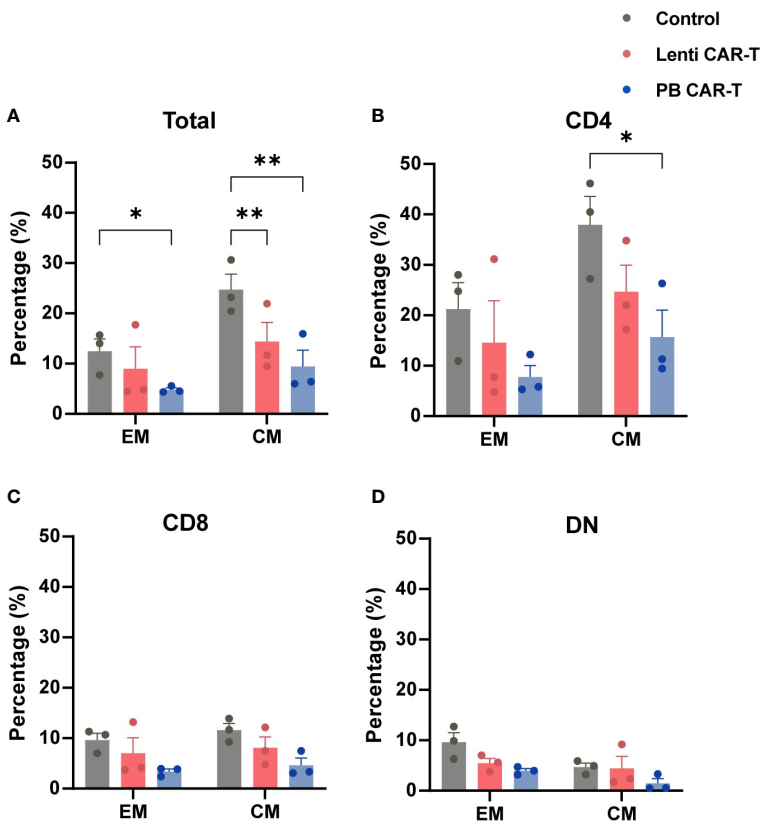

FIGURE 3
Memory phenotypes of total T cells and T cell subsets. CAR-T cells at day 3 post-transfection were analyzed using flow cytometry. T cells were stained with anti-CD45RO and anti-CD62L antibodies. Statistical analysis of CD45RO and CD62L expression in total T cells **(A)**, $CD4^+$ T cells **(B)**, $CD8^+$ T cells **(C)**, and DN T cells **(D)**. $CD45RO^+CD62L^+$ and $CD45RO^+CD62L^-$ represent central memory (CM) and effector memory (EM) phenotypes, respectively (n = 3). One-way ANOVA with Tukey's multiple comparison test. $^*P < 0.05$, $^{**}P < 0.01$.

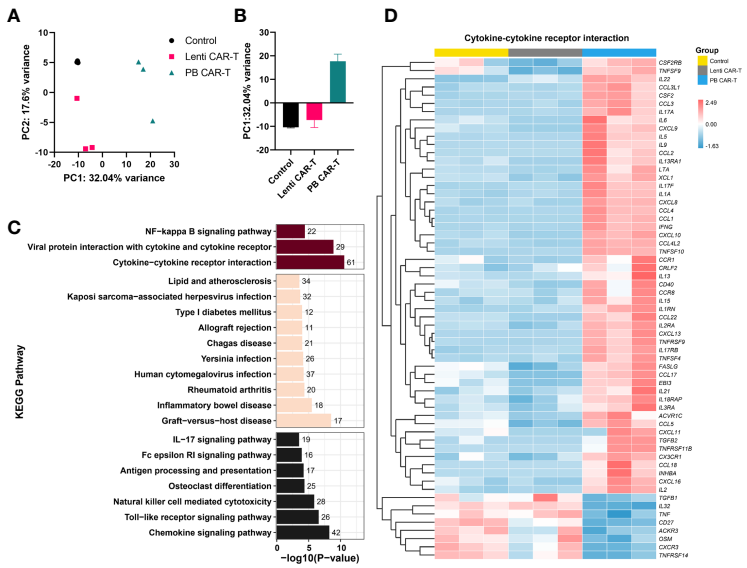

FIGURE 4
Transcriptome analysis. CAR-T cells were sorted on day 3 post-transfection and then rested for 24 hours. The total RNA of sorted CAR-T cells was analyzed using RNA-seq. **(A, B)** PCA analysis of control T cells, PB CAR-T cells, and Lenti CAR-T cells (n =3). **(C)** Kyoto Encyclopedia of Genes and Genomes (KEGG) pathway analysis (PB CAR-T cells *vs.* Lenti CAR-T cells). The purplish red bar represents environmental information processing, the beige bar represents human diseases, and the black bar represents organismal systems. **(D)** Hierarchical cluster analysis for the "cytokine-cytokine receptor interaction" pathway (KEGG enrichment).

10.3389/fimmu.2023.1068625

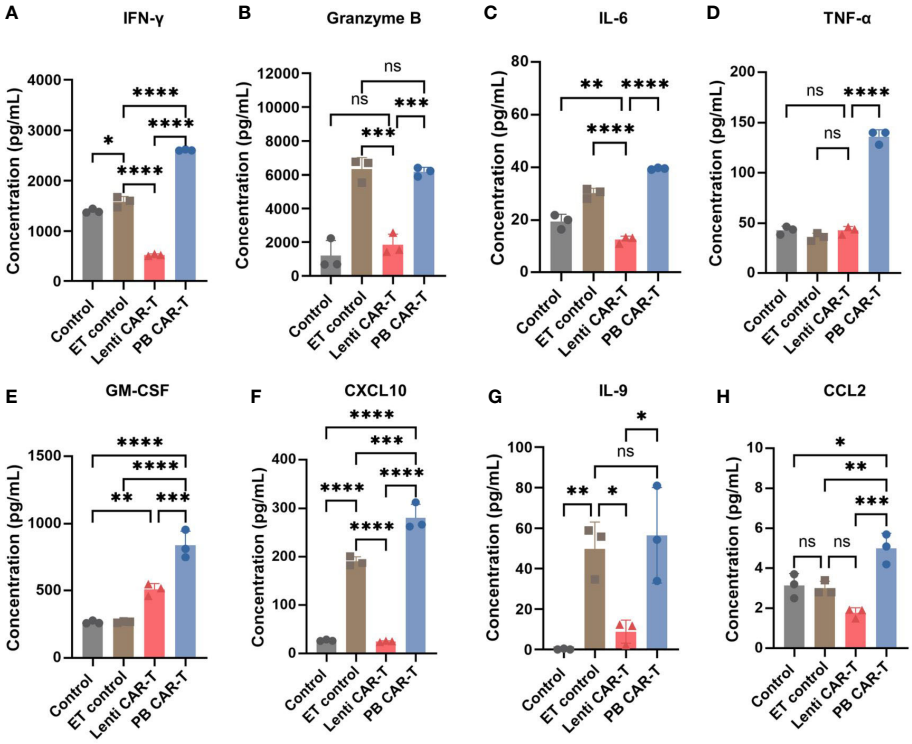

FIGURE 5
Cytokine expression profiles in control T cells, empty transfection (ET) control T cells, Lenti CAR-T cells, and PB CAR-T cells. CAR-T cells were sorted on day 3 post-transfection and rested for 24 hours. ET control T cells were transfected with an empty transposon vector using electroporation, with a total amount of 2.1 μg. Concentrations of IFN-γ **(A)**, granzyme B **(B)**, IL-6 **(C)**, TNF-α **(D)**, GM-CSF **(E)**, CXCL10 **(F)**, IL-9 **(G)**, and CCL2 **(H)** in the medium determined by ELISA (n = 3). One-way ANOVA with Tukey's multiple comparison test. *P < 0.05, **P < 0.01, ***P < 0.001, ****P < 0.0001, ns indicates not significant (P >0.05).

process, we established a control group in which T cells were electroporated with an empty vector. Higher concentrations of granzyme B (Figure 5B), CXCL10 (Figure 5F), and IL-9 (Figure 5G) were observed in this control group, indicating that the electroporation process may have partially contributed to the proinflammatory phenotype of PB CAR-T cells.

3.6 *In vitro* assessment of anti-tumor efficacy

The CD19-expressing luciferase-tagged K562 human leukemia cell line was used as target cells to assess CAR-T and T cell anti-tumor efficacy. K562 cell cytotoxicity in the presence of CAR-T and T cells was evaluated using a luciferin-based assay (31). The results showed that at 4 hours post-co-culture, PB CAR-T cells (effector) induced significantly higher K562 cell (target) cytotoxicity than Lenti CAR-T cells at all effector-to-target ratios (E/T ratios) tested, except for an E/T ratio of 1.25 (Figure 6A). However, at 24 hours post-co-culture, PB CAR-T cells induced similar levels of K562 cell cytotoxicity as Lenti CAR-T cells (Figure 6B). Subsequently, we utilized the RTCA (xCELLigence Real-Time Cell Analyzer) method to continuously monitor the cytotoxicity of CAR-T cells in real-time. The RTCA assay revealed that PB CAR-T cells exhibited a more rapid cytotoxic effect on K562 compared to Lenti CAR-T cells at an E/T ratio of 2.5 (Figure 6C), which was consistent with the results obtained from the luciferin-based assay.

To better understand the difference in the overall cytotoxicity caused by PB and Lenti CAR-T cells, the abundance of numerous cytokines was assessed before and after the cytotoxicity assay (Figures 6D–L). Prior to co-culture, PB CAR-T cells exhibited a proinflammatory phenotype with increased secretion of cytokines, as suggested by the results of RNA-seq. However, at 4 hours post co-culture, Lenti CAR-T cells higher levels of IFN-γ (Figure 6D) and GM-CSF (Figure 6L). Furthermore, at 24 hours post co-culture, Lenti CAR-T cells secreted higher amounts of all tested cytokines except for granzyme B (Figure 6E) and IL-9 (Figure 6G), which was consistent with previous work demonstrating the cytokine release syndrome elicited by Lenti CAR-T cells *in vivo* (13). The rapid and effective cytotoxicity of PB CAR-T cells may be attributed to their initial proinflammatory phenotype and subsequent substantial secretion of IL-9 upon contact with target cells. IL-9 is reportedly important in the anti-tumor immune response (32).

3.7 *In vivo* assessment of anti-tumor efficacy

To evaluate the effects of two CAR-Ts on the anti-tumor response, we conducted evaluation of their *in vivo* efficacy

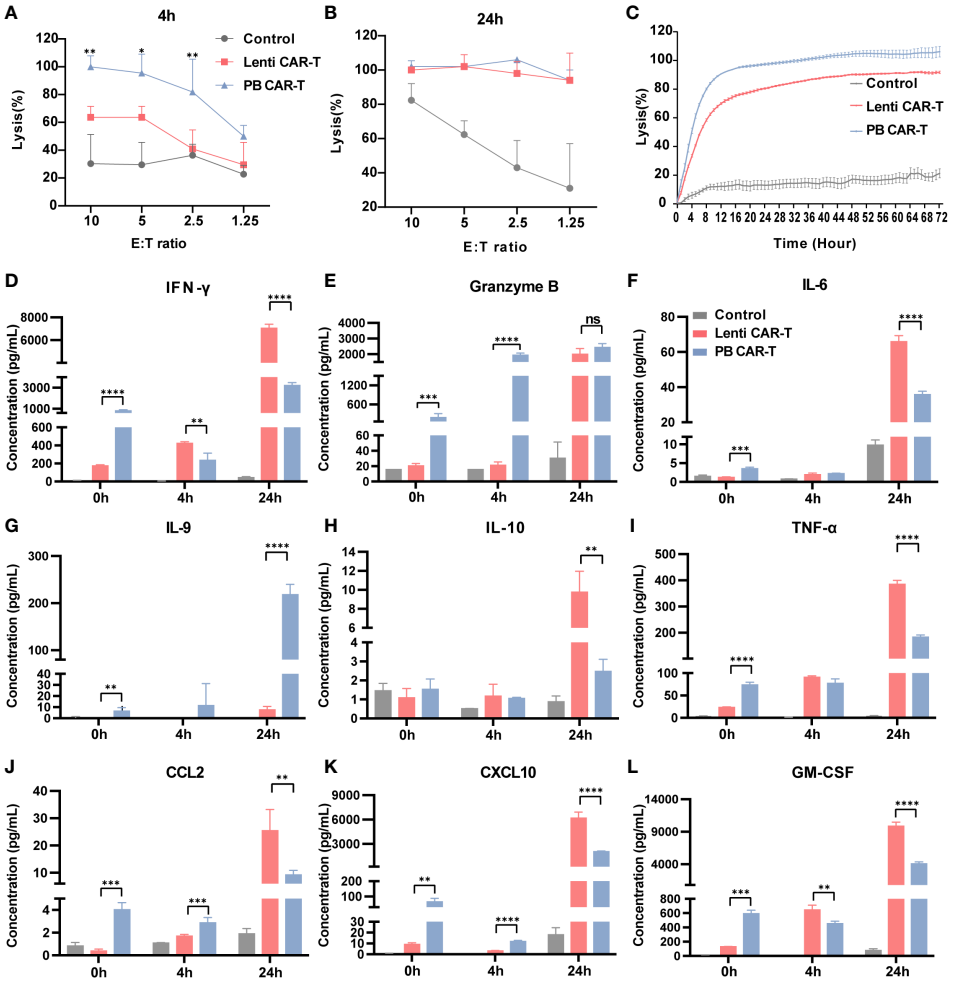

FIGURE 6
In vitro anti-tumor efficacy of PB and Lenti CAR-T cells. CAR-T cells at day 7 post-transfection were tested for anti-tumor efficacy. K562-CD19-luc cells expressing luciferase were used as target cells. **(A, B)** Anti-tumor efficacy determined at 4 hours **(A)** and 24 hours **(B)** post-co-culture. **(C)** Continuous monitoring of the anti-tumor efficacy determined based on the RTCA platform for 72 hours (E:T = 2.5:1). **(D–L)** Detection of human cytokines and chemokines. Concentrations of IFN-γ **(D)**, granzyme B **(E)**, IL-6 **(F)**, IL-9 **(G)**, IL-10 **(H)**, TNF-α **(I)**, CCL2 **(J)**, CXCL10 **(K)** and GM-CSF **(L)** in the medium before co-culture and at 4 and 24 hours post-coculture determined by Ella automated immunoassay or ELISA (n = 3). Significance was determined using an unpaired *t*'-test for **(A, B)** One-way ANOVA with Tukey's multiple comparisons test for **(D–L)**. *P < 0.05, **P < 0.01, ***P < 0.001, ****P < 0.0001, ns, not significant (P >0.05).

(Figure 7A). Specifically, we collected blood PBMC from euthanized NSG (NOD-*Prkdc*^{scid}*Il2rg*^{em1}/Smoc) mice, staining with anti-hCD19 antibody, and analyzed them using flow cytometry. Both PB and Lenti CAR-T groups exhibited a significant reduction in the percentage of CD19^{+} CD3^{-} cells, with no significant difference observed between the two groups (refer to Figure 7B). Furthermore, we quantified the concentrations of cytokines secreted by human T/CAR-T cells in the serum of mice. The results demonstrated that the concentrations of IFN-γ and IL-9 were augmented in PB CAR-T cells relative to Lenti CAR-T cells at 4 hours post-infusion (Figures 7C, D), which subsequently declined to levels below the limit of detection at 24 hours (data not shown). Conversely, all other cytokines, including IL-6, IL-10, IL-12, GM-CSF, TNF-α, CXCL10 and CCL2, were undetectable at both 4 and 24 hours. Overall, these data suggested that PB CAR-T and Lenti CAR-T exhibit comparable *in vivo* anti-tumor efficacy.

4 Discussion

Genetically modified T-cell therapy is a promising and innovative treatment for deleterious leukemia (5). Previous studies have proposed several methods of gene modification to express CARs in T cells, including the prevailing lentivirus/retrovirus and PiggyBac transposon systems (13). In this study, we conducted a rigorous comparative analysis to assess the disparities between Lenti and PB CAR-T cells. Our findings indicated that these two types of CAR-T cells were distinct in terms of their transcriptome and cytokine secretion. Specifically, the PB CAR-T cells exhibited more rapid *in vitro* anti-tumor activity compared to Lenti CAR-T cells, while demonstrating similar tumor eradication ability *in vivo* as Lenti CAR-T cells.

For our analyses, the positivity rates of CAR-T cells manufactured by lentivirus and electroporation were adjusted to a

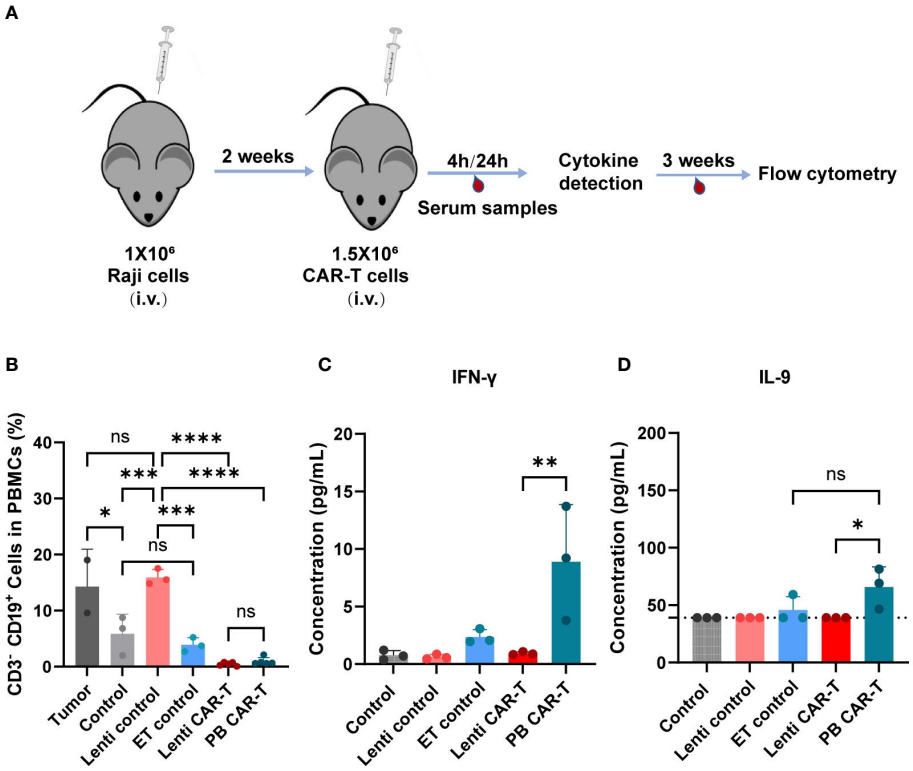

FIGURE 7
In vivo anti-tumor efficacy and cytokine production of PB and Lenti CAR-T. **(A)** Schematic of the mouse model. The Raji cells are injected into the tail vein of mice and are allowed to grow for two weeks after injection. Then 1.5 million CAR-T cells were transferred into the mice *via* tail vein injection on Day 14. After 4 hours and 24 hours, serum samples were collected for cytokine detection *via* facial vein. For three weeks, blood was collected for flow cytometry analysis. **(B)** Percentages of human $CD3^-$ $CD19^+$ cells in mouse PBMCs collected on day 21 after CAR-T infusion determined via Flow cytometry. (Tumor group n=3, *one died; Lenti control and ET control groups n=3; control group n=5, *two died; Lenti CAR-T group n=5; PB CAR-T group n=5). The concentration of human IFN-γ **(C)** and IL-9 **(D)** in serum determined at 4 hours after PB and Lenti CAR-T infusion by ELISA or Ella automated immunoassay. The limit of detection of IL-9 ELISA kits was 39.0 pg/mL and presented as dotted lines. One-way ANOVA with Tukey's multiple comparison test. $^*P < 0.05$, $^{**}P < 0.01$, $^{***}P < 0.001$, $^{****}P < 0.0001$, ns indicates not significant ($P > 0.05$). All data were presented as mean ± standard deviation.

similar level (approximately 30%) to reduce potential confounding variables. Interestingly, at similar CAR positivity rates, PB CAR-T cells exhibited significantly brighter green fluorescence in certain cells than Lenti CAR-T cells, indicating higher CAR expression, which was confirmed by the Protein L staining assay. We postulate that the distinct integration sites (21) may have contributed to the divergent CAR expression profiles. Notably, during lentiviral transfection, several viral components were co-integrated into target cells with the CAR ORF (33–35), which may have hindered the transcriptional efficiency of the target gene.

The number of CM T cells is related to the effectiveness of CAR-T cell therapy (36). CAR-T cells manufactured using the transposon system were previously reported to exhibit a CM phenotype elicited by 4-1BB co-stimulation signaling (37). Moreover, $CD4^+$ CAR-T cells were recently reported to be the dominant cells for persistent remission in leukemia patients treated with CAR-T cell therapy (38). Our data demonstrated that the proportion of $CD4^+$ CM T cell subsets remained highest among subsets after CAR transfection via both methods. For $CD4^+$ CM subsets, PB CAR-T was lower than those in control CAR-T. Although no significant difference was observed between Lenti and PB CAR-T, the mean values of $CD4^+$ CM cells in Lenti CAR-T were higher than those in PB CAR-T. In addition, the frequency of $CD8^+$ memory phenotypes did not differ. Furthermore, in total subsets, the proportion of memory phenotypes of PB CAR-T cells was the lowest among the three groups, which may imply electroporation-associated toxicity against memory phenotypes (29). Taken together, Lenti CAR-T may be more durable than PB CAR-T after infusion due to their induction of T cell memory phenotypes.

An important finding of our study is that PB CAR-T cells exhibited higher basal cytokine levels than Lenti CAR-T cells prior to co-culture with target cells. This result was further supported by our RNA-seq data, which detected elevated expression of cytokines and chemokines in PB CAR-T cells. Moreover, upon antigenic activation *in vitro*, PB CAR-T cells released lower levels of IFN-γ, IL-6, IL-10, TNF-α, CCL2, CXCL10, and GM-CSF than Lenti CAR-T cells, but demonstrated a robust release of IL-9, indicative of a distinct anti-tumor response pathway. In the *in vivo* experiments, the levels of cytokines were not as significant as those observed *in vitro*, possibly due to the lower secretion levels of cytokines that were not effectively detectable.

IL-9, a T-cell growth factor, is a member of the γ-chain-receptor cytokine family and is secreted by Th2 (T helper 2), Th9 (T helper 9), Th17 (T helper 17), and NKT (natural killer T) cells (39). IL-9 has been demonstrated to increase the longevity of Tc9 cells (40). Importantly, the IL-9 signaling pathway has been found to be particularly effective in

enhancing the anti-tumor response of CAR-T cells (41). Our data revealed that the PB transposon system upregulates IL-9 expression in T cells. Although IL-9 expression was reduced by day 7 post-transfection, it was upregulated again in PB CAR-T cells upon encountering tumor cells. The mechanisms underlying IL-9 upregulation in PB CAR-T cells remain to be elucidated.

In comparison to the safety of lentiviral/retroviral systems observed in a cohort of 308 patients (16), a recent clinical trial on PB CAR-T-cell lymphoma reported a concerning oncogenic effect of transposon gene integration system (42). In this study, we did not observe differentially expressed genes in PB CAR-T cells (versus Lenti CAR-T) that were significantly enriched in tumor-associated signaling pathways. However, a small fraction of PB CAR-T cells exhibited a strong green fluorescent signal under similar proportions of CAR positivity (Figure 1E), indicating that the number of inserted CAR copies may be high in a few PB CAR-T cells, which may increase the risk of oncogenic insertion mutagenesis. The oncogenic potential of PB CAR-T cells requires further investigation via single-cell RNA-seq or insertion mutagenesis analysis.

IL-6 is secreted by various immune and stromal cells and exerts multiple functions (43). IL-6 is considered a hub cytokine in CRS triggered by CAR-T cell therapy (30). In fact, the prognosis of CRS was improved by tocilizumab, an IL-6 receptor (IL-6R) monoclonal antibody that blocks IL-6 binding to IL-6R (44). In our study, secretion of IL-6 by PB and Lenti CAR-T cells was unchanged at 4 hours after encountering tumor cells, however, Lenti CAR-T cells released much higher levels of IL-6 into the media than PB CAR-T cells at 24 hours. These data indicate that PB CAR-T may cause less CRS in clinical applications; this conclusion is further supported by a recent report on CAR-T cells manufactured via electroporation (45).

It is important to note that the original PBMCs used to produce both CAR-T cell groups were from several donors; therefore, it will be important to further validate our findings in an expanded group of donors. Despite this limitation, these data revealed a large disparity arising from the two main manufacturing methods used to produce CAR-T cells. These findings shed new light on the effect of different production methods on the phenotypes of seemingly similar cell types and will inform the design of future cell-based therapies.

Data availability statement

The datasets presented in this study can be found in online repositories. The names of the repository/repositories and accession number(s) can be found below: NCBI Gene Expression Omnibus under the accession number GEO: GSE212072.

Ethics statement

The donors' privacy was protected and the study protocol complied with The Helsinki Declaration. All donors provided written informed consent, and this study was approved by Ethics Committees (approval number: AF/SC-08/02.258).

Author contributions

Conceived and designed the experiments: WC, XZ, JZ, and AN; analyzed the data: AN, JZ, and XH; contributed reagents/materials: ZZ, LS, JW, XL and WZ; wrote and revised the paper: AN, JZ, WC, and XZ. All authors contributed to the article and approved the submitted version.

Funding

This research was supported by the National Natural Science Foundation of China (NSFC No. 82173787).

Conflict of interest

The authors declare that the research was conducted in the absence of any commercial or financial relationships that could be construed as a potential conflict of interest.

Publisher's note

Supplementary material

The Supplementary Material for this article can be found online at: https://www.frontiersin.org/articles/10.3389/fimmu.2023.1068625/full#supplementary-material

References

1. Krause A, Guo HF, Latouche JB, Tan C, Cheung NK, Sadelain M. Antigen-dependent CD28 signaling selectively enhances survival and proliferation in genetically modified activated human primary T lymphocytes. *J Exp Med* (1998) 188(4):619–26. doi: 10.1084/jem.188.4.619

2. Philipson BI, O'Connor RS, May MJ, June CH, Albelda SM, Milone MC. 4-1BB costimulation promotes CAR T cell survival through noncanonical NF-kappaB signaling. *Sci Signal* (2020) 13(625):eaay8248. doi: 10.1126/scisignal.aay8248

3. Kalos M, Levine BL, Porter DL, Katz S, Grupp SA, Bagg A, et al. T Cells with chimeric antigen receptors have potent antitumor effects and can establish memory in patients with advanced leukemia. *Sci Transl Med* (2011) 3(95):95ra73. doi: 10.1126/scitranslmed.3002842

4. Mullard A. FDA Approves first CAR T therapy. *Nat Rev Drug Discovery* (2017) 16 (10):669. doi: 10.1038/nrd.2017.196

5. Porter DL, Hwang WT, Frey NV, Lacey SF, Shaw PA, Loren AW, et al. Chimeric antigen receptor T cells persist and induce sustained remissions in relapsed refractory

chronic lymphocytic leukemia. *Sci Transl Med* (2015) 7(303):303ra139. doi: 10.1126/scitranslmed.aac541

6. Park JH, Riviere I, Gonen M, Wang X, Senechal B, Curran KJ, et al. Long-term follow-up of CD19 CAR therapy in acute lymphoblastic leukemia. *N Engl J Med* (2018) 378(5):449–59. doi: 10.1056/NEJMoa1709919

7. Fry TJ, Shah NN, Orentas RJ, Stetler-Stevenson M, Yuan CM, Ramakrishna S, et al. CD22-targeted CAR T cells induce remission in b-ALL that is naive or resistant to CD19-targeted CAR immunotherapy. *Nat Med* (2018) 24(1):20–8. doi: 10.1038/nm.4441

8. Whittington MD, McQueen RB, Ollendorf DA, Kumar VM, Chapman RH, Tice JA, et al. Long-term survival and cost-effectiveness associated with axicabtagene ciloleucel vs chemotherapy for treatment of b-cell lymphoma. *JAMA Netw Open* (2019) 2(2):e190035. doi: 10.1001/jamanetworkopen.2019.0035

9. Neelapu SS, Tummala S, Kebriaei P, Wierda W, Gutierrez C, Locke FL, et al. Chimeric antigen receptor T-cell therapy - assessment and management of toxicities. *Nat Rev Clin Oncol* (2018) 15(1):47–62. doi: 10.1038/nrclinonc.2017.148

10. Gust J, Taraseviciute A, Turtle CJ. Neurotoxicity associated with CD19-targeted CAR-T cell therapies. *CNS Drugs* (2018) 32(12):1091–1101. doi: 10.1007/s40263-018-0582-9

11. Neelapu SS, Locke FL, Bartlett NL, Lekakis LJ, Miklos DB, Jacobson CA, et al. Axicabtagene ciloleucel CAR T-cell therapy in refractory Large b-cell lymphoma. *N Engl J Med* (2017) 377(26):2531–44. doi: 10.1056/NEJMoa1707447

12. Liu E, Marin D, Banerjee P, Macapinlac HA, Thompson P, Basar R, et al. Use of CAR-transduced natural killer cells in CD19-positive lymphoid tumors. *N Engl J Med* (2020) 382(6):545–53. doi: 10.1056/NEJMoa1910607

13. Larson RC, Maus MV. Recent advances and discoveries in the mechanisms and functions of CAR T cells. *Nat Rev Cancer.* (2021) 21(3):145–61. doi: 10.1038/s41568-020-00323-z

14. Schroder AR, Shinn P, Chen H, Berry C, Ecker JR, Bushman F. HIV-1 integration in the human genome favors active genes and local hotspots. *Cell* (2002) 110(4):521–9. doi: 10.1016/s0092-8674(02)00864-4

15. Mitchell RS, Beitzel BF, Schroder AR, Shinn P, Chen H, Berry CC, et al. Retroviral DNA integration: ASLV, HIV, and MLV show distinct target site preferences. *PloS Biol* (2004) 2(8):E234. doi: 10.1371/journal.pbio.0020234

16. Marcucci KT, Jadlowsky JK, Hwang WT, Suhoski-Davis M, Gonzalez VE, Kulikovskaya I, et al. Retroviral and lentiviral safety analysis of gene-modified T cell products and infused HIV and oncology patients. *Mol Ther* (2018) 26(1):269–79. doi: 10.1016/j.ymthe.2017.10.012

17. Lever AM. HIV RNA Packaging and lentivirus-based vectors. *Adv Pharmacol* (2000) 48:1–28. doi: 10.1016/s1054-3589(00)48002-6

18. Frankel AD, Young JA. HIV-1: fifteen proteins and an RNA. *Annu Rev Biochem* (1998) 67:1–25. doi: 10.1146/annurev.biochem.67.1.1

19. Kebriaei P, Singh H, Huls MH, Figliola MJ, Bassett R, Olivares S, et al. Phase I trials using sleeping beauty to generate CD19-specific CAR T cells. *J Clin Invest.* (2016) 126(9):3363–76. doi: 10.1172/JCI86721

20. Zhang Z, Qiu S, Zhang X, Chen W. Optimized DNA electroporation for primary human T cell engineering. *BMC Biotechnol* (2018) 18(1):4. doi: 10.1186/s12896-018-0419-0

21. Monjezi R, Miskey C, Gogishvili T, Schleef M, Schmeer M, Einsele H, et al. Enhanced CAR T-cell engineering using non-viral sleeping beauty transposition from minicircle vectors. *Leukemia* (2017) 31(1):186–194. doi: 10.1038/leu.2016.180

22. Lin Z, Liu X, Liu T, Gao H, Wang S, Zhu X, et al. Evaluation of nonviral piggyBac and lentiviral vector in functions of CD19chimeric antigen receptor T cells and their antitumor activity for CD19(+) tumor cells. *Front Immunol* (2022) 12:802705. doi: 10.3389/fimmu.2021.802705

23. Blom B, Spits H. Development of human lymphoid cells. *Annu Rev Immunol* (2006) 24:287–320. doi: 10.1146/annurev.immunol.24.021605.090612

24. Pimentel H, Bray NL, Puente S, Melsted P, Pachter L. Differential analysis of RNA-seq incorporating quantification uncertainty. *Nat Methods* (2017) 14(7):687–90. doi: 10.1038/nmeth.4324

25. He X, Xu C. PD-1: a driver or passenger of T cell exhaustion? *Mol Cell* (2020) 77 (5):930–1. doi: 10.1016/j.molcel.2020.02.013

26. Lord SJ, Rajotte RV, Korbutt GS, Bleackley RC. Granzyme b: a natural born killer. *Immunol Rev* (2003) 193:31–8. doi: 10.1034/j.1600-065x.2003.00044.x

27. Jin HT, Ahmed R, Okazaki T. Role of PD-1 in regulating T-cell immunity. *Curr Top Microbiol Immunol* (2011) 350:17–37. doi: 10.1007/82_2010_116

28. Sallusto F, Geginat J, Lanzavecchia A. Central memory and effector memory T cell subsets: function, generation, and maintenance. *Annu Rev Immunol* (2004) 22:745–63. doi: 10.1146/annurev.immunol.22.012703.104702

29. Aksoy P, Aksoy BA, Czech E, Hammerbacher J. Electroporation characteristics of human primary T cells. *bioRxiv* (2018), 466243. doi: 10.1101/466243

30. Fajgenbaum DC, June CH. Cytokine storm. *N Engl J Med* (2020) 383(23):2255–73. doi: 10.1056/NEJMra2026131

31. Brown CE, Wright CL, Naranjo A, Vishwanath RP, Chang WC, Olivares S, et al. Biophotonic cytotoxicity assay for high-throughput screening of cytolytic killing. *J Immunol Methods* (2005) 297(1-2):39–52. doi: 10.1016/j.jim.2004.11.021

32. Lu Y, Hong S, Li H, Park J, Hong B, Wang L, et al. Th9 cells promote antitumor immune responses in vivo. *J Clin Invest* (2012) 122(11):4160–71. doi: 10.1172/JCI65459

33. Perry C, Rayat A. Lentiviral vector bioprocessing. *Viruses* (2021) 13(2):268. doi: 10.3390/v13020268

34. De Guzman RN, Wu ZR, Stalling CC, Pappalardo L, Borer PN, Summers MF. Structure of the HIV-1 nucleocapsid protein bound to the SL3 psi-RNA recognition element. *Science* (1998) 279(5349):384–8. doi: 10.1126/science.279.5349.384

35. Fernandes J, Jayaraman B, Frankel A. The HIV-1 rev response element: an RNA scaffold that directs the cooperative assembly of a homo-oligomeric ribonucleoprotein complex. *RNA Biol* (2012) 9(1):6–11. doi: 10.4161/rna.9.1.18178

36. Golubovskaya V, Wu L. Different subsets of T cells, memory, effector functions, and CAR-T immunotherapy. *Cancers (Basel)* (2016) 8(3):36. doi: 10.3390/cancers8030036

37. Kawalekar OU, O'Connor RS, Fraietta JA, Guo L, McGettigan SE, Posey ADJr., et al. Distinct signaling of coreceptors regulates specific metabolism pathways and impacts memory development in CAR T cells. *Immunity* (2016) 44(2):380–90. doi: 10.1016/j.immuni.2016.01.021

38. Melenhorst JJ, Chen GM, Wang M, Porter DL, Chen C, Collins MA, et al. Decade-long leukaemia remissions with persistence of CD4(+) CAR T cells. *Nature* (2022) 602(7897):503–9. doi: 10.1038/s41586-021-04390-6

39. Noelle RJ, Nowak EC. Cellular sources and immune functions of interleukin-9. *Nat Rev Immunol* (2010) 10(10):683–7. doi: 10.1038/nri2848

40. Xiao L, Ma X, Ye L, Su P, Xiong W, Bi E, et al. IL-9/STAT3/fatty acid oxidation-mediated lipid peroxidation contributes to Tc9 cell longevity and enhanced antitumor activity. *J Clin Invest* (2022) 132(7):e153247. doi: 10.1172/JCI153247

41. Kalbasi A, Siurala M, Su LL, Tariveranmoshabad M, Picton LK, Ravikumar P, et al. Potentiating adoptive cell therapy using synthetic IL-9 receptors. *Nature* (2022) 607(7918):360–5. doi: 10.1038/s41586-022-04801-2

42. Bishop DC, Clancy LE, Simms R, Burgess J, Mathew G, Moezzi L, et al. Development of CAR T-cell lymphoma in 2 of 10 patients effectively treated with piggyBac-modified CD19 CAR T cells. *Blood* (2021) 138(16):1504–09. doi: 10.1182/blood.2021010813

43. Copaescu A, Smibert O, Gibson A, Phillips EJ, Trubiano JA. The role of IL-6 and other mediators in the cytokine storm associated with SARS-CoV-2 infection. *J Allergy Clin Immunol* (2020) 146(3):518–34.e1. doi: 10.1016/j.jaci.2020.07.001

44. Le RQ, Li L, Yuan W, Shord SS, Nie L, Habtemariam BA, et al. FDA Approval summary: tocilizumab for treatment of chimeric antigen receptor T cell-induced severe or life-threatening cytokine release syndrome. *Oncologist* (2018) 23(8):943–7. doi: 10.1634/theoncologist.2018-0028

45. Zhang J, Hu Y, Yang J, Li W, Zhang M, Wang Q, et al. Non-viral, specifically targeted CAR-T cells achieve high safety and efficacy in b-NHL. *Nature* (2022) 609:369–374. doi: 10.1038/s41586-022-05140-y

frontiers | Frontiers in Oncology

TYPE Case Report
PUBLISHED 22 May 2023
DOI 10.3389/fonc.2023.1149450

OPEN ACCESS

EDITED BY
Hakim Echchannaoui,
Johannes Gutenberg University
Mainz, Germany

REVIEWED BY
Reona Leo Sakemura,
Mayo Clinic, United States
Yang Su,
Xuzhou Medical University, China
Beate Hauptrock,
Johannes Gutenberg University
Mainz, Germany

*CORRESPONDENCE
Sebastian Zundler
Sebastian.zundler@uk-erlangen.de

RECEIVED 21 January 2023
ACCEPTED 10 May 2023
PUBLISHED 22 May 2023

CITATION
Zundler S, Vitali F, Kharboutli S, Völkl S, Polifka I, Mackensen A, Atreya R, Neurath MF and Mougiakakos D (2023) Case Report: IBD-like colitis following CAR T cell therapy for diffuse large B cell lymphoma.
Front. Oncol. 13:1149450.
doi: 10.3389/fonc.2023.1149450

Case Report: IBD-like colitis following CAR T cell therapy for diffuse large B cell lymphoma

Sebastian Zundler[1,2*], Francesco Vitali[1], Soraya Kharboutli[3], Simon Völkl[3], Iris Polifka[4], Andreas Mackensen[2,3], Raja Atreya[1,2], Markus F. Neurath[1,2] and Dimitrios Mougiakakos[2,3,5]

[1]Department of Medicine 1 – Gastroenterology, Pneumology, Endocrinology, University Hospital Erlangen, Erlangen, Germany, [2]University Hospital Erlangen, Deutsches Zentrum Immuntherapie, Erlangen, Germany, [3]Department of Medicine 5 – Hematology/Oncology, University Hospital Erlangen, Erlangen, Germany, [4]Institute of Pathology, University Hospital Erlangen, Erlangen, Germany, [5]Department for Hematology and Oncology, University Hospital Magdeburg, Magdeburg, Germany

Chimeric antigen receptor (CAR) T cell therapy has become a new mainstay in the treatment of several hematologic malignancies, but the spectrum of associated complications is still incompletely defined. Here, we report the case of a 70-year-old female patient treated with tisagenlecleucel for diffuse large B cell lymphoma (DLBCL), who developed chronic diarrhea with characteristics of inflammatory bowel disease (IBD)-like colitis. CAR T cells were substantially enriched in the colon lamina propria and other diagnoses were ruled out. Thus, we conclude that IBD-like colitis in this patient was associated to CAR T cell therapy and needs to be considered as a rare potential complication.

KEYWORDS

diffuse large B cell lymphoma, inflammatory bowel disease (IBD), tisagenlecleucel, case report, CAR T cells

Case report

Chimeric antigen receptor (CAR) T cell therapy has become a new mainstay in the treatment of several hematologic malignancies (1). However, the spectrum of complications associated with CAR T cell therapy is still incompletely defined (2).

We describe the case of a 70-year-old female patient of Turkish origin with a past history of diffuse large B cell lymphoma (DLBCL) treated with a commercial anti-CD19 CAR T-cell product (i.e., tisagenlecleucel), who presented with chronic diarrhea.

Initially, the patient had been diagnosed with follicular lymphoma in 2007 and received chemotherapy with R-CHOP, R-Bendamustin, R-Gemcitabin/Oxaliplatin and idelalisib over the following years. Transformation into an aggressive B cell non-Hodgkin lymphoma was first noted in 2014 and treated with chemotherapy combining ifosfamid, carboplatin and etoposide followed by high-dose chemotherapy (HDT) with autologous stem cell transplantation (ASCT), R-Revlimid and radiation.

In September 2020, imaging noted a relapse with vertebral and paravertebral involvement. Histology from a punch biopsy as well as on tissue obtained during neurosurgical intervention led to the diagnosis of DLBCL and CAR T cell therapy was performed in November 2020.

Three months after CAR T-cell therapy and being in complete metabolic remission (CMR), the patient reported the development of up to 20 loose stools per day. Over the following weeks, symptoms persisted, and the patient noticed unintentional weight loss. Stool cultures for pathogenic bacteria were repetitiously negative. Similarly, norovirus, astrovirus, and cytomegalovirus infection were ruled out. On ultrasound, we noted a discontinuous pancolitis with bowel wall thickening and hyperemia (Figure 1A). A subsequent colonoscopy confirmed discontinuous pancolitis with redness, swelling, fibrin exudates, and erosions (Figure 1B). Previous FDG-PET scan had not shown any metabolic activity in the colon and, accordingly, histopathologic evaluation ruled out DLBCL infiltration. However, it revealed signs of chronic inflammation of the colon mucosa with crypt distortions and some crypt abscesses (Figure 1C). The patient did not take any non-steroidal anti-inflammatory drugs and there was no indication of atherosclerosis.

Together, these diagnostic results demonstrated presence of an inflammatory bowel disease (IBD). Yet, given the disease and patient history, neither Crohn's disease nor ulcerative colitis were likely.

Further work-up of colon biopsies with immunohistochemistry for CD3 demonstrated a marked enrichment of T cells in the intestinal lamina propria (Figure 2A). Flow cytometry of CAR^+ and CAR^- T cells in the peripheral blood showed that a subset of the CAR T cells expresses the gut-homing receptor α4β7 and that α4β7-expressing cells are enriched within CAR^+ compared to CAR^- T cells (Figure 2B, Supplementary Figure 1). Consistently, we observed a substantial enrichment of CAR T cells in the colon lamina propria (Figure 2C).

A course of prednisolone starting with 50 mg per day was initiated (iv over the first ten days, then orally) and tapered over seven weeks, but no symptomatic improvement was seen. The patient was subsequently scheduled for treatment with the anti-α4β7 integrin antibody vedolizumab. However, this was not initiated, since ultimately before the first planned application and more than four months after symptom onset, diarrhea spontaneously and gradually resolved, and no signs of colitis were detected on follow-up ultrasound. There was no correlation of diarrhea with CAR^+ T cell frequencies in the peripheral blood (Supplementary Figure 2) and, interestingly, resolution occurred following a two-week course of antibiotic treatment with empiric levofloxacin plus vancomycin followed by linezolid for bacteremia due to central venous line infection.

Discussion

We conclude that IBD-like colitis in this patient was triggered by CAR T cells. CAR T cell therapy has revolutionized the treatment of several hematologic malignancies (4–6). Tisagenlecleucel comprises expanded autologous T cells engineered with a CAR to target CD19. Here, it seems that the *ex vivo* expansion of certain gut-homing T cell clones during CAR T cell production led to the recruitment of large numbers of these cells to the large bowel following adoptive transfer. We speculate that their interaction with the intestinal microbiome *via* the original T cell receptor may have triggered local expansion and IBD-like inflammation in this patient (7). Eventually, resolution of colitis following an episode of antibiotic therapy even highlights the possibility that a change in the intestinal microbiota might have limited further stimulation of these intestinal CAR T cell clones.

The trials leading to approval of anti-CD19 CAR T cells were relatively small (6) and, thus, previously unknown adverse events are continuing to emerge. The most common specific side effects of CAR T cell therapy described to date are the cytokine release syndrome (CRS) and the immune effector cell associated neurotoxicity syndrome (ICANS) (8, 9). CRS is triggered by activation of CAR T cells following target antigen recognition, which in turn stimulate (by e.g., abundant GM-CSF, IFN-γ or TNF) the myeloid compartment that releases high levels of IL-6. This activation of myeloid cells can aggravate to macrophage activation syndrome (MAS) or hemophagocytic lymphohistiocytosis (HLH), which are very severe pathologies. Consequently, first-line therapy consists of blocking the IL-6 receptor. In case of therapy failure, primarily steroids are used, but also antibodies against TNF, IL-1 or tyrosine kinase inhibitors can be used, especially in clinically frustrating situations. The

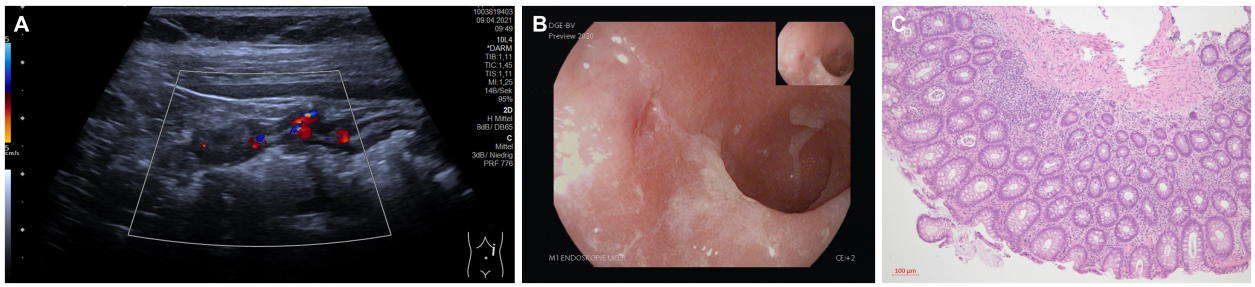

FIGURE 1
(A) Findings on bowel ultrasound (proximal descending colon). **(B)** Findings on colonoscopy (sigmoid colon) **(C)** Findings on histopathology (H/E staining, 10x magnification).

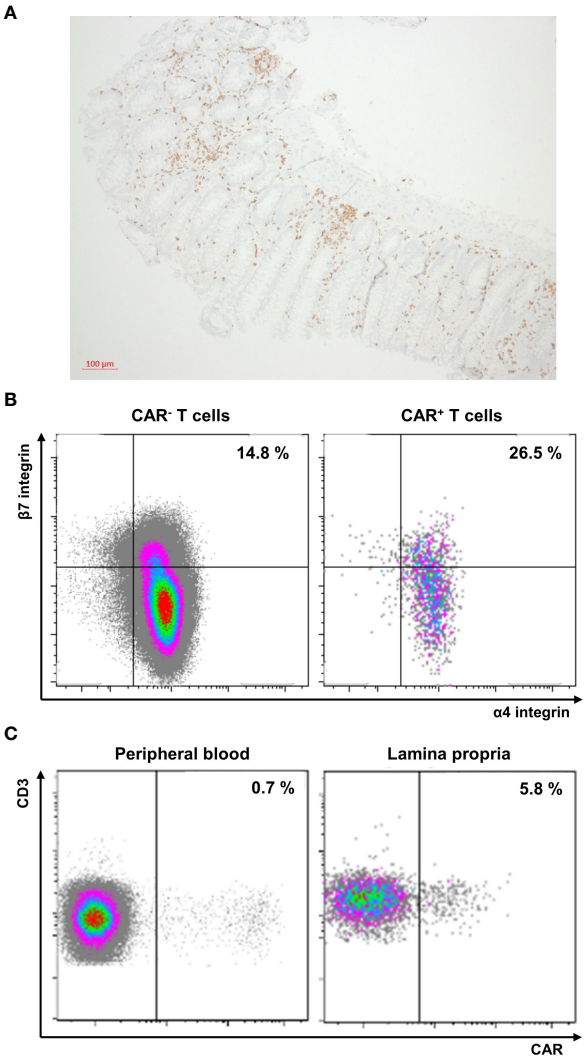

FIGURE 2
(A) Immunohistochemistry of a colon biopsy for CD3 (10x magnification). **(B)** Flow cytometry of peripheral blood T cells expressing the chimeric antigen receptor (CAR) or not. The frequency of $\alpha4^+\beta7^+$ cells is indicated. CAR T cells were analyzed as previously described (3). Briefly, peripheral blood mononuclear cells were isolated by density centrifugation, stained with CD19 CAR detection reagent, washed twice and stained with Biotin antibody (both Miltenyi Biotec, Bergisch-Gladbach, Germany), 7-AAD (BD Biosciences) and a standardized panel of antibodies against CD45, CD3, CD4, CD8 (all BD Biosciences, Heidelberg, Germany), α4 integrin and β7 integrin (both Biolegend). Gating strategies are depicted in the Supplementary Figure 1. Data were acquired on a LSRFortessa (BD Biosciences) and analyzed by Kaluza software v2.1 (Beckman Coulter, Krefeld, Germany). **(C)** Flow cytometry of peripheral blood (left) and lamina propria (right) T cells. The frequency of CAR^+ cells is indicated.

pathophysiology of ICANS is less well understood. It can take place with or without a CRS and the clinical picture is also very inhomogeneous. Vascular permeability, endothelial disruption, and glial cell injury appear to be involved in the clinical picture, and the primary treatment of isolated ICANS is steroid therapy. Another bothersome side effect, which only became apparent as the number of CAR T cell-treated patients increased, was prolonged hematotoxicity. The cause of this phenomenon is not conclusively understood, but an inflammatory milieu appears to be an important trigger (10).

These side effects are in significant part due to overactivation of CAR T cells. Many concepts are being evaluated in this regard, ranging from the preventive administration of IL-6 receptor antagonists to the genetic modification of CAR T cells. Here, the installation of "off-switches", the better adjustment of the signal strength by modification of the affinity to the target antigen or the costimulatory domain and also the suppression of cytokine release are conceivable (11).

Collectively, these adverse events are in one or another way linked to the function of the CAR T cells. However, that also the original T cell receptor (TCR) of the expanded clonotypes might cause side effects has not been acknowledged so far. Such a risk could be avoided by genetic removal of the endogenous TCR as it already occurs during generation of allogeneic CAR T cells (12). However, it is important to consider here that the endogenous TCR also seems to be important for the persistence of CAR T cells (13). Overall, we consider the probability of transduction of T cells carrying an autoreactive TCR with the CAR construct to be very low. However, it cannot be ruled out and should at least be considered, especially in cases of organ-specific complications (beyond generalized inflammation).

In conclusion, this case is the first to report IBD-like CAR T cell-associated colitis following therapy with tisagenlecleucel. Moreover, while a previous report described similar symptoms following therapy with axicabtagene ciloleucel (14), it is also the first to directly demonstrate the presence of CAR T cells in the inflamed intestinal mucosa.

Thus, IBD-like colitis seems to be a rare side effect that should be considered in the differential diagnosis in patients with chronic colitis following CAR T cell therapy.

Data availability statement

The original contributions presented in the study are included in the article/Supplementary Material. Further inquiries can be directed to the corresponding author.

Ethics statement

Ethical review and approval was not required for the study on human participants in accordance with the local legislation and institutional requirements. The patients/participants provided their written informed consent to participate in this study. Written informed consent was obtained from the participant/patient(s) for the publication of this case report.

Author contributions

SZ: ultrasound, endoscopy, data integration and analysis, drafting of the manuscript. FV: endoscopy. SK: outpatient care. SV: flow cytometry. IP: histology. AM: supervision of diagnostic

and therapeutic management. RA: IBD consultation. MN: supervision of diagnostic and therapeutic management. DM: outpatient care, data integration and analysis. All authors contributed to the article and approved the submitted version.

Conflict of interest

The authors declare that the research was conducted in the absence of any commercial or financial relationships that could be construed as a potential conflict of interest.

Publisher's note

All claims expressed in this article are solely those of the authors and do not necessarily represent those of their affiliated organizations, or those of the publisher, the editors and the reviewers. Any product that may be evaluated in this article, or claim that may be made by its manufacturer, is not guaranteed or endorsed by the publisher.

Supplementary material

The Supplementary Material for this article can be found online at: https://www.frontiersin.org/articles/10.3389/fonc.2023.1149450/full#supplementary-material

SUPPLEMENTARY FIGURE 1
Gating strategy for CAR detection: Time parameter was used to monitor instrument stability, doublets were excluded by FSC-H/FSC-A, $CD45^+$ events were gated, lymphocytes were determined by FSC-A/SSC-A, viable T cells were gated by $CD3^+$ and $7\text{-}AAD^-$, and further subdivided in CAR^+ and CAR^- T cells.

SUPPLEMENTARY FIGURE 2
Time course of frequencies (left panel) and numbers (right panel) of CAR^+ T cells in the peripheral blood of the patient as determined by flow cytometry.

References

1. Singh AK, McGuirk JP. CAR T cells: continuation in a revolution of immunotherapy. *Lancet Oncol* (2020) 21:e168–78. doi: 10.1016/S1470-2045(19)30823-X

2. Penack O, Koenecke C. Complications after CD19+ CAR T-cell therapy. *Cancers (Basel)* (2020) 12:E3445. doi: 10.3390/cancers12113445

3. Mackensen A, Müller F, Mougiakakos D, Böltz S, Wilhelm A, Aigner M, et al. Anti-CD19 CAR T cell therapy for refractory systemic lupus erythematosus. *Nat Med* (2022) 28:2124–32. doi: 10.1038/s41591-022-02017-5

4. Bishop MR, Dickinson M, Purtill D, Barba P, Santoro A, Hamad N, et al. Second-line tisagenlecleucel or standard care in aggressive b-cell lymphoma. *New Engl J Med* (2022) 386:629–39. doi: 10.1056/NEJMoa2116596

5. Maude SL, Laetsch TW, Buechner J, Rives S, Boyer M, Bittencourt H, et al. Tisagenlecleucel in children and young adults with b-cell lymphoblastic leukemia. *New Engl J Med* (2018) 378:439–48. doi: 10.1056/NEJMoa1709866

6. Schuster SJ, Bishop MR, Tam CS, Waller EK, Borchmann P, McGuirk JP, et al. Tisagenlecleucel in adult relapsed or refractory diffuse Large b-cell lymphoma. *New Engl J Med* (2019) 380:45–56. doi: 10.1056/NEJMoa1804980

7. Zheng D, Liwinski T, Elinav E. Interaction between microbiota and immunity in health and disease. *Cell Res* (2020) 30:492–506. doi: 10.1038/s41422-020-0332-7

8. Morris EC, Neelapu SS, Giavridis T, Sadelain M. Cytokine release syndrome and associated neurotoxicity in cancer immunotherapy. *Nat Rev Immunol* (2022) 22:85–96. doi: 10.1038/s41577-021-00547-6

9. Bachy E, Le Gouill S, Di Blasi R, Sesques P, Manson G, Cartron G, et al. A real-world comparison of tisagenlecleucel and axicabtagene ciloleucel CAR T cells in relapsed or refractory diffuse large b cell lymphoma. *Nat Med* (2022) 28:2145–54. doi: 10.1038/s41591-022-01969-y

10. Rejeski K, Perez A, Sesques P, Hoster E, Berger C, Jentzsch L, et al. CAR-HEMATOTOX: a model for CAR t-cell–related hematologic toxicity in relapsed/refractory large b-cell lymphoma. *Blood* (2021) 138:2499–513. doi: 10.1182/blood.2020010543

11. Sterner RC, Sterner RM. CAR-T cell therapy: current limitations and potential strategies. *Blood Cancer J* (2021) 11:1–11. doi: 10.1038/s41408-021-00459-7

12. Depil S, Duchateau P, Grupp SA, Mufti G, Poirot L. 'Off-the-shelf' allogeneic CAR T cells: development and challenges. *Nat Rev Drug Discov* (2020) 19:185–99. doi: 10.1038/s41573-019-0051-2

13. Stenger D, Stief TA, Kaeuferle T, Willier S, Rataj F, Schober K, et al. Endogenous TCR promotes *in vivo* persistence of CD19-CAR-T cells compared to a CRISPR/Cas9-mediated TCR knockout CAR. *Blood* (2020) 136:1407–18. doi: 10.1182/blood.2020005185

14. Hashim A, Patten PEM, Kuhnl A, Ooft ML, Hayee B, Sanderson R. Colitis after CAR T-cell therapy for refractory Large b-cell lymphoma responds to anti-integrin therapy. *Inflamm Bowel Dis* (2021) 27:e45–6. doi: 10.1093/ibd/izaa320

frontiers | Frontiers in Immunology

TYPE Original Research
PUBLISHED 27 June 2023
DOI 10.3389/fimmu.2023.1139482

OPEN ACCESS

EDITED BY
Shao-An Xue,
University College London,
United Kingdom

REVIEWED BY
Nina Worel,
Medical University of Vienna, Austria
Magdiel Pérez-Cruz,
Stanford University, United States

*CORRESPONDENCE
Li Yu
ndefy02021@ncu.edu.cn;
zengyulii@126.com

RECEIVED 07 January 2023
ACCEPTED 26 May 2023
PUBLISHED 27 June 2023

CITATION
Yu T, Luo C, Zhang H, Tan Y and Yu L (2023) Cord blood-derived CD19-specific chimeric antigen receptor T cells: an off-the-shelf promising therapeutic option for treatment of diffuse large B-cell lymphoma.
Front. Immunol. 14:1139482.
doi: 10.3389/fimmu.2023.1139482

Cord blood-derived CD19-specific chimeric antigen receptor T cells: an off-the-shelf promising therapeutic option for treatment of diffuse large B-cell lymphoma

Tiantian Yu[1,2], Cancan Luo[1], Huihui Zhang[3], Yi Tan[3] and Li Yu[1]*

[1]Department of Hematology, The Second Affiliated Hospital of Nanchang University, Nanchang, Jiangxi, China, [2]Division of Hematopathology and Department of Pathology, Duke University Medical Center, Durham, NC, United States, [3]R&D Department, Qilu Cell Therapy Technology Co., Ltd., Jinan, Shandong, China

Purpose: Autologous chimeric antigen receptor (CAR) T cell therapy is one of the most significant breakthroughs in hematological malignancies. However, a three-week manufacturing cycle and ineffective T cell dysfunction in some patients hinder the widespread application of auto-CAR T cell therapy. Studies suggest that cord blood (CB), with its unique biological properties, could be an optimal source for CAR T cells, providing a product with 'off-the-shelf' availability. Therefore, exploring the potential of CB as an immunotherapeutic agent is essential for understanding and promoting the further use of CAR T cell therapy.

Experimental design: We used CB to generate CB-derived CD19-targeting CAR T (CB CD19-CAR T) cells. We assessed the anti-tumor capacity of CB CD19-CAR T cells to kill diffuse large B cell lymphoma (DLBCL) *in vitro* and *in vivo*.

Results: CB CD19-CAR T cells showed the target-specific killing of CD19+ T cell lymphoma cell line BV173 and CD19+ DLBCL cell line SUDHL-4, activated various effector functions, and inhibited tumor progression in a mouse (BALB/c nude) model. However, some exhaustion-associated genes were involved in off-tumor cytotoxicity towards activated lymphocytes. Gene expression profiles confirmed increased chemokines/chemokine receptors and exhaustion genes in CB CD19-CAR T cells upon tumor stimulation compared to CB T cells. They indicated inherent changes in the associated signaling pathways in the constructed CB CAR T cells and targeted tumor processes.

Conclusion: CB CD19-CAR T cells represent a promising therapeutic strategy for treating DLBCL. The unique biological properties and high availability of CB CD19-CAR T cells make this approach feasible.

KEYWORDS

cancer immunotherapy, chimeric antigen receptor T cells, CD19, cord blood, diffuse large B-cell lymphoma

Introduction

One of the developmental milestones in immunotherapy of hematologic malignancies is chimeric antigen receptor (CAR) T cell therapy (1). Genetically engineered T cells expressing CARs can specifically target tumor cells (2). CAR is a fusion protein consisting of an extracellular domain binding target antigen and linked to an intracellular signaling domain. First-generation CARs were designed using only the CD3ζ intracellular signaling domain of the TCR/CD3 complex. Second- and third-generation CARs contain costimulatory molecules fused to CD3ζ, such as CD28 and/or 4-1BB, which leads to enhanced proliferation, durable activity, cytokine secretion, apoptotic resistance, and *in vivo* persistence (2). Currently, the Food and Drug Administration has approved the use of four CAR T programs as third-line therapy of large B cell lymphoma (LBCL): BREYANZI (lisocabtagene maraleucel) (3), Novartis's KYMRIAH (tisagenlecleucel) (4), Gilead's YESCARTA (axicabtagene ciloleucel) (5), and Gilead's TECARTUS (brexucabtagene autoleucel) (6) and second-line therapy of LBCL: YESCARTA (7). The overall response rate has been observed to be as high as 73% with 54% complete response (CR) rate (8). With this clinical success, CAR T cells have revolutionized the treatment of relapsed/refractory (R/R) LBCL.

Use of autologous CAR T (auto-CAR T) cells targeting CD19 has led to outstanding data for patients with R/R LBCL (9). However, following leukapheresis, auto-CAR T cell engineering is a bespoke fabrication procedures for all patients, leading to certain well-known shortcomings, such as high out-of-pocket payments and prolonged wait time. Some patients may show disease progression or may lose eligibility for treatment-related complications over the waiting period, causing delayed or failed availability of auto-CAR T cell therapy (10). Moreover, auto-CAR T cells may be ineffective owing to T cell dysfunction, wherein immunosuppression receptors are expressed (11). The functional characteristics of auto-CAR T cells are inversely affected by the previous accumulation effects of chemotherapy (12). For these reasons, some patients fail to receive autologous T cells for producing CAR T cell products (13). Finally, the cost of this auto-CAR T cell therapeutic approach remains high and it is not readily available for all patients, which is a challenge for healthcare systems (14).

The 'off-the-shelf' allogeneic CAR T (allo-CAR T) cells from healthy donors with simplified and standardized manufacturing are expected to address these problems. Allo-CAR T cells host several prospective advantages, for example lower and affordable costs, owing to the application of scaled manufacturing processes and the capacity to generate multiple CAR T cells from a single donor (15). Allo-CAR T cells with pre-prepared and cryopreserved features can be taken as needed, making therapy available instantly for patients (15). In addition, a crucial difference is that allogeneic cell manufacturing involves a batch of products, which can be used if repetition is necessary. In contrast, a collection of autologous cells can only be used to produce a single-cell product. The 'off-the-shelf' allo-CAR T cells also can combinate with antibody targeting co-inhibitory molecule (16). Clinical studies have shown that donor-derived CAR T cells exhibit effective expansion in patients with acute lymphoblastic leukemia (ALL), achieving a high CR and controllable safety (17). However, allogeneic approaches suffer from two significant problems. First, allogeneic T cells may lead to life-threatening graft-versus-host disease (GVHD). Second, the host immune system may rapidly recognize and eradicate allogeneic T cells, thereby limiting their anti-tumor activity (18).

Allo-CAR T cells are primarily derived from peripheral blood mononuclear cells (PBMCs) and not often from cord blood (CB). CB transplantation has been successfully used to cure hematologic malignancies in recent decades, owing to decreased graft failure rates and transplantation-related mortality. Research indicates that the exceptional biological characteristics of CB cells may result in improved anti-cancer efficacy. Therefore, CB could be an ideal option for immunotherapy, offering products that are readily accessible 'off-the-shelf' (19). CB-derived CAR-NK cell therapy has been successfully used to treat hematologic malignancies. 73% (8/11) of patients responded to treatment with CB-derived CARNK cells without developing major toxic effects (20). Through genetic manipulation and stimulation of costimulatory molecules, the formerly naïve CB T-cell has been directed to differentiate into effector T cells (21). In a mouse model of ALL, CB-derived CAR T cells show a higher naïve T cells proportion and better tumor growth inhibition than PB-derived CAR T cells from R/R ALL patients (22). However, the number of clinical trials using CB-derived CAR T cells products is limited. Thus, we generated CB-derived CD19-targeting CAR T cells and assessed the anti-tumor activity of CB CD19-CAR T cells in diffuse large B cell lymphoma (DLBCL).

Materials and methods

Cell lines, cell culture, and animal experiments

SUDHL-4, DB, BV173, and K562 cells were obtained from the Stem Cell Bank of the Chinese Academy of Sciences. All cell lines were cultured in RPMI-1640 medium supplemented with 10% fetal bovine serum (Gibco, Billings, MT, USA). All cell lines were authenticated by Short Tandem Repeat profiling and regularly tested negative for mycoplasma contamination.

This study used male BALB/c nude (BALB/c-nu) mice aged 5-6 weeks, purchased from Hunan Slake Jingda Experimental Co., Ltd. Ethical approval was received from the Medical Research Ethics Committee of the Second Affiliated Hospital of Nanchang University, and written informed consent was obtained. A total of 1×10^6 SUDHL-4 cells suspended in a mixture of 100 µL Matrigel and PBS were subcutaneously injected into the backs of BALB/c-nu immunodeficient mice. Definition tumor engraftment at day 9, mice were then randomly divided and received CB CD19-CAR T cells in treatment groups and CB T cells in control groups at day 10, and tumor measurement was monitored every 3 days (n=7 per group). After experimental observation, the mice were euthanized following the painless cervical dislocation, and their tumors were collected for subsequent analyses.

CD19-CAR construct design and lentiviral vector production

The construct of generating the CD19 CAR lentiviral was performed based on the methods previously published in a patent (CN 108753774 B). The scFv (VL-linker-VH) sequence of CD19 CAR was encoded using synthetic DNA technology (GENEWIZ, China). Next, the CAR was subcloned into a second generation with a 4-1BB costimulatory domain. A truncated version of the CD19 CAR was created by deleting the cytoplasmic domains. 293T cells transfected with packaging plasmids and the scFv vector, including CAR construct, generate lentiviruses products. The viral supernatant was harvested after 48–72h, concentrated and stored at −196°C until further use.

T-cell isolation, culture, and transduction

According to the manufacturer's instructions, we isolated CD3 + T cells from fresh cord blood by CD3 positive selection microbeads (Miltenyi Biotech, Germany). For activating the T cells, we resuspended the isolated CD3+ T cells (1×10^6 cells/ml) in X-VIVO 15 medium (Thermo Fisher Scientific, Waltham, MA, USA) supplemented with 5% human AB serum (Thermo Fisher Scientific) and 200 U/mL recombinant human IL-2 (PeproTech, USA) at 37°C in 5% CO_2. Sterile, non-tissue-culture-treated 24-well plates were coated with Retronectin (Thermo Fisher Scientific) at 6 μg/cm^2 and left to stand overnight at 37°C in 5% CO_2. Next, the lentivirus supernatant was transferred to plates, and then T cells activated using recombinant human interleukin-2 (250 U/mL) were added, followed by incubation at 37°C for 24h after centrifugation. The medium was changed 24h later and every other day afterwards.

Cytotoxicity and multiplex cytokine assay

All anti-human antibodies, including CD45RA-APC (Cat: 550855), CD3-FITC (Cat: 555339), CD4-APC-Cy7 (Cat: 557871), CD8-PerPCy5.5 (Cat: 560662), CCR7-PE (Cat: 552176), CD27-PE-Cy7 (Cat: 560609), CD28-BV711 (Cat: 563131), Fixable Viability Stain (FVS) (Cat: 562247), PD-1-BV421 (Cat: 562584), and TIM-3-BV605 (Cat: 747961), were purchased from BD Pharmingen (BD Biosciences, Franklin Lakes, NJ, USA). Tumor cells were labeled with 2 μM intracellular tracing reagent carboxyfluorescein succinimidyl ester (CFSE) (Invitrogen, Waltham, MA, USA), and dead cells were marked with FVS. All flow cytometric analyses were performed using a BD FACSCanto (BD Biosciences) and analyzed with FlowJo Version 10 (Tree Star, Ashland, OR, USA). The capacity of CB CD19-CAR T cells recognizing and killing target cells was evaluated by analyzing the percentage of CFSE-labelled target cells after coculturing for 24 h at different effector: target (E: T) ratios of 1:1, 2:1, 5:1, 10:1. Supernatants were harvested after 48 h, and multiple cytokines (IL-2, IL-4, IL-6, IL-10, TNF-α, and IFN-γ) were detected using the BD Cytometric Bead Array (CBA) Human Th1/Th2 Cytokine Kit (BD Pharmingen) by flow cytometry.

RNA sequencing analysis

CB T and CB CD19-CAR T cells were collected (three biological replicates) as samples for RNA-seq analysis. This RNA-seq was also used to analyze CB CD19-CAR T cells before and after co-culture with SUDHL-4 cells an E: T ratio of 1:1 for 48h. cDNA library construction, library purification, and transcriptome sequencing were executed using the DNBseq platform according to the instructions provided by Kindstar Global Company (www.kindstar.com.cn). For RNA-seq data, the gene expression levels were quantified in fragments per kb of exon model per million mapped reads exon model. The differentially expressed genes (DEGs) were analyzed using EdgeR software and the significance was adjusted *P*-value of <0.05 and absolute $\log^2$ (absolute ratio value) ≥ 1.

Statistical analyses

Statistical analyses were executed using GraphPad Prism 8.0 (GraphPad Software). Two-tailed Student's *t*-test was used to compare two groups to identify significant differences. A two-way ANOVA with Tukey's multiple comparison test was used for three and more groups. For experiments in the animal tumor model, two-way ANOVA was used to analyze tumor volume and weight. Experimental data were collected from a minimum of three independent experiments for each analysis. Data are presented as the mean ± standard error of means (SEM), and statistical significance was set at $P < 0.05$.

Data availability

The data generated in this study are available upon request from the corresponding author. Data were generated by the authors and included in the article

Results

Generation and characterization of CB CD19-CAR T cells

We generated a CD19scFv-based CAR construct with a 4-1BB costimulatory domain and a CD3ζ signaling domain (Figures 1A, B). CB T cells without CD19 CAR transduction were used as control. Activated CB T cells were transfected with lentiviral vectors, with consequential expression of CD19 CAR (Figure 1C). Subsequently, we tested the immunophenotypes of CB CD19-CAR T and CB T. Flow cytometry data indicated that the proportions of CD4, CD8, TCR-α, and TCR-γ cells did not differ between CB

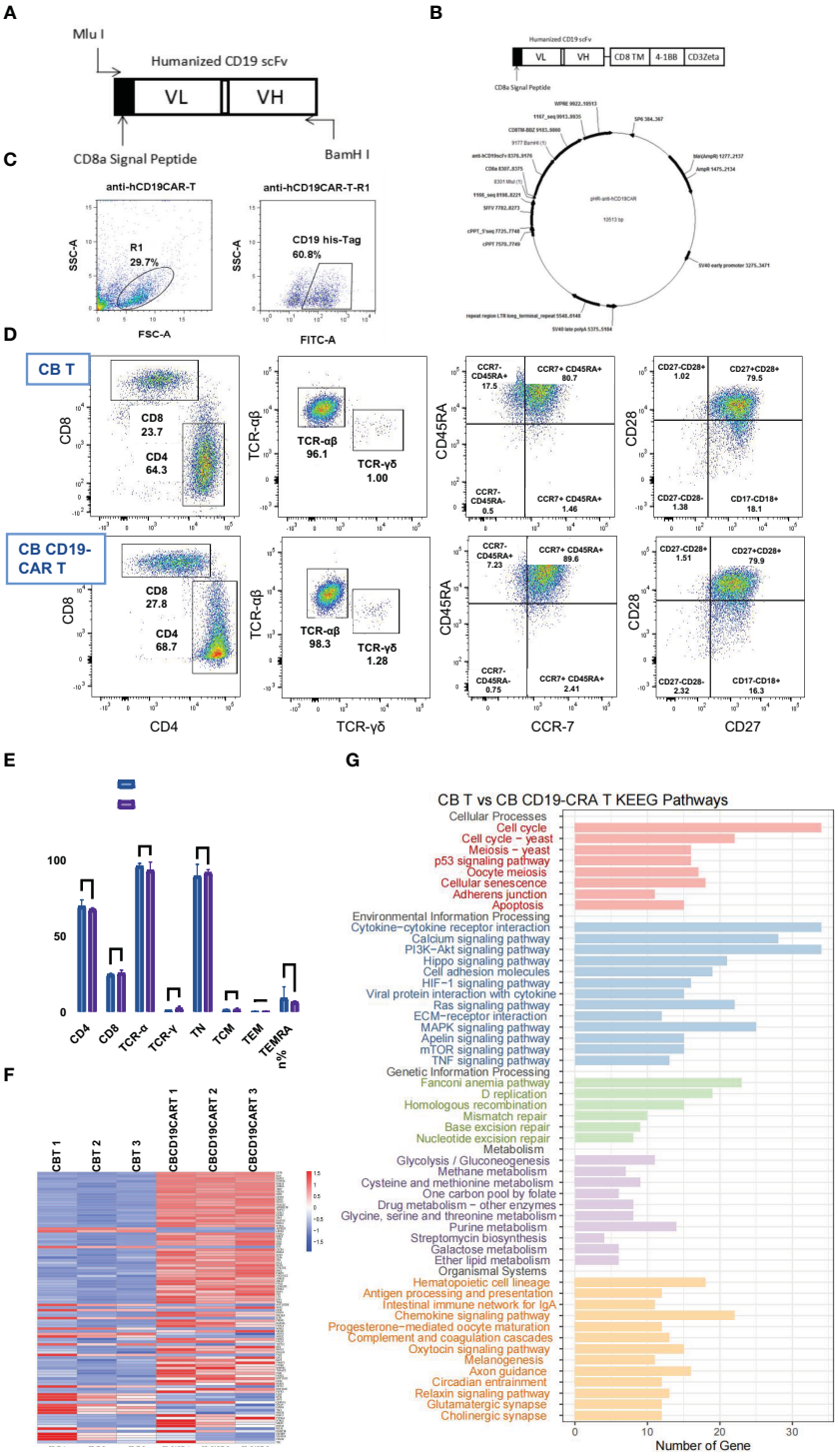

FIGURE 1
The construction, characterization, and gene expression of CB CD19-CAR T. **(A)** Schematic diagram of anti-hCD19 scFv. **(B)** Schematic diagram of plasmid construct for pHR- anti-hCD19CAR. **(C)** Representative flow cytometry analysis of transduction efficiency of CB T cells. **(D)** Representative flow cytometry analysis of the maturation profile shows there is no difference found in either the fraction of CB CD19-CAR T cells or CB T cells. **(E)** Data show mean ± SEM. **(F)** The heatmap of top 50 DEGs expression profiles. **(G)** KEGG pathway functional enrichment analyses of CB CD19-CAR T cells compared with CB T cells. TN, Naive T cell; TCM, Central memory T cell; TEM, effector memory T cell; TEMRA, Terminal effector T cell; DGEs, differentially expressed genes; SEM, standard error of means; ns, non-significant.

CD19-CAR T and CB T (Figures 1D, E). Following expansion, both CB CD19-CAR T and CB T cells were enriched for naïve T cells (CD45RA+CCR7+; CD28+CD27+), indicating that they were similarly cultured with no significant proliferation differences. We performed RNA-seq analysis of CB CD19-CAR and CB T cells (Figures 1F, G). CB CD19-CAR T cells manifested changes in genes related to adherens junction, cytokine-cytokine receptor interaction, chemokine signaling pathway and antigen processing

and presentation. This may be associated with the assembly of CAR to enhance cell membrane's function and T cell immune response.

CB CD19-CAR T cells specifically recognize and kill BV173 cells

To investigate the cytolytic ability of CB CD19-CAR T cells for distinguishing and eliminating CD19+ tumor cells, we first selected BV173 cells (a CD19+ ALL cell line) for verification. Compared with the CB T group and CD19-negative cell line K562 group, CB CD19-CAR T cells mediated cytotoxicity against the CFSE-labelled BV173 cells ($P < 0.05$, n = 3; Figures 2A, B), indicating that CB T cells expressing CAR constructs were able to eliminate tumor cell. We also detected cytokine products of CB CD19-CAR T cells following coculture with target tumor cells for the examination of the effector function. Supernatants analyzed by the CBA assay revealed that only BV173 group could elicit release of multiple cytokines by CB CD19-CAR T cells (Figure 2C and Figure S1A), further indicating that the CB CD19-CAR T cells exhibited specific activation with target cell stimulation.

CB CD19-CAR T has potent anti-tumor efficacy against CD19+ DLBCL cells *in vitro* and *in vivo*

SUDHL-4 cells are DLBCL cells expressing CD19 markers that can be recognized explicitly by CB CD19-CAR T cells. DB cells are DLBCL cells that are not CD19-positive. To confirm their cytotoxicity against CD19+DLBCL cells, we cocultured SUDHL-4 and DB cells with CB T and CB CD19-CAR T cells at different E: T ratios of 1:1, 2:1, 5:1, 10:1. In contrast to CB T cells, CB CD19-CAR T cells showed strong lysis function during coculture with SUDHL-4 cells ($P < 0.05$, n = 3; Figures 3A, B). We observed cytotoxicity towards SUDHL-4 cells but not DB cells, which was mirrored by the anti-tumor activity post antigen stimulation ($P < 0.05$, n = 3; Figures 3A, B). While the outgrowth of SUDHL-4 was not affected by the dose of CB CD19-CAR T cells, the low amount (E: T of 1:1) of CB CD19-CAR T cells still led to anti-tumor activity against CB CD19-CAR T cells. CB CD19-CAR T cells cocultured with SUDHL-4 cells also showed significantly higher cytokine secretion, including IL-2, IL-4, IL-6, IL-10, TNF-α, and IFN-γ (Figure 3C and Figure S1B), further demonstrating the CD19-dependent cytotoxicity of CB CD19-CAR T cells.

To evaluate the anti-lymphoma activity of CB CD19-CAR T cells *in vivo*, we established a murine xenogeneic model using SUDHL-4 cells. Subcutaneous injection of SUDHL-4 cells into the backs of BALB/c-nu mice allowed the tumor to expand. Following confirmation of tumor engraftment on day 9, animals received CB CD19-CAR T cells or CB T cells on day 10. The growth of tumors and their weight were followed in three groups (Figures 3D-F). CB CD19-CAR T cells were able to control the growth of tumor compared with CB T cells and untreated group, the representative images and data from n = 4 mice per group (Figure 3D). No significant decrease in mouse body weight or other toxicity signs was observed in any treatments, including CB T cells and CB CD19-CAR T cells, suggesting little systemic toxicity with good tolerability (Figure 3F). These results support the results of our *in vitro* study and indicate that CB CD19-CAR T cells effectively inhibit tumor growth in a DLBCL model.

Changes in genes expression of CB CD19-CAR T cells following coculture

We analyzed the changes after CB CD19-CAR T cell interaction with tumor cells. After 48h of coculture, CB CD19-CAR T cells showed loss of the CCR-7 phenotype and naïve T cells converted them into terminally differentiated effector memory cells re-expressing CD45RA (T_{EMRA}) T cells; the formerly naïve CB T cell population promptly differentiated into an effector cell (Figure 4A). The upregulation of immune checkpoint proteins might limit the anti-tumor activity causing resistance of immune cell-mediated therapy. Among them, programmed cell death protein-1 (PD-1) and T cell immunoglobulin and mucin domain-containing protein 3 (TIM-3) have recently received increased attention for playing a critical role in inhibition of T cell proliferation and function. Therefore, we investigated changes in the expression of PD-1 and TIM-3 on the surface of CB CD19-CAR T cells. As shown by our flow cytometry results (Figure 4B), mean TIM-3 expression was significantly higher in CB CD19-CAR T cells after coculture with SUDHL-4 cells. PD-1 expression levels were not statistically significant. CB-derived CAR T cells showed elevated immune checkpoints after coculture with SUDHL-4, which might hinder the ability of CB CAR T cells to expand and act continuously *in vivo*.

To elucidate which gene is responsible for these changes, we analyzed the RNA-seq data of CB CD19-CAR T cells cocultured with or without SUDHL-4 cells. The resulting SUDHL-4 cells were cultured for 48 h when CB CD19-CAR T cells were selected using magnetic beads. We identified 3331 DEGs, 1584 upregulated and 1747 downregulated, in the two comparisons (Figure 5A). The top 50 DEGs following coculture was listed in Figure 5B. KEGG analysis of the top DEGs showed that immune-related gene pathways were mainly altered following coculture. A functional enrichment analysis in all two comparisons showed that most of the KEGG pathways were signal "focal adhesion" "cytokine-cytokine receptor interaction," and "chemokine signaling pathway," which are associated with recognition or killing by CAR T cells binding to tumor cells (Figure 5C).

Next, we analyzed DEGs associated with immunity between CB T subsets, CB CD19-CAR T subsets, and CB CD19-CAR T/SUDHL-4 coculture subsets in our combined dataset. Hierarchical clustering of 65 immune-related genes led to the identification of chemokines/chemokine receptors (*CXCL10, CCL2, CX3CR1, CXCR4*, and *CCL5*), costimulation (*TNFRSFs* gene families), exhaustion- (*NR4As* gene families), and memory-associated genes (*IL7R* and *IL2RA*) (Figure 5D). Coculture of CB CD19-CAR T cells with SUDHL-4 cells significantly upregulated canonical exhaustion-associated genes (*NR4A3*), costimulation genes (*TNFSF9, TNFRSF8*, and *TNFRSF9*) and *STAT1*, and downregulated memory-associated

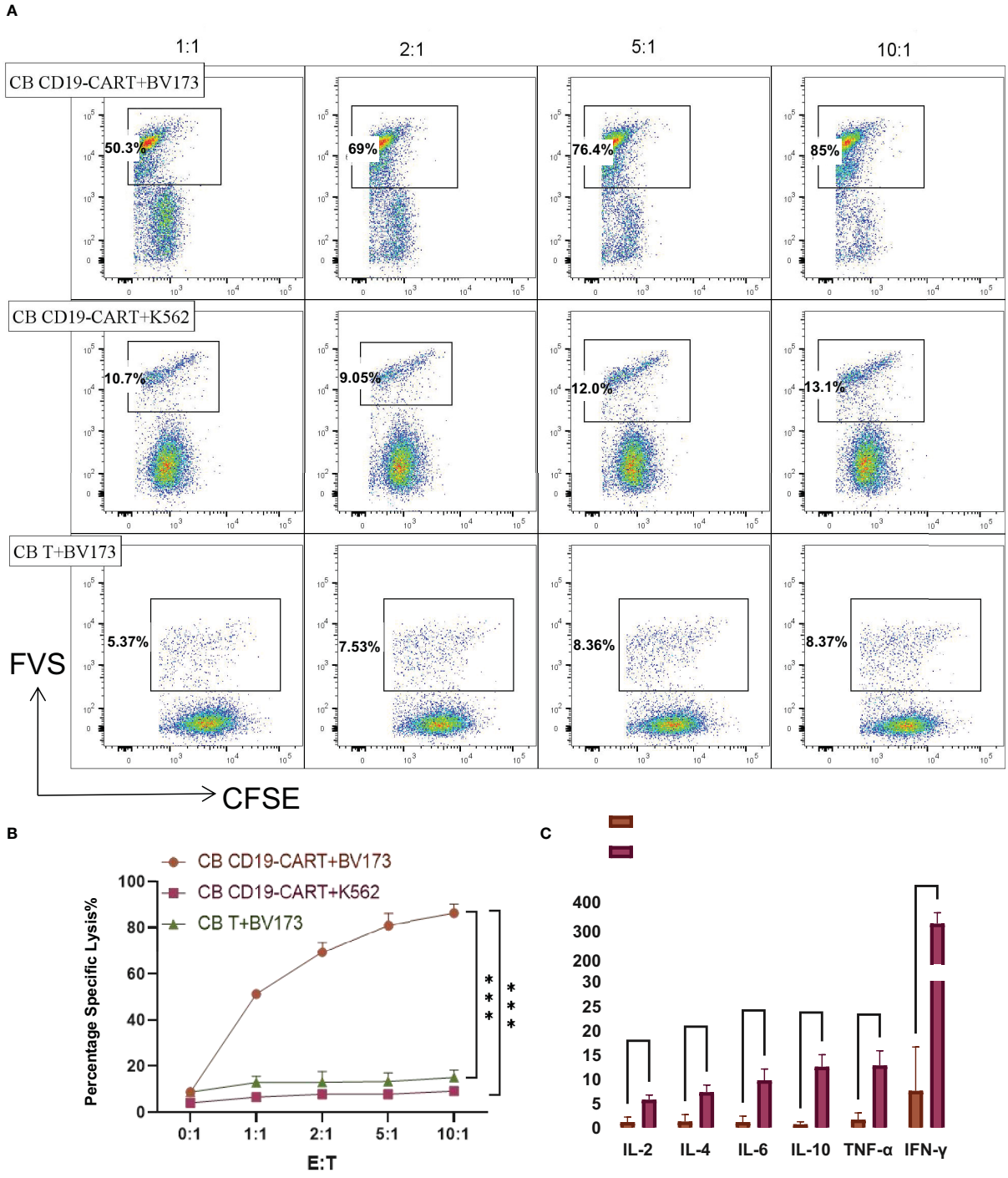

FIGURE 2
CB CD19-CART specifically kills CD19+ BV173 cells. **(A)** Representative dot plots of cytotoxicity assays showing specific on-target killing. The CFSE +FVS+/CFSE+ ratio was used to determine the kill rate. **(B)** Data show mean ± SEM of specific cytotoxicity experiments. **(C)** Statistical diagram of cytokine concentration in CB T or CB-CD19-CAR T cells cocultured with BV173 cells at an E: T ratio of 1:1 for 24h. SEM, standard error of means; ns, non-significant; ***$P < 0.001$, ****$P < 0.0001$.

genes (*IL7R*, *CXCL10*, and *CXCR4*) compared to coculture with CB T cells. Notably, we found that genes associated with ferroptosis (*TFRC* and *SLC40A1*) in CB CD19-CAR T/SUDHL-4 coculture were more likely to be differentially expressed compared to CB T and CB CD19-CAR T. Here, it may indicate the involvement of ferroptosis in CB CD19-CAR T cell death (Figure 5D).

Discussion

CAR T cell therapy has been presented as a second or even first-line treatment in patients with R/R LBCL (23–25). The 'off-the-shelf' product is under intense investigation to enable higher and broader availability of CAR T therapy. Several studies have shown

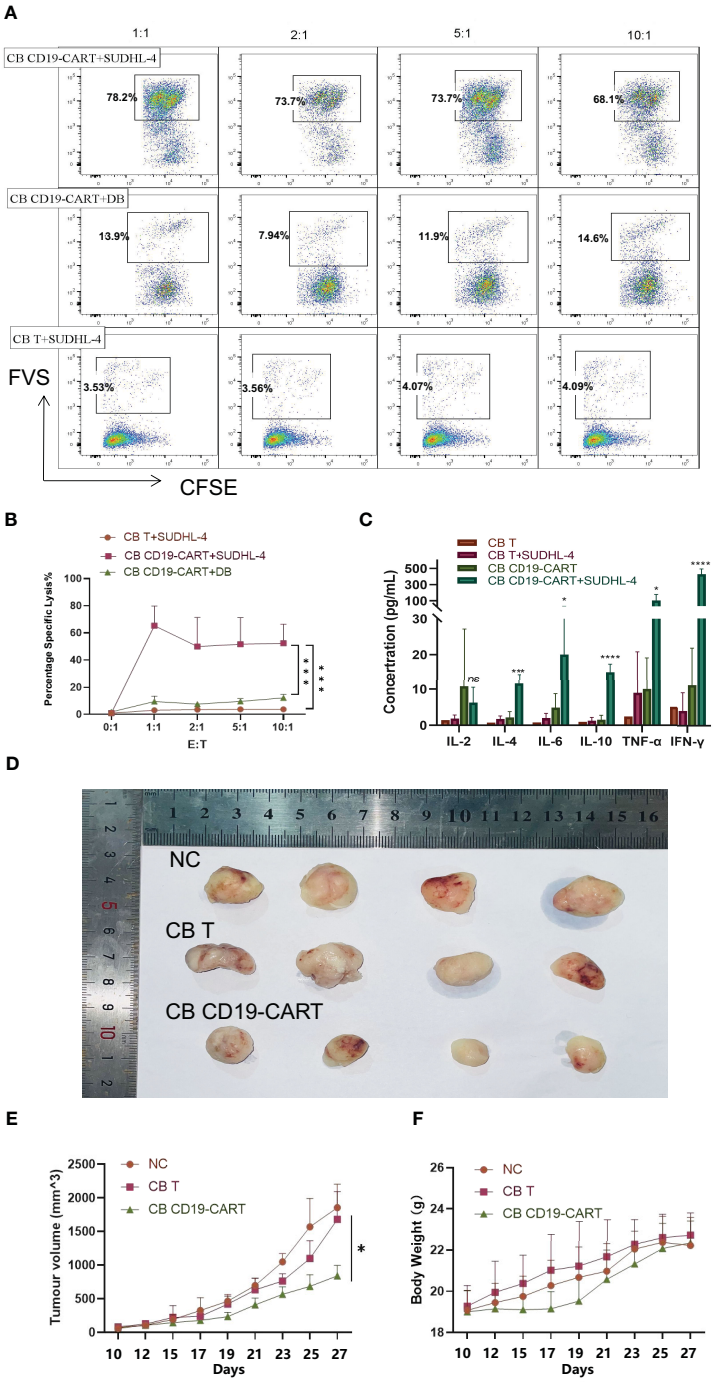

FIGURE 3
Specific cytotoxicity of CB CD19-CAR T cells targeting CD19+ DLBCL cells. **(A)** Representative plots showing specific cytotoxicity of CB CD19-CAR T cells against CD19+ DLBCL cells but not CD19- DLBCL cells. **(B)** Quantitative data of the cytotoxic activity of CB-CD19-CAR T cells and CB T cells against DLBCL cell lines. Error bars represent SEM. **(C)** Cytokine concentration in CB T or CB-CD19-CAR T cells cocultured with SUDHL-4 cells at an E: T ratio of 1:1 for 24h. **(D)** Representative tumor resectates from each group. **(E, F)** Data are expressed as mean ± SEM of tumor masses and body weight (n=4 mice per group). SEM, standard error of means; ns, non-significant; *$P < 0.05$; ***$P < 0.001$; ****$P < 0.0001$.

that CB, a lesser-used source of CAR T cells, is an effective source of cancer immunotherapy (22, 26). For example, studies have used primary cells from CB to culture-specific T cells that target acute myeloid leukemia and ALL (27, 28). The activity of CB-derived CAR T cells has also been confirmed in ALL cell lines and mouse models (22). Additionally, CAR-NK cells from CB cells have been safely administered without complete HLA matching and showed practical anti-tumor effects in NHL. Considering the unique characteristics of CB, we designed a study on the application of CB CD19-CAR T cells in CD19+ DLBCL. CB CD19-CAR T cells

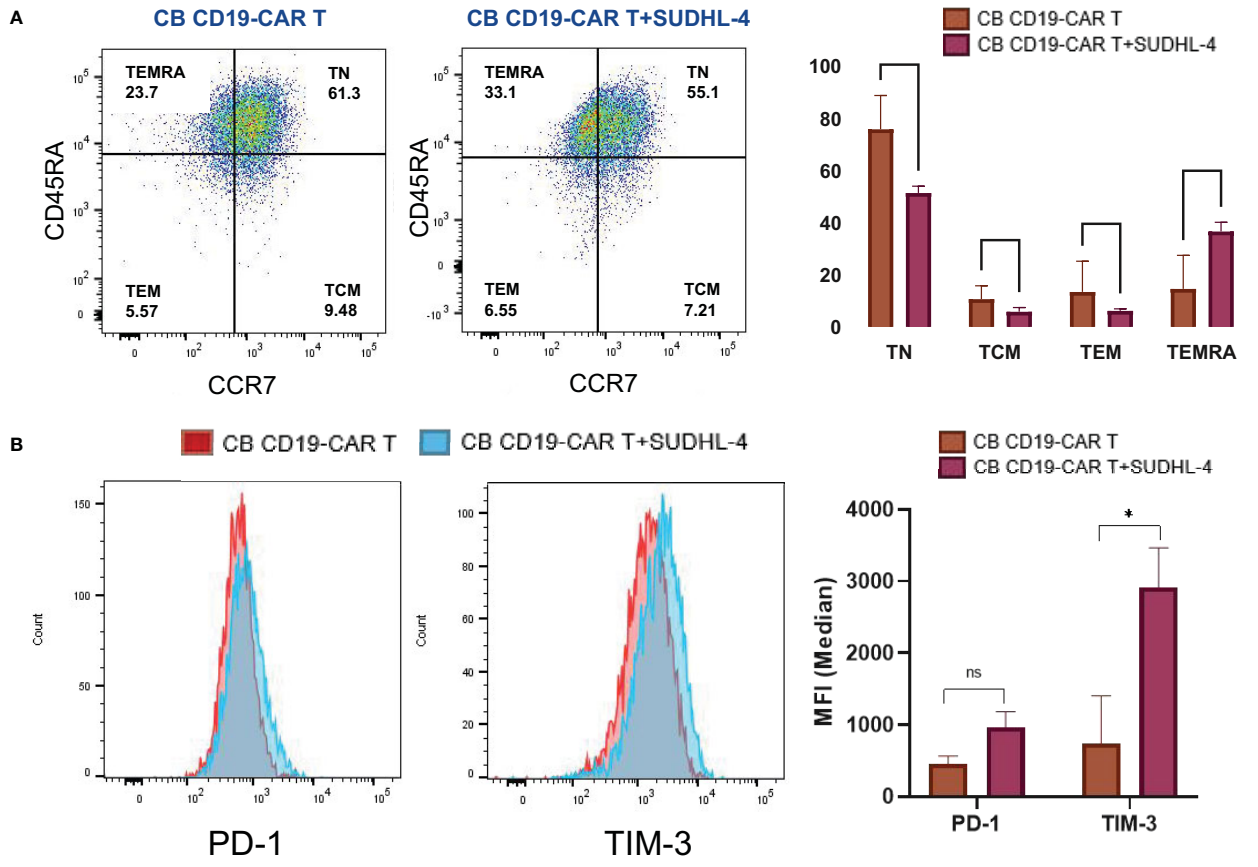

FIGURE 4
Phenotypic and numeric changes of the coculture of CB CD19-CAR T with the DLBCL cells. **(A)** Representative flow cytometric plots of the CB CD19-CAR T after coculture of SUDHL-4 cells (left panel). Data show mean ± SEM (right panel). **(B)** Representative flow cytometry histogram and representative histogram of PD-1 and TIM-3 expression in CB CD19-CAR T alone and after coculture with SUDHL-4 cells (left panel). Bar graphs show mean ± SEM (right panel). TN, Naive T cell; TCM, Central memory T cell; TEM, effector memory T cell; TEMRA, Terminal effector T cell; PD-1, programmed cell death protein-1; TIM-3, T cell immunoglobulin and mucin domain-containing protein 3; SEM, standard error of means; ns, non-significant; $*P < 0.05$; $**P < 0.01$.

displayed cytotoxicity targeting the CD19+ T cell lymphoma cell line BV173 and CD19+ DLBCL cell line SUDHL-4, triggered secretion of multiple cytokines in coculture assays, and limited tumor growth in a mouse model. Gene expression profiles confirmed increased chemokines/chemokine receptors and exhaustion genes in CB CD19-CAR T cells upon challenge with tumor cells compared to CB T cells. Our results show that CB CD19-CAR T cells are a promising therapeutic strategy for treating DLBCL.

A single dose of CB can amplify 10^8 CAR T cells, and CB T cells have an advantage over auto-CAR T cells because of insufficient T cells in post-chemotherapy patients. T cells derived from CB also possess a unique antigen-naïve status (29). There is ample evidence that demonstrates different subsets of naïve T cells play distinct roles in immunity (30) and that the stemness of anti-tumor T cells can increase the potential of immunotherapy (31). CAR T cells constructed with different costimulatory domains show different features. We built CB CD19-CAR T cells using 4-1BB as a costimulatory molecule, as CARs confer longer persistence in the presence of 4-1BB (32). Additionally, 4-1BB-based T cells tend to behave like central memory-like T cells, improving mitochondrial and expiratory capability and fatty acid metabolism (33). Moreover, we argue that CB CD19-CAR T cells could specifically recognize and kill the CD19+ ALL cell line BV173 and DLBCL cell line SUDHL-4 in an antigen-specific manner *in vitro* and control tumor progression *in vivo*. Overall, we determined that CB CD19-CAR T cells show specific cytotoxicity and simultaneous cytokine production can effectively eliminate CD19+ DLBCL cells.

PBMCs-naïve T cells cause severe GVHD in murine models (34). However, T cells derived from CB were transformed into CAR T cells after transfection with a surface antigen specific CAR because these cells lack the CD3/TCRab complex; therefore, their responses are not HLA-restricted (35), which is a characteristic of the placenta. Different from all other tissue cells, extravillous cytotrophoblast cells in the placenta express only HLA-C, HLA-E, and HLA-G, and syncytiotrophoblast cells are HLA-negative (36); these potential features result in minimal risk of GVHD (37). Furthermore, this implies an additional reason for the decreased risk of GVHD. The reactivity of CB T cells is reduced by impaired nuclear factor of activated T cell signaling (38). We observed a

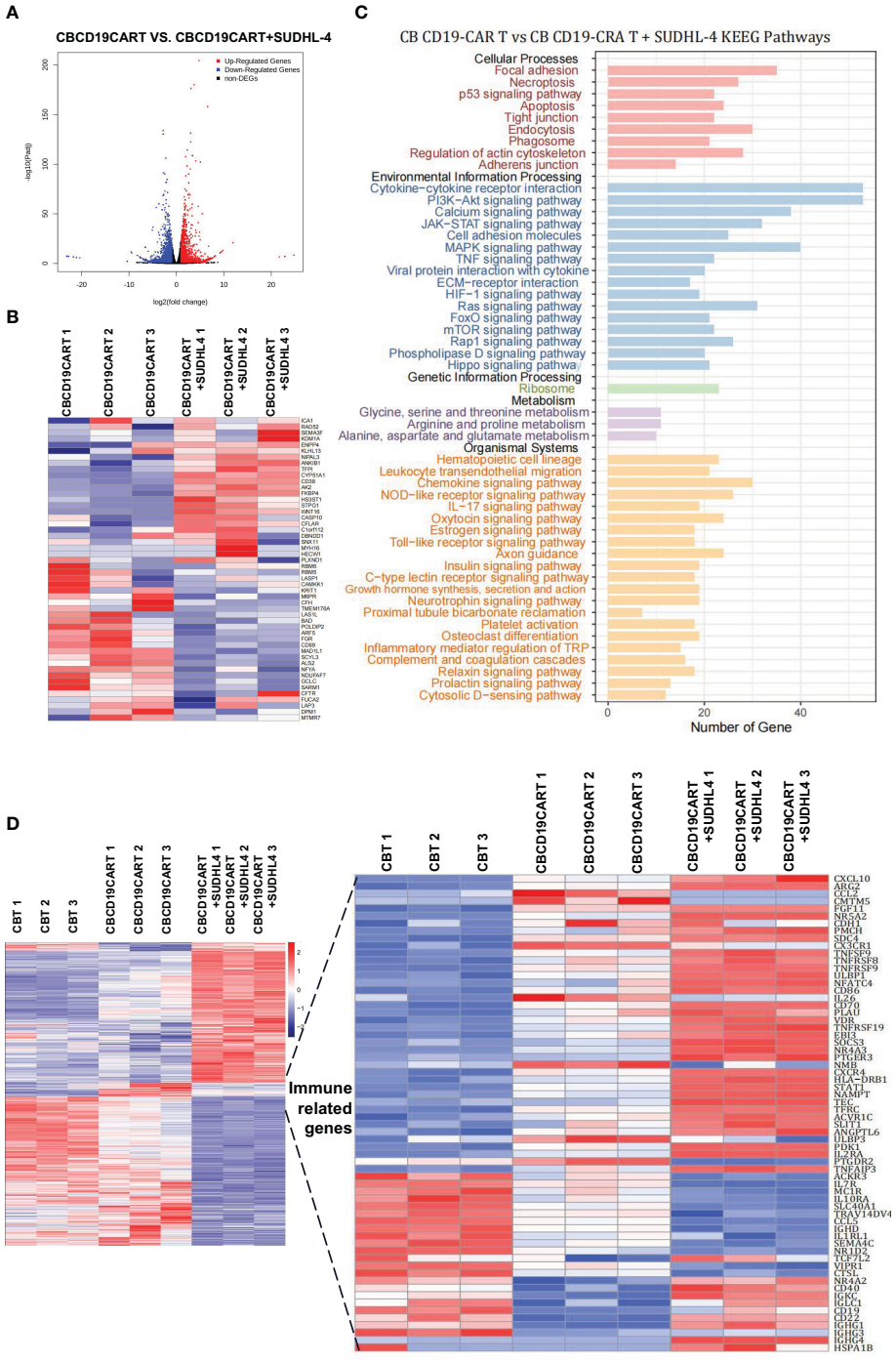

FIGURE 5
RNA-seq analysis of the coculture of CB CD19-CAR T with the DLBCL cells. **(A)** The distribution of DEGs between CB CD19-CAR T alone and after coculture with SUDHL-4 cells. **(B)** Heatmap of top 50 DEGs. **(C)** KEGG pathways of DEGs between CB CD19-CAR T alone and after coculture with SUDHL-4 cells. **(D)** Heatmap for immune-related gene sets of CB T group, CB CD19-CAR T alone group and after coculture with SUDHL-4 cells group. DGEs, differentially expressed genes.

weight reduction in the CB CD19-CAR T cell group after treatment compared with the control group, but it increased again after a week. No diarrhea, rash, or jaundice, which are common symptoms of GVHD, were observed during the observation period. We concluded that CB CD19-CAR T cells were associated with minimal GVHD.

No response and secondary resistance after CAR T cell therapy are clinical conundrums in the CAR T cell therapy era (39). CAR T cell expansion and persistence are essential components for CAR T efficacy, patients achieving CR, and preventing relapse. Defining phenotypic and functional changes in CAR T cells is paramount for developing practical CAR-T strategies (40). Our study also

elucidated that after coculture with DLBCL cell lines, CB CD19-CAR T cells show significantly upregulated *TNFSF9, TNFRSF8, TNFRSF9*, and *STAT1* compared with CB T and CB CD19-CAR T cells. Several TNFR family members participate in sustaining T cell responses after T cell activation (41). Another study demonstrated that the STAT1 pathway defends T cells from NK cell-mediated eradication involved in T cell survival (42). CB CD19-CAR T cells may be activated by naïve CB T cells to initiate the STAT1 signaling pathway and TNK pathway and release cytokines to play an effector role. However, we also found that *NR4As* gene families were upregulated, and IL7R was downregulated in the coculture group compared with CB CD19-CAR T alone. *NR4As* genes play an essential role in T cell dysfunction and cause CAR T cells to enter an exhausted or dysfunctional state in solid tumors (43, 44). Previous reports have shown that *IL7R* blocks the development of T cells, and patients with *IL7R*-inactivating mutations present with severe combined immunodeficiency (45, 46). Short persistence and early exhaustion of T cells are significant limitations to immunotherapy efficacy and its broad application (47, 48). Thus, targeting *IL7R* and *NR4A* is a promising CAR T cell therapy strategy. Many strategies, such as designing CB-derived CAR T cells with specificity to immunodeficiency genes and virus-specific antigens (49), must be explored to address these problems. Nevertheless, our work addresses a significant barrier to the progress of this emerging class of therapeutic agents. These possibilities will be examined in the future to develop CAR T therapy.

In conclusion, we generated CB CD19-CAR T cells and confirmed their anti-tumor activity against DLBCL cells. We also studied the underlying cellular pathways in CB CAR-T cells and explored their exhaustion mechanisms. The development of CB CAR T cells as an 'off-the-shelf' CAR T cell readily available for patients with R/R LBCL in an affordable and timely manner would significantly get patients close to these therapeutics. Our trial results could help inform patients who require immunotherapy of more excellent choices.

Data availability statement

The datasets presented in this study can be found in online repositories. The names of the repository/repositories and accession number(s) can be found below: BioProject *via* accession ID: PRJNA924756 https://dataview.ncbi.nim.nih.gov/object/PRJNA924756?reviewer=ktch835c5g69b09tia6qphv13f.

Ethics statement

The animal study was reviewed and approved by Department of Hematology, The Second Affiliated Hospital of NanChang University.

Author contributions

TY and LY designed the study; TY, CL, and LY performed the experiments and analyzed the data, TY and LY wrote the manuscript. All authors contributed to the article and approved the submitted version.

Funding

This work and LY were supported by the National Natural Science Foundation of China (grant numbers 81460030 and 81770221), and the Leading Talent Foundation of Jiangxi Province (grant numbers 20225BCJ22001).

Acknowledgments

We thank Editage (www.editage.com) for linguistic assistance with the manuscript.

Conflict of interest

Authors HZ and YT were employed by the company Qilu Cell Therapy Technology Co., Ltd.

The remaining authors declare that the research was conducted in the absence of any commercial or financial relationships that could be construed as a potential conflict of interest.

Publisher's note

Supplementary material

The Supplementary Material for this article can be found online at: https://www.frontiersin.org/articles/10.3389/fimmu.2023.1139482/full#supplementary-material

References

1. Lin X, Lee S, Sharma P, George B, Scott J. Summary of us food and drug administration chimeric antigen receptor (Car) T-cell biologics license application approvals from a statistical perspective. *J Clin Oncol* (2022) 40(30):3501–9. doi: 10.1200/JCO.21.02558

2. June CH, O'Connor RS, Kawalekar OU, Ghassemi S, Milone MC. Car T cell immunotherapy for human cancer. *Science* (2018) 359(6382):1361–5. doi: 10.1126/science.aar6711

3. Food and Drug Administration (Fda). *Center for biologics evaluation and research. approval letter-breyanzi* (2021). Available at: https://www.fda.gov/media/145712/download.

4. Food and Drug Administration (Fda). *Center for biologics evaluation and research. approval letter-kymriah* (2017). Available at: https://www.fda.gov/media/106989/download.

5. Food and Drug Administration (Fda). *Center for biologics evaluation and research. approval letter-yescarta* (2017). Available at: https://www.fda.gov/media/108458/download.

6. Food and Drug Administration (Fda). *Center for biologics evaluation and research. approval letter-tecartus* (2020). Available at: https://www.fda.gov/media/140415/download.

7. Food and Drug Administration (Fda). *Center for biologics evaluation and research. approval letter-yescarta* (2022). Available at: https://www.fda.gov/downloads/BiologicsBloodVaccines/CellularGeneTherapyProducts/ApprovedProducts/UCM573941.pdf.

8. Mullard A. Fda approves fourth car-T cell therapy. *Nat Rev Drug Discovery* (2021) 20(3):166. doi: 10.1038/d41573-021-00031-9

9. Park JH, Geyer MB, Brentjens RJ. Cd19-targeted car T-cell therapeutics for hematologic malignancies: interpreting clinical outcomes to date. *Blood* (2016) 127 (26):3312–20. doi: 10.1182/blood-2016-02-629063

10. Kohl U, Arsenieva S, Holzinger A, Abken H. Car T cells in trials: recent achievements and challenges that remain in the production of modified T cells for clinical applications. *Hum Gene Ther* (2018) 29(5):559–68. doi: 10.1089/hum.2017.254

11. Thommen DS, Schumacher TN. T Cell dysfunction in cancer. *Cancer Cell* (2018) 33(4):547–62. doi: 10.1016/j.ccell.2018.03.012

12. Amini L, Silbert SK, Maude SL, Nastoupil LJ, Ramos CA, Brentjens RJ, et al. Preparing for car T cell therapy: patient selection, bridging therapies and lymphodepletion. *Nat Rev Clin Oncol* (2022) 19(5):342–55. doi: 10.1038/s41571-022-00607-3

13. Salmikangas P, Kinsella N, Chamberlain P. Chimeric antigen receptor T-cells (Car T-cells) for cancer immunotherapy - moving target for industry? *Pharm Res* (2018) 35(8):152. doi: 10.1007/s11095-018-2436-z

14. Yip A, Webster RM. The market for chimeric antigen receptor T cell therapies. *Nat Rev Drug Discovery* (2018) 17(3):161–2. doi: 10.1038/nrd.2017.266

15. Depil S, Duchateau P, Grupp SA, Mufti G, Poirot L. 'Off-the-Shelf' allogeneic car T cells: development and challenges. *Nat Rev Drug Discovery* (2020) 19(3):185–99. doi: 10.1038/s41573-019-0051-2

16. Benjamin R. Advances in off-the-Shelf car T-cell therapy. *Clin Adv Hematol Oncol* (2019) 17(3):155–7.

17. Pan J, Tan Y, Wang G, Deng B, Ling Z, Song W, et al. Donor-derived Cd7 chimeric antigen receptor T cells for T-cell acute lymphoblastic leukemia: first-in-Human, phase I trial. *J Clin Oncol* (2021) 39(30):3340–51. doi: 10.1200/JCO.21.00389

18. The quest for off-the-Shelf car T cells. *Cancer Discovery* (2018) 8(7):787–8. doi: 10.1158/2159-8290.CD-ND2018-005

19. Balassa K, Rocha V. Anticancer cellular immunotherapies derived from umbilical cord blood. *Expert Opin Biol Ther* (2018) 18(2):121–34. doi: 10.1080/14712598.2018.1402002

20. Liu E, Marin D, Banerjee P, Macapinlac HA, Thompson P, Basar R, et al. Use of car-transduced natural killer cells in Cd19-positive lymphoid tumors. *N Engl J Med* (2020) 382(6):545–53. doi: 10.1056/NEJMoa1910607

21. Tammana S, Huang X, Wong M, Milone MC, Ma L, Levine BL, et al. 4-1bb and Cd28 signaling plays a synergistic role in redirecting umbilical cord blood T cells against b-cell malignancies. *Hum Gene Ther* (2010) 21(1):75–86. doi: 10.1089/hum.2009.122

22. Liu DD, Hong WC, Qiu KY, Li XY, Liu Y, Zhu LW, et al. Umbilical cord blood: a promising source for allogeneic car-T cells. *Front Oncol* (2022) 12:944248. doi: 10.3389/fonc.2022.944248

23. Locke FL, Miklos DB, Jacobson CA, Perales MA, Kersten MJ, Oluwole OO, et al. Axicabtagene ciloleucel as second-line therapy for Large b-cell lymphoma. *N Engl J Med* (2022) 386(7):640–54. doi: 10.1056/NEJMoa2116133

24. Neelapu SS, Dickinson M, Munoz J, Ulrickson ML, Thieblemont C, Oluwole OO, et al. Axicabtagene ciloleucel as first-line therapy in high-risk Large b-cell lymphoma: the phase 2 zuma-12 trial. *Nat Med* (2022) 28(4):735–42. doi: 10.1038/s41591-022-01731-4

25. Kamdar M, Solomon SR, Arnason J, Johnston PB, Glass B, Bachanova V, et al. Lisocabtagene maraleucel versus standard of care with salvage chemotherapy followed by autologous stem cell transplantation as second-line treatment in patients with relapsed or refractory Large b-cell lymphoma (Transform): results from an interim analysis of an open-label, randomised, phase 3 trial. *Lancet* (2022) 399(10343):2294–308. doi: 10.1016/S0140-6736(22)00662-6

26. Cael B, Galaine J, Bardey I, Marton C, Fredon M, Biichle S, et al. Umbilical cord blood as a source of less differentiated T cells to produce Cd123 car-T cells. *Cancers (Basel)* (2022) 14(13). doi: 10.3390/cancers14133168

27. Hubner J, Hoseini SS, Suerth JD, Hoffmann D, Maluski M, Herbst J, et al. Generation of genetically engineered precursor T-cells from human umbilical cord blood using an optimized alpharetroviral vector platform. *Mol Ther* (2016) 24(7):1216–26. doi: 10.1038/mt.2016.89

28. Micklethwaite KP, Savoldo B, Hanley PJ, Leen AM, Demmler-Harrison GJ, Cooper LJ, et al. Derivation of human T lymphocytes from cord blood and peripheral blood with antiviral and antileukemic specificity from a single culture as protection against infection and relapse after stem cell transplantation. *Blood* (2010) 115 (13):2695–703. doi: 10.1182/blood-2009-09-242263

29. Szabolcs P, Park KD, Reese M, Marti L, Broadwater G, Kurtzberg J. Coexistent naive phenotype and higher cycling rate of cord blood T cells as compared to adult peripheral blood. *Exp Hematol* (2003) 31(8):708–14. doi: 10.1016/s0301-472x(03)00160-7

30. Davenport MP, Smith NL, Rudd BD. Building a T cell compartment: how immune cell development shapes function. *Nat Rev Immunol* (2020) 20(8):499–506. doi: 10.1038/s41577-020-0332-3

31. Arcangeli S, Bove C, Mezzanotte C, Camisa B, Falcone L, Manfredi F, et al. Car T cell manufacturing from Naive/Stem memory T lymphocytes enhances antitumor responses while curtailing cytokine release syndrome. *J Clin Invest* (2022) 132(12). doi: 10.1172/JCI150807

32. Philipson BI, O'Connor RS, May MJ, June CH, Albelda SM, Milone MC. 4-1bb costimulation promotes car T cell survival through noncanonical nf-kappab signaling. *Sci Signal* (2020) 13(625). doi: 10.1126/scisignal.aay8248

33. Kawalekar OU, O'Connor RS, Fraietta JA, Guo L, McGettigan SE, Posey ADJr., et al. Distinct signaling of coreceptors regulates specific metabolism pathways and impacts memory development in car T cells. *Immunity* (2016) 44(2):380–90. doi: 10.1016/j.immuni.2016.01.021

34. Bleakley M, Sehgal A, Seropian S, Biernacki MA, Krakow EF, Dahlberg A, et al. Naive T-cell depletion to prevent chronic graft-Versus-Host disease. *J Clin Oncol* (2022) 40(11):1174–85. doi: 10.1200/JCO.21.01755

35. Lo Presti V, Nierkens S, Boelens JJ, van Til NP. Use of cord blood derived T-cells in cancer immunotherapy: milestones achieved and future perspectives. *Expert Rev Hematol* (2018) 11(3):209–18. doi: 10.1080/17474086.2018.1431119

36. Juch H, Blaschitz A, Dohr G, Hutter H. Hla class I expression in the human placenta. *Wien Med Wochenschr* (2012) 162(9-10):196–200. doi: 10.1007/s10354-012-0070-7

37. Kwoczek J, Riese SB, Tischer S, Bak S, Lahrberg J, Oelke M, et al. Cord blood-derived T cells allow the generation of a more naive tumor-reactive cytotoxic T-cell phenotype. *Transfusion* (2018) 58(1):88–99. doi: 10.1111/trf.14365

38. Kadereit S, Mohammad SF, Miller RE, Woods KD, Listrom CD, McKinnon K, et al. Reduced Nfat1 protein expression in human umbilical cord blood T lymphocytes. *Blood* (1999) 94(9):3101–7. doi: 10.1182/blood.V94.9.3101

39. Bishop MR, Dickinson M, Purtill D, Barba P, Santoro A, Hamad N, et al. Second-line tisagenlecleucel or standard care in aggressive b-cell lymphoma. *N Engl J Med* (2022) 386(7):629–39. doi: 10.1056/NEJMoa2116596

40. Daniels KG, Wang S, Simic MS, Bhargava HK, Capponi S, Tonai Y, et al. Decoding car T cell phenotype using combinatorial signaling motif libraries and machine learning. *Science* (2022) 378(6625):1194–200. doi: 10.1126/science.abq0225

41. Watts TH. Tnf/Tnfr family members in costimulation of T cell responses. *Annu Rev Immunol* (2005) 23:23–68. doi: 10.1146/annurev.immunol.23.021704.115839

42. Kang YH, Biswas A, Field M, Snapper SB. Stat1 signaling shields T cells from nk cell-mediated cytotoxicity. *Nat Commun* (2019) 10(1):912. doi: 10.1038/s41467-019-08743-8

43. Liu X, Wang Y, Lu H, Li J, Yan X, Xiao M, et al. Genome-wide analysis identifies Nr4a1 as a key mediator of T cell dysfunction. *Nature* (2019) 567(7749):525–9. doi: 10.1038/s41586-019-0979-8

44. Chen J, Lopez-Moyado IF, Seo H, Lio CJ, Hempleman LJ, Sekiya T, et al. Nr4a transcription factors limit car T cell function in solid tumours. *Nature* (2019) 567 (7749):530–4. doi: 10.1038/s41586-019-0985-x

45. Puel A, Ziegler SF, Buckley RH, Leonard WJ. Defective Il7r expression in t(-)B(+)Nk(+) severe combined immunodeficiency. *Nat Genet* (1998) 20(4):394–7. doi: 10.1038/3877

46. Han C, Ntziachristos P. T-All and the talented Mr Il7ralpha. *Blood* (2021) 138 (12):1003–4. doi: 10.1182/blood.2021012184

47. Fraietta JA, Lacey SF, Orlando EJ, Pruteanu-Malinici I, Gohil M, Lundh S, et al. Determinants of response and resistance to Cd19 chimeric antigen receptor (Car) T cell therapy of chronic lymphocytic leukemia. *Nat Med* (2018) 24(5):563–71. doi: 10.1038/s41591-018-0010-1

48. Maude SL, Frey N, Shaw PA, Aplenc R, Barrett DM, Bunin NJ, et al. Chimeric antigen receptor T cells for sustained remissions in leukemia. *N Engl J Med* (2014) 371 (16):1507–17. doi: 10.1056/NEJMoa1407222

49. Rossig C, Pule M, Altvater B, Saiagh S, Wright G, Ghorashian S, et al. Vaccination to improve the persistence of Cd19car gene-modified T cells in relapsed pediatric acute lymphoblastic leukemia. *Leukemia* (2017) 31(5):1087–95. doi: 10.1038/leu.2017.39

Frontiers in Immunology

Explores novel approaches and diagnoses to treat immune disorders.

The official journal of the International Union of Immunological Societies (IUIS) and the most cited in its field, leading the way for research across basic, translational and clinical immunology.

Discover the latest Research Topics

See more →

Frontiers

Avenue du Tribunal-Fédéral 34
1005 Lausanne, Switzerland
frontiersin.org

Contact us

+41 (0)21 510 17 00
frontiersin.org/about/contact